



# Summary of Alberta's Shale- and Siltstone-Hosted Hydrocarbon Resource Potential

# **Summary of Alberta's Shale- and Siltstone-Hosted Hydrocarbons**

C.D. Rokosh, S. Lyster, S.D.A. Anderson,  
A.P. Beaton, H. Berhane, T. Brazzoni,  
D. Chen, Y. Cheng, T. Mack, C. Pana and  
J.G. Pawlowicz

Energy Resources Conservation Board

October 2012

©Her Majesty the Queen in Right of Alberta, 2012  
ISBN 978-1-4601-0082-0

The Energy Resources Conservation Board/Alberta Geological Survey (ERCB/AGS), its employees and contractors make no warranty, guarantee or representation, express or implied, or assume any legal liability regarding the correctness, accuracy, completeness or reliability of this publication. Any references to proprietary software and/or any use of proprietary data formats do not constitute endorsement by ERCB/AGS of any manufacturer's product.

If you use information from this publication in other publications or presentations, please acknowledge the ERCB/AGS. We recommend the following reference format:

Rokosh, C.D., Lyster, S., Anderson, S.D.A., Beaton, A.P., Berhane, H., Brazzoni, T., Chen, D., Cheng, Y., Mack, T., Pana, C. and Pawlowicz, J.G. (2012): Summary of Alberta's shale- and siltstone-hosted hydrocarbon resource potential; Energy Resources Conservation Board, ERCB/AGS Open File Report 2012-06, 327 p.

**Published October 2012 by**

Energy Resources Conservation Board  
Alberta Geological Survey  
402, 4999–98th Avenue  
Edmonton, AB T6B 2X3  
Canada

Tel: 780.422.1927

Fax: 780.422.1918

E-mail: [AGS-Info@ercb.ca](mailto:AGS-Info@ercb.ca)

Website: [www.ags.gov.ab.ca](http://www.ags.gov.ab.ca)

## Contents

Acknowledgements .....	ix
Executive Summary .....	x
<b>1 Introduction .....</b>	<b>1</b>
1.1 Introduction to Shale- and Siltstone-Hosted Hydrocarbons .....	1
1.2 Study Overview.....	1
1.3 Definitions and Methodology.....	2
1.4 Data Collection Summary .....	4
1.5 Units Evaluated .....	4
<b>2 Summary of Resource Variables for Each Unit.....</b>	<b>4</b>
2.1 Summary of the Duvernay Formation .....	6
2.2 Summary of the Muskwa Formation .....	20
2.3 Summary of the Montney Formation.....	31
2.4 Preliminary Summary of the Basal Banff and Exshaw Formations .....	42
2.5 Preliminary Summary of the Nordegg Member .....	52
2.6 Preliminary Summary of the Wilrich Member .....	63
2.7 Preliminary Summary of the Rierdon Formation .....	73
2.8 Preliminary Summary of the Colorado Group.....	84
2.8.1 North Colorado Evaluation Area .....	84
2.8.2 South Colorado Evaluation Area .....	85
2.9 Preliminary Evaluation of Additional Units with Shale- and Siltstone-Hosted Hydrocarbon Potential .....	86
<b>3 Summary of Resource Variables Common to Each Assessed Unit: Methodology, Assumptions, and Sources of Errors .....</b>	<b>104</b>
3.1 Reservoir Pressure, Temperature, Gas Compressibility, and Oil Shrinkage Factor.....	104
3.2 Thermal Maturity, Liquid Distribution, and Gas-Oil Ratios.....	104
3.3 Water Saturation.....	105
3.4 Grain Density and Porosity .....	106
3.5 Regional TOC Determination and Adsorbed Gas .....	107
<b>4 Resource Estimation Workflow .....</b>	<b>108</b>
<b>5 Summary of Shale- and Siltstone-Hosted Hydrocarbon Resource Endowment .....</b>	<b>109</b>
5.1 Explanation for Preliminary Hydrocarbon Resource Endowment Status.....	110
5.2 Duvernay Formation Shale-Hosted Hydrocarbon Resource Endowment .....	110
5.3 Muskwa Formation Shale-Hosted Hydrocarbon Resource Endowment .....	121
5.4 Montney Formation Siltstone-Hosted Hydrocarbon Resource Endowment.....	132
5.5 Preliminary Basal Banff/Exshaw Shale-Hosted Hydrocarbon Resource Endowment .....	143
5.6 Preliminary North Nordegg Shale-Hosted Hydrocarbon Resource Endowment.....	154
5.7 Preliminary Wilrich Member Shale-Hosted Hydrocarbon Resource Endowment .....	165
<b>6 Constraints and Considerations for Future Work on Shale- and Siltstone-Hosted Hydrocarbon Resource Analysis and Modelling .....</b>	<b>176</b>
<b>7 Conclusion .....</b>	<b>176</b>
References.....	178
Appendix – Consultant Report – Shale Gas Potential (Source-Rock Geochemistry and Maturity).....	180

## Tables

Table 1	Summary of estimates of Alberta shale- and siltstone-hosted hydrocarbon resource endowment.....	xi
Table 1.3.1	List of key variables, data, and methods used to determine the resources of the assessed units.....	2
Table 1.3.2	List of types of analysis conducted on core and outcrop samples, purpose of analysis, and organization that performed the analyses for the shale- and siltstone-hosted hydrocarbon resource-evaluation project.....	3
Table 3.1.1	Adjoining units and their stratigraphic relationships.....	104
Table 3.2.1	Hydrocarbon-generation zones, gas-oil ratios, and vitrinite reflectance.....	105
Table 5.2.1	Summary of Duvernay Formation shale-hosted hydrocarbon resource endowment: low, medium, and high estimates.....	110
Table 5.2.2	Summary of shale-hosted hydrocarbon resource assessment of the Duvernay Formation.....	111
Table 5.3.1	Summary of Muskwa Formation shale-hosted hydrocarbon resource endowment: low, medium, and high estimates.....	121
Table 5.3.2	Summary of shale-hosted hydrocarbon resource assessment of the Muskwa Formation..	122
Table 5.4.1	Summary of Montney Formation siltstone-hosted hydrocarbon resource endowment: low, medium, and high estimates.....	132
Table 5.4.2	Summary of siltstone-hosted hydrocarbon resource assessment of the Montney Formation.....	133
Table 5.5.1	Preliminary summary of the basal Banff/Exshaw shale-hosted hydrocarbon resource endowment: low, medium, and high estimates.....	143
Table 5.5.2	Summary of shale-hosted hydrocarbon resource assessment of the combined basal Banff and Exshaw formations.....	144
Table 5.6.1	Preliminary summary of the north Nordegg shale-hosted hydrocarbon resource endowment: low, medium, and high estimates.....	154
Table 5.6.2	Summary of shale-hosted hydrocarbon resource assessment of the north Nordegg.....	155
Table 5.7.1	Preliminary summary of the Wilrich Member shale-hosted hydrocarbon resource endowment: low, medium, and high estimates.....	165
Table 5.7.2	Summary of shale-hosted hydrocarbon resource assessment of the Wilrich Member.....	166

## Figures

Figure 1.5.1	Generalized stratigraphic chart for Alberta highlighted with units evaluated in this report..	5
Figure 2.1.1	Index map of the Duvernay Formation.....	8
Figure 2.1.2	Depth to the top of the Duvernay Formation.....	9
Figure 2.1.3	Gross isopach of the Duvernay Formation.....	10
Figure 2.1.4a	Regional stratigraphic cross-section A-A'.....	11
Figure 2.1.4b	Stratigraphic cross-section B-B' of the Duvernay Formation.....	12
Figure 2.1.5	Net-shale isopach of the Duvernay Formation.....	13
Figure 2.1.6	Net-carbonate isopach of the Duvernay Formation.....	14
Figure 2.1.7	Thermal maturity map of the Duvernay Formation.....	15
Figure 2.1.8	Thermal maturity zones for the Duvernay Formation and distribution of Swan Hills oil and gas pools.....	16
Figure 2.1.9	Histogram of total organic carbon of 202 samples from the Duvernay Formation.....	17
Figure 2.1.10	Porosity-thickness map of the Duvernay Formation.....	18
Figure 2.1.11	Histogram of water-saturation analysis results of 20 samples from the Duvernay Formation.....	19

Figure 2.2.1	Index map of the Muskwa Formation .....	21
Figure 2.2.2a	Depth to top of the Muskwa Formation .....	22
Figure 2.2.2b	Structure of the Muskwa Formation .....	23
Figure 2.2.3	Gross isopach of the Muskwa Formation.....	24
Figure 2.2.4	Stratigraphic cross-section C-C' of the Muskwa Formation .....	25
Figure 2.2.5	Net-shale isopach of the Muskwa Formation.....	26
Figure 2.2.6	Thermal maturity map of the Muskwa Formation .....	27
Figure 2.2.7	Histogram of total organic carbon of 50 samples from the Muskwa Formation .....	28
Figure 2.2.8	Porosity-thickness map of the Muskwa Formation.....	29
Figure 2.2.9	Histogram of water-saturation analysis results from 12 samples from the Muskwa Formation .....	30
Figure 2.3.1	Index map of the Montney Formation .....	32
Figure 2.3.2	Depth to top of the Montney Formation .....	33
Figure 2.3.3	Gross isopach of the Montney Formation.....	34
Figure 2.3.4	Stratigraphic cross-section D-D' of the Montney Formation .....	35
Figure 2.3.5	Net-silt isopach of the Montney Formation .....	36
Figure 2.3.6	Net-sand isopach of the Montney Formation.....	37
Figure 2.3.7	Thermal maturity map of the Montney Formation .....	38
Figure 2.3.8	Histogram of total organic carbon of 170 samples from the Montney Formation.....	39
Figure 2.3.9	Porosity-thickness map of the Montney Formation .....	40
Figure 2.3.10	Histogram of water-saturation analysis results from 9 samples from the Montney Formation .....	41
Figure 2.4.1	Index map of the combined basal Banff and Exshaw formations.....	44
Figure 2.4.2	Stratigraphic cross-section E-E' of the basal Banff and Exshaw formations.....	45
Figure 2.4.3	Depth to top of the basal Banff/Exshaw upper shale in the study area.....	46
Figure 2.4.4	Gross isopach of the basal Banff/Exshaw middle unit in the study area .....	47
Figure 2.4.5	Porosity-thickness map of the basal Banff/Exshaw middle unit in the study area .....	48
Figure 2.4.6	Histogram of total organic carbon of 75 samples from the basal Banff and Exshaw formations.....	49
Figure 2.4.7	Thermal maturity map of the combined basal Banff and Exshaw formations in the study area .....	50
Figure 2.4.8	Histogram of water-saturation analysis results from 23 samples from the combined basal Banff and Exshaw formations.....	51
Figure 2.5.1	Index map of the Fernie Formation including the Nordegg Member .....	53
Figure 2.5.2	Depth to top of the north Nordegg.....	54
Figure 2.5.3	Gross isopach of the north Nordegg.....	55
Figure 2.5.4	Stratigraphic cross-section F-F' of the Nordegg Member.....	56
Figure 2.5.5	Net-shale isopach of the Nordegg Member.....	57
Figure 2.5.6	Net-carbonate isopach of the Nordegg Member .....	58
Figure 2.5.7	Thermal maturity map of the north Nordegg.....	59
Figure 2.5.8	Histogram of total organic carbon of 82 samples from the north Nordegg .....	60
Figure 2.5.9	Porosity-thickness map of the north Nordegg.....	61
Figure 2.5.10	Histogram of water-saturation analysis results of 5 samples from the north Nordegg....	62
Figure 2.6.1	Index map of the Wilrich Member .....	64
Figure 2.6.2	Depth to top of the Wilrich Member .....	65
Figure 2.6.3	Gross isopach of the Wilrich Member.....	66
Figure 2.6.4	Stratigraphic cross-section G-G' of the Wilrich Member.....	67
Figure 2.6.5	Net-shale isopach of the Wilrich Member.....	68

Figure 2.6.6	Histogram of total organic carbon of 213 samples from the Wilrich Member .....	69
Figure 2.6.7	Porosity-thickness map of the Wilrich Member.....	70
Figure 2.6.8	Thermal maturity map of the Wilrich Member .....	71
Figure 2.6.9	Histogram of water-saturation analysis results of 25 samples from the Wilrich Member ..	72
Figure 2.7.1	Index map of the Rierdon Formation .....	74
Figure 2.7.2	Structure of the Rierdon Formation .....	75
Figure 2.7.3	Depth to top of the Rierdon Formation .....	76
Figure 2.7.4	Gross isopach of the Rierdon Formation .....	77
Figure 2.7.5	Stratigraphic cross-section H-H' of the Rierdon Formation.....	78
Figure 2.7.6	Net-shale isopach of the Rierdon Formation .....	79
Figure 2.7.7	Porosity-thickness map of the Rierdon Formation.....	80
Figure 2.7.8	Histogram of total organic carbon of 137 samples from the Rierdon Formation .....	81
Figure 2.7.9	Thermal maturity map of the Rierdon Formation.....	82
Figure 2.7.10	Histogram of water-saturation analysis results for 10 samples from the Rierdon Formation .....	83
Figure 2.8.1	Index map of the Colorado Group .....	87
Figure 2.8.2	Thickness of the Colorado Group above the base of groundwater protection .....	88
Figure 2.8.3a	Depth to the top of the lower Colorado unit .....	89
Figure 2.8.3b	Depth to the top of the middle Colorado unit .....	90
Figure 2.8.3c	Depth to the top of the upper Colorado unit .....	91
Figure 2.8.4	Stratigraphic cross-section I-I' of the Colorado Group in the north Colorado evaluation area .....	92
Figure 2.8.5	Gross isopach of the lower Colorado unit.....	93
Figure 2.8.6	Net-shale isopach of the lower Colorado unit.....	94
Figure 2.8.7	Gross isopach of the middle Colorado unit.....	95
Figure 2.8.8	Gross isopach of the upper Colorado unit.....	96
Figure 2.8.9	Net-shale isopach of the middle Colorado unit.....	97
Figure 2.8.10	Net-shale isopach of the upper Colorado unit.....	98
Figure 2.8.11	Histogram of total organic carbon of 83 samples from the Colorado Group in the north Colorado evaluation area .....	99
Figure 2.8.12	Histogram water-saturation analysis results for 12 Colorado samples from the north Colorado evaluation area .....	100
Figure 2.8.13	Stratigraphic cross-section J-J' of the Colorado Group in the south Colorado evaluation area .....	101
Figure 2.8.14	Histogram of total organic carbon of 294 samples from the Colorado Group in the south Colorado evaluation area.....	102
Figure 2.8.15	Histogram of water-saturation analysis results of 16 Colorado Group samples from the Middle and Upper Colorado in south Colorado evaluation area.....	103
Figure 5.2.1	P50 (best estimate) shale-hosted oil initially-in-place in the Duvernay Formation.....	112
Figure 5.2.2	P90 (low estimate) shale-hosted oil initially-in-place in the Duvernay Formation .....	113
Figure 5.2.3	P10 (high estimate) shale-hosted oil initially-in-place in the Duvernay Formation .....	114
Figure 5.2.4	P50 (best estimate) shale-hosted natural-gas liquids initially-in-place in the Duvernay Formation .....	115
Figure 5.2.5	P90 (low estimate) shale-hosted natural-gas liquids initially-in-place in the Duvernay Formation .....	116

Figure 5.2.6	P10 (high estimate) shale-hosted natural-gas liquids initially-in-place in the Duvernay Formation .....	117
Figure 5.2.7	P50 (best estimate) shale-hosted gas initially-in-place in the Duvernay Formation.....	118
Figure 5.2.8	P90 (low estimate) shale-hosted gas initially-in-place in the Duvernay Formation .....	119
Figure 5.2.9	P10 (high estimate) shale-hosted gas initially-in-place in the Duvernay Formation.....	120
Figure 5.3.1	P50 (best estimate) shale-hosted oil initially-in-place in the Muskwa Formation.....	123
Figure 5.3.2	P90 (low estimate) shale-hosted oil initially-in-place in the Muskwa Formation .....	124
Figure 5.3.3	P10 (high estimate) shale-hosted oil initially-in-place in the Muskwa Formation .....	125
Figure 5.3.4	P50 (best estimate) shale-hosted natural-gas liquids initially-in-place in the Muskwa Formation .....	126
Figure 5.3.5	P90 (low estimate) shale-hosted natural-gas liquids initially-in-place in the Muskwa Formation .....	127
Figure 5.3.6	P10 (high estimate) shale-hosted natural-gas liquids initially-in-place in the Muskwa Formation .....	128
Figure 5.3.7	P50 (best estimate) shale-hosted gas initially-in-place in the Muskwa Formation.....	129
Figure 5.3.8	P90 (low estimate) shale-hosted gas initially-in-place in the Muskwa Formation .....	130
Figure 5.3.9	P10 (high estimate) shale-hosted gas initially-in-place in the Muskwa Formation.....	131
Figure 5.4.1	P50 (best estimate) siltstone-hosted oil initially-in-place in the Montney Formation ...	134
Figure 5.4.2	P90 (low estimate) siltstone-hosted oil initially-in-place in the Montney Formation ...	135
Figure 5.4.3	P10 (high estimate) siltstone-hosted oil initially-in-place in the Montney Formation ..	136
Figure 5.4.4	P50 (best estimate) siltstone-hosted natural-gas liquids initially-in-place in the Montney Formation.....	137
Figure 5.4.5	P90 (low estimate) siltstone-hosted natural-gas liquids initially-in-place in the Montney Formation.....	138
Figure 5.4.6	P10 (high estimate) siltstone-hosted natural-gas liquids initially-in-place in the Montney Formation.....	139
Figure 5.4.7	P50 (best estimate) siltstone-hosted gas initially-in-place in the Montney Formation ..	140
Figure 5.4.8	P90 (low estimate) siltstone-hosted gas initially-in-place in the Montney Formation ..	141
Figure 5.4.9	P10 (high estimate) siltstone-hosted gas initially-in-place in the Montney Formation .	142
Figure 5.5.1	P50 (best estimate) shale-hosted oil initially-in-place in the basal Banff/Exshaw middle unit in the study area .....	145
Figure 5.5.2	P90 (low estimate) shale-hosted oil initially-in-place in the basal Banff/Exshaw middle unit in the study area .....	146
Figure 5.5.3	P10 (high estimate) shale-hosted oil initially-in-place in the basal Banff/Exshaw middle unit in the study area .....	147
Figure 5.5.4	P50 (best estimate) shale-hosted natural-gas liquids initially-in-place in the basal Banff/Exshaw middle unit in the study area .....	148
Figure 5.5.5	P90 (low estimate) shale-hosted natural-gas liquids initially-in-place in the basal Banff/Exshaw middle unit in the study area .....	149
Figure 5.5.6	P10 (high estimate) shale-hosted natural-gas liquids initially-in-place in the basal Banff/Exshaw middle unit in the study area .....	150
Figure 5.5.7	P50 (best estimate) shale-hosted gas initially-in-place in the basal Banff/Exshaw middle unit in the study area .....	151
Figure 5.5.8	P90 (low estimate) shale-hosted gas initially-in-place in the basal Banff/Exshaw middle unit in the study area .....	152
Figure 5.5.9.	P10 (high estimate) shale-hosted gas initially-in-place in the basal Banff/Exshaw middle unit in the study area .....	153
Figure 5.6.1	P50 (best estimate) shale-hosted oil initially-in-place in the north Nordegg.....	156
Figure 5.6.2	P90 (low estimate) shale-hosted oil initially-in-place in the north Nordegg .....	157

Figure 5.6.3	P10 (high estimate) shale-hosted oil initially-in-place in the north Nordegg .....	158
Figure 5.6.4	P50 (best estimate) shale-hosted natural-gas liquids initially-in-place in the north Nordegg.....	159
Figure 5.6.5	P90 (low estimate) shale-hosted natural-gas liquids initially-in-place in the north Nordegg.....	160
Figure 5.6.6.	P10 (high estimate) shale-hosted natural-gas liquids initially-in-place in the north Nordegg.....	161
Figure 5.6.7	P50 (best estimate) shale-hosted gas initially-in-place in the north Nordegg.....	162
Figure 5.6.8	P90 (low estimate) shale-hosted gas initially-in-place in the north Nordegg .....	163
Figure 5.6.9	P10 (high estimate) shale-hosted gas initially-in-place in the north Nordegg .....	164
Figure 5.7.1	P50 (best estimate) shale-hosted oil initially-in-place in the Wilrich Member.....	167
Figure 5.7.2	P90 (low estimate) shale-hosted oil initially-in-place in the Wilrich Member .....	168
Figure 5.7.3	P10 (high estimate) shale-hosted oil initially-in-place in the Wilrich Member .....	169
Figure 5.7.4	P50 (best estimate) shale-hosted natural-gas liquids initially-in-place in the Wilrich Member .....	170
Figure 5.7.5	P90 (low estimate) shale-hosted natural-gas liquids initially-in-place in the Wilrich Member .....	171
Figure 5.7.6	P10 (high estimate) shale-hosted natural-gas liquids initially-in-place in the Wilrich Member .....	172
Figure 5.7.7	P50 (best estimate) shale-hosted gas initially-in-place in the Wilrich Member.....	173
Figure 5.7.8	P90 (low estimate) shale-hosted gas initially-in-place in the Wilrich Member .....	174
Figure 5.7.9	P10 (high estimate) shale-hosted gas initially-in-place in the Wilrich Member .....	175

## Acknowledgements

This study was conducted by the Energy Resource Appraisal Group of the Geology, Environmental Science, and Economics Branch of the Energy Resources Conservation Board (ERCB). Funding was provided by Alberta Energy under the Government of Alberta's Emerging Resources and Technologies Initiative announced in May 2010.

The authors thank the following people for their support and advice:

- D. Bradshaw and S. Rauschnig of Alberta Energy;
- ERCB Core Research Centre staff;
- B. Everett and P. Mukhopadhyay (consultants); and
- A. Budinski, D.K. Chao, C.S. Crocq, M. Grobe, F.J. Hein, G. Hippolt-Squair, B. Lawrence, S. Overland, M. Protz, and T. Yeomans of the ERCB.

## Executive Summary

The Energy Resource Appraisal Group of the Energy Resources Conservation Board provides information related to the oil and gas resource endowment of Alberta. The intent of this report is to provide baseline data, information, and understanding of the geology, distribution, reservoir characteristics, and hydrocarbon resource potential of Alberta shales.

Shale formations are under development by industry worldwide. The United States, arguably the world leader in the development of shale-hosted hydrocarbons, may contain up to 750 trillion cubic feet (Tcf) of technically recoverable gas and 24 billion barrels of technically recoverable oil (U.S. Department of Energy, 2011). A wide variety of historical estimates for Alberta's original shale-hosted gas-in-place range from 80 to 10 000 Tcf. Resource evaluation methodologies and classification are still relatively immature. This is due to the scarcity of data (shales were ignored as reservoirs in the past and consequently received little attention) and the fact that shale resources typically cover large regional areas rather than confined hydrocarbon reservoirs, which presents a difficulty for resource evaluation. Nonetheless, it has been recognized that shale- and siltstone-hosted hydrocarbon resources are very large and present a very important potential energy supply for Alberta and the world.

We examined several shale and siltstone formations in Alberta that exhibit favourable hydrocarbon-resource characteristics. We determined the in-place resource estimates for the key shale and siltstone formations in Alberta that we think are most likely to be developed first. The geographic resource distribution, fluid types, and reservoir characteristics conducive to development were also determined. Hydrocarbons hosted in conventional reservoirs were not included in this evaluation. In cases for which conventional, tight, and shale resources were present in a rock formation, only the shale- and siltstone-hosted hydrocarbons were evaluated.

Data and information produced by this study may assist in the evaluation, exploration, and development of shale gas resources. Data can be used by industry to help identify shale gas prospects, plan effective drilling and completions strategies, and guide land acquisition decisions.

The results allow us to understand the size and distribution of shale-gas resources in Alberta and may be used to assist in the planning of resource allocation and conservation, commingling and rights assignment, royalty assessment, land and water use, and environmental stewardship.

Data and information on reservoir characteristics and hydrocarbon resource potential of shale formations are rare because of the historical lack of interest in shale-hosted hydrocarbon reservoirs. Now, industry is looking for data and information on shale gas resources to decide if and where these resources may be developed.

We evaluated the geology, distribution, characteristics, and hydrocarbon potential of key shale and/or siltstone formations (units) in Alberta. Five units show immediate potential: the Duvernay Formation, the Muskwa Formation, the Montney Formation, the Nordegg Member, and the basal Banff and Exshaw formations (sometimes referred to as the Alberta Bakken by industry). The study also includes a preliminary assessment of the Colorado, Wilrich, Rierdon, and Bantry Shale units. These units were systematically mapped, sampled, and evaluated for their hydrocarbon potential. In total, 3385 samples were collected and evaluated for this summary report.

Table 1 summarizes our estimates of Alberta's shale- and siltstone-hosted hydrocarbon resource endowment for six of the investigated units for which available data allowed at least a preliminary determination. The values represent the medium estimate (P50) along with the P90 to P10 range of resource estimates for natural gas, natural-gas liquids, and oil. The P50 value is considered to be the best estimate because it minimizes the expected variance from the unknown true value. The range of uncertainty is summarized by the P90 (low estimate) and P10 (high estimate) values. In this report, natural gas refers to methane (C<sub>1</sub>), natural-gas liquids refer to C<sub>2</sub> to C<sub>6</sub> hydrocarbons, and oil refers to C<sub>7</sub> and larger hydrocarbons. See Section 5 for the metric equivalents of the resource estimates.

**If a single value is required as a quote for a unit, we recommend using the medium (P50) value.**

**Table 1. Summary of estimates of Alberta shale- and siltstone-hosted hydrocarbon resource endowment.**

Unit	Adsorbed Gas Content %*	Natural Gas (Tcf)	Natural-Gas Liquids (billion bbl)	Oil (billion bbl)
Duvernay P50	6.8	443	11.3	61.7
Duvernay P90–P10	5.6–8.5	353–540	7.5–16.3	44.1–82.9
Muskwa P50	6.9	419	14.8	115.1
Muskwa P90–P10	4.1–10.5	289–527	6.0–26.3	74.8–159.9
Montney P50	17.7	2133	28.9	136.3
Montney P90–P10	10.8–26.0	1630–2828	11.7–54.4	78.6–220.5
Basal Banff/Exshaw P50 (preliminary data; see Section 5.1)	5.7	35	0.092	24.8
Basal Banff/Exshaw P90–P10	3.2–10.0	16–70	0.034–0.217	9.0–44.9
North Nordegg P50 (preliminary data; see Section 5.1)	18.2	148	1.4	37.8
North Nordegg P90–P10	4.6–34.8	70–281	0.487–3.5	19.9–66.4
Wilrich P50 (preliminary data; see Section 5.1)	33.7	246	2.1	47.9
Wilrich P90–P10	6.2–59.2	115–568	0.689–4.449	20.2–172.3
Total P50 (medium estimate) resource endowment	n/a	3424	58.6	423.6

\* The percentage of adsorbed gas represents the portion of natural gas that is stored as adsorbed gas.

The resource estimates listed above provide an estimate of total hydrocarbons-in-place. Geological and reservoir engineering constraints, recovery factors, and additional economic factors, as well as social and environmental considerations, will ultimately determine the potential recovery of this large resource.

# 1 Introduction

## 1.1 Introduction to Shale- and Siltstone-Hosted Hydrocarbons

Hydrocarbons are contained in many of the geological formations in the subsurface of Alberta. Most hydrocarbons discovered and produced to date are hosted in distinct carbonate, sandstone, and siltstone bodies with discrete boundaries that trap large accumulations of hydrocarbons, forming pools. The hydrocarbons occur within the spaces between or within grains or in void spaces within the rock matrix (porosity). The buoyant nature of hydrocarbons allows them to migrate into the porous rock bodies via interconnected pores (permeability) in the rock. Hydrocarbons are often trapped or retained in these pools by an overlying caprock or seal.

The caprock is often shale, a rock with clay minerals and a very small grain size. Both of these features contribute to the low permeability and effective porosity of shale. Over millions of years, sediment may be buried and subjected to heat and pressure. Very fine grained, clay-rich sediments compact to form a shale rock that has the potential to be a tight caprock for hydrocarbon trapping. Some shale contains a small amount of organic matter, which consists of the remains of plant and animal matter incorporated in the sediments at the time of deposition. This organic matter also undergoes chemical and physical changes during burial, generating products that may include oil and gas, depending on the original organic matter's chemical makeup and the amount of heat and pressure to which the rock is subjected (thermal maturation). This organic-matter-rich shale is referred to as a source rock.

Generated hydrocarbons may migrate slowly from the organic matter, through the shale, and travel along a more permeable path until trapped, forming a hydrocarbon pool. If gas is generated and the shale has a very low permeability, the gas may remain as free gas in the shale matrix. Some of the gas will also be adsorbed to organic matter. The occurrence of trapped and adsorbed gas in organic-rich shale makes the shale both a potential seal or caprock for hydrocarbon pools and a combination of source and reservoir rock for hydrocarbons. Organic-rich shale that contains both free and adsorbed gas is referred to as a gas shale.

Shale-hosted hydrocarbon reservoirs tend to occur over a broad geographic area rather than in discrete pools. The low porosity and permeability of shale makes producing the hydrocarbons challenging. To economically produce them, the permeability in the rock needs to be increased. This is achieved by artificially enhancing existing, natural fractures or by creating new fractures in the rock (most commonly by hydraulic fracturing). A combination of organic matter content, level of thermal maturation, structure, presence of natural fractures, brittleness, and other rock properties will determine the shale's hydrocarbon production potential.

In Alberta, no less than 15 formations have the potential for shale- and/or siltstone-hosted hydrocarbons, which may represent a valuable resource for the province. Estimates for the total amount of gas in Alberta shale vary widely, from 80 to >10 000 trillion cubic feet (Faraj et al., 2002; Faraj, 2005). This points to the great potential size of the resource, which can contribute to economic benefits and energy security for Alberta.

## 1.2 Study Overview

Energy Resources Conservation Board (ERCB) studies of shale- and siltstone-hosted hydrocarbons began in 2006. Initially, it focused on shale gas in the formations for which industry had shown interest. As our study progressed, we found that many of the formations we were analyzing also contained a significant amount of natural-gas liquids and oil. Therefore, we expanded the study to include all shale- and siltstone-hosted hydrocarbons.

We evaluated the geology, distribution, characteristics, and hydrocarbon potential of key 'shale' units in Alberta. Five units show immediate potential in Alberta: the Duvernay, the Muskwa, the Montney, the Nordegg, and the basal Banff and Exshaw (occasionally referred to as the Alberta Bakken by industry). Strictly speaking, the Montney Formation is not a 'shale' target. In Alberta, the Montney Formation is dominated by siltstone and is included here because it is a target for unconventional resources. The study also includes a preliminary assessment of the Colorado, Wilrich, and Rierdon units, as well as a summary of the Bantry Shale unit.

All units were systematically mapped, sampled, and evaluated for their hydrocarbon potential. The process included

- collecting samples from core and outcrop exposures,
- analyzing the samples to determine the physical and chemical characteristics of the rocks,
- evaluating geophysical well logs to determine rock properties and reservoir characteristics, and
- using geostatistical methodologies to aid in interpolation and to quantify uncertainty.

### 1.3 Definitions and Methodology

The definition of a hydrocarbon-bearing shale is "organic-rich, and fine-grained" (Bustin, 2006). However, the term 'shale' is used very loosely and—by intent—does not specifically describe the lithology of the reservoir. Lithological variations in shale units indicate that hydrocarbons are hosted not only in shale but also in a wide spectrum of lithologies and textures from mudstone (i.e., nonfissile shale) to siltstone and laminations of fine-grained sandstone. Organic-rich 'shale' contains two principal gas-storage mechanisms: adsorbed to organic matter and stored as free gas in pores. The hydrocarbon resource estimation methodology described in this section focuses on the determination of absorbed gas and free hydrocarbon volumes.

Table 1.3.1 lists the key variables used in our resource assessment, as well as the data and methods used to determine each variable.

**Table 1.3.1. List of key variables, data, and methods used to determine the resources of the assessed units.**

Key Variable	Data	Methods
Aerial extent	Stratigraphic picks	Stratigraphic correlations and geological mapping
Depth to top of the unit	Stratigraphic picks and a digital elevation model of ground elevation	Stratigraphic correlations, geological mapping, and data calculation
Gas compressibility	Reservoir and well-test data	Data analysis
Gas-oil and condensate-gas ratios	Thermal maturity	Data analysis and interpolation
Grain density	Mineralogy and total organic carbon	X-ray diffraction; data conversion and calculation
Langmuir pressure and Langmuir volume	Adsorption isotherm, organic geochemistry, total organic carbon, and geophysical well logs	Rock Eval™ pyrolysis; LECO TOC; data analysis, calculation, and interpolation

Key Variable	Data	Methods
Lithology	Mineralogy and geophysical well logs	Core description, sample description, petrographic analysis, SEM analysis, and data analysis
Oil shrinkage factor	Reservoir and well-test data	Data analysis and interpolation
Porosity	Stratigraphic picks, geophysical well logs, grain density, and porosity	Stratigraphic correlations, geological mapping, mercury porosimetry, helium pycnometry, and data analysis
Reservoir temperature and pressure	Pressure and temperature	Reservoir and well testing, data analysis, and interpolation
Thermal maturity	Tmax, vitrinite reflectance, and depth to top of the unit	Rock Eval™ pyrolysis, organic petrography, geological mapping, and data interpolation
Total organic carbon	Organic geochemistry, stratigraphic picks, total organic carbon, and geophysical well logs	Stratigraphic correlations, geological mapping, Rock Eval™ pyrolysis, LECO TOC, and data analysis
Unit thickness	Stratigraphic picks and geophysical well logs	Stratigraphic correlations, geological mapping, and data analysis
Water saturation	Oil, gas, and water saturation	Dean Stark analysis, mercury porosimetry, helium pycnometry, and data analysis

A series of geochemical and geological analyses was conducted on core and outcrop samples to aid in resource evaluation (Table 1.3.2). Rock Eval™ pyrolysis and total organic carbon (TOC) analyses were completed on all samples, whereas all other analyses were completed on only selected samples.

The data and interpretations were subjected to geostatistical analysis to provide a probabilistic resource evaluation, indicating P10, P50, and P90 confidence results of initial petroleum-in-place. Each resource estimate is summarized by a P50 value, which is considered to be the best estimate because it minimizes the expected variance from the unknown, true value. The range of uncertainty is summarized by the P90 (low estimate) and P10 (high estimate) values. These are read as, we are 90% certain there is at least as much resource as the P90 value, and there is a 10% chance there is at least as much as the P10 value. Results indicate the size, distribution, and reservoir quality of key shale units in Alberta and provide insight into the distribution of oil, natural-gas liquids, and natural gas potential.

**Table 1.3.2. List of types of analysis conducted on core and outcrop samples, purpose of analysis, and organization that performed the analyses for the shale- and siltstone-hosted hydrocarbon resource-evaluation project.**

Analysis Type	Purpose	Company
Adsorption isotherm and proximate analysis	Adsorbed gas estimation	RMB Earth Science Consultants; Trican Geological Solutions Ltd.; Schlumberger Limited
Dean Stark analysis	Fluid saturation, porosity, and grain density	Core Laboratories
Mercury porosimetry and helium pycnometry	Porosity, bulk and grain density, and pore-throat size	Department of Physics, University of Alberta; Chalmcoal
Organic petrography	Petrographic characterization of organic matter and thermal maturity	Geological Survey of Canada; Global Geoenergy Research Limited; JP Petrographics

Analysis Type	Purpose	Company
Permeametry	Permeability and presence of seal	Department of Earth and Atmospheric Sciences, University of Alberta
Petrographic analysis	Texture, mineralogy, microstratigraphy, porosity, and microfractures	Trican Geological Solutions Ltd.; Vancouver Petrographics; Calgary Petrographics Ltd.
Rock Eval™ pyrolysis and LECO TOC	Geochemical characterization of shale	Geological Survey of Canada; Schlumberger Limited; GeoMark Research Limited; Trican Geological Solutions Ltd.
SEM with energy-dispersive X-ray	Type and distribution of porosity, mineralogy, and microstratigraphy	Department of Earth and Atmospheric Sciences, University of Alberta
Whole-rock inorganic geochemistry	Mineralogy, stratigraphy, and log analysis	Acme Analytical Laboratories Ltd.
X-ray diffraction (bulk and clay mineral) and grain-size analysis	Mineralogy	Trican Geological Solutions Ltd.; SGS Minerals Services Ltd.; Alberta Innovates Technology Futures

#### 1.4 Data Collection Summary

In total, 3385 samples were analyzed, including duplicates and standards for quality control. Samples were collected from 65 outcrops, and core samples were collected from 316 wells. Of the total number of samples collected, 2746 were from core, 440 were from outcrops, and 199 were standards and duplicates.

Some of the data generated by the ERCB's Energy Resource Appraisal Group for this study will be presented in future digital datasets available at [http://www.ag.gov.ab.ca/publications/abstracts/OFR\\_2012\\_06.html](http://www.ag.gov.ab.ca/publications/abstracts/OFR_2012_06.html).

#### 1.5 Units Evaluated

Figure 1.5.1 is a generalized stratigraphic chart of Alberta, highlighting the 'shale' units evaluated in this report. These units were evaluated for their shale- and siltstone-hosted hydrocarbon resource endowment, which includes gas, natural gas liquids, and oil. In this report, natural gas refers to methane (C<sub>1</sub>), natural-gas liquids refer to C<sub>2</sub> to C<sub>6</sub> hydrocarbons, and oil refers to C<sub>7</sub> and larger hydrocarbons. Based on industry interest, we evaluated the following units: the Duvernay Formation, the Muskwa Formation, the Montney Formation, the combined basal Banff and Exshaw formations, the Nordegg Member, and the Wilrich Member. In addition, preliminary work without resource evaluation was done for the Rierdon Formation, the Colorado Group (and equivalent strata of the Smoky and Fort St. John groups), other Fernie Formation units, and the Bantry Shale member.

## 2 Summary of Resource Variables for Each Unit

The resource variables for each unit are summarized along with a series of maps, graphs, and cross-sections displaying the value or range of values of a particular variable used in the resource analysis. Section 3.1 provides information on the pressure, temperature, compressibility, and oil shrinkage factor for each stratum along with assumptions and potential errors.

# Generalized Stratigraphic Chart

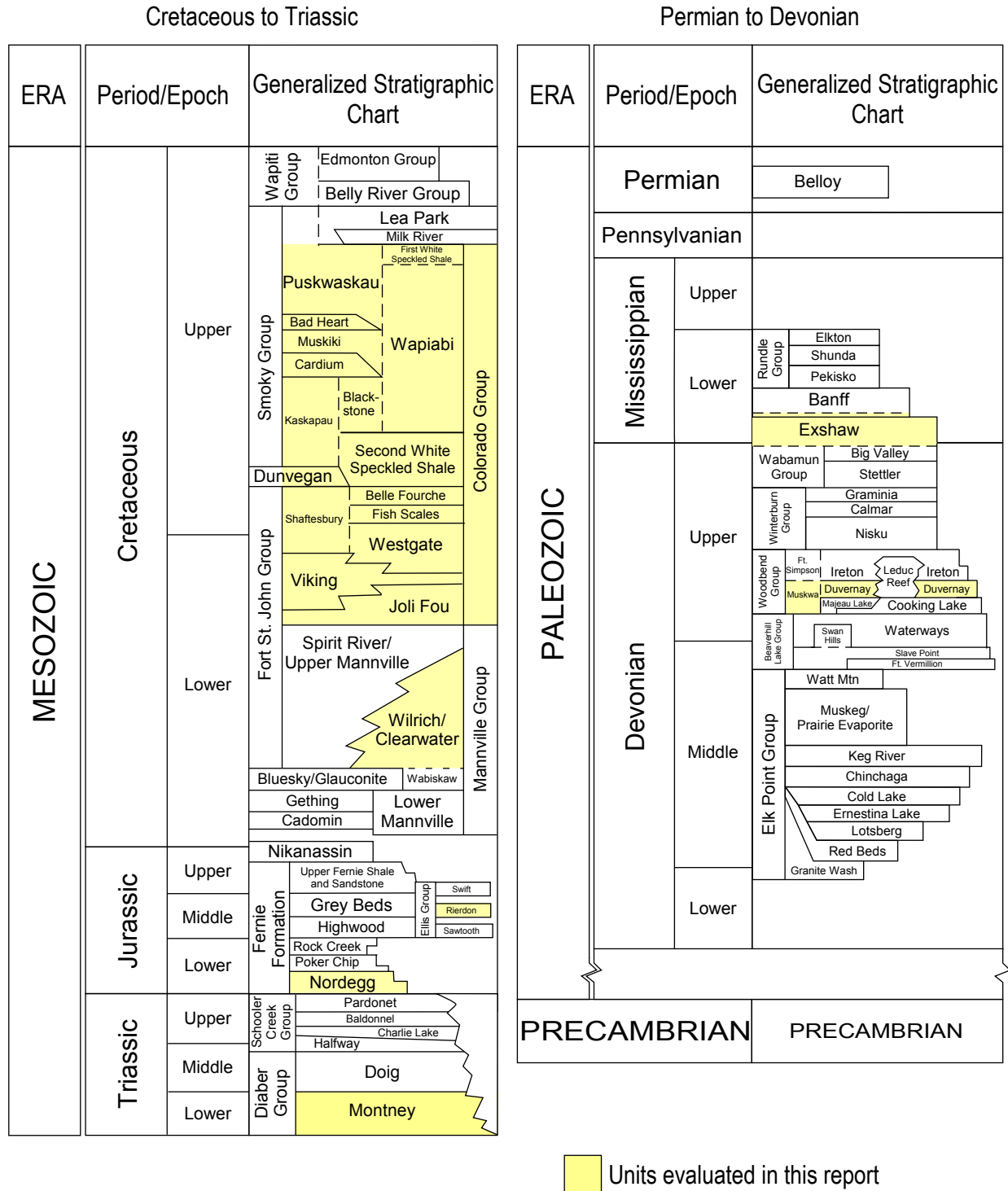


Figure 1.5.1. Generalized stratigraphic chart for Alberta highlighted with units evaluated in this report. Cambrian and Ordovician units are omitted.

## 2.1 Summary of the Duvernay Formation

The Duvernay Formation (Duvernay) is an Upper Devonian source rock that is present in the "East Shale Basin" and "West Shale Basin" of central Alberta (Switzer et al., 1994; Figure 2.1.1). The Duvernay is stratigraphically equivalent to parts of the Muskwa Formation in northern Alberta. The hydrocarbon resource-evaluation parameters for the Muskwa Formation are summarized in Section 2.2. The Duvernay succession is known to have sourced the prolific Leduc and Swan Hills oil and gas reservoirs.

The lithology of the Duvernay in the East Shale Basin is dominated by organic-rich lime-mudstone (i.e., limestone). The Duvernay in the West Shale Basin becomes less calcareous and more shale rich from east to west. In the West Shale Basin, the Duvernay dips to the west-southwest. Depth from the surface to the top of the Duvernay is about 1000 m near the eastern boundary to about 5500 m in the west (Figure 2.1.2).

The thickness of the Duvernay Formation in the West Shale Basin is greatest along the eastern and southern edges, as well as in the west-central area. (Figure 2.1.3). Two southwest to northeast stratigraphic cross-sections (two of more than 50 constructed for the Duvernay) reveal an increase in porous, radioactive shale (identified from gamma and density-porosity logs) in the west and carbonate-rich mudstones in the east (Figures 2.1.4a and 2.1.4b).

A net-shale map was created by calculating the thickness of sediment with a gamma-ray cutoff of >105 API. The map shows a dominance of 'hot' (i.e., radioactive) shale in the West Shale Basin and much less shale (and more carbonate) in the East Shale Basin (Figure 2.1.5). The cutoff was created to exclude clean, organic-rich carbonate from the resource calculation. Where shale is thin, the Duvernay is dominated by organic-rich lime-mudstone, as indicated in the net-carbonate isopach (Figure 2.1.6). The present evaluation uses the net-shale map for the thickness parameter in our resource analysis. Carbonate-rich rocks will be evaluated in a future resource project. Hence, resource values for the Duvernay are dominated by shale-rich strata in the West Shale Basin (Figure 2.1.5).

Vitrinite reflectance data indicate that the Duvernay organic matter exhibits increased thermal maturity to the west (Figure 2.1.7), which corresponds with increased depth below the surface. Dry-gas-rich resources are expected in the extreme west, with more liquids-rich gas and oil-prone strata towards the east. However thermal maturation and migration may be more complex than this. For example, some internal migration of hydrocarbons within the Duvernay may have occurred, as exhibited by the distribution of Swan Hills reef hydrocarbons in Figure 2.1.8. The Swan Hills Formation of the Beaverhill Lake Group directly underlies the Duvernay (Figure 2.1.4a). The Swan Hills oil and gas pools are sourced from the Duvernay, and the hydrocarbon distribution reveals reefs with oil, gassy oil, and oily gas pools with a rather variable distribution. This variation in the hydrocarbon content of the Swan Hills pools suggests that migration may have occurred from the Duvernay gas-rich area towards the oil-rich area and into the Swan Hills. Alternatively, there may be a greater amount of terrestrial organic matter in the Duvernay than has been previously documented. It is also possible that additional gas-prone source rocks (such as from the upper Beaverhill Lake Group) have been sourcing the Swan Hills oil and gas reservoirs. The upper Beaverhill Lake shale and carbonates that surround the Swan Hills reefs are also organic rich, but these sediments have not been included in this resource evaluation. Total organic carbon (TOC) content of the Duvernay varies from 0.1 to 11.1 weight per cent (wt. %) based on 202 samples from 50 wells, with the highest values generally in the East Shale Basin carbonate rocks (Figure 2.1.9).

A porosity-thickness (Phi-h) map of the Duvernay (Figure 2.1.10) was constructed using density-porosity logs calibrated to a grain density of 2.67 grams per cubic centimetre ( $\text{g}/\text{cm}^3$ ) with no porosity cutoff and a >105 API gamma-ray-log cutoff. This grain density accounts for the presence of TOC by converting TOC to kerogen and counting it as a mineral component in the calculation of grain density. Section 3.4 provides the determination of grain density used in our analysis and possible sources of error.

Using Dean Stark analysis and helium pycnometry on select samples, the laboratory calculated water saturation. The distribution of values for the Duvernay shows dominance in the range of about 10% to 30% (Figure 2.1.11), which is used as P90 and P10 constraints in our resource evaluation. Section 3.3 provides information on the methodology used to determine water saturation and possible sources of error.

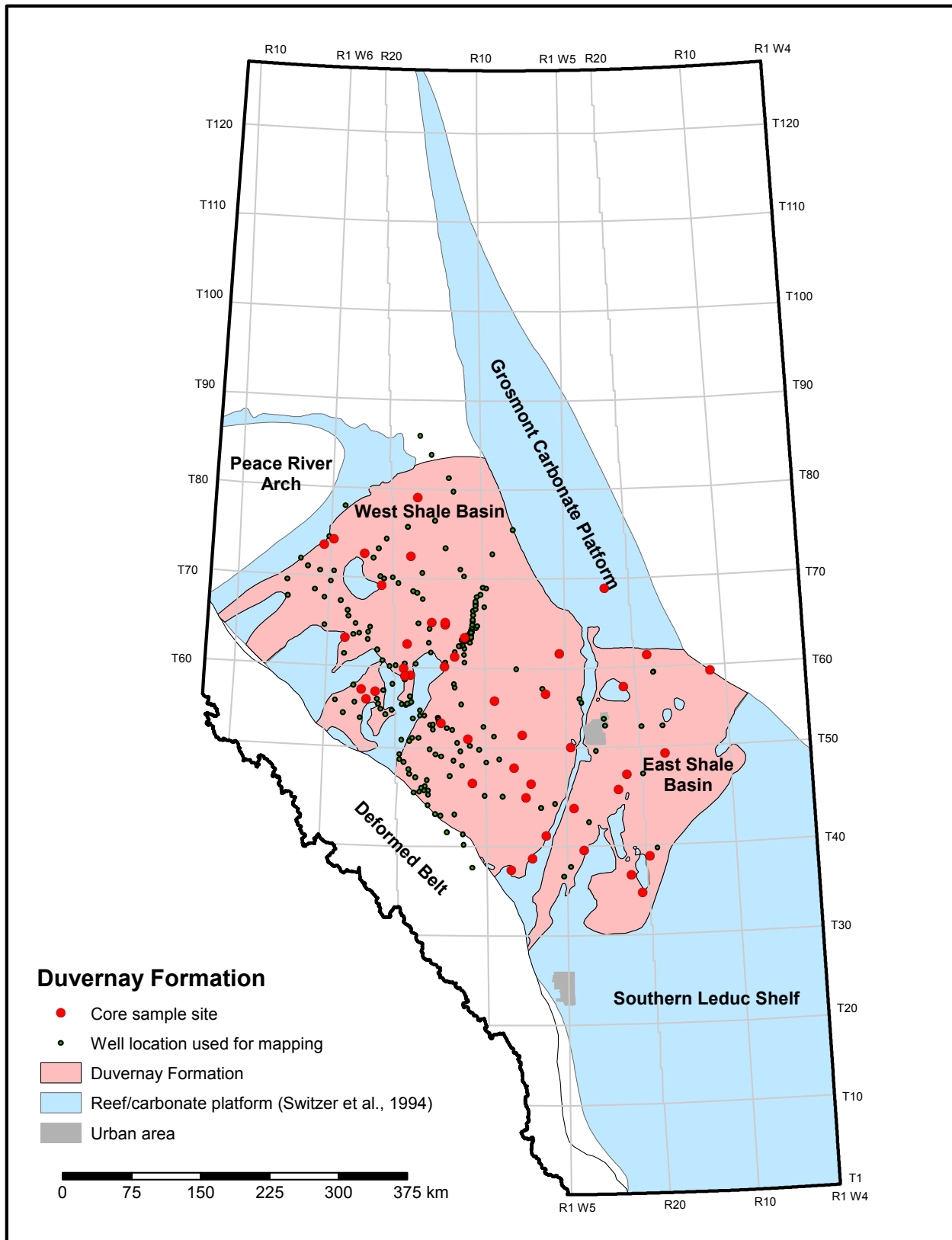


Figure 2.1.1. Index map of the Duvernay Formation.

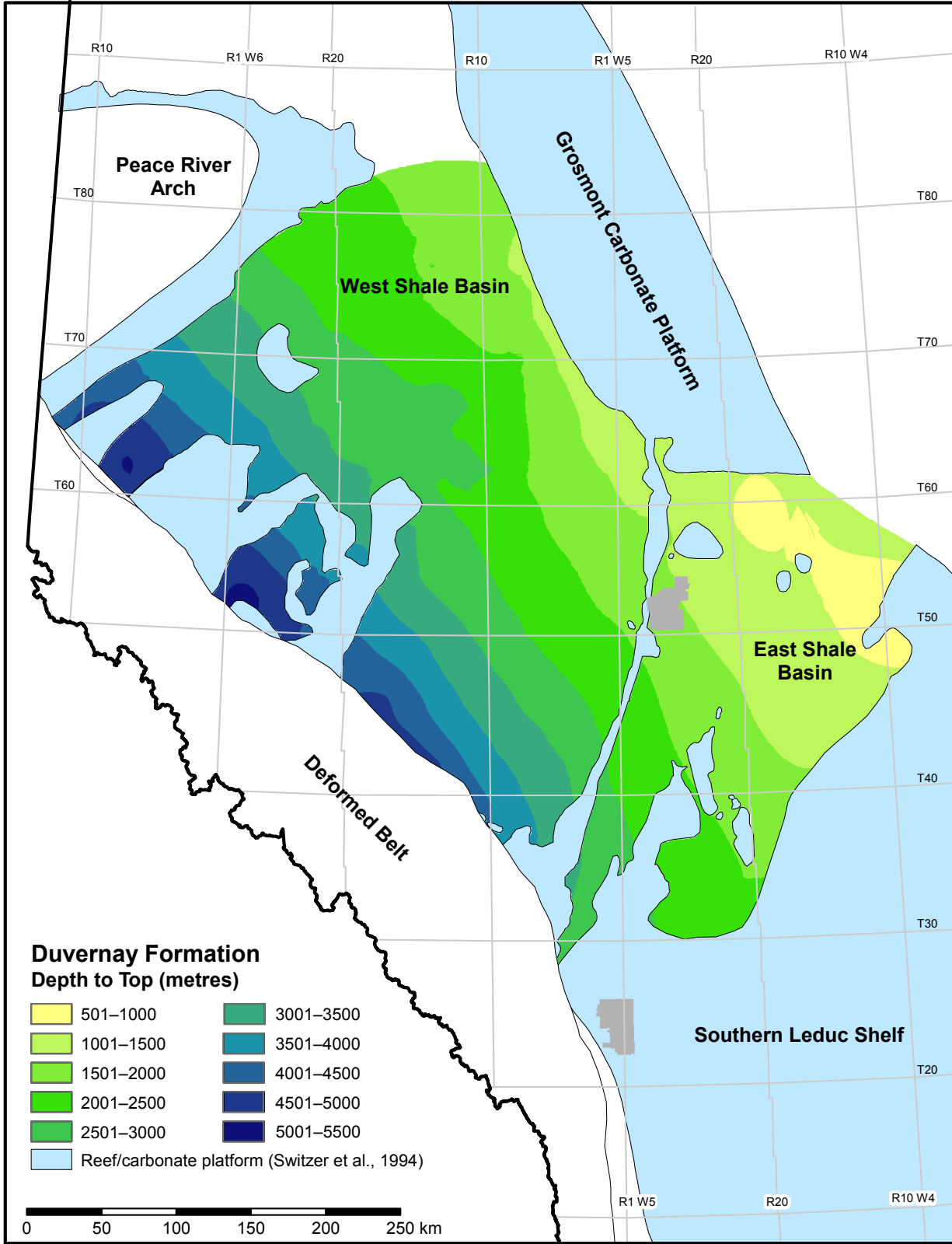


Figure 2.1.2. Depth to the top of the Duvernay Formation.

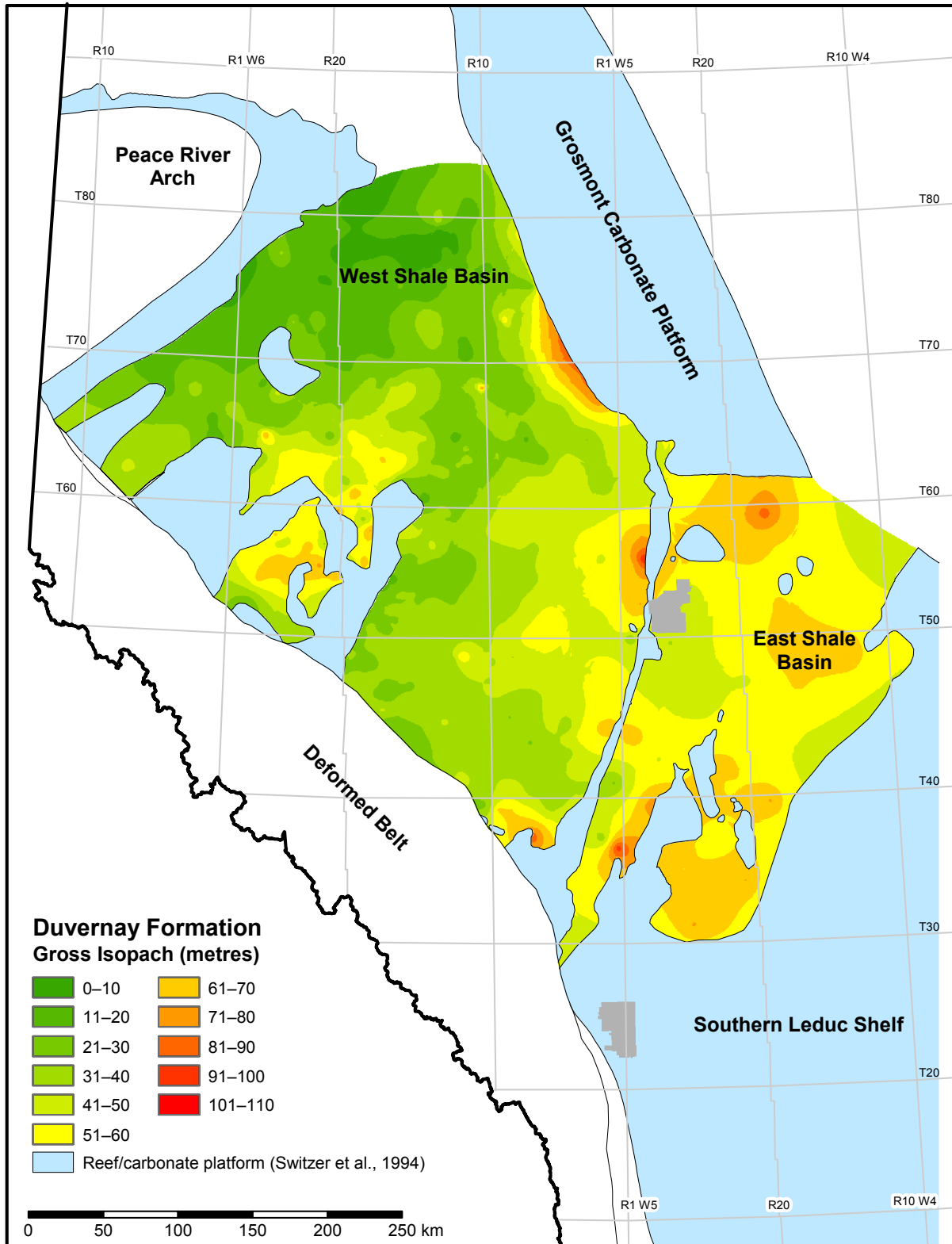


Figure 2.1.3. Gross isopach of the Duvernay Formation.

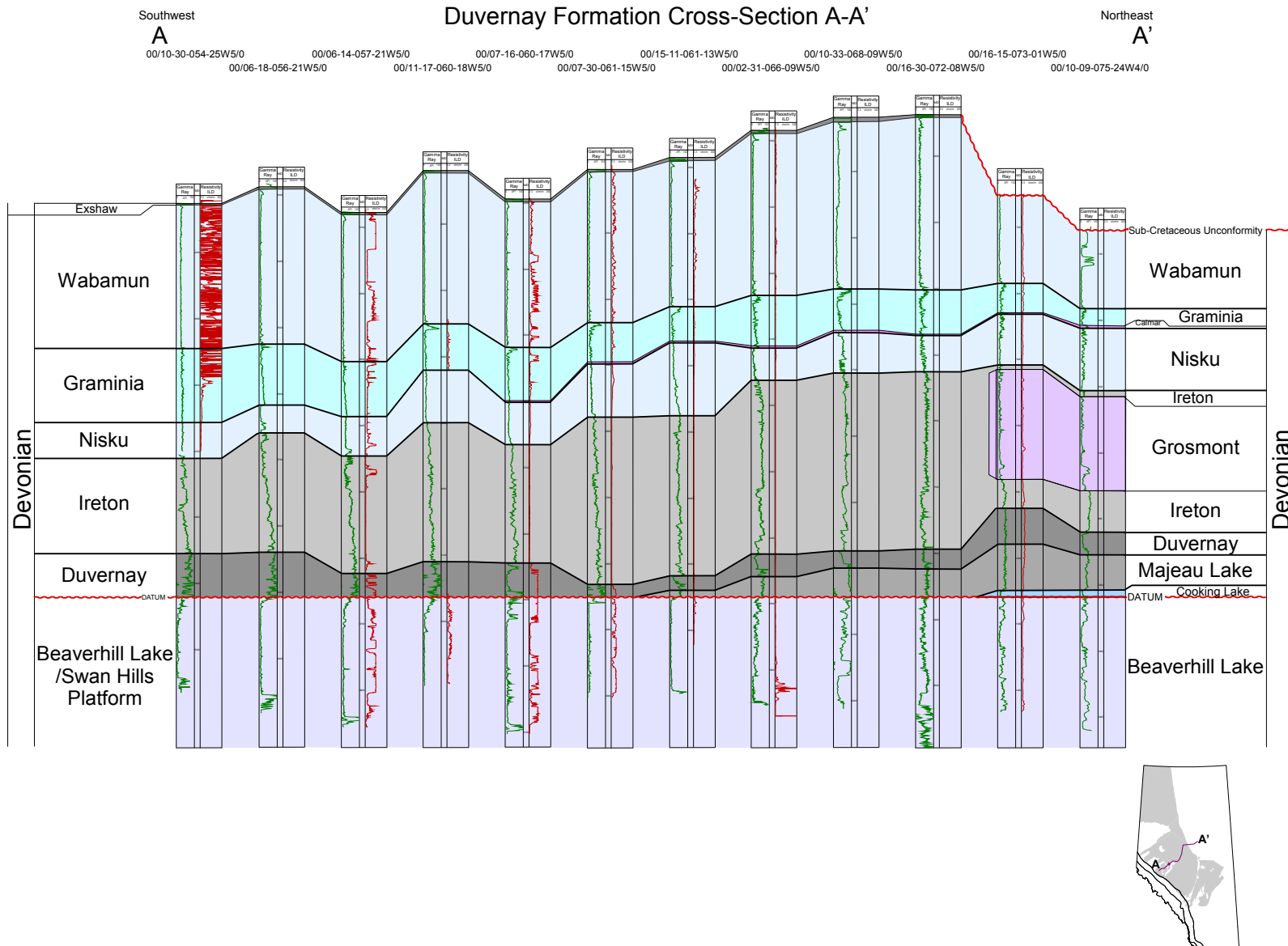


Figure 2.1.4a. Regional stratigraphic cross-section A-A' (see inset map for location).



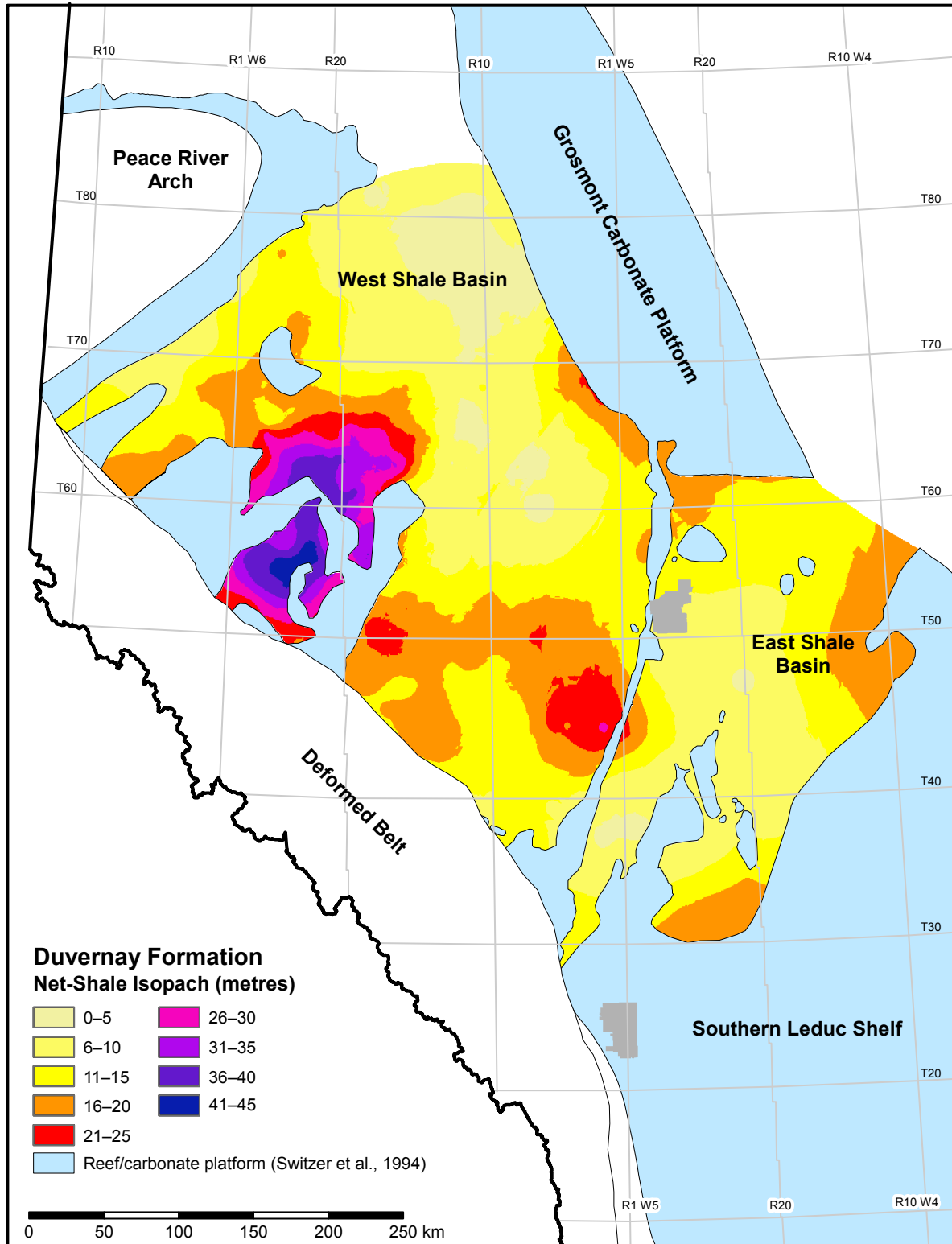


Figure 2.1.5. Net-shale isopach of the Duvernay Formation.

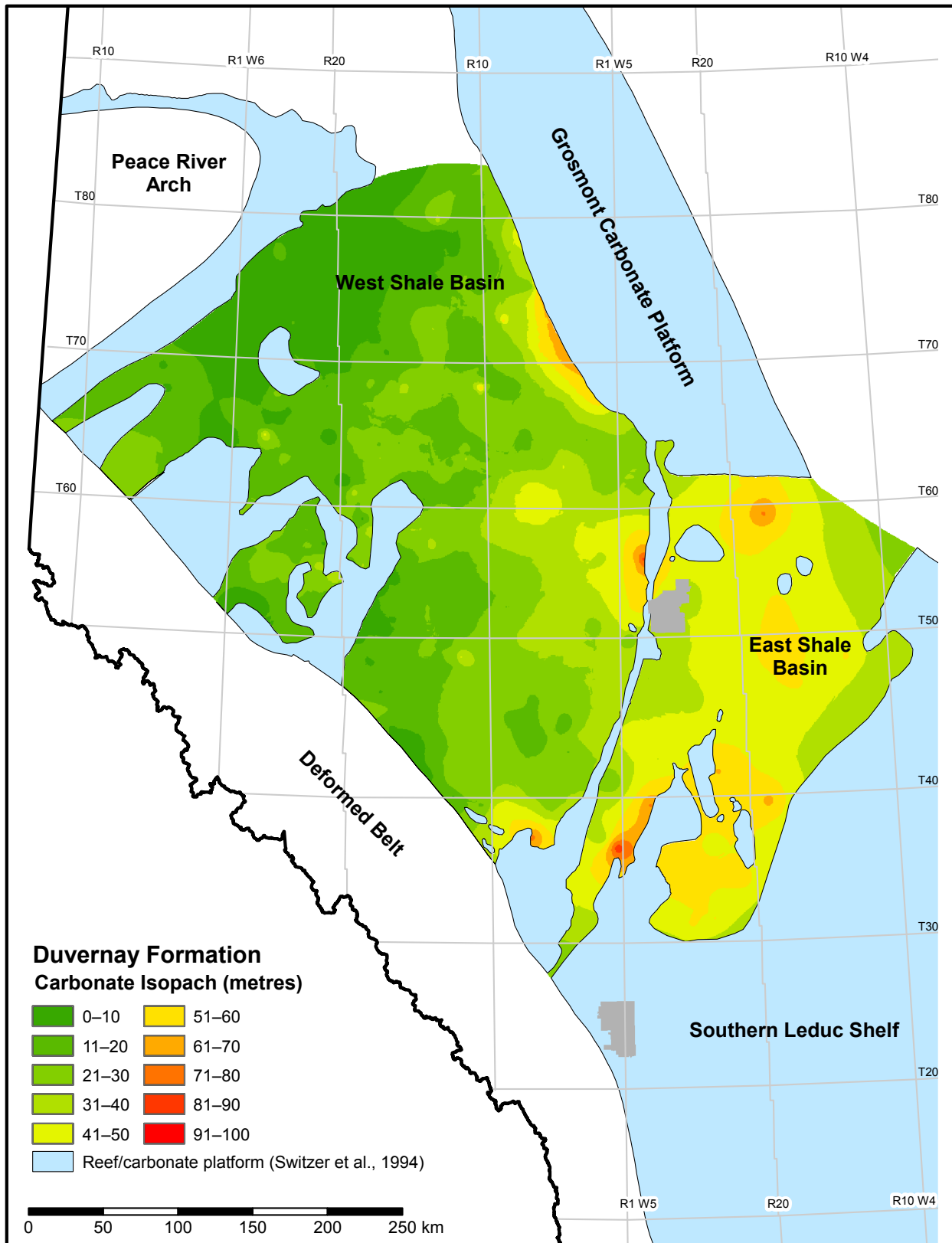


Figure 2.1.6. Net-carbonate isopach of the Duvernay Formation.

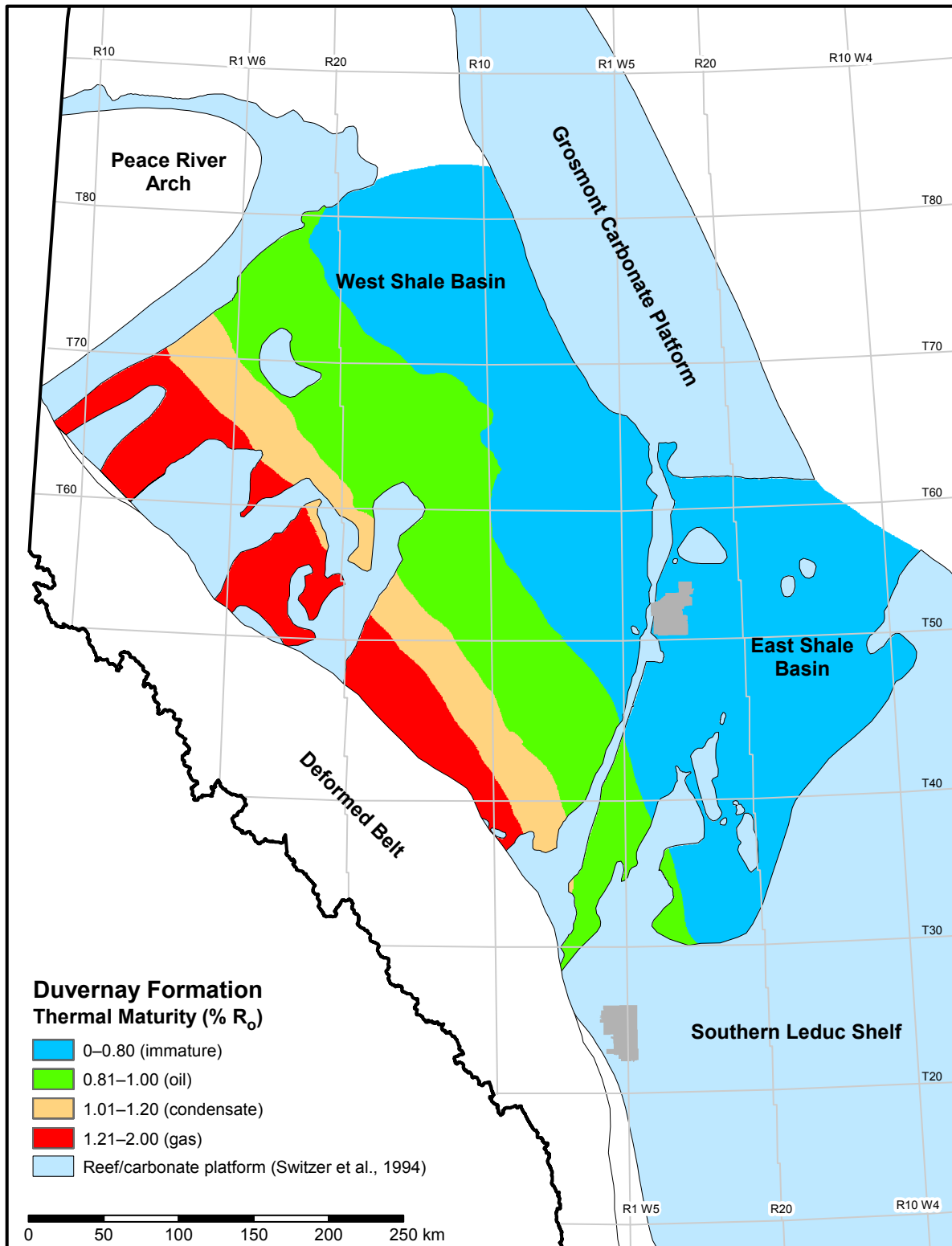


Figure 2.1.7. Thermal maturity map of the Duvernay Formation.

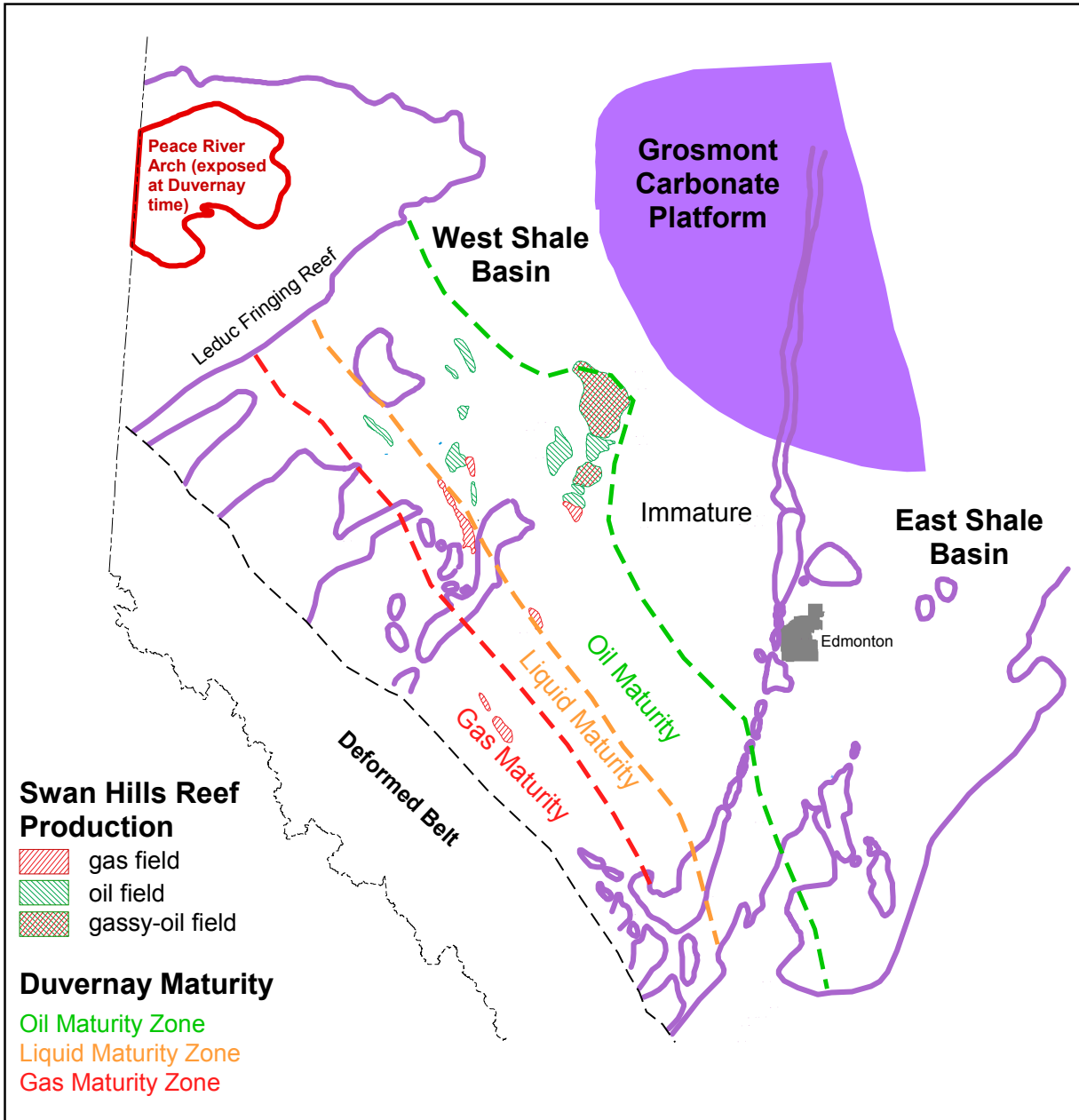


Figure 2.1.8. Thermal maturity zones for the Duvernay Formation and distribution of Swan Hills oil and gas pools. The reef outlines and carbonate platform (in purple) and the oil-, gas-, and gassy-oil-field outlines are from Switzer et al. (1994).

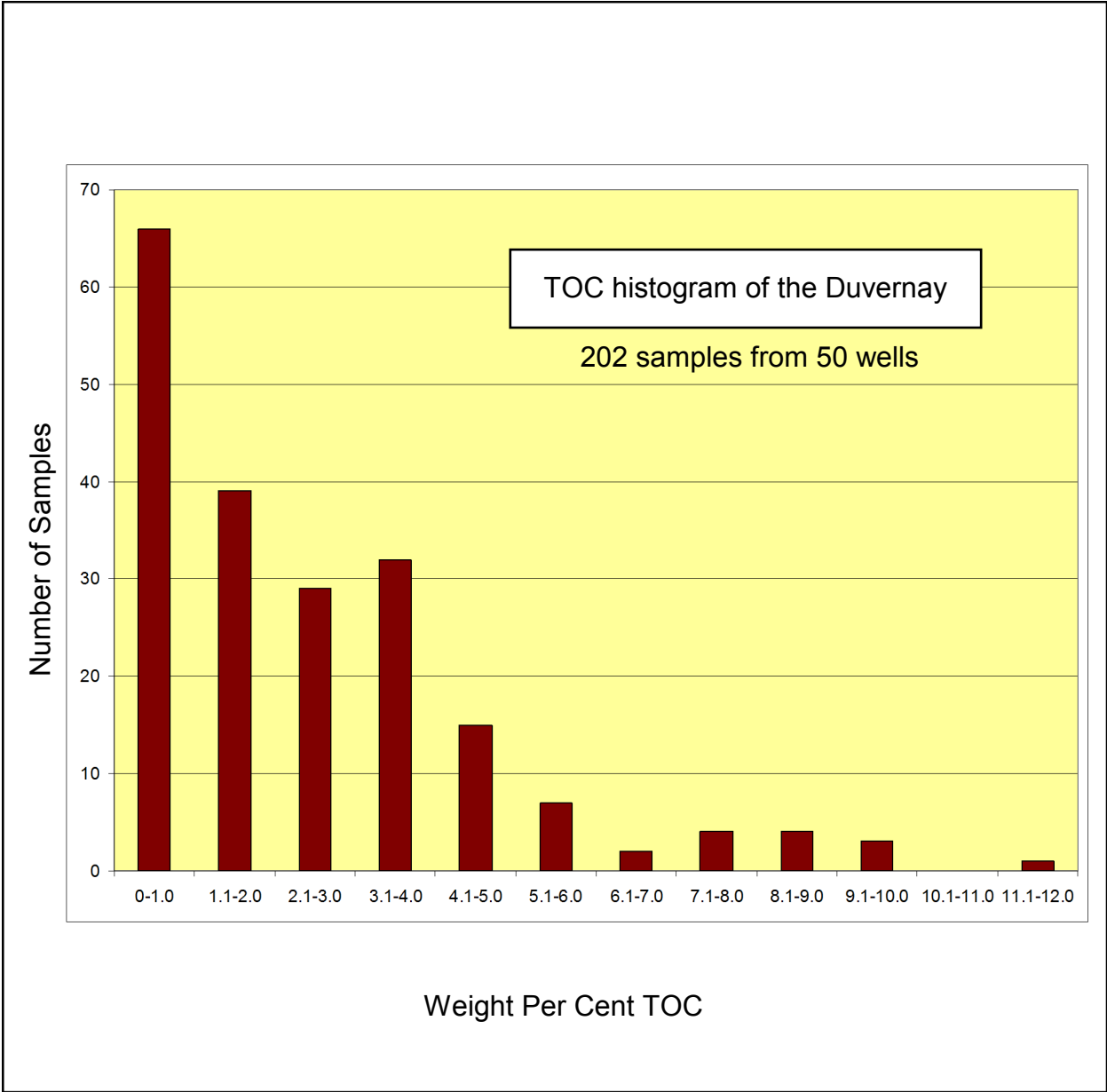


Figure 2.1.9. Histogram of total organic carbon (TOC) of 202 samples from the Duvernay Formation.

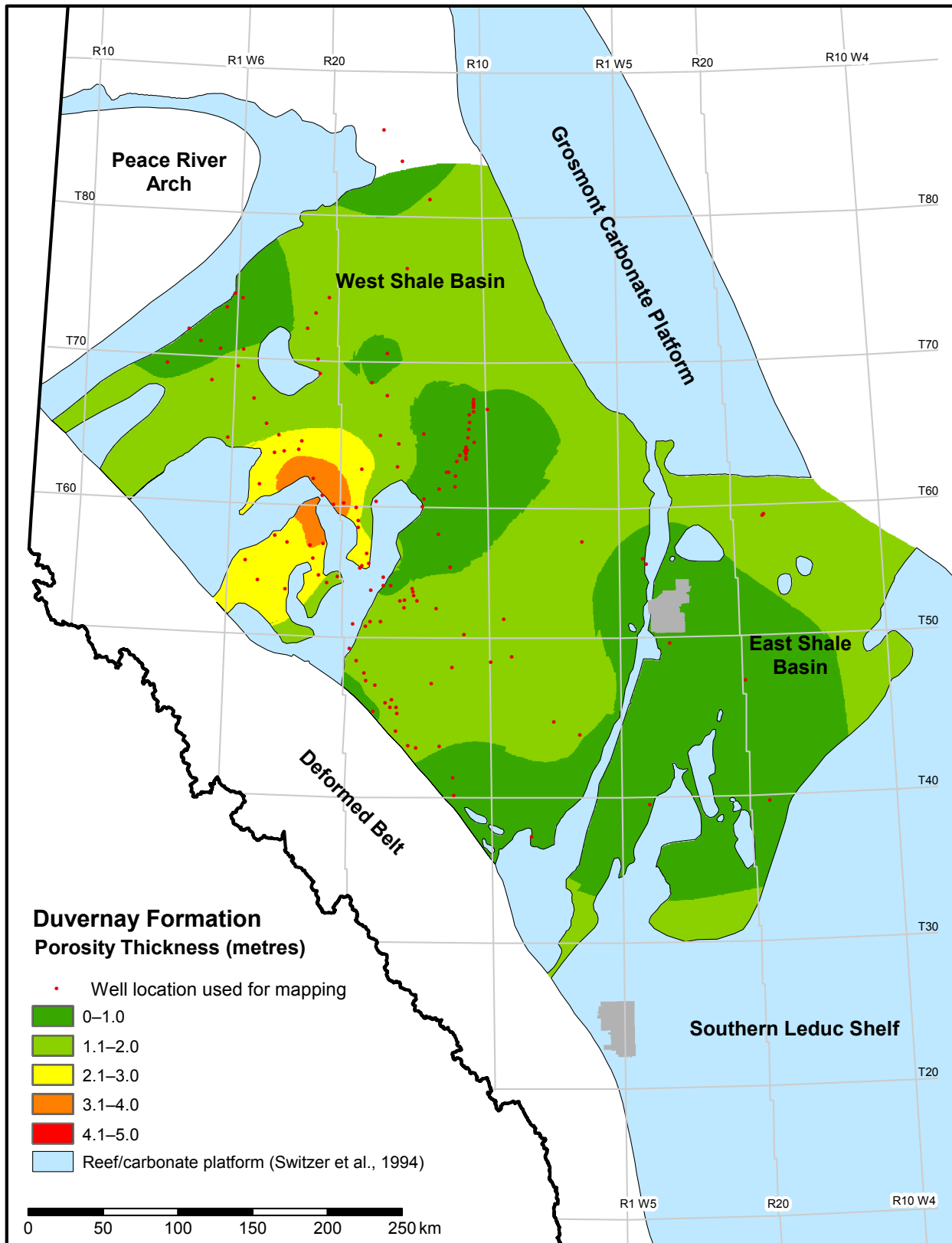


Figure 2.1.10. Porosity-thickness (Phi-h) map of the Duvernay Formation.

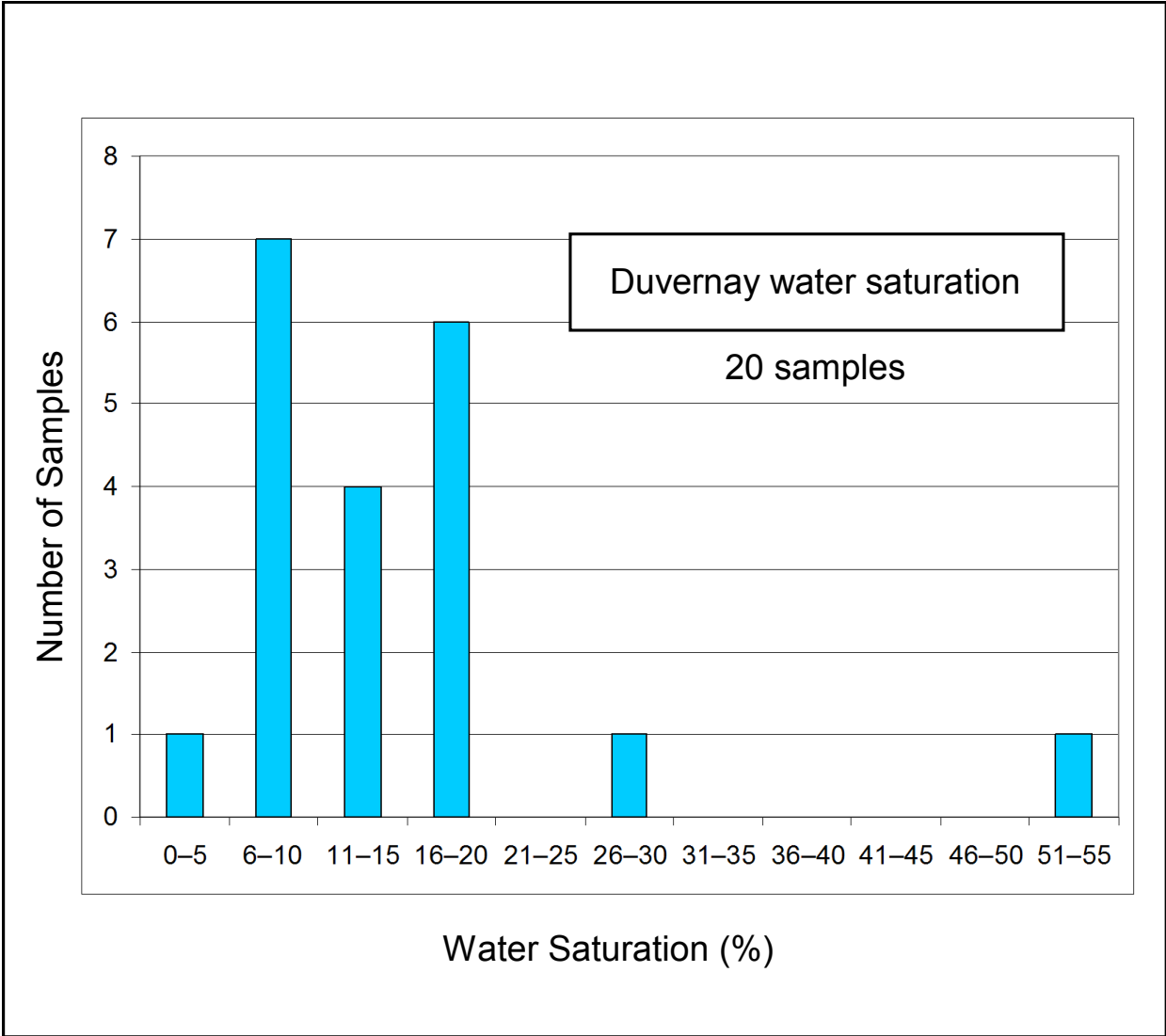


Figure 2.1.11. Histogram of water-saturation analysis results of 20 samples from the Duvernay Formation.

## 2.2 Summary of the Muskwa Formation

The Muskwa Formation (Muskwa) is an Upper Devonian source rock present in the subsurface of northern Alberta (Figure 2.2.1), where it is considered to be approximately stratigraphically equivalent to the Duvernay Formation (Switzer et al., 1994).

Muskwa lithology is dominated by organic-rich calcareous shale representing a relatively deep-water facies interbedded with organic-rich lime-mudstone. Flanking the north side of the Peace River Arch (PRA), Muskwa time-equivalent sandstone was noted in some core. The Muskwa dips from northeast to southwest, with the shallowest depth from the surface at about 800 m in the northeast to 2800 m in the southwest (Figures 2.2.2a and b). Towards the east, the Muskwa calcareous shale gradually changes facies to more shallow-water carbonates and may merge with the lower Grosmont platform-shelf carbonates.

The Muskwa increases in thickness to the north (Figure 2.2.3), away from the PRA. A representative west-to-east stratigraphic cross-section (one of more than 60 constructed for the Muskwa) shows an increase in porous, radioactive shale to the west and an increase in organic-rich lime-mudstone to the east (Figure 2.2.4). A net-shale map was created by calculating the thickness of sediment with a gamma-ray cutoff of >105 API (Figure 2.2.5). This thickness parameter was used in our resource analysis. The cutoff was created to exclude clean (i.e., non-argillaceous), organic-rich carbonate from inclusion in the resource calculation.

The thermal maturity of the Muskwa source rocks, based on vitrinite reflectance, exhibits a broad north-south trend with increased maturity to the northwest and the most immature sediment in the extreme southwest (Figure 2.2.6). The Muskwa in the northwest is structurally higher than the less mature and structurally deeper Muskwa to the southwest (Figures 2.2.2b and 2.2.6), indicating a complex structural history. Liquids-rich resources are expected in the northwest, with oil-prone resources expected in much of the remainder of the study area. Total organic carbon content of the Muskwa varies from 0.7 to 10.5 wt. % (Figure 2.2.7) based on 50 samples from 5 wells.

A porosity-thickness (Phi-h) map of the Muskwa shale (Figure 2.2.8) was constructed using density-porosity logs calibrated to a grain density of 2.67 g/cm<sup>3</sup> with no porosity cutoff and a <105 API gamma-ray-log cutoff. The grain density we used accounts for the presence of TOC by converting TOC to kerogen and counting it as a mineral component in the grain density. Section 3.4 provides the determination of grain density used in our analysis and possible sources of error.

Using Dean Stark analysis and helium pycnometry on select samples, the laboratory calculated water saturation. The distribution of values for the Muskwa shows a range of 6% to 83%, with 20% and 50% used as P90 and P10 constraints, respectively (Figure 2.2.9). Section 3.3 provides information on the methodology used to determine water saturation and possible sources of error.

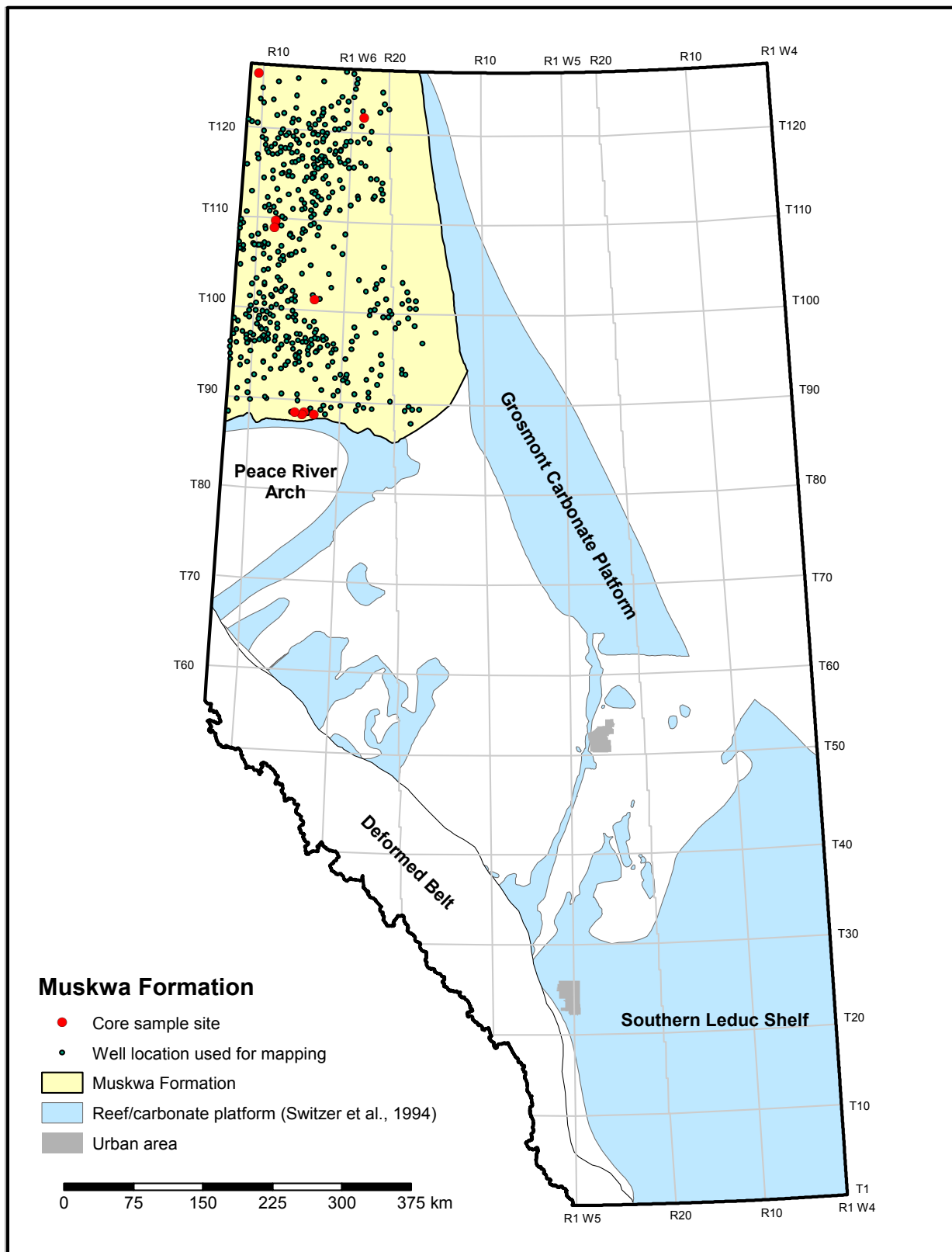


Figure 2.2.1. Index map of the Muskwa Formation.

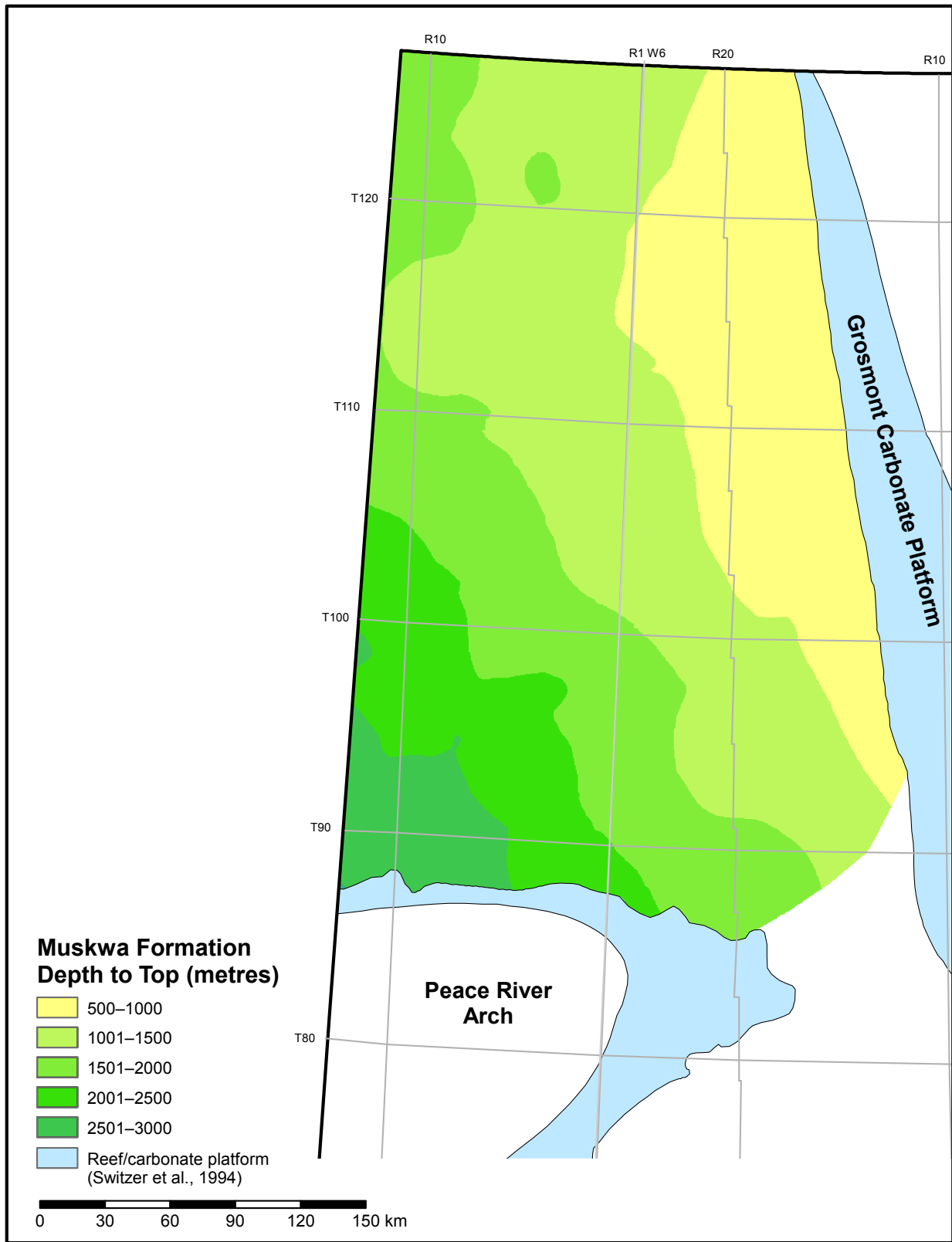


Figure 2.2.2a. Depth to top of the Muskwa Formation.

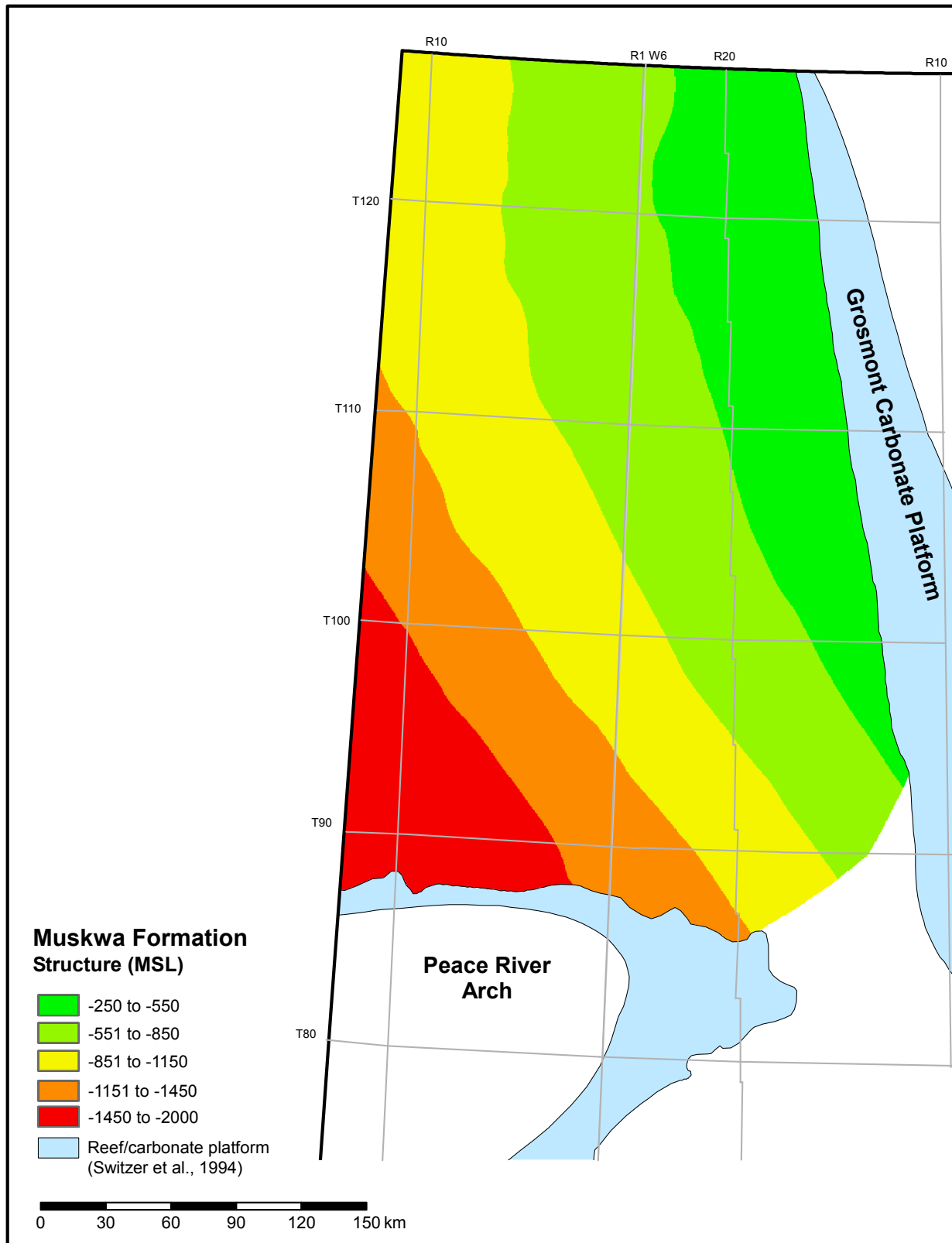


Figure 2.2.2b. Structure of the Muskwa Formation.

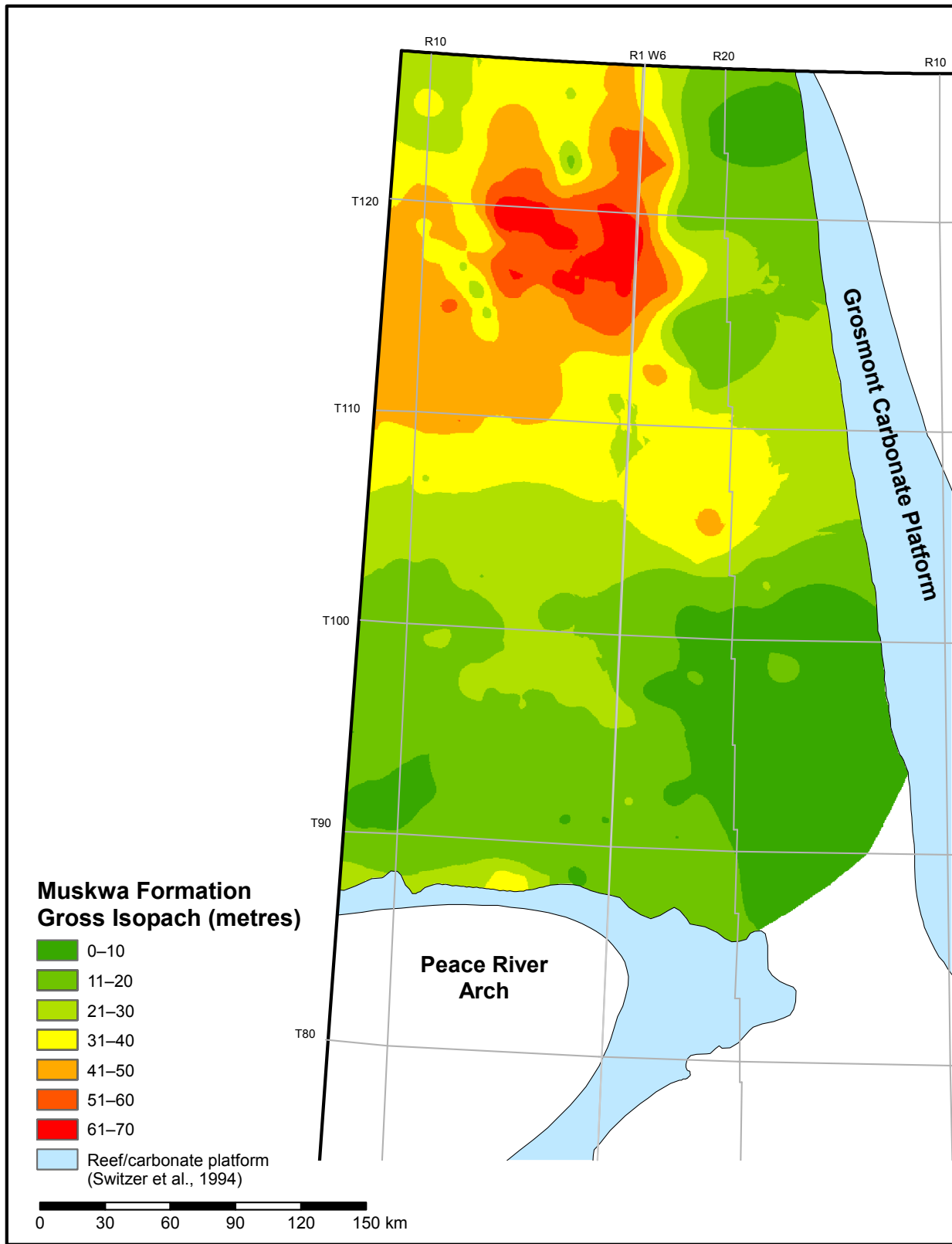


Figure 2.2.3. Gross isopach of the Muskwa Formation.



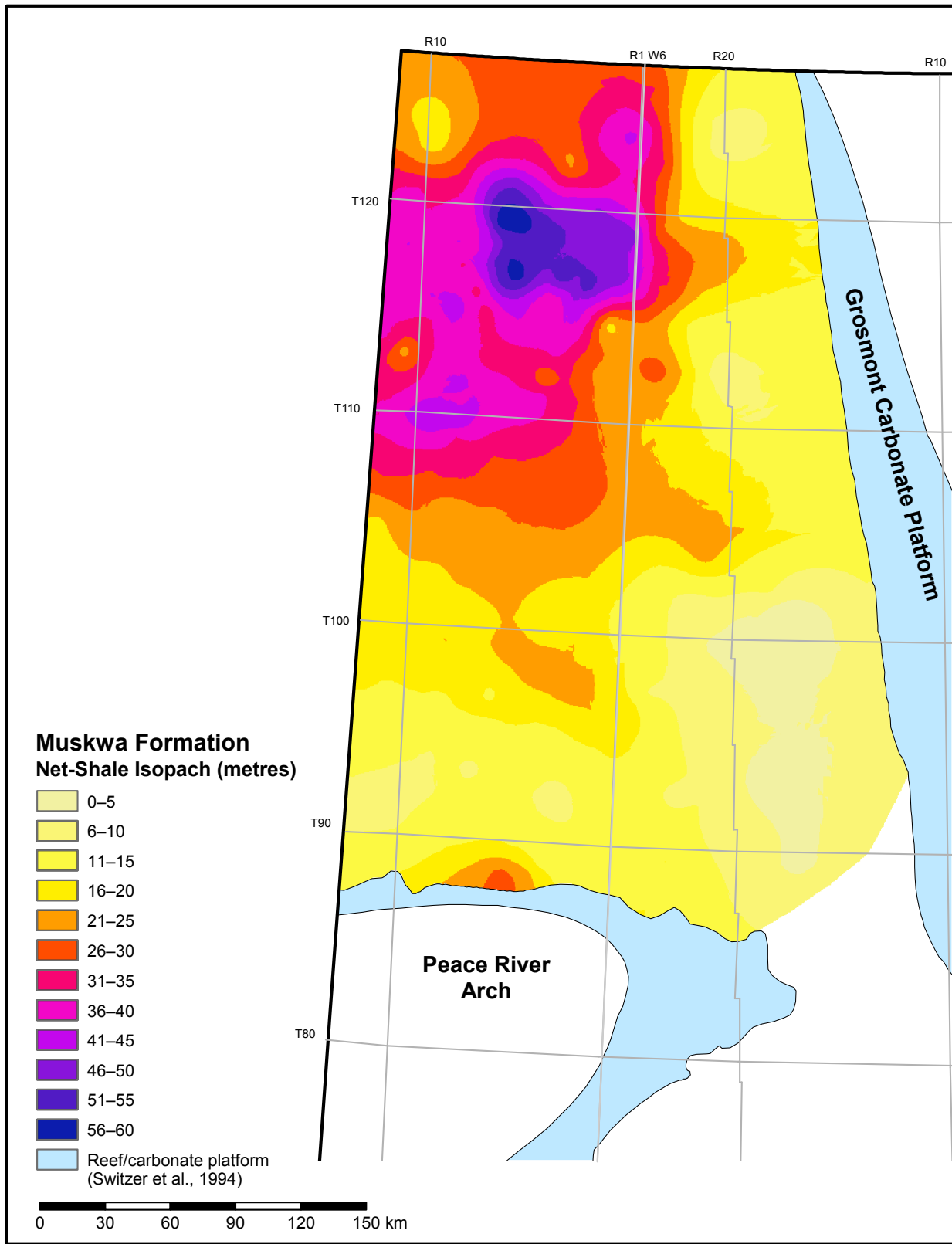


Figure 2.2.5. Net-shale isopach of the Muskwa Formation.

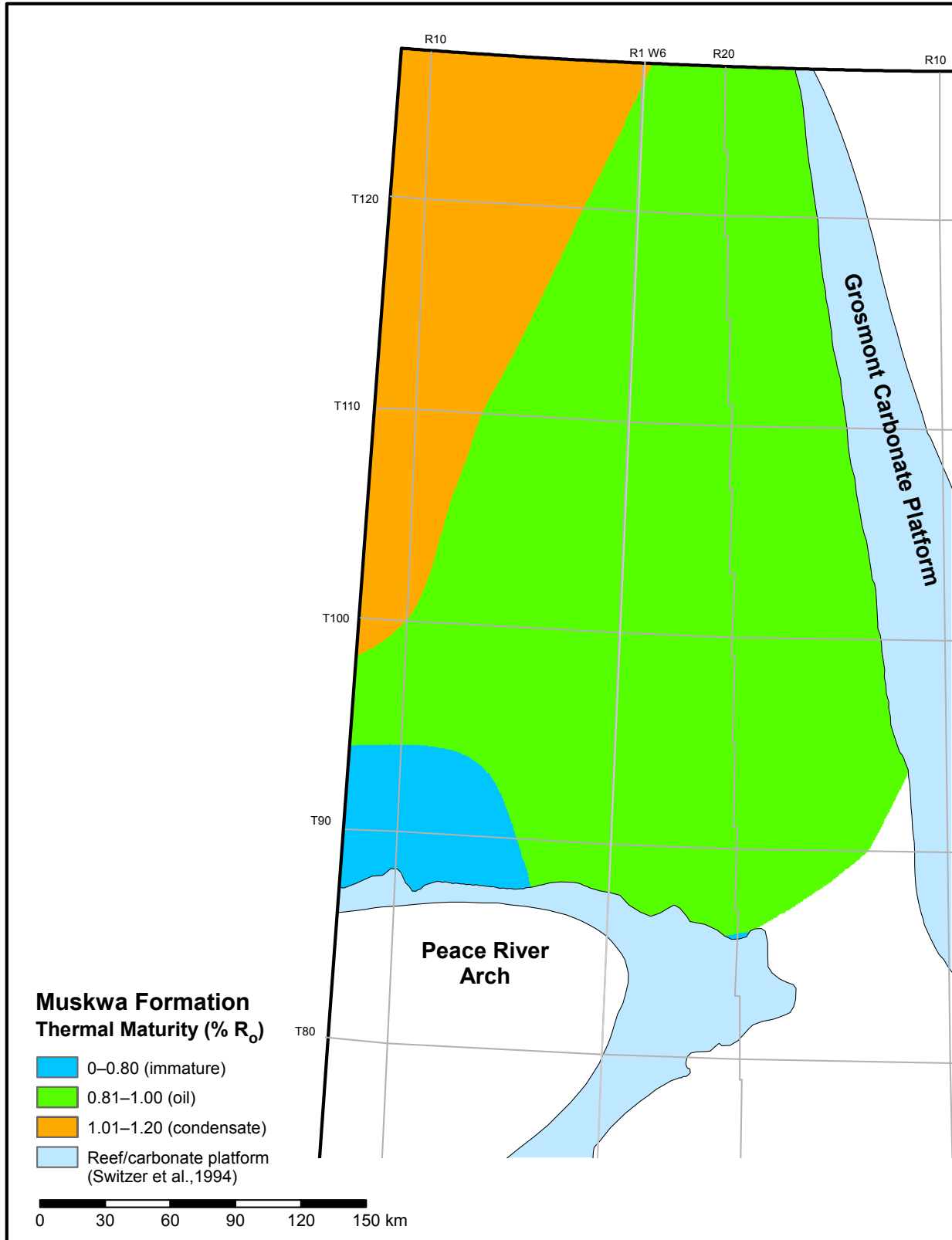


Figure 2.2.6. Thermal maturity map of the Muskwa Formation.

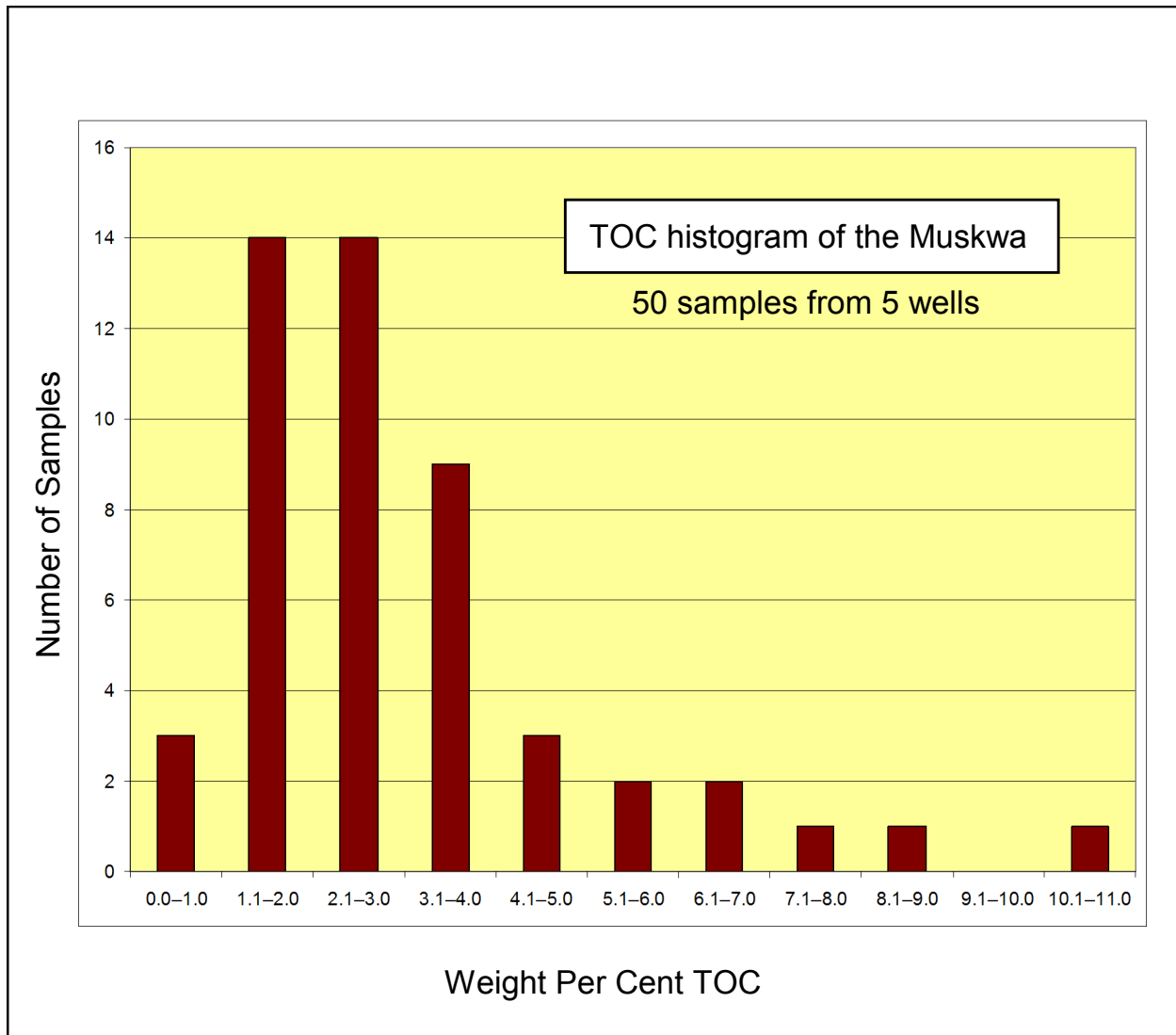


Figure 2.2.7. Histogram of total organic carbon (TOC) of 50 samples from the Muskwa Formation.

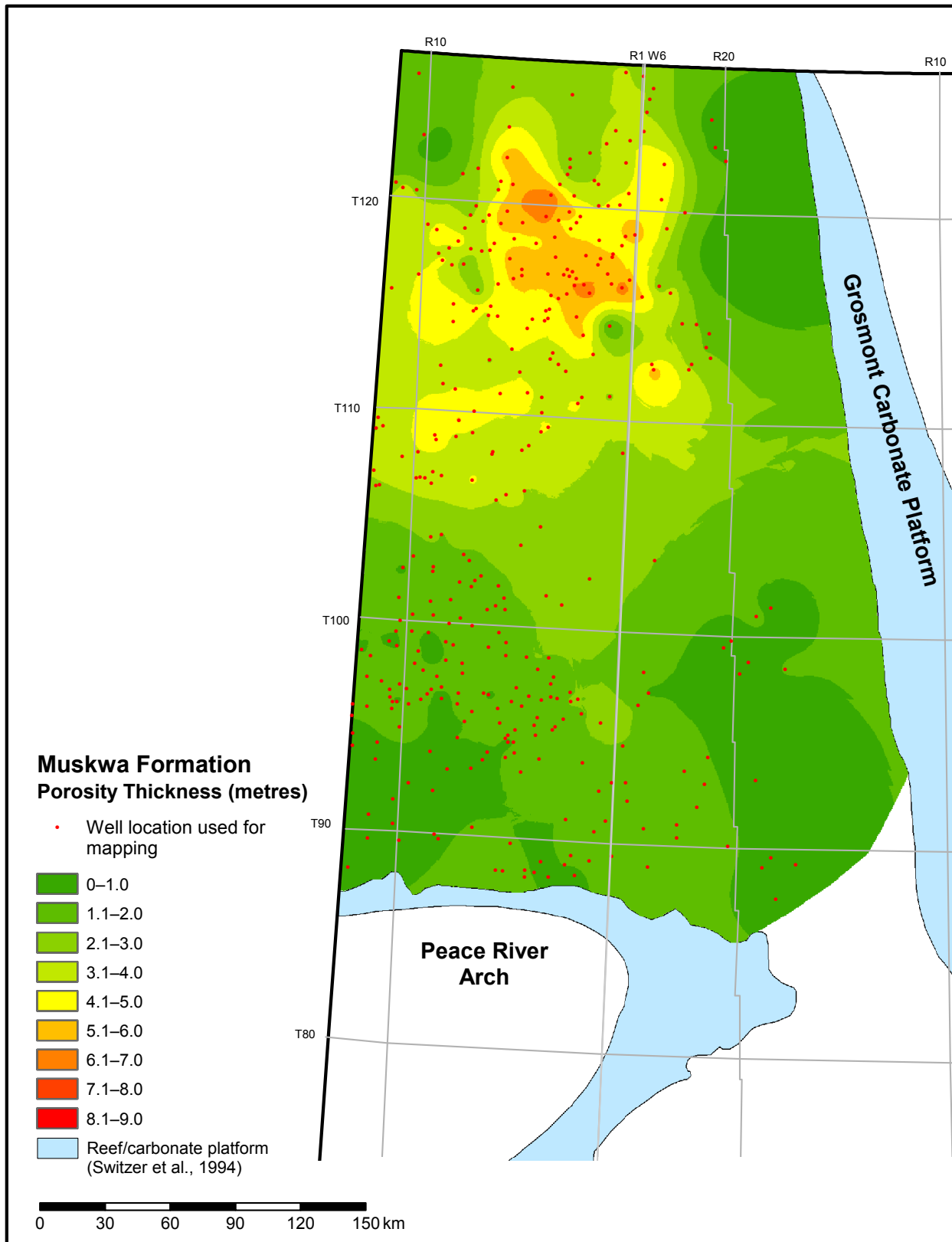


Figure 2.2.8. Porosity-thickness (Phi-h) map of the Muskwa Formation.

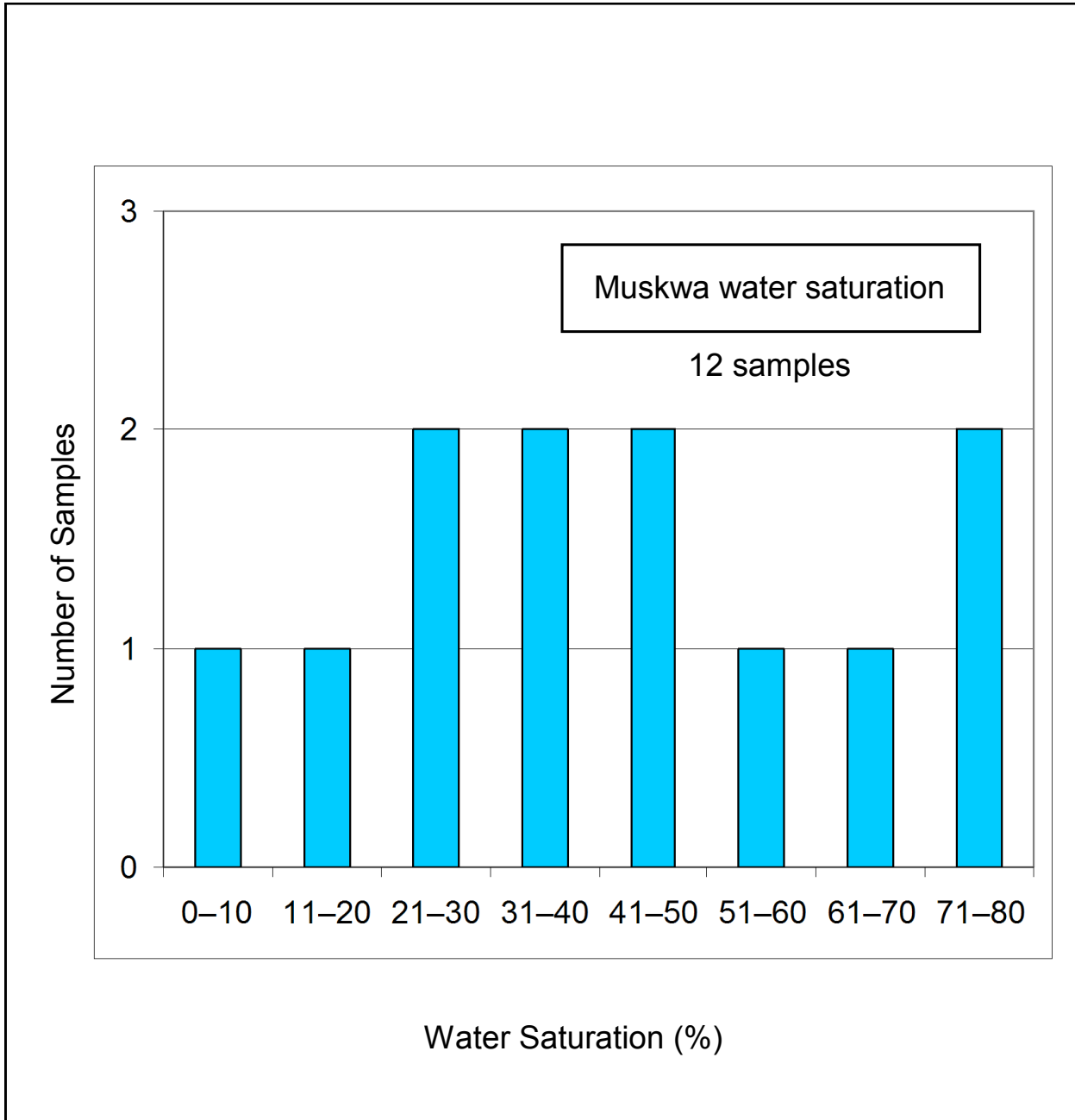


Figure 2.2.9. Histogram of water-saturation analysis results from 12 samples from the Muskwa Formation.

### 2.3 Summary of the Montney Formation

The Montney Formation (Montney) is a Lower to Middle Triassic conventional and tight-reservoir rock in west-central Alberta (Figure 2.3.1) and east-central British Columbia. In Alberta, the upper part of the Montney Formation is often informally referred to as the lower Doig siltstone. For this report, we have excluded the lower Doig siltstone from the Montney evaluation.

Montney lithology is dominated by siltstones with varying degrees of dolomitization. There are fine-grained sandstones and coquinas, which are the main targets of oil and gas exploration.

The depth from the surface to the top of the Montney ranges from about 500 m to about 4500 m (Figure 2.3.2), increasing in depth from northeast to southwest. The thickness of the Montney ranges from 0 m along the eastern erosional edge to about 300 m along the Alberta-British Columbia border (Figure 2.3.3).

More than 70 stratigraphic and structural cross-sections were constructed for the Montney. Figure 2.3.4 is a representative stratigraphic cross-section illustrating the thickness of the Montney and its relationship to overlying formations. A net-silt map (Figure 2.3.5) was created by calculating the thickness of the formation with a gamma-ray cutoff of >75 API. This cutoff eliminated conventional reservoirs in sandstones and coquinas from inclusion in the resource endowment. Figure 2.3.6 is a net-sand map illustrating areas where the Montney has a gamma-ray cutoff of <75 API, highlighting where conventional reservoirs may exist. The present evaluation used only the portion of the rock with a gamma-ray cutoff of >75 API, which we called 'silt,' but may include some organic-rich mudstone or shale, and falls under the loose industry and public definition of 'shale.'

Using vitrinite reflectance data, a map illustrating the thermal maturity of the Montney (Figure 2.3.7) shows the basic trend of increasing maturity to the southwest. This trend corresponds with an increased depth below the surface. Dry-gas resources are expected in the southwest, with more liquids-rich gas and oil-prone strata towards the east. However, some migration of hydrocarbons may have occurred from formations in direct contact with the Montney. For example, in some areas, the Montney directly contacts the Nordegg Member, which is an oil-prone source rock. Where these formations are in contact, the Montney may contain oil sourced from the Nordegg Member.

The average TOC content of the Montney is 0.8 wt. %, with a range of 0.1 to 3.6 wt. % (Figure 2.3.8). This is based on 170 Montney siltstone, sandstone, and coquina samples. Montney organic content varies locally both laterally and vertically, with no indicated regional directional trend of increasing or decreasing TOC.

A porosity-thickness (Phi-h) map of the Montney (Figure 2.3.9) was constructed using density-porosity logs calibrated to a grain density of 2.71 g/cm<sup>3</sup> with no porosity cutoff and a >75 API gamma-ray-log cutoff. The grain density used accounts for the presence of TOC by converting TOC to kerogen and counting it as a mineral component in the grain density. Section 3.4 provides the methodology used to determine grain density; the relationship between grain density, porosity, and TOC content; and possible sources of error.

The Dean Stark and helium pycnometry analyses may not have accurately measured the water saturation of the Montney Formation samples due to the low permeability of the formation. In addition, the water-saturation dataset only contained nine samples (Figure 2.3.10). Therefore, we reviewed publicly available information from which we selected a water-saturation range of 20% to 50% to represent P90 and P10 in our evaluation. The production of water in some wells in the Montney may account for the high end of the saturation range. Section 3.3 provides information on water saturation and possible sources of error.

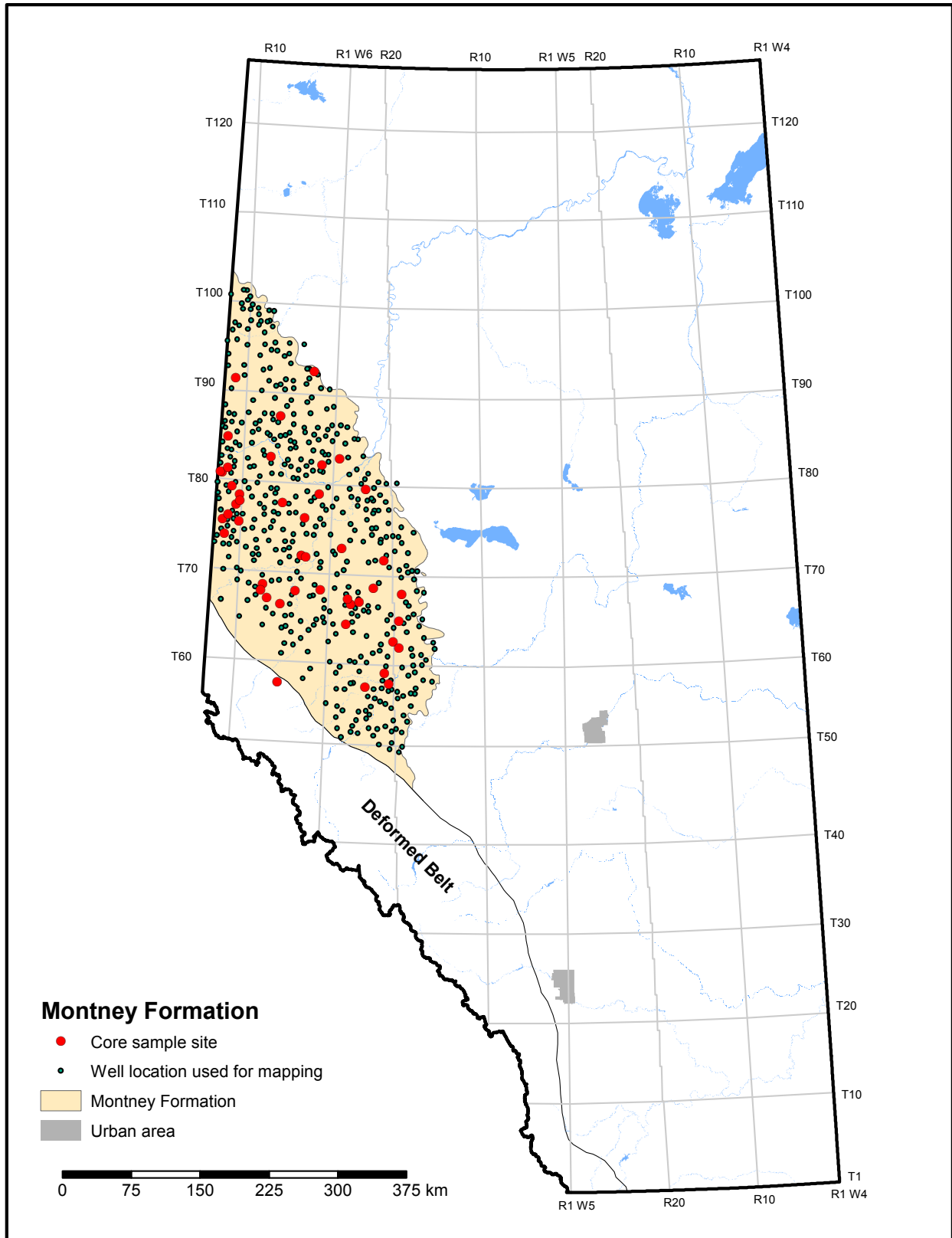


Figure 2.3.1. Index map of the Montney Formation.

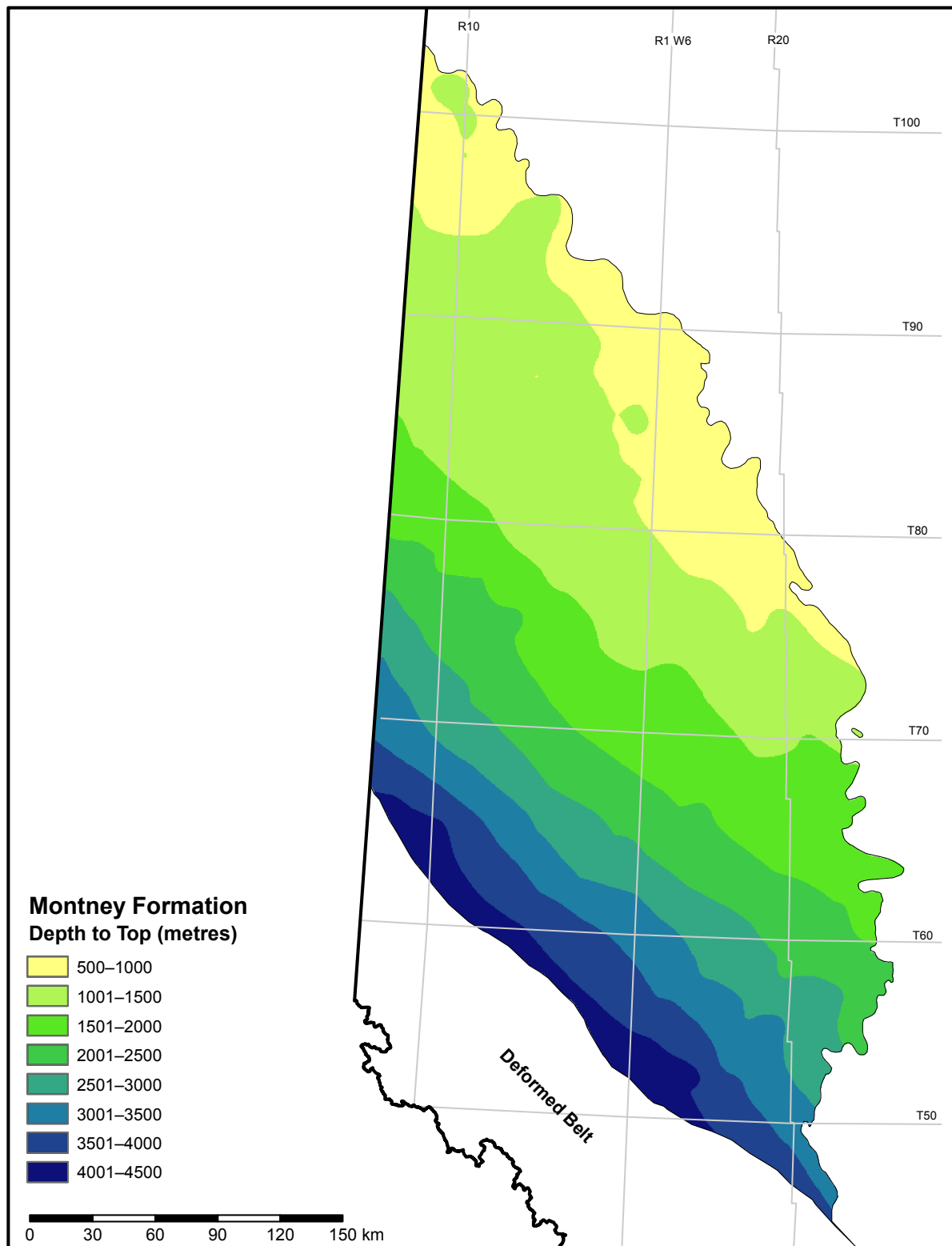


Figure 2.3.2. Depth to top of the Montney Formation.

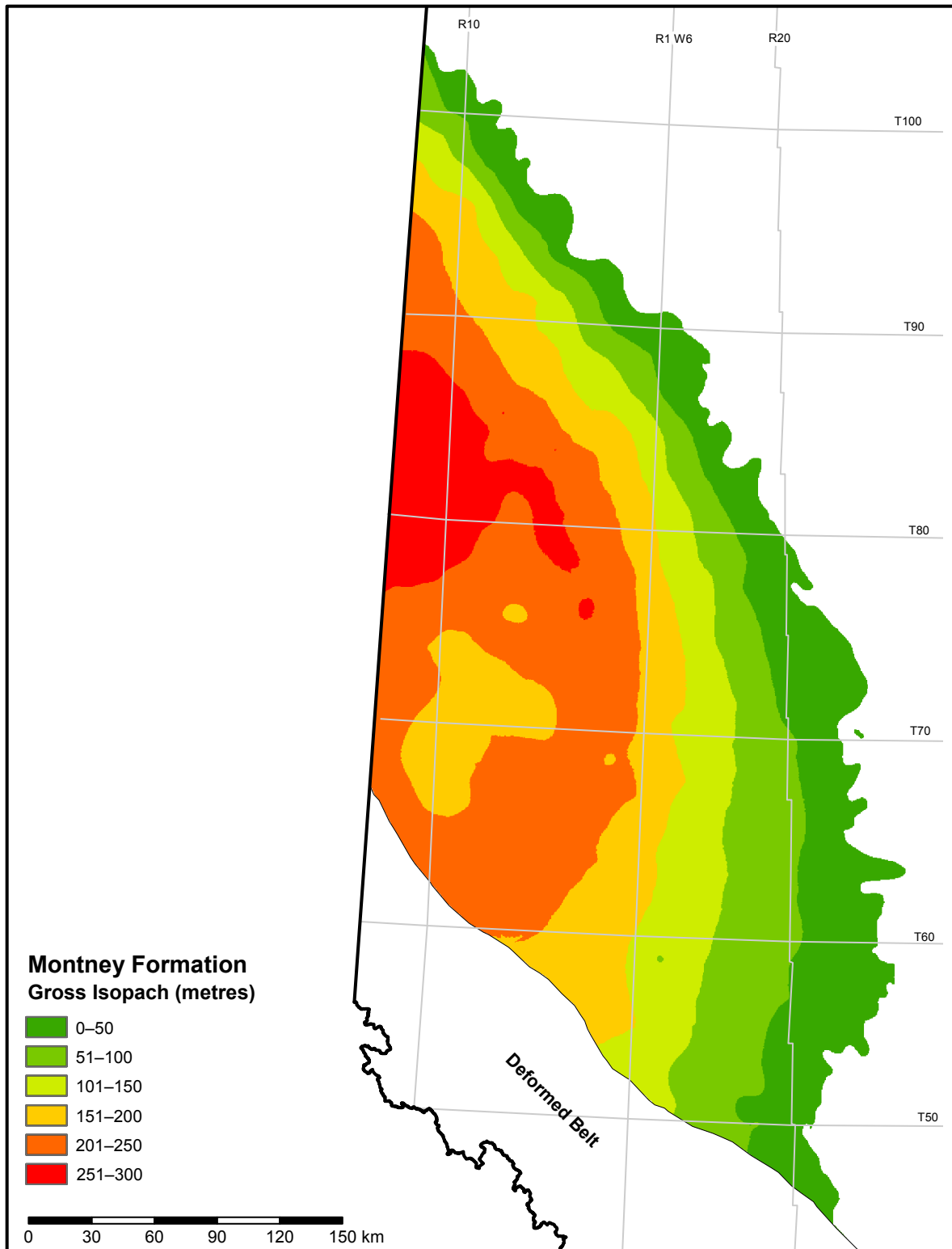


Figure 2.3.3. Gross isopach of the Montney Formation.

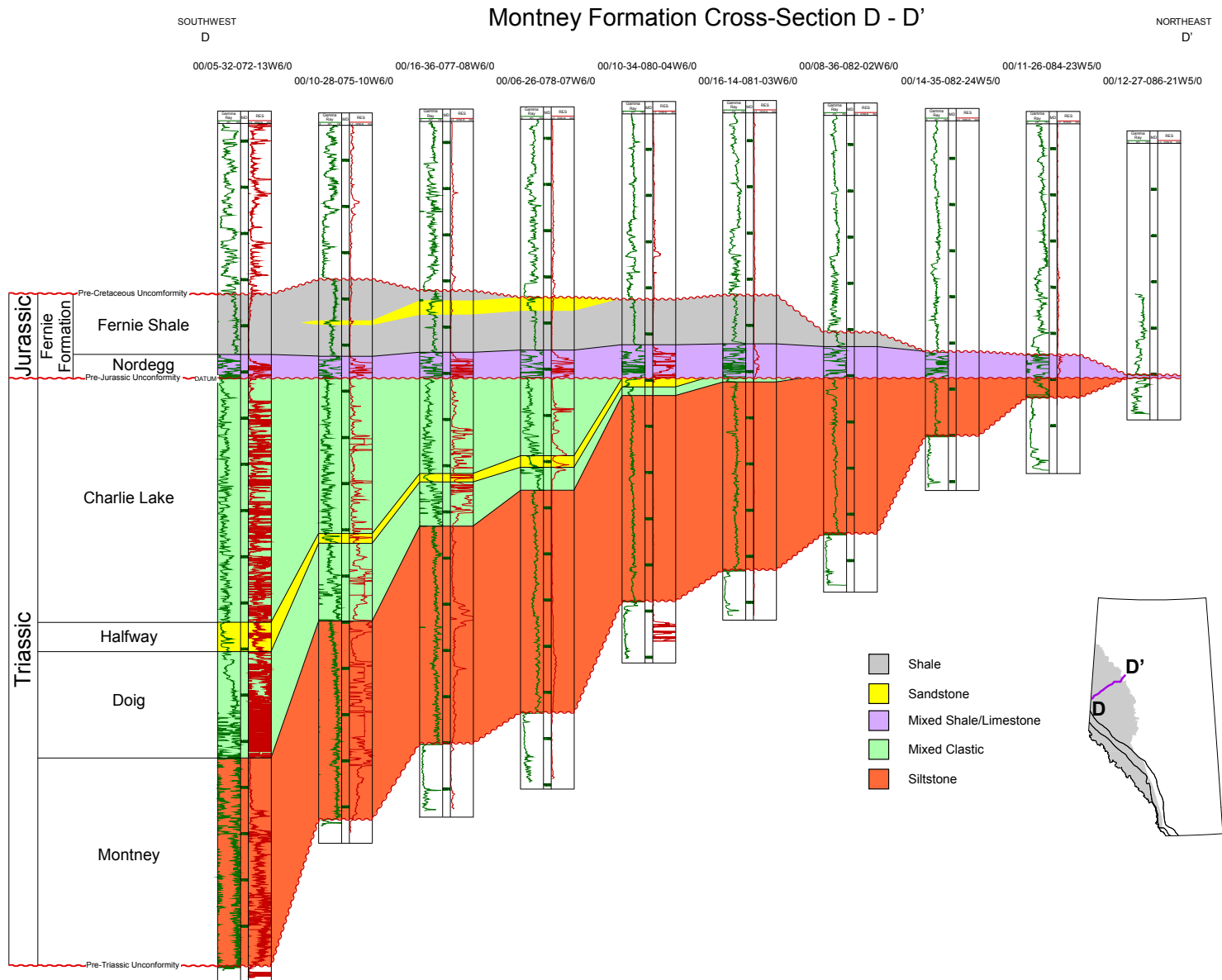


Figure 2.3.4. Stratigraphic cross-section D-D' of the Montney Formation (see inset map for location).

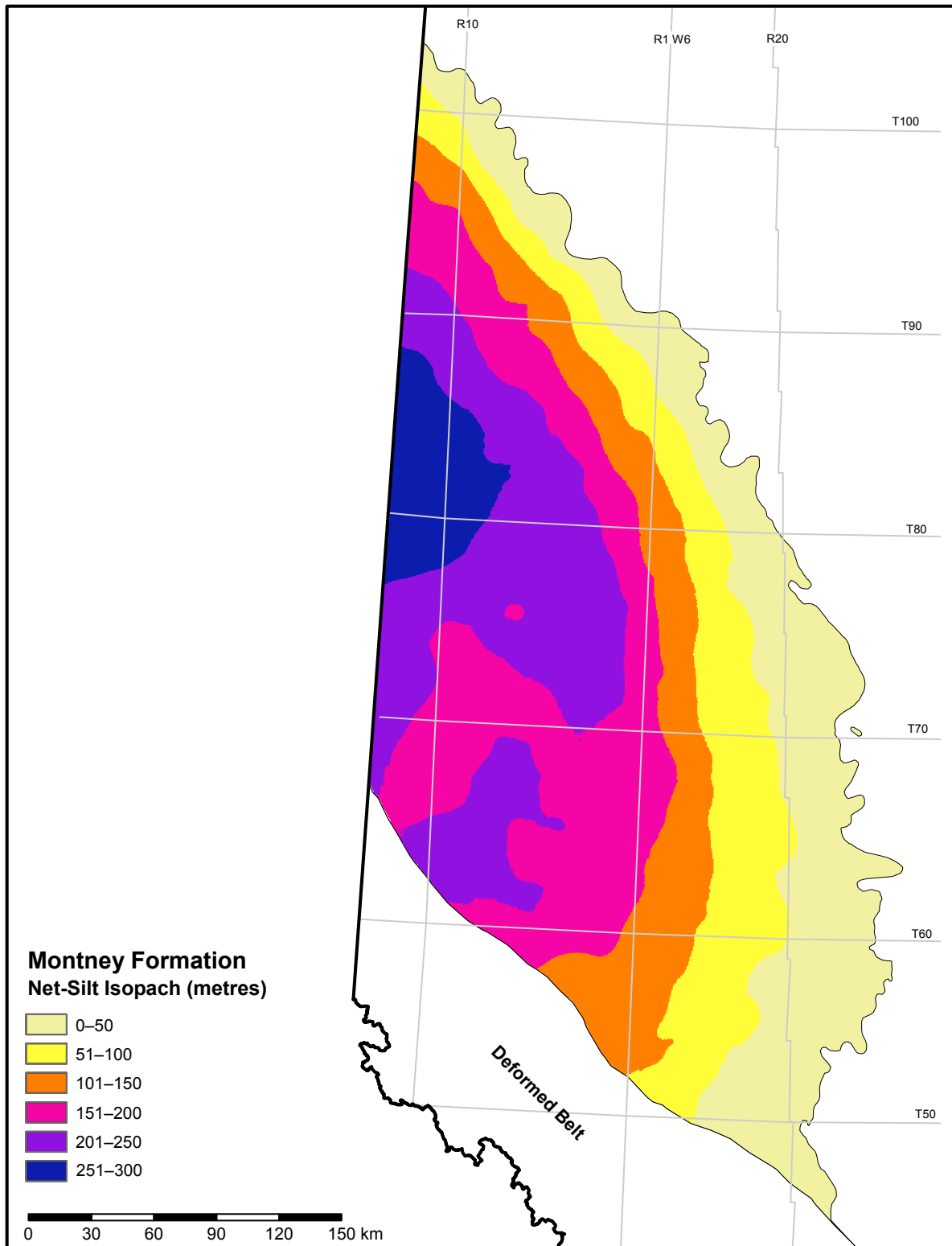


Figure 2.3.5. Net-silt isopach of the Montney Formation.

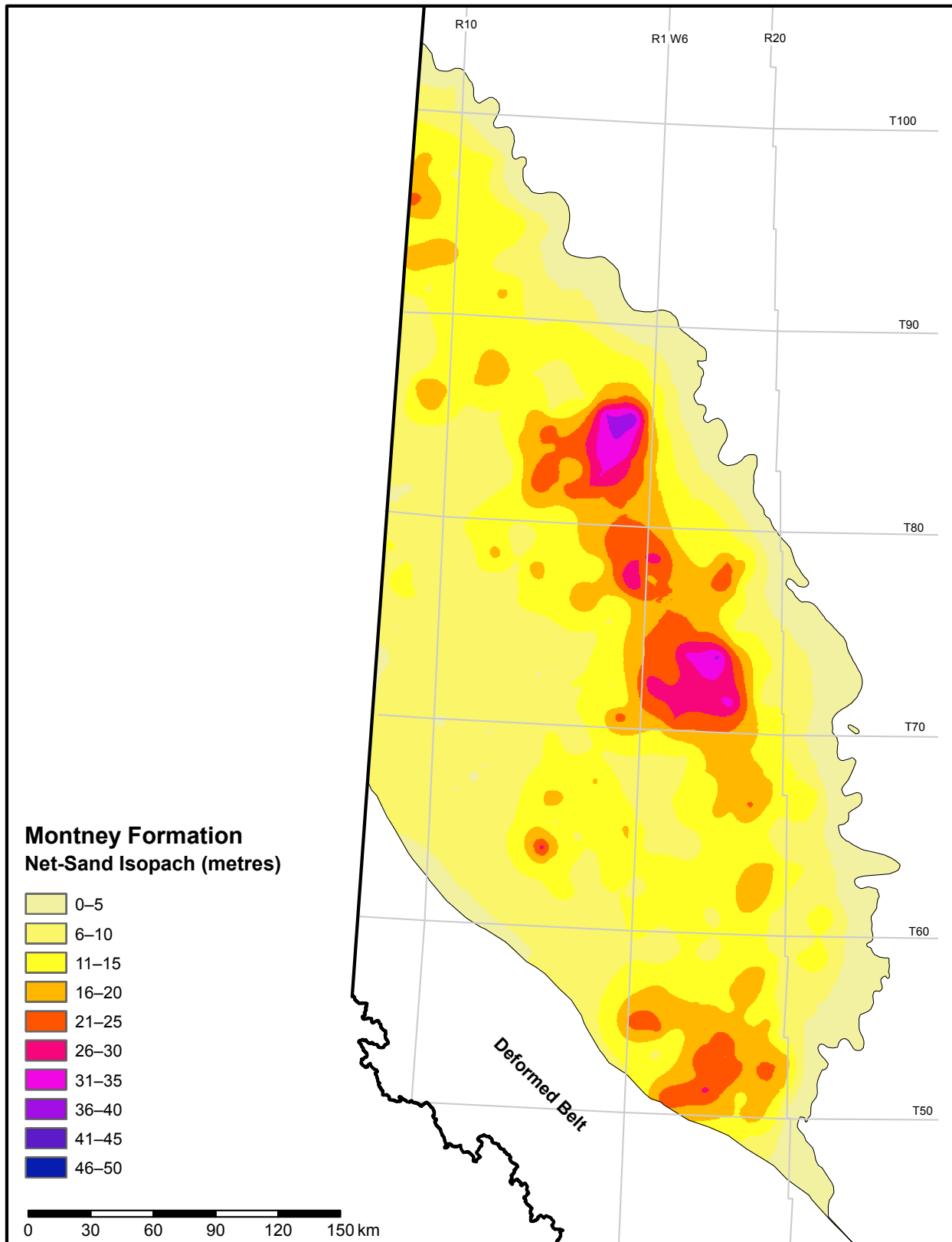


Figure 2.3.6. Net-sand isopach of the Montney Formation.

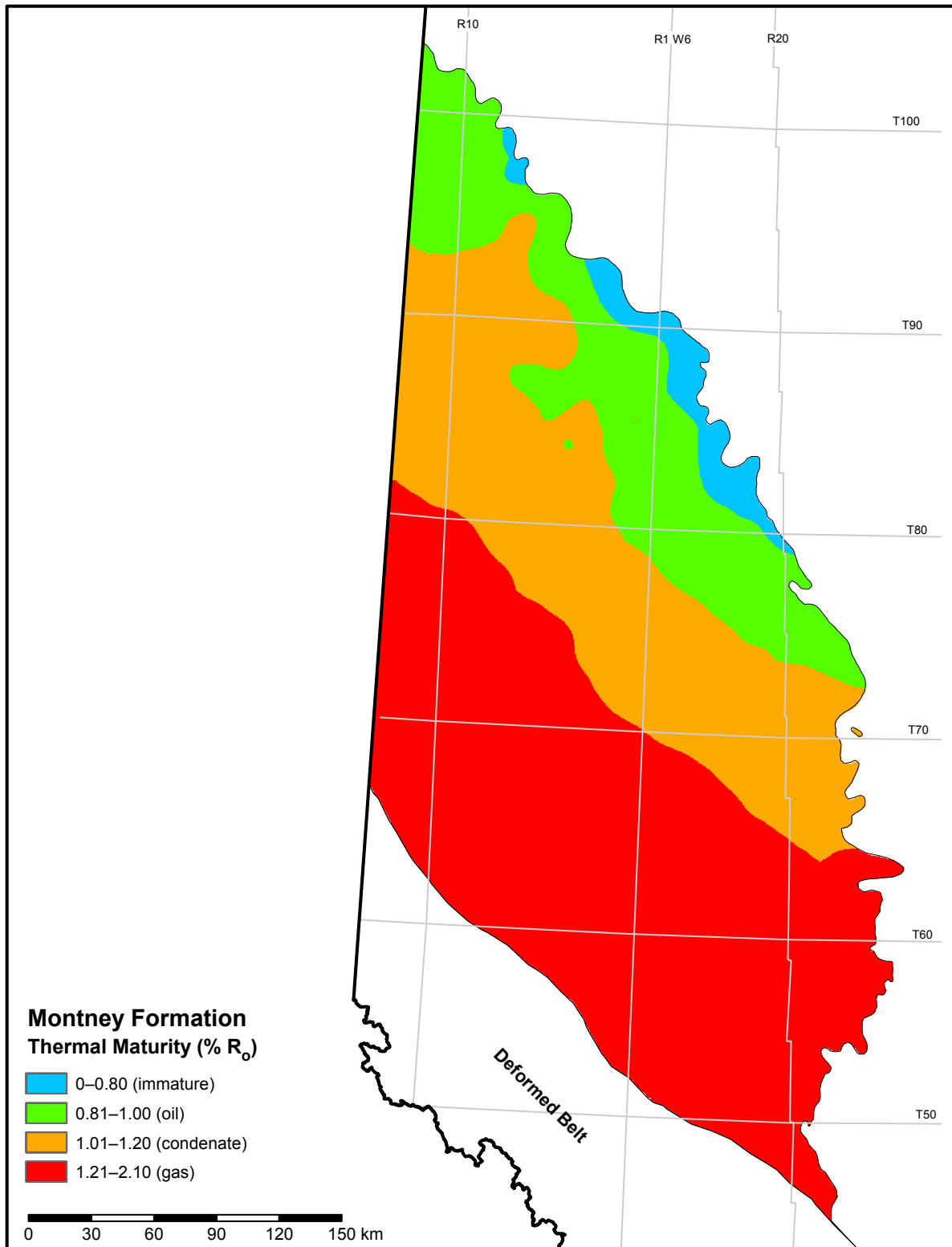


Figure 2.3.7. Thermal maturity map of the Montney Formation.

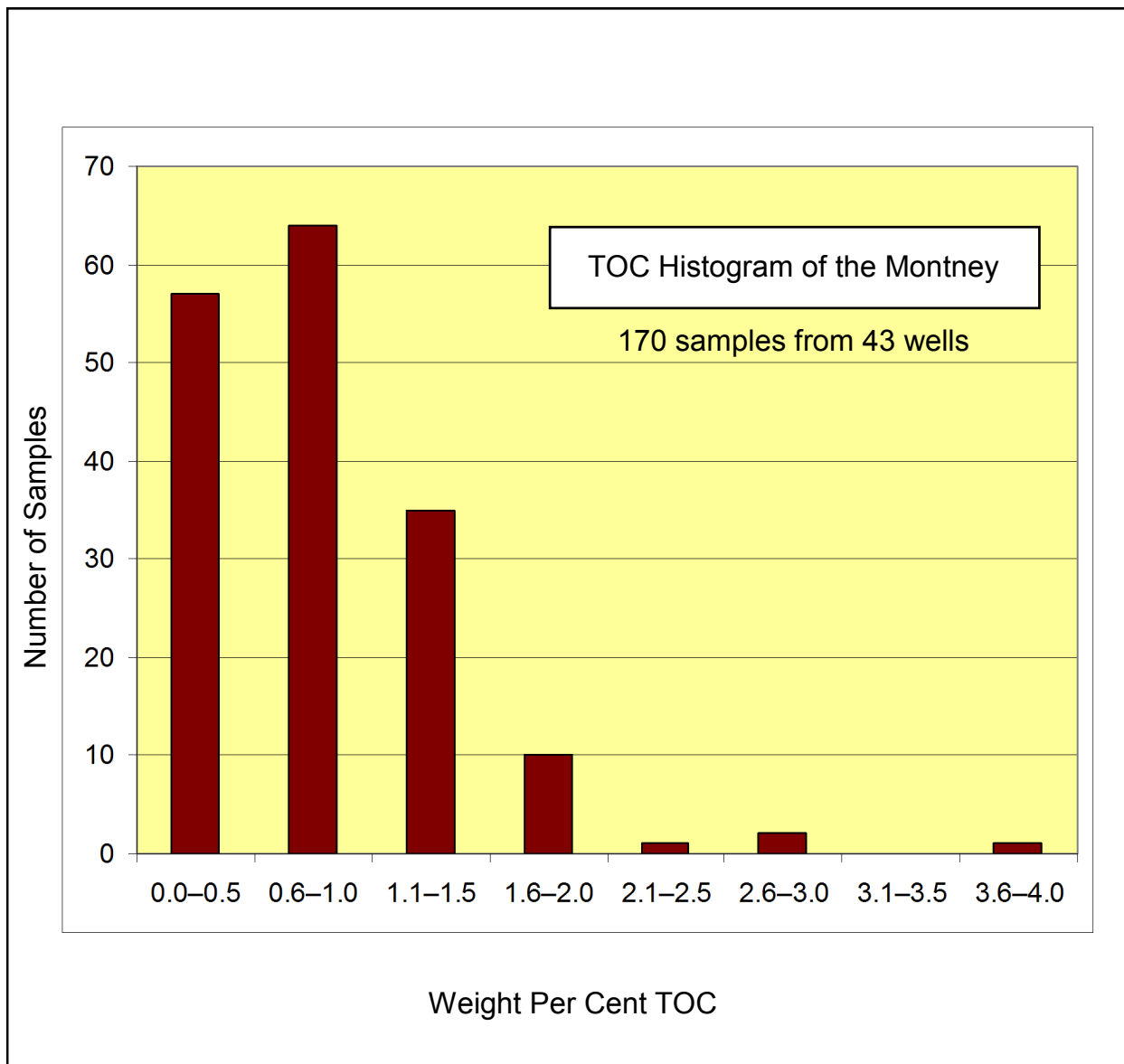


Figure 2.3.8. Histogram of total organic carbon (TOC) of 170 samples from the Montney Formation.

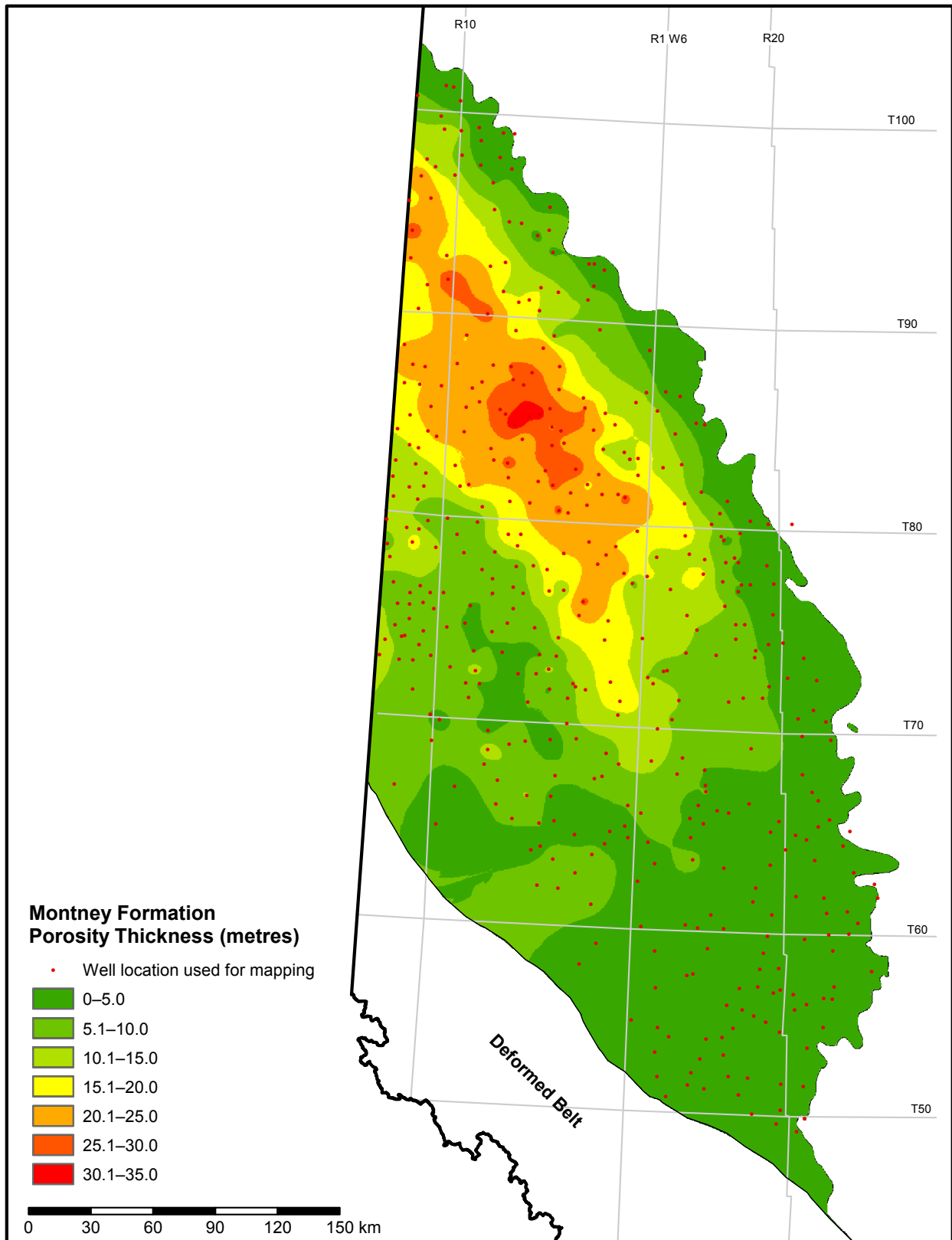


Figure 2.3.9. Porosity-thickness (Phi-h) map of the Montney Formation.

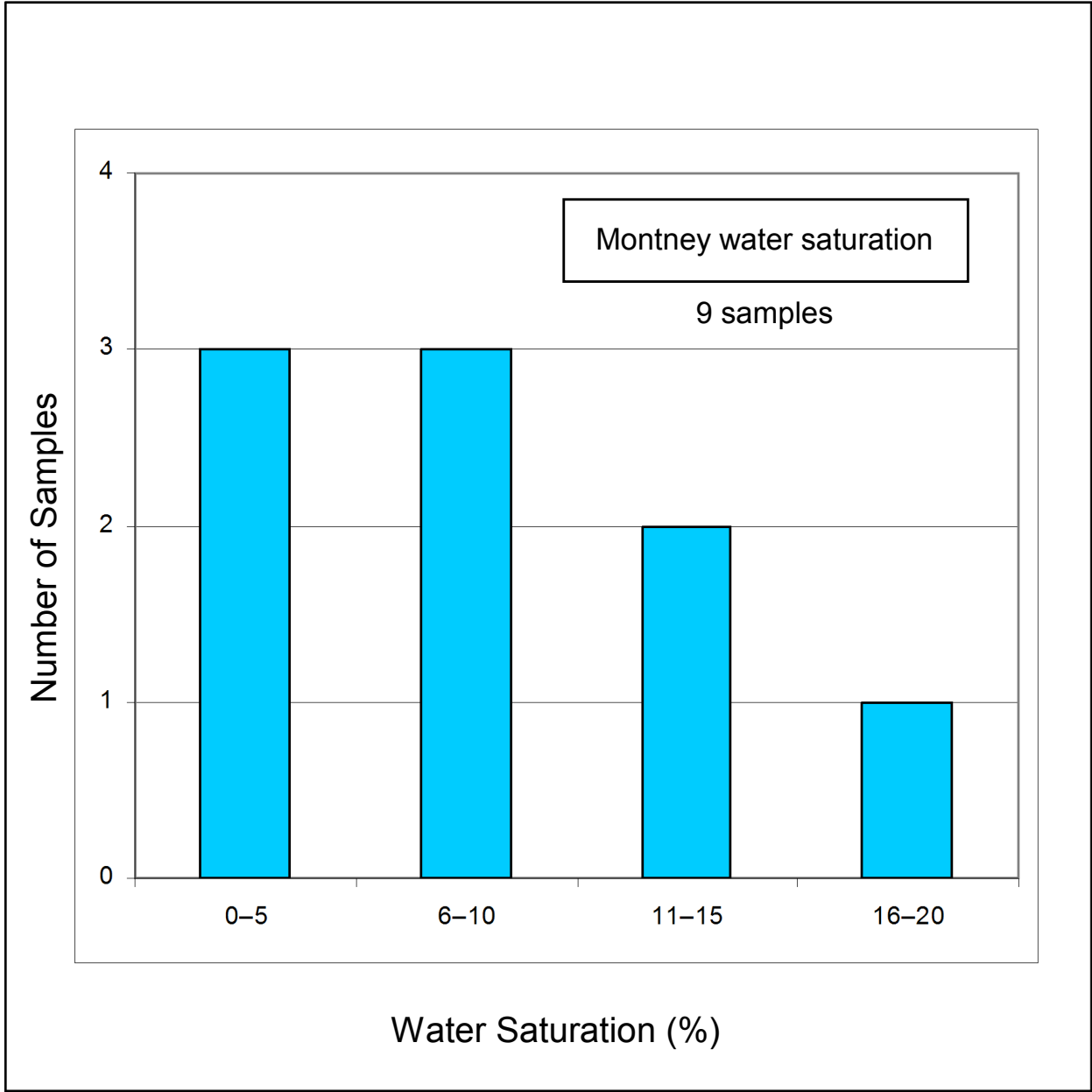


Figure 2.3.10. Histogram of water-saturation analysis results from 9 samples from the Montney Formation.

## 2.4 Preliminary Summary of the Basal Banff and Exshaw Formations

The Banff and Exshaw formations are regionally extensive in the Alberta Basin (Figure 2.4.1). The Exshaw shale is recognized as a major source rock for heavy-oil and bitumen deposits in northern Alberta, in addition to sourcing conventional reservoirs (Smith and Bustin, 2000). The combined interval of the Exshaw Formation and the basal shale of the Banff Formation (basal Banff/Exshaw) is stratigraphically equivalent to the Bakken Formation in the Williston Basin. For this project, the terms lower shale, middle unit, and upper shale correspond to the Exshaw shale (lower Bakken), the upper Exshaw (middle Bakken), and the lower Banff basal black shale (upper Bakken), respectively (Figure 2.4.2). The basal Banff/Exshaw resource assessment was constrained only to southern Alberta (study area) due to data availability and current industry focus (Figure 2.4.1).

The basal Banff/Exshaw has a large variation in primary lithologies. The upper and lower shales are dominated by dark grey to black, fissile, hard-to-soft, calcareous to noncalcareous, organic-rich shale. The middle unit consists of various lithologies, including calcareous sandstone, argillaceous sandstone, dolomitic siltstone, calcareous siltstone, silty lime-mudstone, limestone, and dolostone. The variation in primary lithologies may indicate that the Exshaw and basal Banff merit a more detailed stratigraphic study to determine erosional boundaries and confirm stratigraphic equivalence to the Bakken. In the study area, depth to the top the basal Banff/Exshaw ranges from 500 m near the subcrop erosional edge to about 4000 m along the deformed belt (Figure 2.4.3).

The upper and lower shales are both thin. The thickness of the lower shale ranges from 4 to 13 m. The upper shale is more difficult to correlate and has a smaller aerial extent than the lower shale. The upper shale ranges from <1 to 2.3 m thick. The gross isopach of the middle unit in southeastern Alberta ranges from 0 to 40 m along a roughly northeast-to-southwest trend (Figure 2.4.4). Four wells were selected for a cross-section that displays the stratigraphic relationship of the three units and the correlation to the Bakken (Figure 2.4.2).

A porosity-thickness ( $\Phi$ -h) map of the basal Banff/Exshaw (Figure 2.4.5) was constructed using density-porosity logs calibrated to a grain density of 2.74 g/cm<sup>3</sup> with no porosity cutoff and a >75 API gamma-ray-log cutoff. The gamma-ray cutoff excluded any lithology, such as sandstone or limestone, that was relatively free of argillaceous material. The map shows high porosity-thickness values in the northeast near the erosional edge. Current hydrocarbon exploration is concentrated in the southwest corner of the study area. Section 3.4 provides information on the methodology for the determination of grain density used in our analysis and possible sources of error.

The grain density that we used to determine porosity accounted for the presence of TOC by converting TOC to kerogen and counting it as a mineral component. The methodology that we used works well when the TOC content range spans only a few weight per cent. The TOC content of the upper and lower shale, however, is quite variable (Figure 2.4.6), which may cause significant error in the calculation of the porous volume of shale in our methodology. For the present resource estimation, we chose not to include the porous volume of the shale. A well-by-well evaluation of the data is necessary to achieve a reliable estimate of shale porosity. However, because the upper and lower shales are quite thin, the resource estimate may not change dramatically by this exclusion. In summary, our resource estimate for the basal Banff/Exshaw is based on the adsorbed gas content of the upper and lower shales, as well as the porous volume of the middle unit, which is the primary production unit in the Bakken play in the Williston Basin.

The TOC content ranges from 0.1 to 16.9 wt. % based on 75 samples from 13 wells (Figure 2.4.6). The TOC content of the middle unit is generally <1.0 wt. % in the southern area. There is some indication that the northern area may contain a higher content of TOC. The thermal maturity of the basal Banff/Exshaw source rocks, based on vitrinite reflectance data, exhibits increased maturity to the southwest (Figure 2.4.7), corresponding to an increased depth below the surface.

Using Dean Stark analysis and helium pycnometry on select samples, the laboratory calculated water saturation. The distribution of values for the basal Banff and Exshaw formations in the southern area shows dominance in the range of about 10% to 50% (Figure 2.4.8), which we used as P90 and P10 constraints in our resource evaluation. Section 3.3 provides information on the methodology used to determine water saturation and possible sources of error.

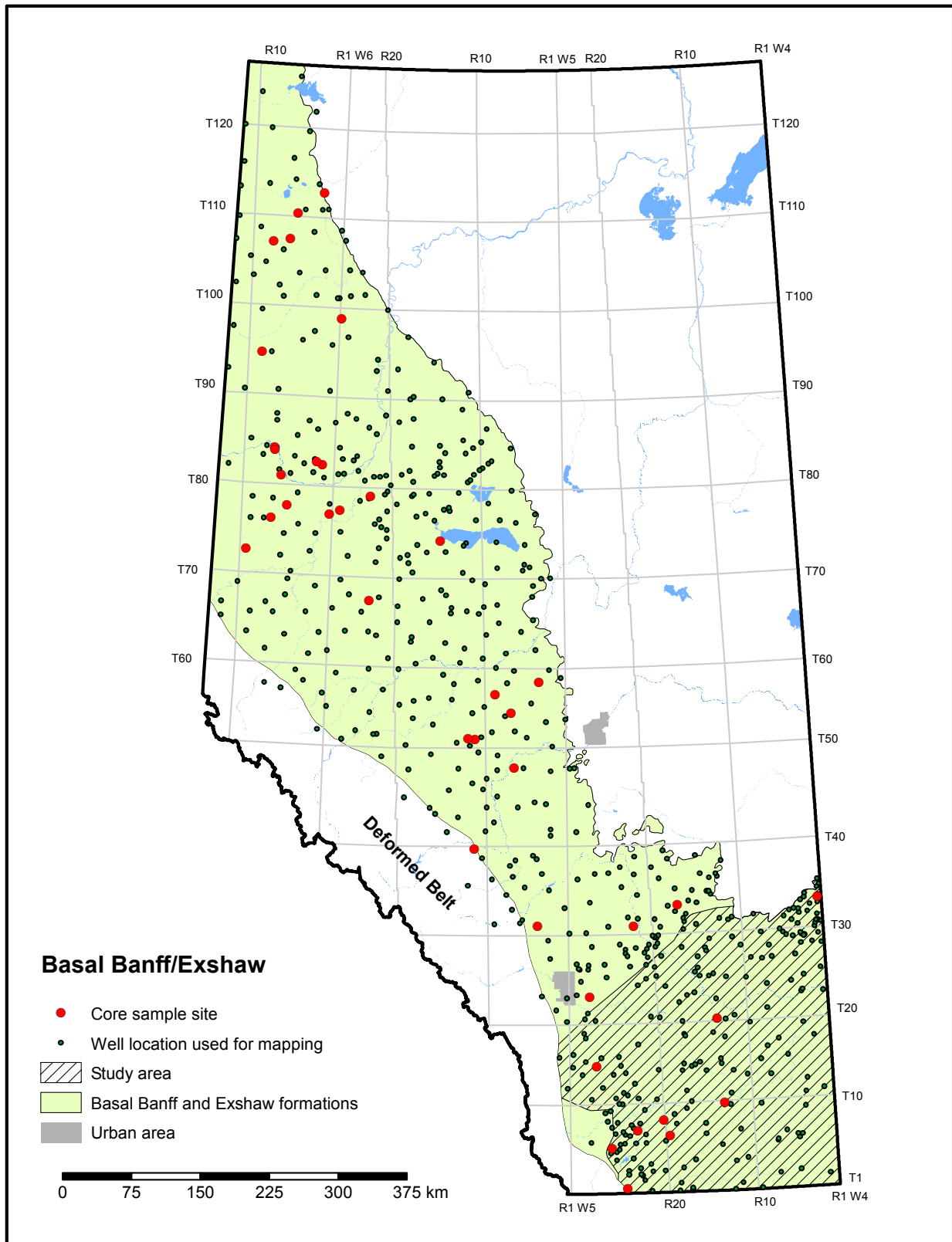


Figure 2.4.1. Index map of the combined basal Banff and Exshaw formations.

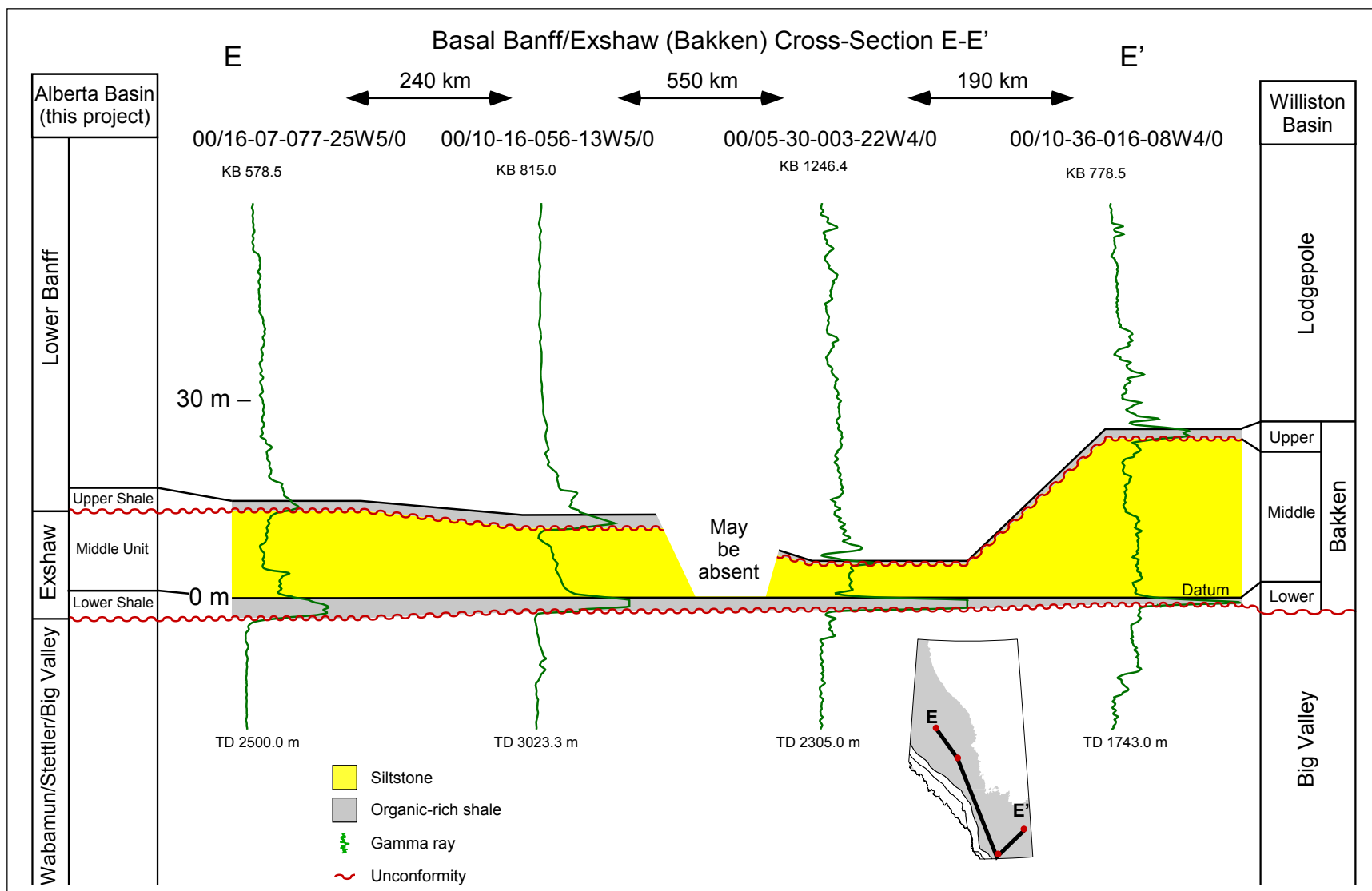


Figure 2.4.2. Stratigraphic cross-section E-E' of the basal Banff and Exshaw formations (see inset map for location).

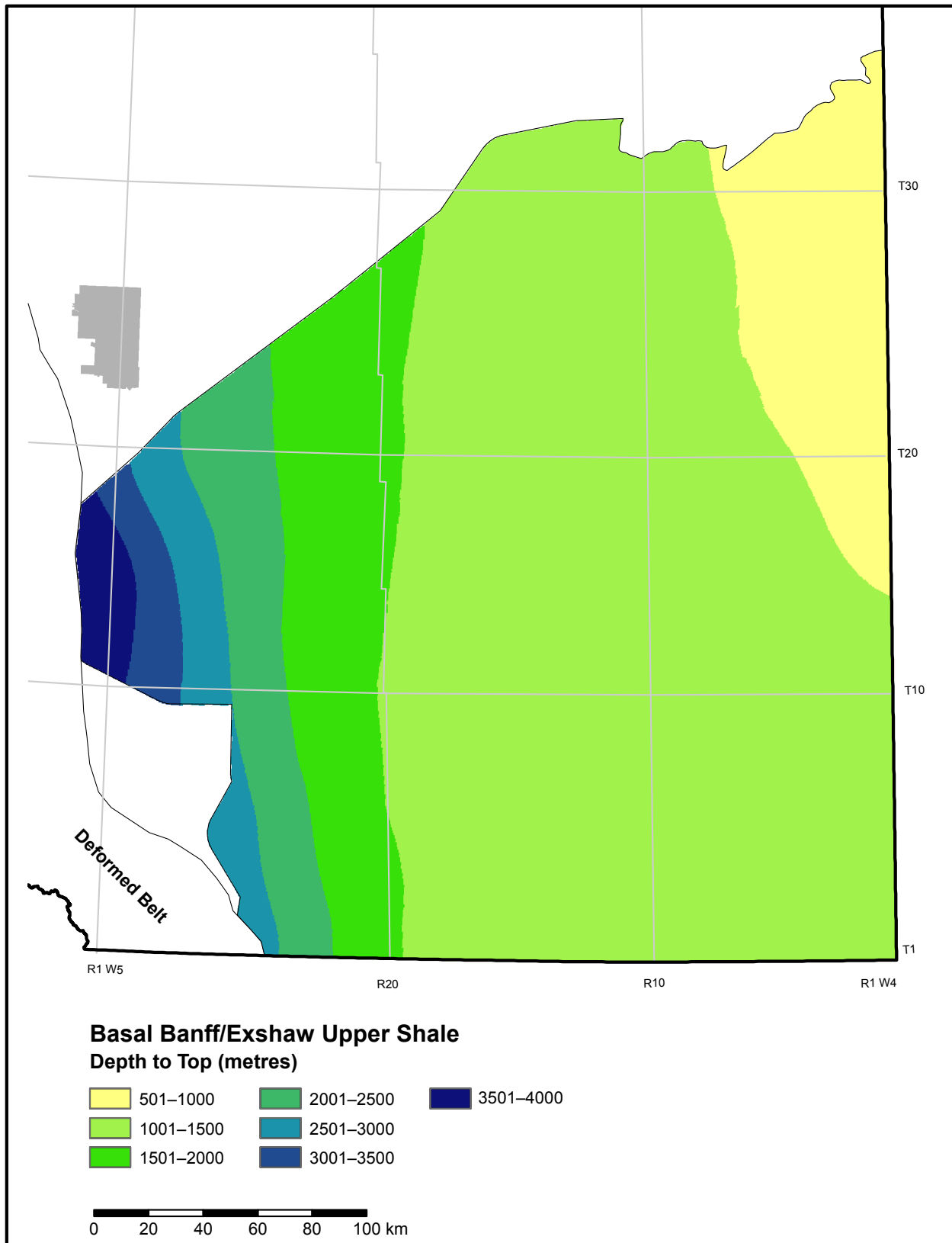


Figure 2.4.3. Depth to top of the basal Banff/Exshaw upper shale in the study area.

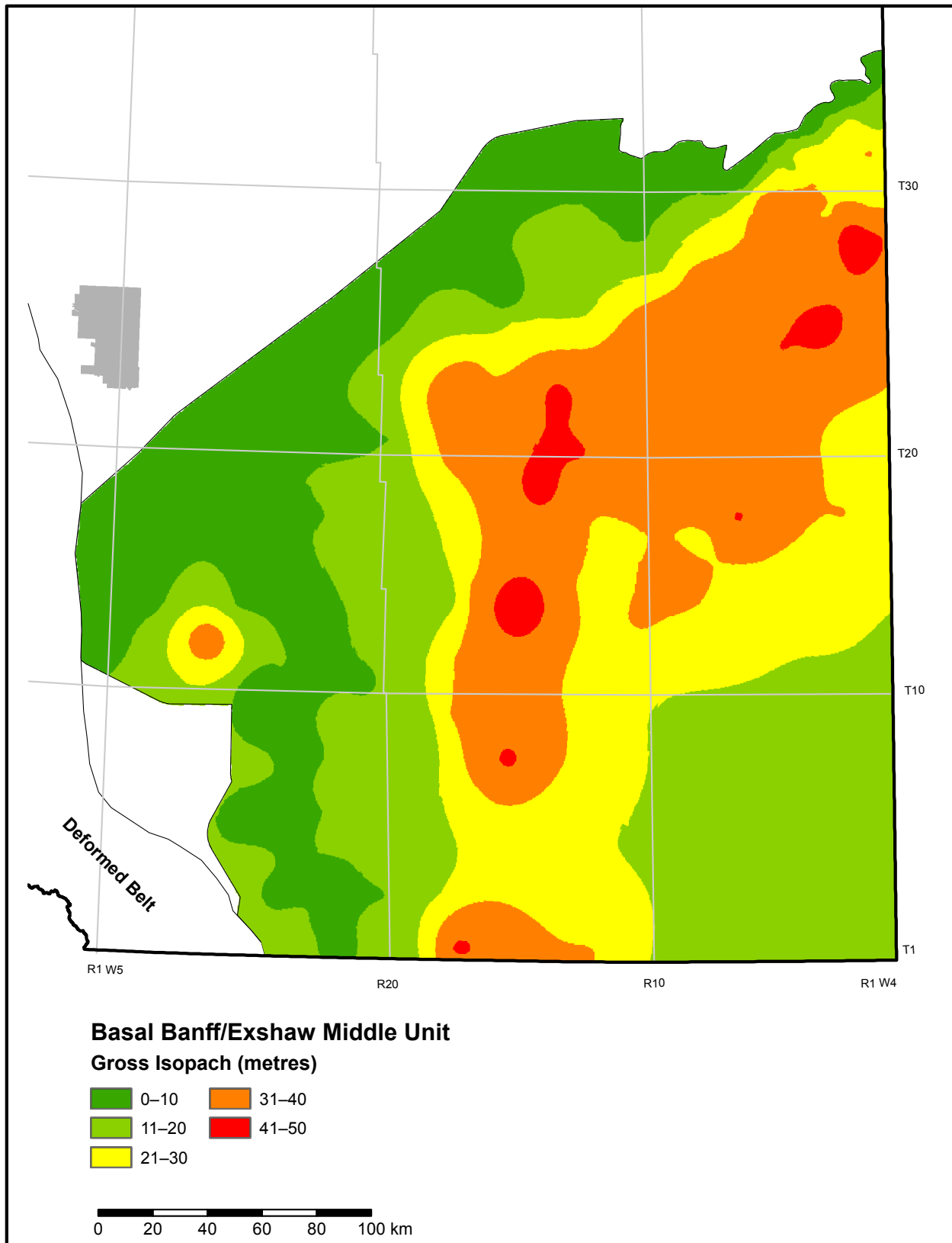


Figure 2.4.4. Gross isopach of the basal Banff/Exshaw middle unit in the study area.

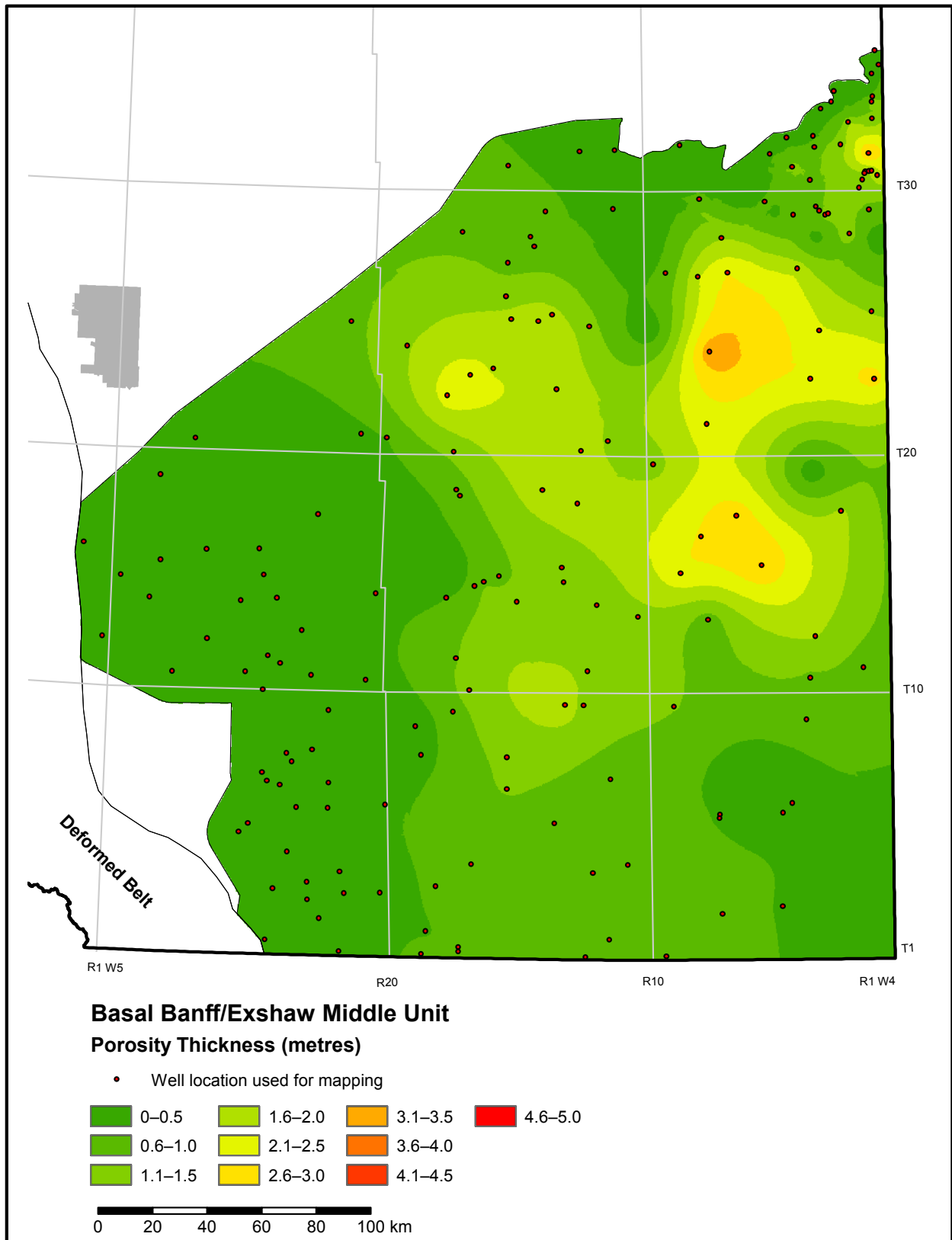


Figure 2.4.5. Porosity-thickness (Phi-h) map of the basal Banff/Exshaw middle unit in the study area.

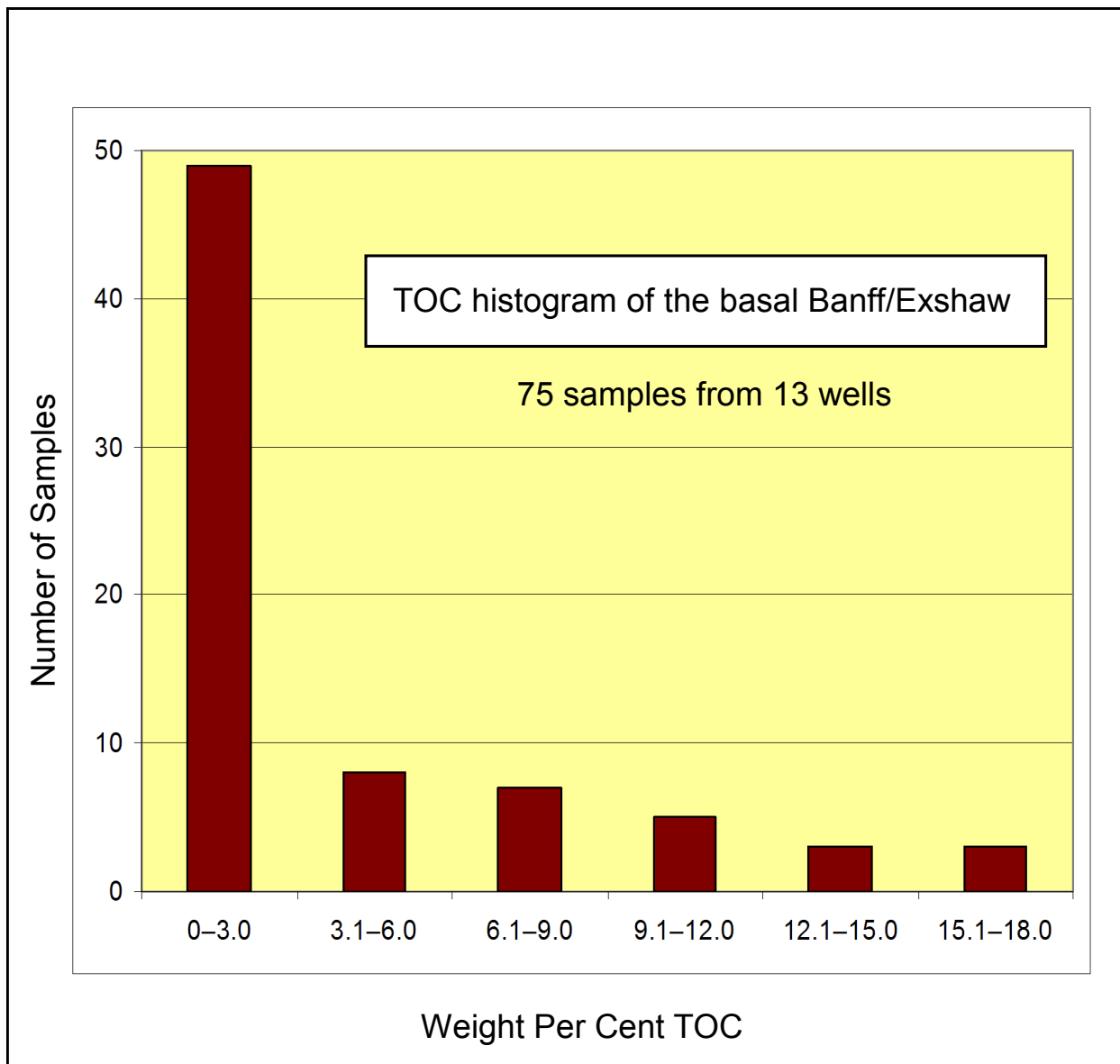


Figure 2.4.6. Histogram of total organic carbon (TOC) of 75 samples from the basal Banff and Exshaw formations.

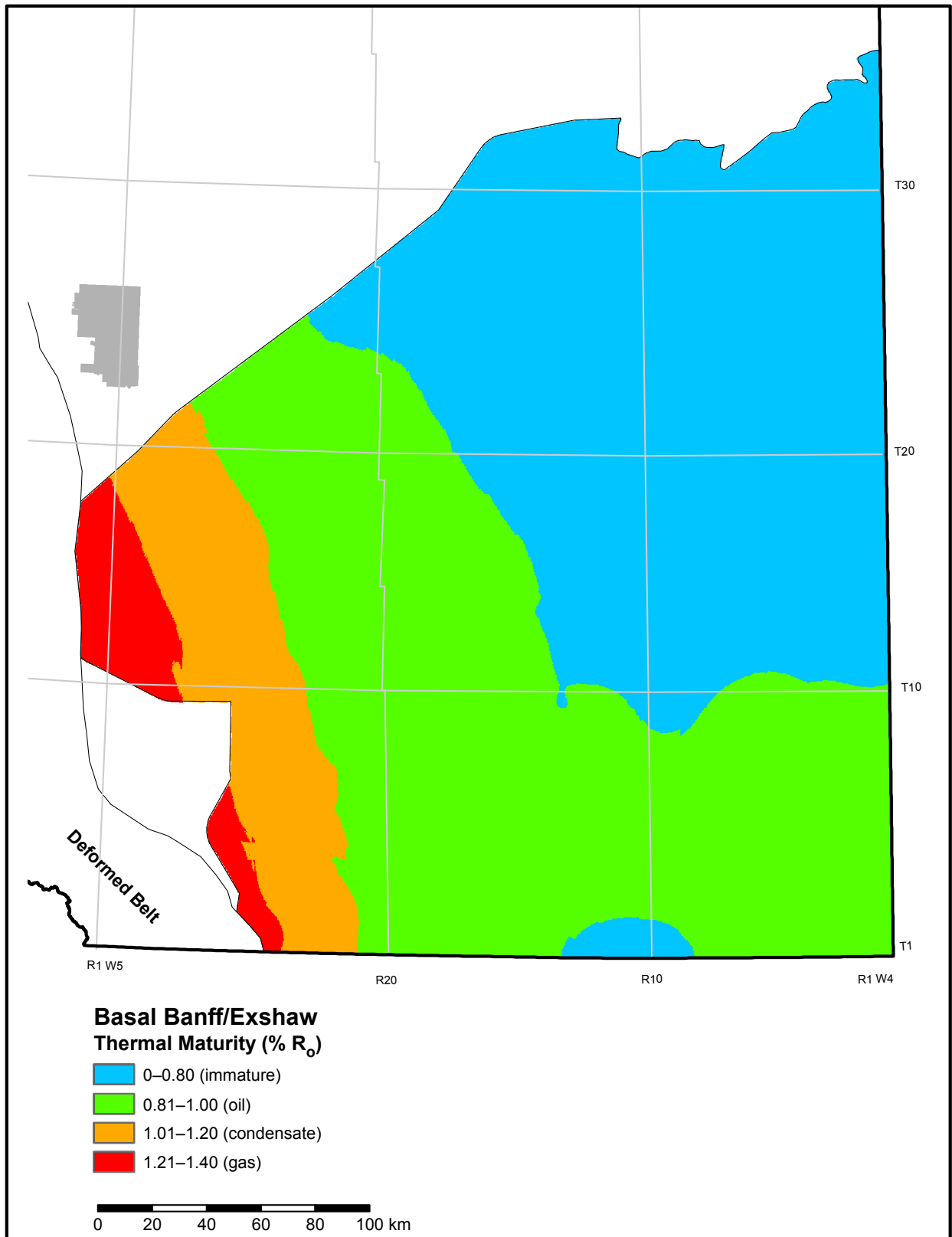


Figure 2.4.7. Thermal maturity map of the combined basal Banff and Exshaw formations in the study area.

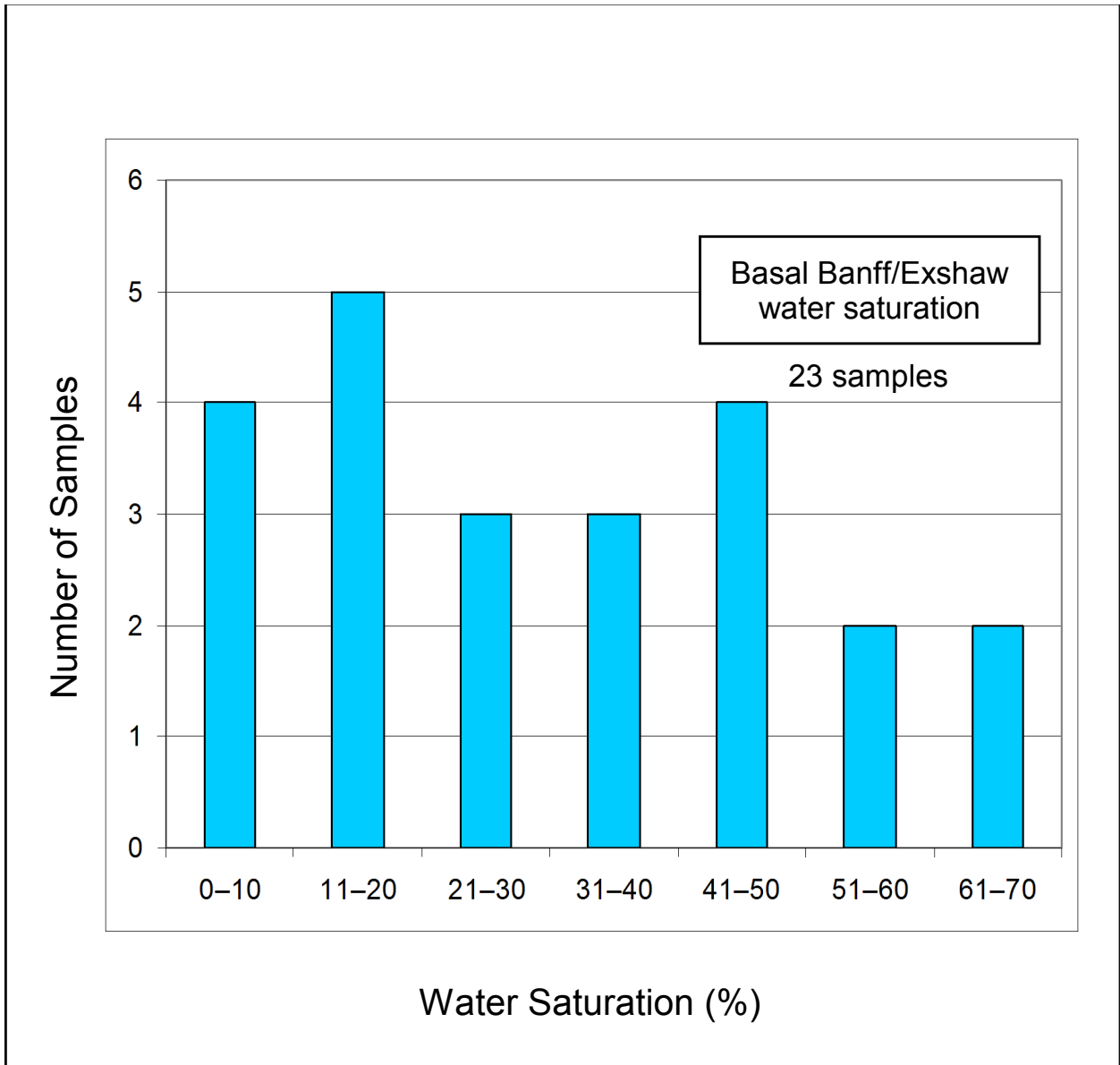


Figure 2.4.8. Histogram of water-saturation analysis results from 23 samples from the combined basal Banff and Exshaw formations.

## 2.5 Preliminary Summary of the Nordegg Member

The Lower Jurassic Nordegg Member (Nordegg) of the Fernie Formation is located in west-central Alberta (Figure 2.5.1). It consists of cherty and phosphatic carbonates and shales, is a prolific source rock, and hosts conventional hydrocarbon reservoirs. For this report, 'north Nordegg' refers to the organic-rich Nordegg in west-central Alberta (informally called the Gordondale member; Asgar-Deen et al., 2004) and does not include the carbonate lithology farther to the south (Figure 2.5.1).

North Nordegg lithology is dominated by mudstones, which can be phosphatic, argillaceous, calcareous, and cherty. The north Nordegg also includes siltstone and some sandstone.

The depth from the surface to the top of the north Nordegg ranges from 430 m to more than 4000 m, increasing in depth from the northeast to the southwest (Figure 2.5.2). The thickness of the north Nordegg ranges from 0 m along the eastern erosional edge to about 45 m (Figure 2.5.3).

More than 50 stratigraphic and structural cross-sections were constructed for the Nordegg. Figure 2.5.4 is a representative stratigraphic cross-section illustrating the thickness of the north Nordegg and its relationship to underlying and overlying units. A net-shale map (Figure 2.5.5; gamma ray >75 API) was created to identify the area where the Nordegg transitions from a thick limestone to an organic-rich sediment. For the present evaluation, we only considered the north Nordegg with no gamma-ray cutoff. The reason for no gamma-ray cutoff was to include the thin limestone/siltstone/sandstone component that developed within the north Nordegg, west of the erosional edge. This component is considered an unconventional reservoir and so is included in the resource assessment.

In the south, the Nordegg transitions to a thick, conventional carbonate reservoir, as shown on the net-carbonate map (Figure 2.5.6). This area was not evaluated.

Using vitrinite reflectance data, a map illustrating the thermal maturity of the north Nordegg (Figure 2.5.7) shows a basic trend of increasing maturity to the southwest. This trend corresponds with an increased depth below the surface. Dry-gas resources are expected in the southwest, with more liquids-rich gas and oil-prone strata towards the northeast.

The average TOC content of the north Nordegg is 11.4 wt. % with a range of 1.2 to 26.3 wt. %; some samples are oil saturated (Figure 2.5.8). These data are based on 82 samples from the north Nordegg. North Nordegg organic content generally increases from southwest to northeast.

A porosity-thickness ( $\Phi$ -h) map of the north Nordegg (Figure 2.5.9) was constructed using density-porosity logs calibrated to a grain density of 2.50 g/cm<sup>3</sup> with no porosity cutoff and no gamma-ray cutoff. The grain density used accounts for the presence of TOC by converting TOC to kerogen and counting it as a mineral component in the grain density. Section 3.4 provides the methodology for the determination of the grain density used in our analysis; the relationship between grain density, porosity, and TOC content; and possible sources of error.

Using Dean Stark analysis and helium pycnometry on select samples, the laboratory calculated water saturation. Due to the small water-saturation dataset we had (Figure 2.5.10), we reviewed publicly available information from which we selected a water-saturation range of 10% to 30% to represent P90 and P10 in our evaluation of the north Nordegg. Section 3.3 provides further information on the determination of water saturation and possible sources of error.

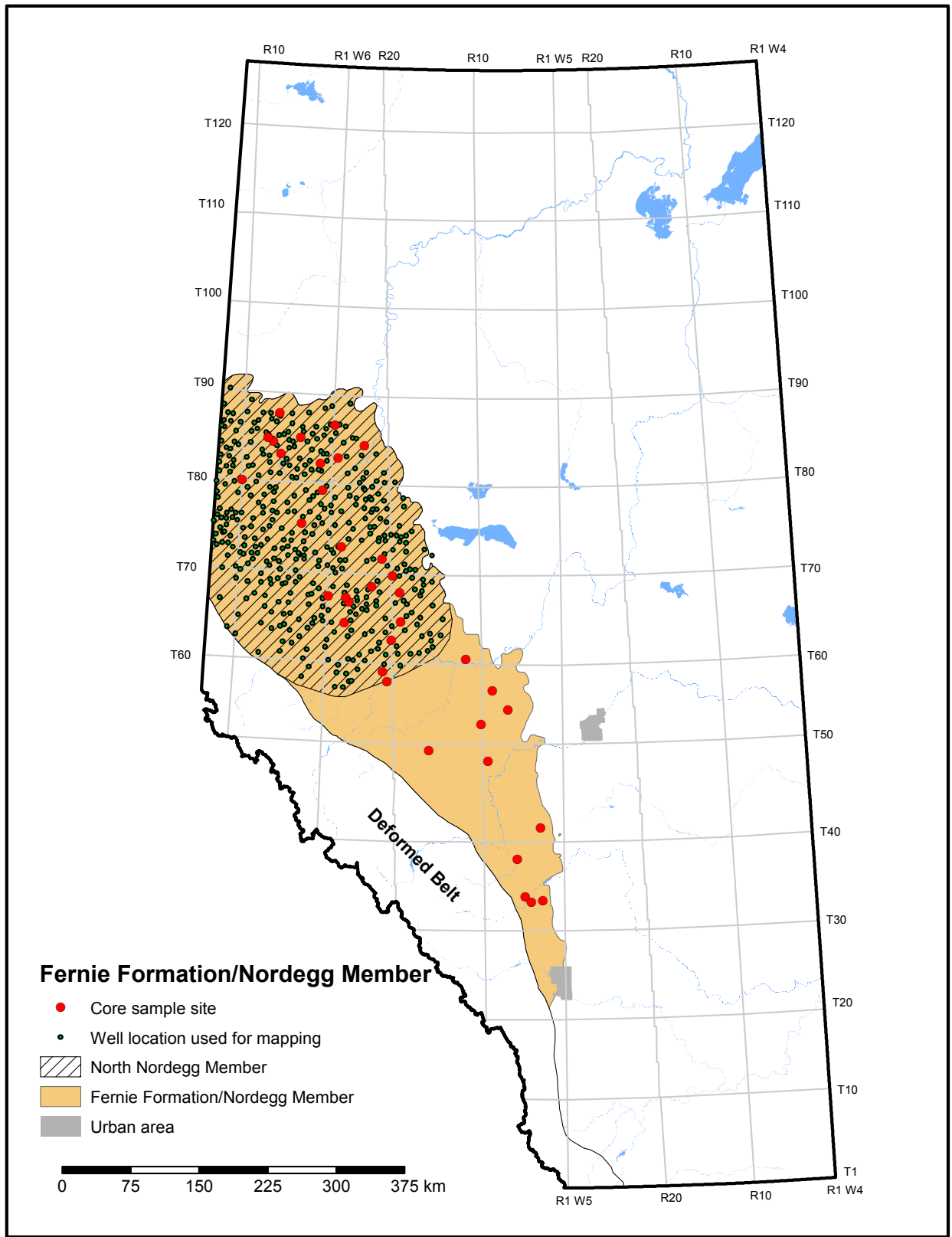


Figure 2.5.1. Index map of the Fernie Formation including the Nordegg Member.

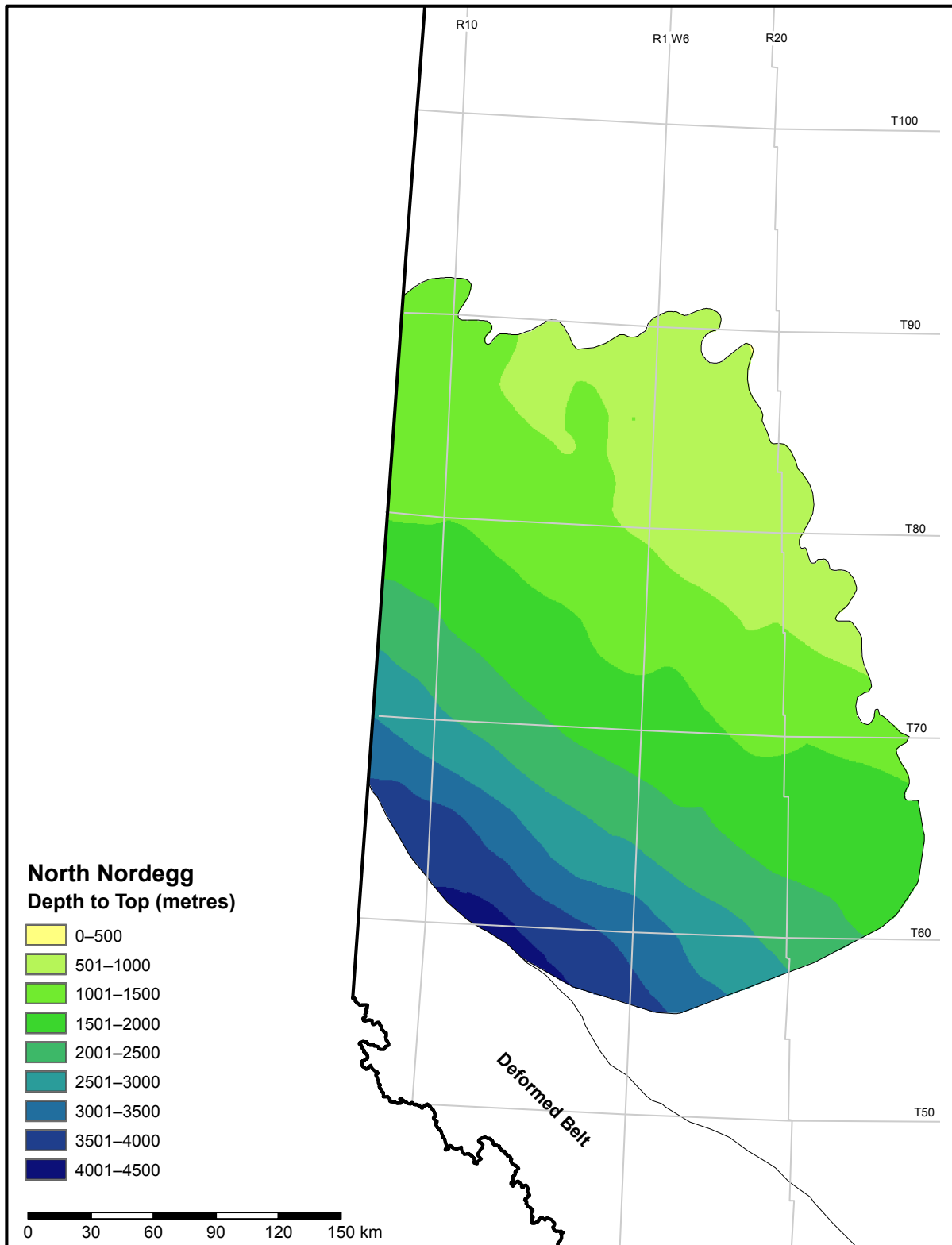


Figure 2.5.2. Depth to top of the north Nordegg.

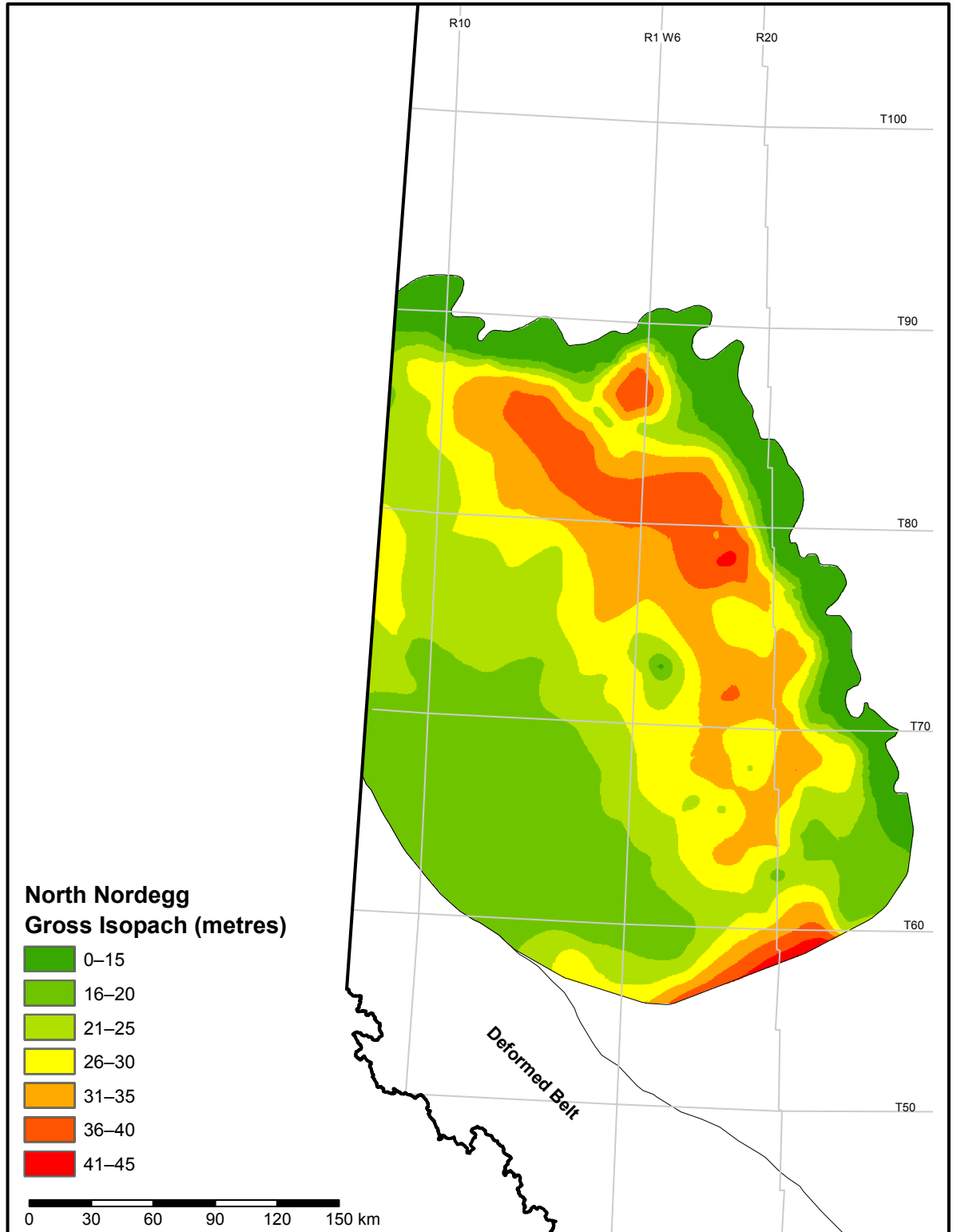


Figure 2.5.3. Gross isopach of the north Nordegg.



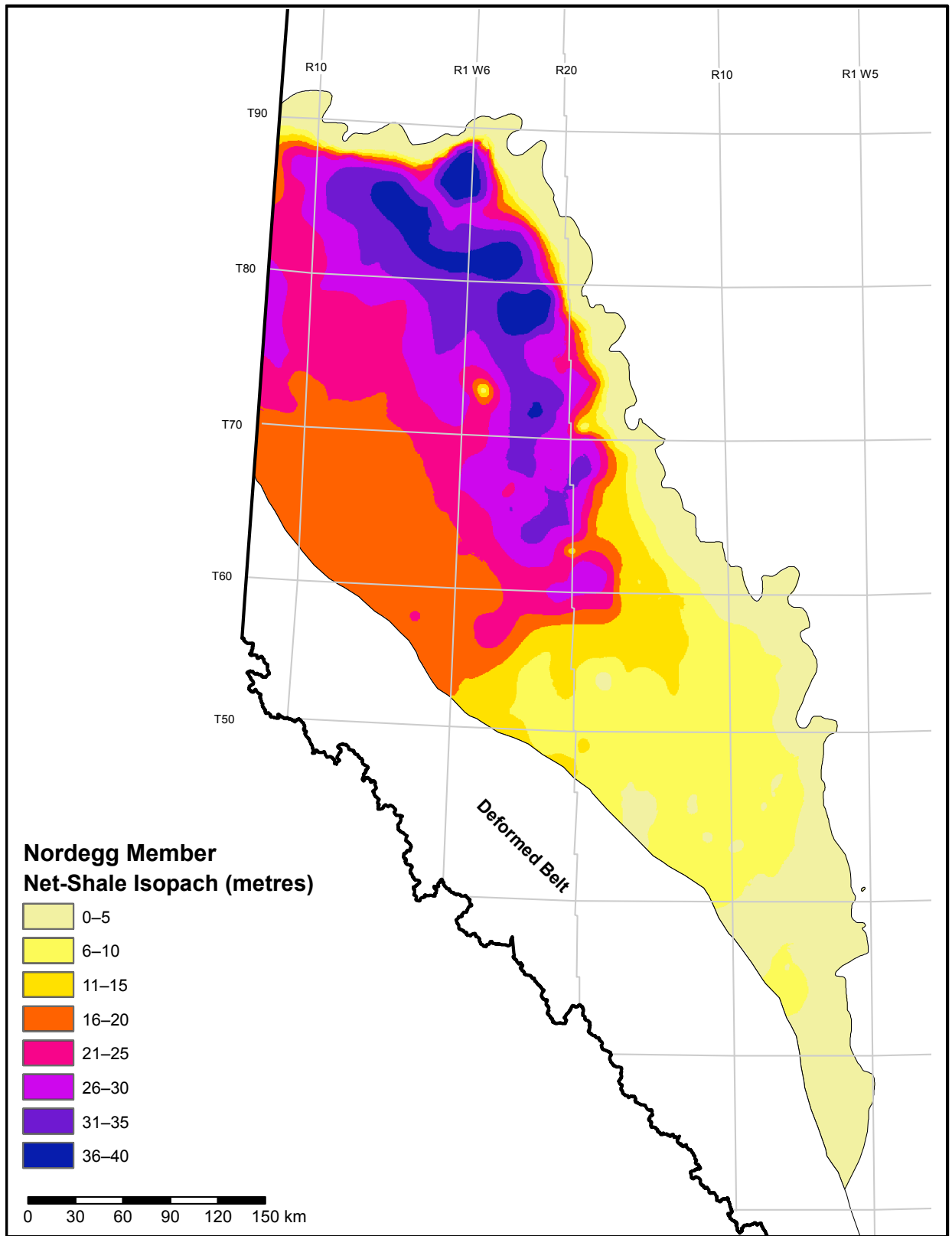


Figure 2.5.5. Net-shale isopach of the Nordegg Member.

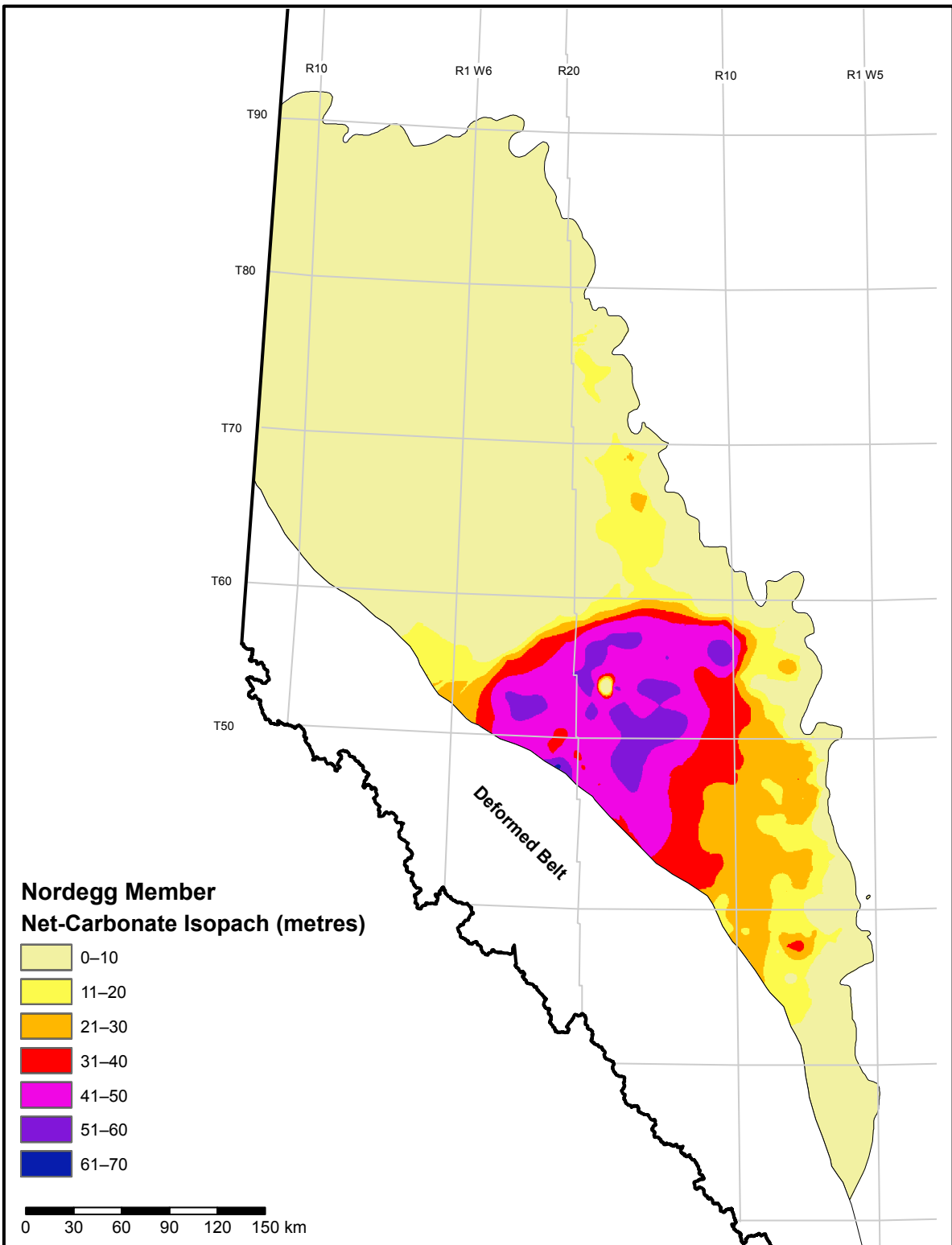


Figure 2.5.6. Net-carbonate isopach of the Nordegg Member.

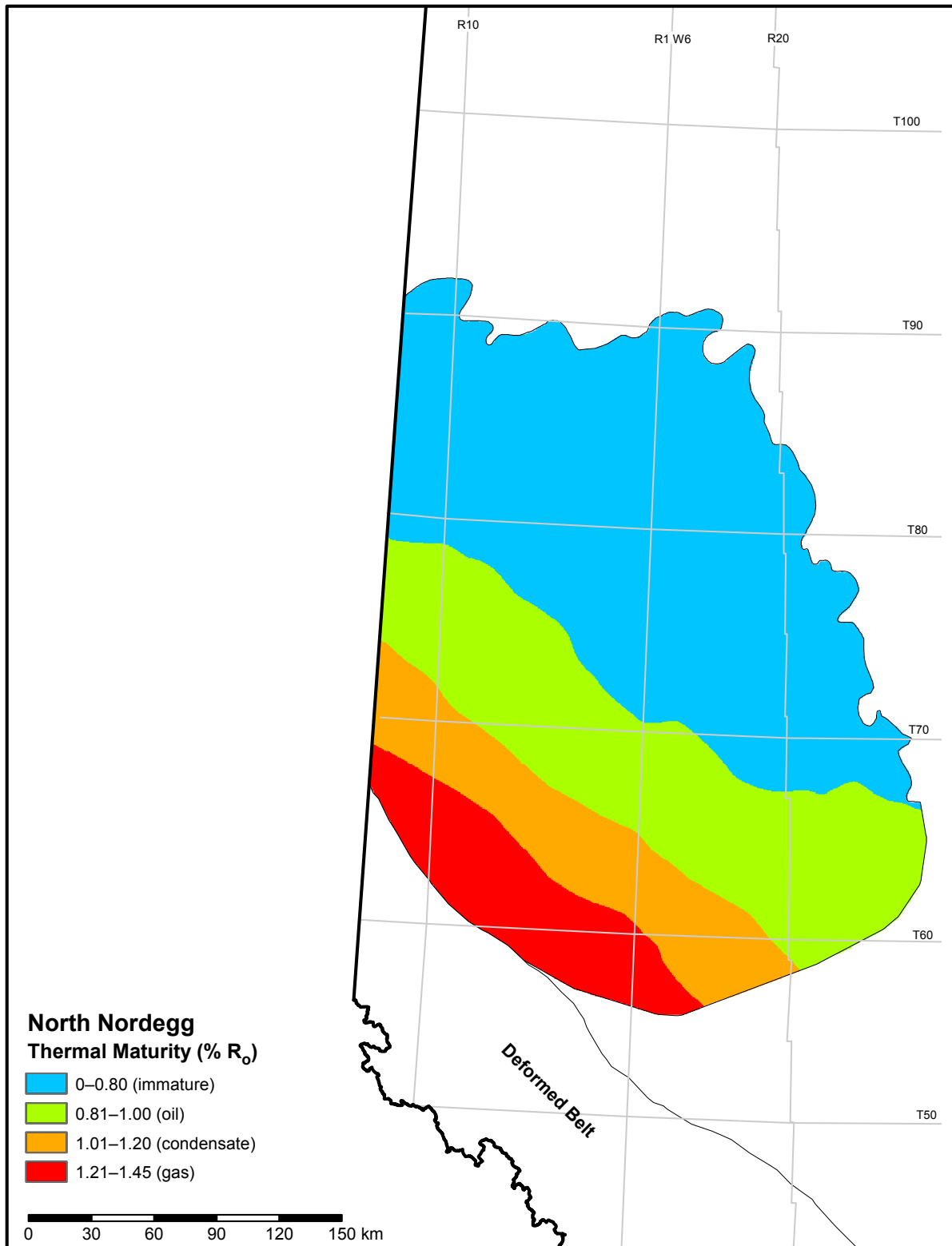


Figure 2.5.7. Thermal maturity map of the north Nordegg.

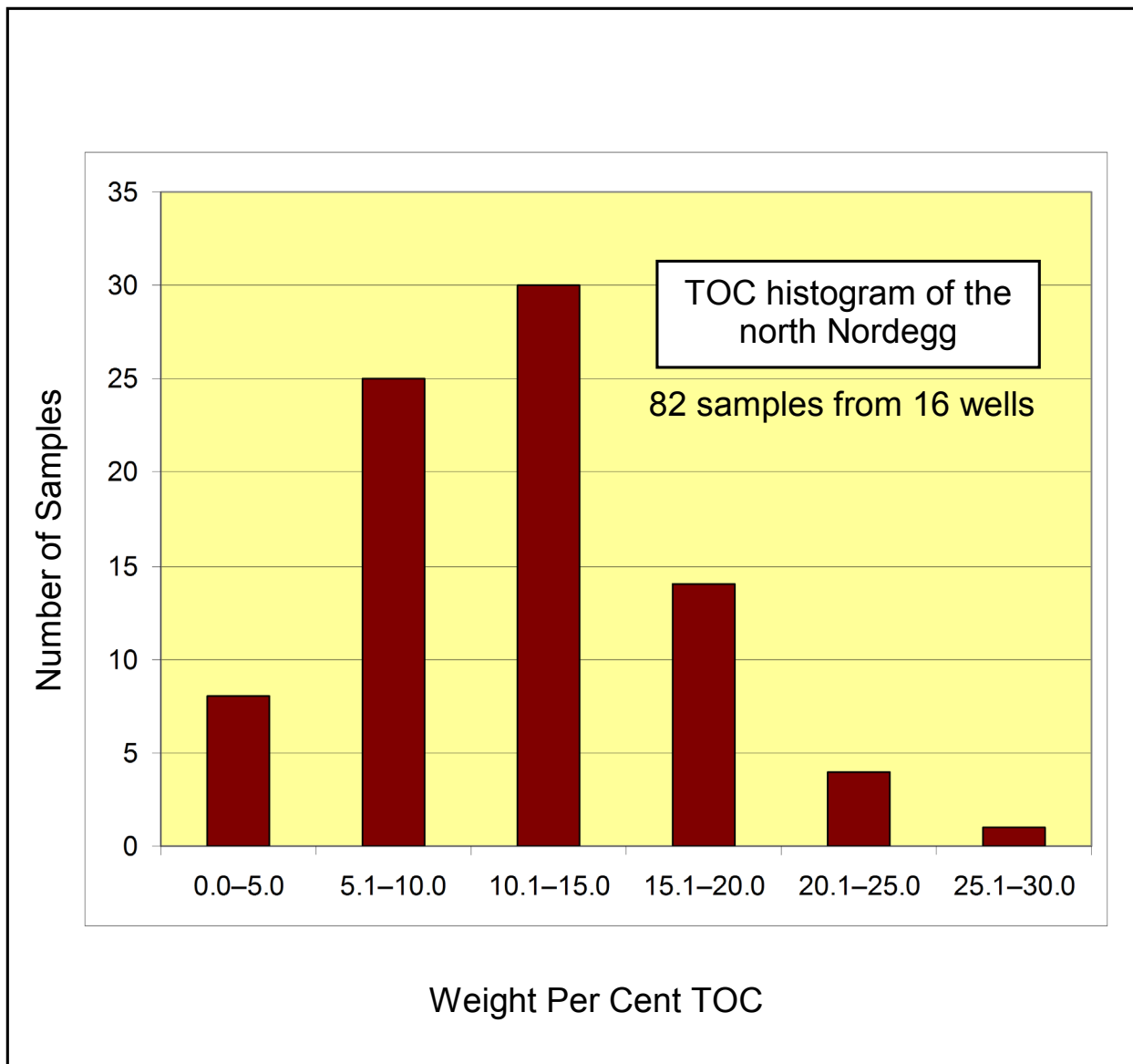


Figure 2.5.8. Histogram of total organic carbon (TOC) of 82 samples from the north Nordegg.

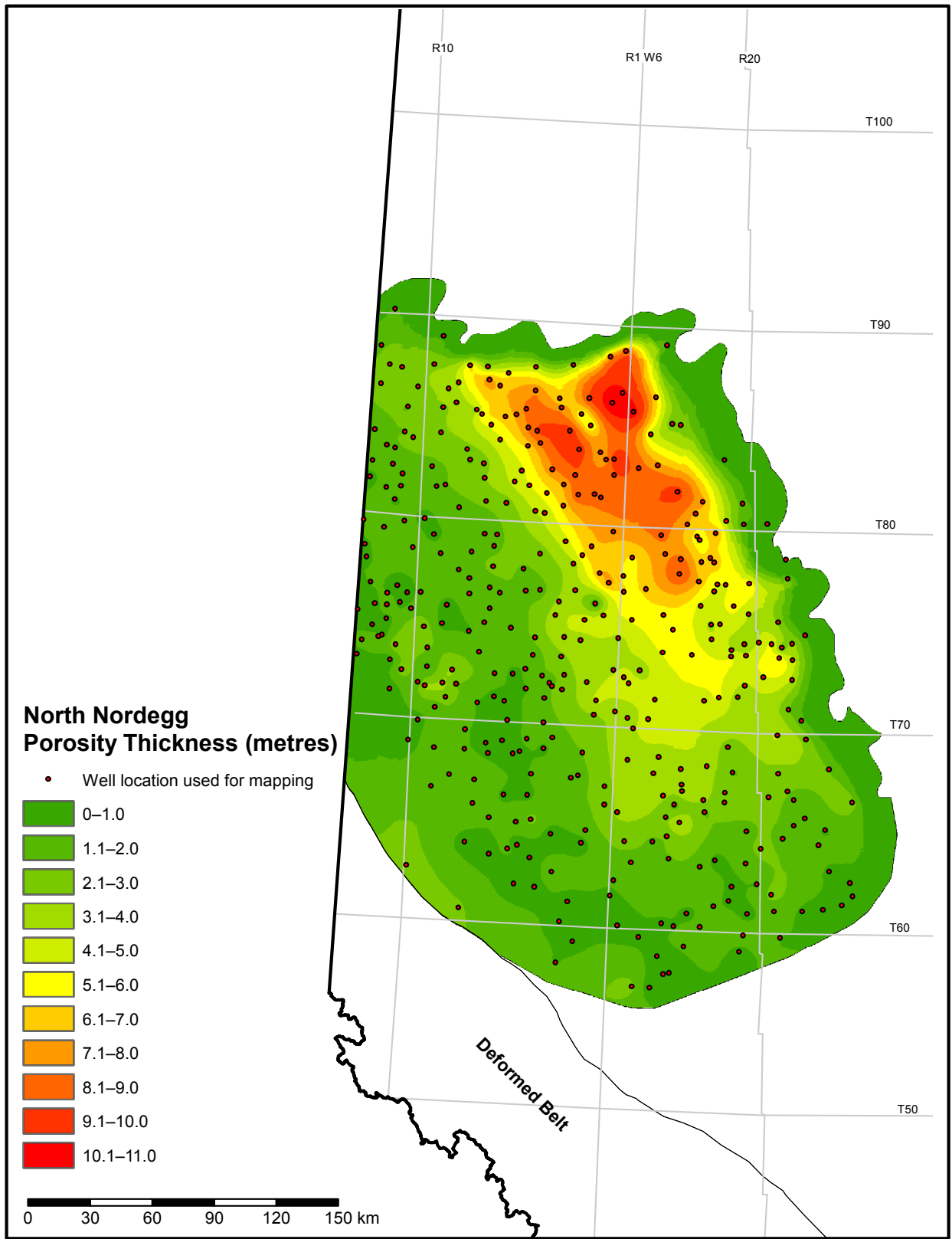


Figure 2.5.9. Porosity-thickness (Phi-h) map of the north Nordegg.

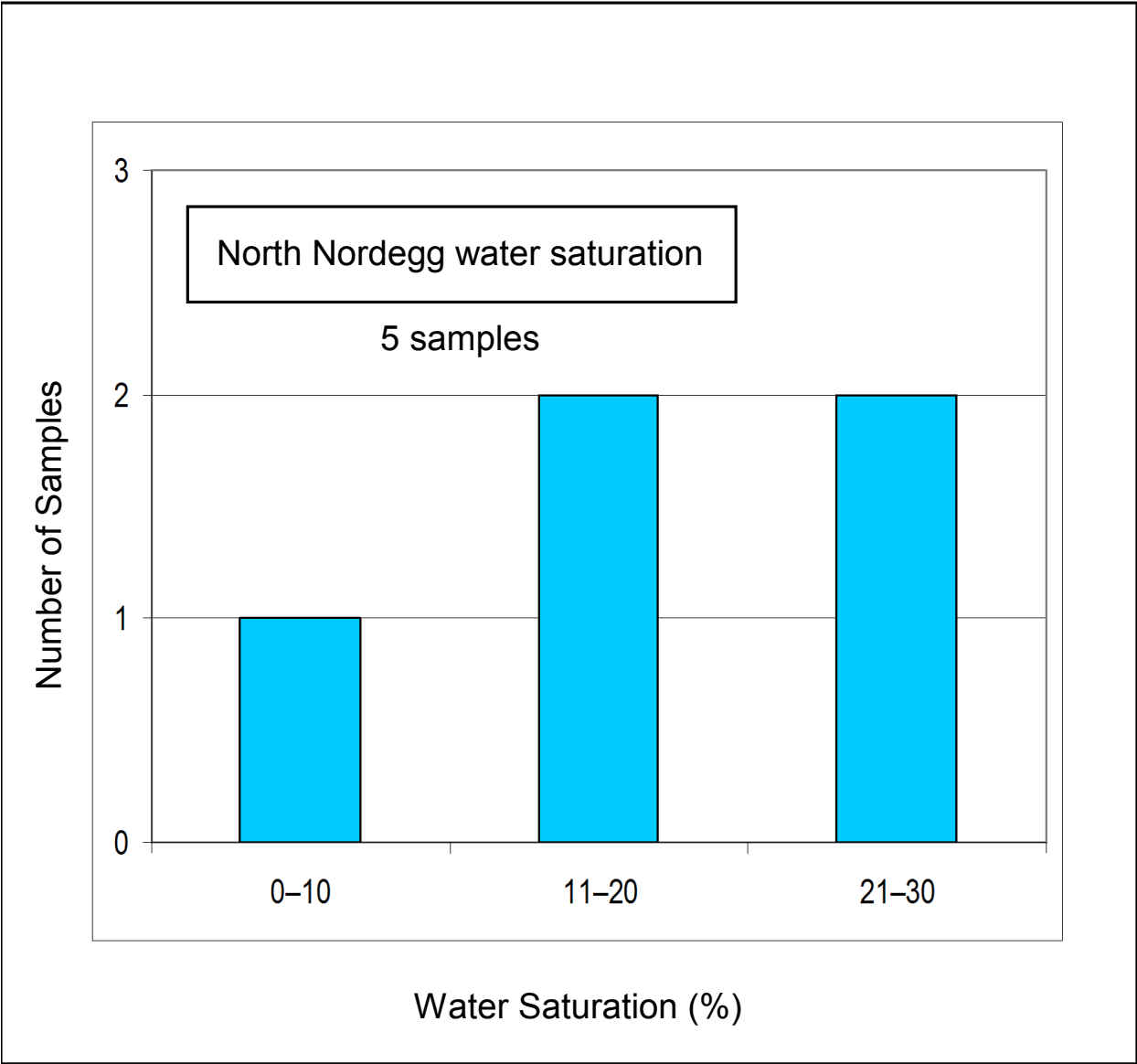


Figure 2.5.10. Histogram of water-saturation analysis results of 5 samples from the north Nordegg.

## 2.6 Preliminary Summary of the Wilrich Member

The Wilrich Member (Wilrich) of the Spirit River Formation is an organic-rich source rock located in west-central Alberta (Figure 2.6.1). It is stratigraphically equivalent to the Moosebar Formation in the northern mountains and foothills and the basal shales of the Clearwater Formation in the northeast plains. The Wilrich is known to have source rock potential and is thought to have contributed to hydrocarbon accumulations in the overlying Falher Member and underlying Bluesky Formation (Ibrahimias and Riediger, 2004).

To the north, the Wilrich lithology is largely dominated by dark grey, shallow marine shales with an increasing occurrence of siltstone and sandstone beds to the south. Depth to the top of the Wilrich ranges from 250 m near the northeastern edge of the study area to about 3700 m near the deformed belt (Figure 2.6.2).

A gross isopach of the Wilrich shows a maximum thickness of about 150 m (Figure 2.6.3). A stratigraphic cross-section illustrates the transition from the thicker part of the Wilrich interval in the west, which includes siltstones and sandstones, to the thinner, more shale-dominated Wilrich interval to the north (Figure 2.6.4). A net-shale map was created using a gamma-ray–log cutoff of >75 API to exclude any clean siltstone or clean sandstone from the resource estimation. The net-shale map (Figure 2.6.5) corresponds well to the cross-section and the gross isopach map, showing thicker shale deposits in the western part of the study area. The present evaluation uses the net-shale map for the thickness parameter in our resource analysis.

The TOC content of the Wilrich varies from 0.1 to 7.7 wt. % (Figure 2.6.6) based on 215 samples from 17 wells. TOC values are generally higher in the north.

A porosity-thickness (Phi-h) map of the Wilrich (Figure 2.6.7) was constructed using density-porosity logs calibrated to a grain density of 2.70 g/cm<sup>3</sup> with no porosity cutoff and a >75 API gamma-ray–log cutoff. The grain density we used accounts for the presence of TOC by converting TOC to kerogen and counting it as a mineral component in the calculation of grain density. Section 3.4 provides the methodology for determination of the grain density used in our analysis and possible sources of error.

A Wilrich thermal maturity map was created to determine zones of oil-, gas-, and liquid-generation potential (Figure 2.6.8). Most of our core samples are from the base of the Wilrich, which may cause sampling bias that will be investigated further as the assessment moves from preliminary to final. Much of the shale in the northern two-thirds of the extent of the Wilrich is presently interpreted as relatively immature; however, more samples need to be analyzed to refine this interpretation. For this reason, we have chosen to estimate Alberta's Wilrich resource endowment only in the southern area of the Wilrich, for which we have better data control.

Using Dean Stark analysis and helium pycnometry on select samples, the laboratory calculated water saturation. The distribution of values for the Wilrich shows dominance in the range of about 10% to 50% (Figure 2.6.9), which is used as P90 and P10 constraints in our resource evaluation. Section 3.3 provides further information on the methodology to determine water saturation and possible sources of error.

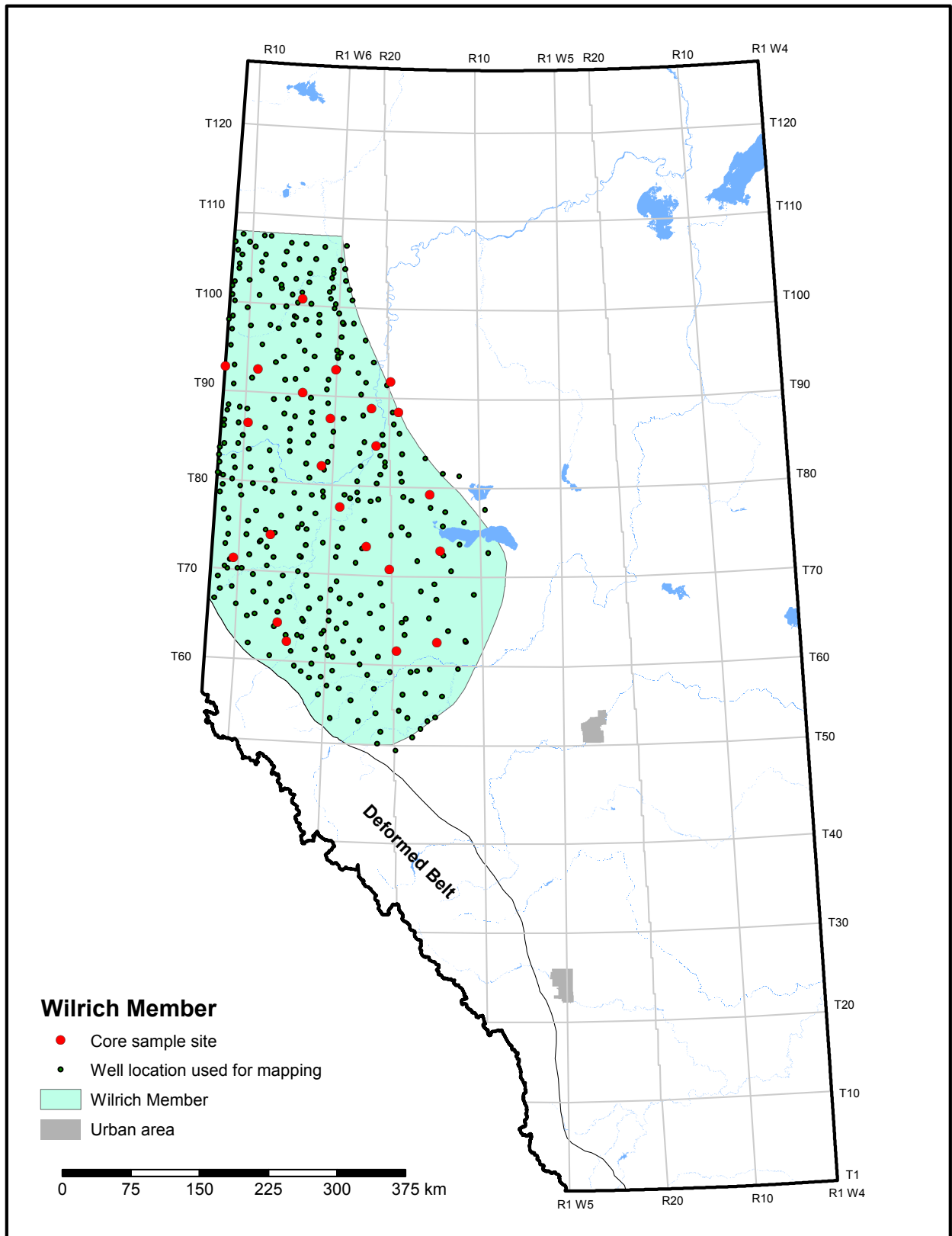


Figure 2.6.1. Index map of the Wilrich Member.

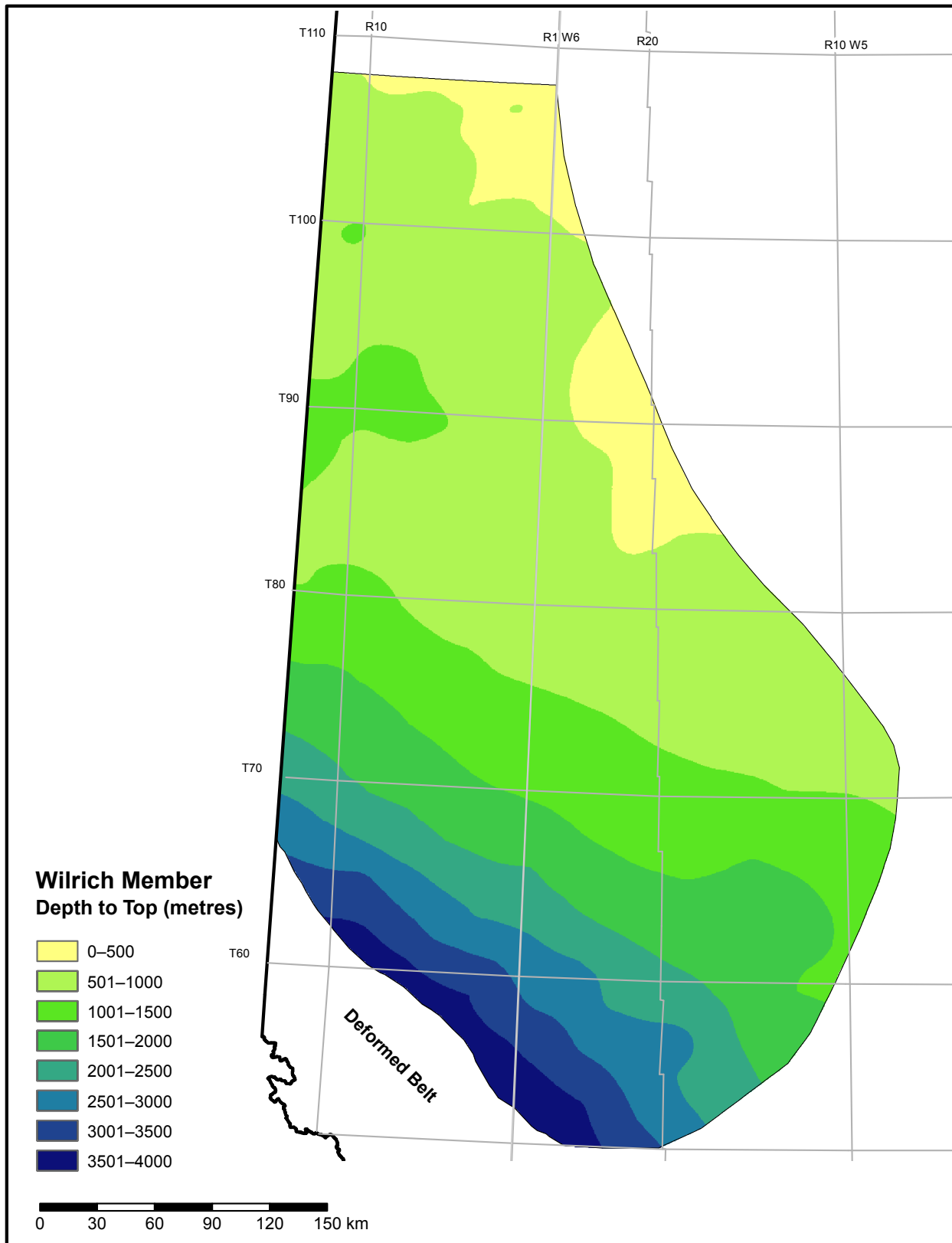


Figure 2.6.2. Depth to top of the Wilrich Member.

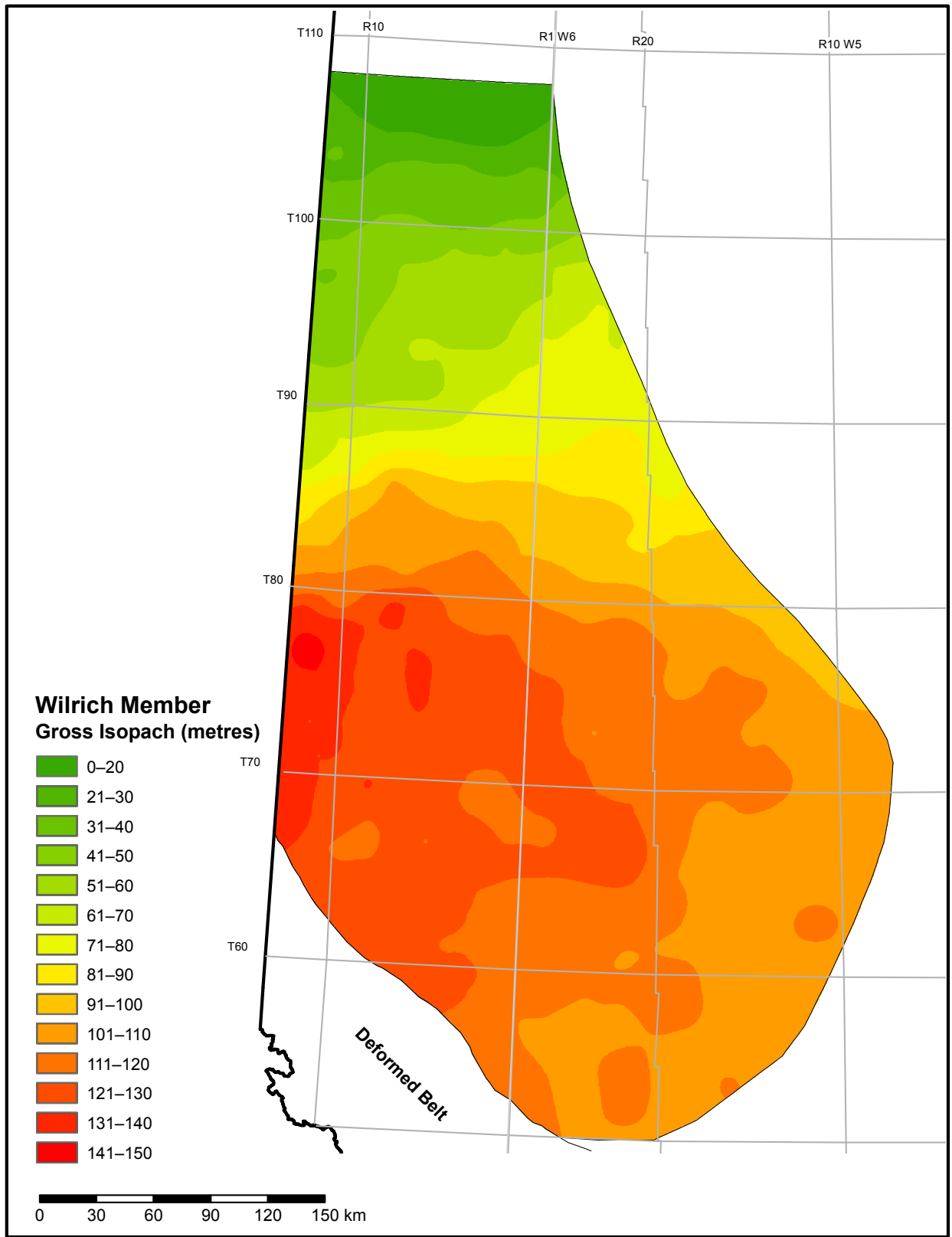


Figure 2.6.3. Gross isopach of the Wilrich Member.

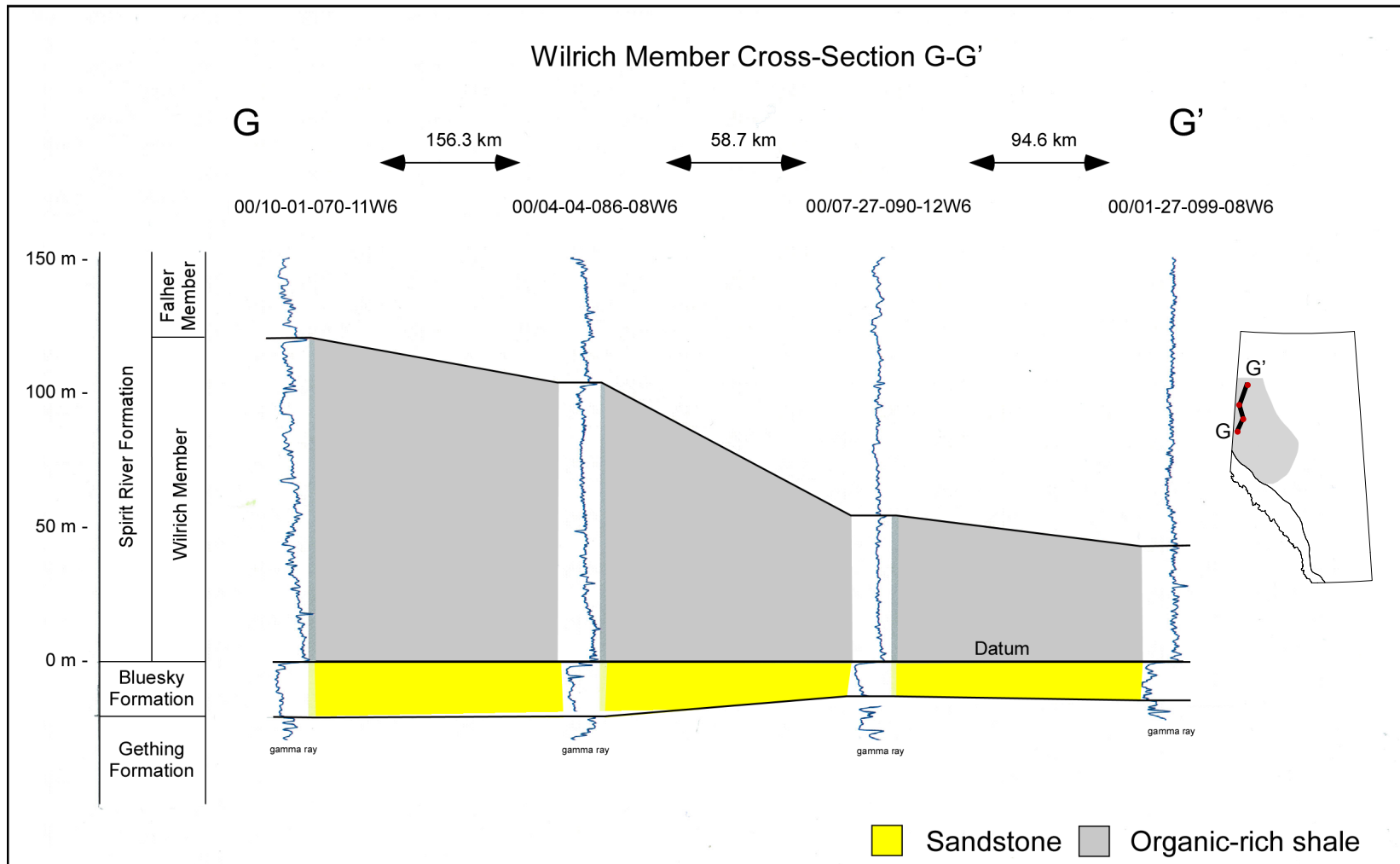


Figure 2.6.4. Stratigraphic cross-section G-G' of the Wilrich Member (see inset map for location).

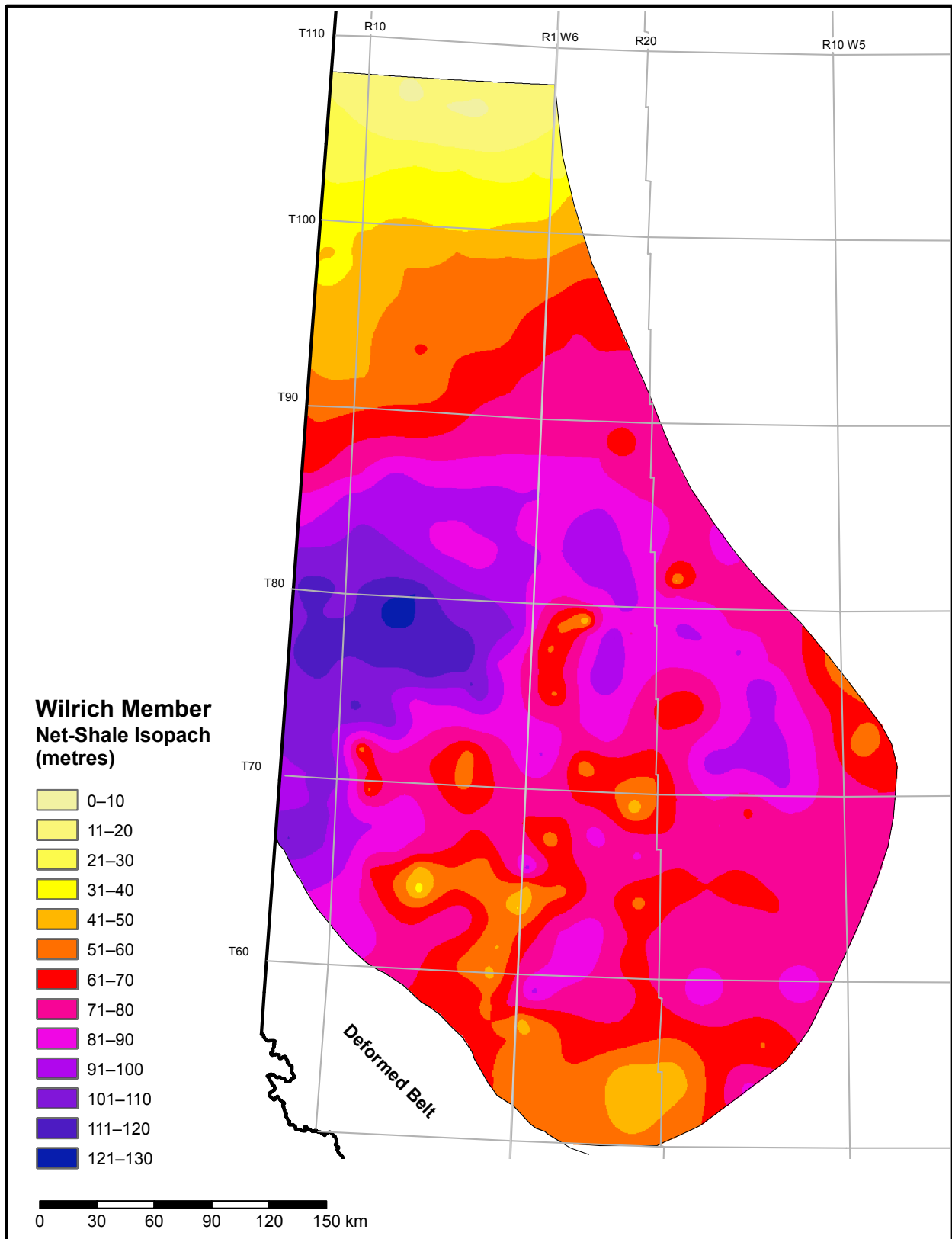


Figure 2.6.5. Net-shale isopach of the Wilrich Member.

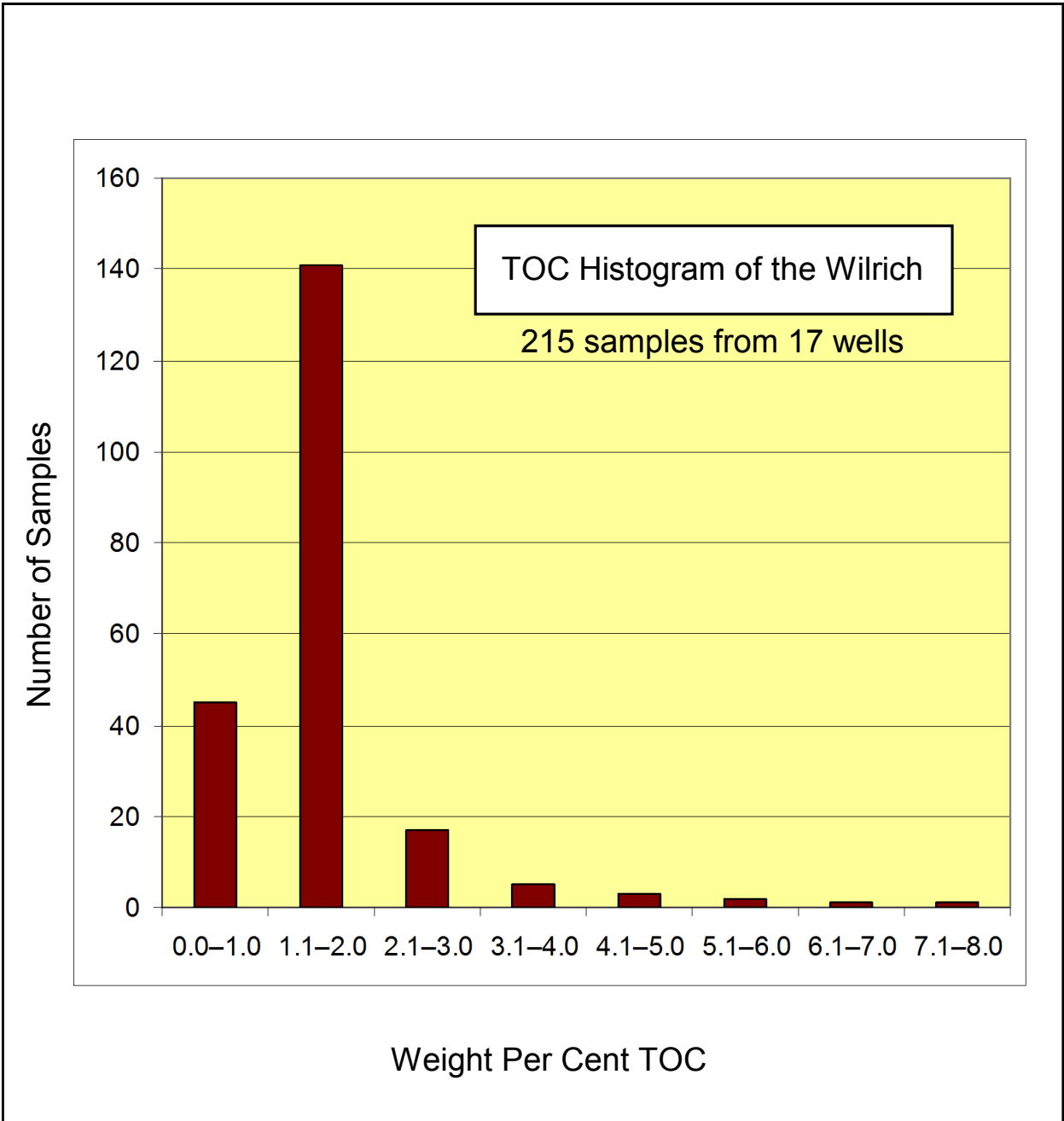


Figure 2.6.6. Histogram of total organic carbon (TOC) of 213 samples from the Wilrich Member.

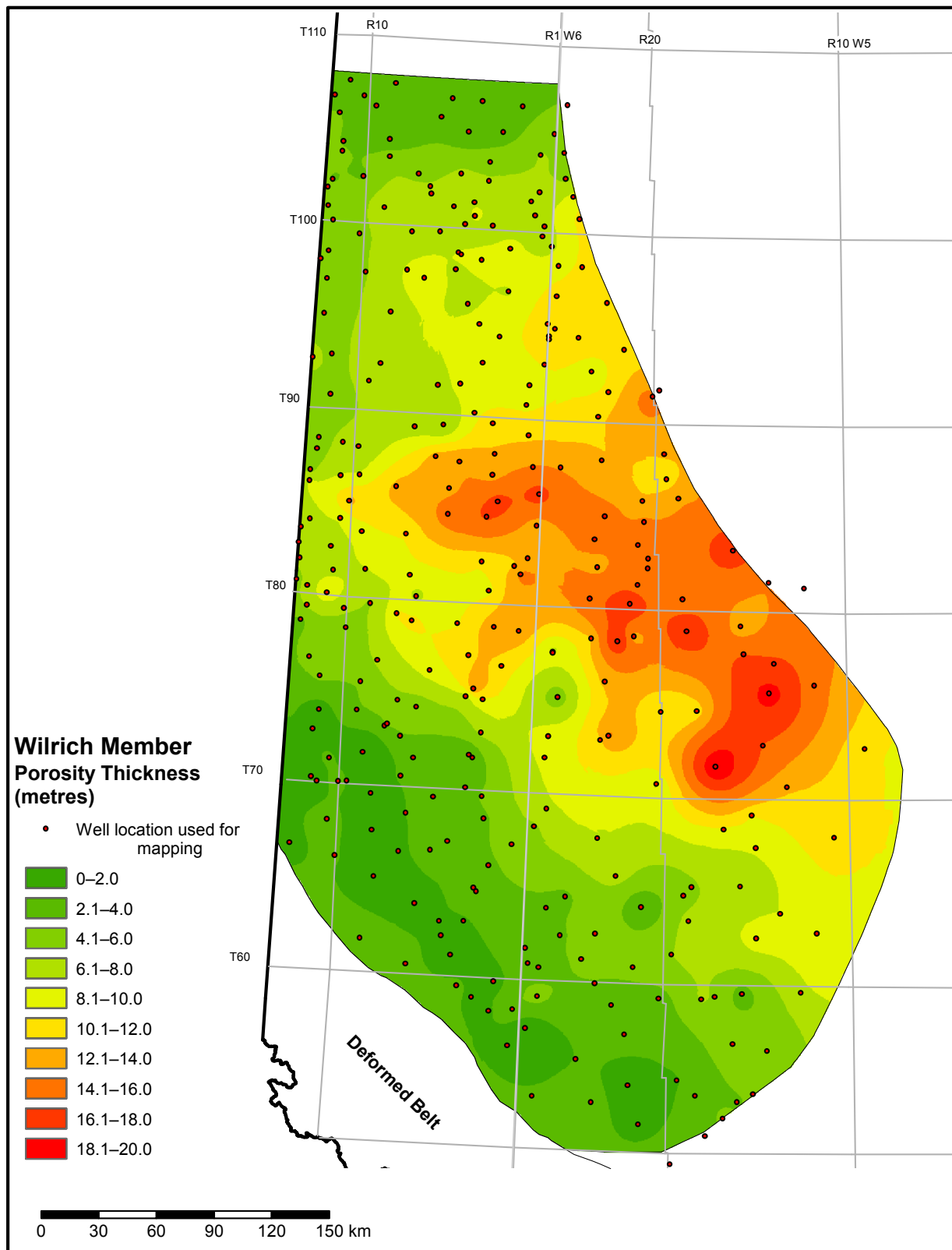


Figure 2.6.7. Porosity-thickness (Phi-h) map of the Wilrich Member.

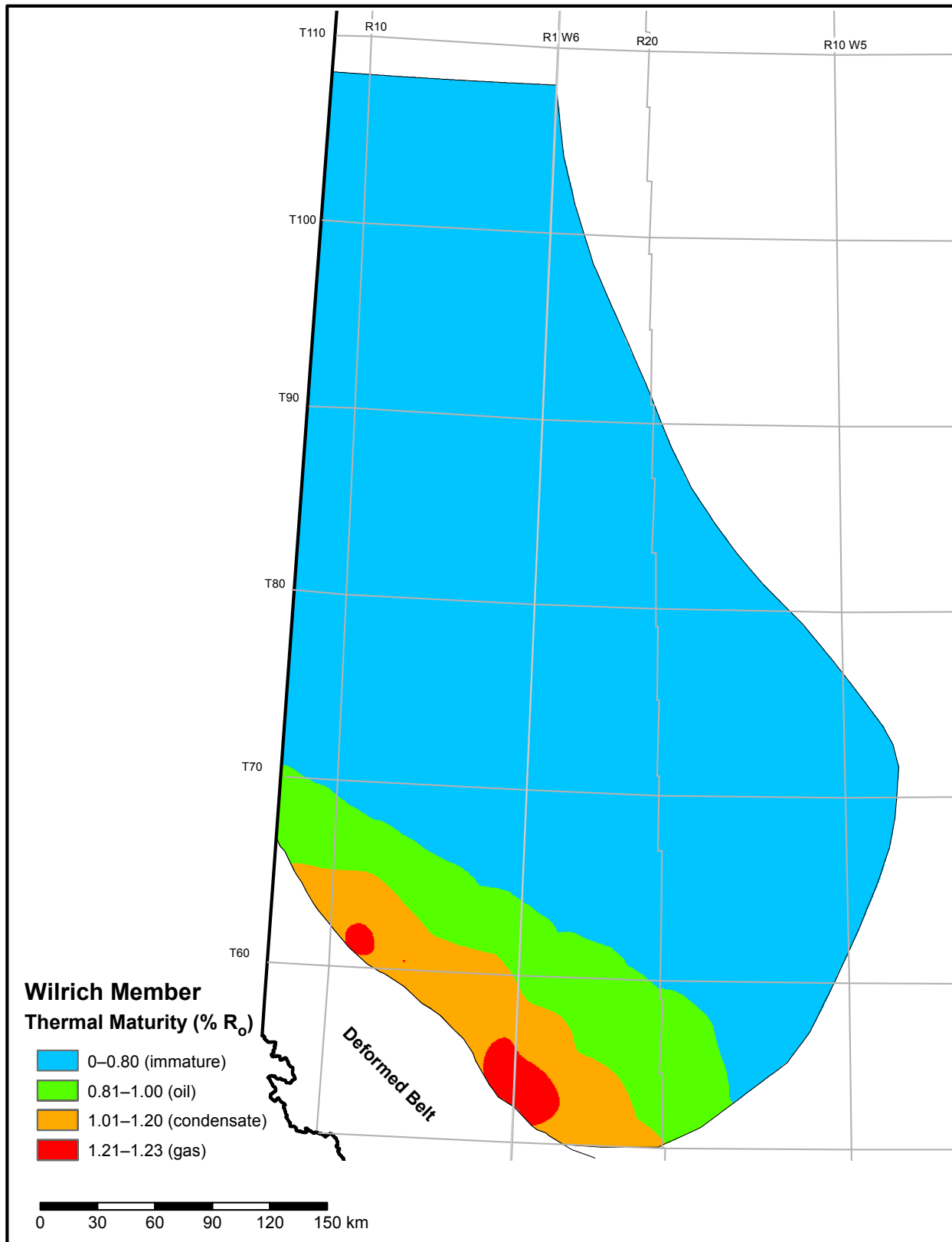


Figure 2.6.8. Thermal maturity map of the Wilrich Member.

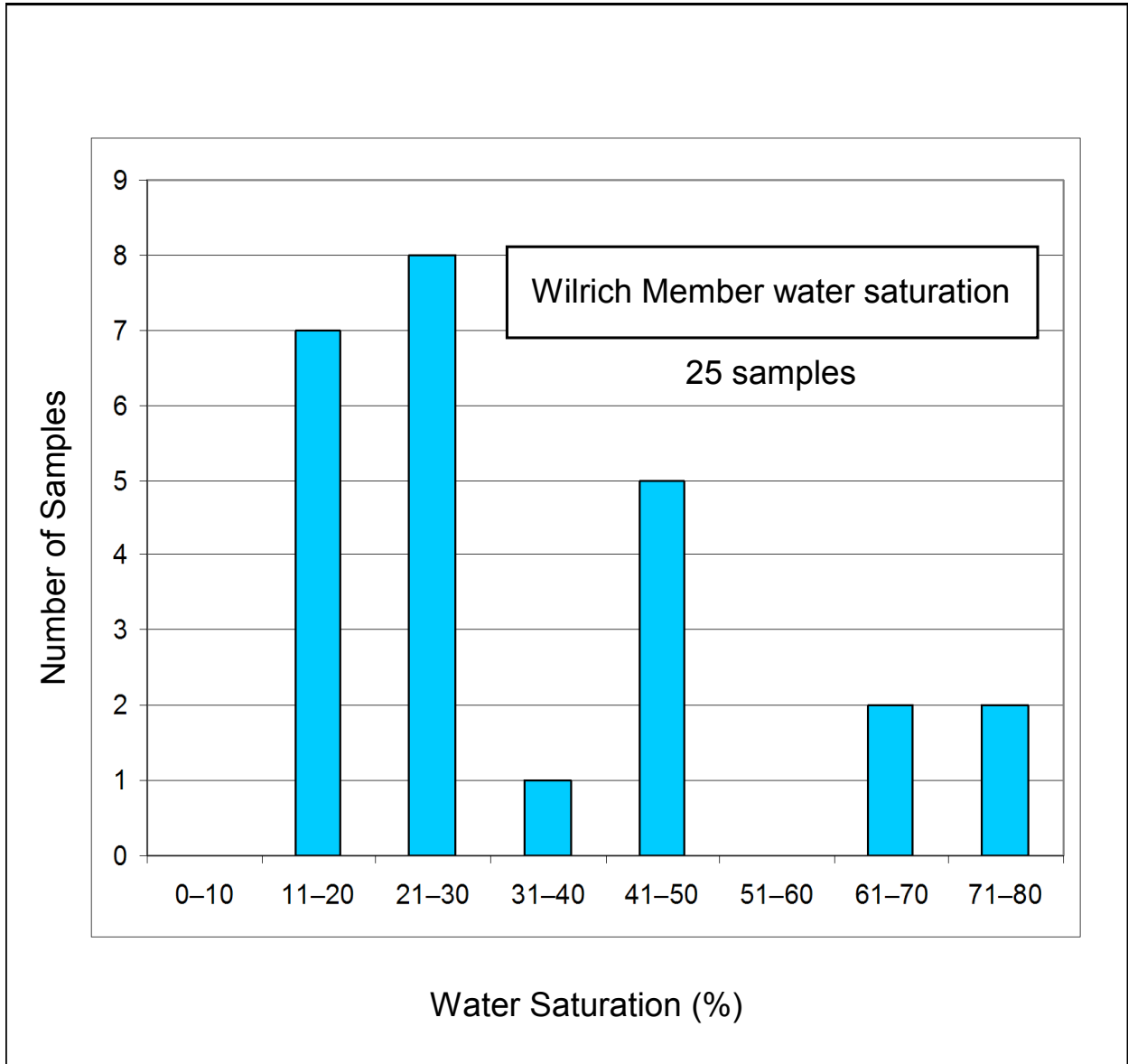


Figure 2.6.9. Histogram of water-saturation analysis results of 25 samples from the Wilrich Member.

## 2.7 Preliminary Summary of the Rierdon Formation

The Rierdon Formation (Rierdon) belongs to the middle to upper Ellis Group in southern Alberta. Its stratigraphic equivalents in western Alberta and the Rocky Mountain Foothills are the Grey Beds of the Fernie Formation. The study area uses the erosional edge of the Swift, Rierdon, and Sawtooth formations as the northern boundary and the Foothills deformation belt as the western boundary (Figure 2.7.1).

The Rierdon is primarily composed of interbedded grey to dark-grey and green, calcareous to noncalcareous, pyrite-rich, fossiliferous shale and brown to light-grey limestone. Figure 2.7.2 shows a structural high in the extreme south of Alberta. This structural high was influenced by the paleostructure of the Sweetgrass Arch. The east flank dips to the east-northeast about 18 to 20 m per km, whereas the west flank dips to the west more steeply, increasing from about 10 to 30 m per km near the Foothills. The shallowest depth to top of the Rierdon is 760 m on the Sweetgrass Arch, whereas the deepest depth to top is 3500 m along the Foothills belt (Figure 2.7.3).

The gross isopach map of the Rierdon indicates that the paleo-Sweetgrass Arch influenced deposition of the Rierdon succession (Figure 2.7.4). There are two Rierdon depocentres in the study area:

1. along the southeastern flank of the Sweetgrass Arch, where the thickness of the Rierdon ranges from 30 to 60 m, and
2. on the western flank, where the thickness ranges from 40 to 80 m.

Above the crest of the Sweetgrass Arch, the thickness ranges from 10 to 40 m. Northwards of the depocentres, the Rierdon thins to 0 m at the erosional edge. A representative stratigraphic cross-section using four wells (two on the western flank and two on the eastern flank of the Sweetgrass Arch) illustrates this thickness variation (Figure 2.7.5).

We generated a net-shale map (Figure 2.7.6) using a gamma-ray cutoff of >75 API. This cutoff eliminated limestone from the evaluation and focused on shale and mudstone. The net-shale map shows similar trends as the gross isopach for the Rierdon.

A porosity-thickness ( $\Phi$ -h) map of the Rierdon (Figure 2.7.7) was constructed using density-porosity logs calibrated to a grain density of 2.72 g/cm<sup>3</sup> with no porosity cutoff and a >75 API gamma-ray-log cutoff. The grain density we used accounts for the presence of TOC by converting TOC to kerogen and counting it as a mineral component in the grain density. Section 3.4 provides information on the determination of grain density used in our analysis and a discussion on sources of error.

Based on 137 samples from 17 wells, TOC content of the Rierdon ranges from 0.1 to 4.0 wt. %, averaging 1.0 wt. %, (Figure 2.7.8).

The thermal maturity map of the Rierdon is based on vitrinite reflectance (%  $R_o$ ) data and indicates that much of the Rierdon is below 0.8%  $R_o$  (Figure 2.7.9), which we have used as a cutoff. Nonetheless, a well located in 00/4-26-015-26W4M is producing oil and condensate from the Rierdon according to ERCB records. We are recommending a preliminary status for the Rierdon and will not generate a resource estimate until the maturity of the Rierdon is studied in more detail.

Using Dean Stark analysis and helium pycnometry for select samples, the laboratory calculated water saturation. The distribution of values for the Rierdon ranges from 30% to 90% (Figure 2.7.10), which is used as P90 and P10 constraints in our resource evaluation. There is one sample with water saturation of approximately 10%, which is from a limestone bed. Section 3.3 provides information on the methodology used to determine water saturation and a discussion of possible sources of error.

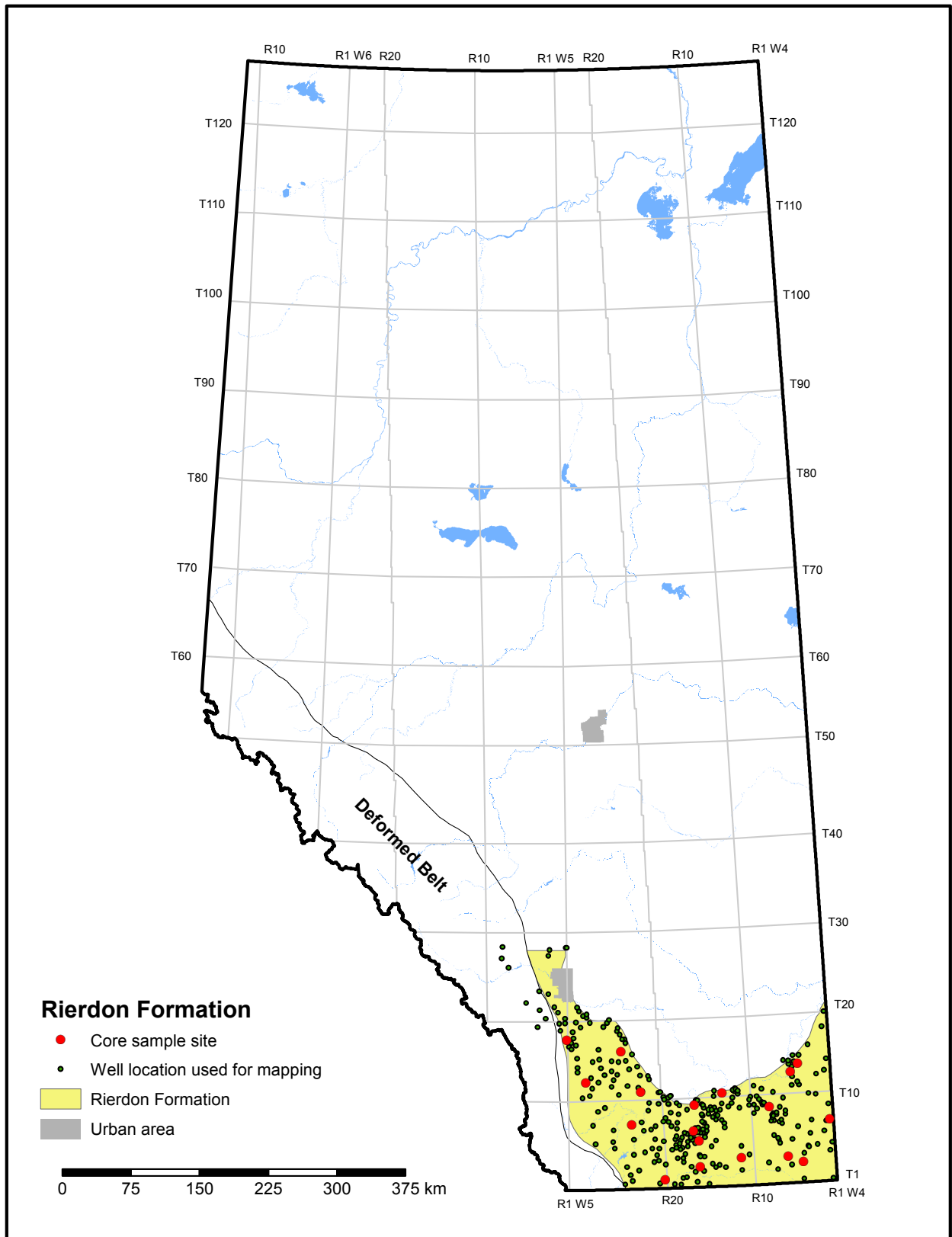


Figure 2.7.1. Index map of the Rierdon Formation.

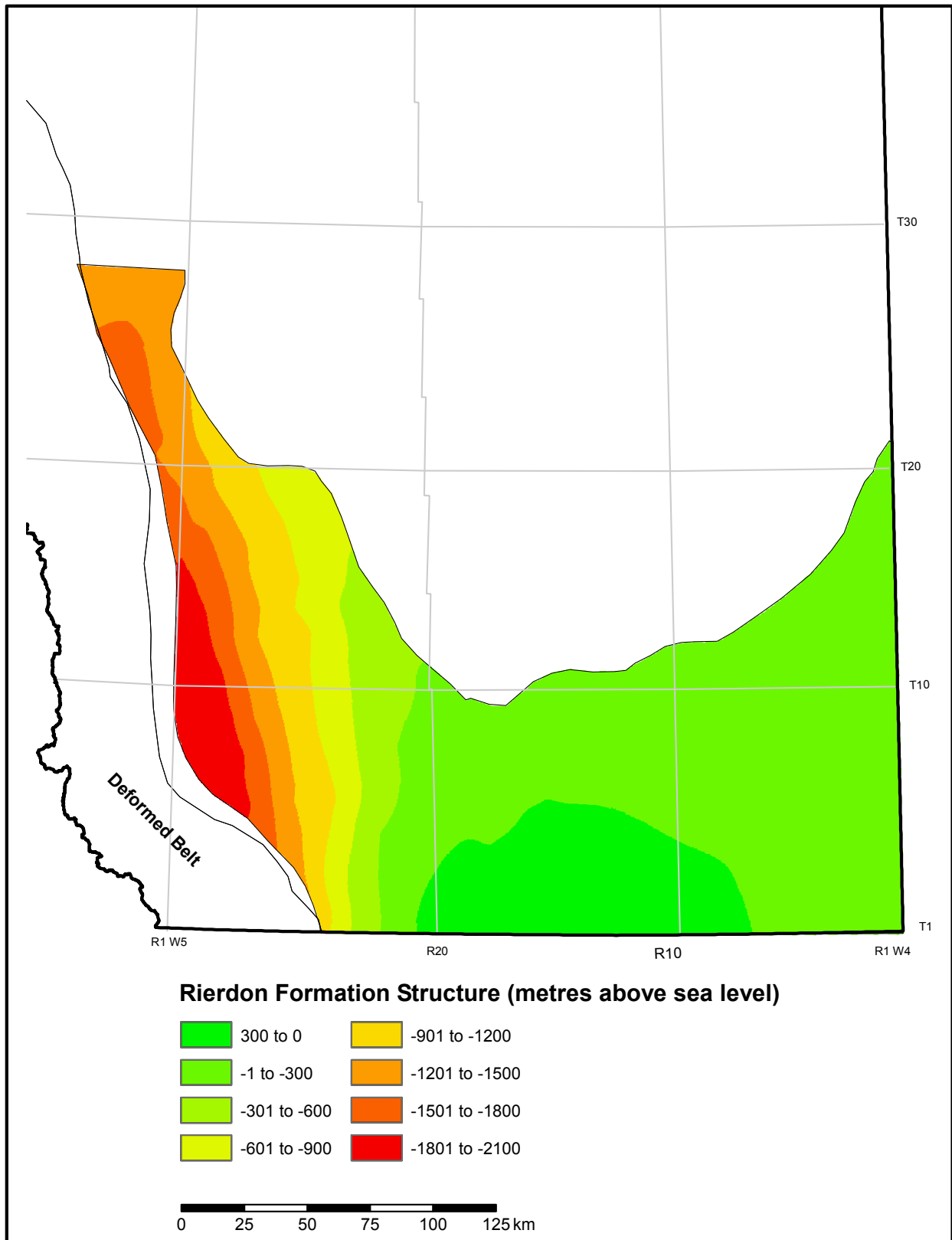


Figure 2.7.2. Structure of the Rierdon Formation.

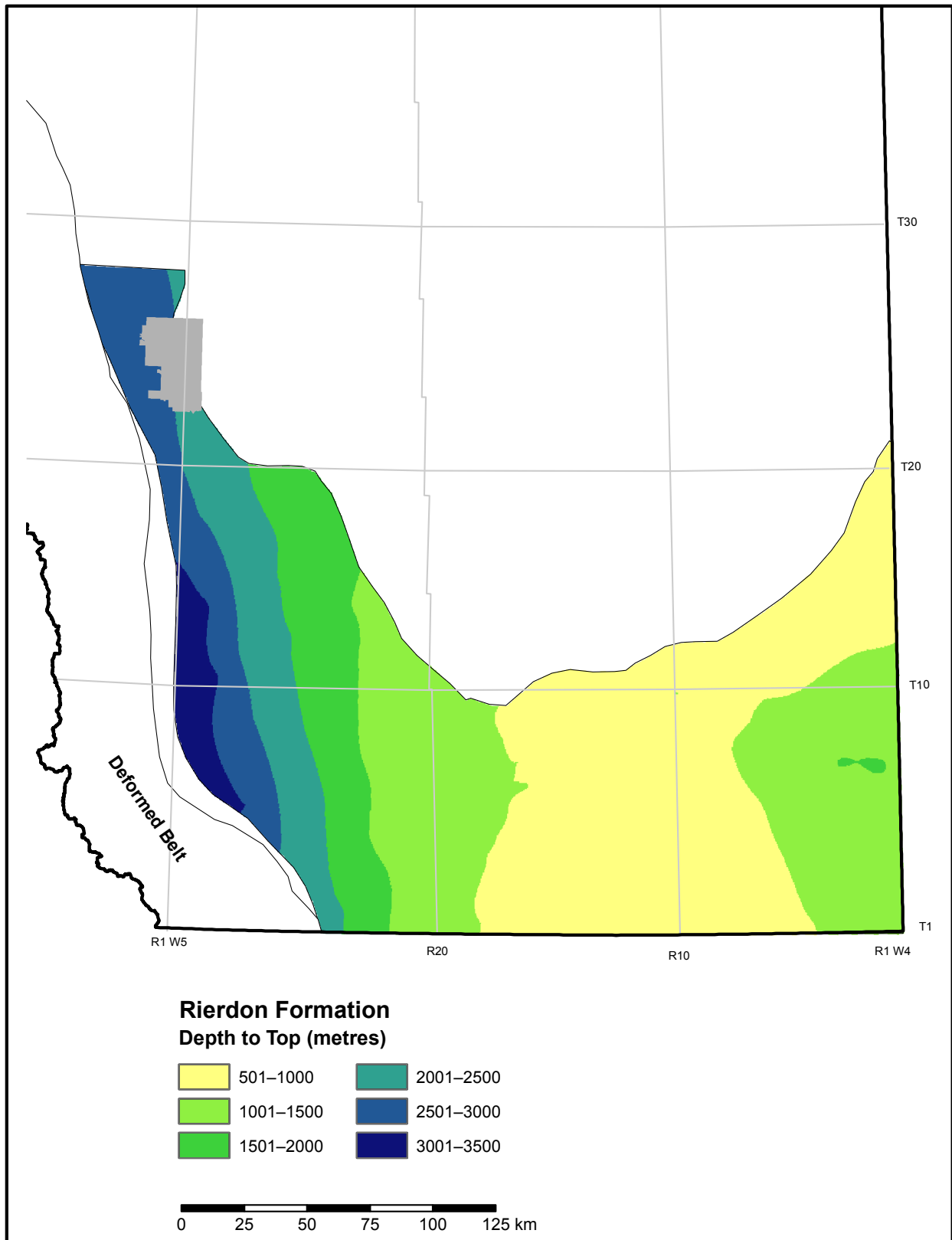


Figure 2.7.3. Depth to top of the Rierdon Formation.

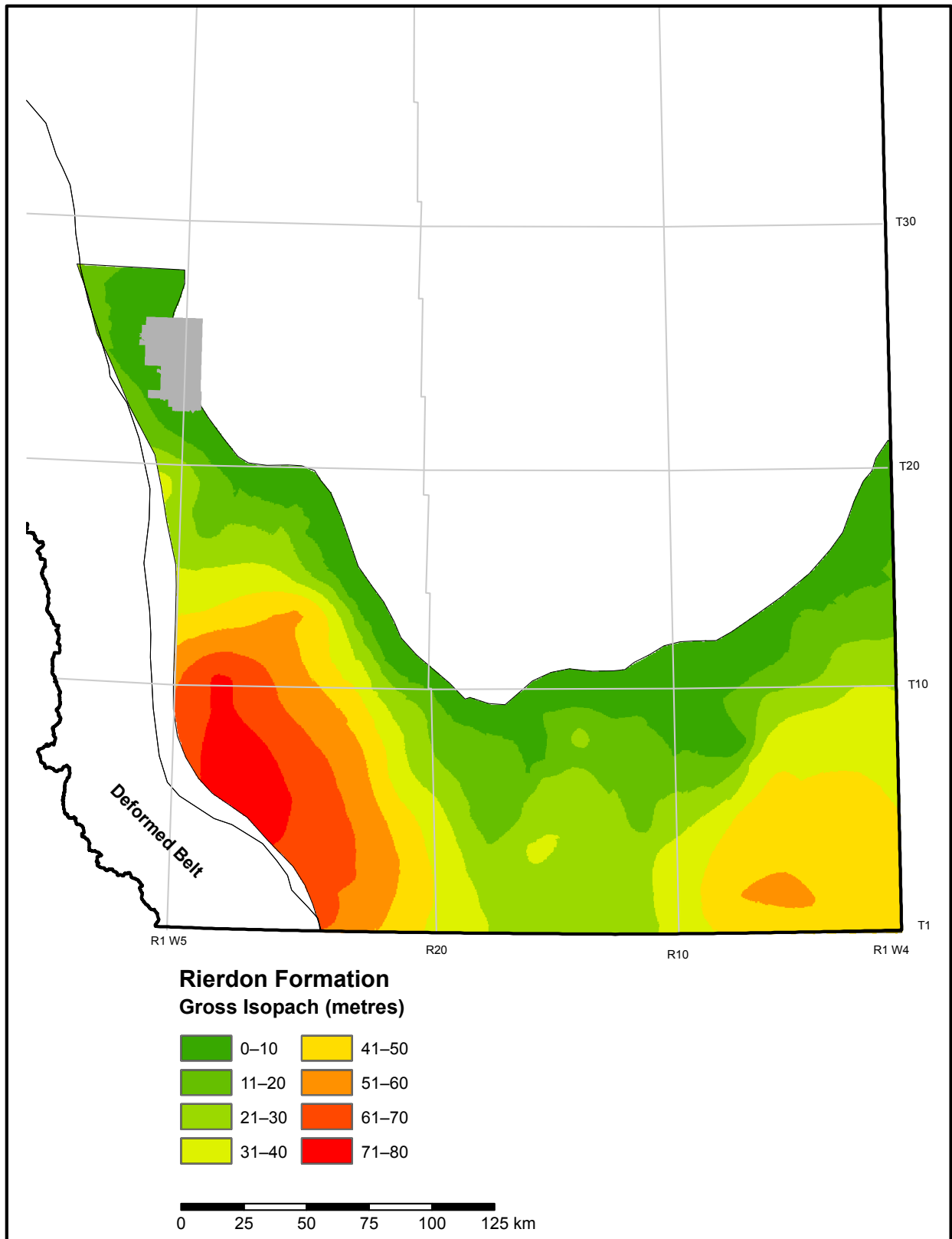


Figure 2.7.4. Gross isopach of the Rierdon Formation.

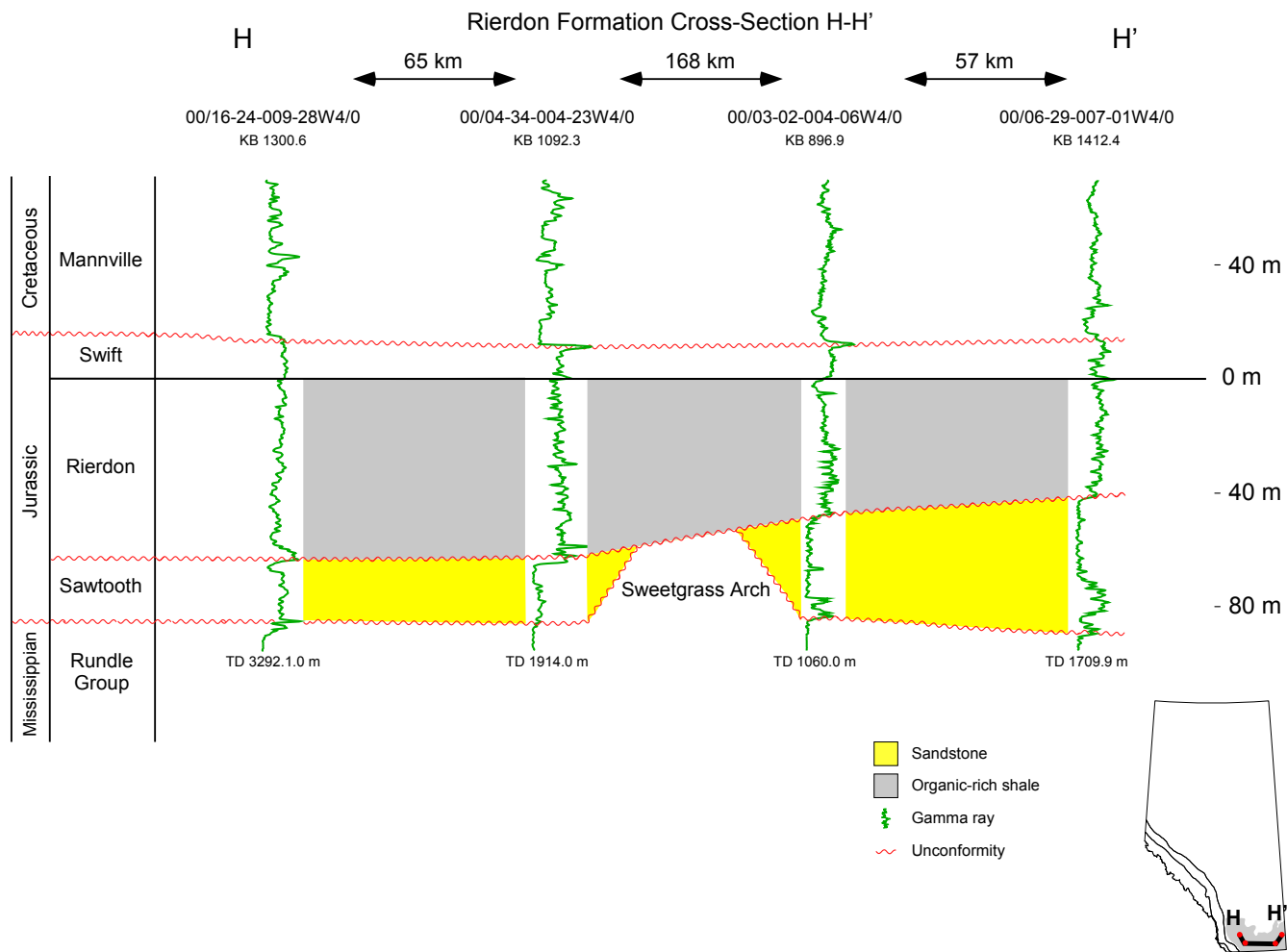


Figure 2.7.5. Stratigraphic cross-section H-H' of the Rierdon Formation (see inset map for location).

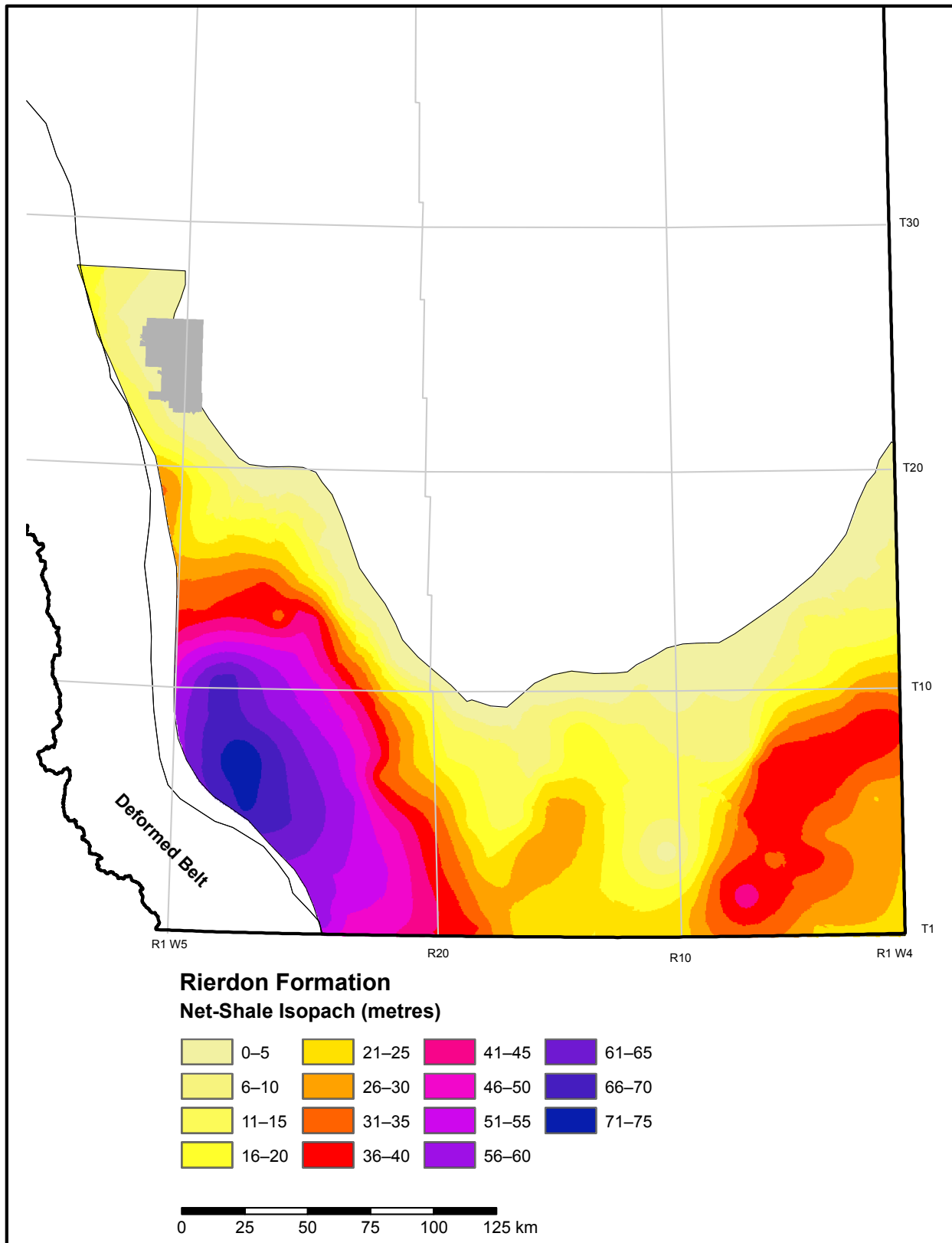


Figure 2.7.6. Net-shale isopach of the Rierdon Formation.

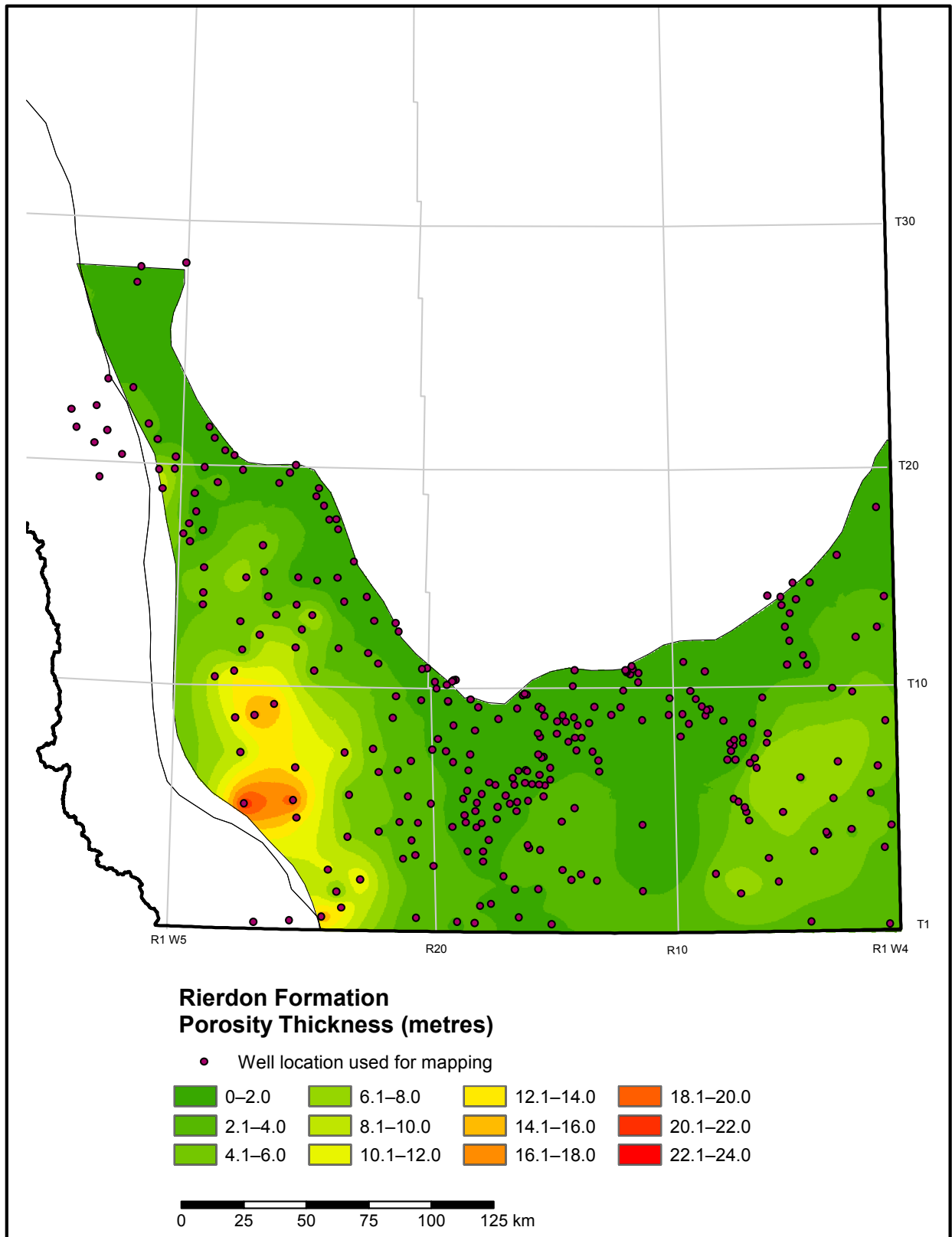


Figure 2.7.7. Porosity-thickness (Phi-h) map of the Rierdon Formation.

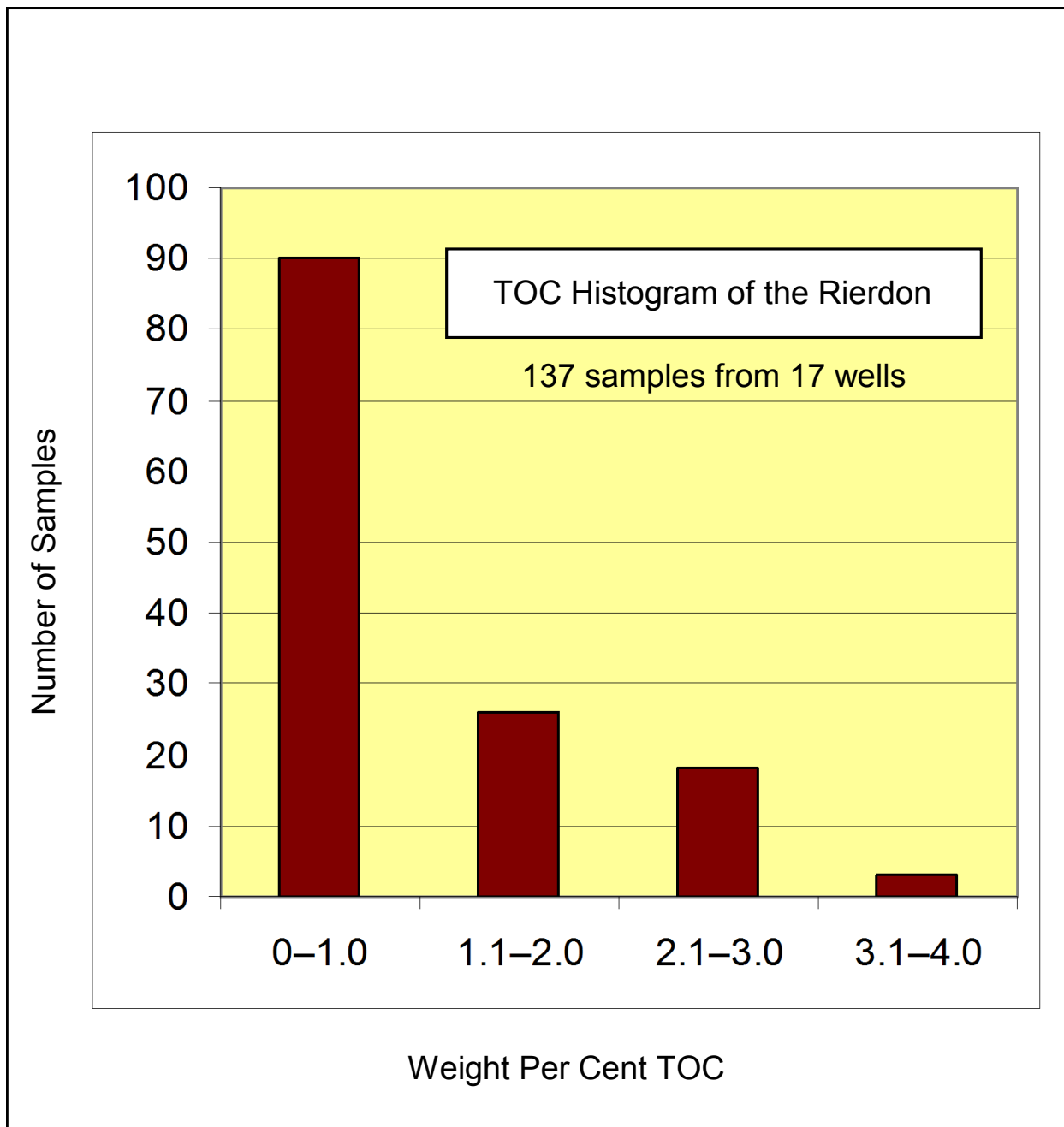


Figure 2.7.8. Histogram of total organic carbon (TOC) of 137 samples from the Rierdon Formation.

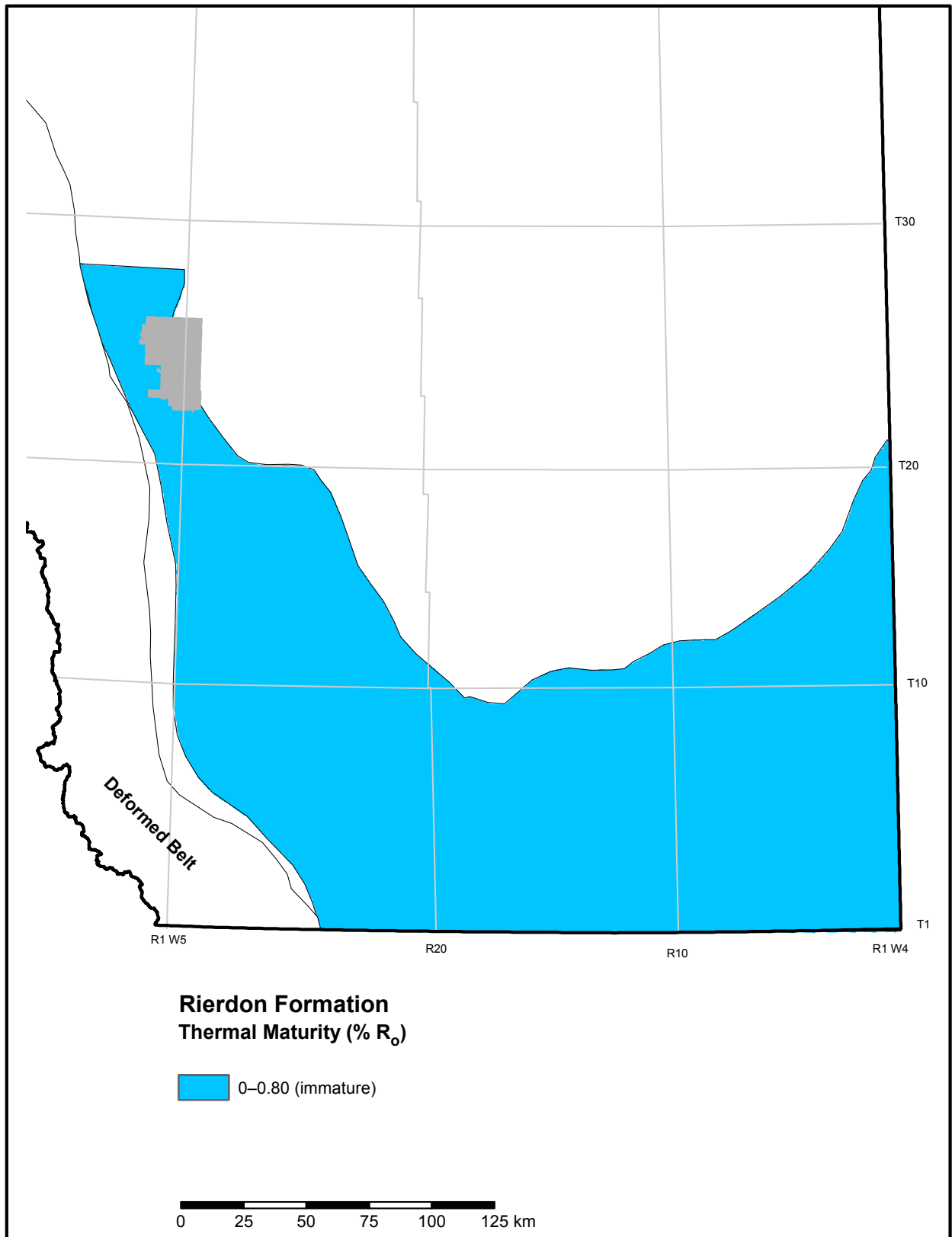


Figure 2.7.9. Thermal maturity map of the Rierdon Formation.

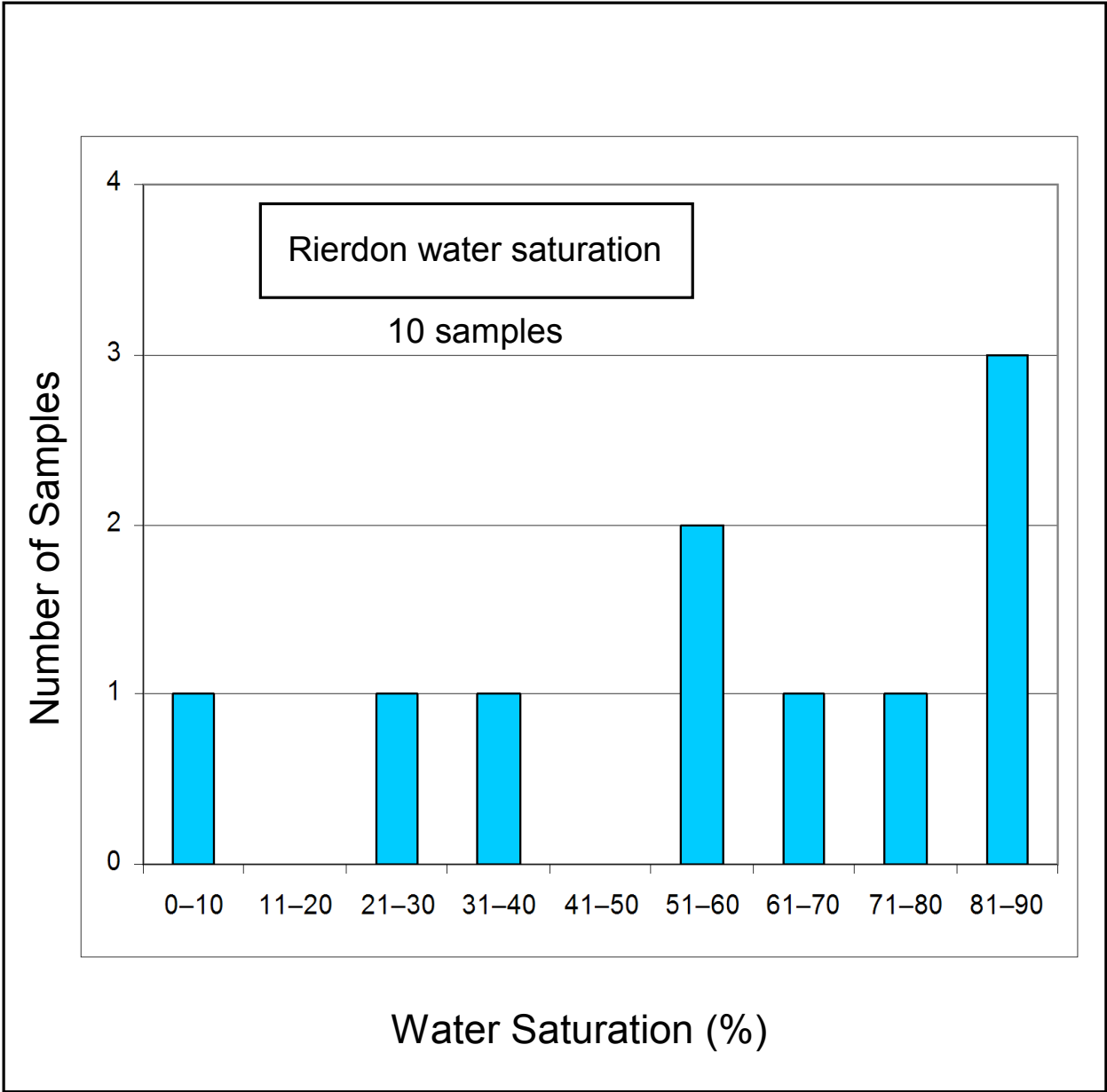


Figure 2.7.10. Histogram of water-saturation analysis results for 10 samples from the Rierdon Formation.

## 2.8 Preliminary Summary of the Colorado Group

Rocks of the Colorado Group, and approximately stratigraphically equivalent strata of the Smoky and Fort. St. John groups in northern Alberta (here collectively called Colorado Group), underlie much of Alberta. To reduce the size of individual study areas, we split the Colorado Group into a northern and a southern resource-evaluation area, informally referred to as the 'north Colorado evaluation area' and the 'south Colorado evaluation area' (Figure 2.8.1).

We have informally divided the Colorado Group into three units: upper, middle, and lower Colorado. The upper unit comprises strata from the top of the Colorado Group (i.e., base of the Lea Park Formation and its equivalents) to the top of the Second White Speckled Shale. The middle unit comprises the strata from the top of the Second White Speckled Shale to the Base of Fish Scales marker. The third unit is defined by the strata below the Base of Fish Scales marker to the top of the Mannville Group and the Spirit River Formation. Cross-sections in the respective summaries for the north and south Colorado evaluation areas display the subdivisions.

The Colorado Group gross isopach exhibits two depocentres in Alberta (Leckie et al., 1994): in the Deep Basin, where the Colorado is more than 1600 m thick, and in southeastern Alberta, under the influence of the Williston Basin, near the Sweetgrass Arch, where it is about 500 m thick.

The thermal maturity data of the Colorado Group follows a similar pattern to the other assessed units by showing increasing maturity with depth. Historical conventional production includes an eastern, relatively immature zone dominated by shallow gas, a central area that is in the oil window, and a western, over-mature zone that is largely dry-gas prone.

The base of groundwater protection (BGP) extends into the north and south Colorado evaluation areas (Figure 2.8.2). Any Colorado Group sediment lying above the BGP will not be evaluated for resources. Depth from the surface to the top of the lower, middle, and upper Colorado ranges from 0 to 3500 m, 0 to 3250 m, and 0 to 2500 m, respectively (Figures 2.8.3a–c). The Colorado units outcrop to the north and are deepest near the deformed belt.

More data are needed to properly assess the resource potential of the vast Colorado Group.

### 2.8.1 North Colorado Evaluation Area

The north Colorado evaluation area consists predominantly of mudstones with thin beds and thick wedges of sandstone and conglomerate: specifically, from geologically youngest to oldest, the Viking, Pelican, Paddy-Cadotte, Dunvegan-Doe Creek, Cardium, and Bad Heart deposits. These relatively coarse siliciclastic rocks, especially the Cardium and the Viking formations, are long-standing, prolific, conventional oil and gas producers.

In the north Colorado evaluation area, the Colorado Group is extensively eroded to the north and east. The edge of the shaded area in Figure 2.8.1, representing the erosional edge of the Colorado Group, delineates the zero edge of the group. A network of 333 wells has been correlated along 35 cross-sections that are consistent with the work of Leckie et al. (1994). A representative cross-section shown in Figure 2.8.4 clearly illustrates that the Colorado Group forms a north- and eastward-thinning wedge with sandstone units that become finer grained and with shale units that merge towards the north and east.

The gross thickness of the lower Colorado displays a pronounced increase in the Deep Basin in northwestern Alberta (Figure 2.8.5). The distribution of net shale of the lower Colorado displays an

increase in thickness in two areas near the British Columbia border, both greater than 130 m (Figure 2.8.6). The net-shale isopachs employed a gamma-ray cutoff of >105 API, which was used to exclude conventional sandstone and siltstone from the resource assessment. The variation in gross thickness of the middle Colorado is similar to the lower Colorado, showing a pronounced increase towards the Deep Basin (Figure 2.8.7). The upper Colorado also increases in thickness in the Deep Basin, but the change is more gradual (Figure 2.8.8). The net-shale isopach of both the middle and upper Colorado increases in thickness to about 500 m and 450 m, respectively, towards a depocenter located in west-central Alberta near the deformed belt (Figures 2.8.9 and 2.8.10).

The TOC histogram for the north Colorado evaluation area contains 83 samples from 20 wells (Figure 2.8.11). The TOC content varies by more than 8.0 wt. %, with a dominance in the range of 1.0 to 2.0 wt. % for all Colorado units. Lower Colorado TOC values range up to 2.2 wt. %, whereas the middle and upper Colorado TOC contents have a much higher range of values, as high as 6.8 wt. % and 8.1 wt. %, respectively.

Using Dean Stark analysis and helium pycnometry for select samples, the laboratory calculated water saturation. The distribution of values for the north Colorado evaluation area ranges from less than 10% to 60% (Figure 2.8.12). For both the TOC and water-saturation data, the number of samples analyzed was too small to discern any reasonably reliable trends. Section 3.3 provides further information on the methodology used to determine water saturation and possible sources of error.

## 2.8.2 South Colorado Evaluation Area

The south Colorado evaluation area represents a mudstone-dominated succession interbedded with sandstone beds, including the Viking Formation, Second White Speckled Shale Formation, Cardium Formation, Bad Heart Formation, and Medicine Hat Member, which contain conventional oil and gas reservoirs (Figure 2.8.13). The shale and mudstone components vary from 25 m to more than 525 m, and the sandstone beds are relatively thin in comparison.

In most parts of the south Colorado evaluation area, the gross thickness of the lower Colorado ranges from 70 to 90 m (Figure 2.8.5), except in the southeast, where it thickens up to 175 m, and towards the northwest, where the unit thins to <50 m. The net-shale isopach of the lower Colorado (Figure 2.8.6) shows a relatively consistent distribution in the southern and east-central part of the province, reaching about 110 m in thickness.

The middle Colorado consists of the Fish Scales Formation (stratigraphically equivalent to the Fish Scales Zone in the north), the Belle Fourche Formation, and the Second White Speckled Shale (2WSPK) Formation. The unit is distinguished by a regionally extensive radioactive, organic-rich layer, referred to as the Fish Scales Zone, and by the 2WSPK, composed mainly of shale and mudstone with skeletal calcarenite, fish-skeletal debris, calcite and siderite concretions, and phosphate, as well as localized occurrences of sandstones and siltstones.

The middle Colorado thickness varies from zero at the erosional edge to about 15 m in eastern Alberta and gradually increases towards the Deep Basin to about 155 m (Figure 2.8.7). The net-shale isopach shows a very similar distribution (Figure 2.8.9).

The First White Speckled Shale occurs at the top of the upper Colorado and is distinguished by white, coccolith-bearing pellets and radioactive layers that exhibit a wide geographic distribution. The upper Colorado comprises several stratigraphic entities that change in name and definition from west to east, similar to the north Colorado evaluation area. The most well-known unit in the upper Colorado is the

Cardium Formation. Below the Cardium are thick, black mudstone units known as the Blackstone and Kaskapau formations. Overlying the Cardium are the mudstones of the Wapiabi and Muskiki formations

The thickness of the upper Colorado in the south Colorado evaluation area ranges between 30 m and 500 m (Figure 2.8.8). The net-shale isopach (Figure 2.8.10) varies from about 30 m in the extreme northeast to about 450 m in the northwest, displaying a gradual increase in thickness parallel to the deformed belt and towards the Deep Basin.

A histogram of TOC content in the three units is shown in Figure 2.8.14 and is based on 294 samples from 43 wells. In the lower, middle, and upper Colorado, the TOC content ranges up to 3.0 wt. %, 8.2 wt. %, and 6.6 wt. %, respectively. In the upper and lower Colorado, the dominant range of TOC is between 1.0 wt. % and 2.0 wt. %, whereas in the middle Colorado most samples fall between 2.0 wt. % and 3.0 wt. %. The highest TOC values occur in central Alberta for each unit of the south Colorado evaluation area.

Using Dean Stark analysis and helium pycnometry for select samples, the laboratory calculated water saturation. The distribution of values for the upper Colorado shows dominance in the range of 19% to 84%, with an average of 36% (Figure 2.8.15). The distribution of values for the middle Colorado shows dominance in the range of 22% to 91%, averaging at 58%. No water-saturation analysis data are available for the lower Colorado. Similar to the north Colorado evaluation area, the number of water-saturation analyses were insufficient to discern any reliable trends. Section 3.3 provides information on the methodology used to determine water saturation and a discussion of possible sources of error.

## **2.9 Preliminary Evaluation of Additional Units with Shale- and Siltstone-Hosted Hydrocarbon Potential**

We mapped and sampled the Bantry Shale member, which is an Early Cretaceous, lower Mannville shale. The shale averages 3 to 5 m thick with a TOC content that is dominantly below 1.0 wt. %, although a few values are as high as 4.0 wt. %.

Fernie Formation shales, such as the Poker Chip Shale Member, were sampled at the same time as the Nordegg Member. Many of the samples are still in the laboratory. Additional work is necessary to properly evaluate the resource potential.

Relatively organic-rich Ordovician strata are located in southeastern Alberta. A prior study by Nowlan et al. (1995) led us to take an initial look at the Ordovician and determine if the unit merits further study. There is a limited suite of logs and core from which to evaluate Ordovician 'shale-hosted' hydrocarbon resources. Additional work is necessary to properly evaluate the resource potential.

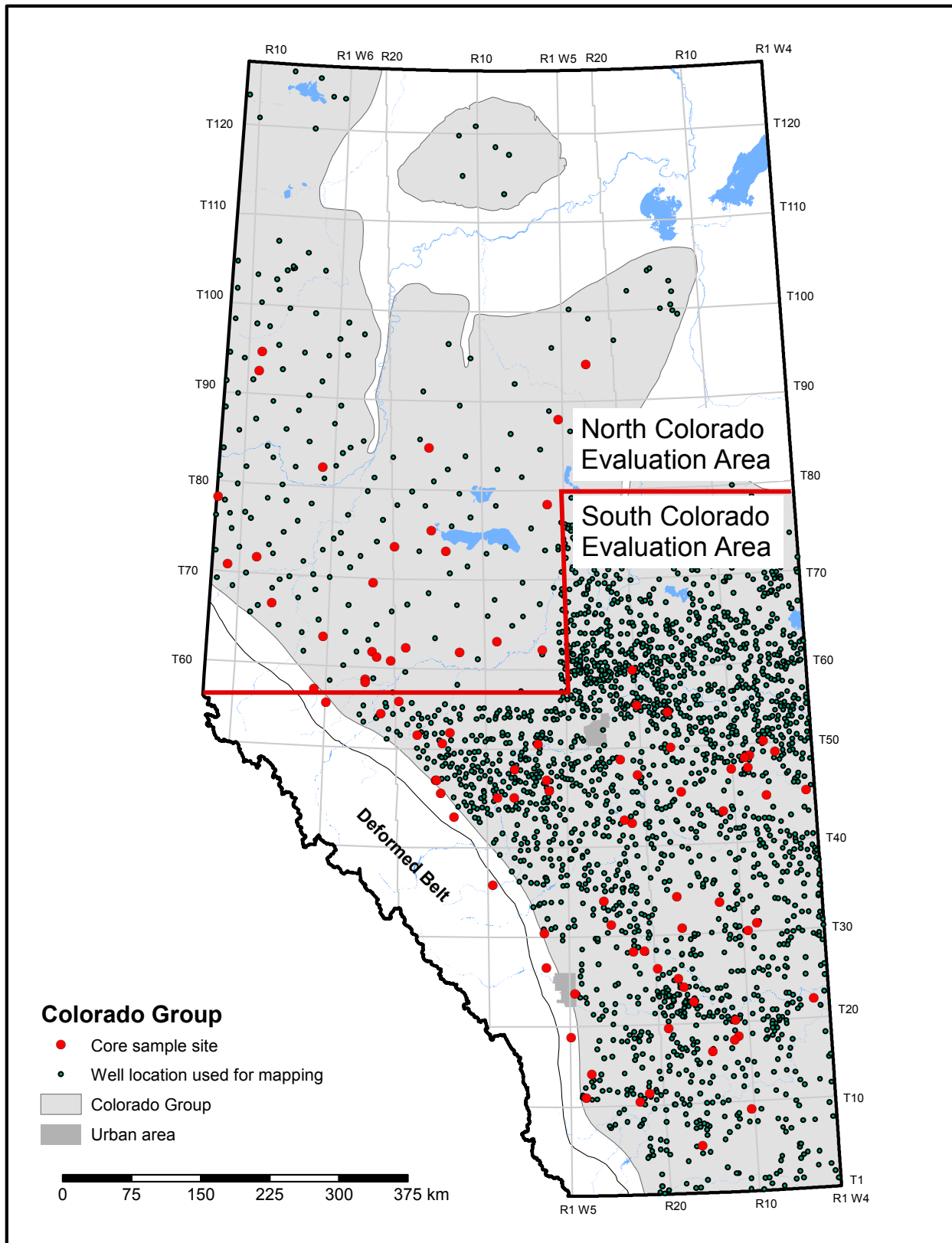


Figure 2.8.1. Index map of the Colorado Group.

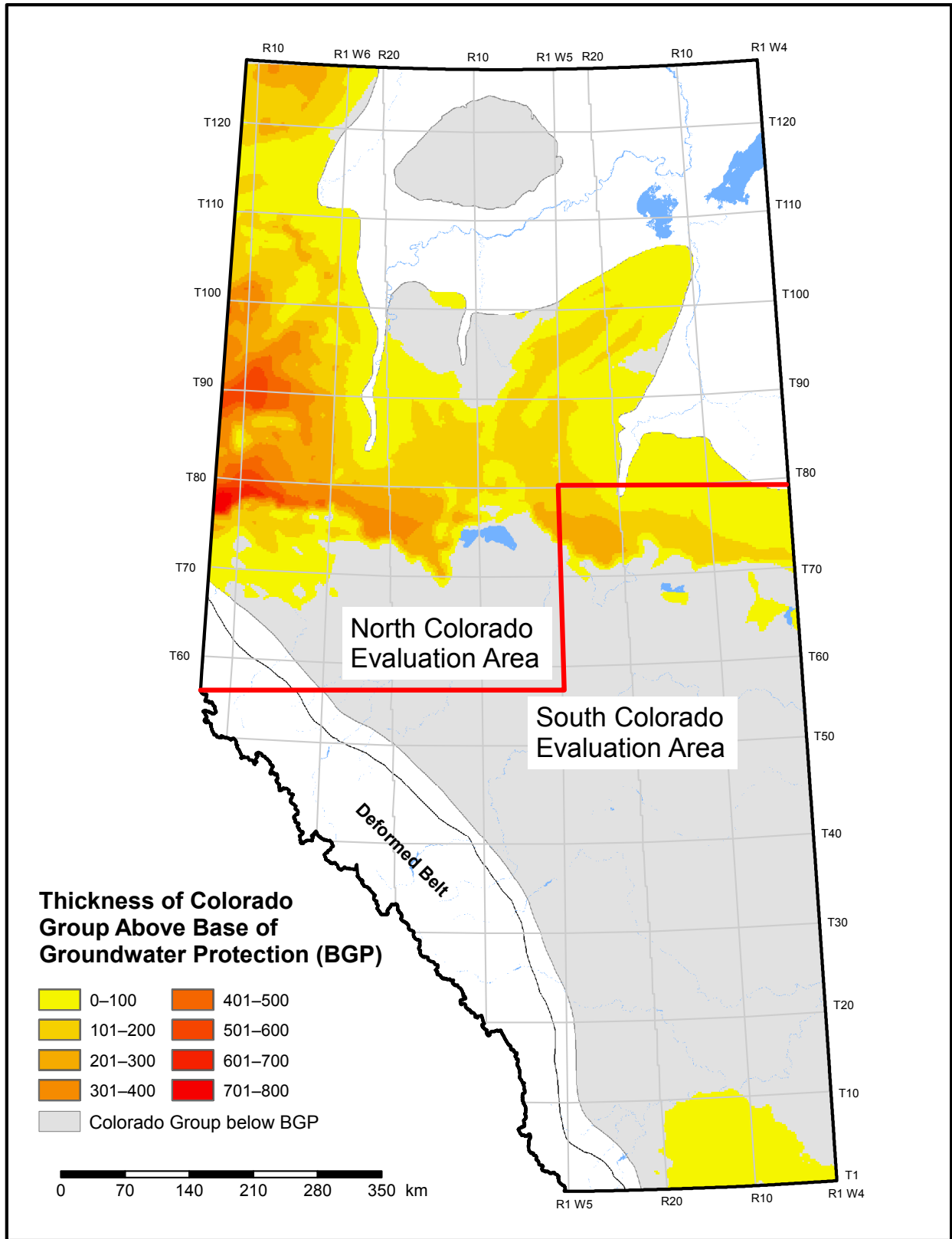


Figure 2.8.2. Thickness of the Colorado Group above the base of groundwater protection (BGP).

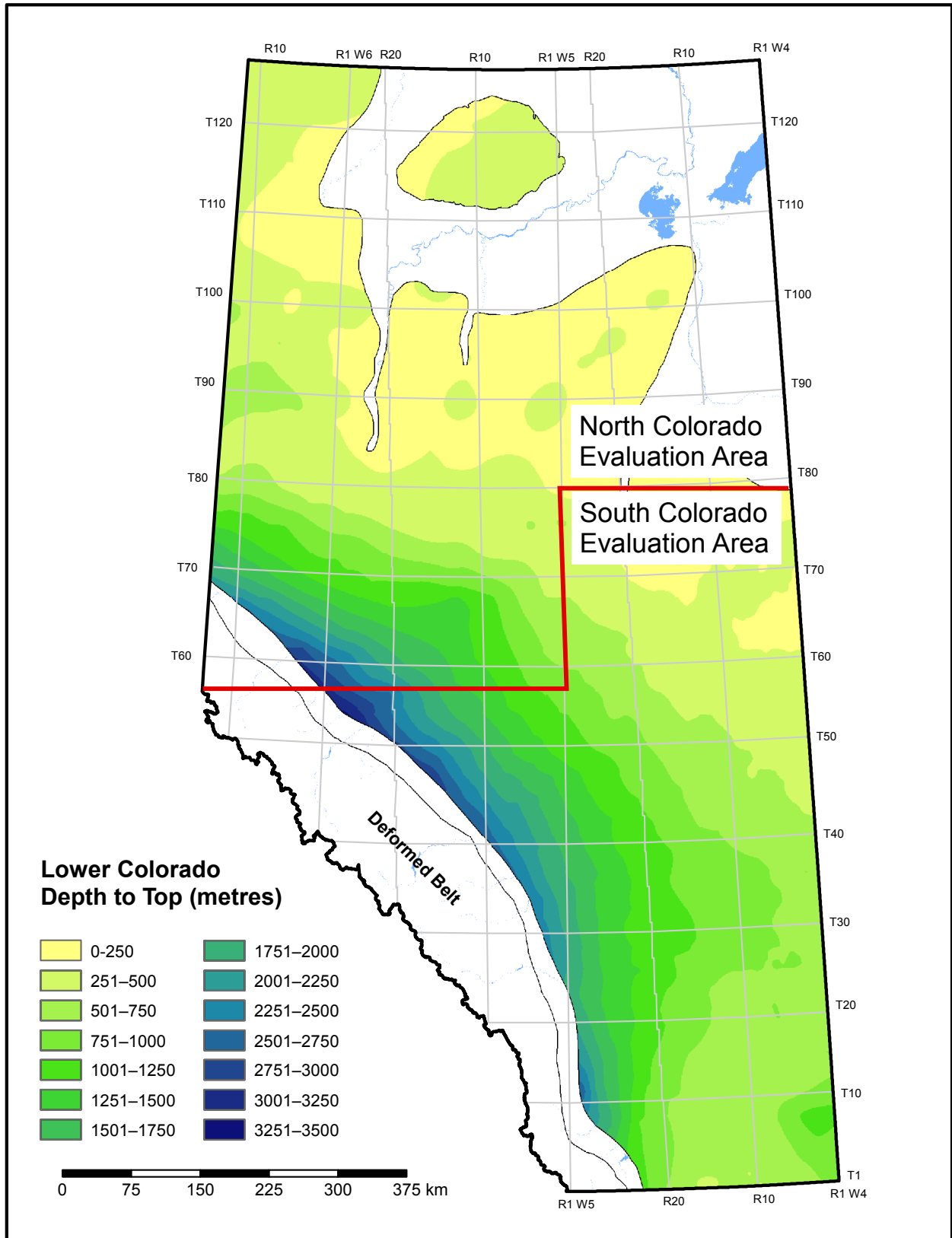


Figure 2.8.3a. Depth to the top of the lower Colorado unit.

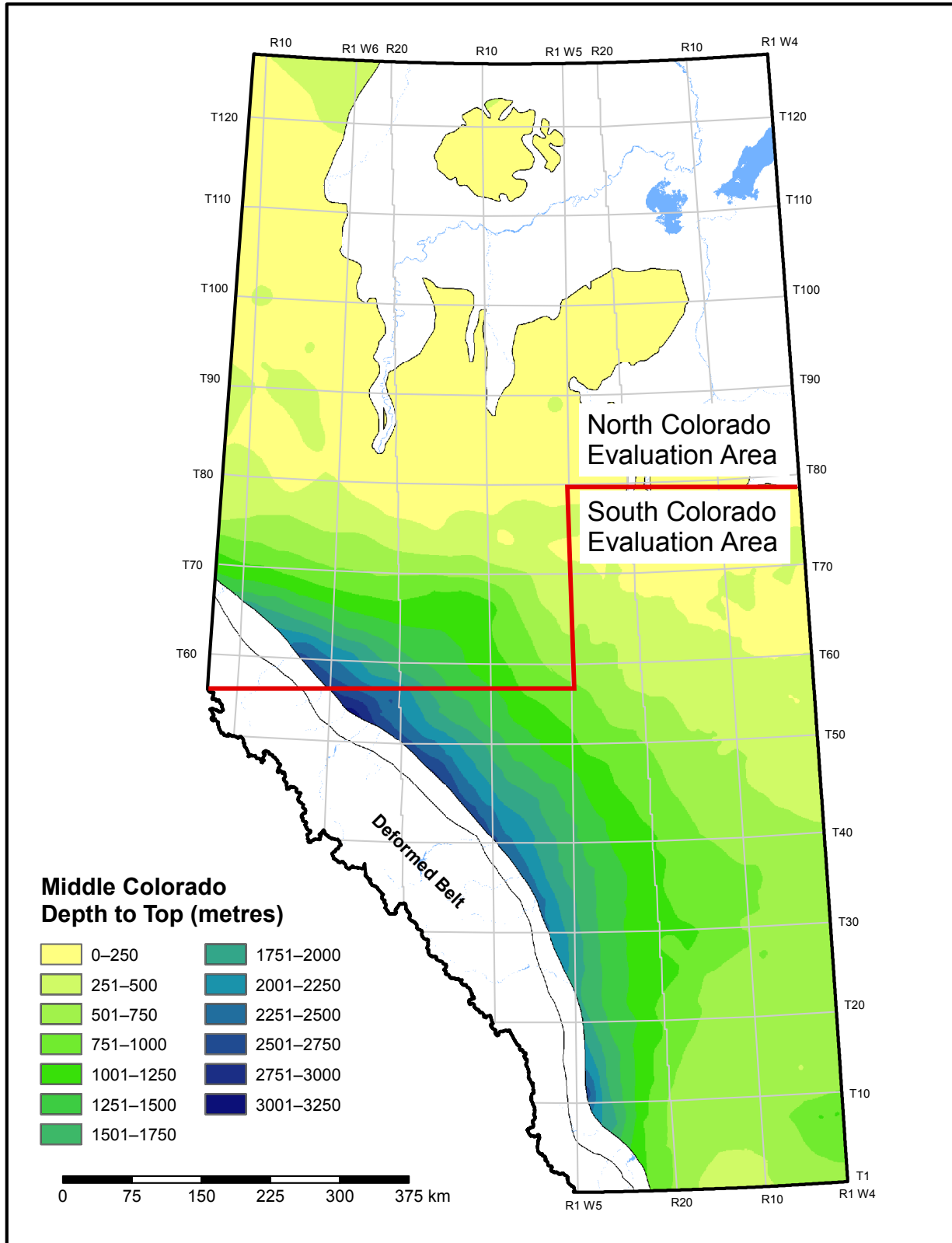


Figure 2.8.3b. Depth to the top of the middle Colorado unit.

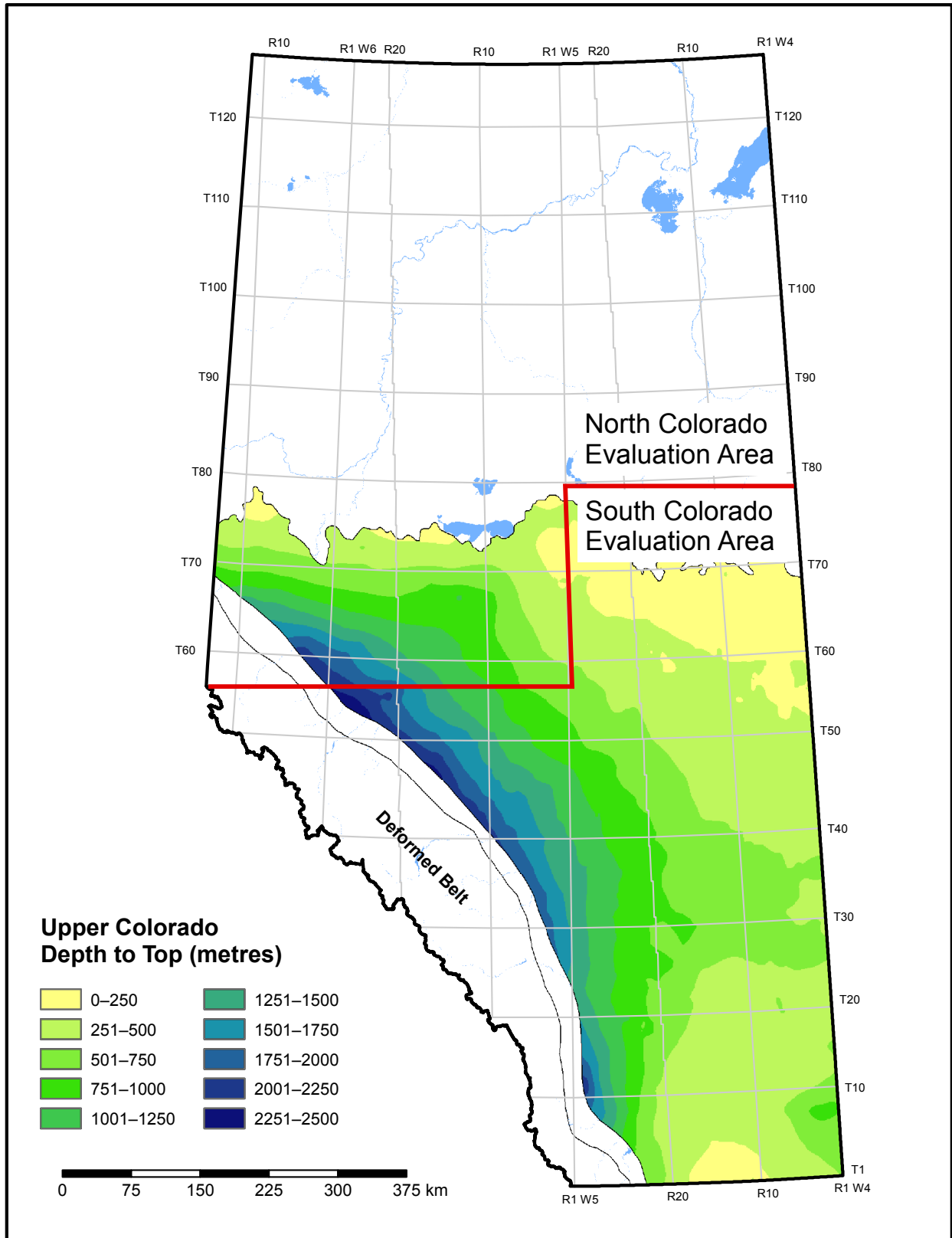


Figure 2.8.3c. Depth to the top of the upper Colorado unit.

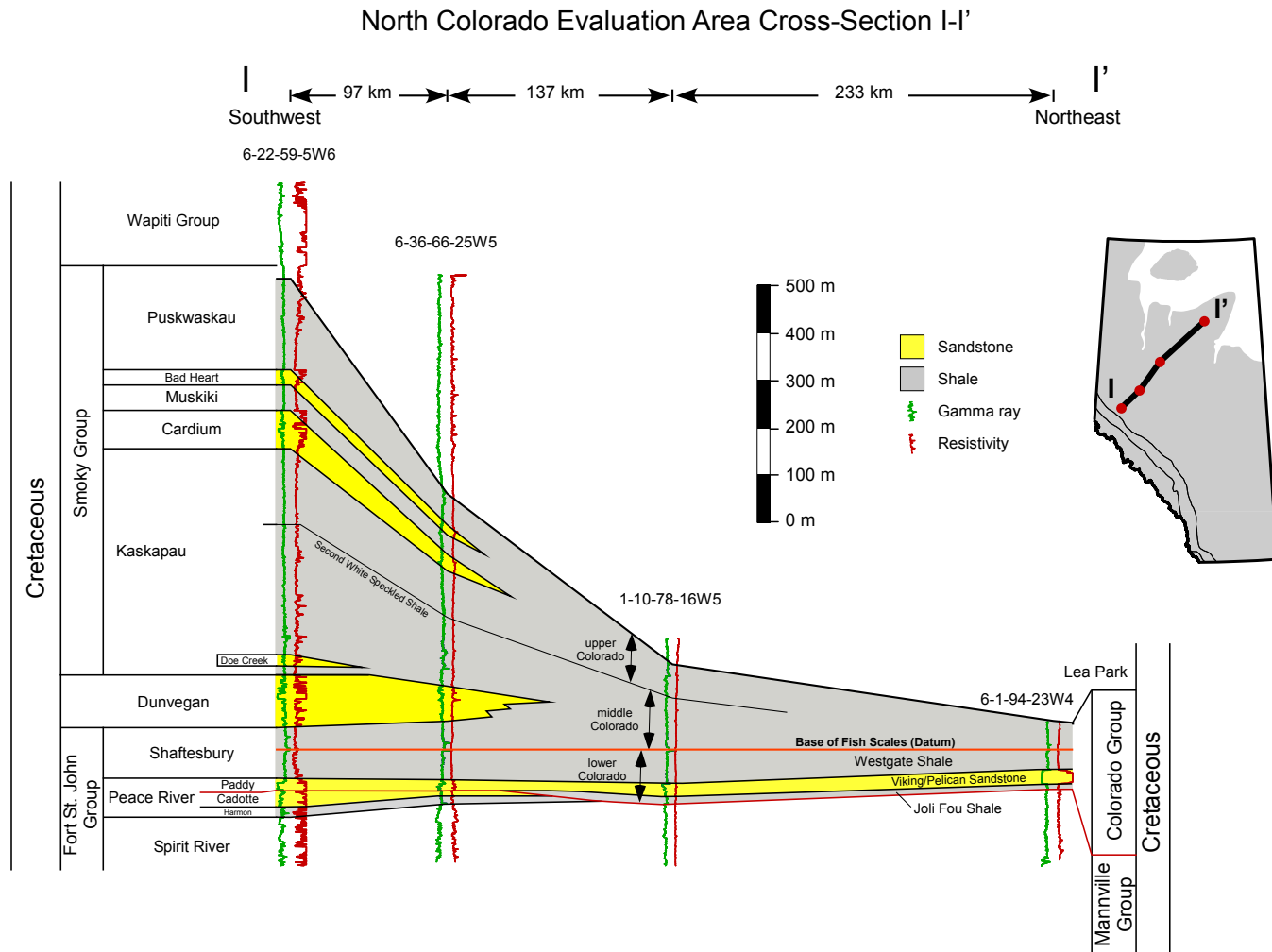


Figure 2.8.4. Stratigraphic cross-section I-I' of the Colorado Group in the north Colorado evaluation area (see inset map for location). We created the informal upper, middle, and lower Colorado subdivisions for resource calculation.

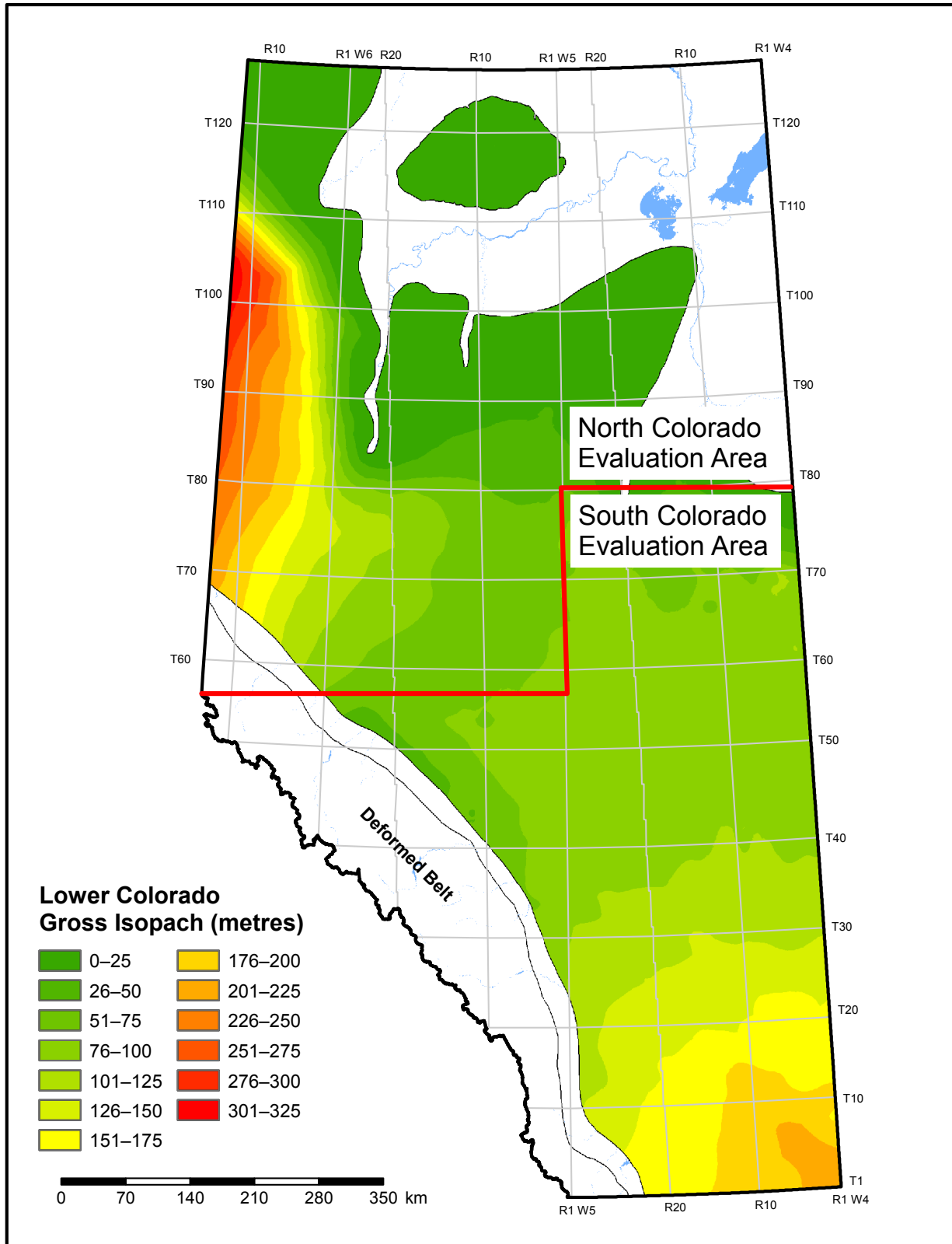


Figure 2.8.5. Gross isopach of the lower Colorado unit.

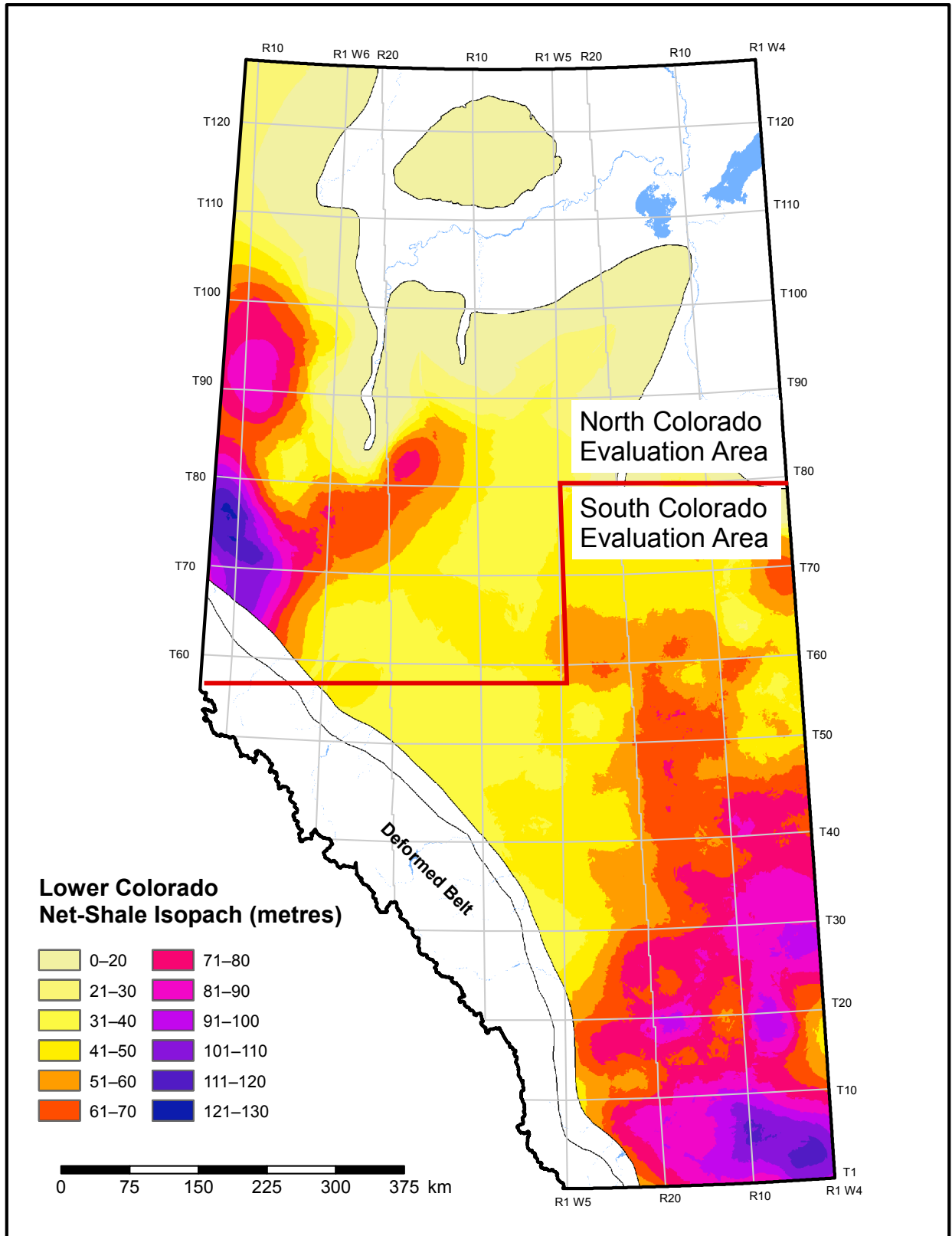


Figure 2.8.6. Net-shale isopach of the lower Colorado unit.

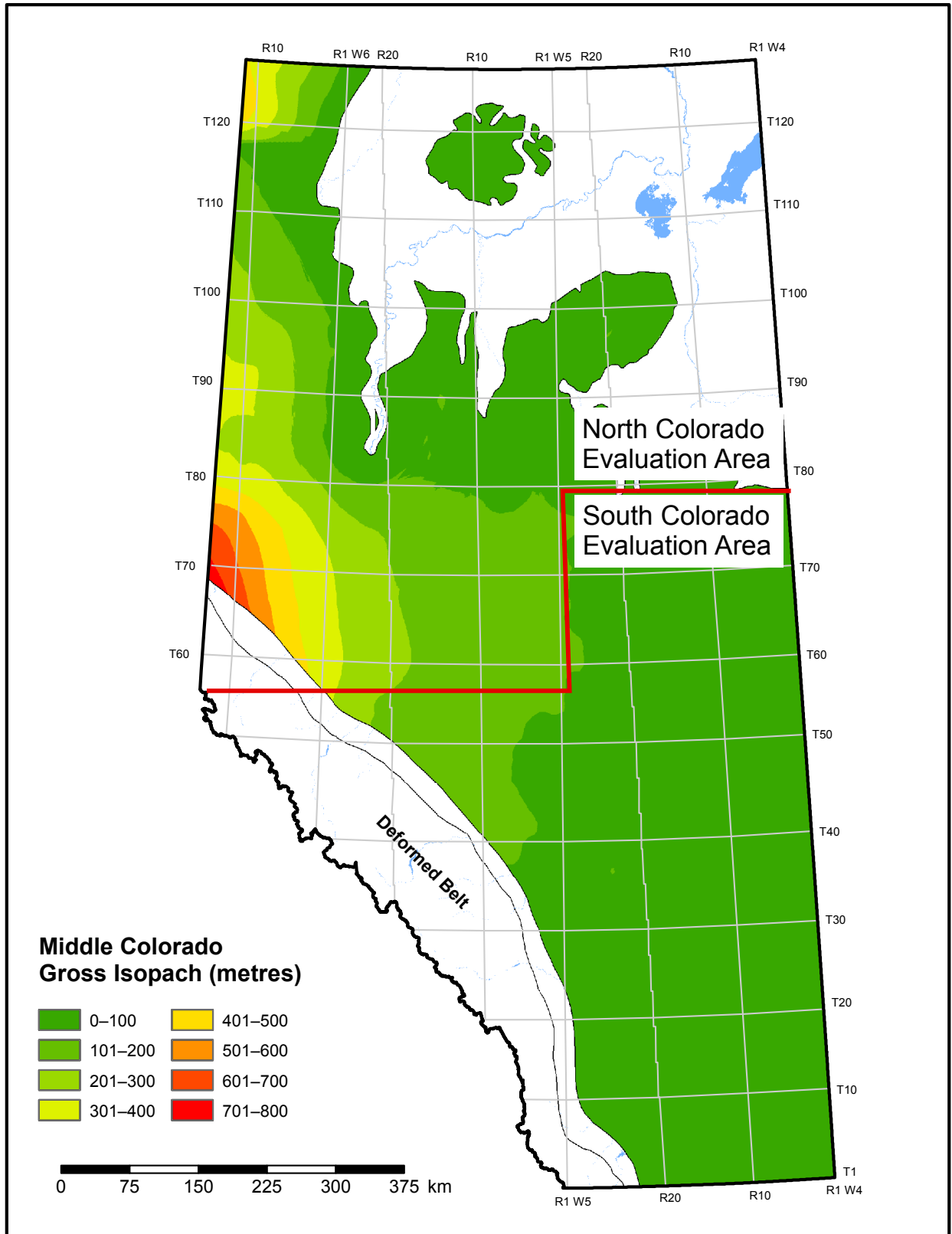


Figure 2.8.7. Gross isopach of the middle Colorado unit.

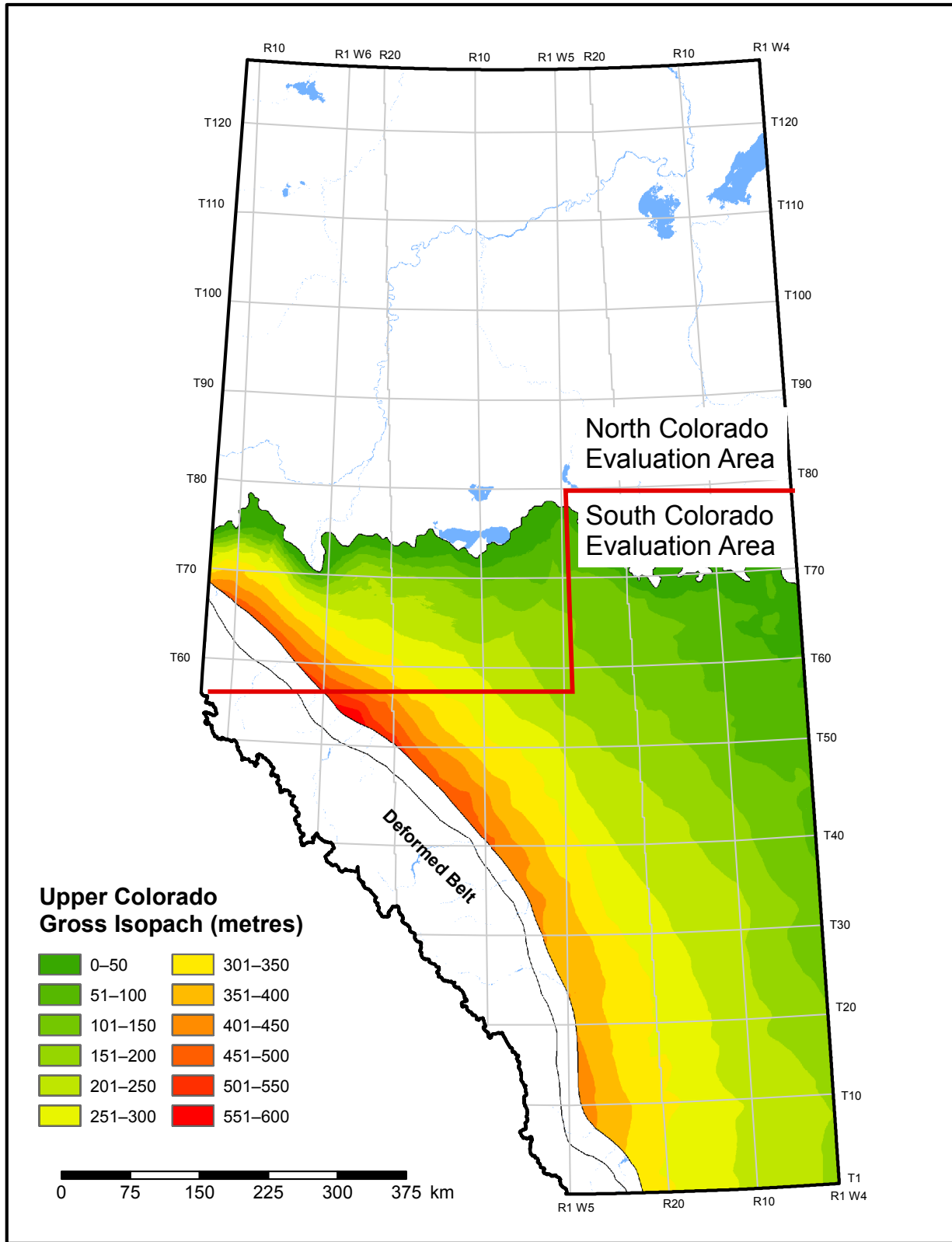


Figure 2.8.8. Gross isopach of the upper Colorado unit.

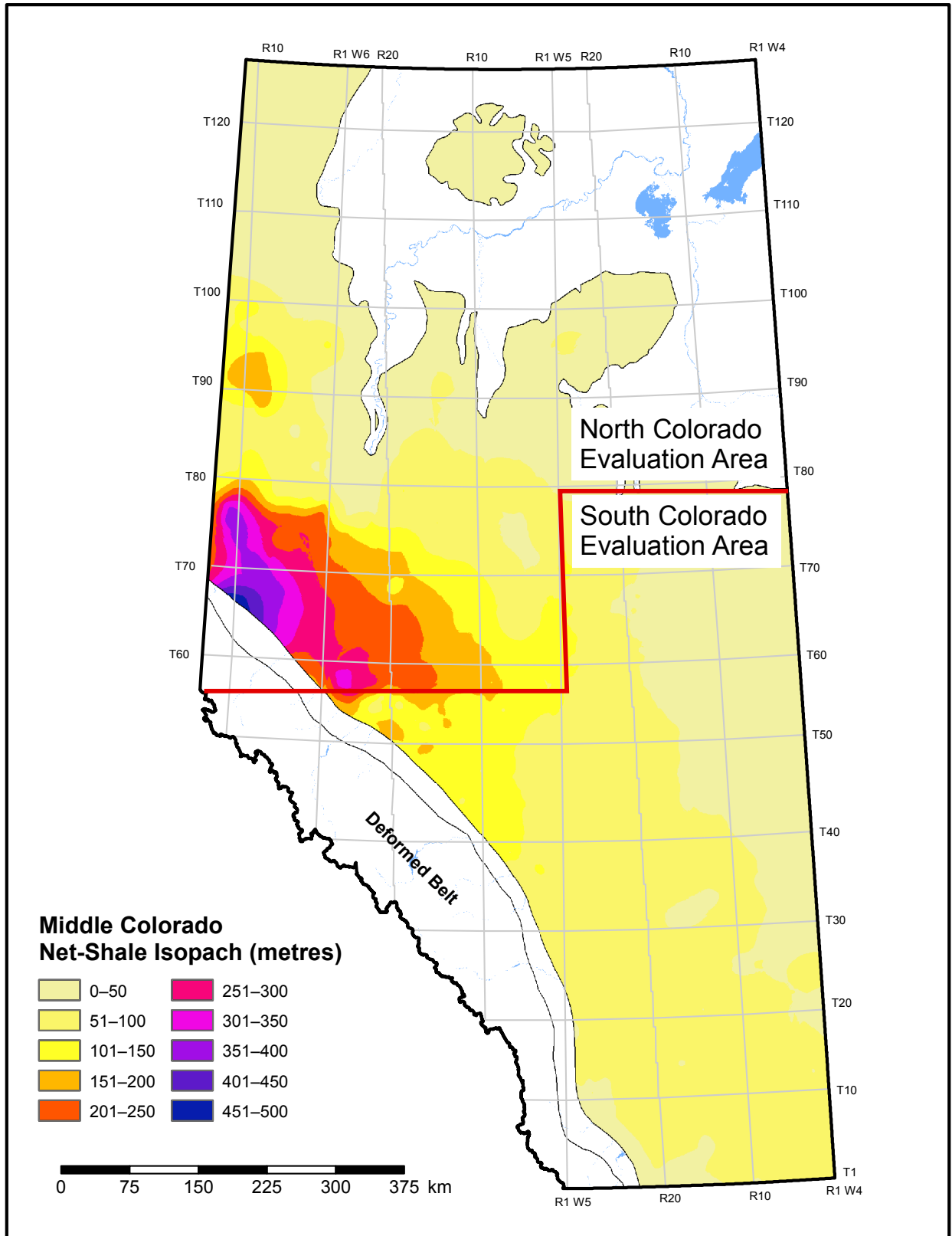


Figure 2.8.9. Net-shale isopach of the middle Colorado unit.

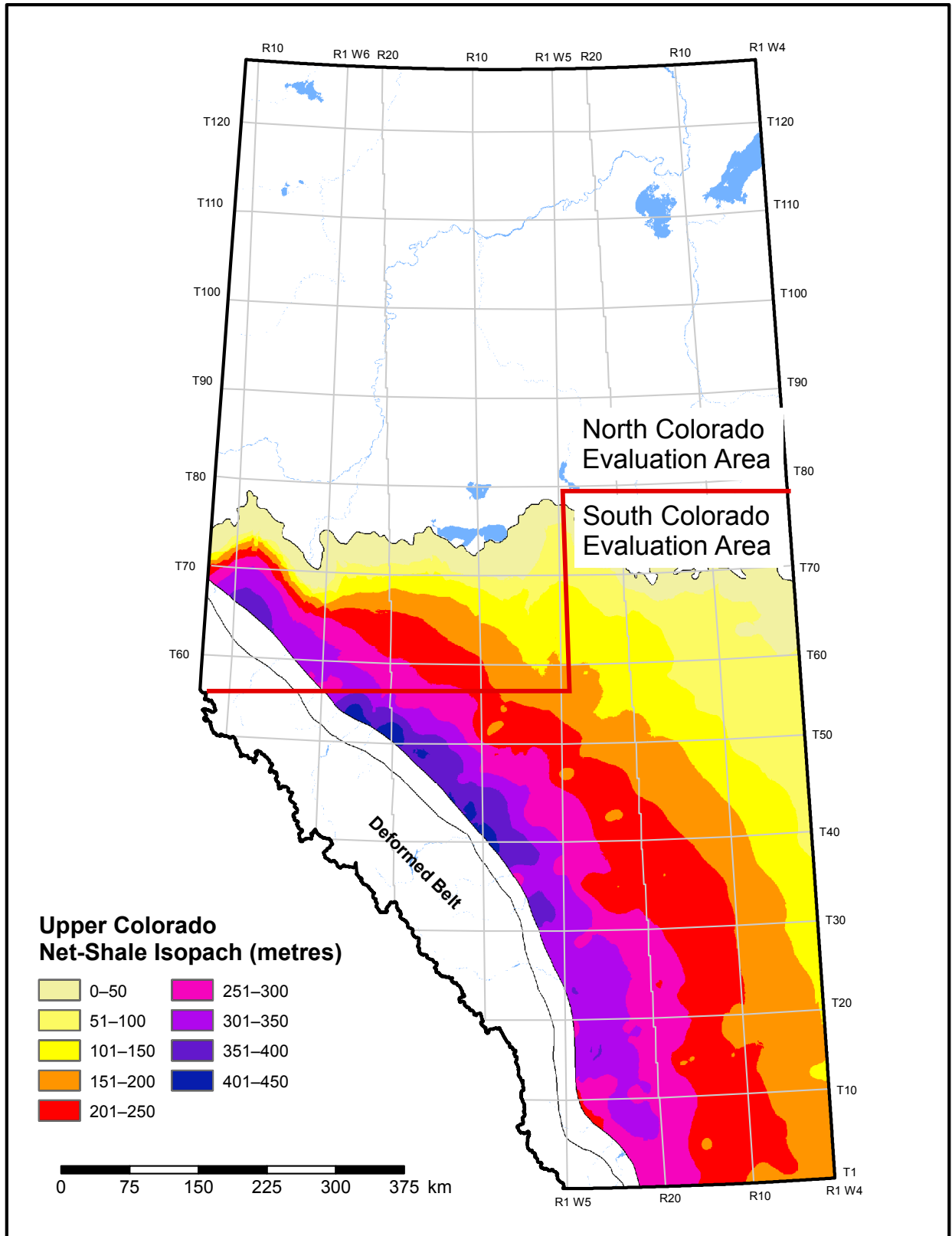


Figure 2.8.10. Net-shale isopach of the upper Colorado unit.

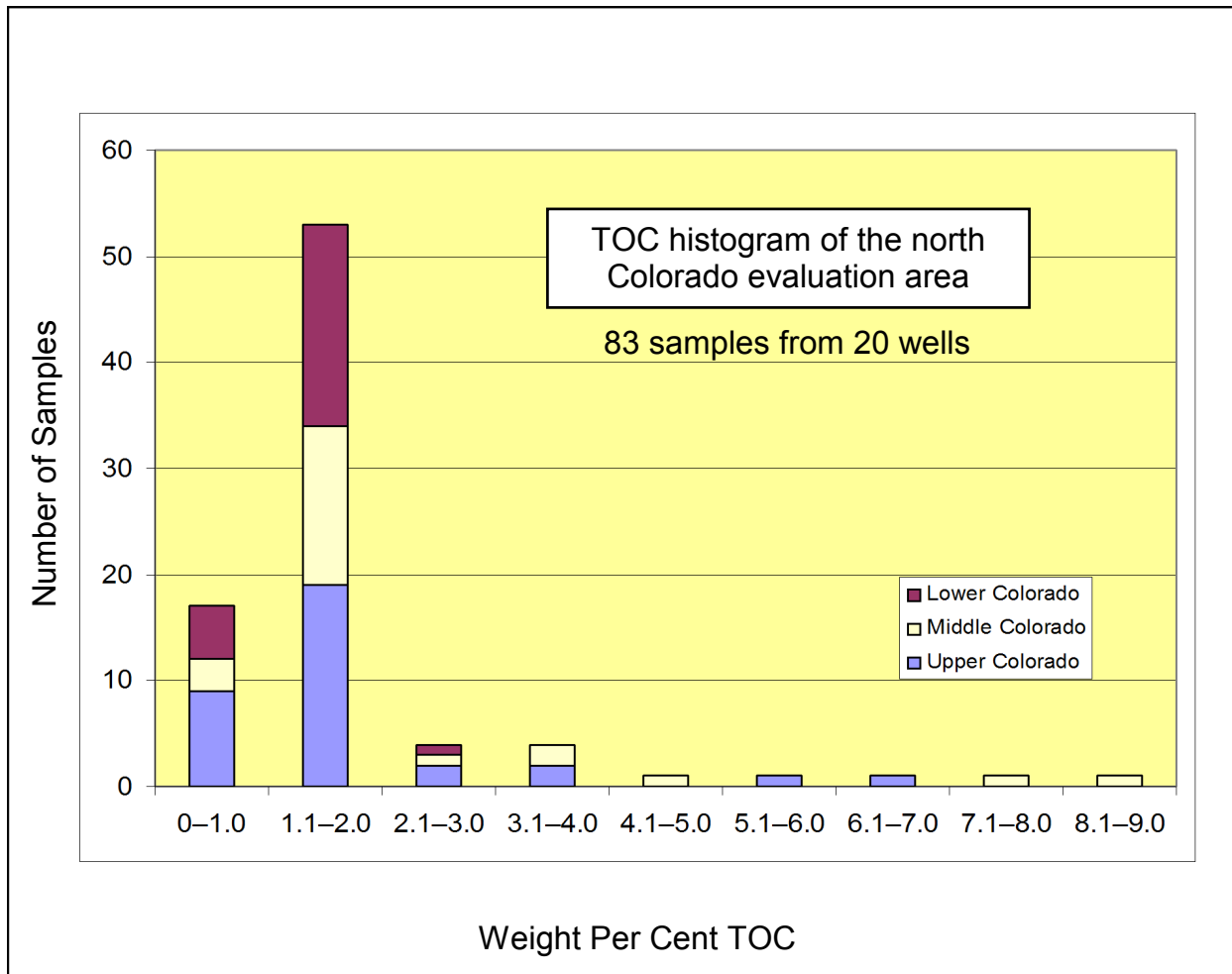


Figure 2.8.11. Histogram of total organic carbon (TOC) of 83 samples from the Colorado Group in the north Colorado evaluation area.

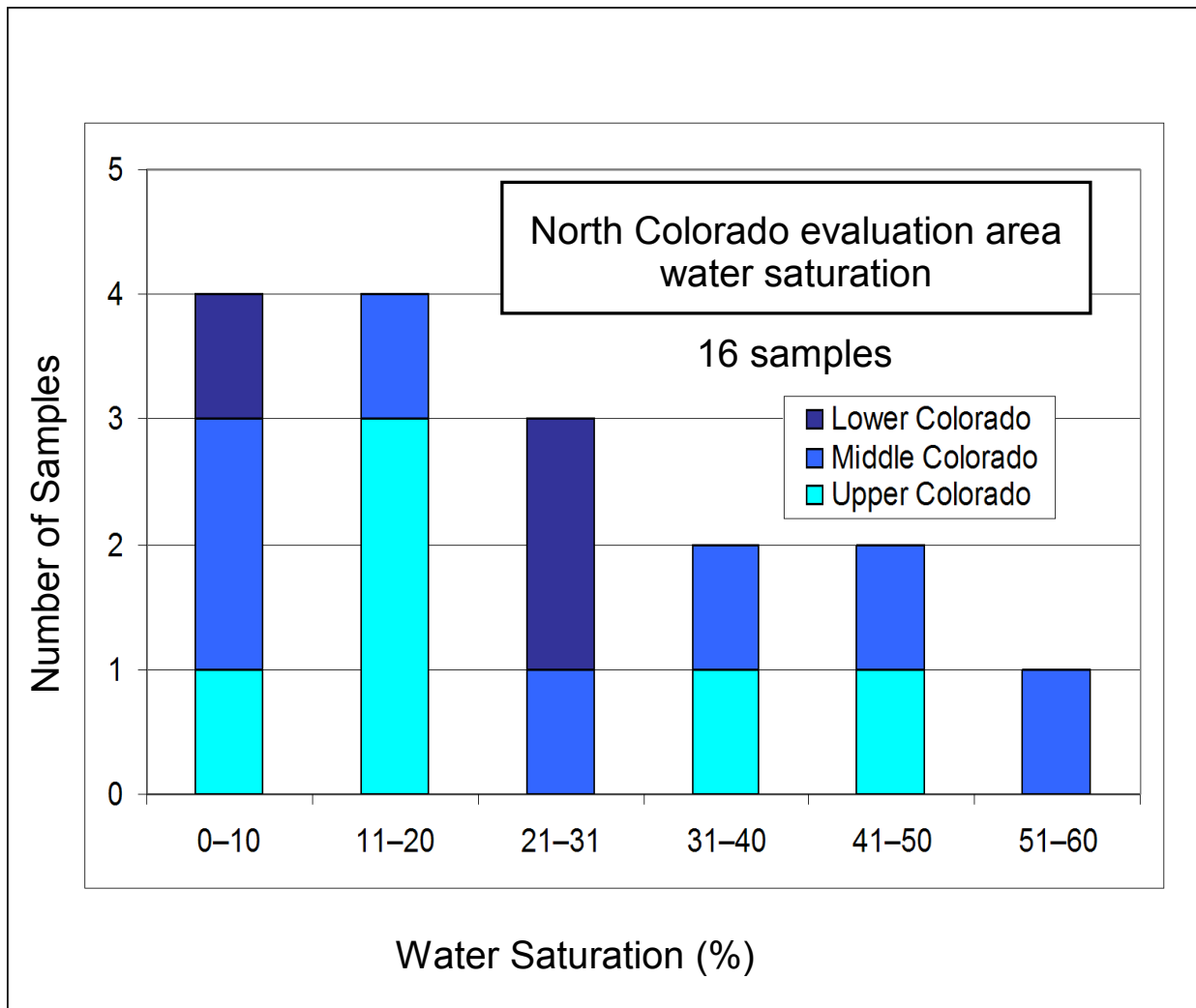
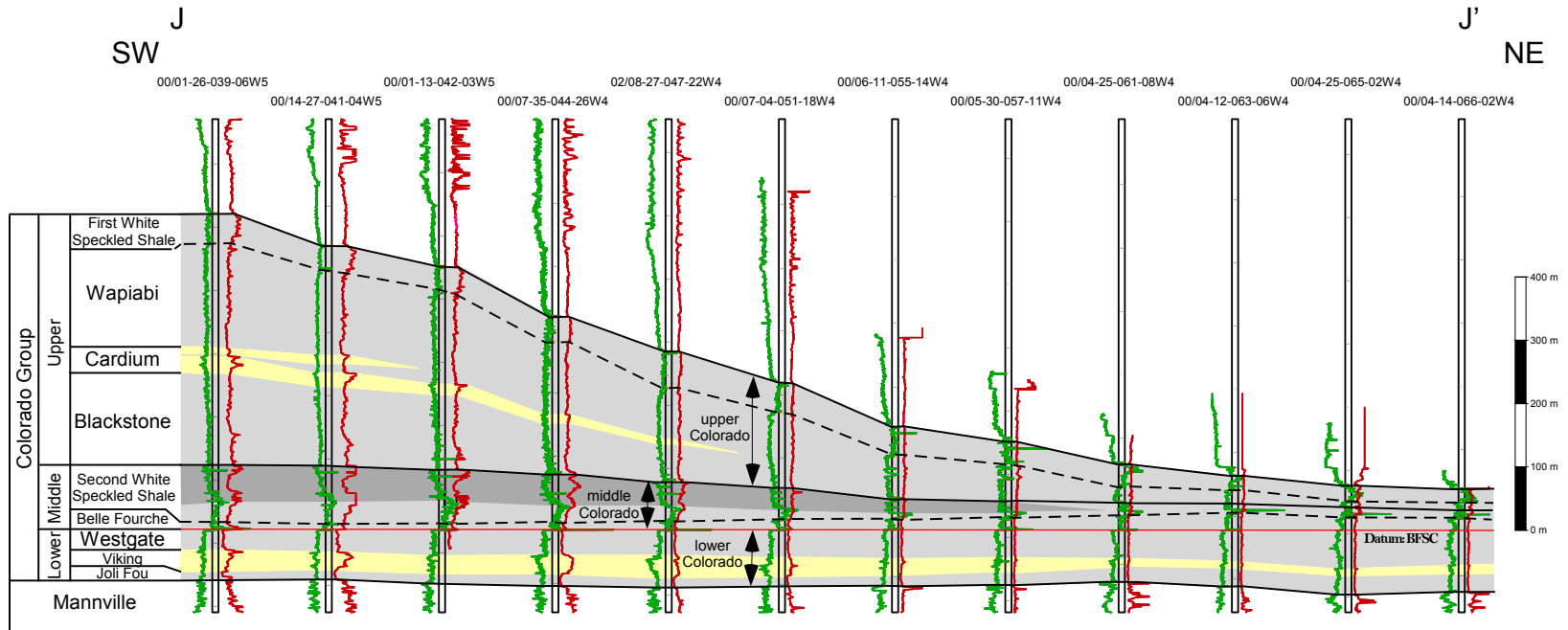


Figure 2.8.12. Histogram water-saturation analysis results for 12 Colorado samples from the north Colorado evaluation area.

# South Colorado Evaluation Area Cross-Section J-J'



- Sandstone
- Shale and siltstone
- Calcareous shale
- Gamma ray
- Resistivity

Figure 2.8.13. Stratigraphic cross-section J-J' of the Colorado Group in the south Colorado evaluation area (see inset map for location). We created the informal upper, middle, and lower Colorado subdivisions for resource calculation.

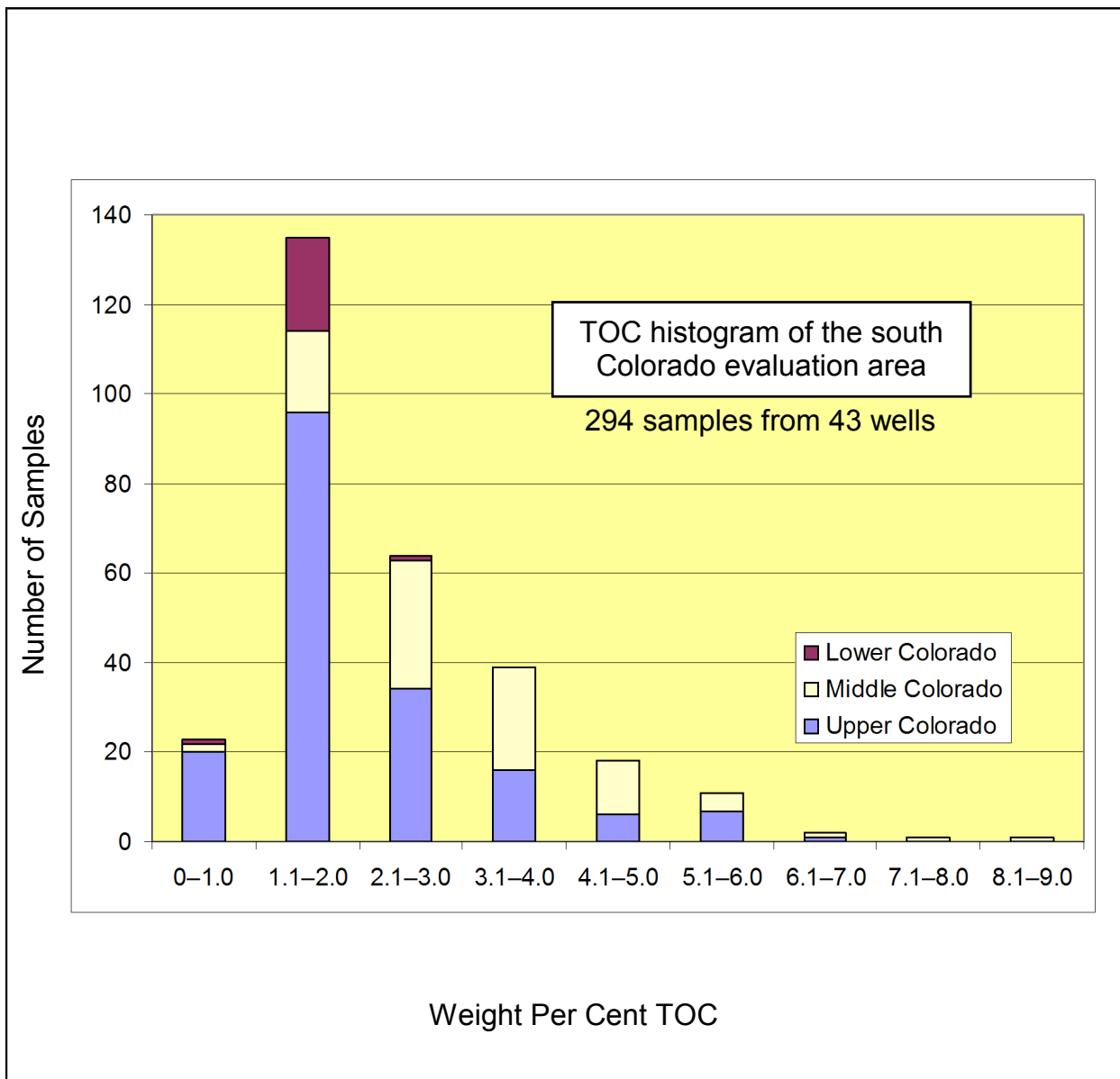


Figure 2.8.14. Histogram of total organic carbon (TOC) of 294 samples from the Colorado Group in the south Colorado evaluation area.

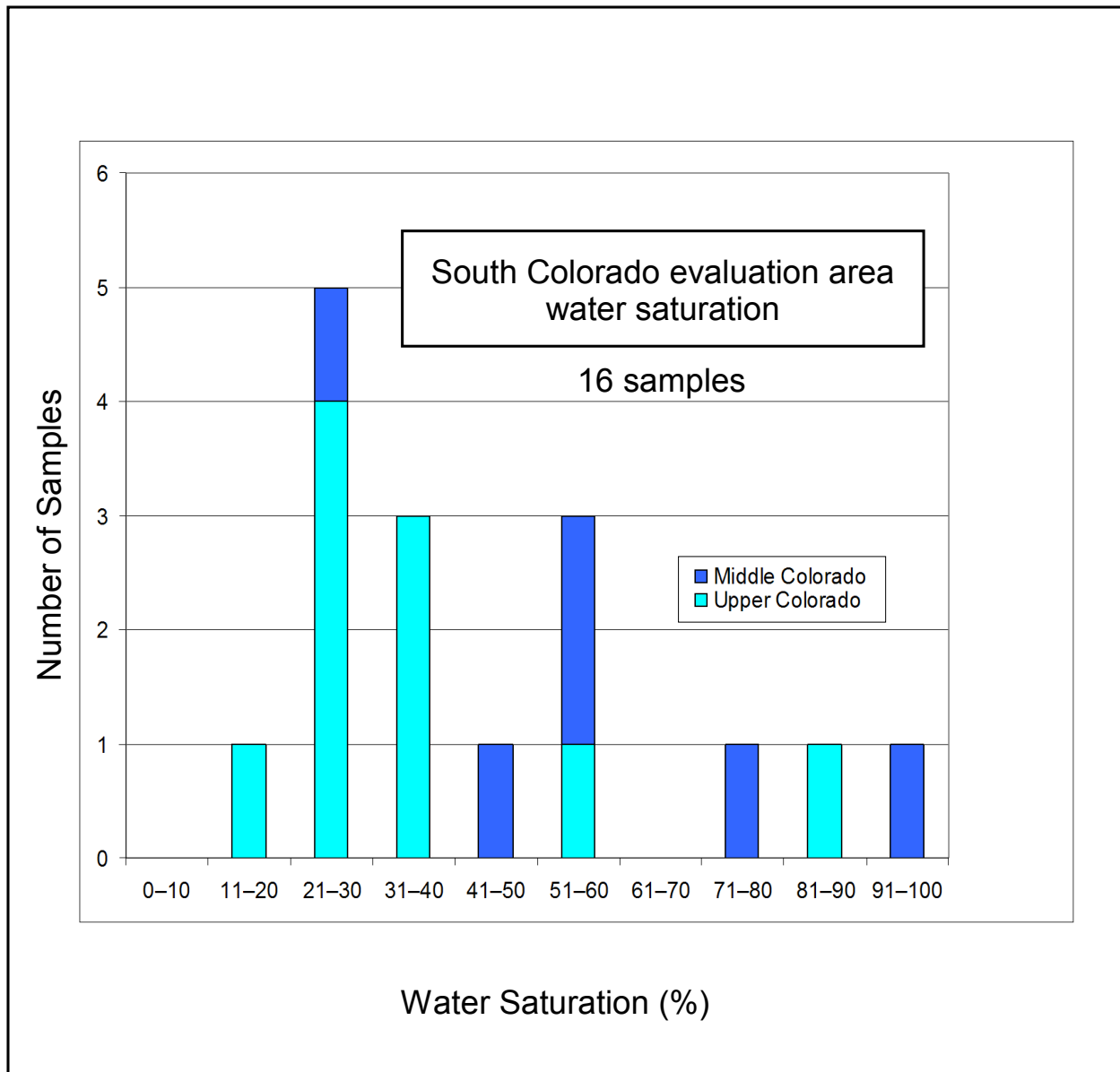


Figure 2.8.15. Histogram of water-saturation analysis results of 16 Colorado Group samples from the Middle and Upper Colorado in south Colorado evaluation area.

### 3 Summary of Resource Variables Common to Each Assessed Unit: Methodology, Assumptions, and Sources of Errors

#### 3.1 Reservoir Pressure, Temperature, Gas Compressibility, and Oil Shrinkage Factor

Reservoir conditions (pressure and temperature) and fluid properties (gas compressibility and oil shrinkage factor) have a major effect on the storage potential of a hydrocarbon reservoir. These variables are normally determined by well tests. All of the units we evaluated had very few wells with well-test data, except for the Montney. For our resource assessment, we used well-test data from conventional reservoirs that adjoin each of the assessed units. For example, for our Duvernay resource assessment, we used data from Swan Hills Formation wells, which have been producing since the 1950s from reefs directly underlying the Duvernay shale.

Table 3.1.1 lists the units from which we collected well-test data to determine resource parameters for each of our assessed units. In all cases, we collected initial pressures and temperatures from hydrocarbon pools within the adjoining units. We then applied the extrapolated data to our assessed units. The pressures used are generally at or slightly lower than the regional pressure gradient. Industry evidence (e.g., investor reports, oil and gas bulletins, and convention presentations) indicates that many organic-rich shale units may be overpressured. However, the scarcity of data severely limited our ability to make such a determination in this study. If one of the units listed in this report is overpressured, then our assessment will underestimate the resource endowment for that unit.

**Table 3.1.1. Adjoining units and their stratigraphic relationships.**

Resource Assessment Unit	Adjoining Unit	Stratigraphic Relationship to Assessed Unit
Duvernay	Swan Hills Formation	Underlying
Muskwa	Slave Point and Sulphur Point formations	Underlying
Montney	Montney Formation	Equivalent
Basal Banff/Exshaw	Wabamun Group	Underlying
North Nordegg	Nordegg Member	Equivalent
Wilrich	Bluesky Formation	Underlying

#### 3.2 Thermal Maturity, Liquid Distribution, and Gas-Oil Ratios

The petroleum-generation window (represented by vitrinite reflectance [%  $R_o$ ]) for oil-prone kerogen ranges from 0.5%  $R_o$  to about 0.8%  $R_o$  at peak generation, with gas generation occurring above about 0.9%  $R_o$  (modified from Peters and Casa (1994) and Baskin (1997)). Below 0.8%  $R_o$ , organic matter is relatively immature, but oil and gas generation may occur dependent, in part, on the type of organic matter. Our upper cutoff point for resource evaluation is 0.8%  $R_o$ , which is conservative and may be modified later for individual units as resources are discovered. In this report, we are not evaluating thermally immature areas for hydrocarbon potential, nor are we estimating the potential for biogenic-gas accumulation in any of the assessed units.

The gas-oil ratio (GOR) of the assessed units in each Alberta Township System section was calculated based on each section's modelled thermal maturity (%  $R_o$ ). Table 3.2.1 lists the GOR and vitrinite reflectance ranges used to identify the hydrocarbon-generation zones for all assessed units. The GOR was linearly interpolated within the vitrinite reflectance ranges.

**Table 3.2.1. Hydrocarbon-generation zones (Danesh, 1998), gas-oil ratios (Danesh, 1998), and vitrinite reflectance (modified from Peters and Casa (1994) and Baskin (1997)).**

Gas-Oil Ratio (m <sup>3</sup> /m <sup>3</sup> )	Zone	Vitrinite Reflectance (% $R_o$ )
Infinity (i.e., no oil)	Dry Gas	>1.35
Infinity (i.e., no oil)	Wet Gas	1.20–1.35
570–10 000	Condensate	1.00–1.20
310–570	Volatile (Gassy) Oil	0.85–1.00
0–310	Black Oil	0.80–0.85
0 (i.e., no gas)	Immature	<0.80

### 3.3 Water Saturation

In shale, organic matter, minerals, pores, microlaminae, and microfractures are distributed heterogeneously. The amount and distribution of formation water (i.e., water saturation) in shale is equally heterogeneous because the rock is composed of components that are hydrophobic (organic matter) and hydrophilic (clays), and the volumetric contribution of these components, and other minerals, may be vertically and laterally variable at the laminar scale. Contributing to the complexity of shale water saturation, open microfractures may be either water-wet or oil-wet, whereas capillary pores, if present, are presumably filled with water.

Water saturation at the laminar scale cannot be determined by the current resolution of log analysis. Nonetheless, allowing for the differences in resolution, we can compare geophysical well-log data and laboratory saturation data. As individual log analysis on thousands of wells for each unit was outside the scope of this study, we determined that laboratory data from Dean Stark analysis and helium pycnometry would contribute the major component of water-saturation data for our resource analysis.

Using Dean Stark analysis and helium pycnometry, the laboratory calculated water saturation for some samples. The data reflect the saturation over about a 10 centimetre interval. If the sample interval is composed of interlaminated strata with variable mineral and/or organic components, then the actual saturation profile of the sample at the laminar scale will be variable. Our results give an average of the interval sampled.

We used cores of a variety of ages for sampling water saturation. We assumed that invasion and contamination of drilling fluid into the cores was minimal. Furthermore, evaporation from the cores may have occurred during retrieval and storage, but because the permeability of most shale is extremely low, we assumed that the degree of evaporation was low. Presumably, evaporation would have occurred primarily from the outer edges of old cores due, in part, to the presence of induced microfractures.

Our method of determining water saturation involved graphing the Dean Stark data to determine the high and low distribution extents that approximate P10 and P90 values. These are illustrated in the water-saturation histograms in Section 2. However, actual water-saturation values may differ.

For example, depth of burial will influence saturation, since water is lost during the conversion of smectite to illite. Hence, more deeply buried and more mature shale may be relatively dry compared to shale at shallower depths. Furthermore, additional gas may be generated by migration or water reforming and Fischer-Tropsch-like reactions (Tang and Xia, 2011), resulting in lower water saturation and higher hydrocarbon storage capacity, as well as possible overpressure in the most mature parts of the study area.

### 3.4 Grain Density and Porosity

Our task in determining porosity was to find a method that can be used to batch-process thousands of geophysical well logs. The difficulty was that any geophysical well-log cutoffs or variables that we used must be applicable over a wide depth range.

To generate a consistent grain density for log analysis and determination of porosity, we used mineralogical data from X-ray diffraction reconciled with X-ray fluorescence data for each sample and converted mineral weight per cent to volume. Total organic carbon (TOC) was converted to kerogen and was included as a mineral component. TOC was converted to kerogen using a conversion factor of 1.2. The conversion factor was used to add the weight of the elements that bond with carbon (e.g., oxygen and hydrogen) to form kerogen and extractable organic matter (i.e., hydrocarbons) in the original sample. Extractable organic matter is normally a very small component (<1%) of the TOC. The conversion factor assumed that the average carbon content of kerogen was about 80%, with the remaining 20% comprising other elements. Furthermore, the conversion factor assumed that all of the carbon in our TOC data was organic. The average content of carbon in hydrocarbons (by atomic weight) varied between 75% and 95%.

In our methodology, a common mineral density was obtained from Mindat.org (Ralph and Chau, 1993) or Herron and Matteson (1993). If a range of grain densities for the mineral was published, we used an average of the values. Kerogen density can range between 1.0 g/cm<sup>3</sup> to 1.5 g/cm<sup>3</sup> and increases with thermal maturity (Tissot and Welte, 1984). We used a density of 1.35 g/cm<sup>3</sup> for kerogen. A grain density was calculated for each sample with kerogen incorporated as a mineral. We then obtained a high, low, and average value for all samples from a given unit.

Since we used the density-porosity log to determine porosity, the presence of organic matter resulted in the density-porosity log reading a higher total porosity than may have been present. By using a grain density with the kerogen (TOC) as a mineral, we reduced the effect of the organic matter on the density-porosity log. However, organic-matter content may be variable within the shale or siltstone sequence, either higher or lower than the value we used, so our method of bulk processing logs cannot account for the variability. If the variability was reasonably constrained, the method worked quite well. The method did not work as well when more pronounced variability was particularly evident, such as in the north Nordegg, for which the TOC can vary from <5.0 wt. % to nearly 30.0 wt. %, and in the basal Banff/Exshaw, where it varies from 1.0 wt. % to about 20.0 wt. %.

To illustrate the influence of TOC content on our porosity determination, we offer the following example:

Sample 9311 from the Duvernay has a laboratory-determined TOC content of 3.73 wt. %. For this sample, we calculated a grain density of 2.745 g/cm<sup>3</sup> without kerogen as a mineral and 2.545 g/cm<sup>3</sup> with kerogen as a mineral. If we use the latter value to derive porosity from geophysical well logs for an interval for which the actual TOC content is 10.0 wt. %, a porosity of 9.6% is calculated. However, the actual porosity is zero because of the influence of the TOC. A grain density of 2.402 g/cm<sup>3</sup> would be needed to derive the true porosity of zero per cent. Hence, we are assigning resources to an interval for which there are no resources.

In summary, the porosity determination methodology that worked for many of the units in our assessment will not work on the basal Banff/Exshaw interval, the north Nordegg, and perhaps part of the Colorado Group.

Furthermore, in the case of the basal Banff/Exshaw, north Nordegg, and Colorado, analysis results for many of the samples sent for mineralogy and TOC analysis have not yet been received; therefore, the interpretations and evaluations for these units are preliminary. For these units, we used the few samples we had available to determine grain density and porosity. When all of the laboratory data are received, we will regenerate the grain density and porosity data, perform log analysis if needed, and rerun the assessment to obtain a refined estimate of resources.

Once porosity was derived and modelled for each unit, we applied a further level of uncertainty analysis by applying a formula that modified the modelled porosities. The formula calculated the equivalent porosities for different grain densities, with a range determined from our methodology, with specified uncertainty distributions.

### **3.5 Regional TOC Determination and Adsorbed Gas**

Total organic carbon was determined from Rock Eval™ pyrolysis on 2375 samples. The TOC data represent convertible hydrocarbons and a residual fraction of oxidized dead carbon. However, if any residual oil or gas is trapped in the sample, the amount of TOC will be overstated, resulting in an overstatement of the amount of adsorbed gas measured in the sample. Due to the insufficient geographic density of TOC data available, we used geophysical well logs to calculate TOC using the method described in Passey et al. (1990) (Passey method).

As there are more geophysical well logs available than core sample data, we applied the Passey method to calculate TOC from geophysical well logs using a sample rate of 0.125 m. This provided sufficient data to create a regional view of TOC distribution of each unit. To verify our calculated TOC data, we compared them with the laboratory-determined TOC data. For the Montney, the Passey method worked well, but it did not work well for the Duvernay and Muskwa. Therefore, we developed a modified Passey method that combines the Passey method for calculating TOC from geophysical well logs with the TOC calculated from the uranium content derived from the spectral gamma-ray logs. These data were more comparable to the laboratory-determined data.

Although we confirmed that the Passey and modified Passey methods provided results comparable to the laboratory-determined data, the Passey method was developed to analyze rocks in the oil-maturity window. Therefore, using this methods for rocks that are relatively over-mature will result in an overestimation of TOC (Passey et al., 2010) and an overestimation of adsorbed gas. In addition, the Passey method is time consuming because each well must be evaluated individually. Therefore, for this report, we evaluated the Duvernay (213 wells) and Muskwa (503 wells) using the modified methods and evaluated the Montney (439 wells) using the Passey method. We did not use either method for the basal Banff/Exshaw, north Nordegg, and Wilrich.

For the basal Banff/Exshaw, north Nordegg, and Wilrich, we used the TOC data from our analyses and assumed that the values were representative of the average for the unit in the specific well. The TOC data were plotted and geostatistically modelled to create a map of regional TOC distribution. With this map, we determined the adsorbed gas content using the relationship of Langmuir volume and Langmuir pressure versus TOC.

Since TOC may vary vertically and laterally within a unit, the assumption that the TOC values from laboratory analyses are representative of the average for the unit may have affected our resource determination for the basal Banff/Exshaw, north Nordegg, and Wilrich. Therefore, the resource evaluation of these units is preliminary. We will re-evaluate these units using either the Passey or modified Passey method for a future report. Although adsorbed gas forms a much smaller portion of the total resources in each unit than free porosity does, we still expect an improvement in the resource assessment and uncertainty values after applying the method.

## 4 Resource Estimation Workflow

We developed a workflow for estimating the resource endowment in unconventional petroleum accumulations, such as shale gas. The workflow is data-driven and incorporates the concept of uncertainty at every step to quantify the wide range of possible values for resources. This workflow is geared towards early appraisal of unconventional resources, and we used it to determine petroleum initially-in-place without addressing whether these resources are technically or economically recoverable. The following summarizes our workflow.

The first step of the workflow was to map the variables, on a section-by-section basis, that have sufficient data density to justify mapping. These variables included depth to the top of the unit (from subsurface picks), the net-shale thickness (from gamma-ray logs using an appropriate cutoff value), and the average porosity of the net shale (from density-porosity logs). The Duvernay, Muskwa, and Montney formations had sufficient geophysical well-log coverage to allow in-depth log analysis to calculate the TOC. This provided enough data to determine the spatial distribution of the TOC. We also mapped the vitrinite reflectance of the units to represent thermal maturity. In most cases, there was a strong correlation between depth of burial and maturity. The mapping methods used geostatistical algorithms (Deutsch, 2002) to calculate estimates and to quantify the uncertainty in the maps.

The second step of the workflow was to determine variables, on a section-by-section basis, that correlated to the mapped variables that also had sufficient data to quantify the relationship. These variables included

- pressure and temperature as functions of depth,
- gas compressibility and oil shrinkage factor as functions of pressure as calculated above, and
- Langmuir volume and Langmuir pressure as functions of TOC.

Most of these relationships used simple linear regression in the modelling, with the uncertainty in the slope and intercept calculated from the empirical data.

The third step of the workflow was to determine the values of the variables that had insufficient data to accurately map them or that had data that were dependent upon other variables. We used the average of the data for these variables over the entire area for each assessed unit. These variables included water saturation, condensate-gas ratio, grain density, and, for some units, TOC. We calculated distributions of these variables and then applied the distributions as average values across the entire unit.

The final step of the workflow was to determine the uncertainty. Once we determined the variables for each unit, either on a section-by-section basis or on average over the whole unit, we used the Monte Carlo simulation in the @RISK software program to calculate the range of uncertainty for the total resource endowments. This method selects a random value from the distribution of each variable and then combines

all of the values to produce a resource estimate. By repeating this procedure (1000 iterations in our analysis), the uncertainties in all of the individual variables were combined to define the uncertainty in the resource estimates. Each resource estimate is summarized by a P50 value, which is considered to be the best estimate because it minimizes the expected variance from the unknown, true value. The range of uncertainty is summarized by the P90 (low estimate) and P10 (high estimate) values. These are read as, we are 90% certain there is at least as much resource as the P90 value, and there is a 10% chance there is at least as much as the P10 value.

Future work will allow us to improve the estimates for individual variables. Once more of the laboratory analyses are completed, the mapping part of the workflow can be expanded to include other variables, with a consequent refinement of existing maps. The relationships between variables can be better quantified and other relationships can be explored. Some examples of this future work include

- applying Rock Eval™ pyrolysis data to improve the adsorption isotherm data,
- performing additional log analysis to provide more TOC data for mapping, and
- obtaining additional Dean Stark analyses allowing us to build a relationship between porosity and water saturation.

Results and interpretation from geochemical analysis conducted in this study are summarized in a consultant report (Appendix). This report integrates organic geochemistry with geology and thermal maturation data, obtained for this study, to characterize the source-rock potential of the Montney/Doig, Banff/Exshaw, and Duvernay/Muskwa units.

## 5 Summary of Shale- and Siltstone-Hosted Hydrocarbon Resource Endowment

In the following sections, we provide overviews of the resource assessment for the units investigated in this study. The results are summarized in tables and illustrated in maps accompanying each section. The resource endowment for each assessed unit has an associated P90 (low estimate), P50 (medium estimate), and P10 (high estimate) value for natural gas, natural-gas liquids, and oil, with a map for each of these levels of uncertainty.

The areas on each map showing where the resources are highest are reasonably representative of the most prospective area within the unit that is likely to be drilled first. Given the present level of industry activity, some of the most prospective areas may have already been drilled. In the future, we will compare our resource maps and estimates with new drilling and production activity.

In all cases, we attempted to use reasonable input variables (guided by scientific analyses), which in many cases were similar to public records from industry, investment houses, or Canadian public institutions. The endowment values are most sensitive to areal extent, thickness, and porosity. Therefore, if any one of these is large, then the endowment values will follow in a similar manner.

**If a single value is required as a quote for an assessed unit, we recommend using the medium value (P50) in all cases.**

## 5.1 Explanation for Preliminary Hydrocarbon Resource Endowment Status

The assessments of the basal Banff/Exshaw, north Nordegg, and Wilrich must be classified as preliminary for the following reasons:

- Results are outstanding for the mineralogy, thermal maturity, and TOC variables.
- TOC data are highly variable. The variability cannot be adequately modelled in our resource-estimation methodology, resulting in a porous volume that is either significantly too high or too low on a well-by-well basis. To rectify this, we will need to do detailed geophysical well-log evaluation on each well in the unit.

We have not determined the resource endowments for the Rierdon Formation and the Colorado Group for the following reasons:

- The stratigraphic units cover much of Alberta, and the geology is complex. More work is required to properly evaluate the resource parameters.
- Results are outstanding for the mineralogy, thermal maturity, and TOC variables.
- TOC data are highly variable. The variability cannot be adequately modelled in our resource-estimation methodology, resulting in a porous volume that is either significantly too high or too low on a well-by-well basis. To rectify this, we will need to do detailed geophysical well-log evaluation on each well in the unit.

## 5.2 Duvernay Formation Shale-Hosted Hydrocarbon Resource Endowment

Shale-hosted natural gas initially-in-place for the Duvernay ranges from a low estimate (P90) of 353 Tcf to a high estimate (P10) of 540 Tcf, with a medium estimate of 443 Tcf. Shale-hosted natural-gas liquids initially-in-place range from a low estimate (P90) of 7.492 billion barrels to a high estimate (P10) of 16.304 billion barrels, with a medium estimate of 11.320 billion barrels. Shale-hosted oil initially-in-place ranges from a low estimate (P90) of 44.077 billion barrels to a high estimate (P10) of 82.889 billion barrels, with a medium estimate of 61.690 billion barrels. Figures 5.2.1 to 5.2.9 illustrate the shale-hosted hydrocarbon resource endowment estimates on a per-section basis. Tables 5.2.1 and 5.2.2 show the hydrocarbon resource endowment and resource assessment summaries.

**Table 5.2.1. Summary of Duvernay Formation shale-hosted hydrocarbon resource endowment: low, medium, and high estimates.**

Hydrocarbon	Low Estimate (P90)	Medium Estimate (P50)	High Estimate (P10)
Oil (billion bbl)	44.1	61.7	82.9
Natural-Gas Liquids (billion bbl)	7.5	11.3	16.3
Natural Gas (Tcf)	353	443	540
Natural Gas-Adsorbed Gas Content (%)	5.6	6.8	8.5

Table 5.2.2. Summary of shale-hosted hydrocarbon resource assessment of the Duvernay Formation.

Duvernay	Area (km <sup>2</sup> )				Depth (m)				Net-Shale Thickness (m)			
	Low	Medium	High	Mean	Low	Medium	High	Mean	Low	Medium	High	Mean
Dry Gas	8704	9850	11 009	9851	4486	4544	4598	4543	17.7	20.2	24.0	20.8
Wet Gas	3496	5635	7468	5554	3815	3881	3948	3881	16.2	18.7	21.2	18.8
Condensate	7782	5635	14 425	11 150	3347	3423	3504	3424	15.4	17.4	18.5	17.2
Volatile Oil	14 736	11 096	28 915	21 942	2790	2884	2989	2886	13.9	15.3	16.8	15.3
Black Oil	1602	11 345	22 994	11 824	2331	2466	2585	2460	8.7	11.1	12.8	11.0
<b>TOTAL</b>	<b>52 596</b>	<b>59 758</b>	<b>69 183</b>	<b>60 321</b>	<b>3129</b>	<b>3271</b>	<b>3390</b>	<b>3265</b>	<b>14.7</b>	<b>16.0</b>	<b>17.3</b>	<b>16.0</b>
Duvernay	Porosity (%)				TOC (%)							
	Low	Medium	High	Mean	Low	Medium	High	Mean	Low	Medium	High	Mean
Dry Gas	6.69	7.78	8.94	7.79	2.42	2.63	2.91	2.66				
Wet Gas	6.59	7.76	8.90	7.76	2.47	2.66	2.74	2.63				
Condensate	6.71	7.87	8.99	7.87	2.59	2.72	2.88	2.73				
Volatile Oil	6.62	7.78	8.86	7.74	2.57	2.65	2.82	2.68				
Black Oil	6.75	7.93	9.06	7.93	2.31	2.45	2.60	2.46				
<b>TOTAL</b>	<b>6.68</b>	<b>7.82</b>	<b>8.91</b>	<b>7.81</b>	<b>2.55</b>	<b>2.63</b>	<b>2.73</b>	<b>2.64</b>				
Duvernay	Gas (billion m <sup>3</sup> )				NGL (million m <sup>3</sup> )				Oil (million m <sup>3</sup> )			
	Low	Medium	High	Mean	Low	Medium	High	Mean	Low	Medium	High	Mean
Dry Gas	2981	3969	5135	4043	-	-	-	-	-	-	-	-
Wet Gas	1109	1888	2743	1923	219	331	464	339	-	-	-	-
Condensate	2065	3049	4230	3112	885	1458	2213	1530	492	725	1030	745
Volatile Oil	1750	2611	3579	2632	-	-	-	-	4071	6039	8241	6103
Black Oil	119	752	1 516	804	-	-	-	-	402	2791	6210	3133
<b>TOTAL</b>	<b>9934</b>	<b>12 479</b>	<b>15 219</b>	<b>12 514</b>	<b>1190</b>	<b>1798</b>	<b>2589</b>	<b>1869</b>	<b>7004</b>	<b>9803</b>	<b>13 172</b>	<b>9981</b>
Duvernay	Gas (Bcf)				NGL (MMbbl)				Oil (MMbbl)			
	Low	Medium	High	Mean	Low	Medium	High	Mean	Low	Medium	High	Mean
Dry Gas	105 801	140 892	182 244	143 504	-	-	-	-	-	-	-	-
Wet Gas	39 352	67 029	97 354	68 243	1377	2086	2919	2133	-	-	-	-
Condensate	73 306	108 206	150 143	110 474	5573	9183	13 934	9 636	3095	4565	6480	4691
Volatile Oil	62 099	92 678	127 017	93 423	-	-	-	-	25 617	38 001	51 861	38 404
Black Oil	4235	26 690	53 826	28 523	-	-	-	-	2533	17 564	39 076	19 717
<b>TOTAL</b>	<b>352 610</b>	<b>442 913</b>	<b>540 174</b>	<b>444 167</b>	<b>7492</b>	<b>11 320</b>	<b>16 304</b>	<b>11 769</b>	<b>44 077</b>	<b>61 690</b>	<b>82 889</b>	<b>62 812</b>

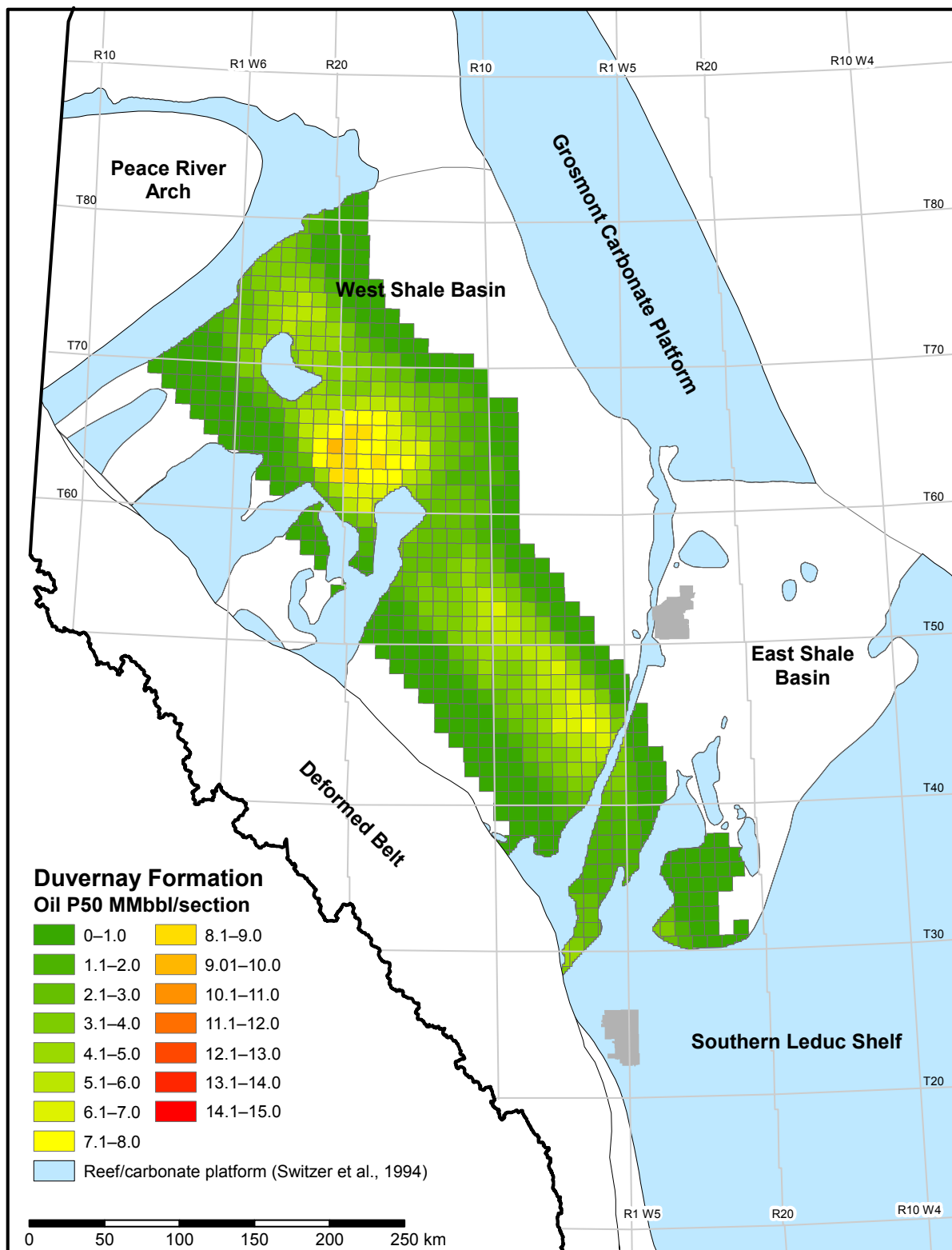


Figure 5.2.1. P50 (best estimate) shale-hosted oil initially-in-place in the Duvernay Formation.

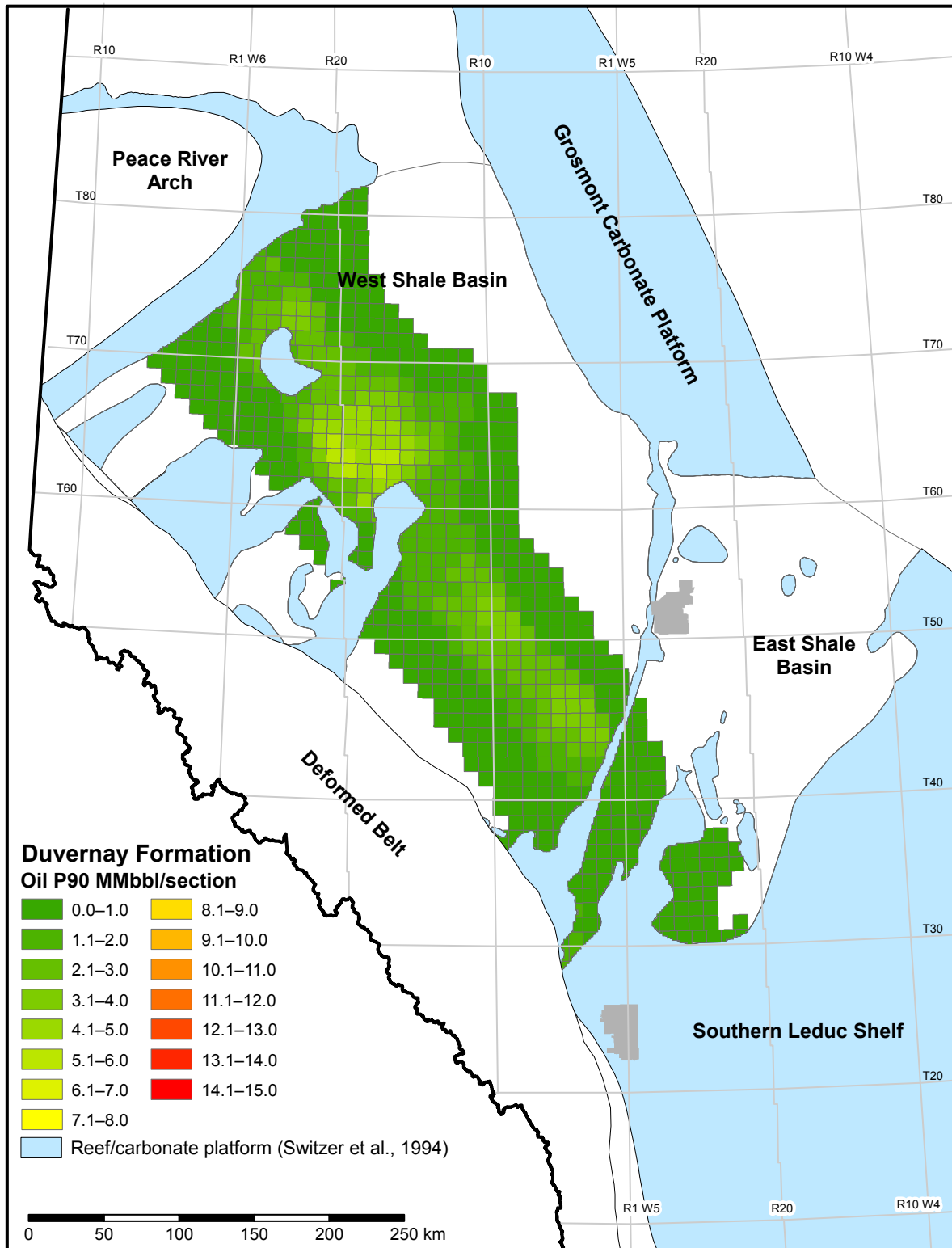


Figure 5.2.2. P90 (low estimate) shale-hosted oil initially-in-place in the Duvernay Formation.

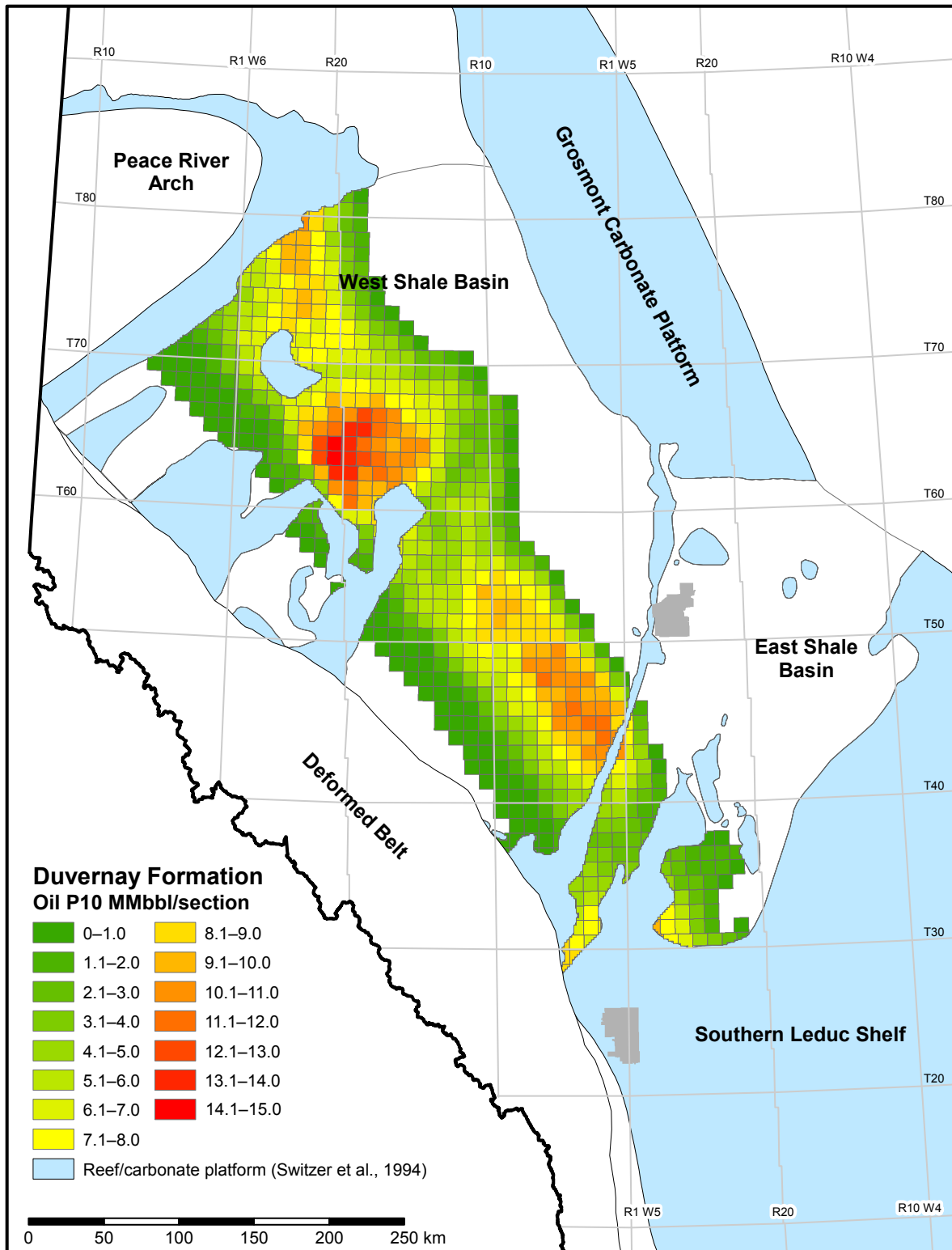


Figure 5.2.3. P10 (high estimate) shale-hosted oil initially-in-place in the Duvernay Formation.

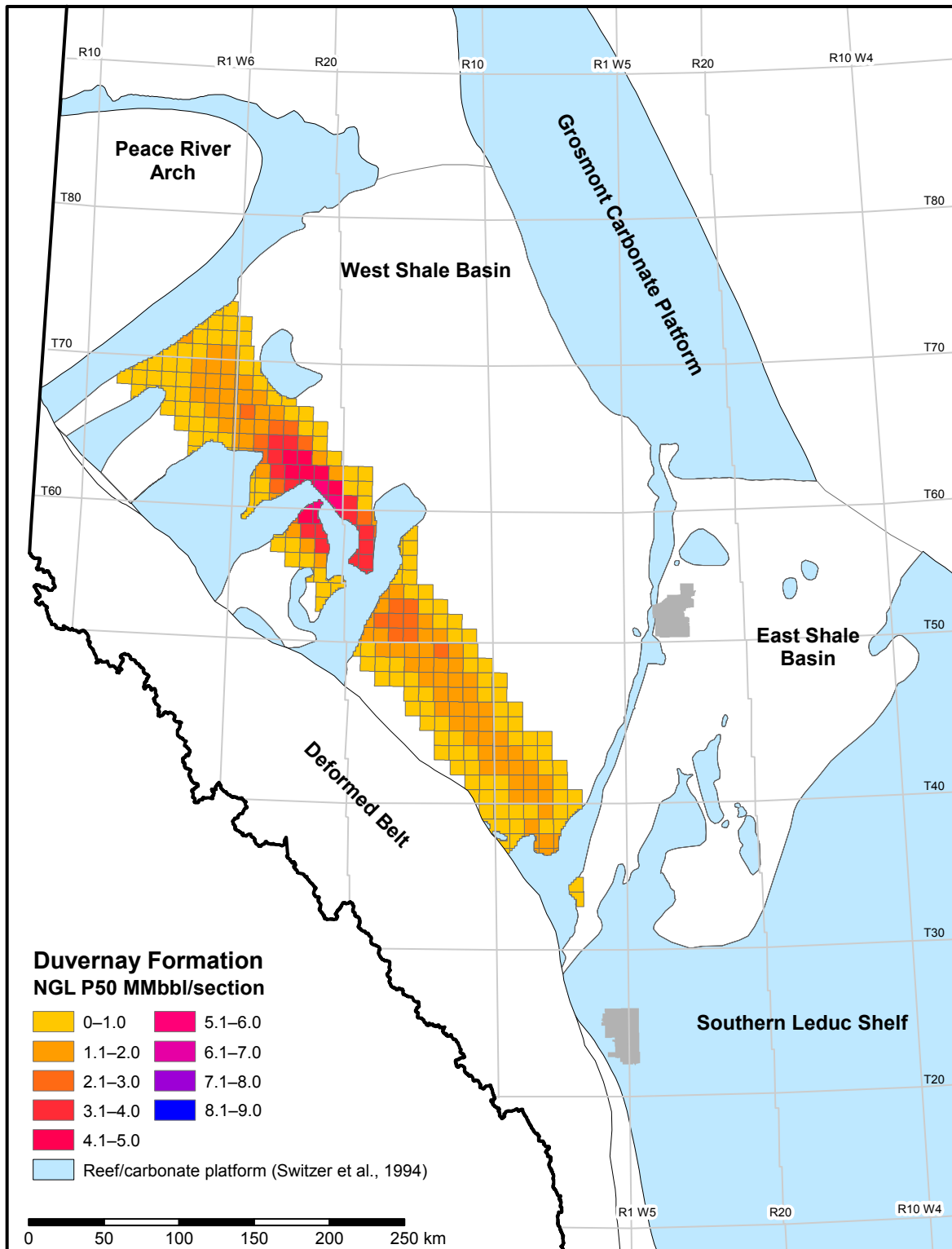


Figure 5.2.4. P50 (best estimate) shale-hosted natural-gas liquids initially-in-place in the Duvernay Formation.

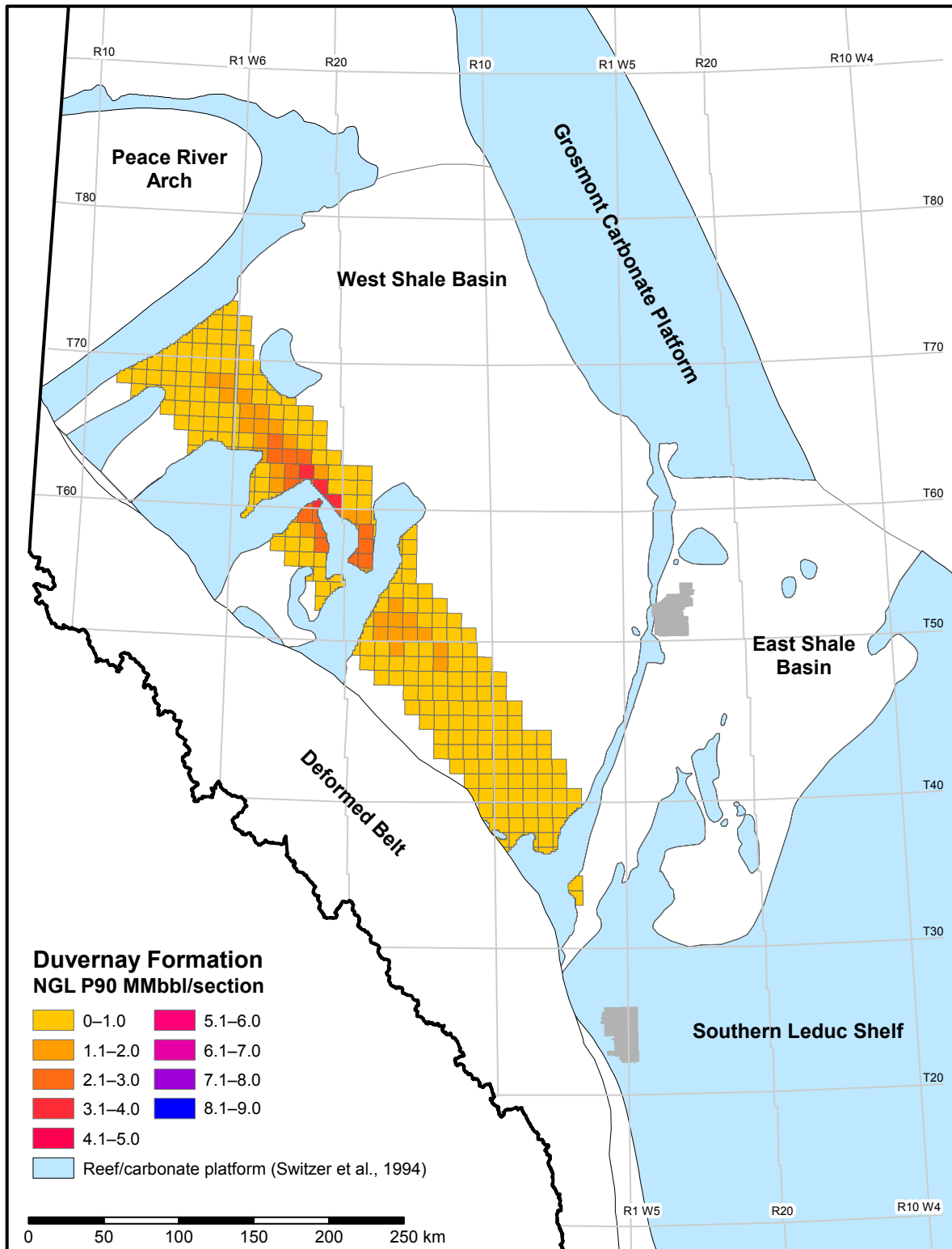


Figure 5.2.5. P90 (low estimate) shale-hosted natural-gas liquids initially-in-place in the Duvernay Formation.

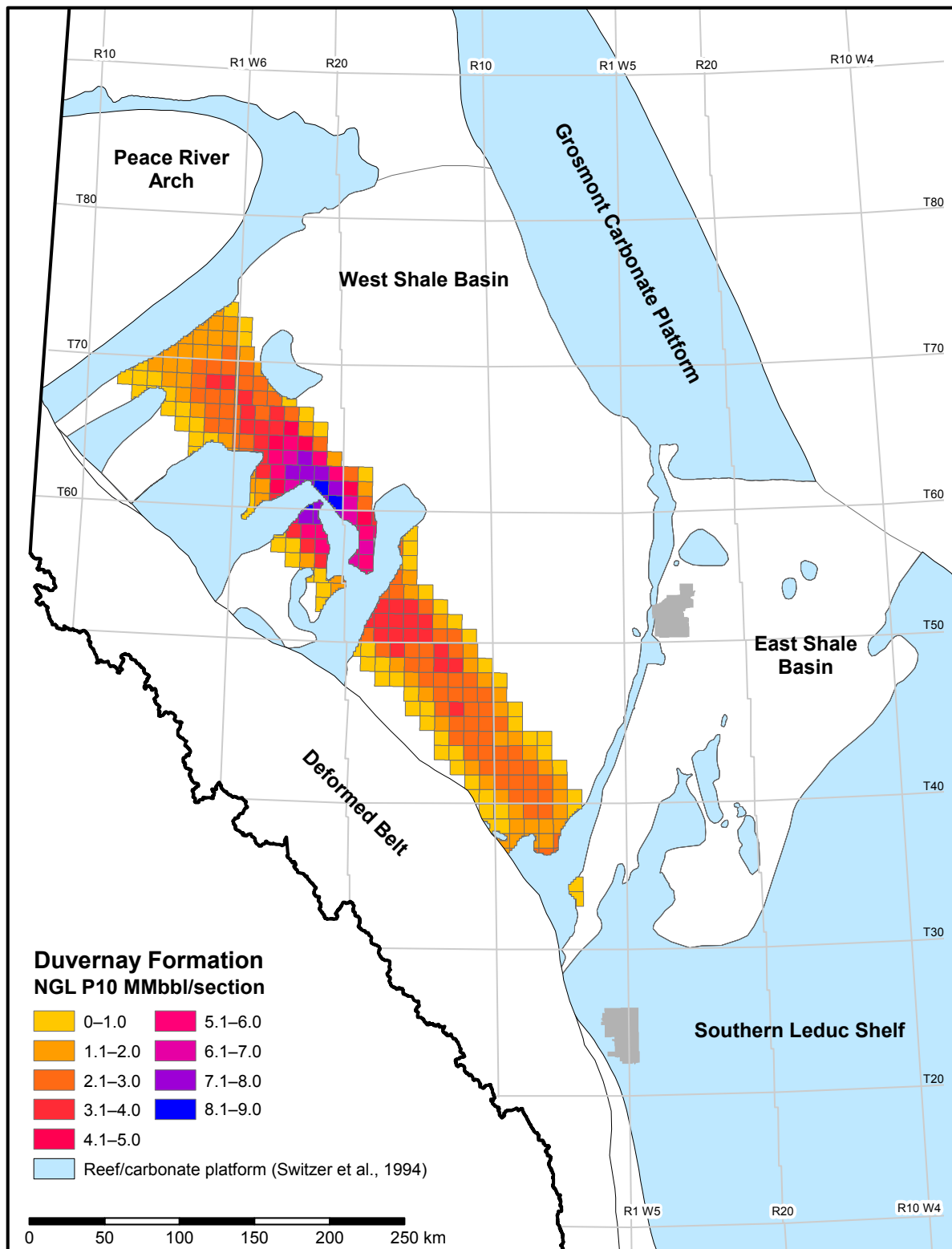


Figure 5.2.6. P10 (high estimate) shale-hosted natural-gas liquids initially-in-place in the Duvernay Formation.

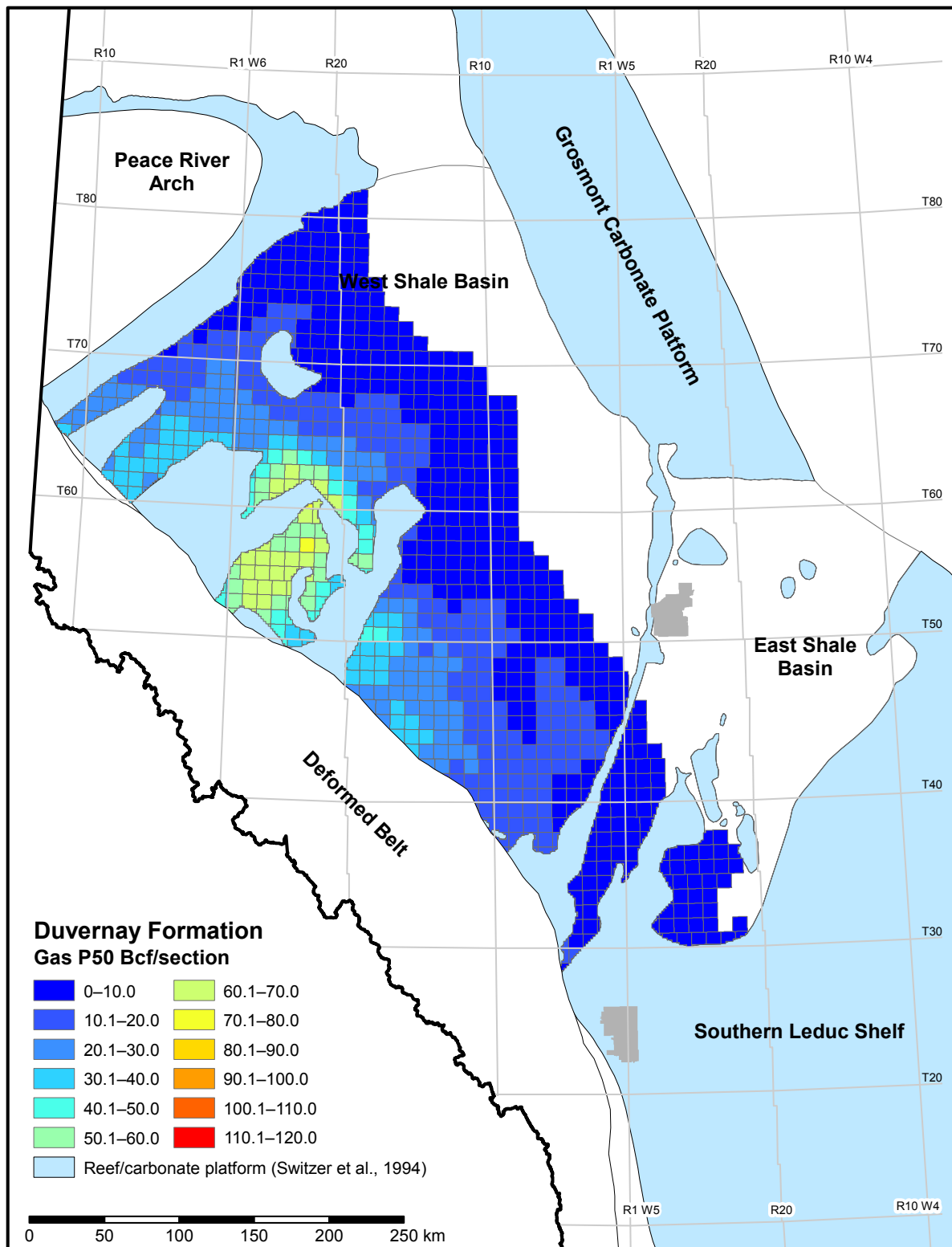


Figure 5.2.7. P50 (best estimate) shale-hosted gas initially-in-place in the Duvernay Formation.

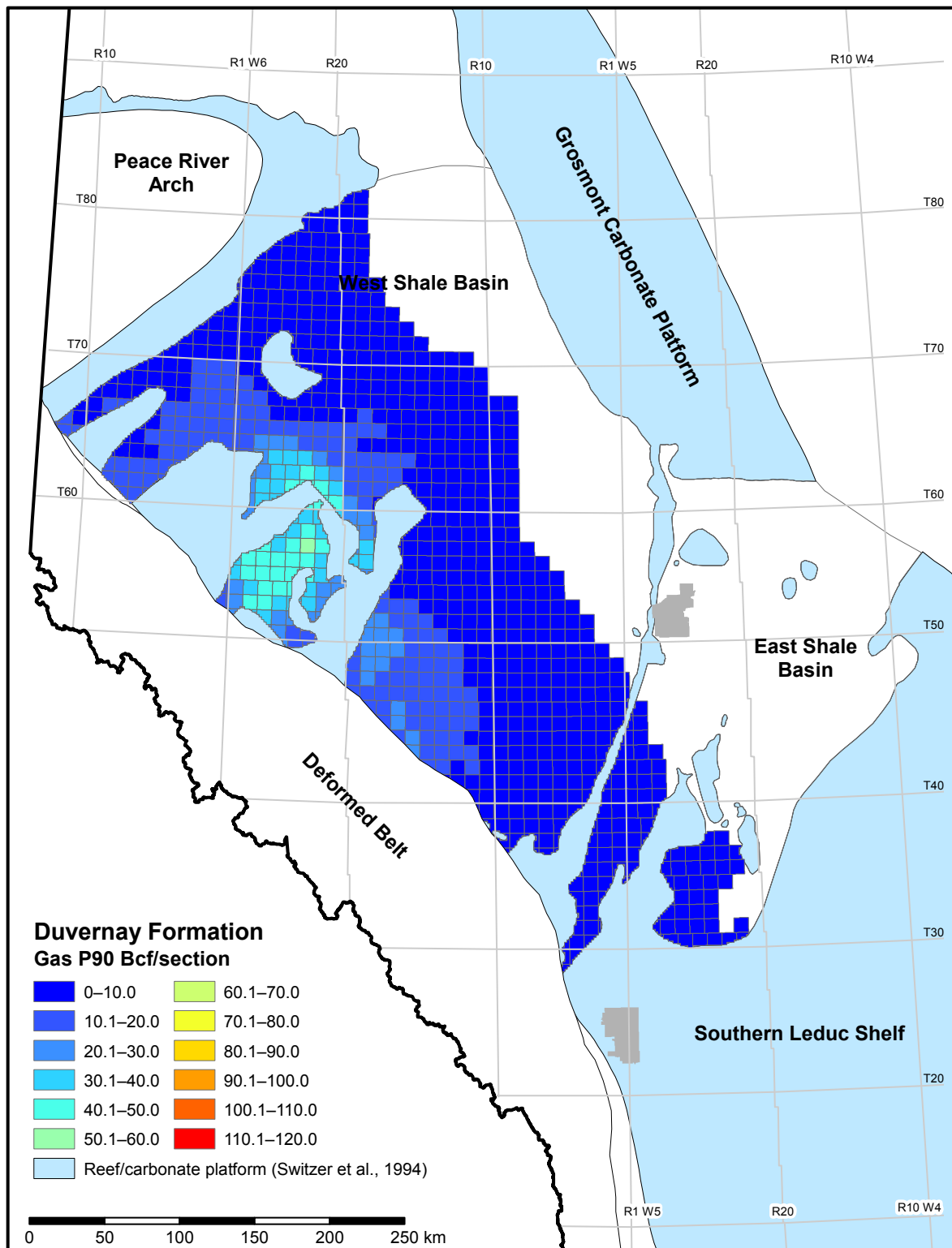


Figure 5.2.8. P90 (low estimate) shale-hosted gas initially-in-place in the Duvernay Formation.

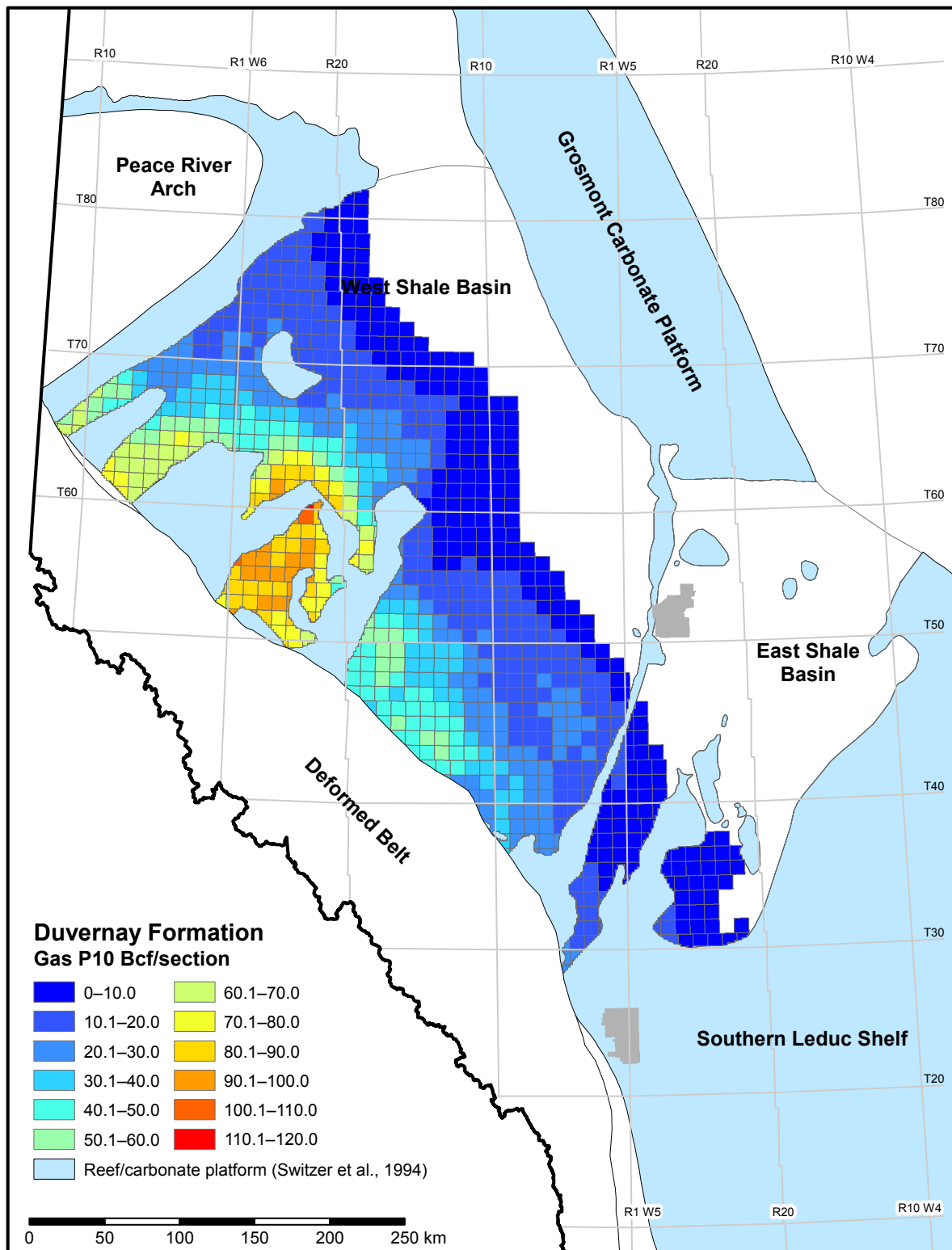


Figure 5.2.9. P10 (high estimate) shale-hosted gas initially-in-place in the Duvernay Formation.

### 5.3 Muskwa Formation Shale-Hosted Hydrocarbon Resource Endowment

In the Muskwa study area, there was no area of dry-gas maturity and only a small area of wet-gas maturity.

Shale-hosted gas initially-in-place for the Muskwa Formation ranges from a low estimate (P90) of 289 Tcf to a high estimate (P10) of 527 Tcf, with a medium estimate of 419 Tcf. Shale-hosted natural-gas liquids initially-in-place range from a low estimate (P90) of 5.976 billion barrels to a high estimate (P10) of 26.329 billion barrels, with a medium estimate of 14.797 billion barrels. Shale-hosted oil initially-in-place ranges from a low estimate (P90) of 74.784 billion barrels to a high estimate (P10) of 159.917 billion barrels, with a medium estimate of 115.137 billion barrels. Figures 5.3.1 to 5.3.9 illustrate the shale-hosted hydrocarbon resource endowment estimates on a per-section basis. Tables 5.3.1 and 5.3.2 show the hydrocarbon resource endowment and resource assessment summaries.

**Table 5.3.1. Summary of Muskwa Formation shale-hosted hydrocarbon resource endowment: low, medium, and high estimates.**

Hydrocarbon	Low Estimate (P90)	Medium Estimate (P50)	High Estimate (P10)
Oil (billion bbl)	74.8	115.1	159.9
Natural-Gas Liquids (billion bbl)	6.0	14.8	26.3
Natural Gas (Tcf)	289	419	527
Natural Gas–Adsorbed Gas Content (%)	4.1	6.9	10.5

Table 5.3.2. Summary of shale-hosted hydrocarbon resource assessment of the Muskwa Formation.

Muskwa	Area (km <sup>2</sup> )				Depth (m)				Net-Shale Thickness (m)			
	Low	Medium	High	Mean	Low	Medium	High	Mean	Low	Medium	High	Mean
Dry Gas	-	-	-	-	-	-	-	-	-	-	-	-
Wet Gas	-	-	1207	331	1540	1560	1591	1562	16.3	22.6	27.2	22.3
Condensate	9383	17 687	28 637	18 544	1414	1549	1562	1520	29.5	32.5	33.9	32.0
Volatile Oil	39 783	47 527	56 395	47 971	1147	1228	1339	1238	13.7	17.8	24.0	18.4
Black Oil	1465	11 932	23 839	12 393	1484	1727	2540	1868	9.3	11.4	13.6	11.5
<b>TOTAL</b>	<b>72 579</b>	<b>81 268</b>	<b>82 637</b>	<b>79 238</b>	<b>1323</b>	<b>1369</b>	<b>1389</b>	<b>1361</b>	<b>19.5</b>	<b>20.1</b>	<b>21.3</b>	<b>20.3</b>
Muskwa	TOC (%)				Porosity (%)							
	Low	Medium	High	Mean	Low	Medium	High	Mean				
Dry Gas	-	-	-	-	-	-	-	-				
Wet Gas	1.78	2.15	2.39	2.13	4.88	7.06	8.93	6.98				
Condensate	1.88	1.94	2.04	1.95	8.45	9.46	10.49	9.45				
Volatile Oil	1.73	1.84	1.95	1.84	10.55	11.51	12.46	11.51				
Black Oil	1.92	2.22	3.54	2.48	7.73	11.01	12.48	10.52				
<b>TOTAL</b>	<b>1.82</b>	<b>1.91</b>	<b>1.98</b>	<b>1.91</b>	<b>10.23</b>	<b>11.08</b>	<b>11.88</b>	<b>11.08</b>				
Muskwa	Gas (billion m <sup>3</sup> )				NGL (million m <sup>3</sup> )				Oil (million m <sup>3</sup> )			
	Low	Medium	High	Mean	Low	Medium	High	Mean	Low	Medium	High	Mean
Dry Gas	-	-	-	-	-	-	-	-	-	-	-	-
Wet Gas	-	-	218	69	-	-	7	3	-	-	-	-
Condensate	2611	5575	8913	5688	949	2350	4179	2464	265	717	1629	844
Volatile Oil	3655	5404	6739	5313	-	-	-	-	8712	12 599	15 703	12 407
Black Oil	56	346	1391	561	-	-	-	-	444	5145	10 583	5167
<b>TOTAL</b>	<b>8132</b>	<b>11 812</b>	<b>14 839</b>	<b>11 631</b>	<b>949</b>	<b>2350</b>	<b>4181</b>	<b>2467</b>	<b>11 884</b>	<b>18 296</b>	<b>25 412</b>	<b>18 418</b>
Muskwa	Gas (Bcf)				NGL (MMbbl)				Oil (MMbbl)			
	Low	Medium	High	Mean	Low	Medium	High	Mean	Low	Medium	High	Mean
Dry Gas	-	-	-	-	-	-	-	-	-	-	-	-
Wet Gas	-	-	7748	2451	-	-	45	19	-	-	-	-
Condensate	92 670	197 874	316 359	201 902	5976	14 797	26 313	15 517	1665	4511	10 248	5310
Volatile Oil	129 726	191 809	239 196	188 566	-	-	-	-	54 826	79 284	98 817	78 077
Black Oil	1995	12 278	49 376	19 900	-	-	-	-	2796	32 374	66 597	32 517
<b>TOTAL</b>	<b>288 618</b>	<b>419 243</b>	<b>526 687</b>	<b>412 820</b>	<b>5976</b>	<b>14 797</b>	<b>26 329</b>	<b>15 537</b>	<b>74 784</b>	<b>115 137</b>	<b>159 917</b>	<b>115 903</b>

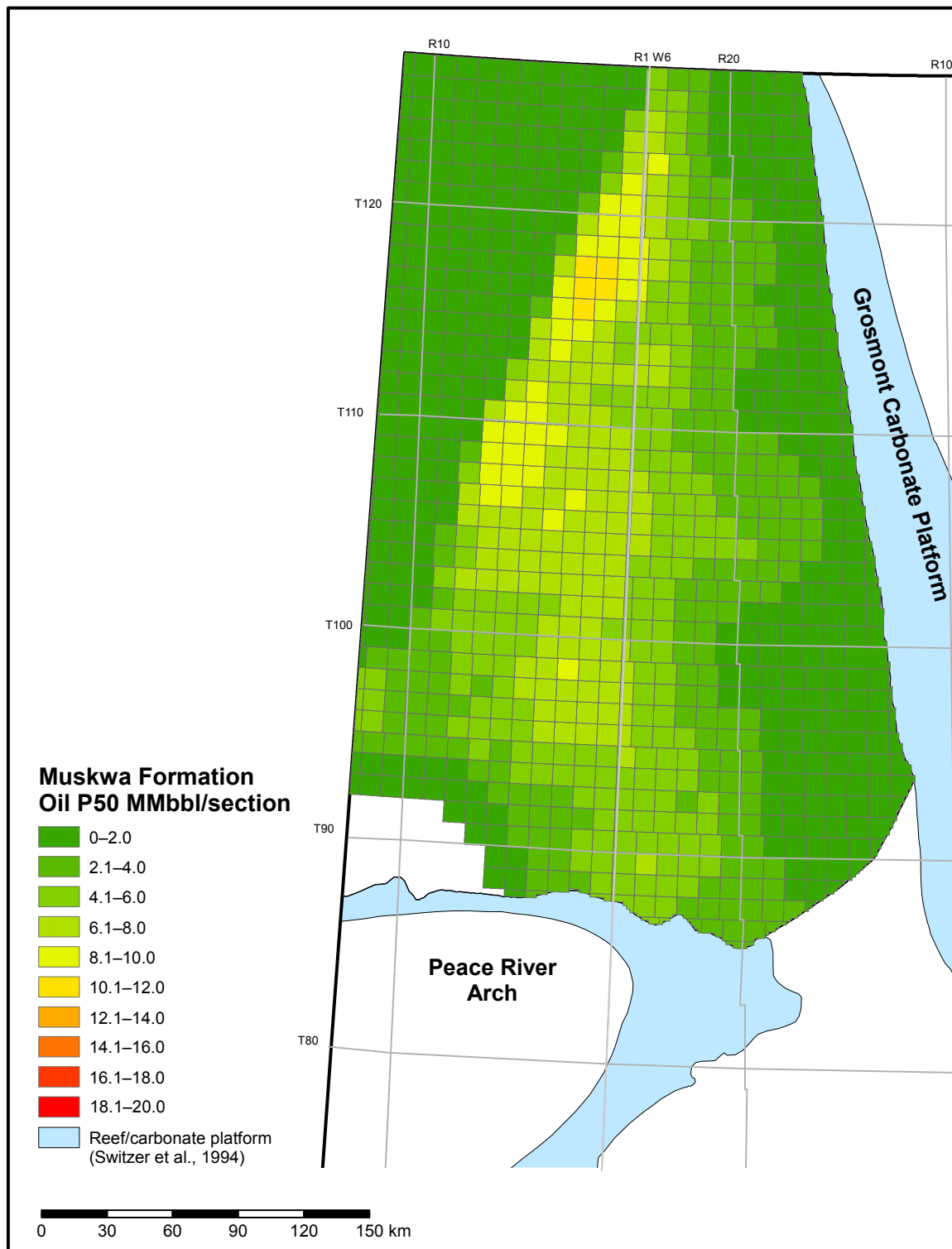


Figure 5.3.1. P50 (best estimate) shale-hosted oil initially-in-place in the Muskwa Formation.

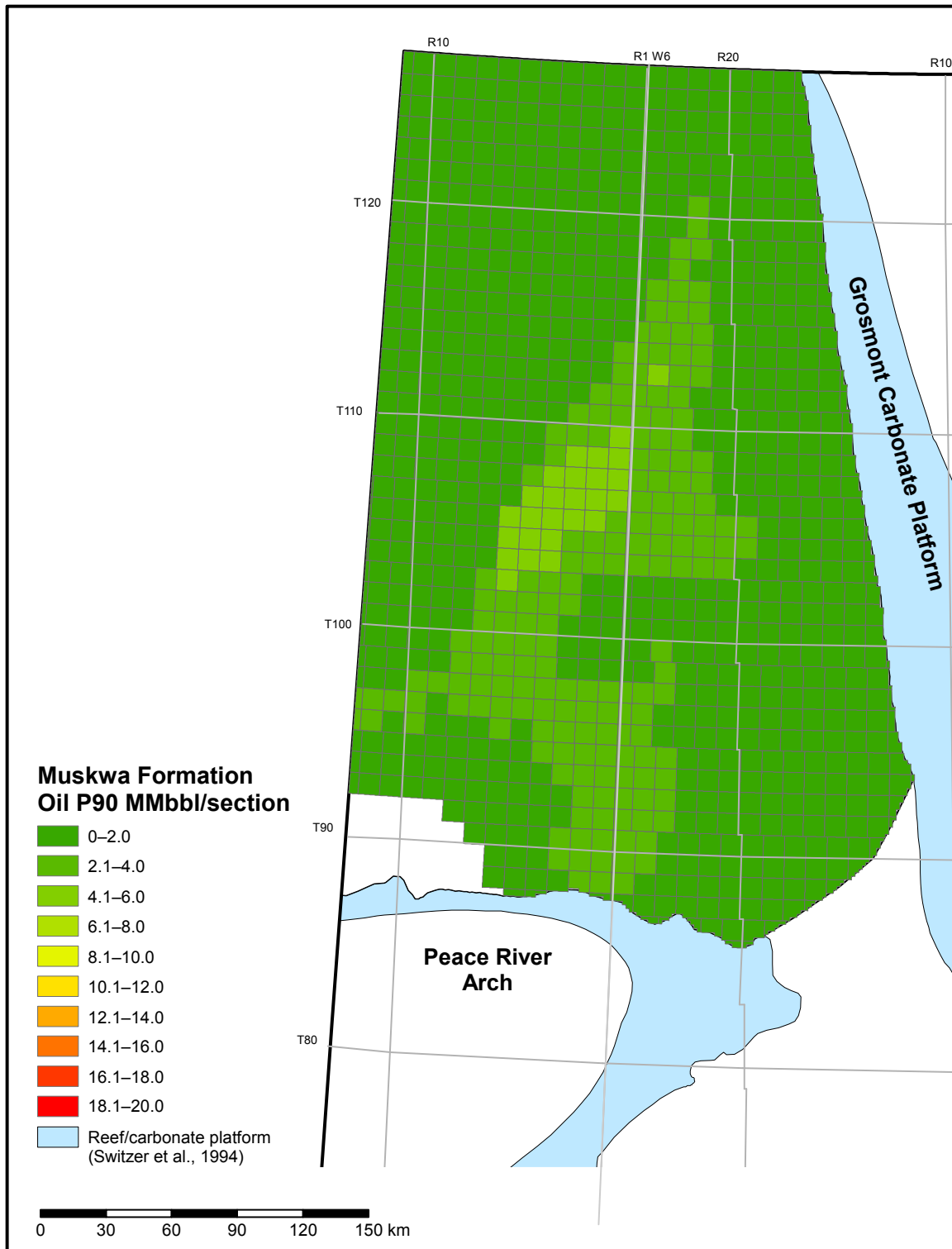


Figure 5.3.2. P90 (low estimate) shale-hosted oil initially-in-place in the Muskwa Formation.

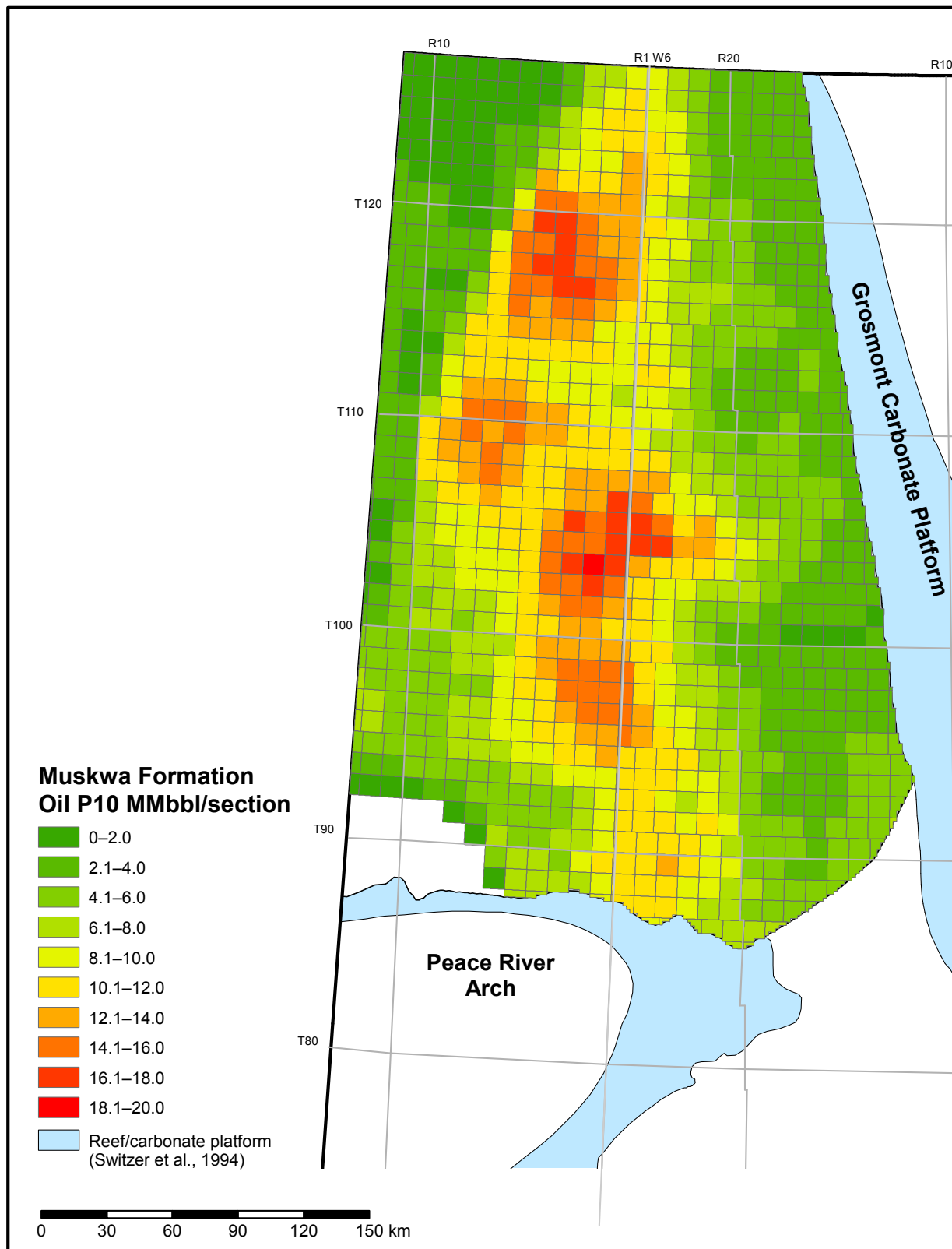


Figure 5.3.3. P10 (high estimate) shale-hosted oil initially-in-place in the Muskwa Formation.

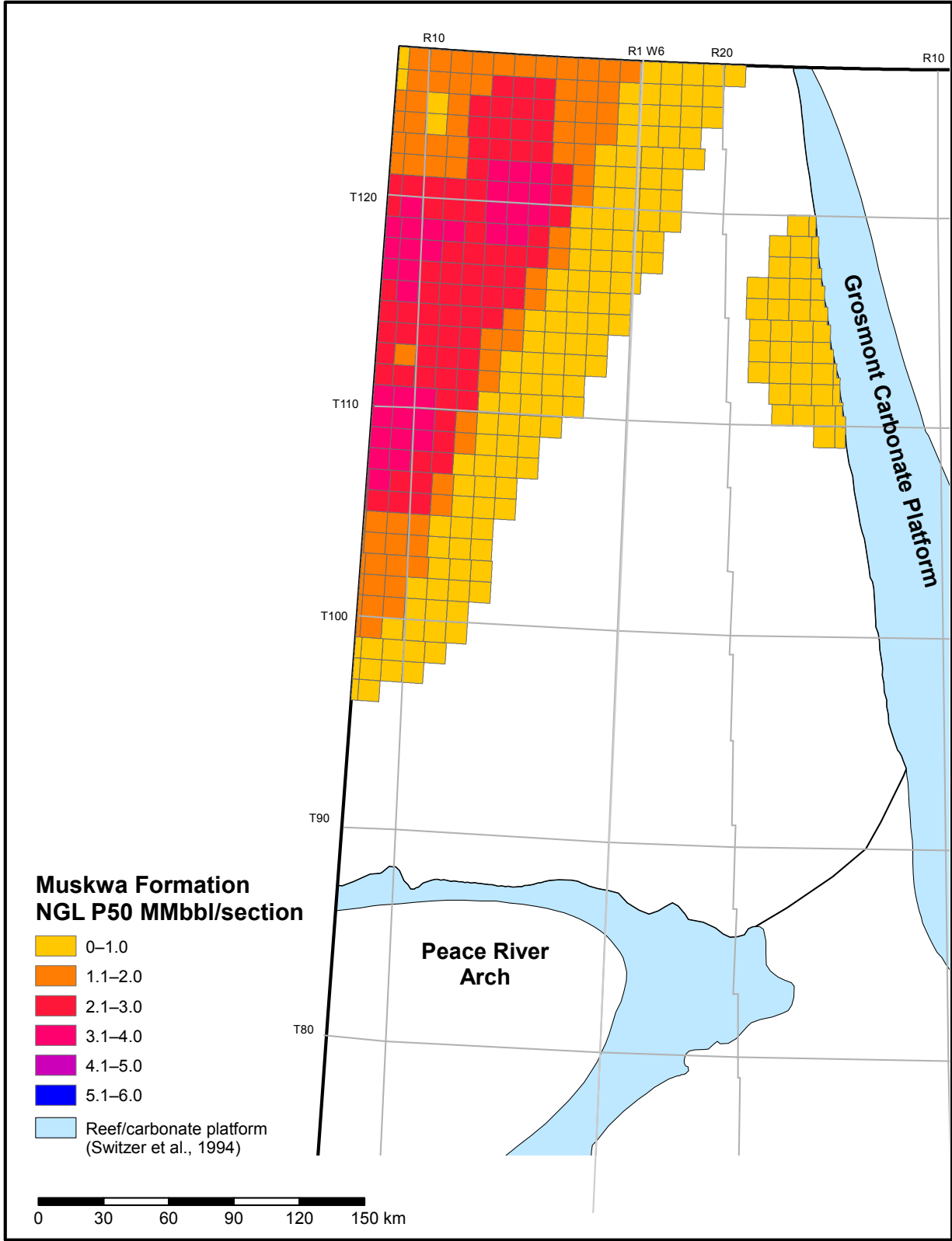


Figure 5.3.4. P50 (best estimate) shale-hosted natural-gas liquids initially-in-place in the Muskwa Formation.

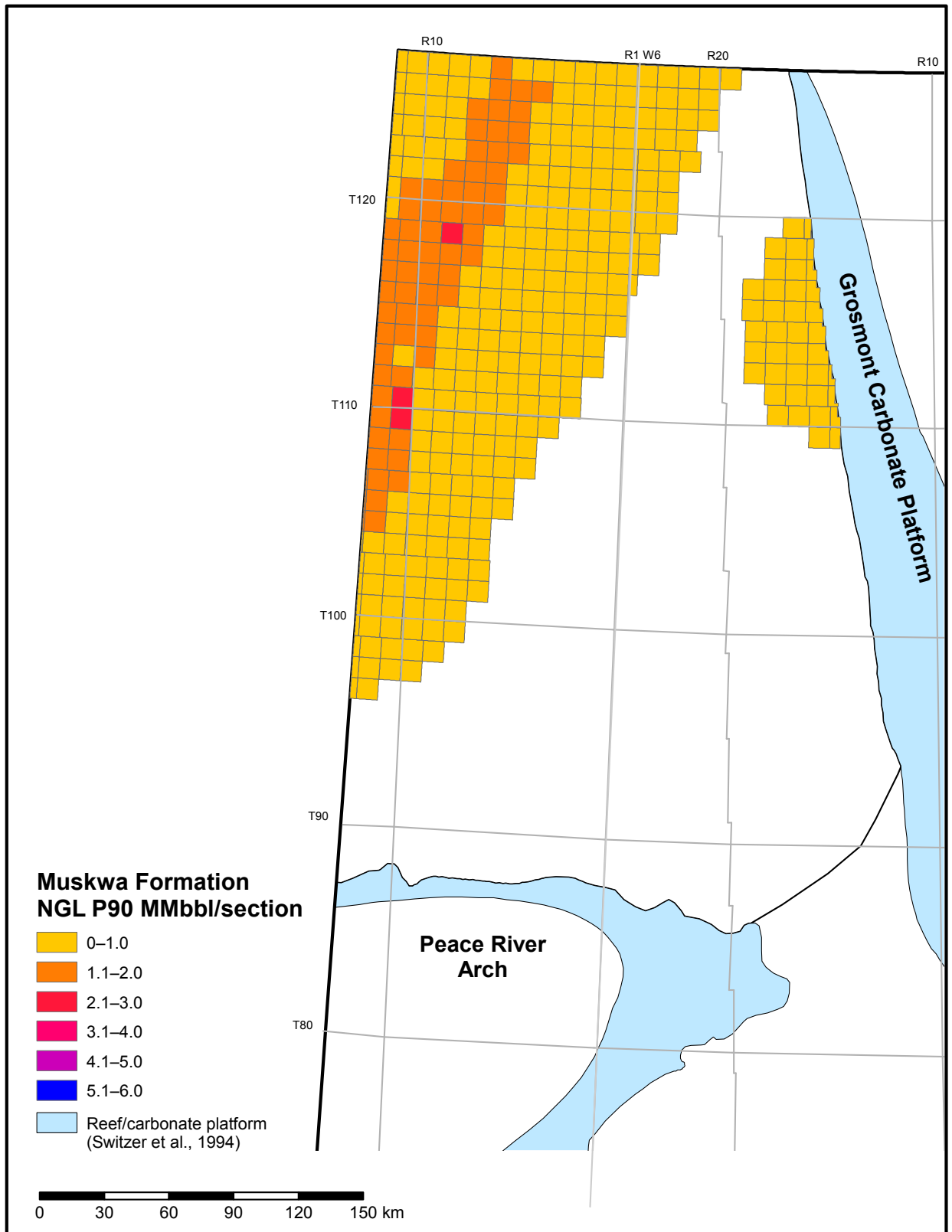


Figure 5.3.5. P90 (low estimate) shale-hosted natural-gas liquids initially-in-place in the Muskwa Formation.

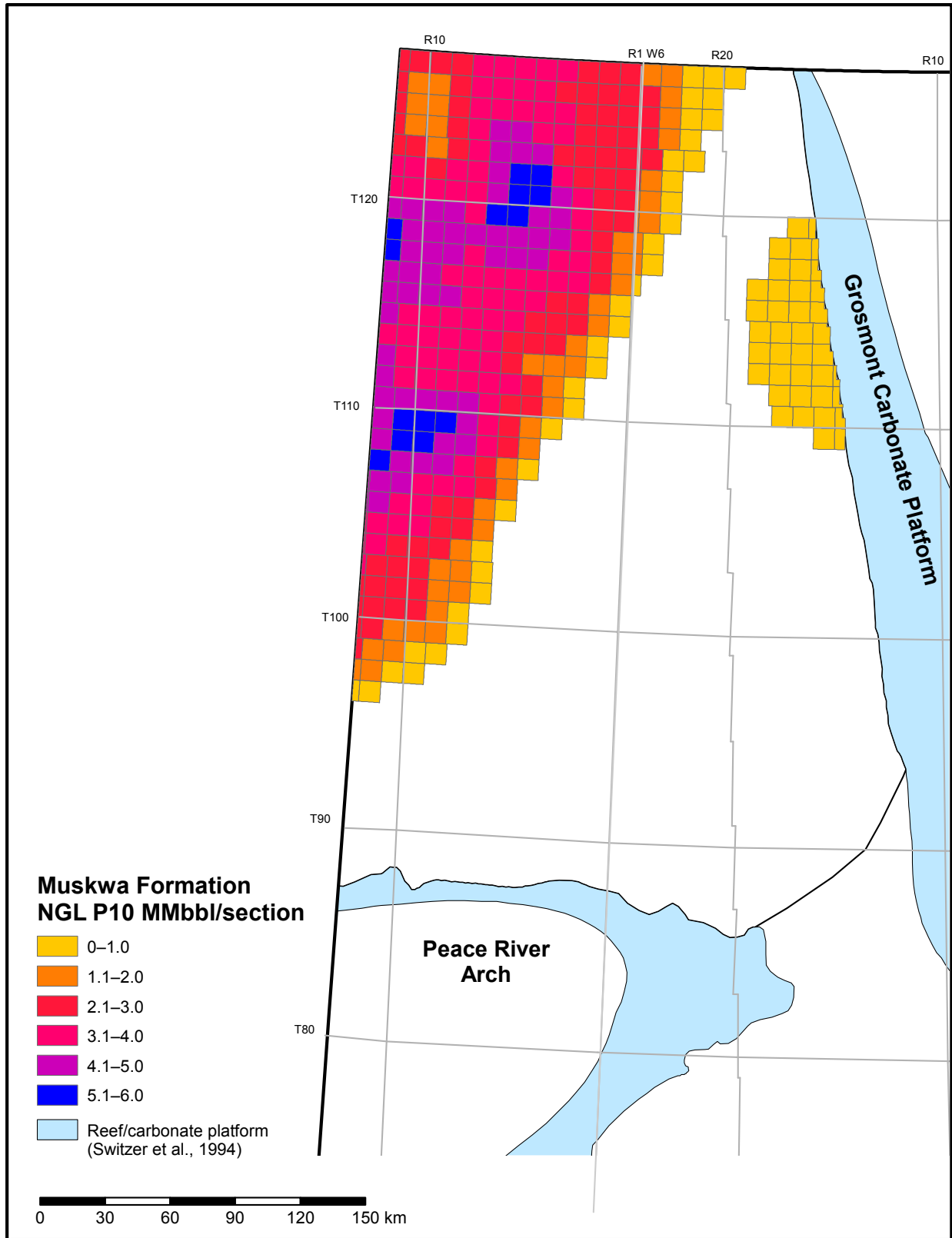


Figure 5.3.6. P10 (high estimate) shale-hosted natural-gas liquids initially-in-place in the Muskwa Formation.

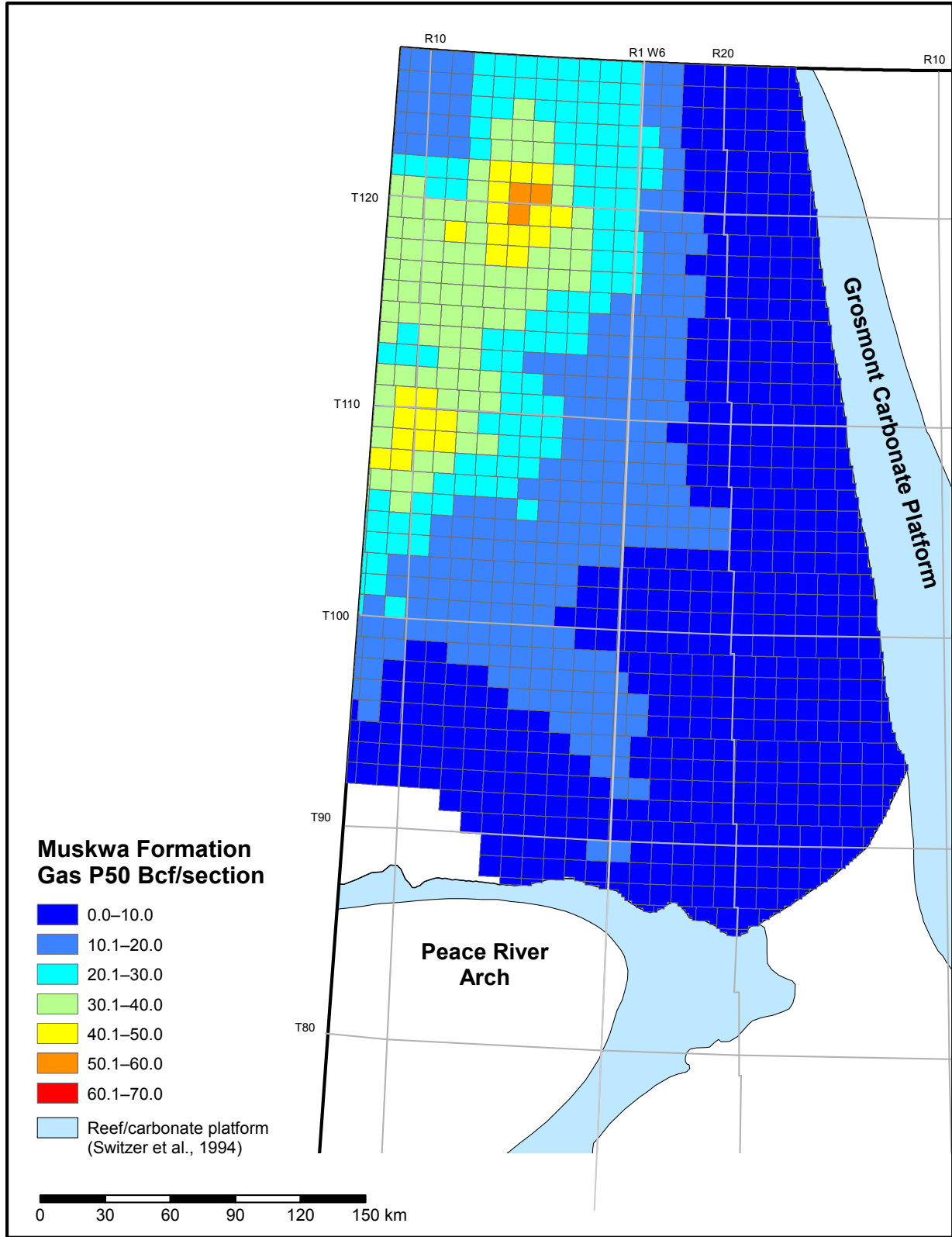


Figure 5.3.7. P50 (best estimate) shale-hosted gas initially-in-place in the Muskwa Formation.

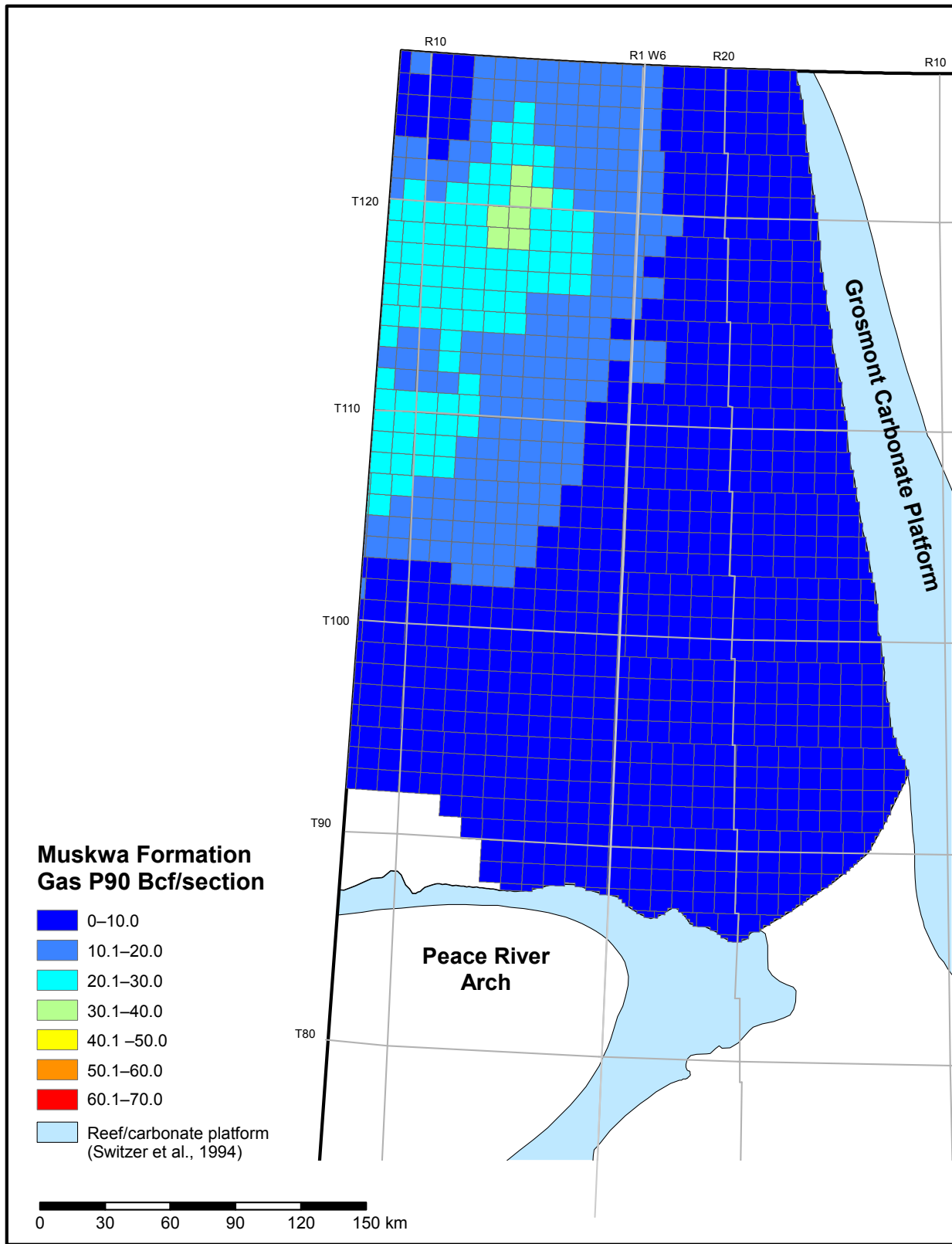


Figure 5.3.8. P90 (low estimate) shale-hosted gas initially-in-place in the Muskwa Formation.

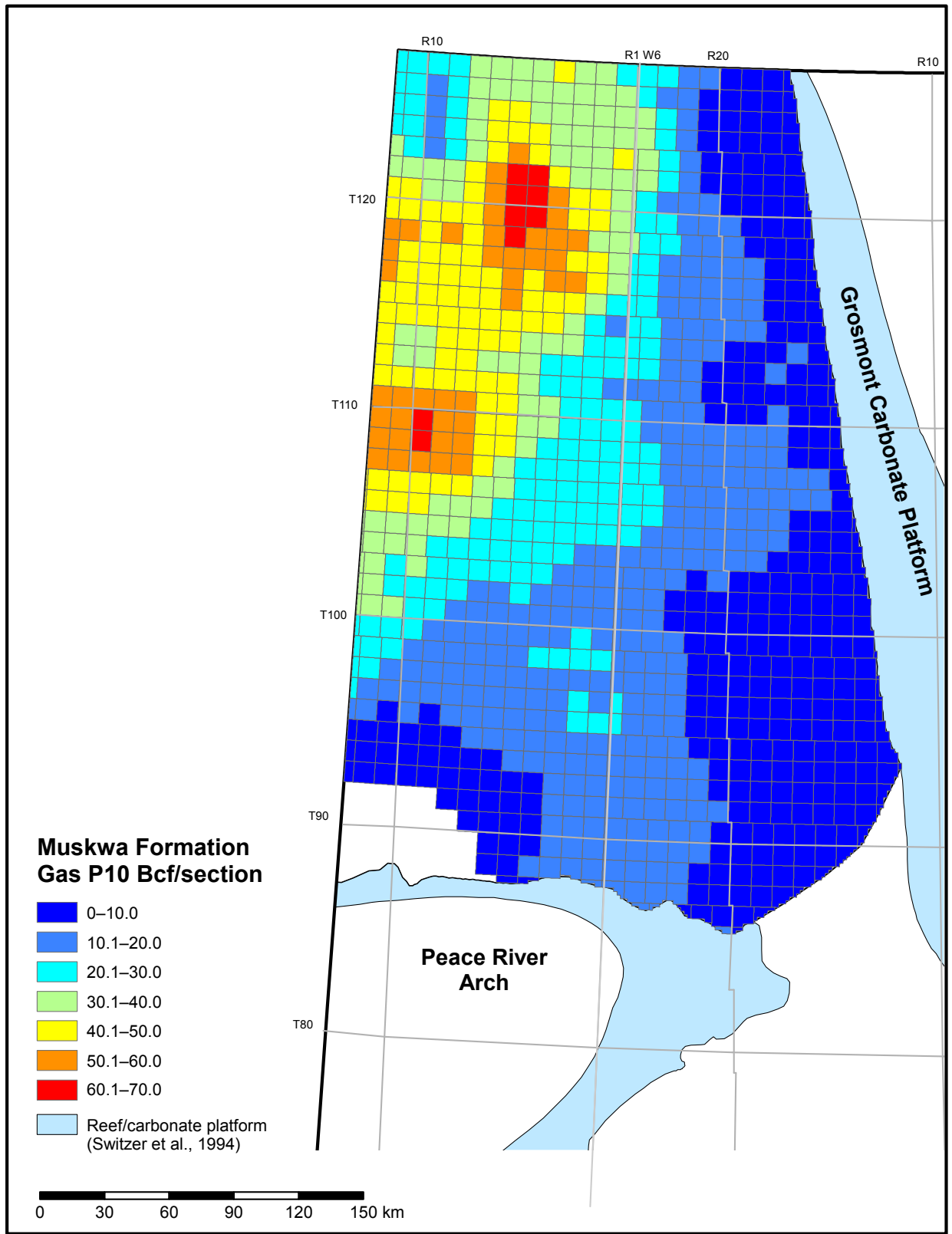


Figure 5.3.9. P10 (high estimate) shale-hosted gas initially-in-place in the Muskwa Formation.

#### 5.4 Montney Formation Siltstone-Hosted Hydrocarbon Resource Endowment

Siltstone-hosted gas initially-in-place for the Montney Formation ranges from a low estimate (P90) of 1630 Tcf to a high estimate (P10) of 2828 Tcf, with a medium estimate of 2133 Tcf. Siltstone-hosted natural-gas liquids initially-in-place range from a low estimate (P90) of 11.660 billion barrels to a high estimate (P10) of 54.353 billion barrels, with a medium estimate of 28.858 billion barrels. Siltstone-hosted oil initially-in-place ranges from a low estimate (P90) of 78.634 billion barrels to a high estimate (P10) of 220.473 billion barrels, with a medium estimate of 136.260 billion barrels. Figures 5.4.1 to 5.4.9 illustrate the siltstone-hosted hydrocarbon resource endowment estimates on a per-section basis. Tables 5.4.1 and 5.4.2 show the hydrocarbon resource endowment and resource assessment summaries.

**Table 5.4.1. Summary of Montney Formation siltstone-hosted hydrocarbon resource endowment: low, medium, and high estimates.**

Hydrocarbon	Low Estimate (P90)	Medium Estimate (P50)	High Estimate (P10)
Oil (billion bbl)	78.6	136.3	220.5
Natural-Gas Liquids (billion bbl)	11.7	28.9	54.4
Natural Gas (Tcf)	1630	2133	2828
Natural Gas-Adsorbed Gas Content (%)	10.8	17.7	26.0

Table 5.4.2. Summary of siltstone-hosted hydrocarbon resource assessment of the Montney Formation.

Montney	Area (km <sup>2</sup> )				Depth (m)				Net-Silt Thickness (m)			
	Low	Medium	High	Mean	Low	Medium	High	Mean	Low	Medium	High	Mean
Dry Gas	20 573	25 549	32 160	25 977	3112	3325	3503	3317	132.3	134.7	135.9	134.4
Wet Gas	12 468	13 753	14 781	13 703	1827	2123	2399	2118	138.0	141.9	149.5	143.2
Condensate	20 249	22 955	23 684	22 350	1269	1442	1637	1449	153.1	159.4	161.8	158.0
Volatile Oil	9065	11 884	14 609	11 920	971	1037	1111	1040	62.5	86.0	118.0	88.6
Black Oil	1168	2051	3112	2117	834	891	950	892	23.7	37.6	53.8	38.3
<b>TOTAL</b>	<b>74 484</b>	<b>76 242</b>	<b>77 325</b>	<b>76 067</b>	<b>2099</b>	<b>2117</b>	<b>2147</b>	<b>2120</b>	<b>132.0</b>	<b>133.7</b>	<b>136.1</b>	<b>133.9</b>
Montney	TOC (%)				Porosity (%)							
	Low	Medium	High	Mean	Low	Medium	High	Mean				
Dry Gas	0.81	0.88	0.95	0.88	1.35	2.08	3.52	2.29				
Wet Gas	0.60	0.75	0.83	0.73	2.06	3.31	5.24	3.51				
Condensate	0.24	0.34	0.47	0.34	5.80	7.56	9.22	7.55				
Volatile Oil	0.19	0.21	0.23	0.21	7.98	8.99	10.49	9.14				
Black Oil	0.16	0.19	0.22	0.19	5.98	7.53	9.05	7.55				
<b>TOTAL</b>	<b>0.55</b>	<b>0.57</b>	<b>0.59</b>	<b>0.57</b>	<b>4.38</b>	<b>5.07</b>	<b>6.46</b>	<b>5.30</b>				
Montney	Gas (billion m <sup>3</sup> )				NGL (million m <sup>3</sup> )				Oil (million m <sup>3</sup> )			
	Low	Medium	High	Mean	Low	Medium	High	Mean	Low	Medium	High	Mean
Dry Gas	10 664	16 667	26 545	17 896	-	-	-	-	-	-	-	-
Wet Gas	7392	10 872	16 201	11 491	203	517	1112	603	-	-	-	-
Condensate	19 196	26 255	33 506	26 345	1618	4048	7624	4454	4036	6016	7996	6049
Volatile Oil	2311	5112	9814	5686	-	-	-	-	5973	12 979	24 637	14 387
Black Oil	44	182	458	225	-	-	-	-	495	2017	4505	2362
<b>TOTAL</b>	<b>45 917</b>	<b>60 095</b>	<b>79 684</b>	<b>61 642</b>	<b>1852</b>	<b>4583</b>	<b>8631</b>	<b>5057</b>	<b>12 496</b>	<b>21 653</b>	<b>35 035</b>	<b>22 798</b>
Montney	Gas (Bcf)				NGL (MMbbl)				Oil (MMbbl)			
	Low	Medium	High	Mean	Low	Medium	High	Mean	Low	Medium	High	Mean
Dry Gas	378 522	591 585	942 191	635 202	-	-	-	-	-	-	-	-
Wet Gas	262 362	385 896	575 048	407 847	1277	3257	7002	3799	-	-	-	-
Condensate	681 334	931 884	1189 241	935 070	10 187	25 489	48 008	28 047	25 398	37 856	50 317	38 065
Volatile Oil	82 010	181 453	348 326	201 803	-	-	-	-	37 589	81 678	155 039	90 535
Black Oil	1578	6473	16 273	7979	-	-	-	-	3114	12 691	28 348	14 863
<b>TOTAL</b>	<b>1 629 764</b>	<b>2 133 010</b>	<b>2 828 271</b>	<b>2 187 903</b>	<b>11 660</b>	<b>28 858</b>	<b>54 353</b>	<b>31 846</b>	<b>78 634</b>	<b>136 260</b>	<b>220 473</b>	<b>143 463</b>

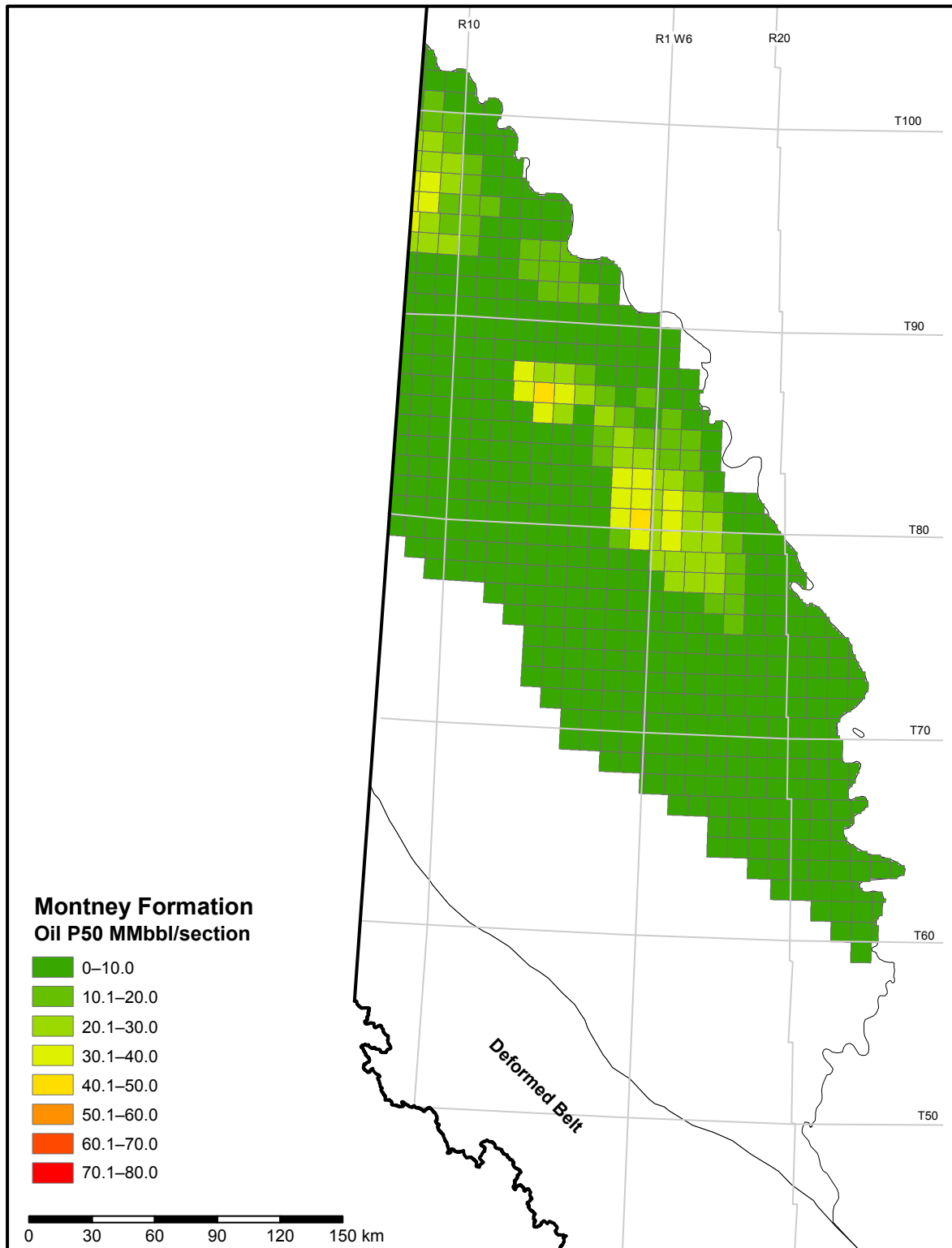


Figure 5.4.1. P50 (best estimate) siltstone-hosted oil initially-in-place in the Montney Formation.

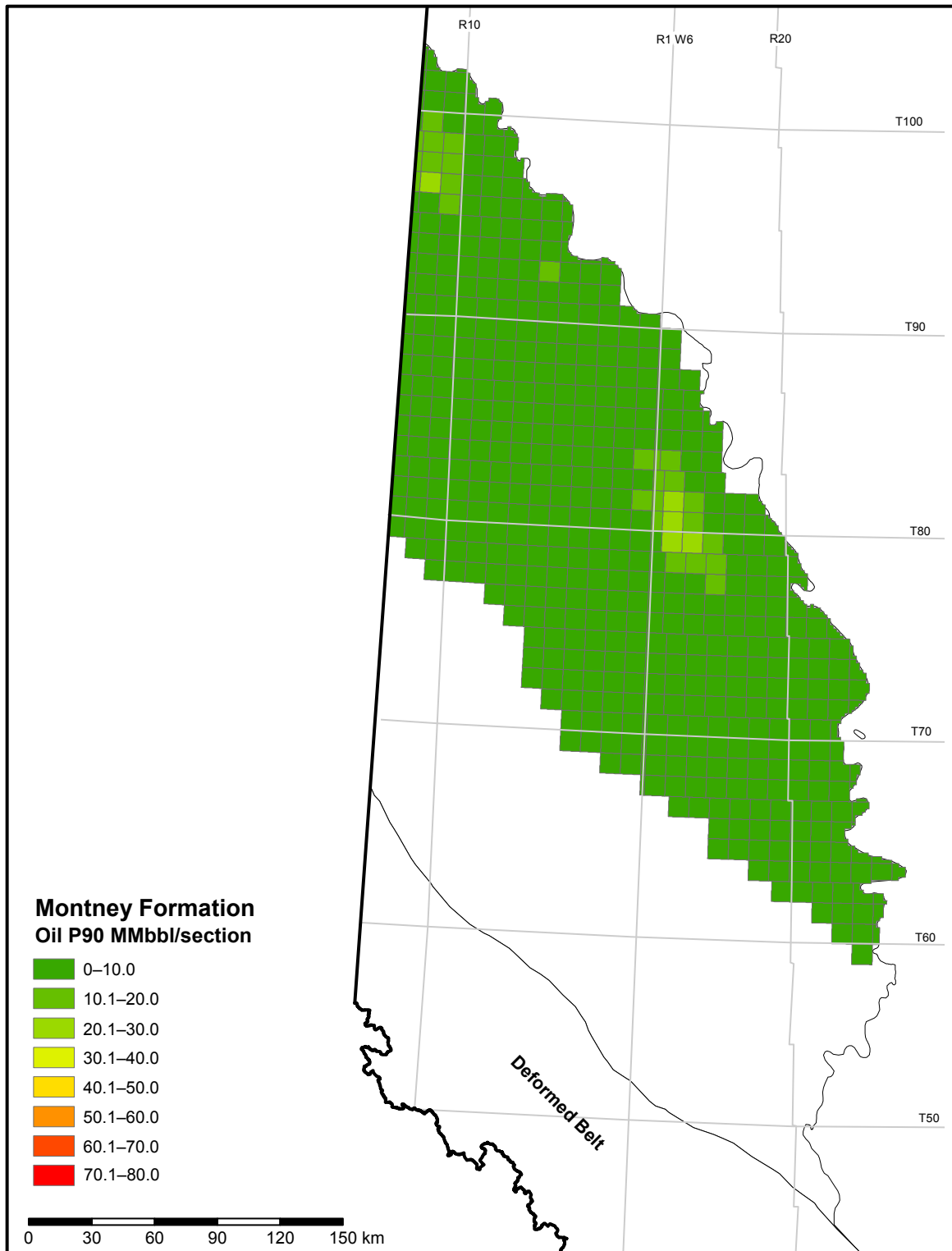


Figure 5.4.2. P90 (low estimate) siltstone-hosted oil initially-in-place in the Montney Formation.

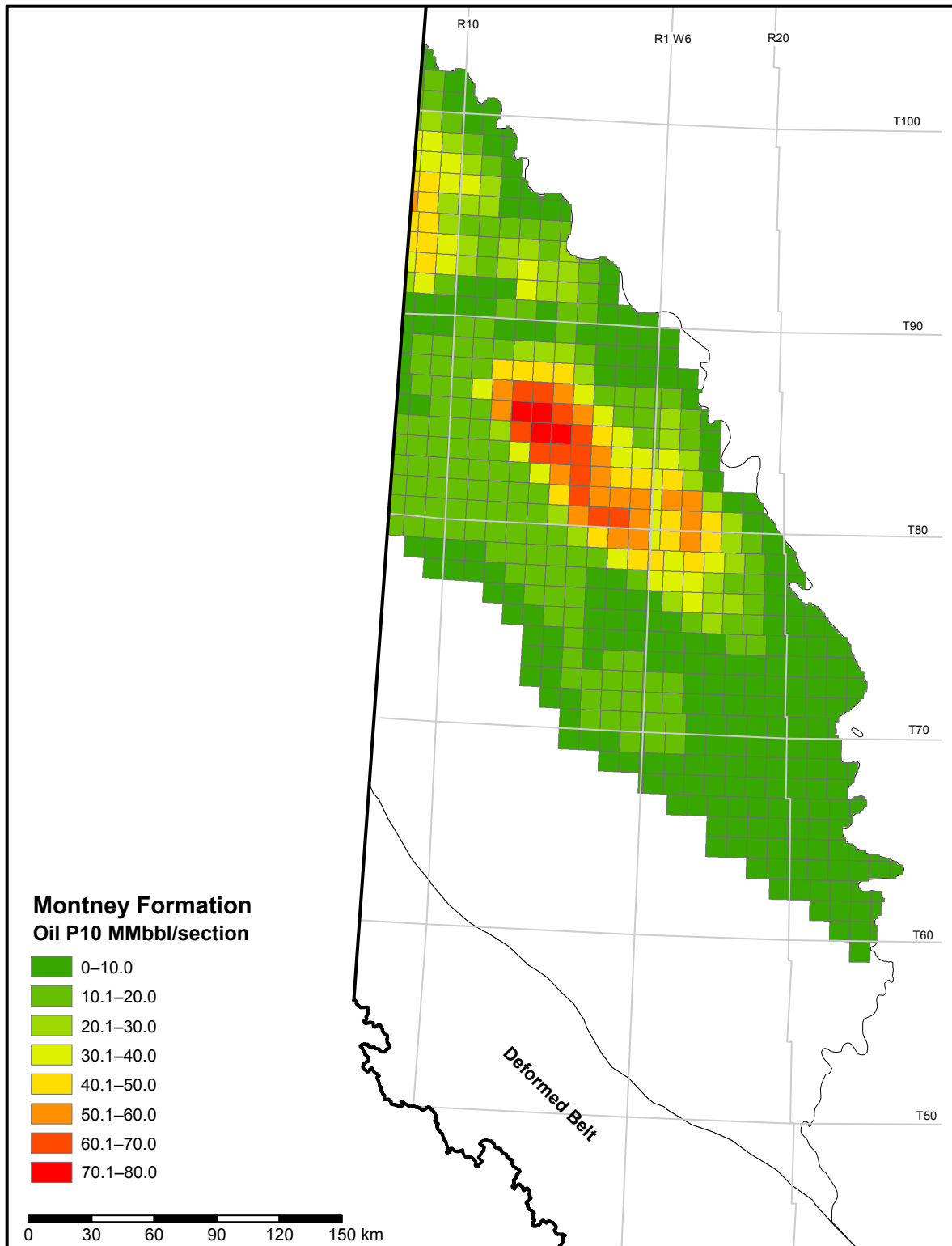


Figure 5.4.3. P10 (high estimate) siltstone-hosted oil initially-in-place in the Montney Formation.

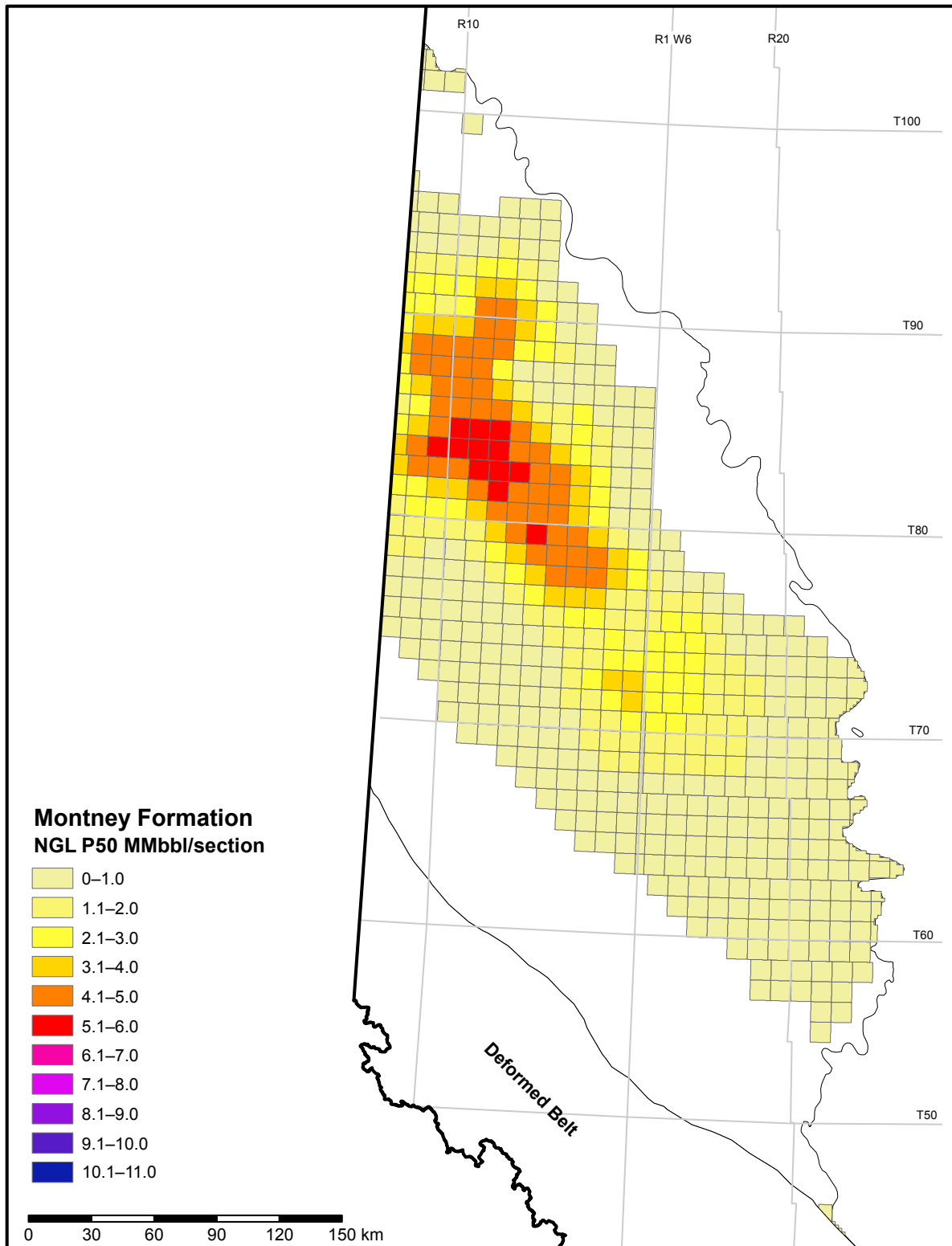


Figure 5.4.4. P50 (best estimate) siltstone-hosted natural-gas liquids initially-in-place in the Montney Formation.

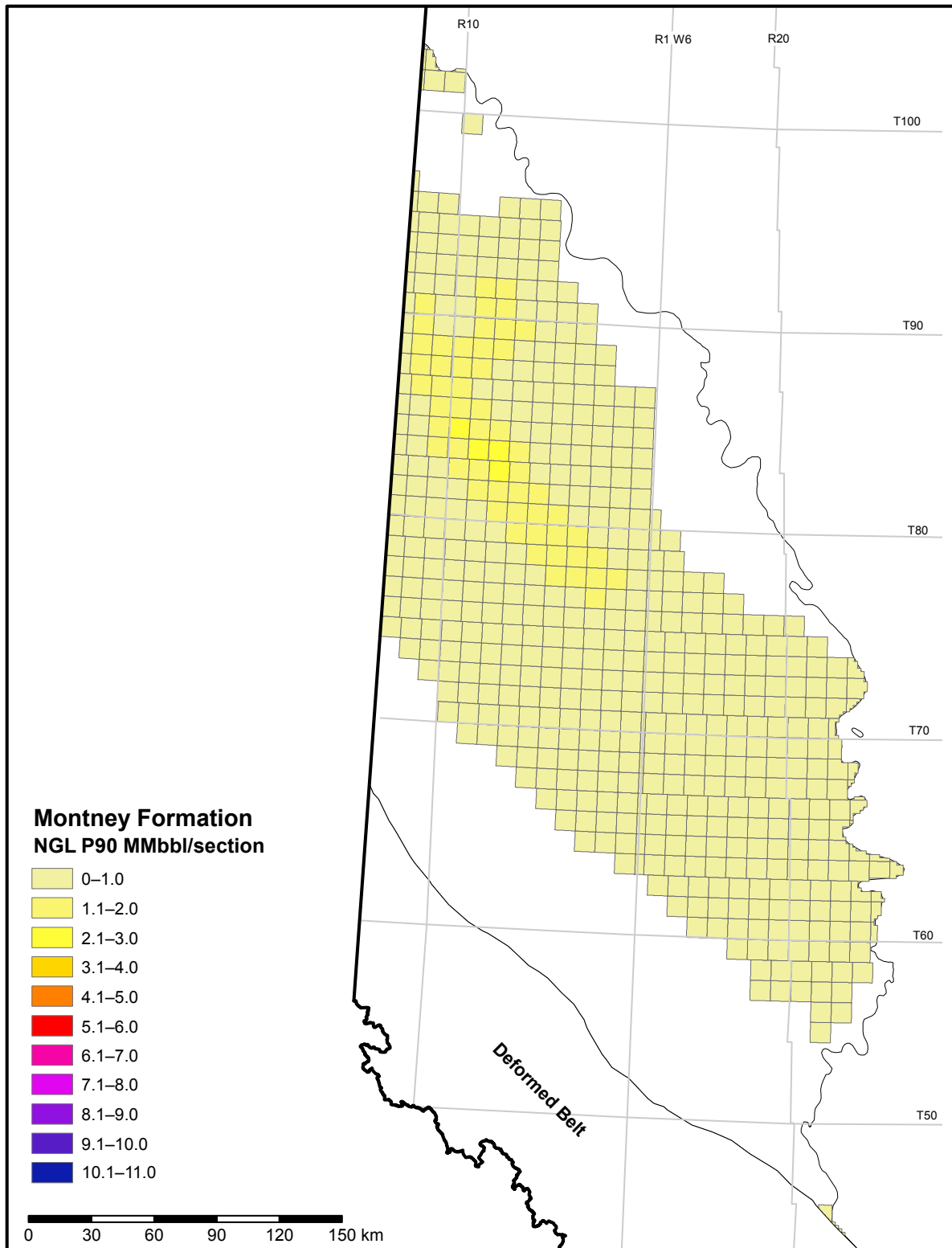


Figure 5.4.5. P90 (low estimate) siltstone-hosted natural-gas liquids initially-in-place in the Montney Formation.

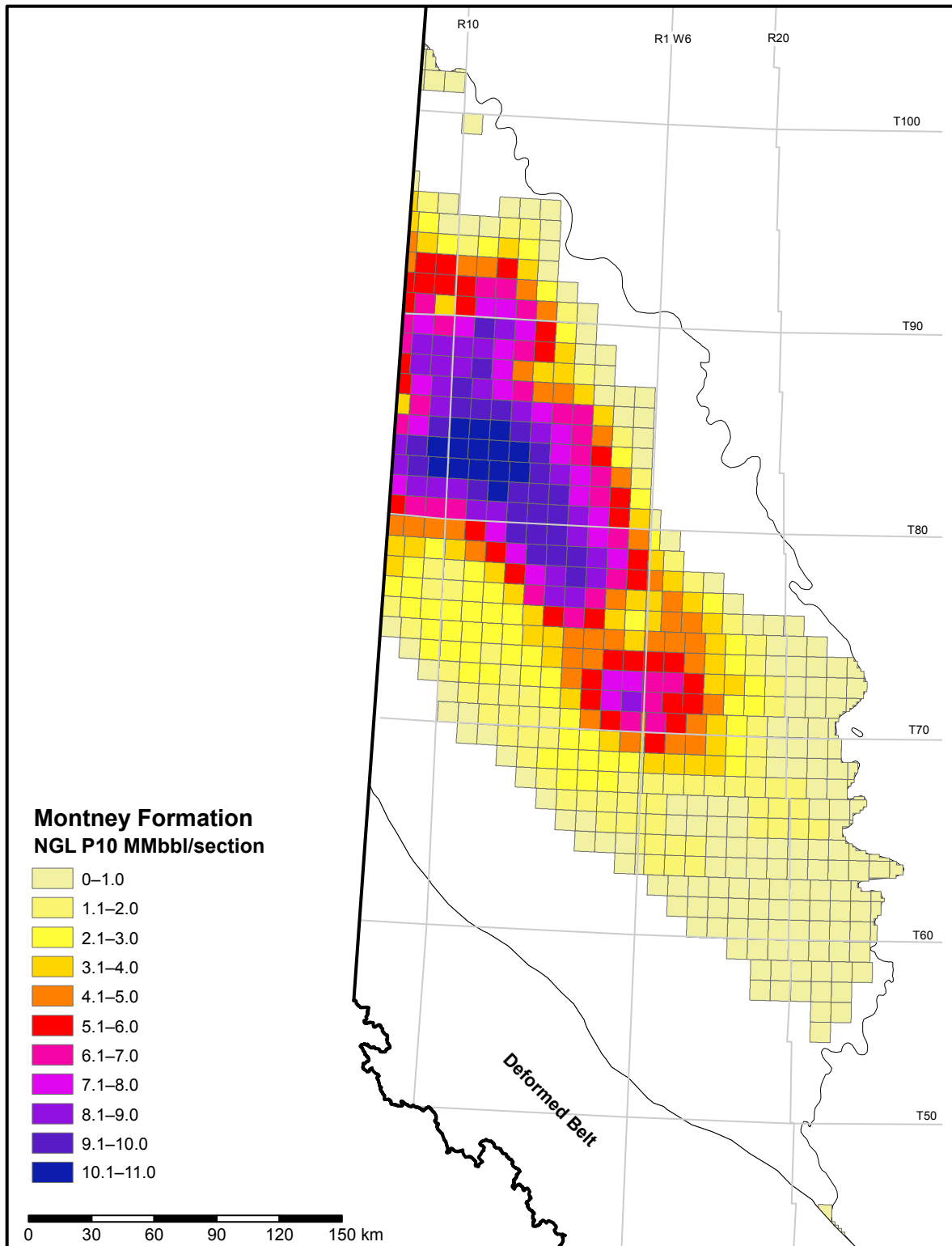


Figure 5.4.6. P10 (high estimate) siltstone-hosted natural-gas liquids initially-in-place in the Montney Formation.

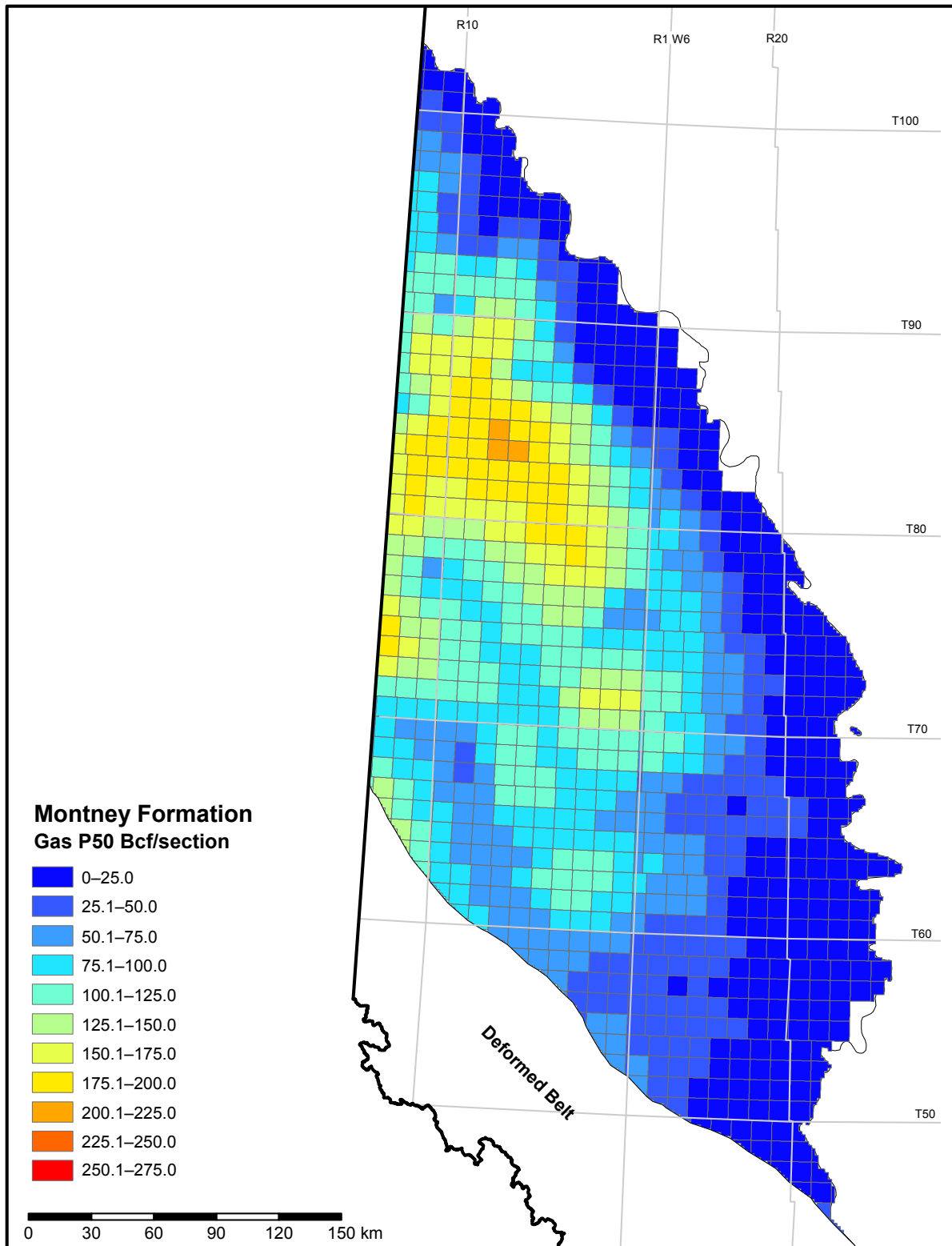


Figure 5.4.7. P50 (best estimate) siltstone-hosted gas initially-in-place in the Montney Formation.

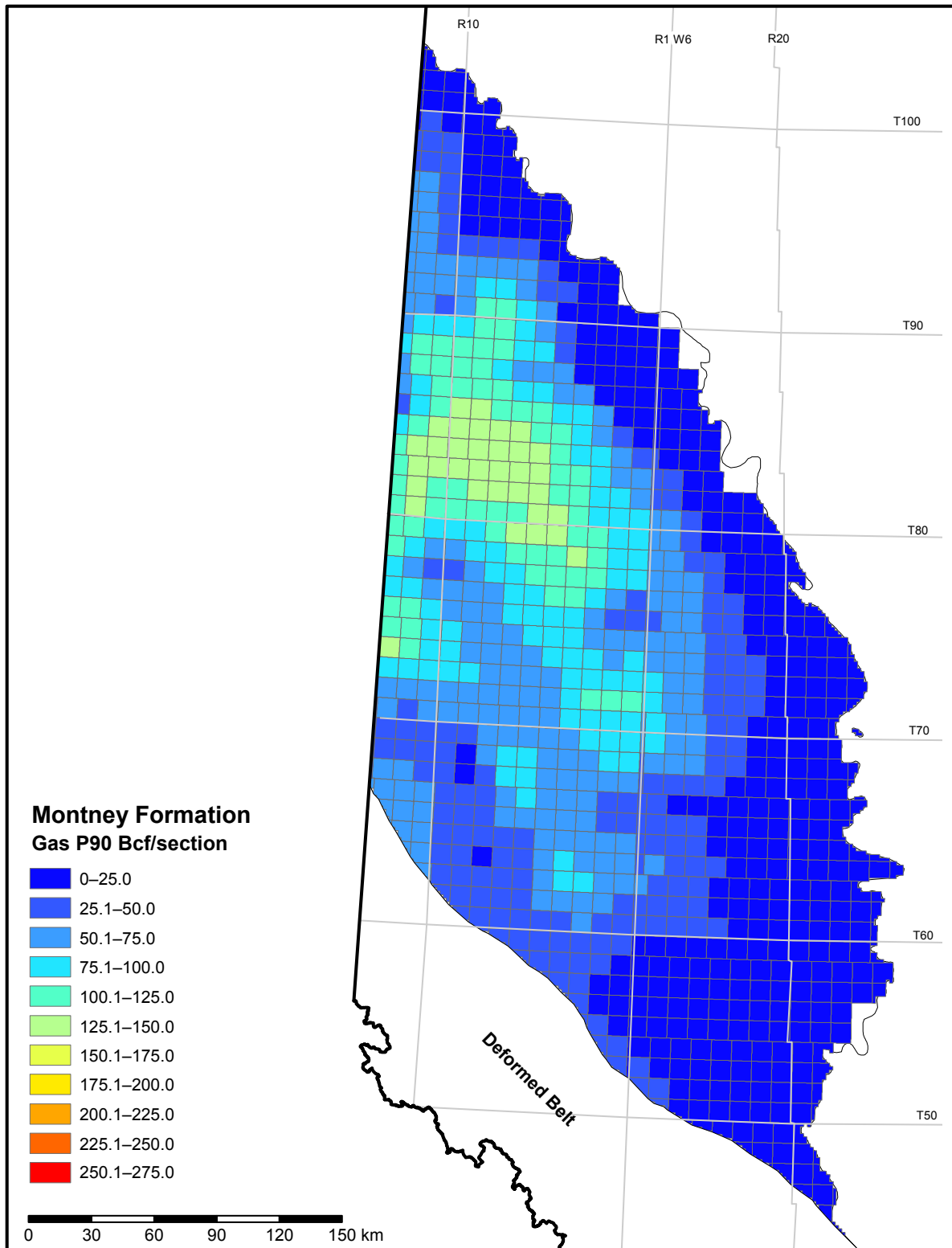


Figure 5.4.8. P90 (low estimate) siltstone-hosted gas initially-in-place in the Montney Formation.

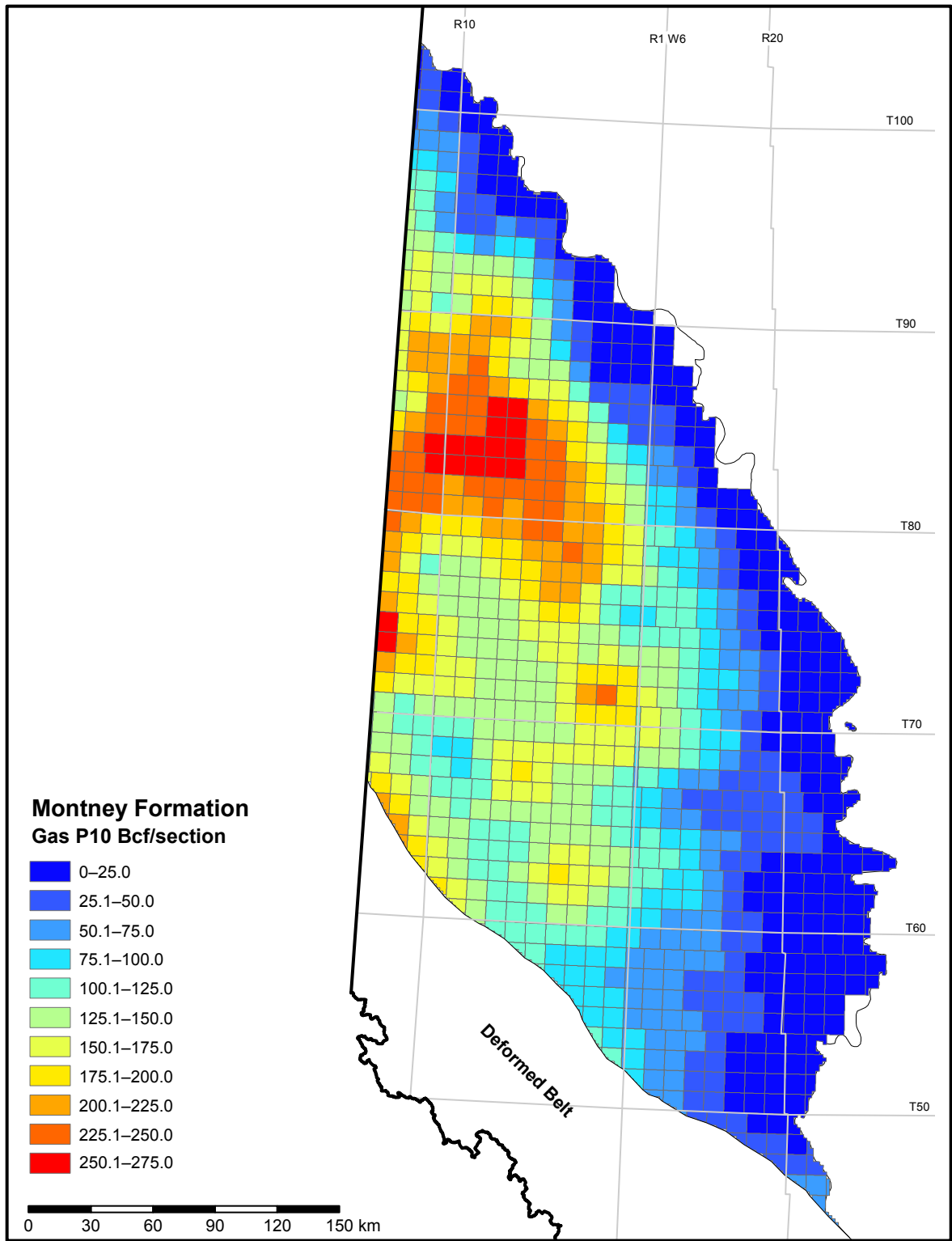


Figure 5.4.9. P10 (high estimate) siltstone-hosted gas initially-in-place in the Montney Formation.

## 5.5 Preliminary Basal Banff/Exshaw Shale-Hosted Hydrocarbon Resource Endowment

Shale-hosted gas initially-in-place for the combined basal Banff/Exshaw ranges from a low estimate (P90) of 16 Tcf to a high estimate (P10) of 70 Tcf, with a medium estimate of 35 Tcf. Shale-hosted natural-gas liquids initially-in-place range from a low estimate (P90) of 0.034 billion barrels to a high estimate (P10) of 0.217 billion barrels, with a medium estimate of 0.092 billion barrels. Shale-hosted oil initially-in-place ranges from a low estimate (P90) of 8.971 billion barrels to a high estimate (P10) of 44.947 billion barrels, with a medium estimate of 24.829 billion barrels. Figures 5.5.1 to 5.5.9 illustrate the shale-hosted hydrocarbon resource endowment estimates on a per-section basis. Tables 5.5.1 and 5.5.2 show the hydrocarbon resource endowment and resource assessment summaries.

**Table 5.5.1. Preliminary summary of the basal Banff/Exshaw shale-hosted hydrocarbon resource endowment: low, medium, and high estimates.**

Hydrocarbon	Low Estimate (P90)	Medium Estimate (P50)	High Estimate (P10)
Oil (billion bbl)	9.0	24.8	44.9
Natural-Gas Liquids (billion bbl)	0.034	0.092	0.217
Natural Gas (Tcf)	16	35	70
Natural Gas–Adsorbed Gas Content (%)	3.2	5.7	10.0

Table 5.5.2. Summary of shale-hosted hydrocarbon resource assessment of the combined basal Banff and Exshaw formations.

Basal Banff/Exshaw	Area (km <sup>2</sup> )				Depth (m)				Net-Silt (Middle unit) Thickness (m)			
	Low	Medium	High	Mean	Low	Medium	High	Mean	Low	Medium	High	Mean
Dry Gas	-	406	1110	475	3684	3869	3940	3834	1.2	2.7	5.0	2.9
Wet Gas	1216	2186	3493	2290	2759	3169	3681	3199	1.7	2.4	3.4	2.5
Condensate	6198	7325	8830	7445	2068	2332	2557	2323	2.1	2.8	3.6	2.8
Volatile Oil	9938	15 707	26 348	16 848	1385	1571	1821	1588	4.3	6.6	9.5	6.8
Black Oil	9914	13 048	14 903	12 745	1192	1287	1416	1298	8.1	11.3	14.0	11.2
<b>TOTAL</b>	<b>27 265</b>	<b>40 451</b>	<b>51 419</b>	<b>39 803</b>	<b>1603</b>	<b>1717</b>	<b>1926</b>	<b>1744</b>	<b>5.2</b>	<b>7.3</b>	<b>8.9</b>	<b>7.2</b>
Basal Banff/Exshaw	Shale (upper and lower) Thickness (m)				Porosity (%)							
	Low	Medium	High	Mean	Low	Medium	High	Mean				
Dry Gas	1.1	1.8	2.5	1.8	3.58	5.49	7.66	5.56				
Wet Gas	1.5	1.9	2.3	1.9	1.94	3.48	5.57	3.62				
Condensate	1.7	2.0	2.3	2.0	1.55	2.65	4.14	2.76				
Volatile Oil	2.7	3.5	3.9	3.4	3.32	4.78	6.66	4.90				
Black Oil	2.9	3.5	4.2	3.5	5.04	6.98	10.54	7.34				
<b>TOTAL</b>	<b>2.9</b>	<b>3.1</b>	<b>3.3</b>	<b>3.1</b>	<b>3.69</b>	<b>5.07</b>	<b>6.90</b>	<b>5.17</b>				
Basal Banff/Exshaw	Gas (billion m <sup>3</sup> )				NGL (million m <sup>3</sup> )				Oil (million m <sup>3</sup> )			
	Low	Medium	High	Mean	Low	Medium	High	Mean	Low	Medium	High	Mean
Dry Gas	-	11	38	15	-	-	-	-	-	-	-	-
Wet Gas	27	46	72	48	1	2	5	2	-	-	-	-
Condensate	74	117	201	127	5	13	30	16	8	17	31	19
Volatile Oil	135	378	1021	489	-	-	-	-	286	768	2099	1000
Black Oil	191	427	700	442	-	-	-	-	1147	3118	5156	3168
<b>TOTAL</b>	<b>446</b>	<b>993</b>	<b>1975</b>	<b>1122</b>	<b>5</b>	<b>15</b>	<b>35</b>	<b>18</b>	<b>1426</b>	<b>3946</b>	<b>7143</b>	<b>4187</b>
Basal Banff/Exshaw	Gas (Bcf)				NGL (MMbbl)				Oil (MMbbl)			
	Low	Medium	High	Mean	Low	Medium	High	Mean	Low	Medium	High	Mean
Dry Gas	-	380	1353	543	-	-	-	-	-	-	-	-
Wet Gas	962	1640	2569	1716	4	13	31	16	-	-	-	-
Condensate	2627	4141	7148	4524	28	79	190	98	53	107	198	119
Volatile Oil	4804	13 408	36 248	17 340	-	-	-	-	1798	4832	13 207	6295
Black Oil	6792	15 150	24 859	15 688	-	-	-	-	7218	19 621	32 444	19 933
<b>TOTAL</b>	<b>15 819</b>	<b>35 253</b>	<b>70 092</b>	<b>39 811</b>	<b>34</b>	<b>92</b>	<b>217</b>	<b>114</b>	<b>8971</b>	<b>24 829</b>	<b>44 947</b>	<b>26 347</b>

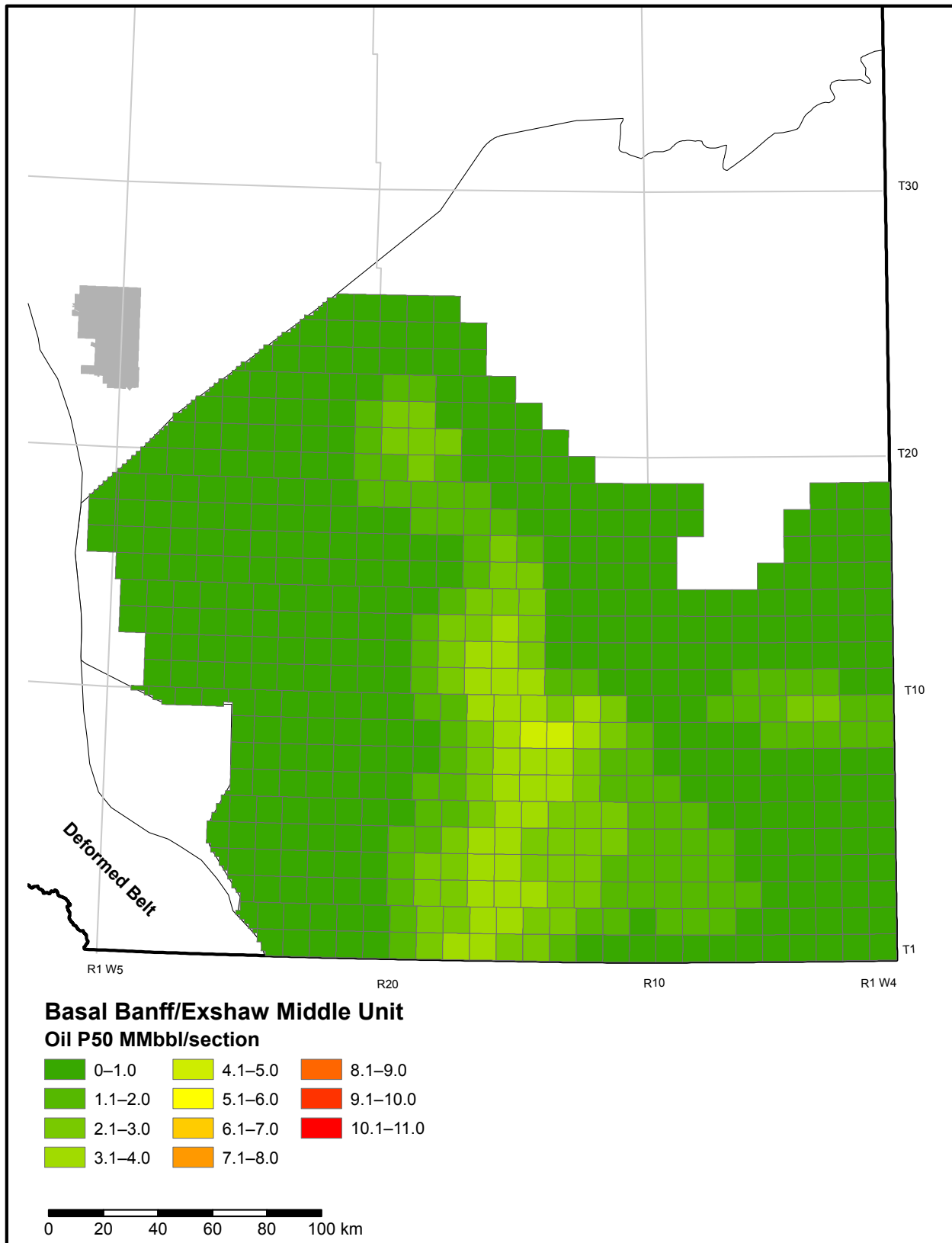


Figure 5.5.1. P50 (best estimate) shale-hosted oil initially-in-place in the basal Banff/Exshaw middle unit in the study area.

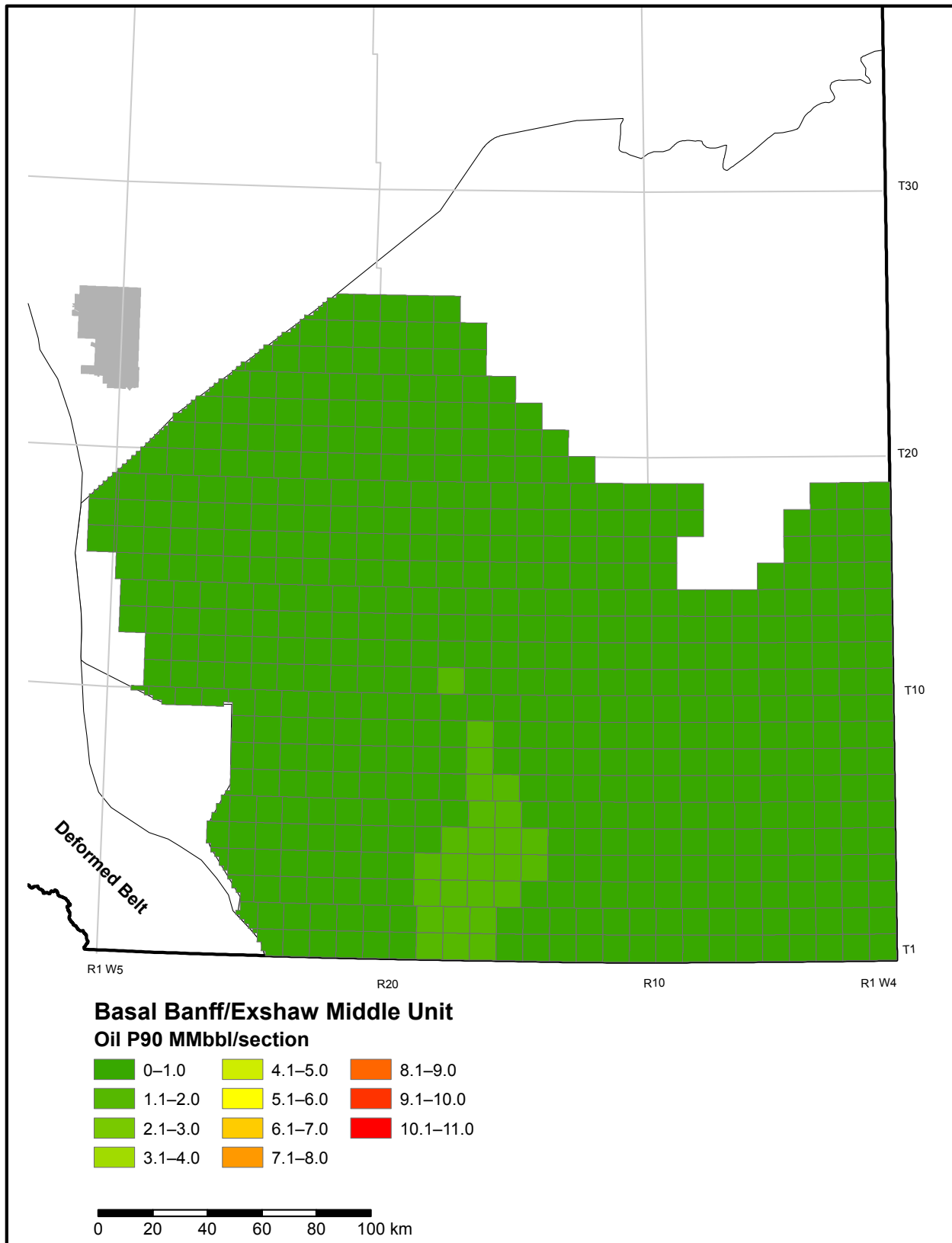


Figure 5.5.2. P90 (low estimate) shale-hosted oil initially-in-place in the basal Banff/Exshaw middle unit in the study area.

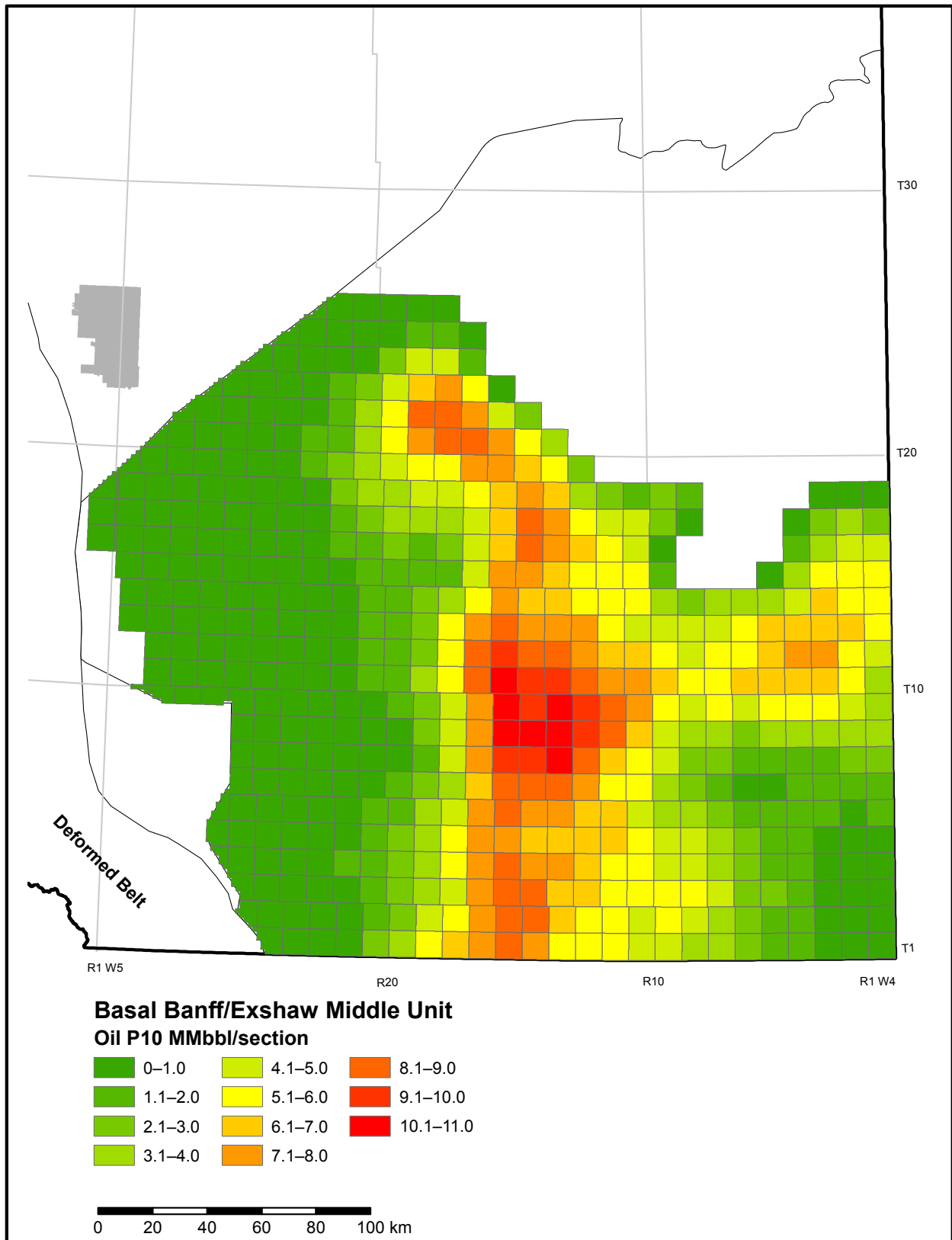


Figure 5.5.3. P10 (high estimate) shale-hosted oil initially-in-place in the basal Banff/Exshaw middle unit in the study area.

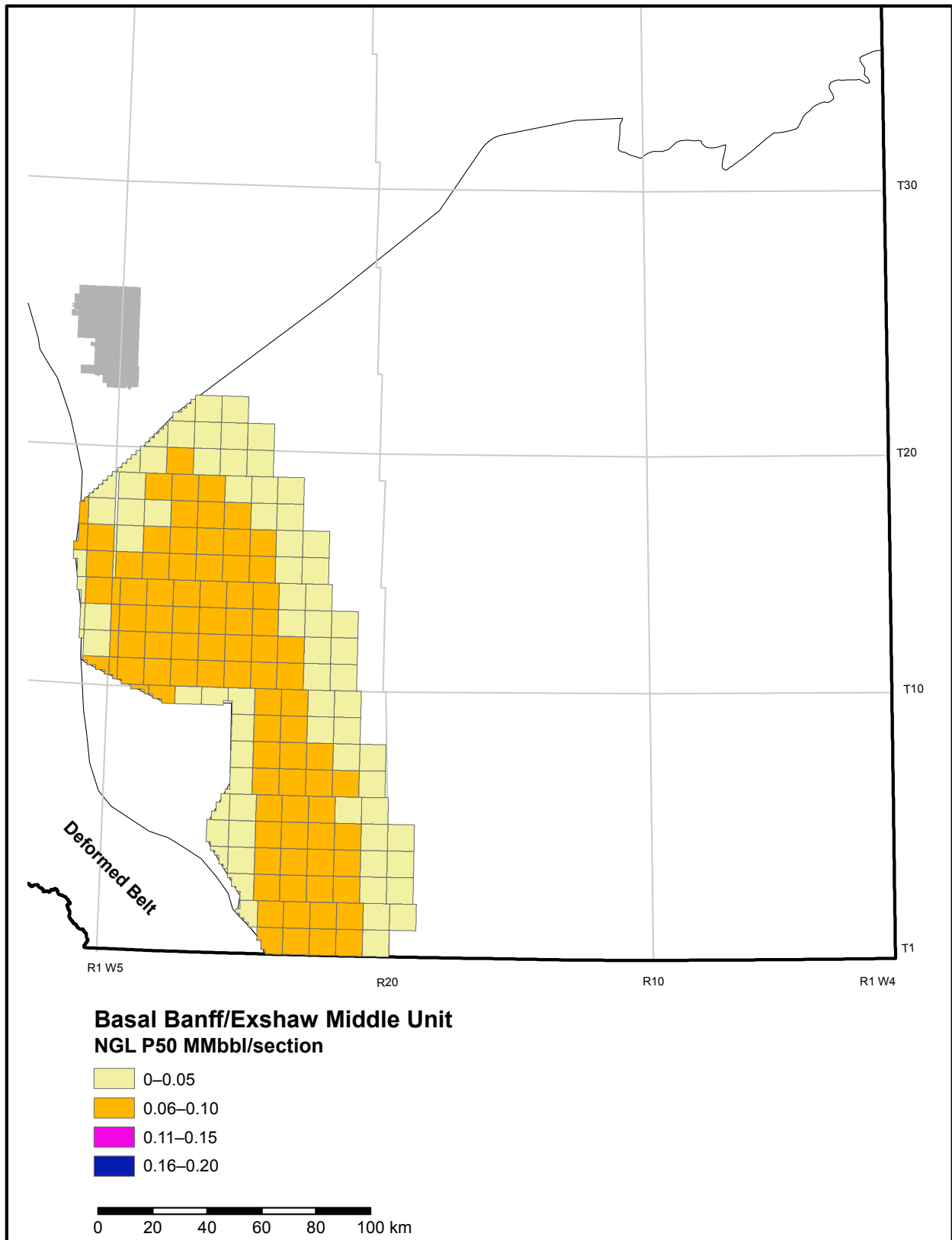


Figure 5.5.4. P50 (best estimate) shale-hosted natural-gas liquids initially-in-place in the basal Banff/Exshaw middle unit in the study area.

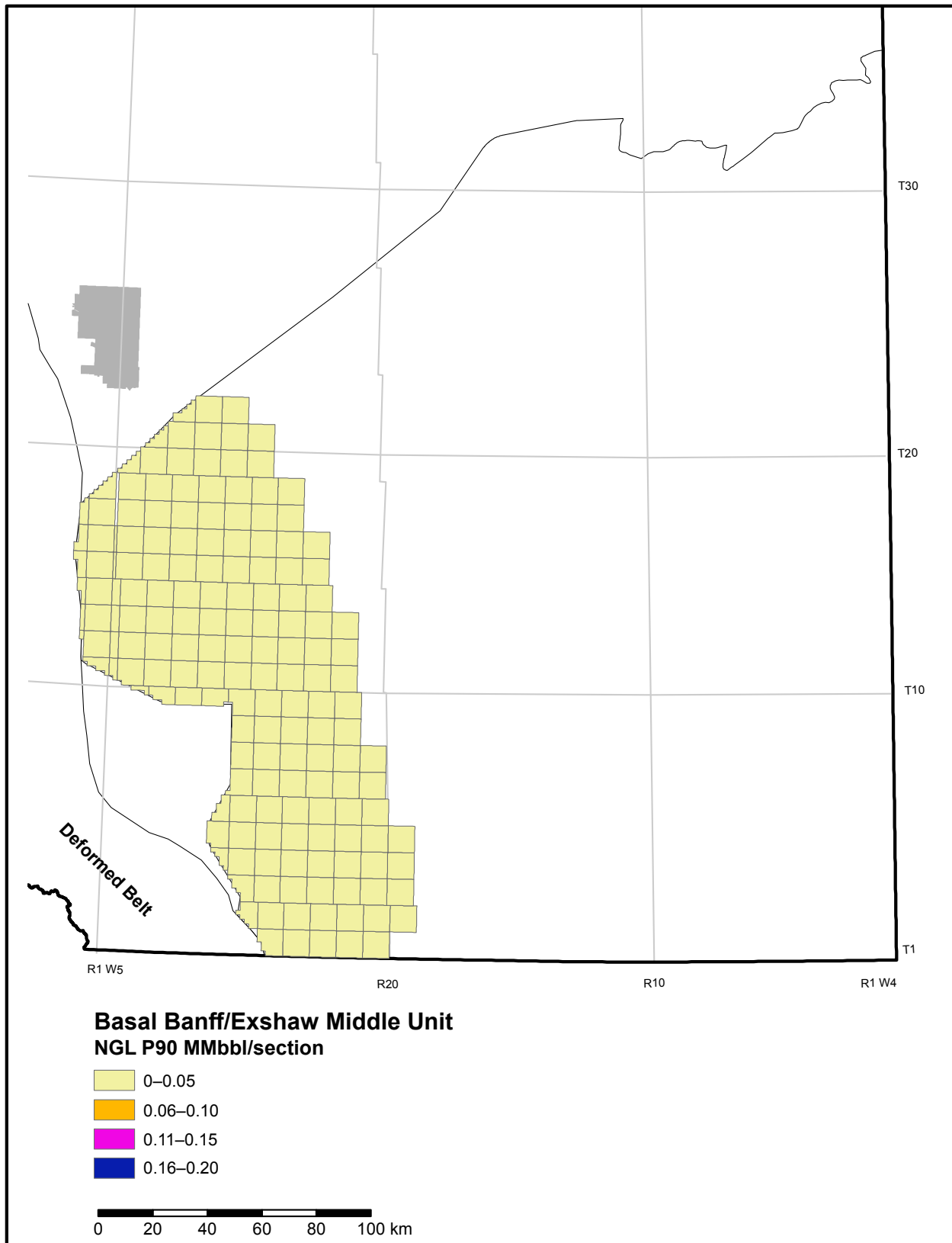


Figure 5.5.5. P90 (low estimate) shale-hosted natural-gas liquids initially-in-place in the basal Banff/Exshaw middle unit in the study area.

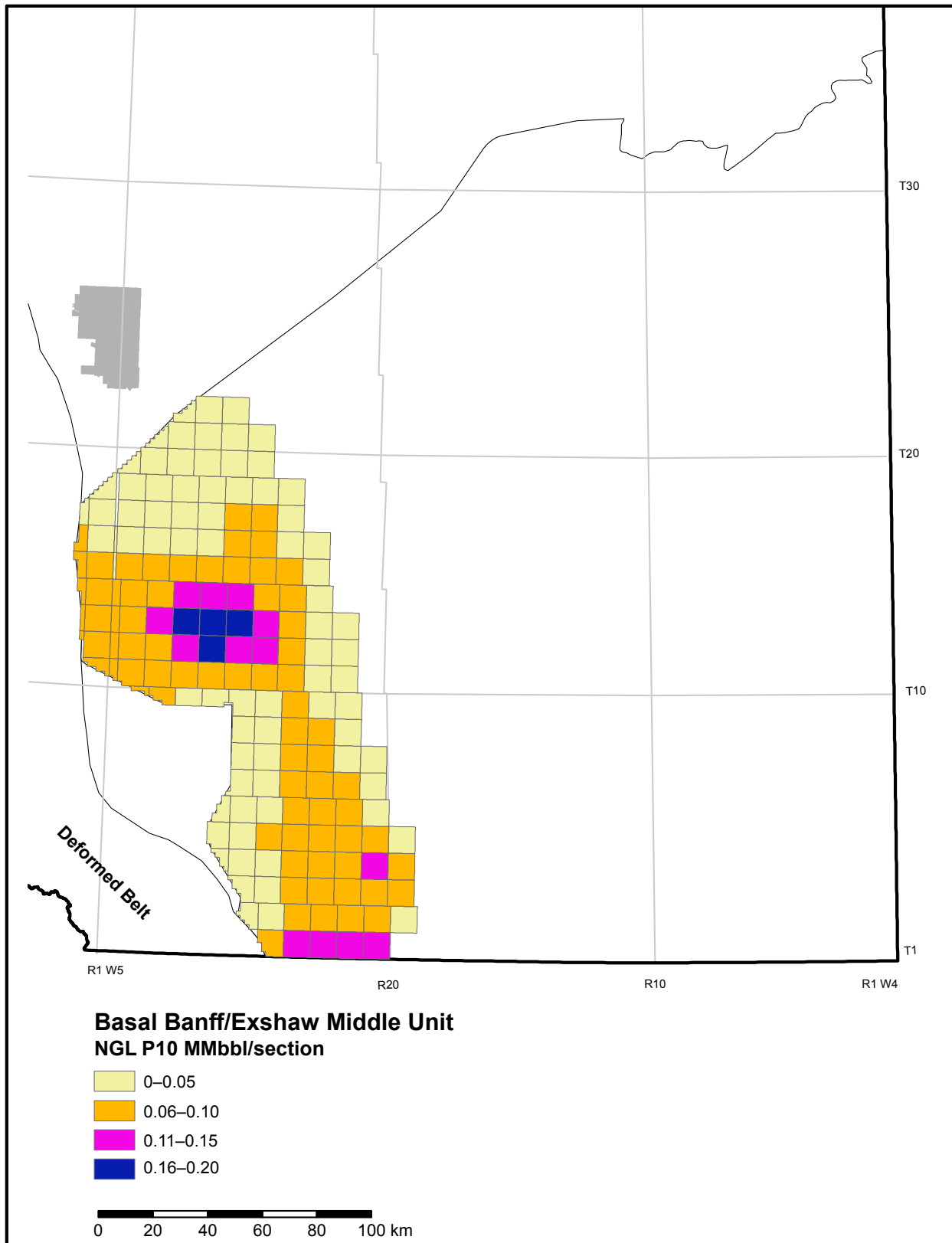


Figure 5.5.6. P10 (high estimate) shale-hosted natural-gas liquids initially-in-place in the basal Banff/Exshaw middle unit in the study area.

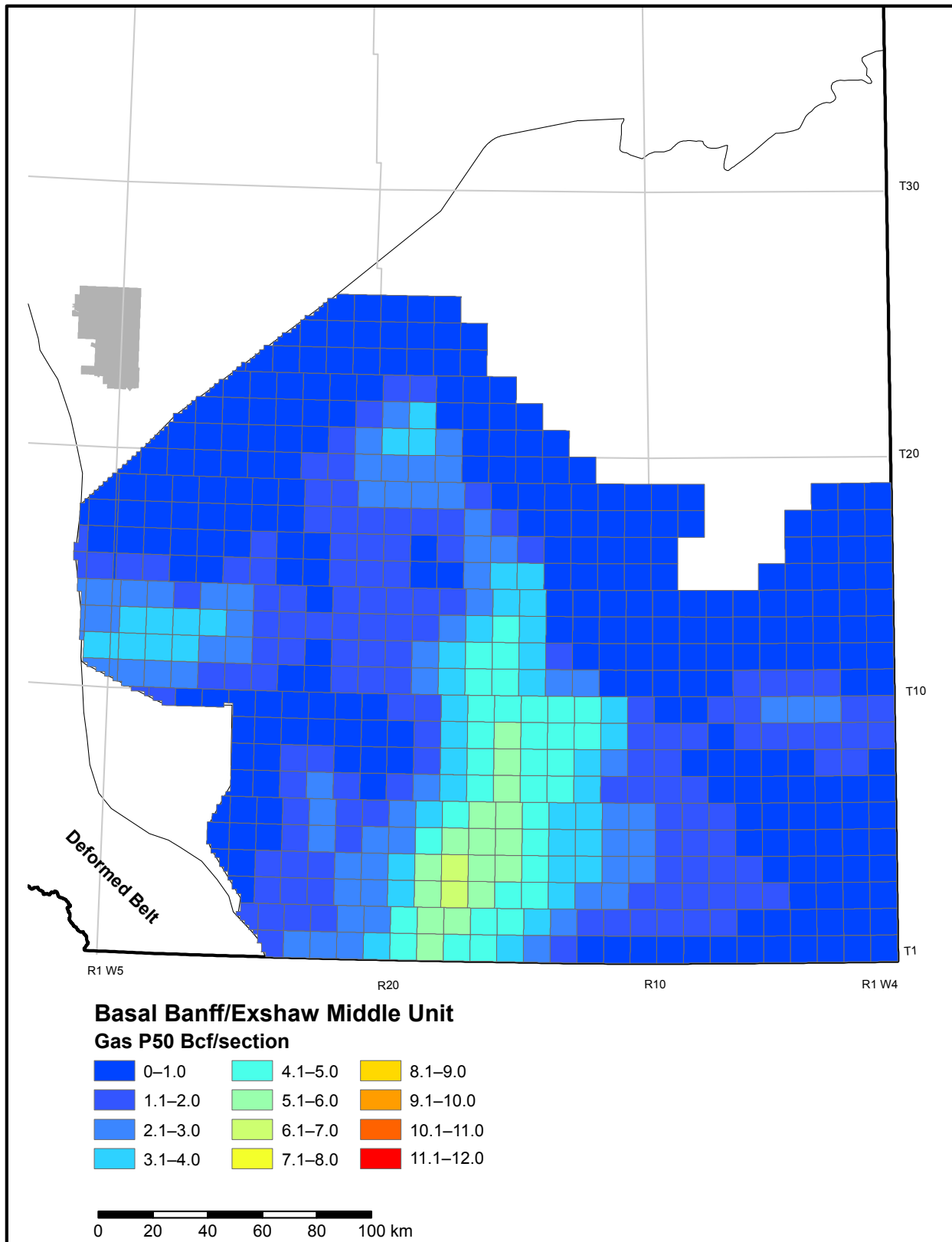


Figure 5.5.7. P50 (best estimate) shale-hosted gas initially-in-place in the basal Banff/Exshaw middle unit in the study area.

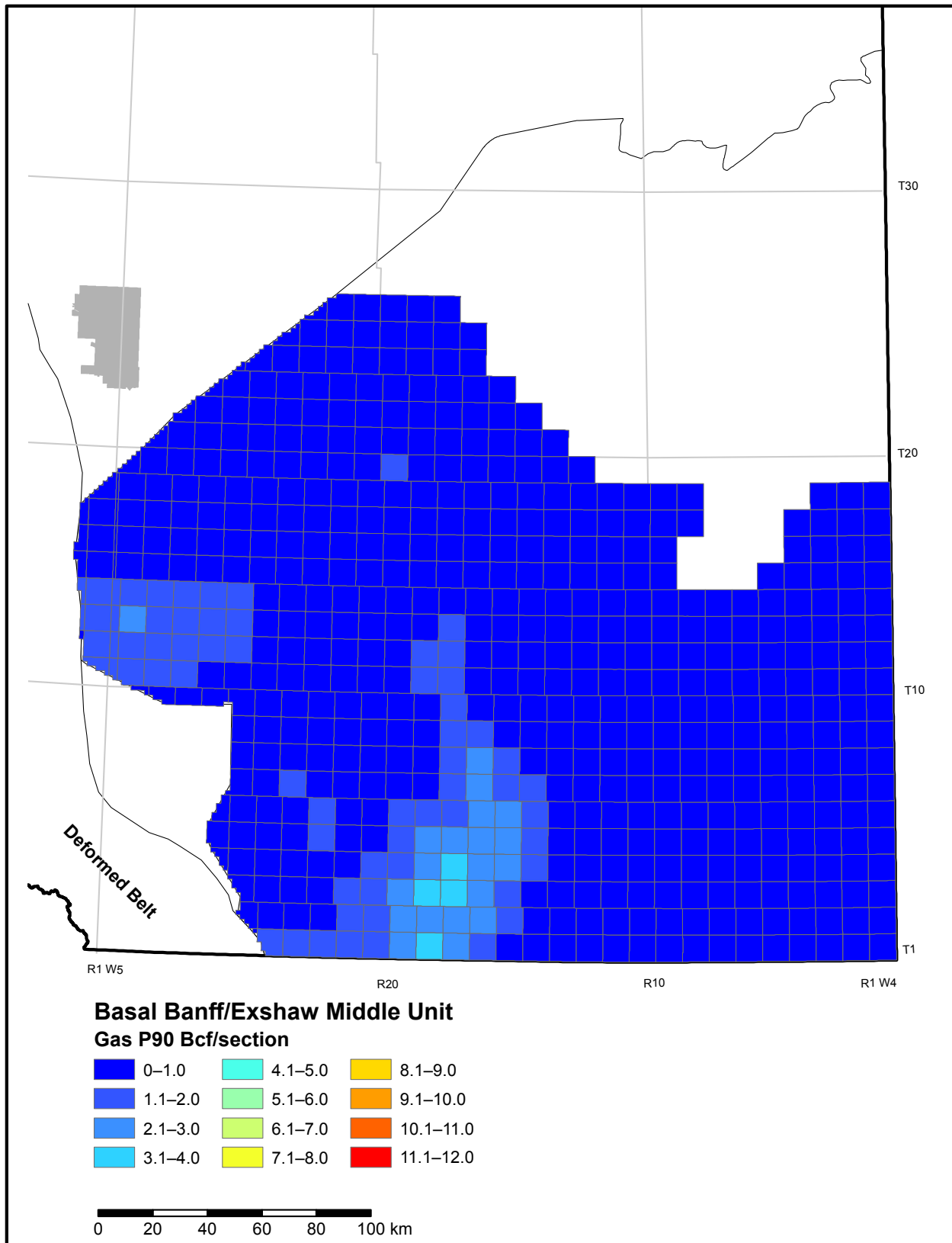


Figure 5.5.8. P90 (low estimate) shale-hosted gas initially-in-place in the basal Banff/Exshaw middle unit in the study area.

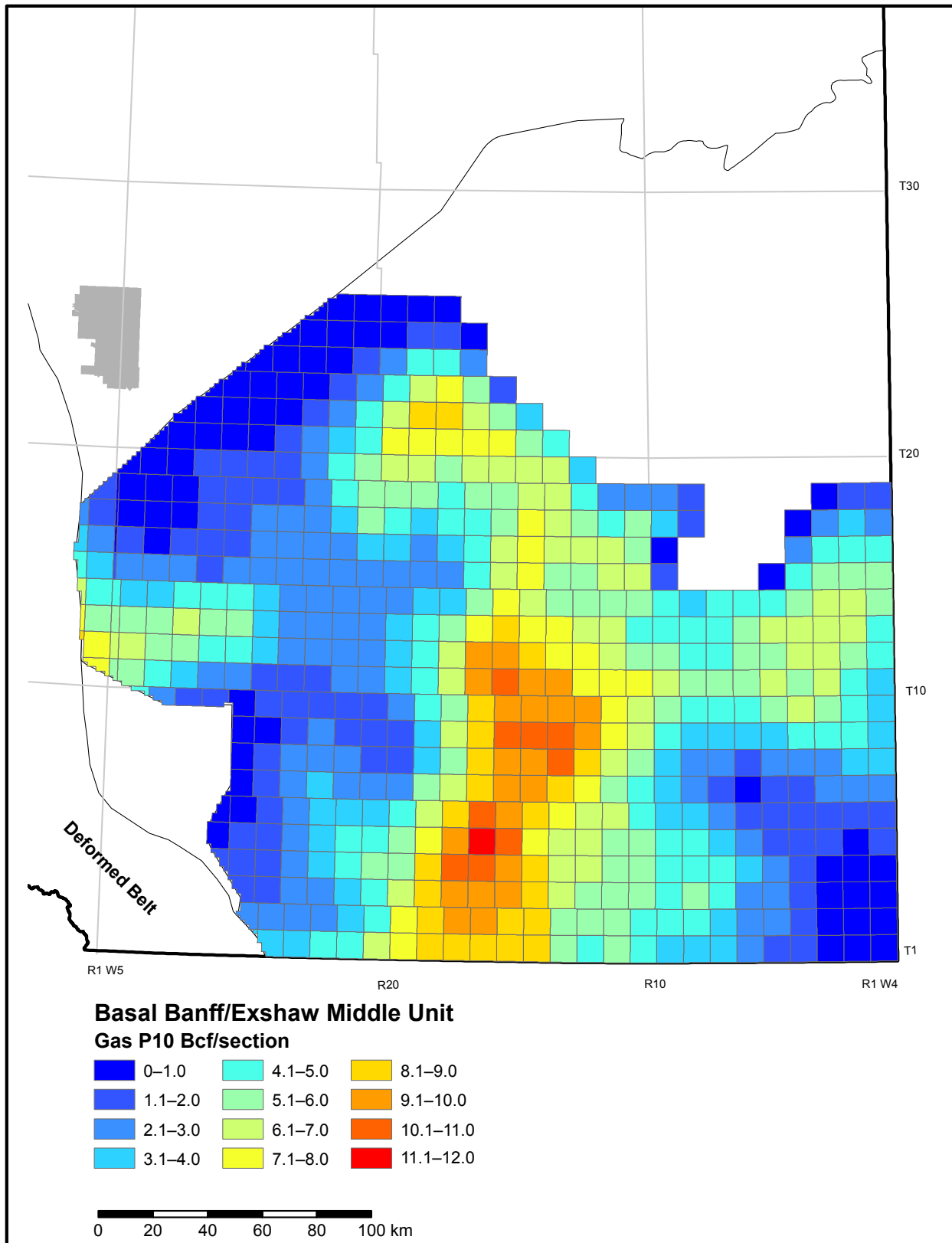


Figure 5.5.9. P10 (high estimate) shale-hosted gas initially-in-place in the basal Banff/Exshaw middle unit in the study area.

## 5.6 Preliminary North Nordegg Shale-Hosted Hydrocarbon Resource Endowment

Shale-hosted gas initially-in-place for the north Nordegg ranges from a low estimate (P90) of 70 Tcf to a high estimate (P10) of 281 Tcf, with a medium estimate of 148 Tcf. Shale-hosted natural-gas liquids initially-in-place range from a low estimate (P90) of 0.487 billion barrels to a high estimate (P10) of 3.497 billion barrels, with a medium estimate of 1.433 billion barrels. Shale-hosted oil initially-in-place ranges from a low estimate (P90) of 19.891 billion barrels to a high estimate (P10) of 66.388 billion barrels, with a medium estimate of 37.829 billion barrels. Figures 5.6.1 to 5.6.9 illustrate the shale-hosted hydrocarbon resource endowment estimates on a per-section basis. Tables 5.6.1 and 5.6.2 show the hydrocarbon resource endowment and resource assessment summaries.

**Table 5.6.1. Preliminary summary of north Nordegg shale-hosted hydrocarbon resource endowment: low, medium, and high estimates.**

Hydrocarbon	Low Estimate (P90)	Medium Estimate (P50)	High Estimate (P10)
Oil (billion bbl)	19.9	37.8	66.4
Natural-Gas Liquids (billion bbl)	0.5	1.4	3.5
Natural Gas (Tcf)	70	148	281
Natural Gas-Adsorbed Gas Content (%)	4.6	18.2	34.8

Table 5.6.2. Summary of shale-hosted hydrocarbon resource assessment of the north Nordegg.

Nordegg	Area (km <sup>2</sup> )				Depth (m)							
	Low	Medium	High	Mean	Low	Medium	High	Mean				
Dry Gas	-	1879	7724	2974	3510	3826	4177	3843				
Wet Gas	-	4399	5096	3632	2826	3416	3972	3410				
Condensate	6844	8467	9733	8123	2319	2763	3495	2835				
Volatile Oil	9242	11 598	14 385	11 676	1825	2070	2583	2157				
Black Oil	3835	5445	7427	5602	1515	1718	2062	1768				
<b>TOTAL</b>	<b>23 925</b>	<b>33 154</b>	<b>38 394</b>	<b>32 007</b>	<b>2372</b>	<b>2509</b>	<b>2778</b>	<b>2547</b>				
Nordegg	Net-Shale Thickness (m)				Porosity (%)							
	Low	Medium	High	Mean	Low	Medium	High	Mean				
Dry Gas	18.8	21.4	23.1	21.1	1.57	4.02	8.18	4.61				
Wet Gas	19.0	21.3	22.9	21.1	1.24	3.22	6.58	3.62				
Condensate	20.3	22.2	24.3	22.3	1.68	3.51	6.60	3.94				
Volatile Oil	22.8	24.9	25.8	24.6	2.49	4.45	7.56	4.79				
Black Oil	24.5	26.3	27.9	26.2	3.27	5.99	9.30	6.20				
<b>TOTAL</b>	<b>22.5</b>	<b>23.6</b>	<b>24.3</b>	<b>23.5</b>	<b>2.31</b>	<b>4.15</b>	<b>7.21</b>	<b>4.50</b>				
Nordegg	Gas (billion m <sup>3</sup> )				NGL (million m <sup>3</sup> )				Oil (million m <sup>3</sup> )			
	Low	Medium	High	Mean	Low	Medium	High	Mean	Low	Medium	High	Mean
Dry Gas	-	402	1696	643	-	-	-	-	-	-	-	-
Wet Gas	-	652	1269	684	-	30	89	40	-	-	-	-
Condensate	679	1490	2539	1561	70	197	480	251	78	231	499	266
Volatile Oil	599	1167	2173	1289	-	-	-	-	1306	2576	4843	2863
Black Oil	238	420	704	454	-	-	-	-	1682	3111	5216	3330
<b>TOTAL</b>	<b>1968</b>	<b>4164</b>	<b>7905</b>	<b>4632</b>	<b>77</b>	<b>228</b>	<b>555</b>	<b>291</b>	<b>3161</b>	<b>6011</b>	<b>10 550</b>	<b>6459</b>
Nordegg	Gas (Bcf)				NGL (MMbbl)				Oil (MMbbl)			
	Low	Medium	High	Mean	Low	Medium	High	Mean	Low	Medium	High	Mean
Dry Gas	-	14 272	60 191	22 840	-	-	-	-	-	-	-	-
Wet Gas	-	23 143	45 027	24 270	-	187	563	253	-	-	-	-
Condensate	24 089	52 878	90 124	55 414	439	1241	3022	1581	493	1455	3139	1671
Volatile Oil	21 257	41 406	77 131	45 740	-	-	-	-	8218	16 209	30 478	18 019
Black Oil	8463	14 922	24 990	16 131	-	-	-	-	10 588	19 575	32 824	20 956
<b>TOTAL</b>	<b>69 836</b>	<b>147 809</b>	<b>280 587</b>	<b>164 394</b>	<b>487</b>	<b>1433</b>	<b>3497</b>	<b>1834</b>	<b>19 891</b>	<b>37 829</b>	<b>66 388</b>	<b>40 645</b>

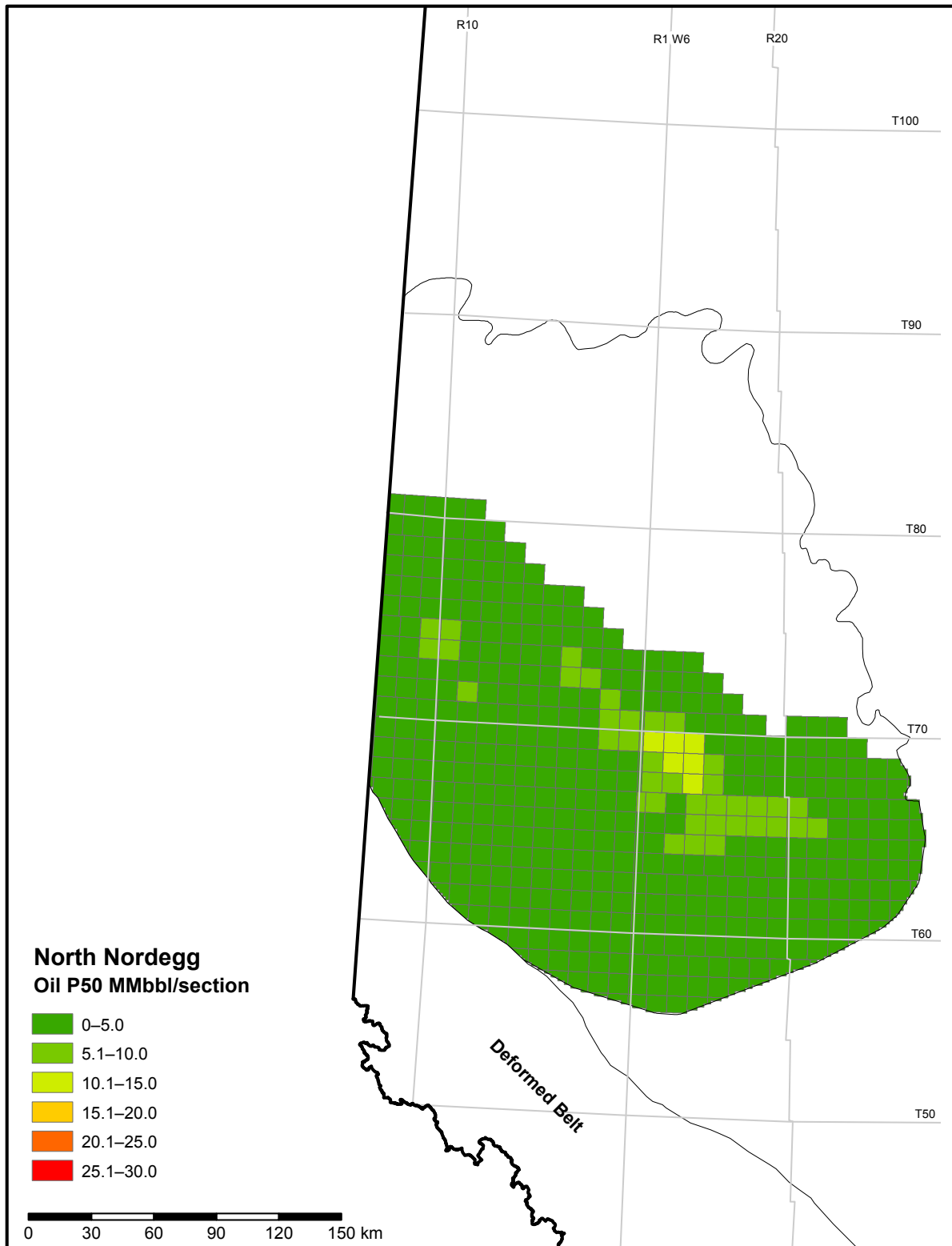


Figure 5.6.1. P50 (best estimate) shale-hosted oil initially-in-place in the north Nordegg.

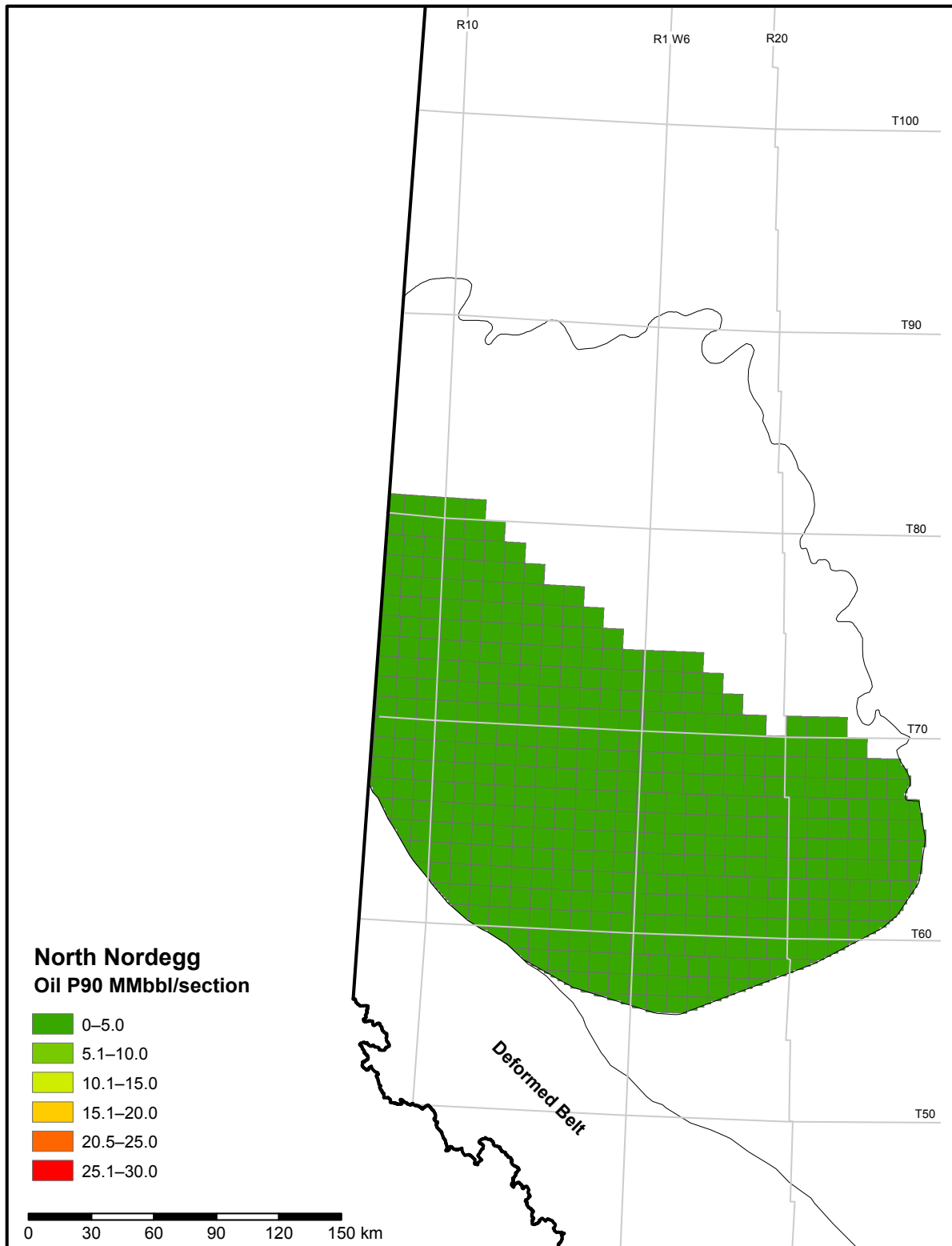


Figure 5.6.2. P90 (low estimate) shale-hosted oil initially-in-place in the north Nordegg.

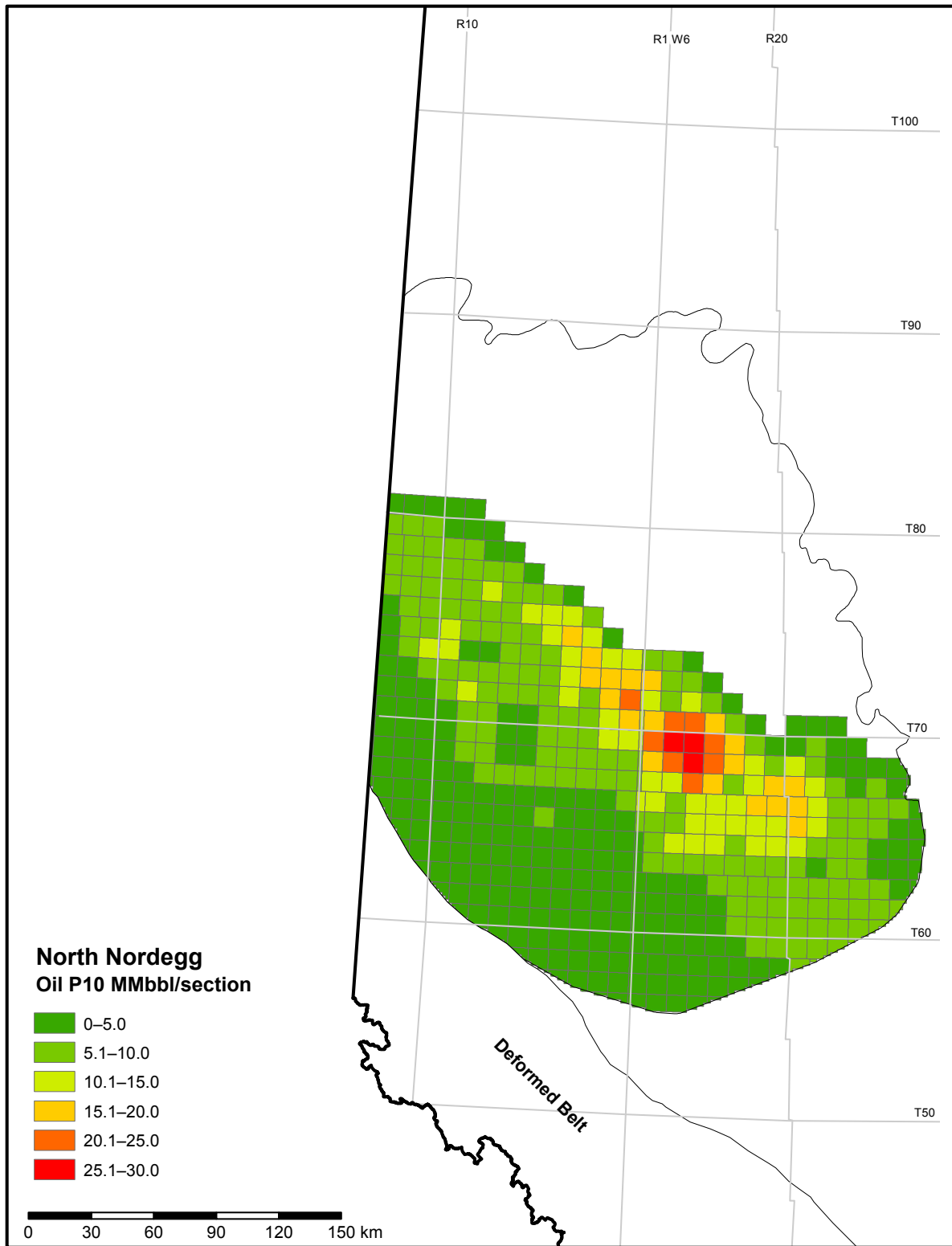


Figure 5.6.3. P10 (high estimate) shale-hosted oil initially-in-place in the north Nordegg.

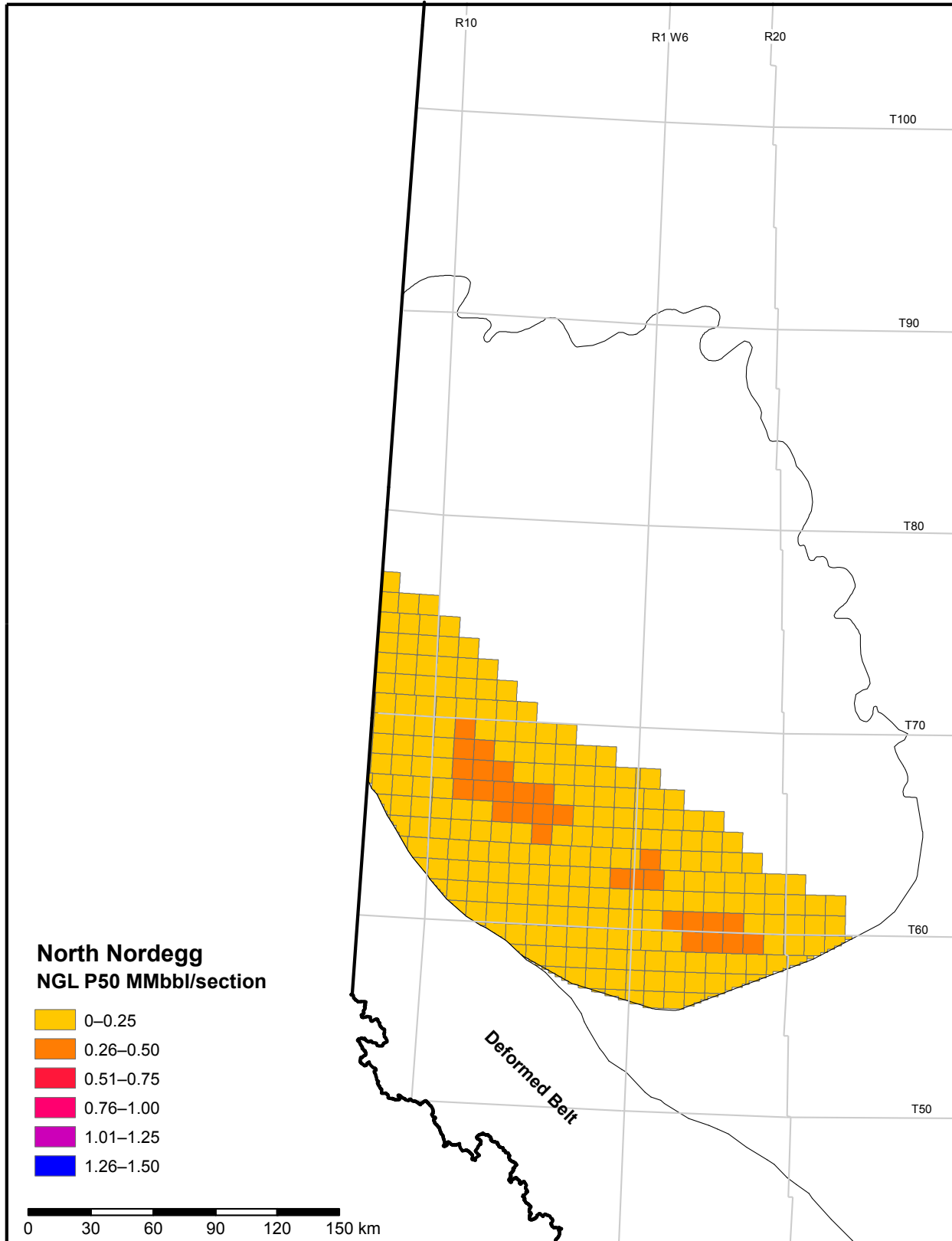


Figure 5.6.4. P50 (best estimate) shale-hosted natural-gas liquids initially-in-place in the north Nordegg.

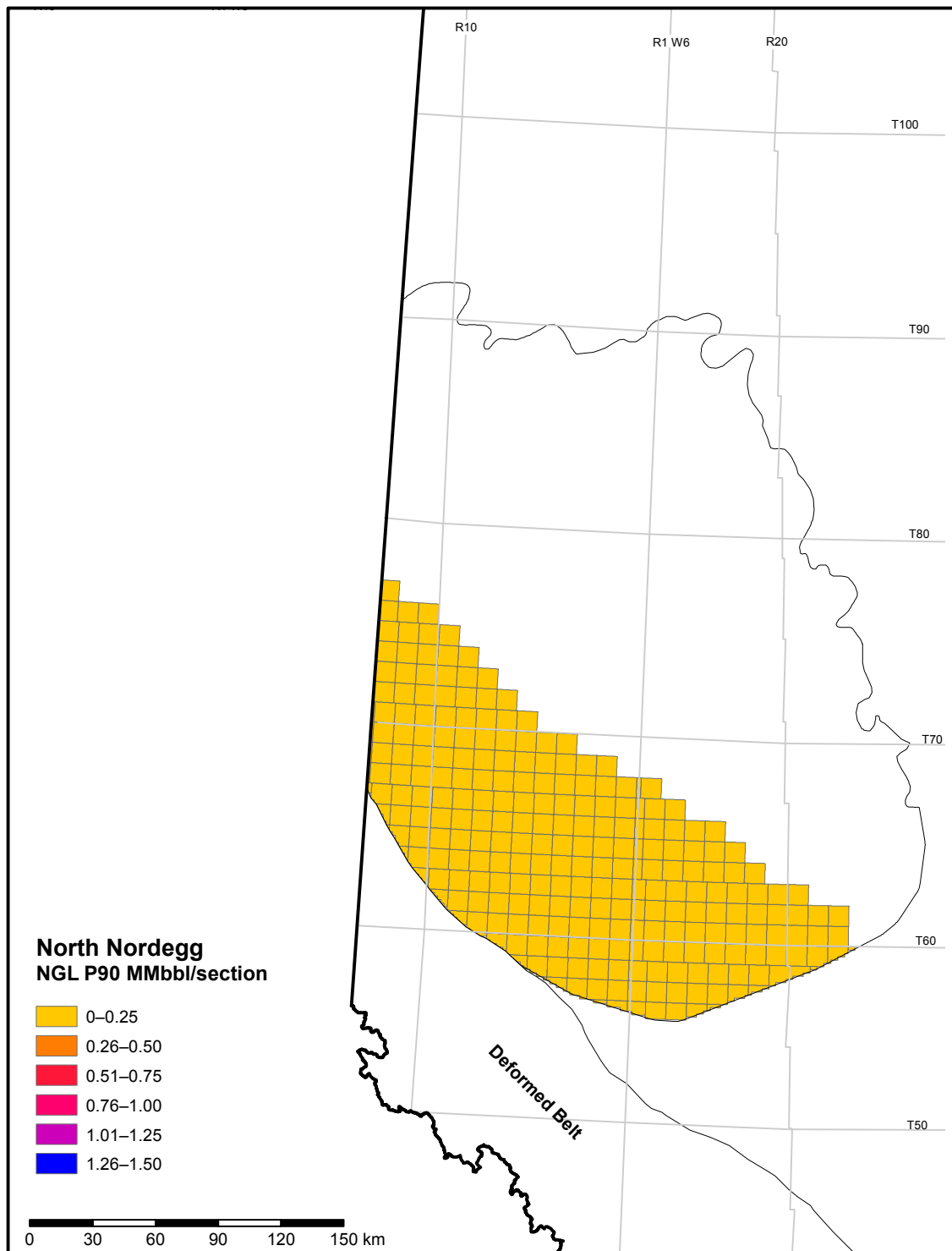


Figure 5.6.5. P90 (low estimate) shale-hosted natural-gas liquids initially-in-place in the north Nordegg.

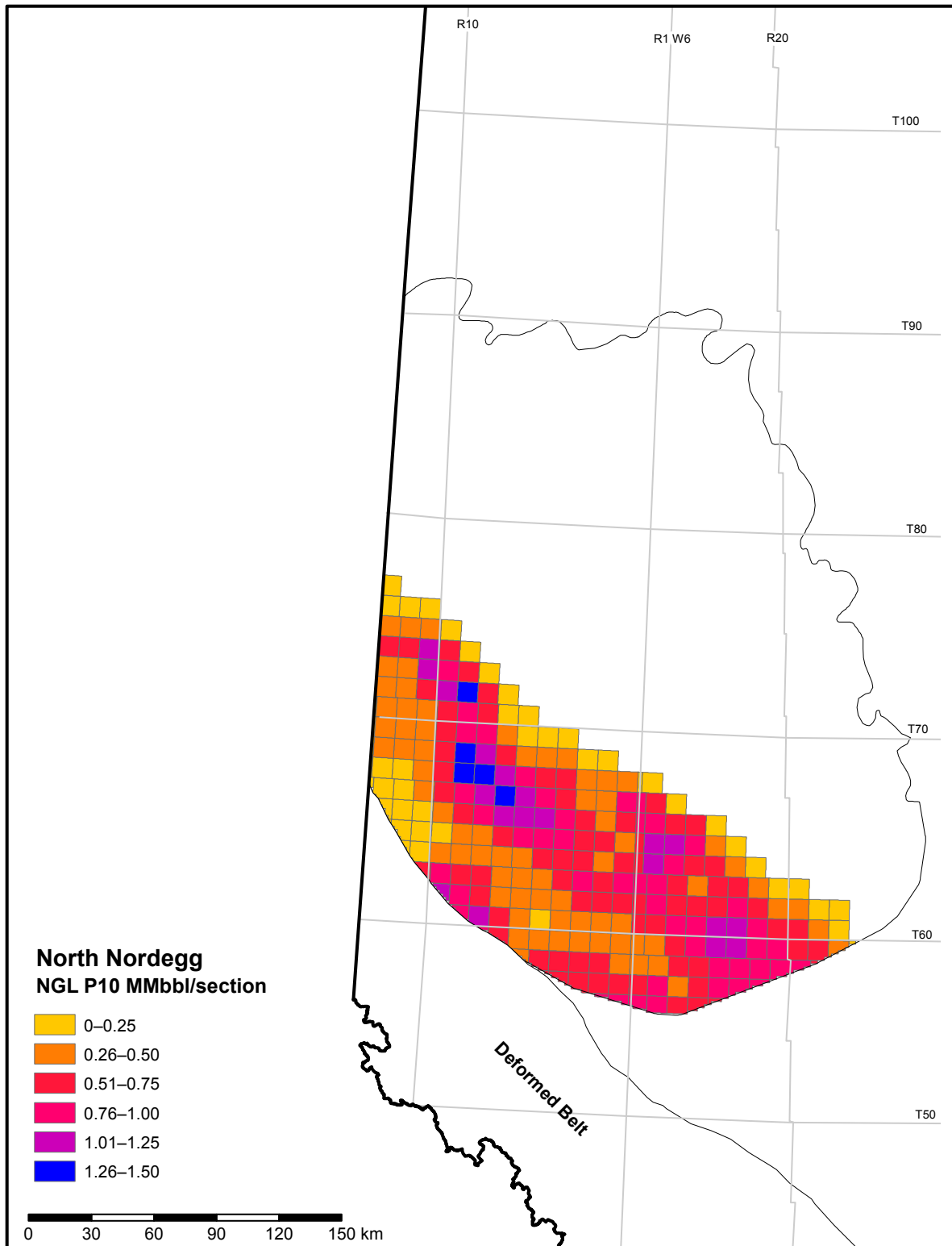


Figure 5.6.6. P10 (high estimate) shale-hosted natural-gas liquids initially-in-place in the north Nordegg.

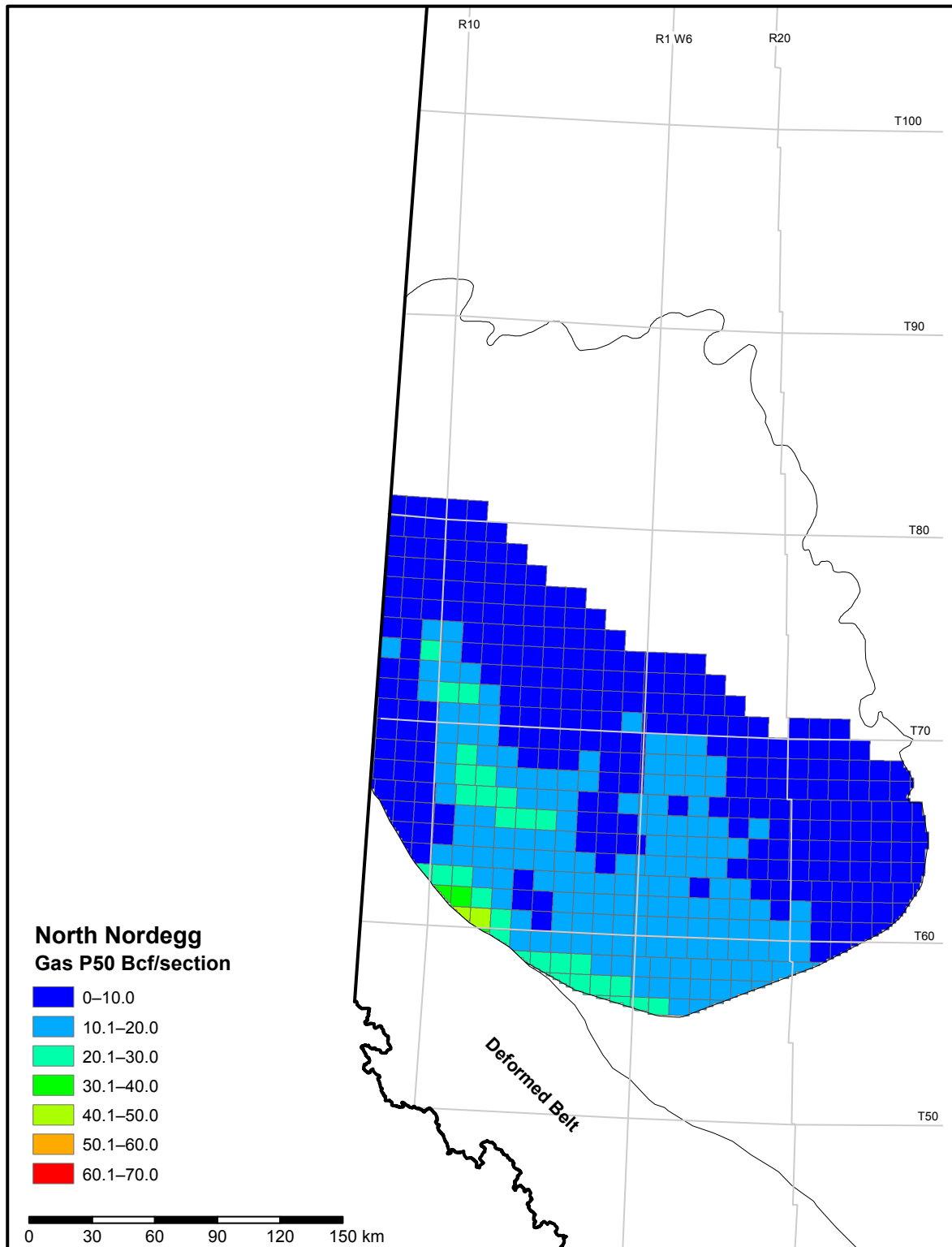


Figure 5.6.7. P50 (best estimate) shale-hosted gas initially-in-place in the north Nordegg.

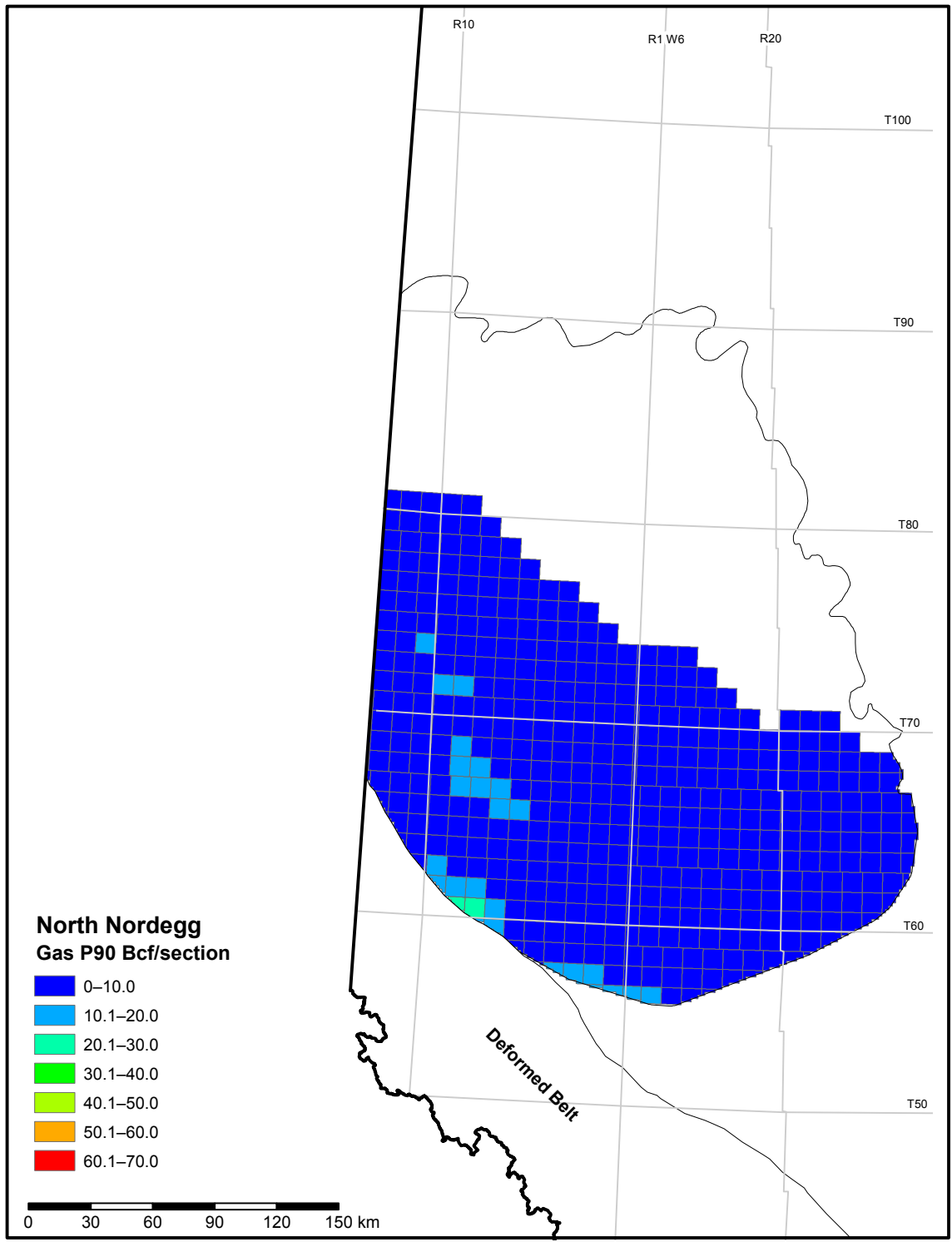


Figure 5.6.8. P90 (low estimate) shale-hosted gas initially-in-place in the north Nordegg.

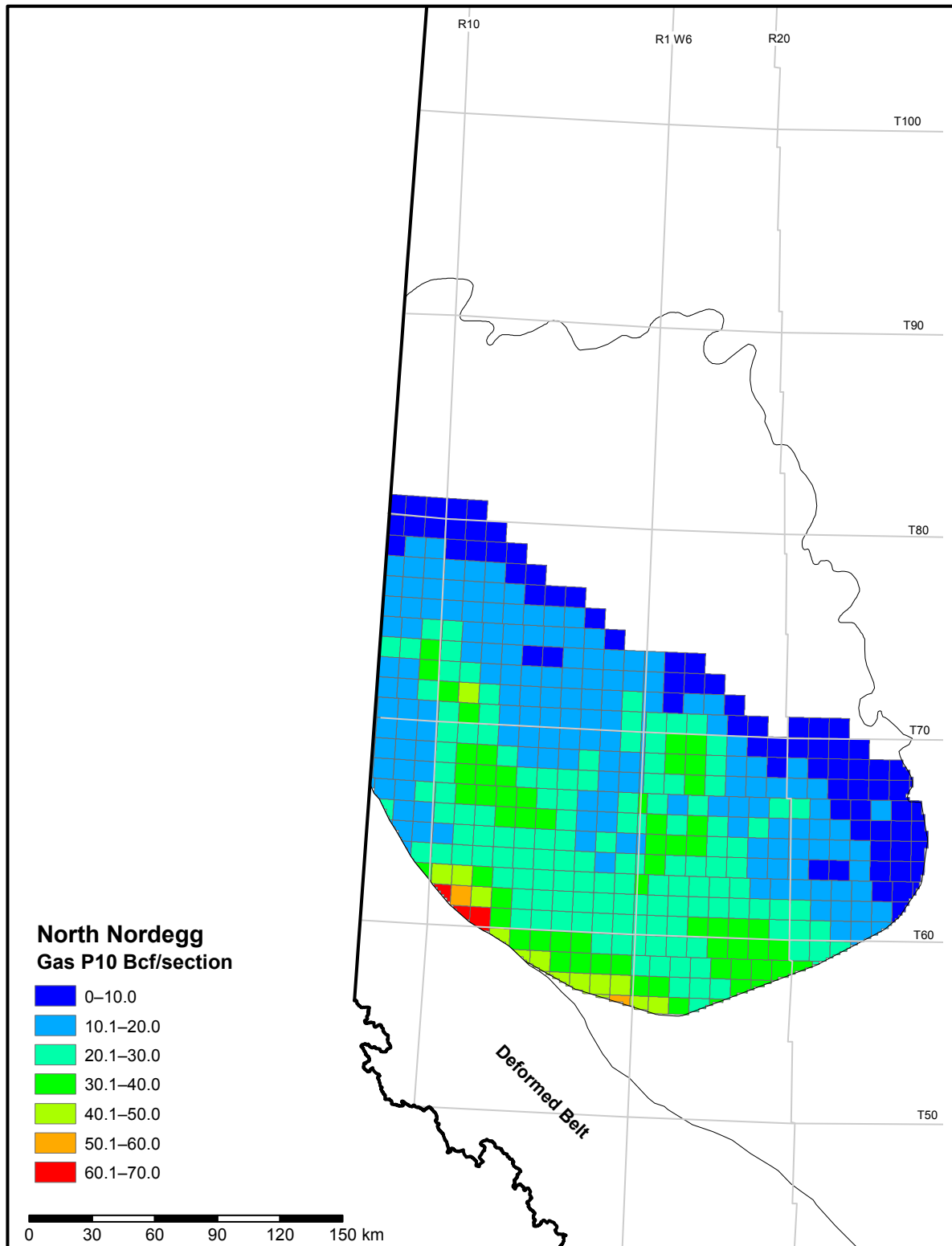


Figure 5.6.9. P10 (high estimate) shale-hosted gas initially-in-place in the north Nordegg.

## 5.7 Preliminary Wilrich Member Shale-Hosted Hydrocarbon Resource Endowment

Shale-hosted gas initially-in-place for the Wilrich Member ranges from a low estimate (P90) of 115 Tcf to a high estimate (P10) of 568 Tcf, with a medium estimate of 246 Tcf. Shale-hosted natural-gas liquids initially-in-place range from a low estimate (P90) of 0.689 billion barrels to a high estimate (P10) of 4.449 billion barrels, with a medium estimate of 2.062 billion barrels. Shale-hosted oil initially-in-place ranges from a low estimate (P90) of 20.176 billion barrels to a high estimate (P10) of 172.300 billion barrels, with a medium estimate of 47.898 billion barrels. Figures 5.7.1 to 5.7.9 illustrate the shale-hosted hydrocarbon resource endowment estimates on a per-section basis. Tables 5.7.1 and 5.7.2 show the hydrocarbon resource endowment and resource assessment summaries.

**Table 5.7.1. Preliminary summary of the Wilrich Member shale-hosted hydrocarbon resource endowment: low, medium, and high estimates (preliminary evaluation).**

Hydrocarbon	Low Estimate (P90)	Medium Estimate (P50)	High Estimate (P10)
Oil (billion bbl)	20.2	47.9	172.3
Natural-Gas Liquids (billion bbl)	0.7	2.1	4.4
Natural Gas (Tcf)	115	246	568
Natural Gas-Adsorbed Gas Content (%)	6.2	33.7	59.2

Table 5.7.2. Summary of shale-hosted hydrocarbon resource assessment of the Wilrich Member.

Wilrich	Area (km <sup>2</sup> )				Depth (m)							
	Low	Medium	High	Mean	Low	Medium	High	Mean				
Dry Gas	-	-	4355	944	3497	3640	3763	3636				
Wet Gas	-	3680	5438	2957	3139	3581	3736	3513				
Condensate	6151	6984	8393	7157	2697	3114	3445	3095				
Volatile Oil	6566	8626	15 733	9942	1990	2562	2819	2483				
Black Oil	3481	4422	11 348	6053	1515	2158	2482	2071				
<b>TOTAL</b>	<b>17 323</b>	<b>23 100</b>	<b>44 087</b>	<b>27 053</b>	<b>2255</b>	<b>2812</b>	<b>3012</b>	<b>2718</b>				
Wilrich	Net-Shale Thickness (m)				Porosity (%)							
	Low	Medium	High	Mean	Low	Medium	High	Mean				
Dry Gas	56.2	64.0	68.0	63.0	1.94	3.34	4.58	3.26				
Wet Gas	58.3	64.1	67.9	63.3	1.76	3.02	4.39	3.05				
Condensate	61.4	65.2	69.5	65.4	1.53	2.77	3.91	2.78				
Volatile Oil	67.1	70.4	74.8	70.6	2.07	3.33	5.07	3.51				
Black Oil	69.4	74.2	78.3	74.0	2.71	4.24	7.75	4.73				
<b>TOTAL</b>	<b>65.7</b>	<b>68.7</b>	<b>72.2</b>	<b>68.8</b>	<b>2.09</b>	<b>3.41</b>	<b>5.10</b>	<b>3.53</b>				
Wilrich	Gas (billion m <sup>3</sup> )				NGL (million m <sup>3</sup> )				Oil (million m <sup>3</sup> )			
	Low	Medium	High	Mean	Low	Medium	High	Mean	Low	Medium	High	Mean
Dry Gas	-	-	2327	518	-	-	-	-	-	-	-	-
Wet Gas	-	1476	3305	1532	-	27	140	52	-	-	-	-
Condensate	1368	3282	5567	3325	92	279	598	325	184	427	773	455
Volatile Oil	626	1417	4105	1941	-	-	-	-	1379	3128	8808	4202
Black Oil	236	567	2417	945	-	-	-	-	1558	3774	17 278	6490
<b>TOTAL</b>	<b>3237</b>	<b>6918</b>	<b>16 007</b>	<b>8261</b>	<b>109</b>	<b>327</b>	<b>707</b>	<b>377</b>	<b>3206</b>	<b>7611</b>	<b>27 380</b>	<b>11 148</b>
Wilrich	Gas (Bcf)				NGL (MMbbl)				Oil (MMbbl)			
	Low	Medium	High	Mean	Low	Medium	High	Mean	Low	Medium	High	Mean
Dry Gas	-	-	82 589	18 375	-	-	-	-	-	-	-	-
Wet Gas	-	52 382	117 302	54 379	-	170	884	330	-	-	-	-
Condensate	48 560	116 480	197 598	118 026	580	1759	3765	2044	1157	2690	4861	2866
Volatile Oil	22 227	50 292	145 696	68 898	-	-	-	-	8680	19 683	55 426	26 442
Black Oil	8369	20 128	85 791	33 528	-	-	-	-	9804	23 752	108 729	40 843
<b>TOTAL</b>	<b>114 908</b>	<b>245 557</b>	<b>568 134</b>	<b>293 205</b>	<b>689</b>	<b>2062</b>	<b>4449</b>	<b>2374</b>	<b>20 176</b>	<b>47 898</b>	<b>172 300</b>	<b>70 151</b>

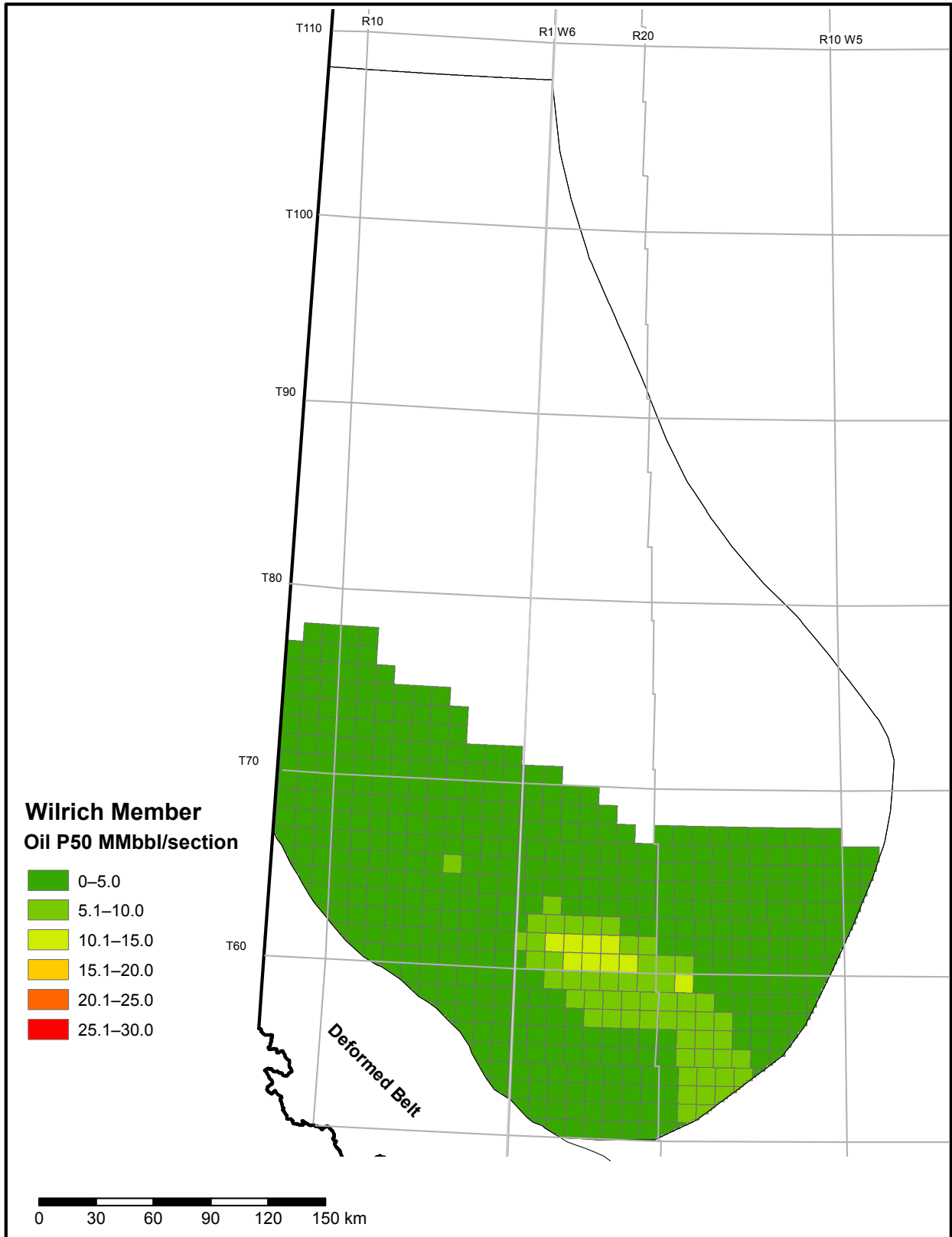


Figure 5.7.1. P50 (best estimate) shale-hosted oil initially-in-place in the Wilrich Member.

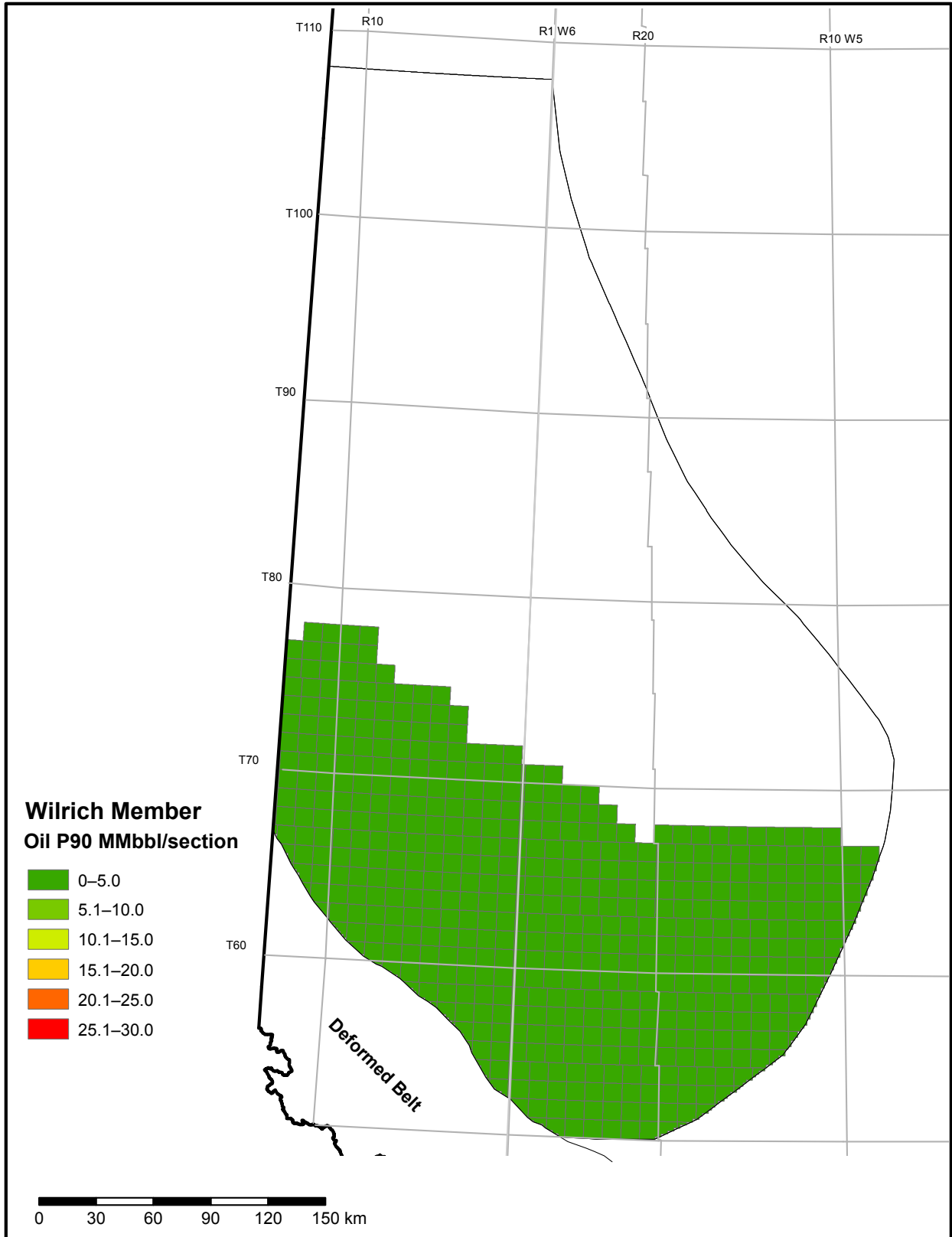


Figure 5.7.2. P90 (low estimate) shale-hosted oil initially-in-place in the Wilrich Member.

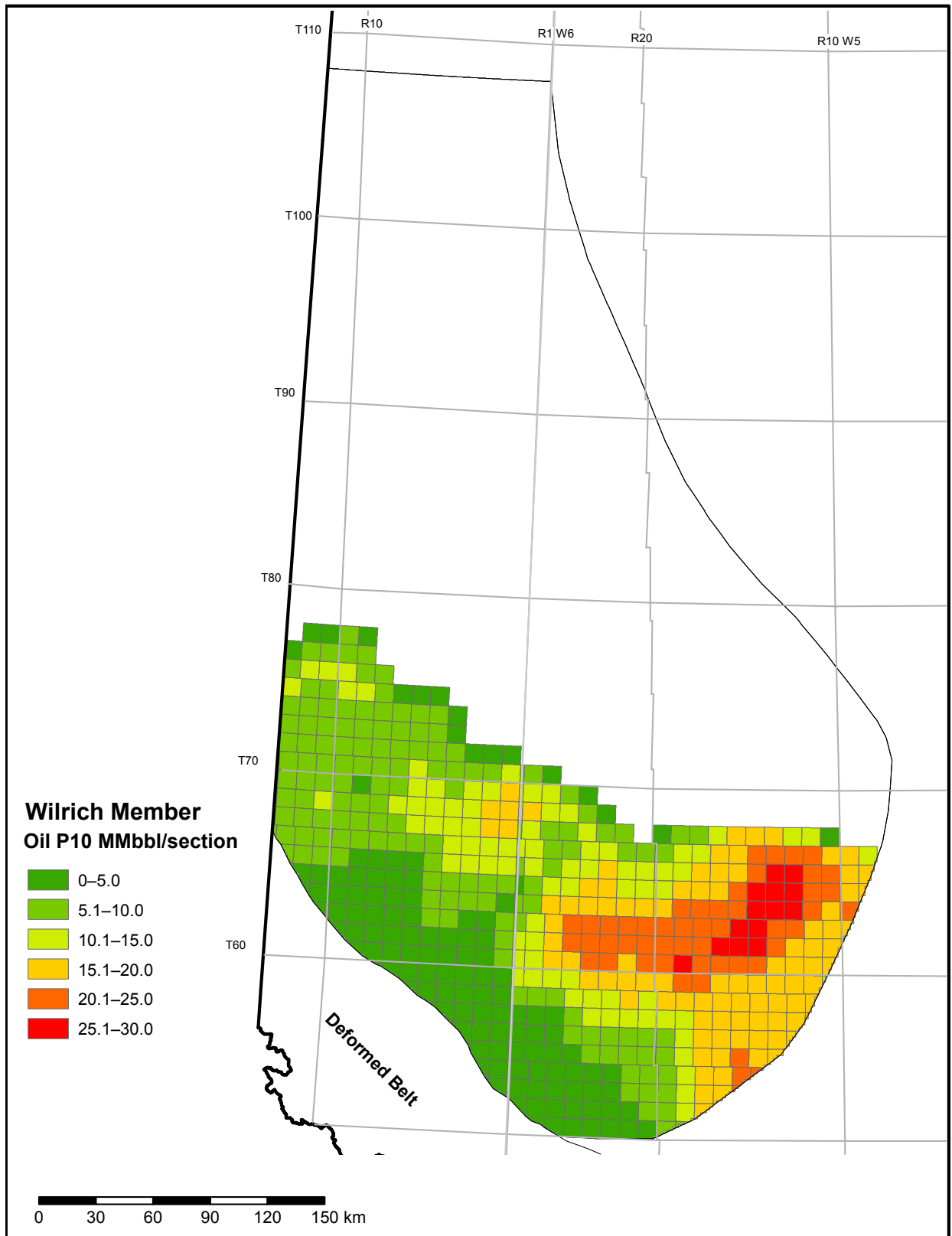


Figure 5.7.3. P10 (high estimate) shale-hosted oil initially-in-place in the Wilrich Member.

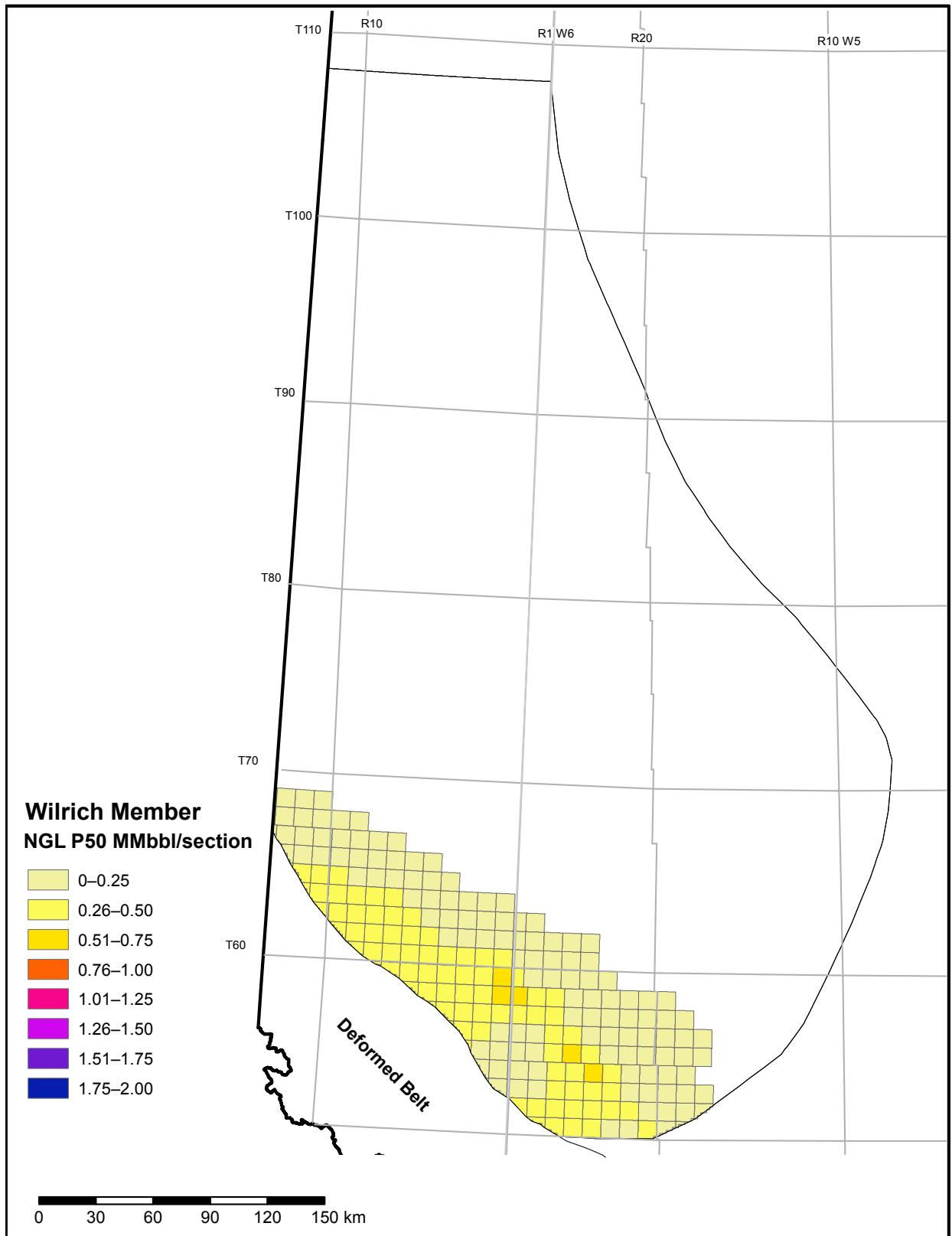


Figure 5.7.4. P50 (best estimate) shale-hosted natural-gas liquids initially-in-place in the Wilrich Member.

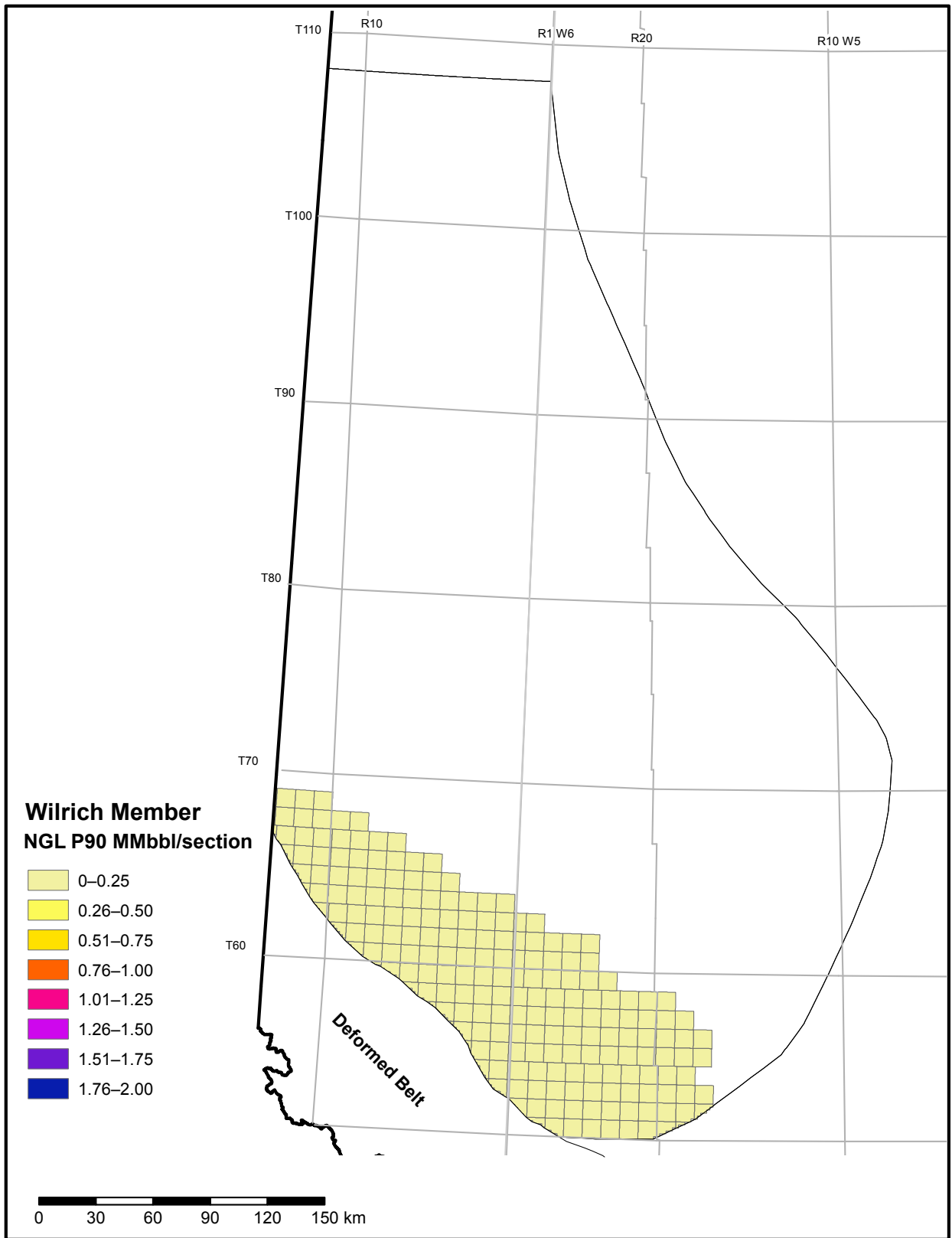


Figure 5.7.5. P90 (low estimate) shale-hosted natural-gas liquids initially-in-place in the Wilrich Member.

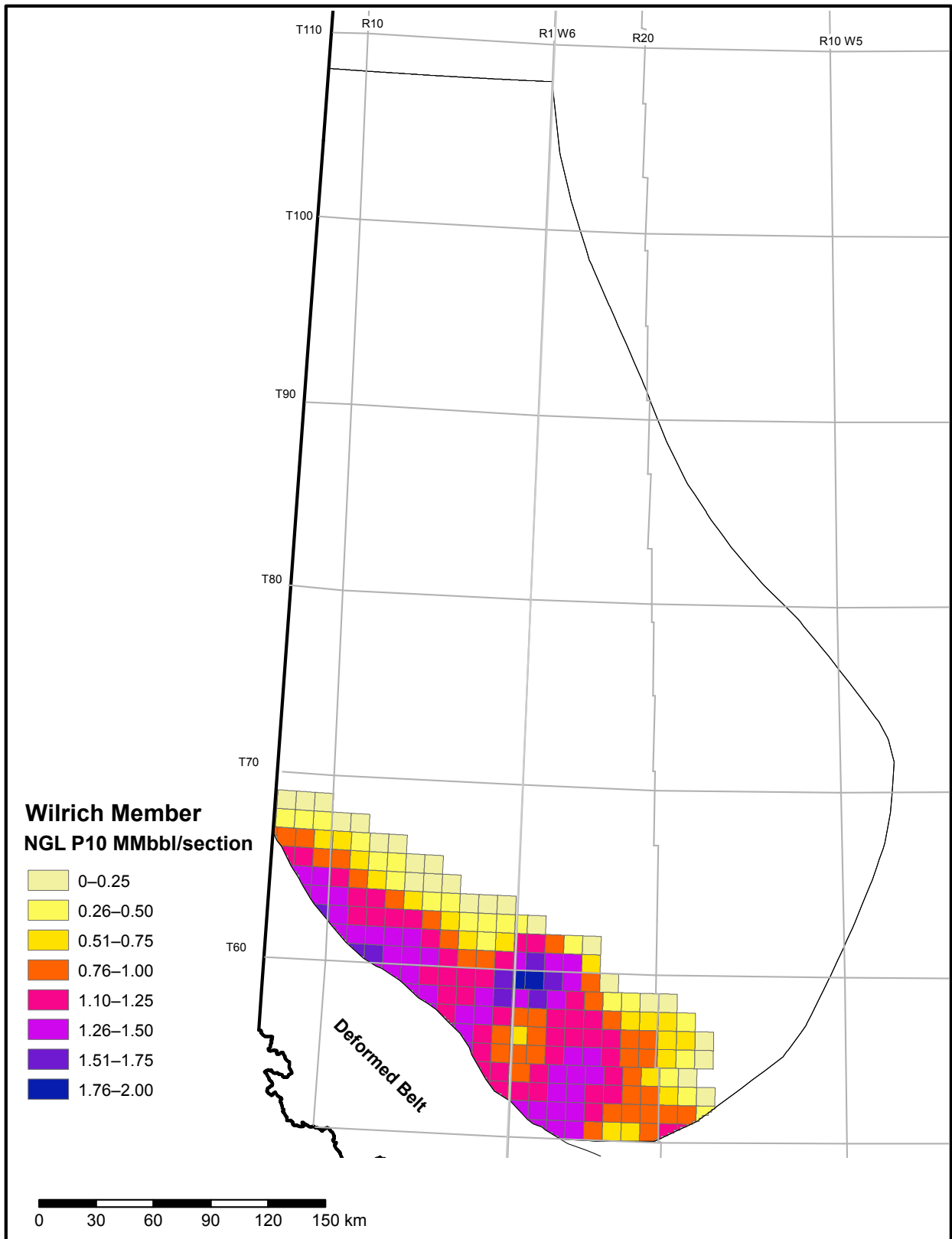


Figure 5.7.6. P10 (high estimate) shale-hosted natural-gas liquids initially-in-place in the Wilrich Member.

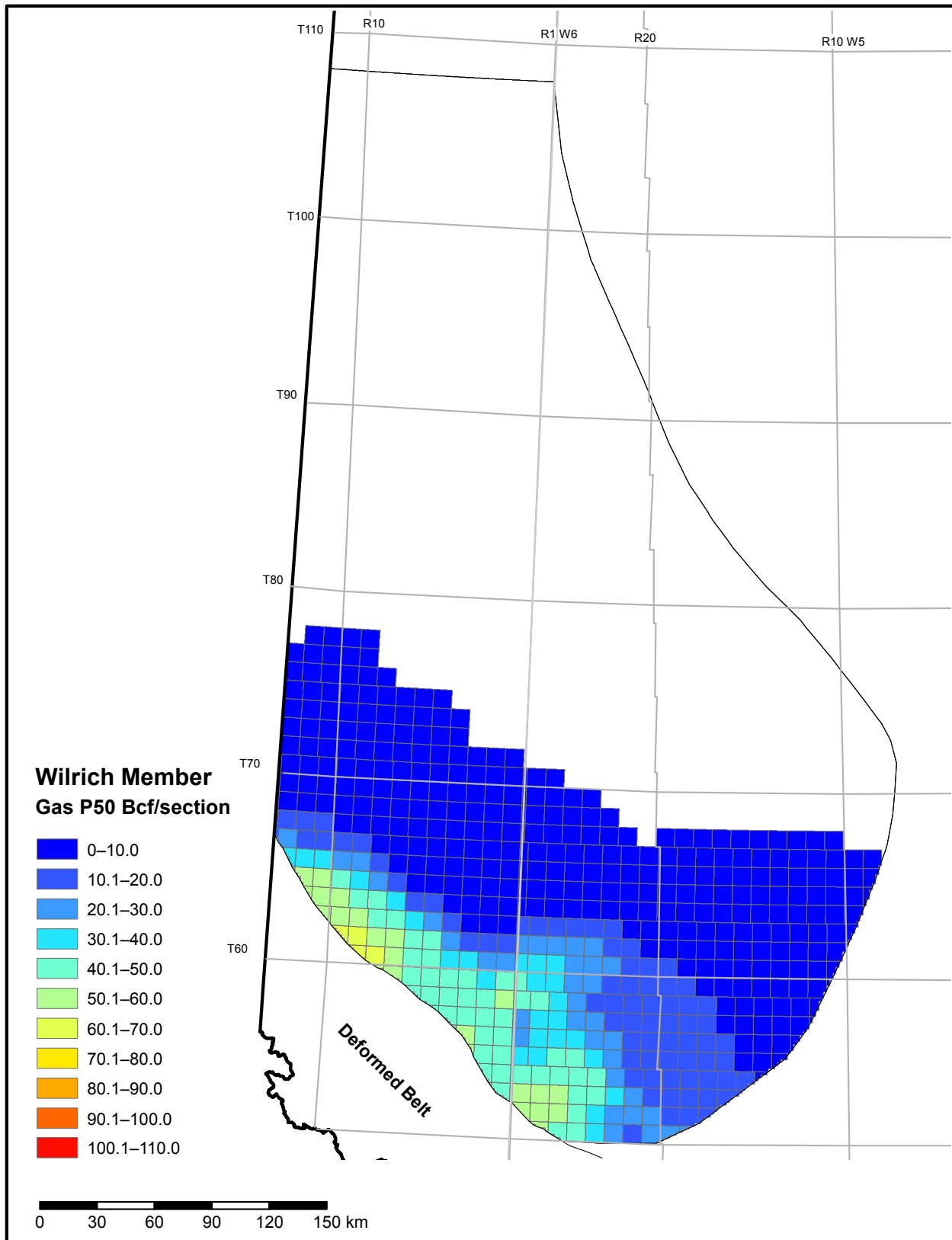


Figure 5.7.7. P50 (best estimate) shale-hosted gas initially-in-place in the Wilrich Member.

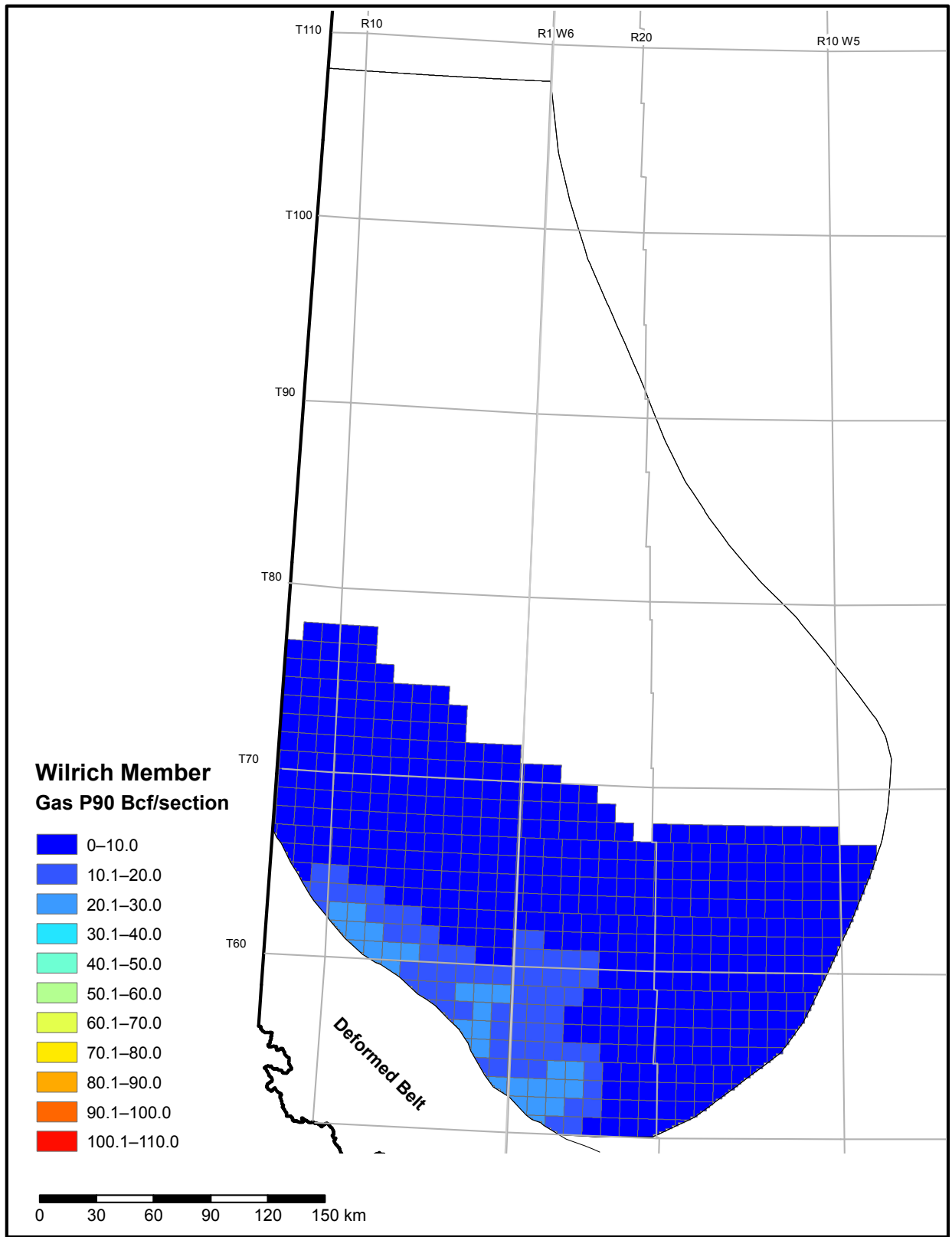


Figure 5.7.8. P90 (low estimate) shale-hosted gas initially-in-place in the Wilrich Member.

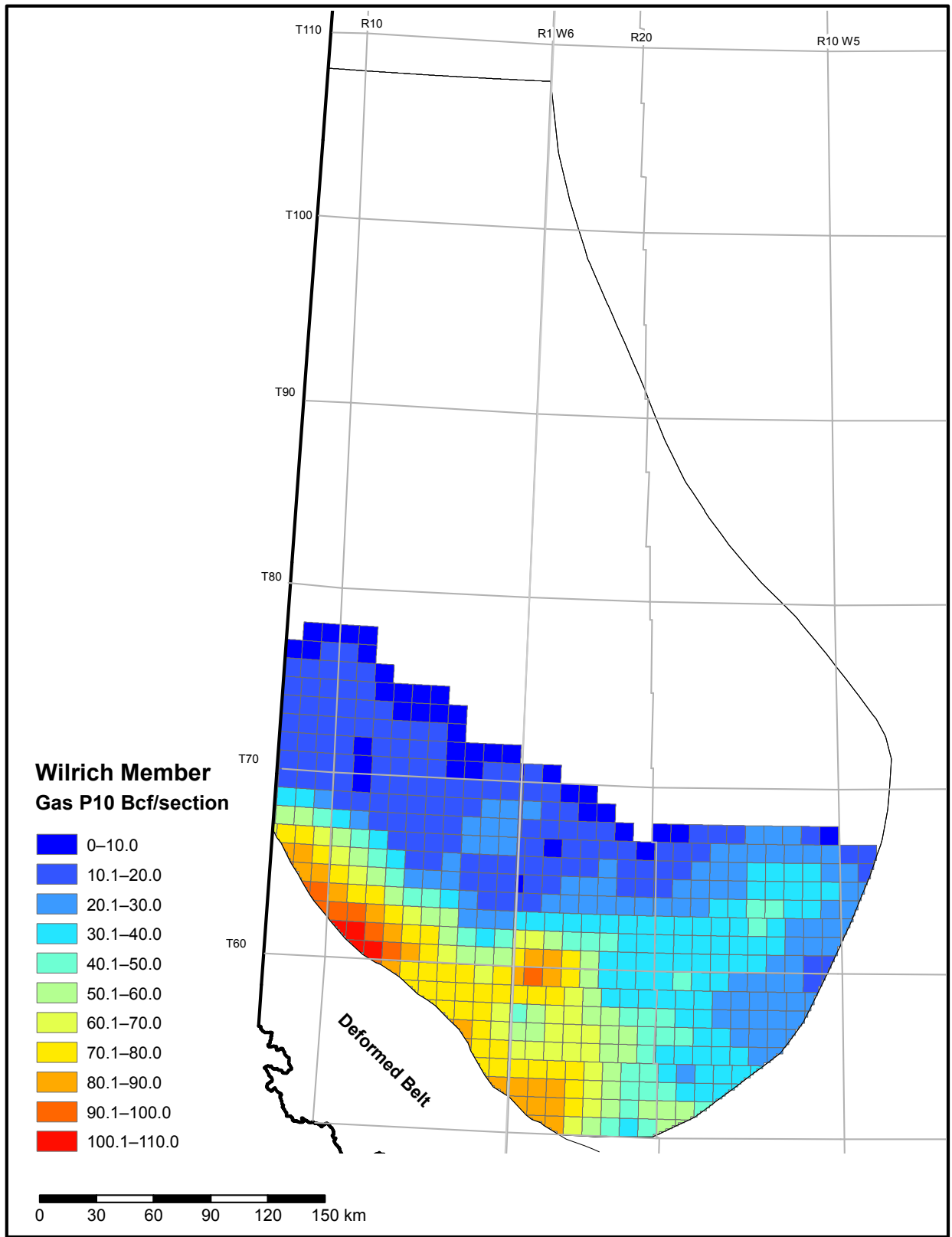


Figure 5.7.9. P10 (high estimate) shale-hosted gas initially-in-place in the Wilrich Member.

## 6 Constraints and Considerations for Future Work on Shale- and Siltstone-Hosted Hydrocarbon Resource Analysis and Modelling

- 1) Due to the lack of pressure and temperature data from the individual units evaluated, we used data from adjacent formations that host conventional hydrocarbon reservoirs. As more data on formations are collected, we will use data specific to the individual assessed units to better characterize pressure and temperature conditions.
- 2) Our porosity evaluation methodology (using a gamma-ray cutoff and density-porosity logs) assigned a single grain-density value to the entire unit. Future work will involve a more detailed geophysical well-log evaluation on each well or at least an evaluation of a selection of geophysical well logs for areas that have consistent mineralogy and grain density. For the gamma-ray cutoff, we were not able to normalize the gamma-ray logs for a unit's entire area of extent. Whenever possible, we used post-1980 gamma-ray logs because gamma-ray logging tools were typically more consistent. We will continue to explore for new methodologies that will allow for normalizing logs over areas as large as the province.
- 3) Although our evaluation should account for all types of porosity, it would be prudent to determine the various types of porosity in each unit (e.g., organic porosity, intraparticle porosity, interparticle porosity, microfracture porosity) and their relative contributions to resources and, eventually, to reserves.
- 4) We will continue to explore the issue of water saturation in shale and siltstone, in terms of the values calculated from Dean Stark analysis, the correlation of geophysical well-log parameters to water saturation, and the issue of contamination from drilling fluids in very low permeability rocks.
- 5) Our determination of the areas of gas, liquid, and oil generation depended, in part, on the gas-oil ratio (GOR) we calculated. Production data from the shale and siltstone reservoirs will help determine the actual GOR and help delineate actual gas-liquid and liquid-oil boundaries. Furthermore, as indicated in Section 2.1, the generation and migration of hydrocarbons are more complex processes than we were able to capture in this study.
- 6) Water-reforming and Fischer-Tropsch-like reactions that may occur in organic-rich shale and siltstone (Tang and Xia, 2011) in the more mature parts of a basin have not been taken into account. The results of this reaction could be lower water saturation, higher gas generation, higher formation pressure, and fewer liquids than we have determined for the dry-gas zone.

## 7 Conclusion

The hydrocarbon-resource estimates presented here are based on a new geostatistical model and are expressed as a probability range of P90 (low estimate), P50 (medium or best estimate) and P10 (high estimate). The total combined P50 values for the Duvernay, Muskwa, Montney, basal Banff/Exshaw, Wilrich, north Nordegg, and Rierdon show significant resources in place for Alberta, specifically, 3424 Tcf of natural gas, 58.6 billion barrels of natural-gas liquids, and 423.6 billion barrels of oil. Estimates for each unit are for unconventional reservoirs only. Conventional pools or conventional potential resources/reserves are not included in this assessment.

Estimates for the basal Banff/Exshaw, Wilrich, and north Nordegg have been included in the total resources in-place for Alberta, but they must be classified as preliminary. The initial results for these units show significant potential.

The study does not include an estimate for the shale and siltstone units of the Colorado Group and equivalent strata. However, the data and initial interpretations we have provided demonstrate significant potential for this group.

The resource endowment estimates that we provided used a novel methodology for resource estimation, developed within the ERA Group of the ERCB, that has not been used elsewhere. Therefore, the estimates may not be comparable to other resource-estimation methodologies used for the assessed units or their equivalents within or outside Alberta. A detailed description and discussion of the methodology will be published separately.

The resource endowment estimates provided in this report must not be confused with recoverable reserves. It is not likely that the entire area evaluated in any unit will be economically producible, even assuming that the technology used in hydrocarbon recovery continues to improve in the future. We have evaluated each unit to its zero edge. Even the most optimistic views of price and technology developments will not result in the entire area being economically productive. As more production occurs and more data become available, we will revisit our estimates and revise and improve as necessary.

Finally, the scientific analyses of variables, such as porosity and water saturation, for shale and siltstone are evolving compared to conventional hydrocarbon reservoirs. Two recent publications that review the merits and problems associated with shale parameter analysis are Passey et al. (2010) and Sondergeld et al. (2010). We urge interested readers to review these documents. As shale analytical methods become more sophisticated and provide more precise and accurate values, we will revisit our analyses for a comparison of data. We have attempted, within reason, to use the best methods available to us and, at the same time, use our expertise to properly evaluate each unit.

## References

- Asgar-Deen, M., Riediger, C. and Hall, R. (2004): The Gordondale Member: designation of a new member in the Fernie Formation to replace the informal "Nordegg Member" nomenclature of the subsurface of west-central Alberta; *Bulletin of Canadian Petroleum Geology*, v. 52, no. 2, p. 201–214.
- Baskin, D.K. (1997): Atomic H/C ratio of kerogen as an estimate of thermal maturity and organic matter conversion; *American Association of Petroleum Geologists Bulletin*, v. 81, no. 9, p. 1437–1450.
- Bustin, M.R. (2006): Geology report: where are the high-potential regions expected to be in Canada and the U.S.? Capturing opportunities in Canadian shale gas; *The Canadian Institute's 2nd Annual Shale Gas Conference*, January 31–February 1, 2006, Calgary, Alberta, 64 p.
- Danesh, A. (1998): PVT and phase behaviour of petroleum reservoir fluids, Elsevier; Science B.V., London, UK. 388 p.
- Deutsch, C.V. (2002): *Geostatistical reservoir modeling*; Oxford University Press, New York, New York, 376 p.
- Faraj, B. (2005): Opening remarks from the chair; *The Canadian Institute, Capturing Opportunities in Canadian Shale Gas conference*, The Canadian Institute, conference proceedings, January 31–February 1, 2005.
- Faraj, B., Williams, H., Addison, G., Donalessen, R., Sloan, G., Lee, J., Anderson, T., Leal, R., Anderson, C., Lafleur, C. and Ahlstrom, J. (2002): Gas shale potential of selected Upper Cretaceous, Jurassic, Triassic and Devonian shale formations in the WCSB of Western Canada: implications for shale gas production; report prepared for the Gas Technology Institute, GRI-02/0233, 285 p.
- Herron, M.M. and Matteson, A. (1993): Elemental composition and nuclear parameters of some common sedimentary minerals; *International Journal of Radiation applications and Instrumentation, Part E, Nuclear Geophysics*, v. 7, no. 3, p. 383–406.
- Ibrahimias, A. and Riediger, C. (2004): Hydrocarbon source rock potential as determined by Rock-Eval/TOC pyrolysis, northeast British Columbia and northwest Alberta; *British Columbia Ministry of Energy and Mines, Resource Development and Geoscience Branch, Summary of Activities 2004*, p. 7–18.
- Leckie, D.A., Bhattacharya, J.P., Bloch, J., Gilboy, C.F. and Norris, B. (1994): Cretaceous Colorado/Alberta Group of the Western Canada Sedimentary Basin; *in Geological Atlas of the Western Canada Sedimentary Basin*, G.D. Mossop and I. Shetsen (comp.), Canadian Society of Petroleum Geologists and Alberta Research Council, URL <[http://www.ags.gov.ab.ca/publications/wcsb\\_atlas/a\\_ch20/ch\\_20.html](http://www.ags.gov.ab.ca/publications/wcsb_atlas/a_ch20/ch_20.html)> [February 2012].
- Nowlan, G.S., Hein, F.J., Coskun, S.B., Stasiuk, L.D., Fowler, M.G., Norford, B.S., Palmer, B.R. and Addison, G.D. (1995): Characterization of Cambrian and Ordovician strata in the subsurface or Alberta using lithostratigraphy, biostratigraphy, organic petrology and image analysis; *CSPG/CWLS 1995 Core Session: The Economic Integration of Geology and Formation Evaluation*, 20 p.
- Passey, Q. R., Creaney, S., Kulla, J.B., Moretti, F.J. and Stroud, J.D. (1990): A practical model for organic richness from porosity and resistivity logs; *American Association of Petroleum Geologists Bulletin*, December 1990, v. 74, no. 12, p. 1777–1794.

- Passey, Q.R., Bohacs, K.M., Esch, W.L., Kilmentidis, R. and Sinha, S. (2010): From oil-prone source rocks to gas-producing shale reservoir—Geologic and petrophysical characterization of unconventional shale gas reservoirs; Chinese Petroleum Society/Society of Petroleum Engineers International Oil and Gas Conference and Exhibition, June 8–10, 2010, Beijing, China, paper SPE-131350, 29 p.
- Peters, K.E. and Cassa, M.R. (1994): Applied source rock geochemistry; *in* The petroleum system - from source to trap, L.B. Magoon and W.G. Dow (ed.), American Association of Petroleum Geologists, Memoir 60, p. 93–120.
- Ralph, J. and Chau, I. (1993): Mineralogy database; Mindata.org, URL <<http://www.mindat.org>> [May 2012].
- Smith, M.G. and Bustin, R.M. (2000): Late Devonian and Early Mississippian Bakken and Exshaw black shale source rocks, Western Canada Sedimentary Basin: a sequence stratigraphic interpretation; American Association of Petroleum Geologists Bulletin, v. 84, no. 7, p. 940–960.
- Sondergeld, C.H., Newsham, K.E., Comisky, T.E., Rice, M.C. and Rai, C.S. (2010): Petrophysical Considerations in evaluating and producing shale gas resources; Society of Petroleum Engineers Unconventional Gas Conference, February 23–25, 2010, Pittsburgh, Pennsylvania, SPE-131768, 34 p.
- Switzer, S.B., Holland, W.G., Graf, G.C., Hedinger, A.S., McAuley, R.J., Wierzbicki, R.A. and Packard, J.J. (1994): Devonian Woodbend-Winterburn strata of the Western Canada Sedimentary Basin; *in* Geological Atlas of the Sedimentary Basin, Canadian Society of Petroleum Geologists and Alberta Research Council, p. 165–202.
- Tang, Y. and Xia, D. (2011): Quantitative assessment of shale gas potential based on its special generation and accumulation processes; adapted from poster presentation at American Association of Petroleum Geologists Annual Convention and Exhibition, April 10–13, 2011, Houston, Texas, 4 p.
- Tissot, B.P. and Welte, E.H. (1984): Petroleum formation and occurrence; Springer-Verlag Telos, New York, New York, 699 p.
- U.S. Department of Energy (2011): Review of emerging resources: U.S. shale gas and shale oil plays; U.S. Energy Information Administration, 82 p., URL <<ftp://ftp.eia.doe.gov/natgas/usshaleplays.pdf>>, [May 2012].

## **Appendix – Consultant Report – Shale Gas Potential (Source-Rock Geochemistry and Maturity)**

We have attached a consultant report that was generated to help us understand and interpret organic petrography and geochemical data as they relate to shale resources. This consultant used data generated from this study to characterize and evaluate source-rock potential, thermal maturity, and reservoir characteristics for the Montney/Doig, Banff/Exshaw, and Duvernay/Muskwa units.

**Preliminary Review on the Shale Gas Potential  
Of Selected Triassic to Upper Devonian Source Rocks  
from Alberta  
(Montney/Doig, Banff/Exshaw (Bakken)  
and Duvernay/Muskwa formations)  
By  
Dr. Prasanta K. Mukhopadhyay (Muki)**

## **1. INTRODUCTION**

The current report includes a review of various geochemical (Rock-Eval, TOC), petrological (vitrinite reflectance data and data from organic facies analysis), mineralogy, selected petrophysical, and scanning electron microscopic and methane adsorption isotherm data of three major source rock units from Alberta. The data was obtained from the current ERCB ERA Shale resource project. These source rocks units are: (a) the Triassic Montney and Doig Formations; (b) Mississippian to Upper Devonian Banff and Exshaw (Bakken) Formations; and (c) Upper Devonian Duvernay and Muskwa Formations (Plate 1). Therefore, the current review has evaluated preliminary shale gas potential of six major source rock units in Alberta. The report will be divided into three parts based on the geochemical and physico-chemical properties of: (1) the Montney and Doig Formations; (2) Banff and Exshaw (Bakken) Formations; and (3) Duvernay and Muskwa Formations. These source rocks have provided more than 40% of Alberta's entire conventional oil and gas reservoirs. Moreover, these source rocks have significant potential for future unconventional shale oil and gas shale exploration in Alberta. Various oil companies are already involved in unconventional oil and gas production.

The objectives of the proposed research are to document the following pertinent information for three target source rocks (Triassic Montney/Doig, Mississippian Banff/Exshaw/Bakken, and Upper Devonian Duvernay/Muskwa formations; Plate 1) from Alberta using all the relevant current data (provided by ERCB) and earlier publications as provided by the ERCB scientists:

- Define the variability of the source rock maturity; source rock facies, richness, potential, and their conversion to oil & gas
- Variability of porosity and permeability using analysis and Selected Scanning Electron Microscopic interpretation
- A preliminary assessment of the variability of the shale gas potential of three major source rocks from Alberta using all data previously mentioned and the adsorption isotherm data.

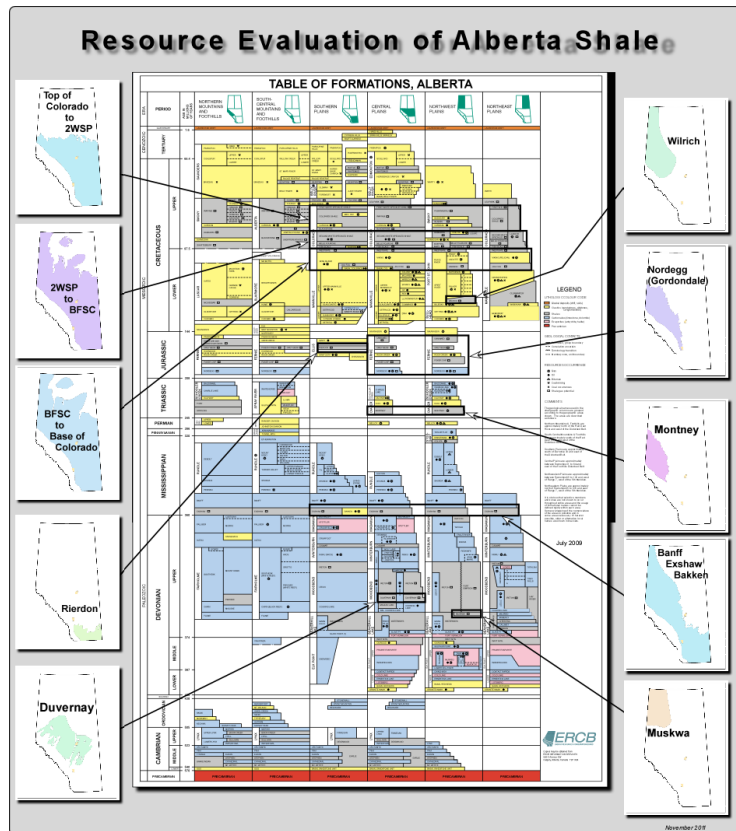


**Plate 1.** A composite formation table showing three candidate source rocks used for this contract (preliminary shale gas evaluation)

## 2. MONTNEY AND DOIG FORMATIONS: SCIENTIFIC REVIEW

### 2.1. INTRODUCTION

In the Alberta Basin, the Triassic strata extends eastward up to 1200 m in thickness to an eroded zero edge. They consist of marine to marginal-marine siliciclastic, carbonate rocks and lesser amounts of evaporites. These strata form a sedimentary wedge deposited on a westward-deepening stable continental shelf and shoreline. The strata ranges in age from the early Triassic (Griesbachian) to late Triassic (Norian). Triassic rocks in the Alberta Basin extend from the Canada-United States border to the Liard River area of northeastern British Columbia and southern Yukon (Plate MD-1).

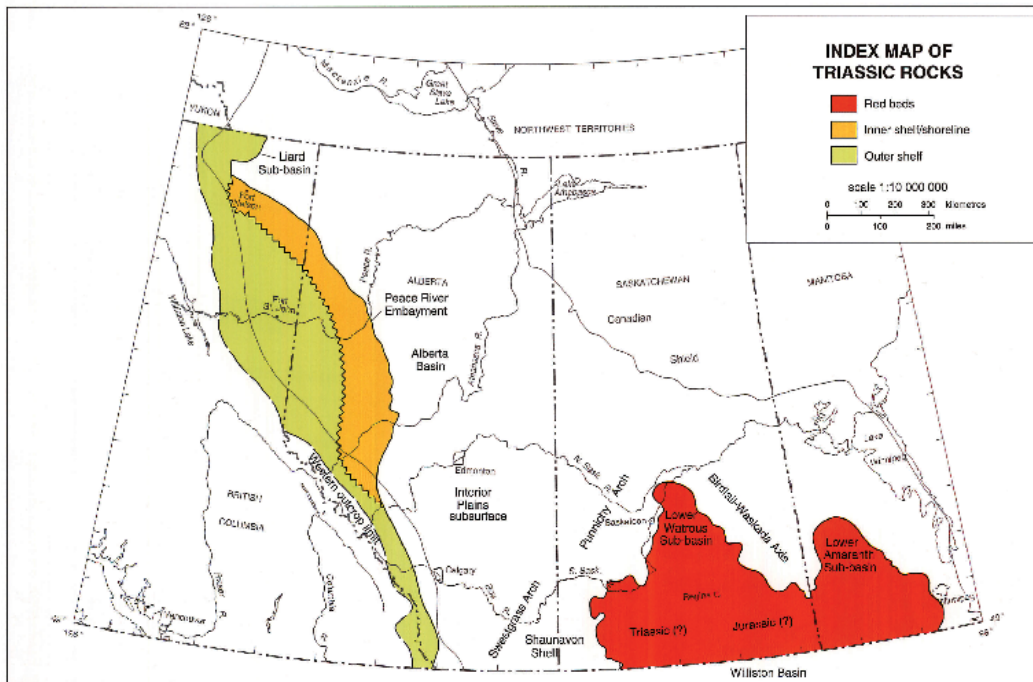


**Plate MD-1.** Index map of Triassic sediments in Alberta, BC, Yukon, and Saskatchewan (Edwards et al., ERCB/AGS Report, 2008)

Maximum thickness for the Montney Formation sediment is approximately 350 m. The formation also displays a local thinning trend to the west and south, probably because of slower rates of sedimentation (GSC Report, 2001).

Although significant shale gas exploration activities could be documented in

the Montney and Doig formations in Alberta at the present time, only a few publications or reports are available on these two major source rocks in Alberta especially on their geochemical and physicochemical properties (Plate MD-2; Figure MD-A; Anderson et al., 2010; Beaton et al., 2010<sup>a</sup>; Beaton et al., 2010<sup>b</sup>; Faraj et al., 2002; Riediger et al., 1990).

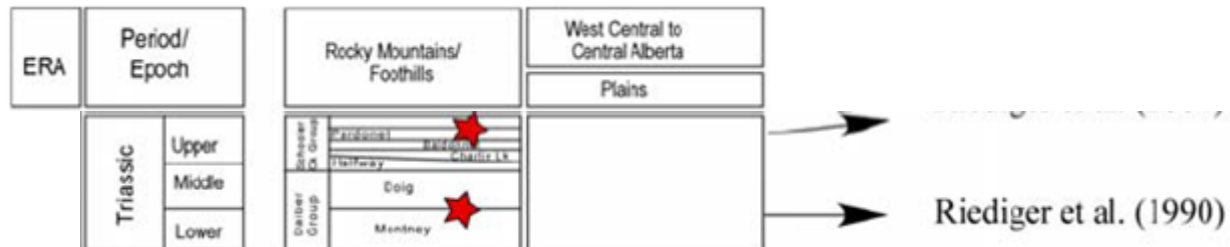


**Plate MD-2:** List of Potential Source Rocks from Triassic to Recent age within Alberta with potential list of publications (after Rokosh et al., 2009).

The Montney and Doig Formations were deposited in western Alberta and northeast British Columbia in the Early to Middle Triassic periods. The Montney Formation consists of shallow water sandstone in the east and deep-water mudstone in the west. The Doig Formation overlies the Montney formation and consists largely of shallow water sands and muds that filled the remainder of the Montney Basin. The lithology of the Montney Formation includes mainly organic-rich and organic lean sandy siltstone to silty sandstone with occasional thin shale and the rare presence of coquina and thin phosphate layers.

The Montney and Doig Formations are mainly concentrated within the west-central part of Alberta where the Montney Formation extends towards the southwestern part of Alberta (Figure MD-B1). They are restricted to the shallower part (top at 389 m) of the basin in the northwest whereas the deep Montney Formation is located within the southwestern part of Alberta (Figure MD-B2). The southwest to northeast cross sections, isopach and the structure contour maps of the Montney and Doig formations revealed that the thickest

section of these two source rocks (250m to 275 m) is close to the northwestern part of the basin (Zone T90 to T70; Figures MD-B3a; MD-B3b, MD-B4, MD-B5). The Doig formation is pinching out in the northeastern section of the basin where the Montney Formation directly underlies the sediments from the Jurassic Nordegg Formation (Figure MD-B3b).

## **2.2. ANALYTICAL RESULTS AND DISCUSSION**

Altogether more than 400 samples from the Montney and Doig formations from Alberta have been analyzed with locations in various parts of Alberta (Figure MD-C). Most of these samples were mainly analyzed to evaluate the organic richness, source rock potential and maturation by Rock-Eval pyrolysis and Leco Carbon Analyzer. Selected samples have been analyzed for organic petrography (visual kerogen and vitrinite reflectance analysis), mineralogical analysis by XRD and X-Ray Fluorescence, porosity and permeability, pore fabric analysis by scanning electron microscope. Only a few selected samples have also been analyzed for determining methane adsorption isotherms for shale gas evaluation.

### **2.2.1. Organic Petrography**

The organic petrography data (Beaton et al., 2010) of various samples (sample numbers within 8117 to 9260) revealed a variability of these sediments. Similar to the Stasiuk and Fowler (2004) organic facies definition of the Devonian to Mississippian source rocks, various organic facies could also be recognized within the studied samples of the Montney and Doig formations that are related to the anoxicity and depth of sedimentary water column.

Two major organic facies types are recognized (Figures MD-D1 and MD-D2): (1) major contribution is of amorphous kerogen that was partially oxidized (with rare brown fluorescence) with minor concentrations of both *Telalginite* (*Tasmanites*) and *Lamalginite* (*Prasinophyte*), vitrinite, fluorescent bitumen and trace amounts of oil inclusion (Figure MD-D1). This facies contains abundant

framboidal pyrite and was deposited in a fluctuating anoxic and dysoxic depositional facies forming Type II, II-III and III source rocks. Most of the silty sandstone and sandstone are of this organic facies; (2) The other organic facies is a mixture of *Prasinophyte* type *Lamalginite* with acanthomorphic Acritarchs, vitrinite, and amorphinite 2 (AOM 2) forming kerogen Type II source rocks (Figure MD-D2). They also include abundant solid bitumen, oil fluid inclusion or yellow fluorescent oil, selected siliceous microfossils and rare *Tetralginite* (*Tasmanites*). In the eastern part of the Montney sediment area, selected silty sandstone and coquina are kerogen-rich and contain abundant amorphinite 2 (AOM 2) forming kerogen Type II source rocks. In the western part of the basin, the AOM 2 converted mainly to micrinite and granular nonfluorescent bitumen forming a more porous network (Figure MD-D2). Most of the Doig Formation shale and silty shale are more organic rich than most of the Montney formation. They contain abundant amorphinite 2 (AOM 2), asphaltene and solid bitumen that have possibly been expelled at an earlier oil generation stage than the Montney formation silty shale or silty sandstone. The few samples of siltstone, sandstone and coquina from the Montney Formation were analyzed in the south-western part of the basin. They are organic lean.

As the westcentral part of the sediment area contains mostly mature or overmature source rocks, the source rocks are partially depleted in hydrocarbons and the kerogen network includes an abundant presence of micrinite and rank-inertinite (metalginite or meta-AOM2). Therefore, the amorphous liptinite rich Type II silty shale and shale source rocks changes to Type III source rocks. Therefore, organic petrography can only define the original organic framework of these source rocks and evaluate the mass balance of hydrocarbons expelled or remained *in situ*. Moreover, the overmature source rocks in the western part of basin (associated with the deformation front) illustrate the formation of abundant organic porosity which are mostly located along the junction of the solid bitumen and amorphous kerogen network.

### 2.2.2. Source Rock Richness, Potential, and Maturation

Figures MD-E1 to MD-E4 illustrate various parameters of the Rock-Eval pyrolysis and total organic carbon analysis illustrating the source rock richness and potential of all sediments; Figures MD-E5 and MD-E6 depict depthwise plots of TOC, hydrogen Index, maturity (Ro or Tmax), production index showing the main oil and gas generation zones. Four major parameters on organic richness, source rock potential, maturation and oil/gas conversion (data on organic carbon content; hydrogen index; Tmax or vitrinite reflectance; and production index) from four sectors (north; west and northwest; east, and south) of the basin are as follows:

#### **West and Northwest:**

Montney: TOC = 0.12 to 3.64%; HI = 11 to 641; Tmax = 418 to 543; Ro = 0.43 to 2.5%; PI = 0.04 to 0.95;

Doig: TOC = 0.48 to 9.77%; HI = 85 to 470; Tmax = 433 to 607; Ro = 0.64 to 0.69 ; PI = 0.1 to 0.73;

**East:** Montney: TOC = 0.11 to 1.72% ;HI = 39 to 514 ;Tmax = 414 to 448; Ro = 0.43 to 1.15%; PI = 0.05 to 0.69;

**North:** Montney: TOC = 0.43 to 6.31%; HI = 89 to 737; Tmax = 407 to 439; Ro = 0.68 to 1.1%; PI = 0.08 to 0.67;

**South:** Montney: TOC = 0.05 to 0.36%; HI = 20 to 62; Tmax = no data ; Ro = no data; PI = 0.21 to 0.77;

TOC= wt %; HI = mg HC/g TOC; Tmax = oC; Ro = %; PI = a ratio of S1/S1 S2

The plot of S2 versus TOC and van Krevelen plot of hydrogen index and oxygen index of all samples indicate that about 30% of the analyzed samples from the Montney and Doig formations are oil prone Type II kerogen. They are considered to have good to excellent source rock potential (Figures MD-E1 and MD-E2). The deeper source rocks (>3000 m) mostly show an excellent source rock potential. A vast majority of the source rocks may possibly have been depleted in hydrocarbons indicating a currently fair hydrocarbon potential because of their advanced maturity (Figure MD-E1). Currently, these source rocks have transformed to kerogen Type II-III or III similar to gas/low oil or gas prone organics because of their loss of hydrocarbons and TOC due to their advanced maturity (Figures MD-E1 and MD-E2).

The plot of Tmax versus hydrogen index clearly eliminated this problem by showing how a Type II kerogen will behave with increasing maturity (Plate 4; Figure MD-E3). Only a few samples are considered to be higher oil prone Type I-II kerogen. All those samples from both Montney and Doig formations are closely related to a depth lower than 2000 m. All kerogen Type I and II source rocks below 3000 m depth have been transformed to kerogen Type II-III and III source rocks because of their loss of TOC and hydrocarbons.

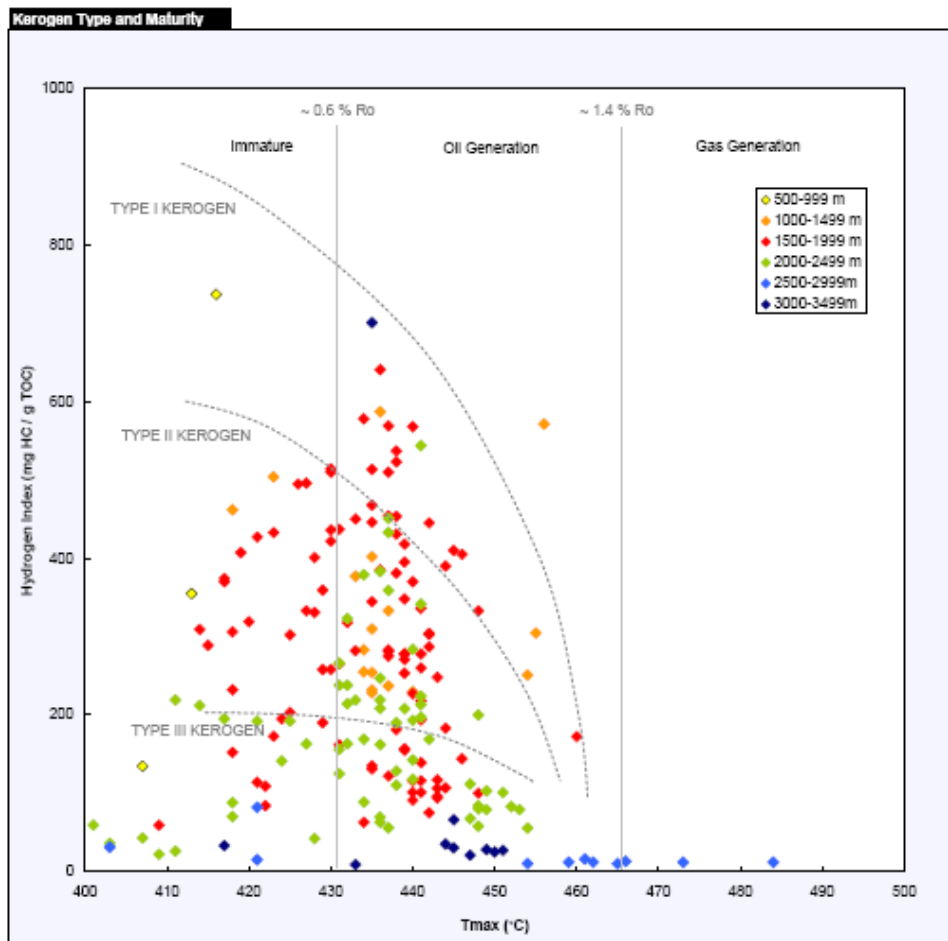


**Plate MD-3.** Maturity (using Tmax) versus hydrogen index X-Y plot showing the variability of source rock potential from various samples analyzed from Alberta. Colour indicates depth range of the samples analyzed by Rock-Eval pyrolysis

The hydrocarbon transformation based on Tmax and production index values indicate that the vast majority of the source rocks could be included within the

main oil generation zone and they are partially depth dependant (Figure MD-E4). This data may have suggested various possibilities: (a) some variability of heat flow within various zones and areas of Alberta; (b) the source rocks may have two different hydrocarbon generation phases based on the chemical kinetics; and (c) the Tmax values of S2 are suppressed because of the abundance of oil like components in advanced maturity.

The depth plot of organic carbon content, oil potential, and the hydrogen index values of the Montney and Doig formations indicate that they are mostly organic rich (>5% TOC), fair to excellent source potential, have mainly mixed oil and gas potential (Figure MD-E5). On the other hand, the depth plot of the normalized content of S1 clearly indicates that the oil zone is mainly restricted to 1250 m to 2250 m depth Figure MD-E5). The depth plot of production index values may indicate that the main dry gas starts beyond 2000 m depth (Figure MD-E6). However, only about 30% of the source rocks from the Montney/Doig Formations beyond 2500 m depth may have a clean dry methane zone (Figure MD-E6). This dry gas zone is mainly restricted to the northwest sector of the Basin near the deformation front. In Alberta, a vast majority of the Montney and Doig formation source rocks between 2000 m to 3000m mainly contain oil or condensate mixed with wet gas and minor dry gas. However, the production index versus depth plot (middle plot of Figure MD-E6) indicates that the vast majority of the source rocks are restricted mainly to the gas generation phase within 1500 m to 2000 m depth. This may suggest the possible dependence of chemical kinetics on the Montney Formation source rocks in different areas thereby showing early oil and gas generation. As seen from organic petrography, the Doig Formation source rock includes higher organic rich amorphinite 2 and solid bitumen as well as containing a higher extract yield (59.2 to 95.7 mg HC/g TOC; Riediger et al., 1990). This data indicates that they have high to excellent source rock capability for oil generation. Based on the GC-MS data, the abundance of tricyclic terpanes relative to hopane may

suggest its origin from specific bacterial membrane supported by organic petrography (Riediger et al., 1990).

As pointed out earlier that because of the abundance of oil within the kerogen fabric of the Montney and Doig formations, both maturity parameters have shown a suppression of maturity generating abundant low values of vitrinite reflectance and Tmax values from the Rock-Eval pyrolysis (Figures MD-E7 and MD-E8). The other reason could be the extremely low concentrations of vitrinite macerals within both the Montney and Doig formation samples. By correlating organic petrography and Rock-Eval pyrolysis, it has been indicated that the type of organic components could be an important issue in the suppression of maturity for these samples. A mixture of abundant organic rich AOM 2 and lamalginite (*Prasinophyte*) associated source rocks (Type II kerogen) generate major migratory bitumen or oil within the kerogen matrix in the early stages of source rock maturity (Ro less 0.8%). On the other hand, high concentrations of telalginite (*Tasmanites*) associated with solid bitumen show major oil generation around 1.0% Ro and low maturity suppression. In the former case because of early migratory bitumen, it always shows a certain degree of maturity suppression. Detailed work is needed in the future to justify the reasons for maturity suppression within the Montney and Doig samples.

Two trends of thermal gradients and a trend of suppressed reflectance (based on Tmax or Ro values) could be identified (Plate MD-4; Figures MD-E7 and MD-E8). Leaving the suppressed vitrinite reflectance trend and using the depth plot of vitrinite reflectance data, two thermal gradients of the Montney and Doig source rock samples could be identified (Figure MD-E7). These thermal gradients are: (a) sediments between 550 to 2000m depth; and (b) the sediments between 2000 m to 3000m. In the first case, the Ro values change from 0.5% to 0.9% with a gradient of 0.03% per 100 m (main oil zone). Maximum suppression of Ro values could be identified within this zone. The maturity gradient of the sediments in the lower part of the source rocks from the Montney Formation is high (0.13% Ro per 100 m) and the reflectance

values sharply change from 0.9% to 2.2% Ro (Plate 4; Figure MD-E7). These sediments belong to wide zones containing condensate, wet gas, and dry gas.

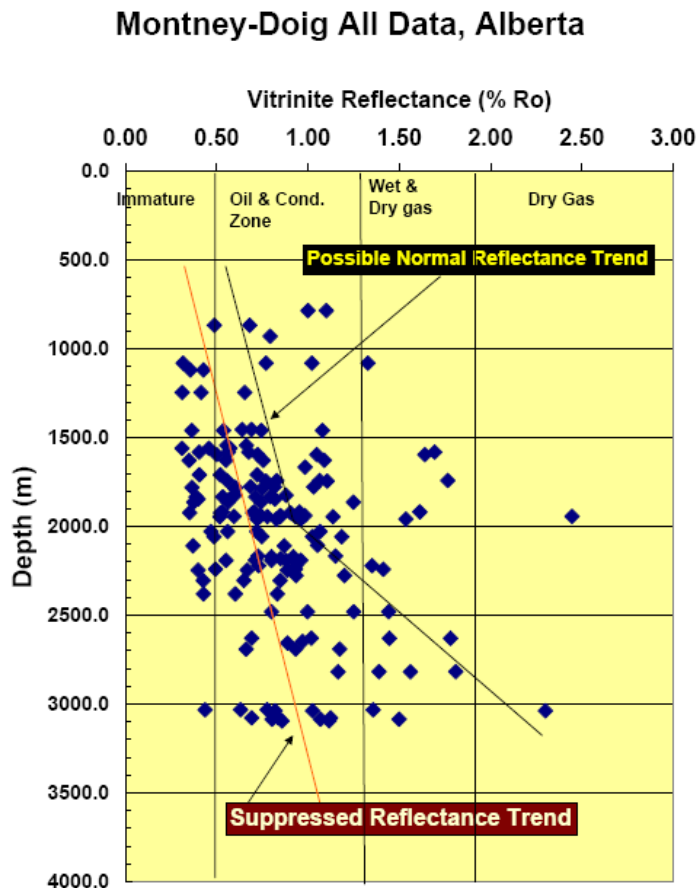


**Plate MD-4.** Montney and Doig formation samples shows two maturity gradients: a. normal reflectance gradient; and b. suppressed reflectance gradient

As defined in the earlier publications in Alberta and British Columbia, our current data indicates that generally the Doig Formation source rocks are anoxic, have a better source rock quality (mostly Type I-II and II oil prone), and possibly show early stages of oil generation in particular (Riediger et al., 1990; Faraj et al., 2002). Montney Formation silty shale, shale, and silty sandstone have deposited within an anoxic to dysoxic depositional environments and have wide variability of organic rich and organic lean oil and gas prone Type II, II-III, and III source rocks. The maturity is mostly dependant on the depth of the samples. A vast majority of the source rocks are either within the oil window or

in the condensate/wet gas zones. Most mature source rocks of both the Montney and Doig formations lie within the northwestern sector of Alberta near the deformation zone and west-central section along the deformation front of the foothills of Alberta (samples M34, M10). Mostly dry and wet gas in this region could be connected to a higher maturity gradient which is possibly related to major faults or higher stress regimes. Most of the immature to early oil rich source rocks are restricted to the eastern part of Alberta (samples M32, M12, M18).

### **2.2.3. Mineralogy**

The mineralogical variability of selected sediments from the Montney and Doig formations indicate that these sediments are clastic rich (with >60% quartz and feldspar with high SiO<sub>2</sub>, Al<sub>2</sub>O<sub>3</sub>, K<sub>2</sub>O) (Figures MD-F1 and MD-F2). Among the clay minerals, all analyzed sediments are low in kaolinite and high in muscovite (mostly >10%). Dolomite is the dominant component among the carbonate minerals. Based on the quantitative perspective, quartz is the major component (>30%) while carbonate minerals (calcite, dolomite, ankerite) and one sample with illite are of moderate concentrations (10-30%)( Figure MD-F3). Feldspars and clay minerals concentrated as minor components (<10%). Pyrite, gypsum, and apatite occur as trace proportions.

### **2.2.4. Permeability and Grain Density**

The permeability of selected Montney Formation source rock samples were analyzed using nitrogen and air as pore fluids (Anderson et al., 2009). The permeability of most samples is low and varies from 0.02 to 0.05 Ka (air) and 0.006 to 0.01 Kl (liquid) in mD. The permeability of these samples suggest that Montney samples have either similar or higher permeability than the Barnett samples. Samples with visible fractures, the permeability varies from 1.7 to 24 Ka in mD showing the future prospects of flow through various natural fractures. The grain density of few selected samples varies from 2.584 to 2.656

g/cm<sup>3</sup> (Figure MD-G). The moderate grain density of selected sediments implies the feasibility for easier '*fracking* capabilities' of these analyzed shale.

### **2.2.5. Mineralogy and Porosity: Scanning Electron Microscope**

Selected scanning electron microscopic photomicrographs demonstrated the distribution and association of various mineral species and the possible development of porosity within the Montney source rock matrix in association with the organics (Figures MD-H1 to MD-H5). Although organic components (maceral) are intimately associated with various minerals, using the interpretation associated with the SEM images could not document the relationship between the organic components and the minerals and the possible development of pores in advanced maturity. Within the mineral porosity, quartz overgrowth and formation of the authigenic dolomite crystals generates porosity that is greater than 5 micrometer. Illite growth occludes porosity (Figures MD-H4 and MD-H5). Systematic analysis of organics and minerals using organic petrological methods, SEM and EDS would be necessary to develop a porosity map of the kerogen-mineral matrix. This will also demonstrate the primary porosity and permeability changes within the same source rock (example: Montney siltstone) with advanced maturity.

### **2.2.6. Adsorption Isotherms**

The adsorption isotherm data of selected samples indicated that the highest adsorption of methane could be observed in samples that are closely connected to the deformational front (area around M2, M29, M34: Figures MD-I, MD-J1, MD-J2; Plate MD-5). These samples have 11 to 26.5 scf/ton of methane adsorption capacity.

Sample No.	Site No.	Depth (Metres)	TOC wt. %	Analysis Temperature Celsius	As Received Moisture wt. %	PL Raw Basis MPa	VL Raw Basis scc/g	PL Raw Basis psia	VL Raw Basis scf/ton
9255	M23	2816.4 - 2823.3	1.83	72	0.20	6.93	0.50	1,005.2	16.1
9256	M10	3088.4 - 3093.7	1.17	72	0.13	6.92	0.30	1,003.7	11.0
9257	M2	2646.6 - 2650.2	1.14	60	0.17	5.66	0.80	820.8	26.5
9258	M6	2297.3 - 2306.9	0.47	61	0.60	5.71	0.40	828.1	12.0
9259	M8	3030.6 - 3044.1	0.93	80	0.28	8.61	0.40	1,248.3	11.9
9260	M34	1827.7 - 1839.1	0.66	55	0.13	6.72	0.50	974.3	14.9

Legend

Column Label	Label Description
Sample No.	AGS sample number
Site No.	AGS sample location number
Depth (Metres)	Sample depth in metres (measured from core)
TOC wt. %	Total organic carbon in weight per cent
Analysis Temperature Celsius	Temperature in degrees Celsius
As Received Moisture wt. %	Sample moisture content in weight per cent
PL Raw Basis MPa	Pressure - Langmuir pressure raw basis in megapascals
VL Raw Basis scc/g	Volume - Langmuir volume raw basis in standard cubic centimetres per gram
PL Raw Basis psia	Pressure - Langmuir pressure raw basis in pounds per square inch absolute
VL Raw Basis scf/ton	Volume - Langmuir volume raw basis in standard cubic feet per ton
Point No.	Individual measurement
Gas Content Raw Basis scc/g	Gas content in standard cubic centimetres per gram
Pressure Raw Basis psia	Pressure raw basis in pounds per square inch absolute
Gas Content Raw Basis scf/ton	Gas content in standard cubic feet per ton

**Plate MD-5.** Adsorption Isotherm analysis of selected samples from various sites and depths (mean data of selected depth intervals).

## 2.3. REFERENCES

Anderson, S. D. A., C. D. Rokosh., J. G. Pawlowicz, H. Berhane, and A. P. Beaton. 2010. Minerology, permeability, mercury porosimetry, pycnometry, and scanning electron microscope of the Montney Formation in Alberta: Shale Gas data Release. ERCB/AGS Open File Report 2010-03. 61p.

Beaton, A. P., J. G. Pawlowicz, S. D. A. Anderson, H. Berhane, and C. D. Rokosh. 2010. Rock-Eval, Total Organic Carbon, and Adsorption Isotherms of the Montney Formation in Alberta: Shale Gas data Release. ERCB/AGS Open File Report 2010-05. 31p.

Beaton, A. P., J. G. Pawlowicz, S. D. A. Anderson, H. Berhane, and C. D. Rokosh. 2010. Organic Petrography of the Montney Formation in Alberta: Shale Gas data Release. ERCB/AGS Open File Report 2010-07. 129p.

Creaney, S., Allan, J., Cole, K.S., Fowler, M.G., Brooks, P.W., Osadetz, K.G., Macqueen, R.W., Snowdon, L.R. and Riedger, C.L. 1994. Petroleum generation and migration; *in* Geological Atlas of the Western Canada Sedimentary Basin, G.D. Mossop and I. Shetsen (comp.), Canadian Society of Petroleum Geologists and Alberta Research Council, Special Report 4, URL [January 15, 2009] <[www.ags.gov.ab.ca/publications/wcsb\\_atlas/atlas.html](http://www.ags.gov.ab.ca/publications/wcsb_atlas/atlas.html)>

Edwards, D. E. Et al. Triassic Strata of the Western Canadian Sedimentary Basin, Chapter 16. ERCB/AGS Report. 2008.

Fowler, M. G., L. D. Stasiuk, H. Hearn, and M. Obermajer, 2001. Bull. Can Petrol. Geol. V. 49, No. 1. p. 117-148.

NEB Energy Report. 2011. Tight Oil Developments in the Western Canada Sedimentary Basin –Energy Briefing Note. December 2011. ISSN 1917-506X

Faraj, B., Williams, H., Addison, G., Donalessen, R., Sloan, G., Lee, J., Anderson, T., Leal, R., Anderson, C., Lafleur, C. and Ahlstrom, J. 2002. Gas shale potential of selected Upper Cretaceous, Jurassic, Triassic and Devonian shale formations in the WCSB of Western Canada: implications for shale gas production; report prepared for the Gas Technology Institute, GRI-02/0233, 285 p.

Rokosh, C.D., J. G. Pawlowicz, H. Berhane, Anderson, S. D. A. and A. P. Beaton. 2008. What is Shale Gas? An Introduction to Shale Gas Geology in Alberta. ERCB/AGS Open File Report 2008-08. 26p

Riediger, C. L., M. G. Fowler, P. W. Brooks and L. R. Snowdon. 1990. Triassic oils and potential source rocks, Peace River Arch area, Western Canada Basin. In *Advances in Organic Geochemistry 1989*, *Org. Geochem.*v. 16, Nos. 1-3, pp. 295-305. Pergamon Press, Great Britain.

### 3. BANFF/EXSHAW/BAKKEN FORMATIONS: SCIENTIFIC REVIEW

#### 3.1. INTRODUCTION

Over the last few years there has been a major increase in the exploration for hydrocarbon reservoirs hosted by the uppermost Wabamun Group (Famennian) to the lowermost Banff Formation (Tournaisian), informally called "the Alberta Bakken", in southern Alberta (Hartel, Willem Langenberg & Barry Richards, Webpage 2012). The repeated black shale source rock sequences (lower, middle, and upper depositional units from the top of the Wabamun to the Lower Banff formations) are comprised of the Exshaw-Bakken-Banff formations within Alberta that forms the main "Alberta Bakken Fairway or Alberta-Banff-Exshaw-Bakken Fairway" for future major oil and gas resources (Figure BEB-1a; Plate BEB-1A; PIE Industry News, 2011) (Figure BEB-1b)

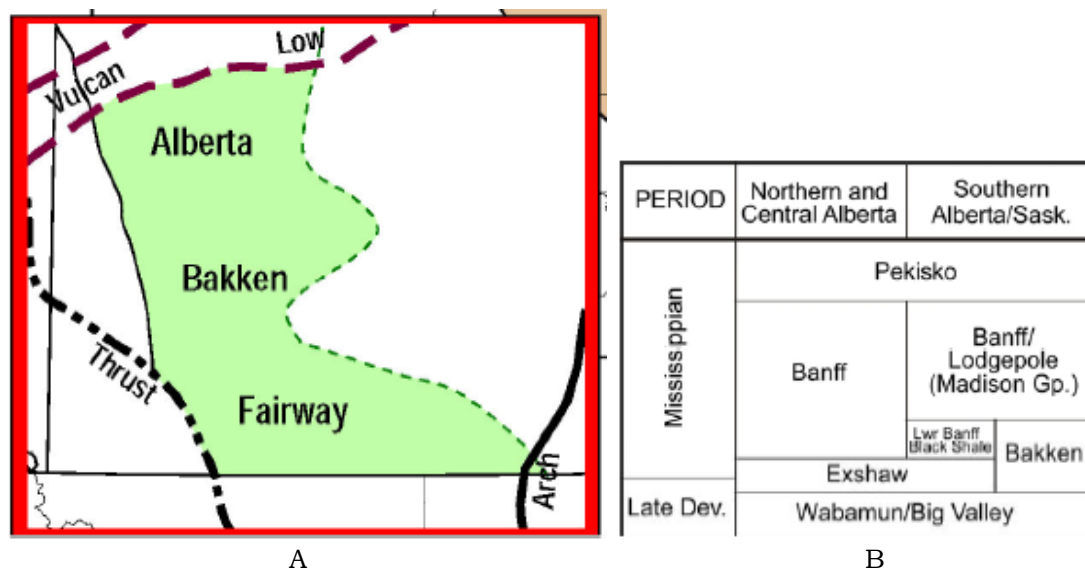


Plate BEB-1. Sketch map of Alberta Bakken Fairway (after Zeitlin et al., 2010) (Plate BEB-1A) and the stratigraphy of the Upper Devonian-Mississippian Banff/Exshaw/Bakken formations within Northern/Central Alberta and Southern Alberta/Saskatchewan (After Rokosh et al., 2009) (Plate BEB-1B)

The Banff-Exshaw-Bakken formations in Alberta is typically composed of (a) Lower Banff organic carbonate and shale unit at the top of the upper Exshaw shale (Figures BEB-2a and BEB-2b); (b) upper Exshaw black shale unit

(Figures BEB-2a and BEB-2b); (c) middle Bakken or Exshaw siltstone-sandstone ; and (d) lower Exshaw-Bakken black shale unit. The lowermost Bakken-Exshaw unit unconformably overlies the Wabamun/Big Valley Formation sandstone and mudstone (Smith and Bustin, 2000). Richards et al (1994 and Rokosh et al (2009) have defined the following depositional facies of these units illustrated within Plate BEB-2.

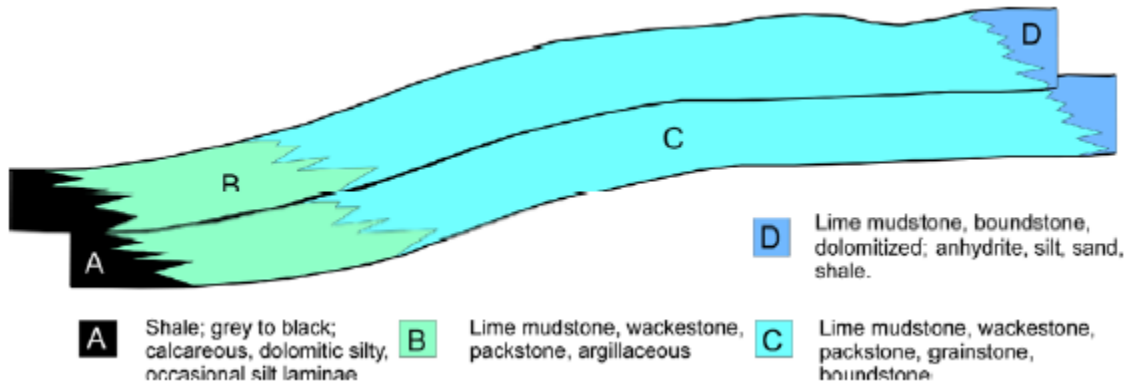


Plate BEB-2. Model of various sedimentary facies of the Upper Devonian-Mississippian Banff-Exshaw-Bakken formation based on change in water depth (after Richards et al., 1994; Rokosh et al., 2009).

Two stratigraphic cross-sections (one at the middle of the basin and one at the south) of the Banff-Exshaw-Bakken (BEB) depositional systems within Alberta illustrated that the thickest Banff-Exshaw-Bakken source rocks are present within the northeast and central parts of Alberta (Figures BEB-Ba, BEB-3b and BEB-3c). The isopach map of the BEB formation shows that the thickest (up to 300m) Banff-Exshaw formation lies within the northwestern section of Alberta (T110 to T80 sectors; Figure BEB-4). In the southeastern section of Alberta , the Banff-Exshaw-Bakken is slightly thinner and merges with the Williston Basin Bakken in Montana (USA) and Saskatchewan.

### 3.2. PREVIOUS STUDIES

Smith and Bustin (2000) demonstrated that the two upper and lower black shale sequences of the Exshaw-Bakken formations beneath the Alberta Plains and Rocky Mountain foothills contain up to 35% TOC. The middle member is a

major reservoir unit with substantial economic potential. These black shale sequences, siltstone, and sandstone are divisible into three sequence system tracks with two transgressive sequences. The basal Banff Formation black shale is the second organic rich interval which is underlain by the Exshaw-Bakken formation sediments. Stasiuk and Fowler (2004) studied various sections of the Exshaw-Bakken formation black shale sequences. The potential source rocks of the BEB formation showed five distinct organic facies zonation that have distinctly different alginite, acritarchs, sporinite, siliceous microfossils, and algal mat microtextures (Figure BEB-5a), sedimentary depths in various areas (Figure 5b) and differences in various TOC and hydrogen index from the Rock-Eval pyrolysis (Figure BEB-5c). The deepwater organic facies A is mostly connected to algal dominated kerogen Type I and II source rocks that plotted within the pseudo-van Krevelen diagram for source rock potential (Stasiuk and Fowler, 2004)(Figure BEB-5C). Similarly, the intermediate water depth related organic facies B plots both in Type I to II kerogen and also in kerogen Type II-III source rocks (Figure BEB-5C). The shallow water organic facies C also plots in kerogen Type I and II fields within the pseudo-van Krevelen diagram (Figure BEB-5c). However, this facies definition often overlaps based on a slight fluctuation of water depth and anoxicity which could not be identified within the TOC versus the S<sub>2</sub> plot of source rock richness.

Two major evaluation reports carried out by the BMO Capital Market News (Zaitlin et al., October 2010) and Scotia Capital Equity Research Industry Report (Bryden, March 2011) have defined well defined facts about the prospects of the Banff-Exshaw-Bakken formations in Alberta based on the geology, source rock evaluation, maturity, and possible production capabilities. However, at this stage, the report shows some limitations of predicting shale gas/oil prediction because of their limited availability of maturity data.

### 3.3. RESULTS AND DISCUSSION

For this report, the data points that were analyzed from various wells have been illustrated in Figure BEB-6. This figure illustrates that the data is mainly concentrated in the northern and southern parts of Alberta.

#### 3.3.1. Organic Petrography

The organic petrography data of the 6000 series sample numbers (6514, 6932) from the Banff and Exshaw formations contain mainly amorphinite 2, few lamalginite and possible fecal pellets with abundant micrinite (Figures BEB-7a and BEB-7b). The kerogen microfabric clearly indicates an overmature sequence. Moreover, the combination of various macerals that are present within these source rocks may possibly suggest a deep water anoxic depositional condition. The 8000 series samples (8020 and 8680) are mixtures of both tel- and lamalginite rich source rocks with amorphous kerogen and solid bitumen that are generated in a mixed anoxic and dysoxic depositional environments (BEB-7c and BEB-7d). The maceral assemblages suggest that these sediments were deposited in intermediate water depths. The fluorescence data of these source rocks may suggest that these sediments currently lie within the late oil to early gas generation stages. The 8900 series source rocks include dominant *Telalginite* (*Tasmanites*, *Leiosphaeridia*) with associated amorphinite 2 and abundant framboidal pyrite suggesting deposition of the Banff-Exshaw formation sediments in a shallow water anoxia. These source rocks lie in the main phase of oil generation.

#### 3.3.2. Source Rock Richness, Potential, and Maturation

Figures BEB-8a to BEB-8D illustrate various parameters of the Rock-Eval pyrolysis and total organic carbon analysis illustrating the source rock richness and potential of all sediments; Figures BEB-8e and BEB-8f depict depthwise plots of TOC, hydrogen Index, maturity ( $R_o$  or  $T_{max}$ ), production index showing the main oil and gas generation zones. Three major classes

based on the depth (1000 m – 2000 m, 2000m-3000 m and 2000 m-3000) of both the Banff and Exshaw formations have been divided to document the changes on organic richness, source rock potential, maturation and oil/gas conversion. Based on that data on organic carbon content, hydrogen index, Tmax or vitrinite reflectance, the production index for both the Banff and Exshaw formations from all three sectors (W4, W5, and W6) of the basin are as follows:

**Table 2**

**Banff** (W4): 0-1000 m: TOC = 1.15 to 2.64%; HI = 409 to 710; Tmax = 430 to 432; Ro = 0.58 to 0.63%; PI = 0.36 to 0.56 (this is Banff Sand)

**Banff** (W4): 1000-2000 m: TOC = 0.16 to 17.1); HI = 48 to 750; Tmax = 422 to 435; Ro = 0.44 to 0.67%; PI = 0.03 to 0.46;

**Banff** (W5): 2000-3000 m: TOC = 0.14 to 5.7%; HI = 37 to 204; Tmax = 432 to 451; Ro = 0.63 to 0.96%; PI = 0.24 to 0.51;

**Banff** (W6) (0-1000m): TOC = 0.12 to 2.81%; HI = 50 to 394; Tmax = 420 to 431; Ro = 0.4 to 0.6; PI = 0.11 to 0.51

**Banff** (W6) > 2000-3000 m: TOC = 0.12 to 2.04%; HI = 6 to 275; Tmax = 426 to 489; Ro = 1.53 to 1.64%; PI = 0.2 to 0.42;

**Banff** (W5): >3000 m: TOC = 0.09 to 1.2%; HI = 23 to 154; Tmax = 419 to 459 (possibly suppressed); Ro = 0.4 to 1.1% (suppressed); PI = 0.13 to 0.66;

**Banff** (W6): >3000 m: TOC = 0.12 to 2.04%; HI = 6 to 275; Tmax = 426 to 489; Ro = 1.53 to 1.64%; PI = 0.20 to 0.42;

**Exshaw**: (W4): 0-2000 m: TOC = 0.21 to 17.0%; HI = 157 to 703; Tmax = 421 to 439; Ro = 0.42 to 0.74%; PI = 0.02 to 0.30.

**Exshaw** (W4): 2000-3000 m: TOC = 0.14 to 8.64%; HI = 33 to 50; Tmax = 459 to 542; Ro = 1.1 to 2.6%; PI = 0.37 to 0.61

**Exshaw** (W5): 2000-3000 m: TOC = 2.32 to 3.67%; HI = 302 to 372; Tmax = 443 to 445; Ro = 0.81 to 0.85%; PI = 0.12 to 0.15

**Exshaw**: (W6): 2000 - 3000 m: TOC = 5.57 to 11.1%; HI = 300 to 590; Tmax = 441 to 448; Ro = 0.78 to 0.90; PI = 0.06 to 0.07

**Exshaw** (W6; one data): TOC = 3.1%; HI = 20; Tmax = 480; Ro = 1.48%; PI = 0.25

TOC= wt %; HI = mg HC/g TOC; Tmax = oC; Ro = %; PI = a ratio of S1/S1 S2

The plot of S2 and total organic carbon data and above data indicates that with a few exceptions, most of the source rocks from the Exshaw source rocks are organic rich (mostly >2% TOC) especially within the W5 and W6 sectors of Alberta (Figure BEB-8a). On the other hand, the lower Banff black shale source rocks have a wide variability of organic richness especially within the W5 and

W6 sectors. They are usually 0.5 to 2% TOC. However, rare anomalously high organic richness (14-17% TOC) within the lower Banff sediments may suggest the possible presence of algal bloom with *Tasmanites algae*. This feature may also suggest that the sporadic development of anoxia within these sediments may occur when these macerals are associated with abundant framboidal pyrite and amorphinite 2 (mixture of sapropel and fine pyrite).

The plot of hydrogen index and oxygen index suggests that a majority of Banff-Exshaw sediments (especially most of the Exshaw source rocks) include typical marine oil prone Type I, I-II, and II kerogen (Figure BEB-8b). However, the colour index (as sample depth indicator) indicates that the kerogen Type I and II source rocks are restricted to a sediment depth of 0-2000 m (mostly within 0-1500m). The anoxia was possibly developed in an intermediate water depth forming a mixture of *Telalginite* (*Tasmanites* and *Leiosphaeridia*), *Lamalginites* (*Prasinophytes*) and amorphinite 2. The current source rock potential plot is quite comparable to the plot from Stasiuk and Fowler (2004) for other source rocks from Alberta, BC, and Saskatchewan (Figures BEB-5c and BEB-8b).

As defined earlier, most of the Banff-Exshaw Formation source rocks have a close relationship with both depth and maturity. In the W4 sector, most of the immature to early mature source rocks are associated to a depth of 0-2000 m (<0.6% Ro; Table 2; Plate BEB-2; Figure BEB-8c). Most of the source rocks from the Banff and Exshaw Formation within a depth of 2000-3000 m of the W4, W5, W6 sectors lie within the main oil generation zone (0.6-1.4% Ro). Most of the Banff source rocks from the W6 sector of sediments >2000 m lie within the main gas generation zone (>1.4% Ro) as well as all the source rocks within the W5 sector of the Exshaw sediments.

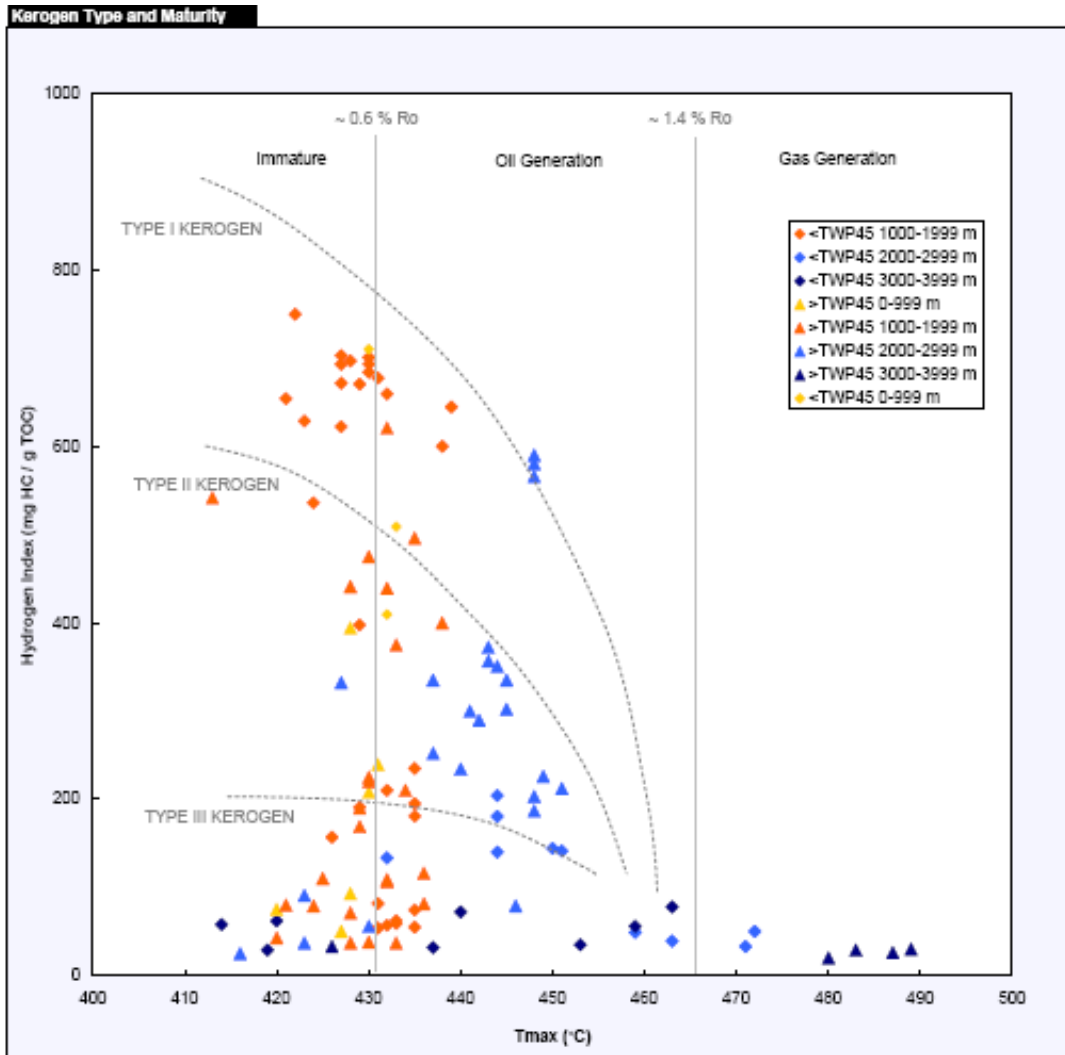


Plate BEB-3. Kerogen maturity in relation to source rock potential

Before discussing the hydrocarbon transformation related to advanced maturity, this report will use the interpretation based on measured maturity available in ERCB compiled geochemical and other data (2012) and from three maturity contour plots (Figures BEB-9a, BEB-9b, and BEB-9c). The ERCB database (2012) on measured vitrinite reflectance suggests that the maturity data shows the following variability in various parts of the basin: North (northeast to southwest): from 0.45% to 0.73% Ro; Central (northeast to southwest): 0.56% to 0.81%; South: (southeast to southwest) 0.89 to 1.79%. The maturity contour lines based on Zeitlin et al (2010) show two highly

reflecting maturity zones (1.00% Ro contour line): one close to the northwest in the foothills and the other is in the southwest close to the USA and Saskatchewan border. They are closely similar to the current database of ERCB (2012). The high maturity zones (1.00% Ro contour line) are connected with major overpressure sediments.

The Ro contour map from Scotia Capital (2011) and the other Ro plot from Higley and Lewan (2009) clearly correlate with the current ERCB database. Most of the data points from Higley and Lewan (2009) are limited and restricted only to the immature to early oil generation zone. However, earlier GSC data (2002; from Scotia Capital, 2011) and current ERCB data indicates that the major dry to wet gas potential is mostly associated with the deformational front starting from the border of the NW Territories and Northern Alberta down to Calgary in the south (close to the USA border). The main wet gas and oil zone lies east and south of the deformational front. Therefore, most of the areas south of Calgary and the area between Calgary and Edmonton would lie within the main phase of the oil generation zone (0.75% to 1.1% Ro) for the Banff-Exshaw-Bakken source rocks.

As the report has already explained maturity zones of the Banff-Exshaw-Bakken source rocks, the interpretation on hydrocarbon transformation and migration aspects based on the Rock-Eval pyrolysis would be more meaningful. The plot of production index and Tmax values indicate that most of the sediments from both the Banff and Exshaw source rocks within 1000 m depth did not show much hydrocarbon transformation and they are restricted to the immature zone (Figure BEB-8d). The highest transformation to oil for the Exshaw source rocks lie within 2000 m to 3000 m depth with low residual hydrogen index and TOC. However, there are striking differences in the production index values (0.35 to 0.61 and 0.13 to 0.15) and hydrogen index values (33 to 50 and 302 to 372) between the W4 and W5 sectors for the Exshaw source rocks within the same depth zone of the sediments (2000-3000 m). This data illustrates that both the depth and maturity of the sediments are

critical for hydrocarbon transformation for these source rocks. This data also suggests differences in heat flow histories in these two sectors of Alberta. Most of the BEB source rocks below 3000 m lie within the condensate/wet gas to dry gas zone (Figure BEB-8d). Although good to excellent oil generating BEB source rocks could be documented from all depth intervals, the highest oil generation and expulsion are mainly restricted to 1000 m to 2500 m (Figures BEB-8e and BEB-8f). Although the dry gas zone is mainly limited between 2500 m to 4000 m depth for the kerogen Type I and II source rocks (Figures BEB-8e and BEB-8f), selected kerogen type II-III source rocks from the W4 sector have also generated dry gases within 500-1000 m depth intervals. In general, the Exshaw source rocks are organic rich, have comparatively higher oil potential, and possibly generate oil at the early stages of maturity (0.5% to 0.85% for Exshaw compared to 0.65% to 1.1% for Banff Formation).

### **3.3.3. Mineralogy**

The bulk mineralogy data of both the outcrop and core samples suggest that they have two different mineral assemblages (Pawlowicz et al., 2009): (a) more carbonates (more calcite) and less clastics (quartz and feldspar); (b) rich in clastics (quartz and feldspar) with associated illite or muscovite as clay minerals (Figure BEB-10a and BEB-10b). Similar features of two mineral assemblages could also be documented within the analysis of major oxides (Figure BEB-10c). However, the quantitative X-Ray diffraction analysis suggests that illite is the major component of both the Banff and Exshaw source rocks; both quartz and calcite can be found in moderate concentrations (Figure BEB-10d). The kaolinite and chlorite remain in minor proportions and pyrite, ankerite, and siderite constitutes only in trace amounts.

Rokosh et al (2009) has identified the differences in mineralogical assemblages within both the Banff and Exshaw source rocks using the XRD analysis. They suggested that the major minerals within the Banff Formation source rocks are quartz (up to 13-51%) and muscovite (3-37%) with varying percentages of

calcite (0-62%), dolomite (0-34) and orthoclase (0-23%). They have also documented that the major minerals within the Exshaw Formation source rocks are quartz (7-82%), calcite (1-37), orthoclase (1-71), and illite (0-43%).

#### **3.3.4. Permeability and Grain Density**

The permeability data for selected Banff and Exshaw formation source rocks are as follows (Figure BEB-11) (Pawlowicz et al., 2009): **Banff**: outcrop - 0.002 mD<sup>3</sup> (lower Banff) to 0.648 mD<sup>3</sup> (upper Banff); core – 0.003 to 3.775 mD<sup>3</sup> (lower Banff); **Exshaw**: outcrop: 0.153 to 0.965 mD<sup>3</sup>.

The grain density of the selected samples from the Banff and Exshaw formation source rocks are as follows (ERCB database, 2012): **Banff** – north: 2.782 to 2.749 gm/cm<sup>3</sup>, central: 2.744 to 2.676 gm/cm<sup>3</sup>, and south: no data; **Exshaw** – north: no data; central: no data; and south: 2.834 to 2.275. This data suggests that the high grain density of selected Banff source rocks may create problems during the “fracking” procedures for better release of gases.

#### **3.3.5. Mineralogy and Porosity: Scanning Electron Microscope**

The mineralogy and porosity data could be utilized from only three selected scanning electron microscope photographs from the upper and lower Banff formation source rocks. The SEM-EDS mineralogy data of the upper Banff lime mudstone shows the porosity development in association with the quartz overgrowth and dolomitization centers (Figure BEB-12a). On the other hand, the porosity within the lower Banff shale possibly developed at the junction of clay minerals and quartz grains (Figures BEB-12b and BEB-12c).

The mercury porosimetry data of two selected mid and lower Banff source rocks shows that both the middle and lower Banff source rock samples contain all three types of porosity (microporosity: 0.002 micrometer, mesoporosity: 0.002-0.005 micrometer, and macroporosity: 0.05 micrometer to 50 nm) development (Figures BEB-13a and BEB-13b).

### **3.3.6. Adsorption Isotherms**

Adsorption isotherms for five outcrop and core samples of lower Banff and one outcrop sample from the Exshaw formation (no. 6517) have been analyzed.

This data suggests that the Exshaw and one lower Banff source rock shows a higher methane adsorption capacity (20 scf/ton) than the other Banff outcrop and core samples (6-15 scf/ton) (Figure BEB-14a). The maximum gas capacity of the core samples is higher than the outcrop samples (0.3 to 1.3 Bcf/ml) for both the Banff and Exshaw source rocks. The Langmuir pressure and volume are similar for both outcrop and core samples (Figures BEB-14b and BEB-15). However, more work is needed on the adsorption capacity of source rocks with variable maturity.

### **3.3.7. Stress Analysis and Shale Oil/Gas Shale Production**

The stress analysis associated with major source rock shale sequences may have two major implications: (a) shale area associated with higher stress may influence advanced maturity because of a possible increase of hot brine flow during the period of maximum sedimentation; and (b) development of oriented fractures which are sometimes parallel or perpendicular to a major stress alignment. This will eventually influence the “fracking” patterns during both shale oil and gas shale production. The maximum and minimum stress directions as defined by Bell and Babcock (1986) for the Alberta part of the Western Canadian Sedimentary Basin clearly defined the possible directions maturity variability within Alberta where major stresses are aligned (Figure BEB-16). High maturity contours should be associated with the minimum stress directions basement arch. More work is needed to review this issue for choosing an unconventional well combining all these parameters.

## **3.4. REFERENCES**

Beaton, A.P, Pawlowicz, J.G, Anderson, S.D.A. and Rokosh, C.D. 2009. Rock Eval™, total organic carbon, adsorption isotherms and organic petrography of

the Banff and Exshaw formations: shale gas data release; Energy Resources Conservation Board, ERCB/AGS Open File Report 2008-12, 65 p.

Bryden, P. 2011. Exploration of the Alberta Bakken: A Resource Play Mosaic in the Making? Scotia Capitol Equity Research Industry Report – A Brief Tour through the School of Rock. Oil & Gas Research Play Spotlight. Scotia Capital Report March 2011. 63p.

Smith, M. G. and R. Marc Bustin. 2000. Late Devonian to Early Mississippian Bakken and Exshaw source rocks, Western Canada Sedimentary Basin. Amer. Assoc. Petrol. Geol. V. 84, no. 7, p. 940-960.

Pawlowicz, J.G., Anderson, S.D.A., Rokosh, C.D. and Beaton, A.P. 2009. Mineralogy, permeametry, mercury porosimetry and scanning electron microscope imaging of the Banff and Exshaw formations: shale gas data release; Energy Resources Conservation Board, ERCB/AGS Open File Report 2008-13, 59 p.

Rokosh, C.D., Pawlowicz, J.G., Berhane, H., Anderson, S.D.A. and Beaton, A.P. (2009b): Geochemical and sedimentological investigation of Banff and Exshaw formations for shale gas potential: initial results; Energy Resources Conservation Board, ERCB/AGS Open File Report 2008-10, 46 p.

Stasiuk, L. D. and Fowler, M. G. 2004. Organic facies in Devonian and Mississippian strata of Western Canada Sedimentary Basin: Relation to kerogen type, paleoenvironment, and paleogeography. Bull. Can. Geol. Geol. V. 52, no. 3, p. 234-255.

Zeitlin, B., Kennedy, J and Kehoe, S. 2010. The Alberta Bakken: A New Unconventional Tight Oil Resource Play October 2010. 21p

## 4. DUVERNAY/MUSKWA FORMATIONS: SCIENTIFIC REVIEW

### 4.1. INTRODUCTION

The Duvernay and Muskwa shale sequences belong to the same formation of the lower part of Frasnian age (Late Devonian) (Figures DM-A1, DM-A2), but named differently in different areas: the shale is called the Duvernay in central Alberta and called the Muskwa in northwestern Alberta and Northeast British Columbia (Reinson et al., 2003; Rokosh et al., 2009). In Alberta, both Duvernay and Muskwa (DM) formation source rocks are widely distributed in specific areas as illustrated in Figure DM-A3 (source: GeoSCOUT, MacQuarie Research 2011).

EPOCH / AGE		NORTHERN BRITISH COLUMBIA	NORTHERN ALBERTA	CENTRAL ALBERTA	WILLISTON BASIN		
LATE DEVONIAN	MISST. TOURNASIAN	EXSHAW		EXSHAW	BAKKEN		
	FAMENNIAN	KOTCHO		KOTCHO	WABAMUN	BIG VALLEY	
		TETCHO		TETCHO		STETTNER	
		BESA RIVER	TROUT RIVER	TROUT RIVER		THREE FORKS	
		KAKISA		KAKISA	GRAMINIA SILT	TORQUAY	
		RED KNIFE		RED KNIFE	BLUE RIDGE		
	FRASNIAN	UPPER MEMBER	JEAN MARIE	JEAN MARIE	CALMAR		
		FORT SIMPSON		WOOD BEND	WINTERBURN	NISKU	WOLF LAKE CYNTHIA BIGORAY LOBSTICK
		MUSKWA		WOOD BEND	WOOD BEND	CAMROSE	SASKATCHEWAN
						LEDUC	BIRDBEAR
				IRETON	DUPEROW		
				DUVERNAY			
				COOKING LAKE / MAJEAU LAKE			

Plate DM-1. Stratigraphic correlation of Duvernay-Muskwa formations in Alberta and BC, and Saskatchewan

The Duvernay and Majeau Lake units represent accumulations under marine, deep-water, low-energy, anoxic basin conditions. The anoxic or euxinic depositional setting of the sediments are based on the absence of fauna, preservation of amorphous lipid organic material, colour of the sediment and the presence of framboidal pyrite. Evidence suggests that euxinic conditions existed in water depths around 100 m in the East Shale Basin (Stoakes, 1980). Undoubtedly the presence of anoxic conditions combined with slow sedimentation rates within this depositional basin is the main reasons for the preservation of abundant organic material in this organic rich source rock.

Earlier publications suggest that euxinic laminites within the late Devonian often show the highly organic rich source rocks (>5% TOC) that are also associated with the bioturbated dysaerobic sediments exhibiting markedly lower organic contents (less than 1.0 percent by weight) (Creaney et al., GSC, 1990). The Duvernay Formation sediments are divided into three major stratigraphic units: (a) lower member is the 20 m thick argillaceous limestone; (b) middle member is black shale with reefal fragments; and (c) the upper member is a mixture of brown bituminous shale and argillaceous limestone (mostly >20m).

The Duvernay formation has long been known as the organic-rich source rock for oil and gas surrounding and within the Leduc reefs where some of the best and first largest discoveries of Alberta took place in 1953. Creaney et al (1990) has defined these two source rock units as the Duvernay Petroleum System (Figure DM-A4). In Alberta, interbedded limestones and organic rich shales of the Duvernay Formation which is part of the Woodbend Group (Upper Devonian) are laterally equivalent to the Muskwa Formation.

The Muskwa Formation is a dark gray to black, organic shale interval which is variably calcareous and pyritic. The Muskwa Formation was deposited on the continental shelf with low sedimentation rates and increased subsidence that resulted in a starved, anoxic basin forming the organic rich shale of the Muskwa Formation.

A schematic geological cross-section of the Duvernay-Muskwa formations from NW to SE of Alberta shows that in the northwest, the Muskwa formation develops as a shallow water equivalent of basinal facies of the Duvernay Formation in the central and southeastern part of Alberta (Figure DM-B). Two stratigraphic cross-sections of Duvernay and Muskwa formations illustrated the variability of the thicknesses of both Muskwa (A-A' cross-section) and Duvernay (B-B') formations within Alberta (Figure DM-C1). The central and southcentral cross-section (line B-B') from log correlation shows that the

Duvernay formation got thicker from the northeast to the southwestern part of Alberta (Figure DM-C2). The structure contour and isopach maps of the Duvernay formation suggests that the thickness changes from 50 m to 10 m from the southeast to the northwest/northcentral part of Alberta (Figures DM-D1, DM-D2, and DM-D3). The northern cross-section of the Muskwa formation (line A-A'; Figure DM-C1; DM-C3) and the structure contour and isopach map of the Muskwa Formation show that the thickness of this formation is 35 m from the north to the central part of Alberta (Figures DM-D4 and DM-D4a).

## **4.2. PREVIOUS STUDIES**

Similar to the Banff-Exshaw source rocks, three main former publications have also evaluated the source rock potential (especially on the shale and shale oil issues) of the late Devonian Duvernay and Muskwa formations within Alberta (Creaney et al., 1990; Fowler et al, 2001; Stasiuk and Fowler, 2004). Stasiuk and Fowler (2004) have defined that organic facies B (with intermediate water depth) dominate the central and west-central part of Alberta, whereas the organic facies D with siliceous microfossils dominate within northern and western Alberta (Figure DM-E1). Coccocoidal alginite rich organic facies C dominates in the eastern part of Alberta (Stasiuk and Figure DM-E1). They also observed from the Rock-Eval pyrolysis plots (hydrogen index versus oxygen index) that the Duvernay Formation source rocks have a wide range of source rock potential similar to the wide variability of their organic facies types (kerogen Type I, II, II-III; Figure DM-E2). However, based on the S2 and TOC data, all the Duvernay Formation source rocks belong to the oil prone kerogen Type II (Figure DM-E2). From similar Rock-Eval pyrolysis plots (Figure DM-E2), Fowler et al (2001) indicated that most of the analyzed Duvernay Formation source rocks were included within the organic rich Type II kerogen as previously suggested by Creaney et al (1990).

### 4.3. RESULTS AND DISCUSSION

For the Duvernay and Muskwa formation source rocks, the analyzed data points of ERCB for this report were divided into two sectors. The Duvernay Formation data points lie within the central and southern parts of Alberta while the Muskwa Formation points lie mainly within the northern sectors (Figure DM-F1). Similar to BEB and MD source rocks, the sample location points were taken from the W4, W5 and W6 sectors which are on the north to south meridian lines dividing Alberta (Figure DM-F2).

#### 4.3.1. Organic Petrography

The organic petrography data of the Duvernay and Muskwa formations show some major differences in maceral distributions and association of oil or bitumen content. Figures DM-G1 and DM-G2 illustrated two plates (12 photomicrographs) both of which have originated from the Duvernay and Muskwa Formation source rocks with variable depths and maturity and have illustrated the following:

Figure DM-G1 (sample no. 8454): Duvernay Formation; 1054.6 m. Immature, highly organic and hydrogen index rich (kerogen Type II: HI - 681) calcareous mudstone with pyrite have shown the presence of abundant Telalginite (*Tasmanites*) and Lamalginite (Prasinophyte algae and acanthomorphic acritarchs) with low concentrations of Amorphinite 2 (low fluorescence). This source rock was possibly deposited in a deep marine sedimentary environment similar to the Organic Facies A as assigned by Stasiuk and Fowler (2004).

Figure DM-G2 (sample no. 8456): Duvernay Formation; 2356.6 m. Mature within Oil Window. The shale has a high TOC and moderate hydrogen rich (Hydrogen Index: ~250-300 mg HC/g TOC). This sample also includes abundant nonfluorescent Amorphinite 2 and low concentrations of visible Tel- or Lamalginite as sample number 8454. The hydrocarbon transformation from the kerogen network was mainly visible with the presence of abundant solid

bitumen and micrinite with rare oil releasing small Lamalginite (*Prasinophyte* algae and possibly from *acanthomorphic* marine *acritarch* and *Tasmanites*) even at a low maturity (sample: 9382)

Figure DM-G3 and DM-G4 (sample no. 8997): Muskwa Formation; 2413.4 m. Mature Early Oil Window (VRo ~ 0.63%). The shale contains abundant TOC (>7%) with high hydrogen index (581) forming kerogen Type II source rock. Petrographically, the shale contains abundant framboidal pyrite associated with abundant Amorphinite 2 (nonfluorescent to dark brown fluorescent) and low concentrations of *Tasmanites* (Telalginite), *Prasinophyte* (Lamalginite) (similar to sample DM-G2) and micrinite. This data may suggest that the Muskwa source rock may have been deposited in a highly anoxic shallow marine environment similar to the Organic Facies C of Stasiuk and Fowler (2004). The sample also contains abundant oil and oil fluid inclusions of oil, solid and adsorbed bitumen within the amorphous lipid matrix. Figure DM-G4 clearly indicates that fluid oil was released from the kerogen macromolecule at an early stage of maturity compared to the Duvernay Formation.

#### **4.3.2. Source Rock Richness, Potential, and Maturation**

The depthwise classes of Rock-Eval data for the Duvernay Formation shows wide variability based on the position of the samples (W4/W5/W6 Meridians and TWP sites) that have controlled the changes on organic richness, source rock potential, maturation and oil/gas conversion (Table 2). On the other hand, the Muskwa Formation sediments are restricted only to the W6 Meridian site. Based on these issues, the average organic carbon content, hydrogen index, Tmax or calculated vitrinite reflectance (based on Tmax) and production index values from both the Duvernay and Muskwa formations for all three sectors (W4, W5, and W6) within the basin are illustrated in Table 2:

## **Table 2**

**Duvernay (W4) TWP 57, 59, 61, 68, 57, 50:** 0-1220 m: TOC = 0.24 to 8.63% (mostly high); HI = 74 to 681 (mostly high); Tmax = 413 to 438; calc. Ro = 0.33 to 0.72%; PI = 0.03 to 0.12 (rare 0.31 Or 0.37)

**Duvernay (W4) TWP 46, 38, 51, 36, 44, 39:** 1700-2290 m: TOC = 0.09 to 11.13% (mostly low); HI = 122 to 582 (mostly high); Tmax = 431 to 452; calc. Ro = 0.42 to 0.87%; PI = 0.06 to 0.56 (several 0.15 to 0.25);

**Duvernay (W5) TWP 47, 48:** 2600-3000 m: TOC = 0.4 to 5.82%; HI = 43 to 260; Tmax = 439 to 472; Ro = 0.74 to 1.34%; PI = 0.17 to 0.54;

**Duvernay (W5): TWP 47, 37** >3300-3700 m: TOC: 0.2 to 4.22%; HI: 49 to 129; Tmax: 448 to 479; calc. Ro: 0.94 to 1.46; PI: 0.30 to 0.53;

**Duvernay (W6) TWP 47, 37:** > 3000 m: TOC = 0.45 to 4.19%; HI = 6 to 275; Tmax = 434 to 456; calc. Ro = 0.65 to 1.05%; PI = 0.33 to 0.59;

**Duvernay (W5) TWP 85, 56, 57, 72:** 1700-2350m: TOC: 0.6 to 7.02 %; HI: 149 to 540; Tmax: 424 to 453; calc. Ro%: 0.47 to 0.99; PI = 0.07 to 0.25 (mostly less than 0.15)

**Duvernay (W5) TWP 62, 65, 59, 72, 74:** 2700-3057m: TOC: 0.51 to 4.93 %; HI: 57 380 (mostly high); Tmax: 432 to 456; calc. Ro: 0.58 to 1.05; PI: 0.16 to 0.65 (mostly high);

**Duvernay (W5) TWP 59 and 63:** 3300-3576m: TOC: 0.39 to 4.51% (mostly high); HI: 6 to 90 (mostly 40-70); Tmax: 437 to 517; calc. Ro: 0.71 to 2.15% (mostly high); PI: 0.30 to 0.73;

**Duvernay (W5) TWP 57 an 56:** 3875-4150m: TOC: 1.19 to 4.7%; HI: 3 to 18; Tmax: 438 to 543; calc. Ro: 0.72 to 2.61% (mostly high); PI: 0.48 to 0.81.

**Muskwa: (W6):** 1515-1652 m: TOC = 0.7 to 10.5% (mostly >2%); HI = 57 to 539 (mostly >250); Tmax = 440 to 460; calc. Ro = 0.76 to 1.26% (mostly >0.8); PI = 0.13 to 0.49 (mostly >0.2).

**Muskwa: (W6):** 2317-2472 m: TOC = 0.92 to 7.54% (mostly >2%); HI = 314 to 517 (mostly >350); Tmax = 434 to 442; calc. Ro = 0.63 to 0.76% (mostly >0.65); PI = 0.04 to 0.13.

TOC= wt %; HI = mg HC/g TOC; Tmax = oC; Ro = %; PI = a ratio of S1/S1 S2

The high and low values of total organic carbon, S2 (mg/HC of Rock), and hydrogen index (mg Hc/g TOC) data of current analyzed ERCB samples have been illustrated in Figures DM-H1, DM-H2, and DM-H3., respectively. These three plots show the variability of these two source rocks on Rock-Eval and Leco TOC parameters in different basins in Alberta. This data shows that in the area between sectors W6 and W5 close to the Peace River Arch (westcentral), the Duvernay Formation has the highest average TOC, S2 and hydrogen index values. This area may have the highest potential for oil within a depth between 1800-2600 m and for dry gas beyond 3000 m. In the W4 and W5 sectors of

eastern Alberta, the calcareous shale source rocks also contain high TOC and HI but the primary oil generation may occur within a depth range of 2400-3000 m.

As discussed earlier, Muskwa Formation organic rich shales are all concentrated around the USA and British Columbia border and possibly formed a different petroleum system from the Duvernay carbonate and calcareous shales in central and southern Alberta.

Figures DM-I1a to DM-I3b illustrate various X-Y plots using selected Rock-Eval pyrolysis and total organic carbon data depicting the source rock richness and potential of all sediments from the Duvernay and Muskwa formations; all three figures with an “a” belong to the Duvernay Formation and the plot marked with a “b” indicate Muskwa Formation samples. Figures DM-I4a and DM-I4b shows the hydrocarbon transformation of all Duvernay and Muskwa formation source rocks. Figures DM-I5a and DM-I6b depict the depth plot of TOC, hydrogen Index, maturity ( $R_o$  or  $T_{max}$ ), and production index that show the main zones for oil and gas generation and expulsion.

The TOC and  $S_2$  plots clearly suggest that both source rock samples are organic rich, high hydrogen generation and expulsion potential and a partial loss of hydrocarbons based on depth (Figures DM-I1a, DM-I1b, DM-I1c). The Duvernay source rocks are categorized to contain best to excellent source rock potential (DM-I1c).

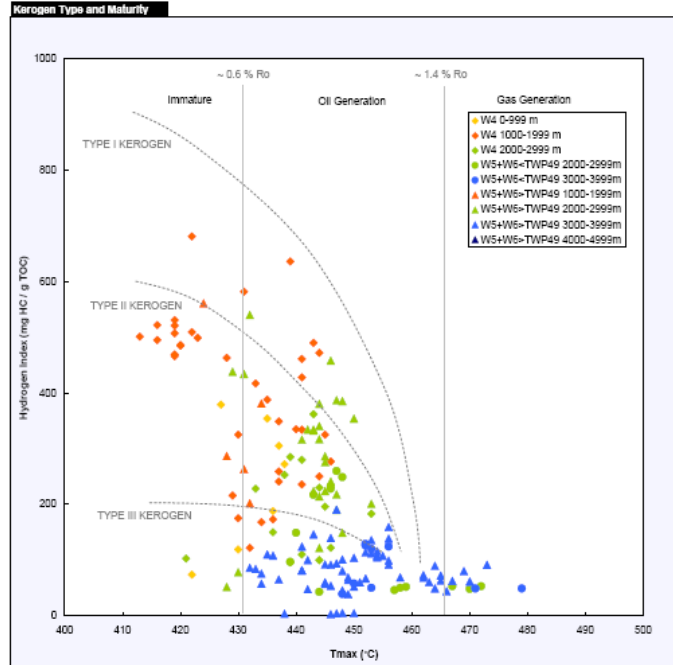


Plate DM-2. Tmax versus hydrogen index showing the variability of source rock potential of Duvernay Formation, Alberta (source: by John Pawlowicz, ERCB).  
 Colour indicates depth range of the samples

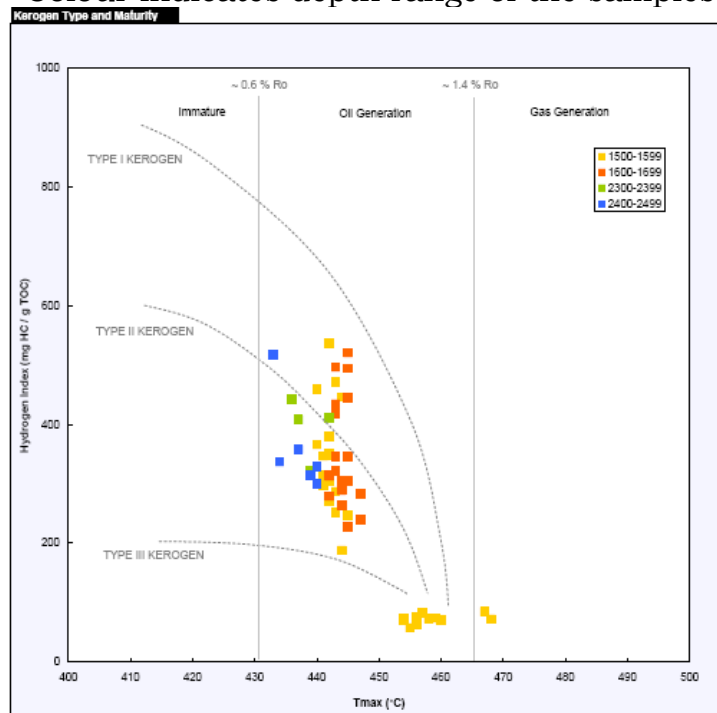


Plate DM-3. Tmax versus hydrogen index showing the variability of source rock potential of Duvernay Formation, Alberta (source: by John Pawlowicz, ERCB).  
 Colour indicates depth range of the samples

The pseudo van Krevelen diagram (HI and OI) suggest that Duvernay organic rich carbonate and calcareous sediments can be designated as oil prone kerogen Type I-II, II to oil and gas prone II-III and III source rocks (Figure DM-I2a); organic rich black shale sequences of Muskwa Formation are considered to be oil prone kerogen Type II and II-III (Plate DM-3; Figure DM-I2b). As suggested earlier, the low oxygen index values of all Muskwa Formation samples clearly indicate that they were deposited in an anoxic depositional environment (Figure DM-I2b). As the sample depth is possibly related to the maturity of the samples (especially for the Duvernay Formation), the Tmax versus hydrogen index plot shows that the Duvernay Formation source rocks are classified to have kerogen Types I, II, II-III, and III source rocks (Figure DM-I3a); all samples within 0-1500 m belong to the immature stage and samples below 3000 m depth clearly indicate advanced maturity (Plate DM-2).

The current report does not include any samples from the Muskwa Formation sediments below 2500 m and the majority of the source rocks were collected from depths between 1500m and 2500 m. These source rocks are organic rich (mostly >2.5% TOC) oil prone Type II and II-III kerogen and lie within the oil generation zone (Figure DM-I3b; Plate DM-3). This feature clearly indicates the close relationship between maturities, the sample depth, and hydrocarbon transformation closeness to the deformational front area.

The hydrocarbon transformation based on the maturity (Tmax) and transformation ratio of the Duvernay Formation sediment suggest that most of the Duvernay source rocks are within the main oil to condensate/wet gas generation and expulsion phase stages (Figure DM-I4a). Only the sediments below 3000 m depth and within the W4, W5, and W6 sectors lie within the dry gas zone. All Muskwa formation source rocks are mature and lie within the principle phase of oil generation and expulsion (Figure DM-I4b).

The depthwise plot of the Duvernay Formation indicates that the main oil generation zone lies within 1500-3000 m depth and have fair to excellent

kerogen Type II oil potential (Figure DM-I5a). In the Muskwa Formation, the source rocks have the main Type II oil potential within a narrow zone (1300-1700 m) (Figure DM-I5b). This data suggests a possible early oil generation for Muskwa Formation source rocks compared to the Duvernay shales. This may also give rise to the generation of early wet and dry gases within the Muskwa Formation compared to the Duvernay source rocks (Figure DM-I6). On the other hand, the main dry generation clearly starts beyond 3000m depth (Figure DM-I7a). Depth-wise plot of oil and gas generation for the Muskwa Formation may indicate two phases of both oil and gas generation from this source rock: wet gas/dry gas around 1500-1700 m and oil, wet, and dry gas around 2300-2500 m respectively (Figure DM-I7b).

This report did not include separate maturity contour maps for both the Duvernay and Muskwa formation source rocks based on the vitrinite reflectance data from the ERCB database. That will be included in a separate contract report later. However, the current report includes an interpretation of two maturity (% Ro) contour maps of the Duvernay Formation acquired from a recent publication (Macquarie Equities Research, 2011; Figures DM-J1 and DM-J2). From the ERCB database, the vitrinite reflectance data of the Duvernay Formation from various parts of Alberta are as follows (ERCB Database, 2011): (a) East (sector W4) Duvernay: %Ro of primary vitrinite varies between 0.56% and 1.13%; (b) South (W5) Duvernay: 0.78% to 1.42%; (c) West (Duvernay): W5 sector wells: 0.55% to 2.74% Ro; West (Duvernay): W6 sector wells: 0.76% to 1.27% Ro; West (Duvernay-Swan Hills): W5 sector wells: 0.7% to 1.28% Ro.

The maturity of the Muskwa Formation in the W5 sector from Northern Alberta varies between 0.47% (early mature) to 1.18% with a rare high of 1.64%. The presence of oil within a maturity of 0.47% to 0.55% Ro suggests either suppression of Ro data or early generation of oil due to low activation energy. In the W6 sector in northern Alberta, the primary vitrinite values vary between

0.52% and 0.97% Ro. In the south, the primary Ro values varies between 0.52% and 0.97%.

These two Ro and isopach contour maps of the Duvernay Formation are associated with two specific areas where a lot of shale gas development activities currently predominate: Greater Keyboob Region and Greater Pembina Areas within Alberta (Figures DM-J1 and DM-J2). In the Greater Keybob region, the maximum shale development of the Duvernay Formation is concentrated in an area where the source rock thickness is between 20-40 m and approximately 1.6% Ro. In the Pembina region, the maximum shale gas and oil development is restricted to the region that is close to the deformational front where the source rock thickness is between 40 to 80m within 1.00 to 1.6% Ro. The 1.6% Ro line runs parallel to the Paleozoic deformational front.

#### **4.3.3. Mineralogy**

The mineralogy data from the XRD analysis suggests that quartz, calcite, and muscovite are the dominant mineral species. The dominant oxides are SiO<sub>2</sub>, Al<sub>2</sub>O<sub>3</sub>, CaO (Figures DM-K1 and DM-K2). The quantitative X-Ray diffraction data suggests that quartz (30%) is the major mineral with calcite and muscovite (10-30) are the moderate minerals, and the illite and chlorite are the minor (<10%) components of the mineral assemblages (DM-K3). A comparable study of the mineralogy of various important shale sequences from North America has revealed that Muskwa shale source rock mineralogy is comparable to the Eagleford shale source rock from Texas (Figure DM-K4). The quartz in the Muskwa shale is also comparable to the Barnett shale (DM-K4).

#### **4.3.4. Grain Density**

The grain density with TOC for the Duvernay and Muskwa Formation source rock samples from various sectors are as follows: (a) south (W5) Duvernay: 2.517 to 2.63 gm/cc<sup>3</sup>, south (W6) Muskwa: 2.696 gm/cc<sup>3</sup> (one data); (b) west (W5) Duvernay: 2.574 to 2.762 gm/cc<sup>3</sup>; West (W5) Swan Hills: 2.725 gm/cc<sup>3</sup>;

West (W6) Duvernay: 2.742 gm/cc<sup>3</sup>; (c) east (W4) Duvernay: 2.377 to 2.755 gm/cc<sup>3</sup>; (d) north (W5) Muskwa: 2.788 gm/cc<sup>3</sup>; north (W6) Muskwa: 2.562 to 2.702 gm/cc<sup>3</sup>.

No permeability data of the Duvernay and Muskwa Formation source rocks could be found in any of the earlier reports from the ERCB or within the current ERCB database.

#### **4.3.5. Mineralogy and Porosity: Scanning Electron Microscope**

In the SEM images, the porosity development within the Duvernay Formation could be visible along the boundary of the clay minerals (illite and spectite), calcite, and quartz grain boundaries (Figures DM-L1 and DM-L2). More work is needed to evaluate the organic porosity within these source rock grains as both the Duvernay and Muskwa Formation source rocks are organic rich and have abundant amorphinite associated with clay minerals, calcite, and pyrite.

#### **4.3.6. Adsorption Isotherms**

Adsorption isotherm analysis of four samples from the Duvernay and Muskwa Formation source rock has been illustrated in Figure DM-M. All plots contain both the adsorption capacity and Langmuir Pressure-Volume analysis which illustrated the variability of methane capacity for both samples. Both Muskwa Formation source rock has an adsorption capacity of 10-15 scf/ton while the Duvernay Formation source has an adsorption capacity of 10-14 scf/ton of methane. This data may suggest that the Muskwa Formation source rock may have slightly higher adsorption capacity of methane at the same depth (maturity interval). The current methane capacity data of the Muskwa formation from Alberta is quite similar to the Muskwa Formation source rocks from six wells drilled in the northeastern British Columbia (Bustin, 2007).

Figure DM-M illustrated the relation between the maturity zones and the possible presence of various types of oil and gas fields derived from the Duvernay Formation source rocks in Alberta. This relationship supports the

discovery of the gas and condensate zones within the W6 sector which is associated with the deformational front (Figure DM-O).

#### **4.4. REFERENCES**

Anderson, S. D. A., C. D. Rokosh., J. G. Pawlowicz, H. Berhane, and A. P. Beaton. 2010. Minerology, permeability, mercury porosimetry, pycnometry, and scanning electron microscope imaging of the Duvernay and Muskwa Formations in Alberta: Shale Gas data Release. ERCB/AGS Open File Report 2010-02. 61p.

Beaton, A. P., J. G. Pawlowicz, S. D. A. Anderson, H. Berhane, and C. D. Rokosh. 2010. Rock-Eval, Total Organic Carbon, and Adsorption Isotherms of the Duvernay and Muskwa Formations in Alberta: Shale Gas data Release. ERCB/AGS Open File Report 2010-04. 33p.

Beaton, A. P., J. G. Pawlowicz, S. D. A. Anderson, H. Berhane, and C. D. Rokosh. 2010. Organic Petrography of the Duvernay and Muskwa Formations in Alberta: Shale Gas data Release. ERCB/AGS Open File Report 2010-06. 147p

Creaney, S., J. Allan, K.S. Cole, M.G. Fowler, P.W. Brooks, K.G. Osadetz, R.W. Macqueen, L.R. Snowdon, C.L. Riediger. 1990. Petroleum Generation and Migration in the Western Canada Sedimentary Basin, Chapter 31, The Duvernay Petroleum System.

Fowler, M. G., L. D. Stasiuk, H. Hearn, and M. Obermajer, 2001. Bull. Can Petrol. Geol. V. 49, No. 1. p. 117-148.

MacQuarie Equities Research 2011. Go the 'Dew'vernay. Big liquids, Big costs, Big payoffs: Duvernay Shales – Canada's Eagle Ford. MacQuarie Equities Global Oil & Gas Specialist's Report. 47p.

Stasiuk, L. D. and Fowler, M. G. 2004. Organic facies in Devonian and Mississippian strata of Western Canada Sedimentary Basin: Relation to kerogen type, paleoenvironment, and paleogeography. Bull. Can. Geol. Geol. V. 52, no. 3, p. 234-255.

Stokes, F.A. 1980. Nature and control of shale basin fill and its effect on reef growth and termination: Upper Devonian Duvernay and Ireton formations of Alberta, Canada. Bulletin of Canadian Petroleum Geology, v. 28, p. 345-410

## **LIST OF FIGURES**

### **MONTNEY AND DOIG FORMATIONS**

MD-A. Straigraphy of the Triassic sedimentary systems of Alberta and British Columbia

MD-B1. Distribution of Montney and Doig Formations

MD-B2. Depth to Montney/DOIG Formations Top

MD-B3a. Dip section of G-G' covering the sediments from the Montney Formation (below) to Fernie Group (topmost)

MD-B3b. Another stratigraphic cross-section covering the sediments from the Montney and Doig Formations (thick section) to Fernie Group (Nordegg and Fernie shale formations)

MD-B4. Montney Formation thickness (isopach) contours

MD-B5. Montney Formation Struction Contour Map

MD-C. Analyzed sample locations for sediments from the Montney and Doig Formations

MD-D1. Photomicrographs of various Montney Polished Samples (sample no. 8765; Ro%: 0.82)(after Beaton et al. 2010)

MD-D2. Photomicrographs of various Montney Polished Samples (sample no. 8117; Ro: 1.02%)(after Beaton et al., 2010)

MD-E1. Kerogen quality plot of total organic carbon and remaining hydrocarbon potential (S2 in mg HC/g rock) of various source rock samples from Montney and Doig Formations , Alberta (source: John Pawlowicz, ERCB). Colour indicates various sample depths.

MD-E2. Pseudo van Krevelen plot of hydrogen index versus oxygen index showing various source rock potential of samples from the Montney and Doig Formations, Alberta (source: John Pawlowicz, ERCB). Colour indicates various sample depths.

MD-E3. Maturity (using Tmax) versus hydrogen index showing the variability of source roc potential of various source rock samples from Montney and Doig formations, Alberta (source: John Pawlowicz, ERCB). Colour indicates various sample depths.

## **MONTNEY AND DOIG FORMATIONS (FIGURES CONTINUED)**

MD-E4. Hydrocarbon transformation versus maturity showing samples connected immature, oil, condensate, wet gas, and dry gas zones of various source rocks from the Montney and Doig Formations (source: John Pawlowicz, ERCB). Colour indicates various sample depths.

MD-E5. Depthwise plot of TOC, oil potential, and hydrogen index of various source rock samples from the Montney and Doig Formations, Alberta (source: John Pawlowicz, ERCB).

MD-E6. Depthwise plot of normalized oil content, production indices and maturity of various source rock samples from the Montney and Doig Formations, Alberta (source: John Pawlowicz, ERCB).

MD-E7. Reflectance versus depth plot of all analyzed samples from the Montney and Doig Formation source rocks showing two different reflectance trends: a. Normal reflectance gradient; b. Suppressed Reflectance gradient

MD-E8. Correlation of two main maturity data (Tmax from Rock-Eval pyrolysis and measured vitrinite reflectance) of various source rock samples from Montney and Doig Formations, Alberta (source: John Pawlowicz, ERCB, 2012) showing areas where Ro values are suppressed and other where Tmax values are suppressed.

MD-F1. Mineralogy from XRD from selected Montney Formation source rocks (source: Anderson et al., 2010)

MD-F2. X-Ray Fluorescence analysis from various oxides of selected Montney & Doig Formation source rocks (source: Anderson et al., 2010)

MD-F3. Quantitative mineral assemblages from selected source rocks of Montney & Doig Formation, Alberta (source: Anderson et al., 2010)

MD-G. Measured porosity, permeability, and grain density of selected Montney Formation source rocks (source: Anderson et al., 2010)

MD-H1. SEM photomicrographs of sample 8705 showing various mineralogical assemblages and porosity distribution, Montney Formation (source: Anderson et al. 2010).

## **MONTNEY AND DOIG FORMATIONS (FIGURES CONTINUED)**

MD-H2. SEM photomicrographs of sample 8709 showing various mineralogical assemblages and porosity distribution, Montney Formation (source: Anderson et al. 2010).

MD-H3. SEM photomicrographs of sample 8731 showing various mineralogical assemblages and porosity distribution, Montney Formation (source: Anderson et al. 2010).

MD-H4. SEM photomicrographs of sample 8739 showing various mineralogical assemblages and porosity distribution, Montney Formation (source: Anderson et al. 2010).

MD-I. Adsorption isotherm analysis of six selected samples from the Montney Formation (Source: Beaton et al., 2010).

MD-J1. Adsorption isotherm analysis of samples from various depths

MD-J1. Changes of gas content during pressure changes for the adsorption isotherm analysis of samples from various depths.

## **LIST OF FIGURES**

### **BANFF AND EXSHAW (BAKKEN) FORMATIONS**

BEB-1a. Devonian to Mississippian basins of Alberta, BC, Saskatchewan, Manitoba, and selected states of northeast USA highlighting the Banff-Exshaw-Bakken Depositional Systems (source: Bryden, Scotia Capital, 2011)

BEB-1b. Stratigraphic correlation of the Fammenin to Tournaisian (Upper Devonian to Mississippian) Banff-Bakken-Exshaw formation sediments within western Canada and USA (source: ERCB, 2011)

BEB-2a. Field photos of Banff and Exshaw Formation source rocks: (A) Banff Formation near Nordegg (arrow 2m in length); (B) Exshaw Formation near type section (at Jura Creek near Kenmore) underlying the Banff Formation source rock (After Rokosh et al., 2009)

BEB-2b. Stratigraphic interlayering of Banff and Exshaw formations at Goat Creek, Alberta (source: Bryden, Scotia Capital, 2011)

BEB-3a. Geological cross-section index map for Banff-Exshaw-Bakken formations

## **BANFF AND EXSHAW (BAKKEN) FORMATIONS (FIGURES CONTINUED)**

BEB-3b. Stratigraphic cross-section of B-B' line that crosses through various wells highlighting Banff-Exshaw-Bakken formations

BEB-3c. Stratigraphic cross-section of C-C' line that crosses through various wells highlighting Banff-Exshaw-Bakken formations

BEB-4. Isopach map of stratigraphic units from the top of Banff Formation to the top of the Wabamum Formation (including Bakken & Exshaw formations)

BEB-5a. Photomicrographs of the organic petrological variability of source rocks within the Banff-Baken-Exshaw source rocks from Alberta and Saskatchewan (after Stasiuk and Fowler, 2004)

BEB-5b. Model of various subdivisions of the organic facies scheme of the Upper Devonian-Mississippian Banff-Exshaw-Bakken formation source rocks within different regions of Alberta based on organic petrological interpretation (after Stasiuk and Fowler, 2004)

BEB-5c. Rock-Eval pyrolysis data Banff-Exshaw-Bakken source rocks along with their variability in organic facies distribution (after Stasiuk and Fowler, 2004)

BEB-6. Sample Locations of Banff-Exshaw source rocks within Alberta

BEB-7a. Photomicrographs of overmature Banff-Exshaw black shale source rocks showing presence nonfluorescent amorphinite and bitumen (sample 6514 (Beaton et al., 2010)

BEB-7b. Amorphous kerogen rich (Amorphinite 2) source rock with solid bitumen (sample 6932) (after Beaton et al., 2009)

BEB-7c. Mixture of amorphinite 2 and Telalginite (*Tasmanites*) source rock from Banff-Exshaw formation (sample 8010) (after Beaton et al., 2009)

BEB-7d: Photomicrographs of algal dominated (both *Telalginite* and *Lamalginitite* - *Tasmanites*, *Leiosphaeridia*, and *Prasinophyphytes*) source rocks from the Banff-Exshaw Formation black shale (sample 8680) (source: Beaton et al., 2009).

BEB-8a. Kerogen quality plot of total organic carbon and remaining hydrocarbon potential (S2 in mg/g rock) for only Exshaw source rocks (source: John Pawlowicz, ERCB, 2012). Colour indicates depth range of the samples

## **BANFF AND EXSHAW (BAKKEN) FORMATIONS (FIGURES CONTINUED)**

BEB-8b. Pseudo-van Krevelen plot of hydrogen index versus oxygen index showing various source rock potential from various samples analyzed from Banff-Exshaw source rocks, Alberta (source: John Pawlowicz, ERCB, 2012). Colour indicates area depth range of the samples

BEB-8c. Maturity (using Tmax) versus hydrogen index showing the variability of source rock potential from various samples from both Banff and Exshaw source rocks, Alberta (source John Pawlowicz, ERCB, 2012). Colour indicates depth range of the samples

BEB-8d. HC transformation versus maturity showing samples connected immature, oil, condensate and dry gas zones areas (source John Pawlowicz, ERCB, 2012). Colour indicates depth range of the samples

BEB-8e. Depthwise plot of TOC, Oil Potential, and Hydrogen Index of various samples from Alberta (source: John Pawlowicz, ERCB, 2012).

BEB-8f. Depthwise plot of Oil Content, Production Index, and Maturity Index of various samples from Alberta (source John Pawlowicz, ERCB, 2012).

BEB-9a. Maturation trend of Baken-Exshaw source rocks from Alberta, Saskatchewan, and Montana (USA) (source: Zeitlin et al., 2010)

BEB-9b. Maturation windows based on selected vitrinite reflectance (data from Higley and Lewan (2009) (source: Bryden, Scotia Capital, 2011)

BEB-9c. Vitrinite reflectance contour map of Alberta (from Geological Survey of Canada, 2002; source: Bryden, Scotia Capital , 2011)

BEB-10a. Bulk mineralogy of Selected outcrop samples from the Banff-Bakkem-Exshaw Formation (after Pawlowicz et al., 2009)

Figure BEB-10b. Bulk mineralogy of selected mixtures of outcrop and core samples from the Banff-Bakkem-Exshaw Formation (after Pawlowicz et al., 2009)

BEB-10c. Oxides of various elements of selected mixture of outcrop and core samples (after Pawlowicz et al., 2009)

BEB-10d. Quantitative X-Ray Deffraction of three selected source rocks (after Pawlowicz et al., 2009)

## **BANFF AND EXSHAW (BAKKEN) FORMATIONS (FIGURES CONTINUED)**

BEB-11. Average permeability of selected Banff and Exshaw outcrop and core samples (after Pawlowicz et al., 2009)

BEB-12a. SEM image of dolomitic lime mudstone (sample 6922) with Banff Formation with less than 5% silt-sized quartz grains and showing dolomitization. The sample show microporosity within the grain boundaries.

BEB-12b. Porosity Distribution within Lower Banff Formation source rock (Pawlowicz et al., 2009)

BEB12c. Porosity Distribution within Lower Banff Formation source rock same image as of Figure 12b in higher magnification (Pawlowicz et al., 2009)

BEB-13a. Pore diameter of selected Middle Banff Fm source rock.

BEB-13b. Pore diameter of selected Lower Banff Fm source rock

BEB-14a. Methane adsorption capacity of six selected samples from Lower Banff and Exshaw Formation source rocks (both outcrop & well)(samples: 6517; 6525; 6534; 6548; 8046; and 8047) (after Beaton et al., 2009)

BEB-14b. Amount of gas from methane adsorption capacity of various samples. (6500 series are high maturity) (after Beaton et al., 2009)

BEB-15. Gas Capacity Banff-Exshaw (after Rokosh et al., 2009)

BEB-16. Stress regime of the western Canadian Sedimentary Basin especially highlighting the area around Alberta

## **LIST OF FIGURES**

### **DUVERNAY AND MUSKWA FORMATIONS**

DM-A1. Sedimentary Basins showing the position of Duvernay and Muskwa formations (after Reinson et al., 2003)

DM-A2: List of potential source rocks from Precambrian to Permian age within Alberta with potential list of publications (after Rokosh et al., 2009)

DM-A3. Distribution of Duvernay and Muskwa formation sediments with specific organic shale rich areas within Alberta (source” GeoSCOUT, Macquarie Research, 2011)

## **DUVERNAY AND MUSKWA FORMATIONS (FIGURES CONTINUED)**

DM-A4. Duvernay Petroleum System after Creaney et al. 1990 (GSC Atlas, WCSB, 1990)

DM-B. Stratigraphic cross section of Duvernay Formation from NW to SE of Alberta (from Alberta Geological Survey, Macquarie Research, 2011) showing the Duvernay shale source rocks occur within basinal part.

DM-C1. Stratigraphic extent map of both Duvernay and Muskwa formations within Alberta

DM-C2. Well log stratigraphic correlation with stratigraphic section B-B' showing the Duvernay Formation shale section

DM-C3. Well log stratigraphic correlation with stratigraphic section A-A' showing the Muskwa Formation shale section

DM-D1. Depth to top of the Duvernay Formation from northwest to southeast section of Alberta

DM-D2. Isopach map of Durvenay Formation from northwest to southeast of Alberta

DM-D3. Structure contour map of Duvernay Formation from north west to southeast Alberta.

DM-D4. Muskwa Formation structure contour map within the north-western section of Alberta

DM-4a. Muskwa Formation isopach map Alberta (Sayer Energy Advisor Report, 2011)

DM-E1. Photomicrographs of various source rocks from the upper Devonian Woodbend Group (Duvernay and Muskwa formations) (after Stasiuk and Fowler, 2004)

DM-E2. Source rock potential of Duvernay and Muskwa formations from Alberta (after Stasiuk and Fowler, 2004)

DM-E3. Rock-Eval pyrolysis data of Duvernay Formtion source rocks from central Alberta (source: Fowler et al., 2001)

DM-F1. Sample Location for Muskwa and Duvernay formations (source: John Pawlowlicz, ERCB)

## **DUVERNAY AND MUSKWA FORMATIONS (FIGURES CONTINUED)**

DM-F2. Sample Location for Duvernay formations with Rock-Eval data locations (source: John Pawlowicz, ERCB 2012)

DM-G1. Photomicrographs of various whole rock kerogen that includes mainly mixtures of Telalginite (*Tasmanites*) and Amorphinite 2 and minor lamalginite (*Prasinophytes*); Duvernay Formation shale – sample 8454 (source: Beaton et al. 2010)

DM-G2. Photomicrographs of various whole rock kerogen that includes mainly framboidal pyrite rich amorphinite 2 and solid bitumen and minor lamalginite (*Prasinophytes*); Duvernay Formation shale - sample 8456 (Source: Beaton et al. 2010)

DM-G3a. Photomicrographs of whole rock kerogen that includes mainly amorphous liptinite (amorphinite 2) with minor algodetrinite, sporinite and solid bitumen; Muskwa Formation carbonate mudstone – sample 8997; depth: 2413.4 m (source: Beaton et al. 2010)

DM-G3a. Photomicrographs of whole rock kerogen in blue light excitation. The photo includes mainly amorphous liptinite (amorphinite 2)(mostly nonfluorescent) with minor telalginite (*Tasmanites*) algodetrinite, sporinite (sp) and abundant oil (oil); Muskwa Formation carbonate mudstone – sample 8997; depth: 2413.4 m (source: Beaton et al. 2010)

DM-H1. Average distribution of the Total Organic Carbon (TOC) values of the Duvernay Formation within Alberta (source: John Pawlowicz, ERCB 2012)

DM-H2. Average distribution of the S2 (mg pyrolyzed hydrocarbons in mg) values from the Rock-Eval pyrolysis of the source rocks from the Duvernay Formation within Alberta (source: John Pawlowicz, ERCB 2012)

DM-H3. Average distribution of the hydrogen index (mg HC/g TOC) values from the Rock=Eval pyrolysis of the source rocks from the Duvernay Formation within Alberta (source: John Pawlowicz, ERCB 2012)

DM-I1a. Kerogen quality plot of total organic carbon and remaining hydrocarbon potential (S2 in mg/g rock) from Duvernay Formation source rock. Colour indicates depth range of the samples (Source: John Pawlowicz, ERCB, 2012)

## **DUVERNAY AND MUSKWA FORMATIONS (FIGURES CONTINUED)**

DM-I1b. Kerogen quality plot of total organic carbon and remaining hydrocarbon potential (S2 in mg/g rock) from Muskwa Formation source rock. Colour indicates depth range of the samples (Source: John Pawlowlicz, ERCB, 2012)

DM-I1c. Cross plots of S2 and TOC values of the sediments from the Duvernay Formation within Alberta showing the quality of the source rock potential (Dean Rokosh, ERCB; 2012)

DM-I2a. Pseudo-van Krevelen plot of hydrogen index versus oxygen index showing source rock potential from Duvernay Formation, Alberta (source: by John Pawlowlicz, ERCB 2012). Colour indicates depth range of the samples

DM-I2b. Pseudo-van Krevelen plot of hydrogen index versus oxygen index showing source rock potential from Muskwa Formation source rocks, Alberta (source: by John Pawlowlicz, ERCB 2012). Colour indicates depth range of the samples

DM-I3a. Maturity (using Tmax) versus hydrogen index showing the variability of source rock potential from various samples from Duvernay Formation, Alberta (source: by John Pawlowlicz, ERCB 2012). Colour indicates depth range of the samples

DM-I3b. Maturity (using Tmax) versus hydrogen index showing the variability of source rock potential from various samples from Duvernay Formation, Alberta (source: by John Pawlowlicz, ERCB 2012). Colour indicates depth range of the samples

DM-I4a. HC transformation versus maturity showing samples connected immature, oil, condensate and dry gas zones areas from Duvernay Formation, Alberta (source: by John Pawlowlicz, ERCB 2012). Colour indicates depth range of the samples

DM-I4b. HC transformation versus maturity showing samples connected immature, oil, condensate and dry gas zones areas from Muskwa Formation, Alberta (source: by John Pawlowlicz, ERCB 2012). Colour indicates depth range of the samples

DM-I5a. Depthwise plot of TOC, Oil Potential, and Hydrogen Index of various samples from Duvernay Formation, Alberta (source: by John Pawlowlicz, ERCB 2012)

## **DUVERNAY AND MUSKWA FORMATIONS (FIGURES CONTINUED)**

DM-I5b. Depthwise plot of TOC, Oil Potential, and Hydrogen Index of various samples from Muskwa Formation, Alberta (source: John Pawlowlicz, ERCB 2012)

DM-I6. Cross plots of the depth versus Production index values for Duvernay & Muskwa Formation source rock samples (source: Deam Rokosh, ERCB 2012)

DM-I7a. Depthwise plot of normalized oil content, production indices, and maturity from various samples analyzed with Rock-Eval pyrolysis from Duvernay Formation, Alberta (source: John Pawlowlicz, ERCB 2012)

DM-I7b. Depthwise plot of normalized oil content, production indices, and maturity from various samples analyzed with Rock-Eval pyrolysis from Muskwa Formation, Alberta (source: John Pawlowlicz, ERCB 2012)

DM-J1. Vitrinite Ro (red lines) contours and the isopach thickness (green letters) of the Duvernay Formation along with Land Sales ages within the Greater Keybob area (source: Macquarie Equities Research, 2011)

DM-J2. Vitrinite Ro (red lines) contours and the isopach thickness (green letters) of the Duvernay Formation along with Land Sales ages within the Greater Pembina area (source: Macquarie Equities Research, 2011)

DM-K1. Bulk sample XRD analysis of the Duvernay and Muskwa formations shale (source: Anderson et al., 2010 ERCB Report)

DM-K2. Major oxides of the Duvernay and Muskwa formations shale from X-ray Fluorescence analysis (source: Anderson et al., 2010 ERCB Report)

DM-K3. Clay Mineralogy of the Duvernay and Muskwa formations shale (source: Anderson et al., 2010 ERCB Report)

DM-K4. Mineralogy of the Duvernay formation shale and its comparison with other important shale gas resources of the world (source: Macquarie Equities Research, 2011)

DM-L. SEM images of Duvernay source rock showing the porosity development within Duvernay Shale (sample 8479)

DM-L2. SEM images of Duvernay source rock showing relatively high porosity surrounding the quartz and clay grains (source: Anderson et al., 2010 ERCB Report)

DM-M. Adsorption isotherms of four samples from the Duvernay and Muskwa Formation source rocks (source: Beaton et al., 2009)

DM-N. The distribution of various types of hydrocarbons (black oil, condensate, and dry gas) with northeast to southwest section of Alberta (source: Dean Rokosh,ERCB, 2011)

DM-O. The distribution of oil, condensate and gas wells within the northwest (source: Dean Rokosh,ERCB, 2011)

# **Montney and Doig Formations**

## **Figures and Tables**

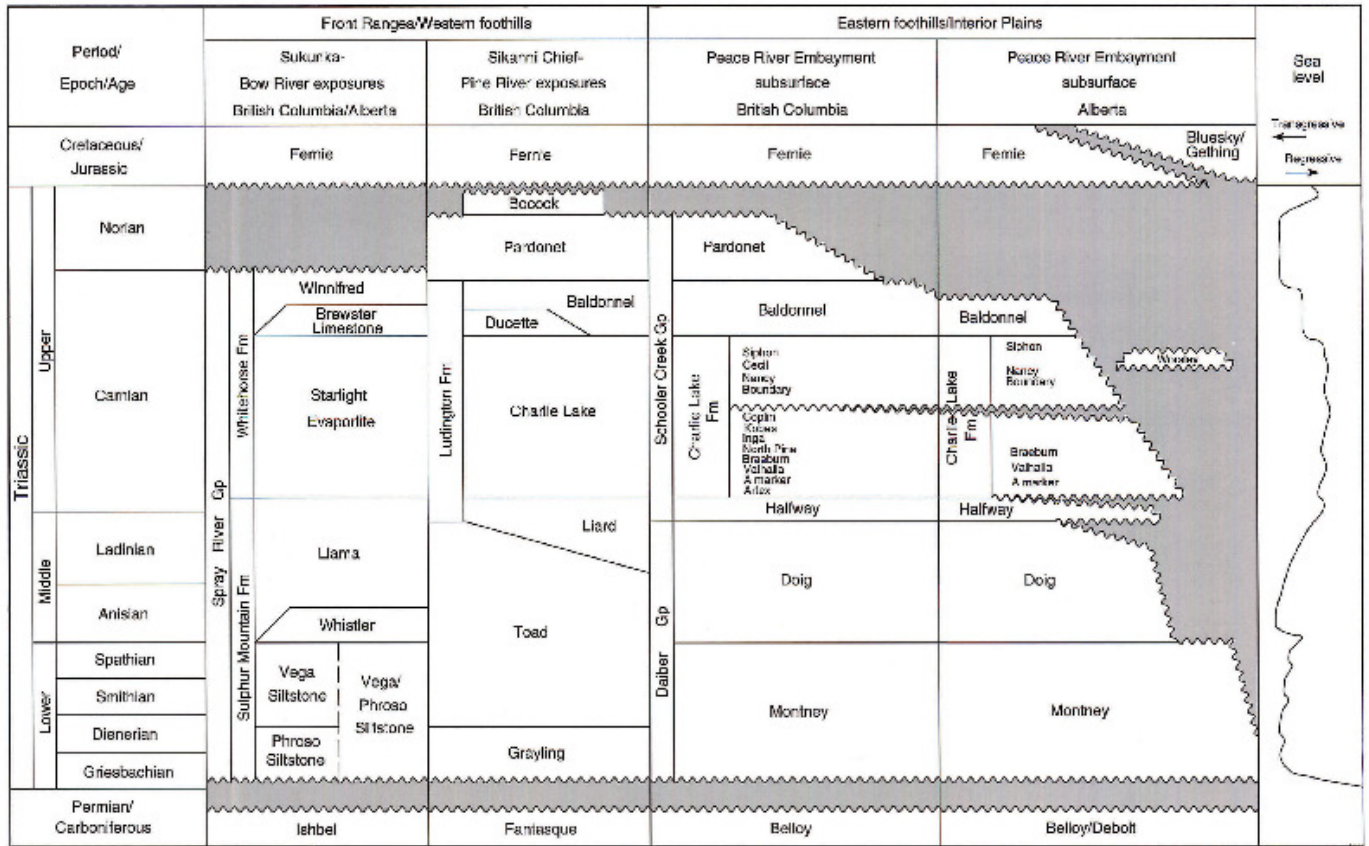


Figure MD-A. Stratigraphy of Triassic sedimentary rocks in Alberta and BC.

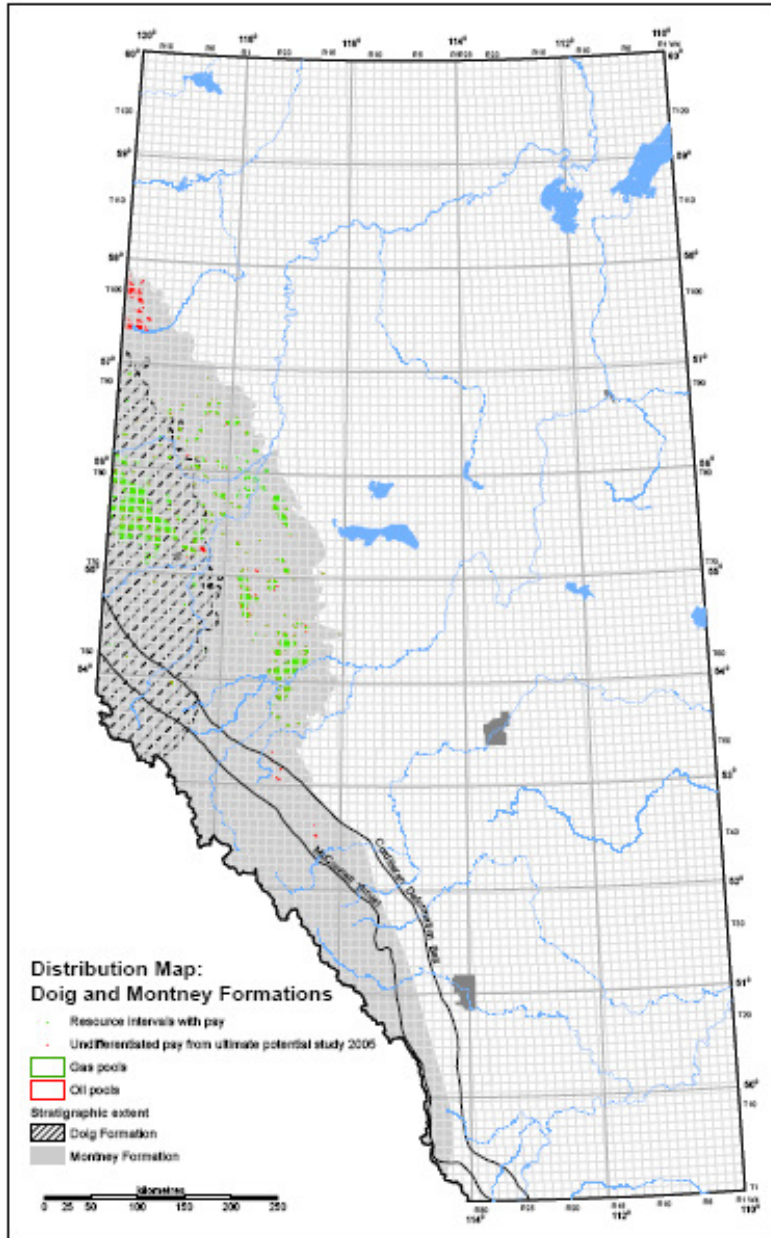


Figure MD-B1. Distribution of Montney and Doig Formation

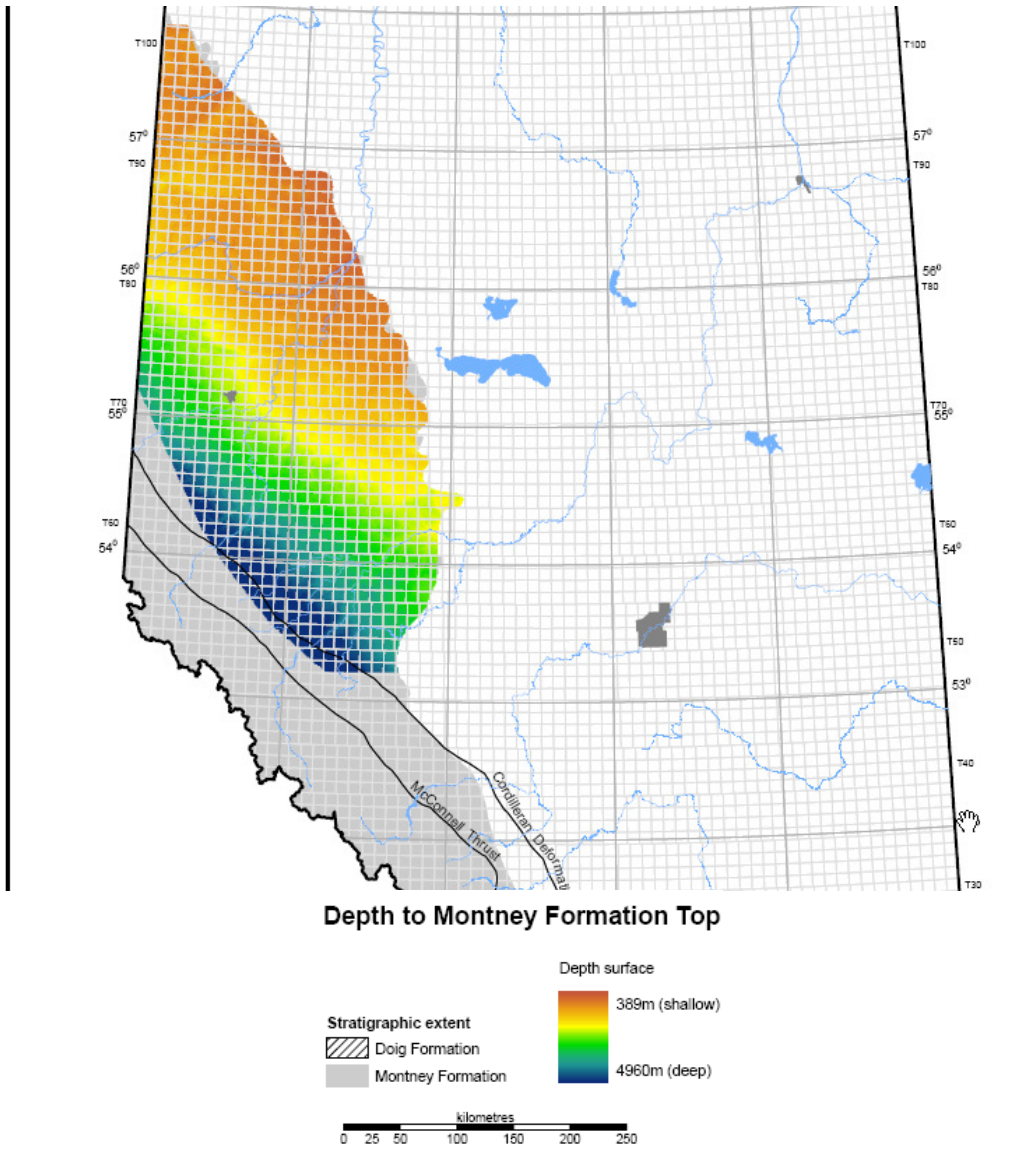


Figure MD-B2. Depth to Montney/Doig formations Top

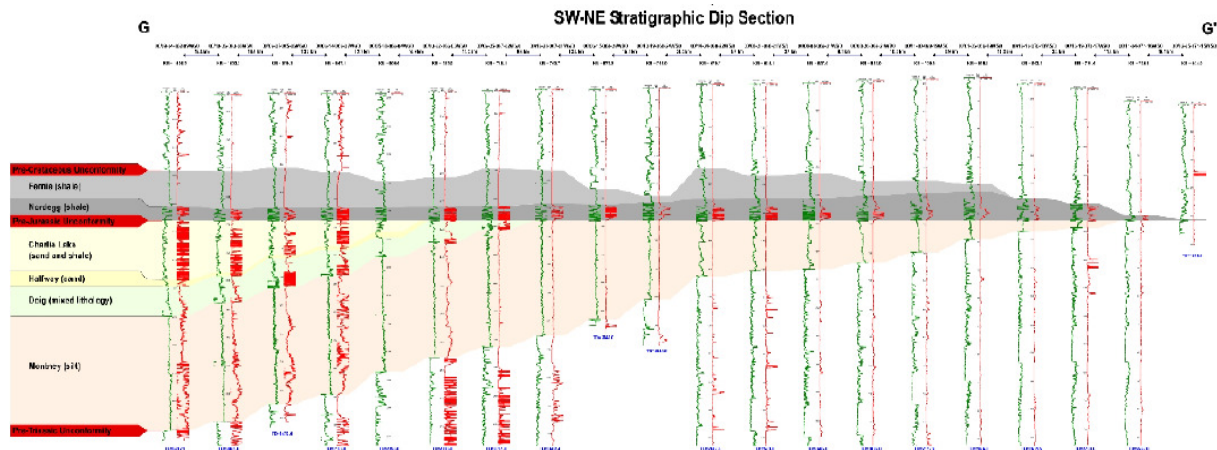


Figure MD-B3a. Dip section of G-G' covering the sediments from Montney Formation (below) to Fernie Group (topmost)

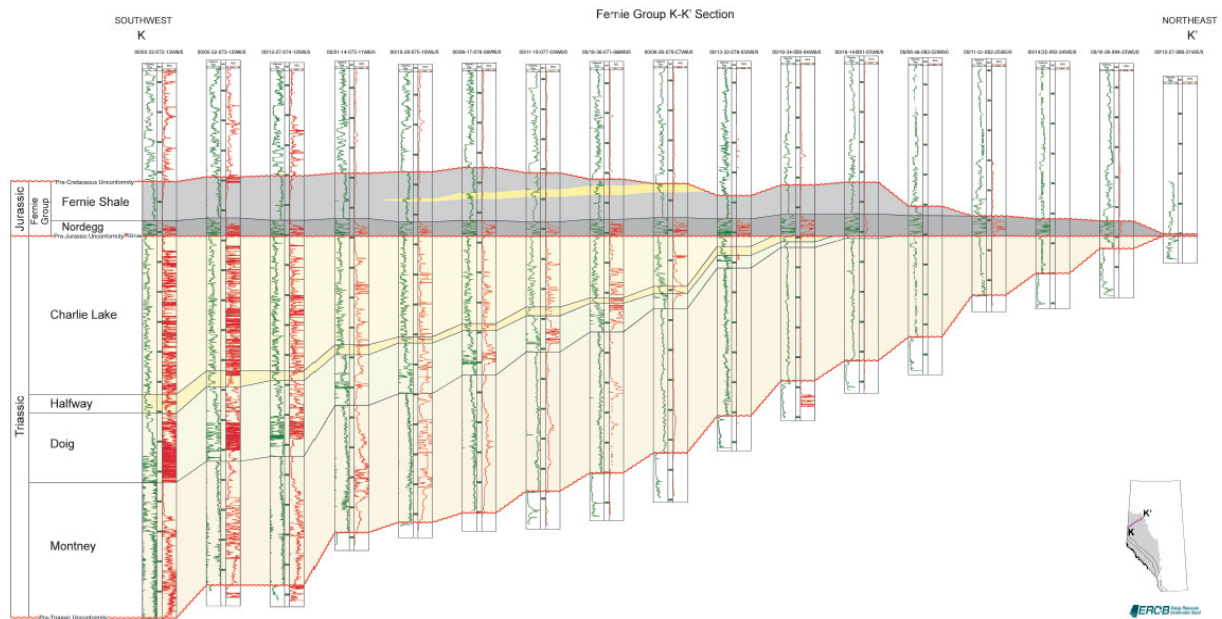
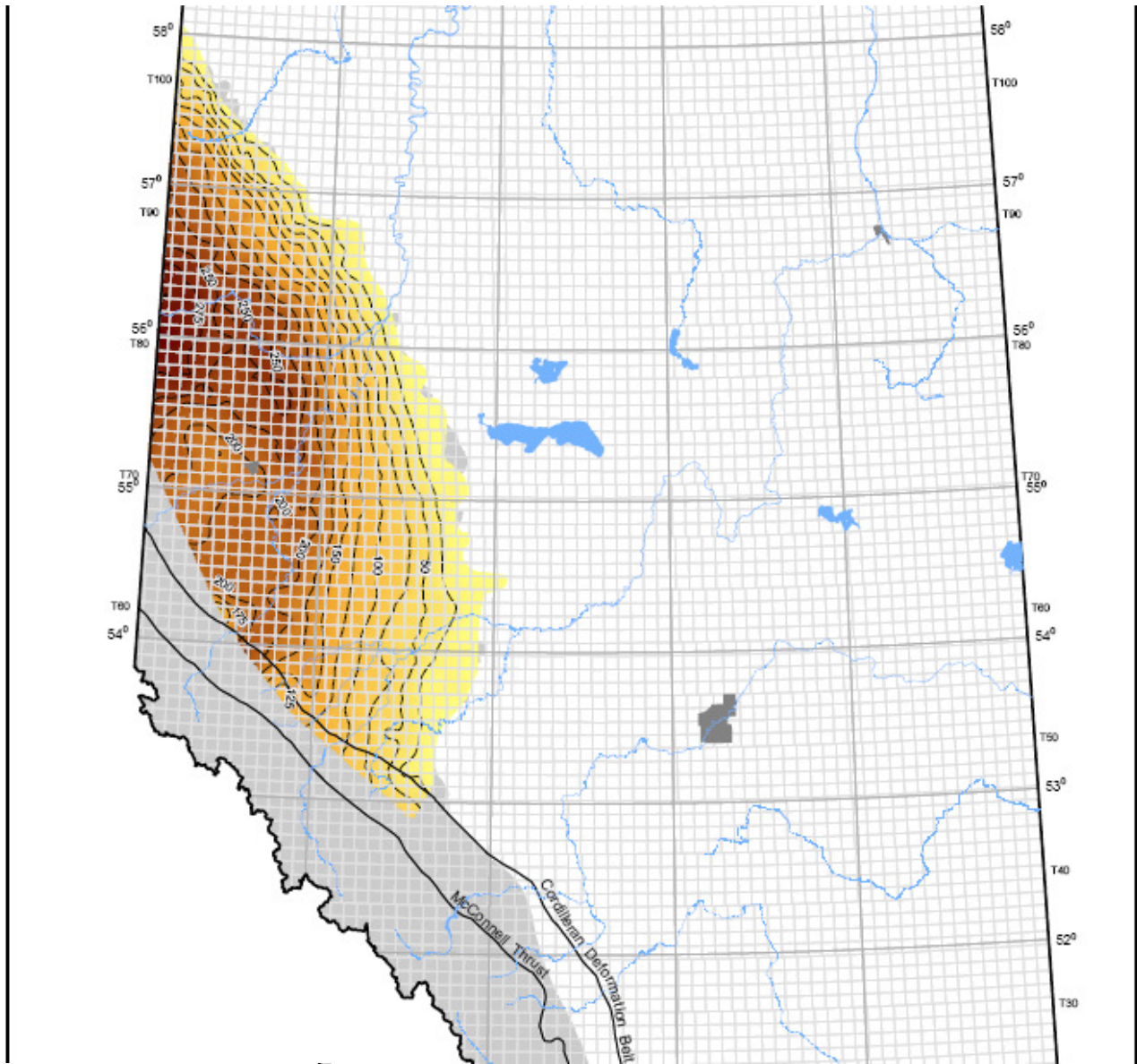


Figure MD-B3b. Another stratigraphic cross section of K-K' covering the sediments from Triassic Montney and Doig formations (thick section) to Fernie Group (Nordegg and Fernie Shale formations)



Montney Formation Thickness

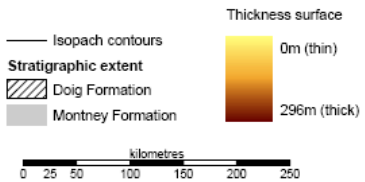


Figure MD-B4. Montney Formation thickness (isopach) contours

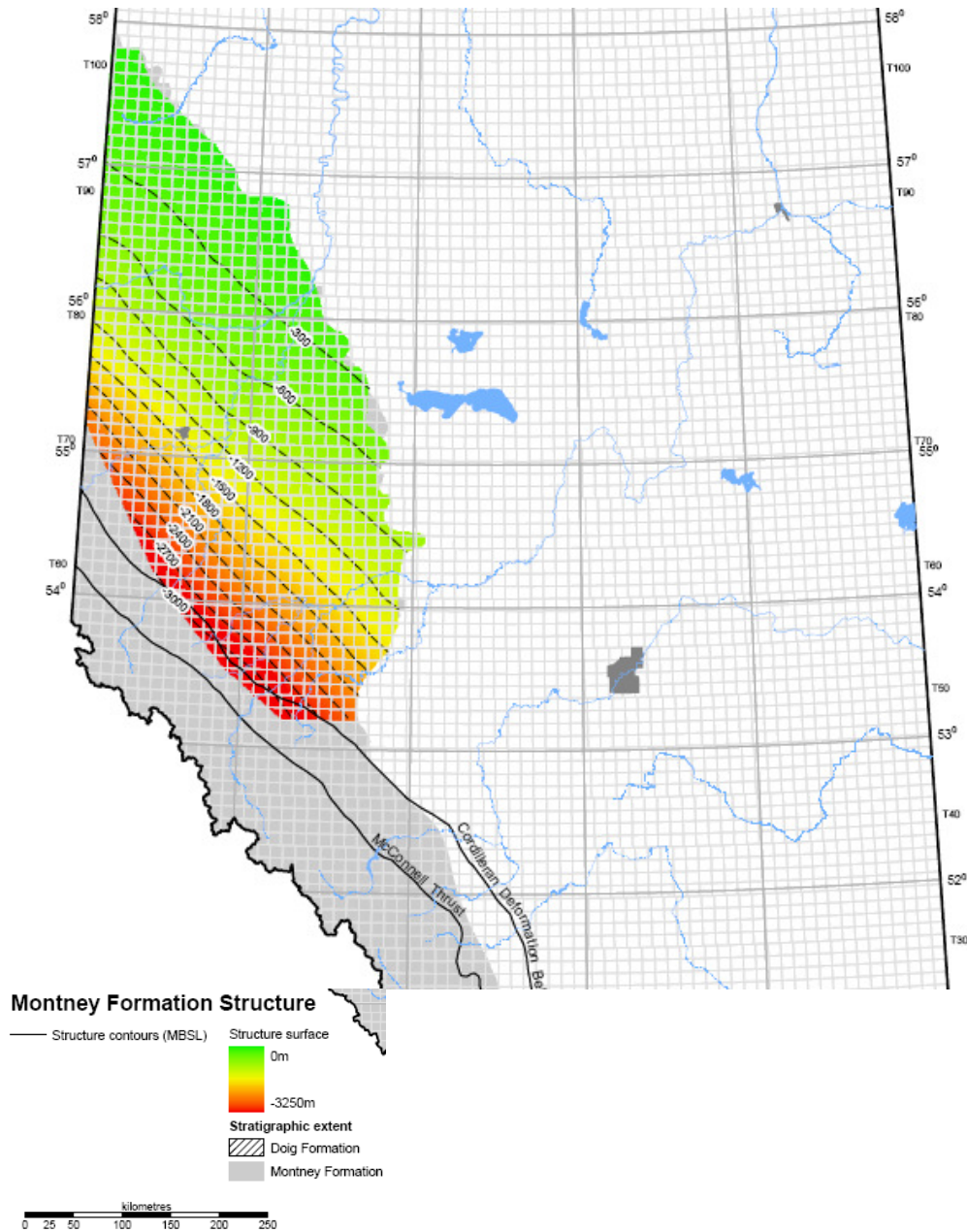


Figure MD-B5. Montney Formation structure contour map

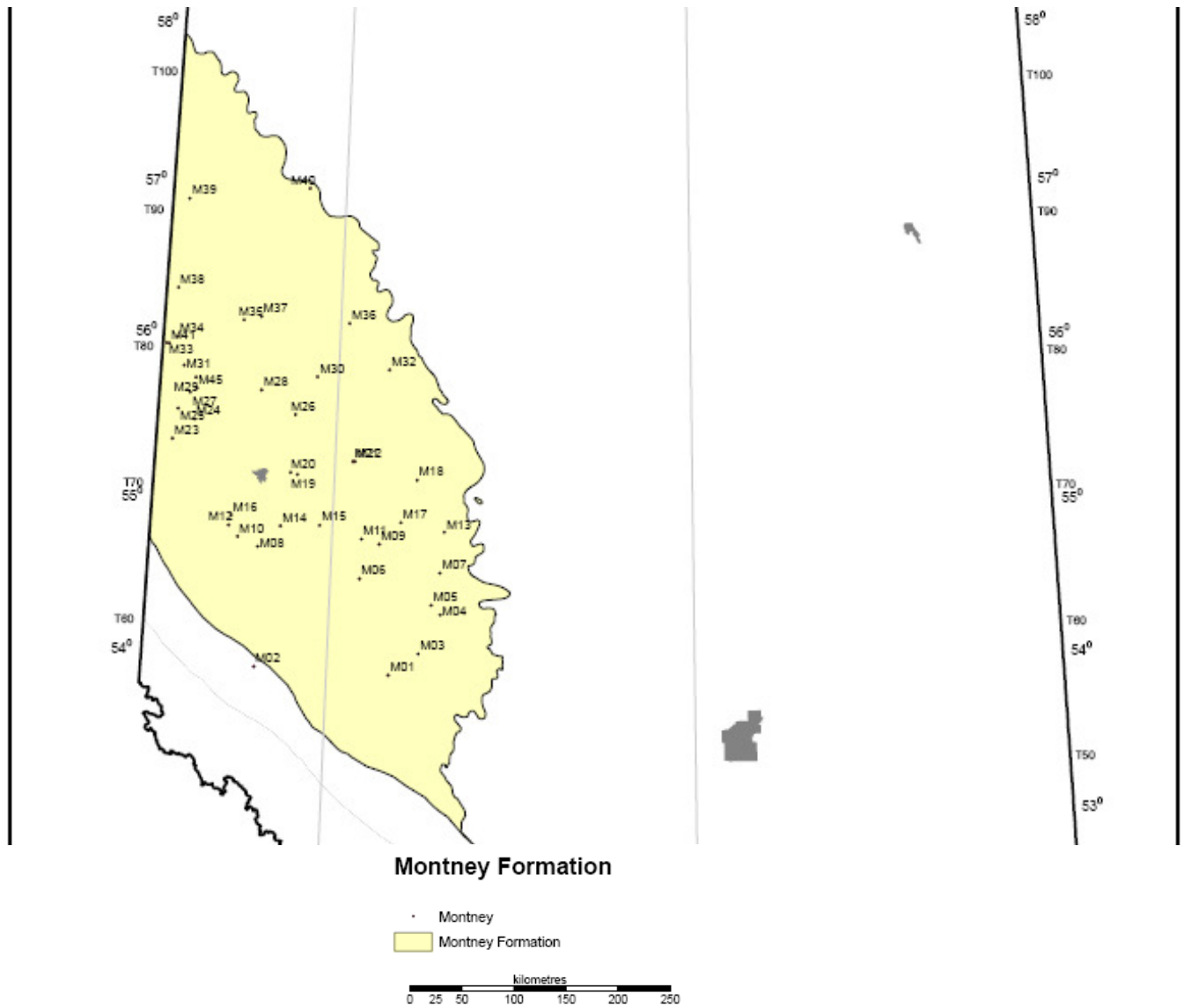
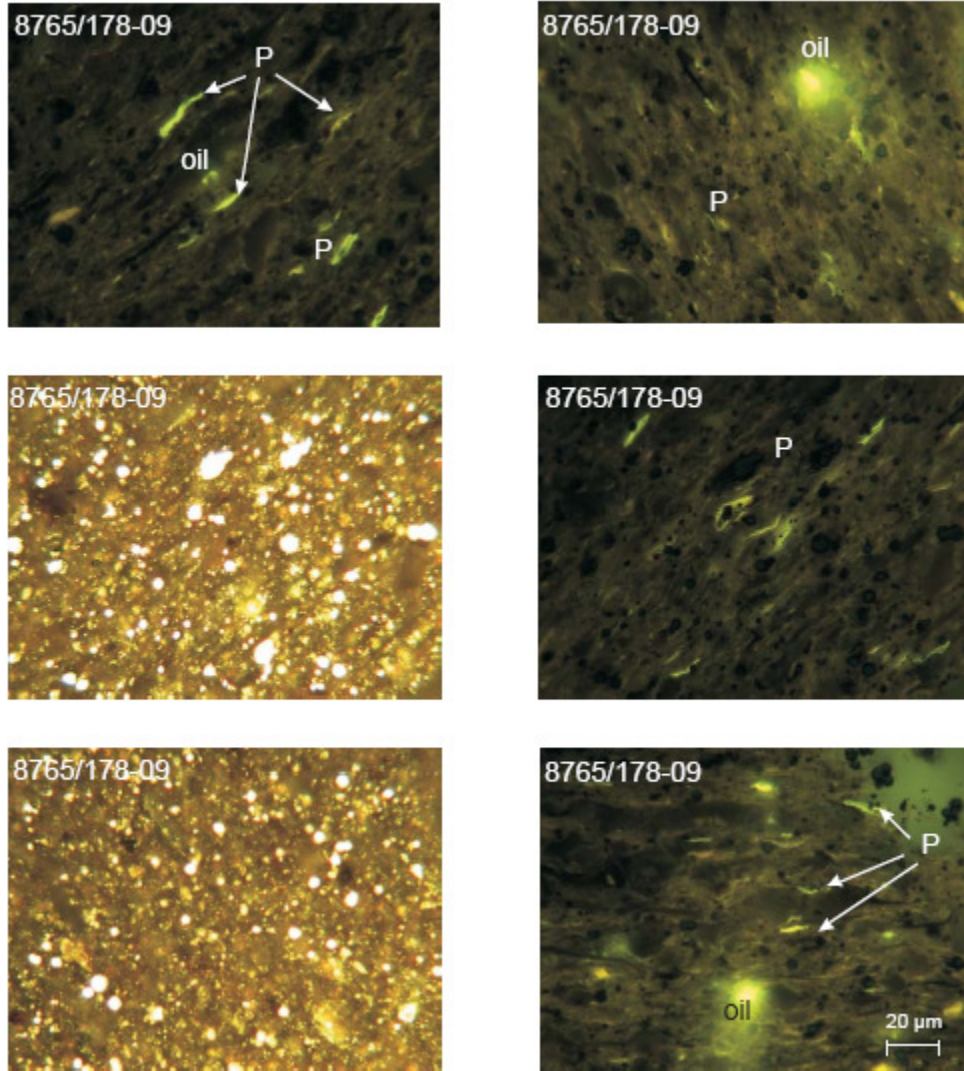
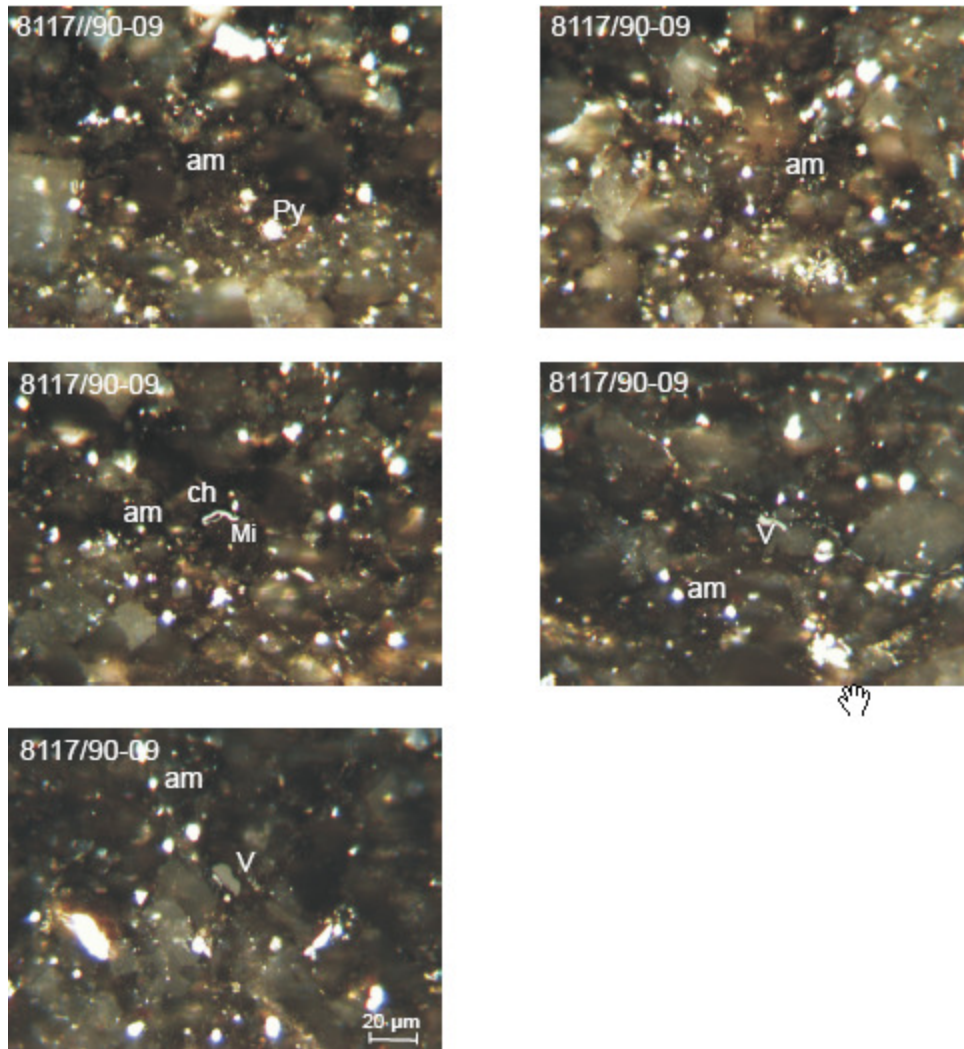


Figure MD-C. Analyzed sample locations for sediments from the Montney and Doig Formations.



AGS 8765/GSC 178-09 (Montney; 100/11-28-071-03W6/00, 1845.8 m core depth). Brown, silty shale with a major amount of dull yellow-fluorescing Prasinophyte (P) alginite widely dispersed within framboidal pyrite-rich amorphous kerogen. Major to minor amounts of bright yellow-fluorescing soluble oil/asphaltine (oil) causing staining and partial saturation. Rare, yellow-fluorescing spiny acanthomorphic acritarch (ac) and possibly chrysophytes. Rare, orange-fluorescing bitumen and non-fluorescing primary bitumen (B) within intergranular pores. Very rare allocthonous inertinite maceral (I). Scale bar applies to all images. (In oil, polished surface, fluorescence and reflected white light, 50X magnification). ch = chitinous microfossil

Figure MD-D1: Photomicrographs of various Montney Polished samples ( Sample no 8765; Ro = 0.82) (after Beaton et al., 2010)



AGS 8117/GSC 90-09 (Montney; 100/06-03-076-12W6/00, 2629.1 m core depth). Mainly a thin, interconnected network of dark brown amorphous kerogen (am) with major micrinite (Mi, bright whitish-yellow particle) and framboidal pyrite (Py) inclusions brecciated within the intergranular pores of a medium- to coarse-grained siltstone. A trace of vitrinite (V) maceral and rare, inert chitinous (ch) lenses are also observed within the matrix. Scale bar applies to all images. (In oil, polished surface, fluorescence and reflected white light, 50X magnification).

Figure MD-D2. Various photomicrographs from the polished Montney samples ( Sample no 8117; Ro = 1.02) (after Beaton et al., 2010)

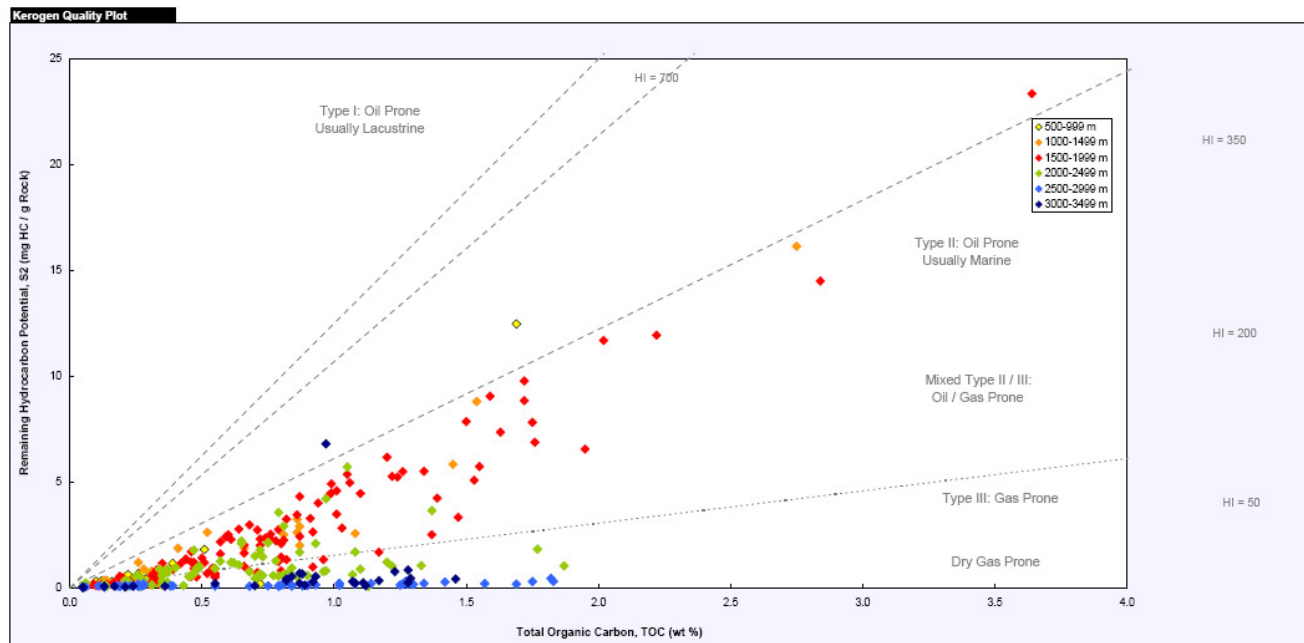


Figure MD-E1. Kerogen quality plot of total organic carbon and remaining hydrocarbon potential (S<sub>2</sub> in mg/g rock) of various source rock samples from the Montney and Doig formations, Alberta (source: John Pawlowicz, ERCB, 2012). Colour indicates depth range of the samples

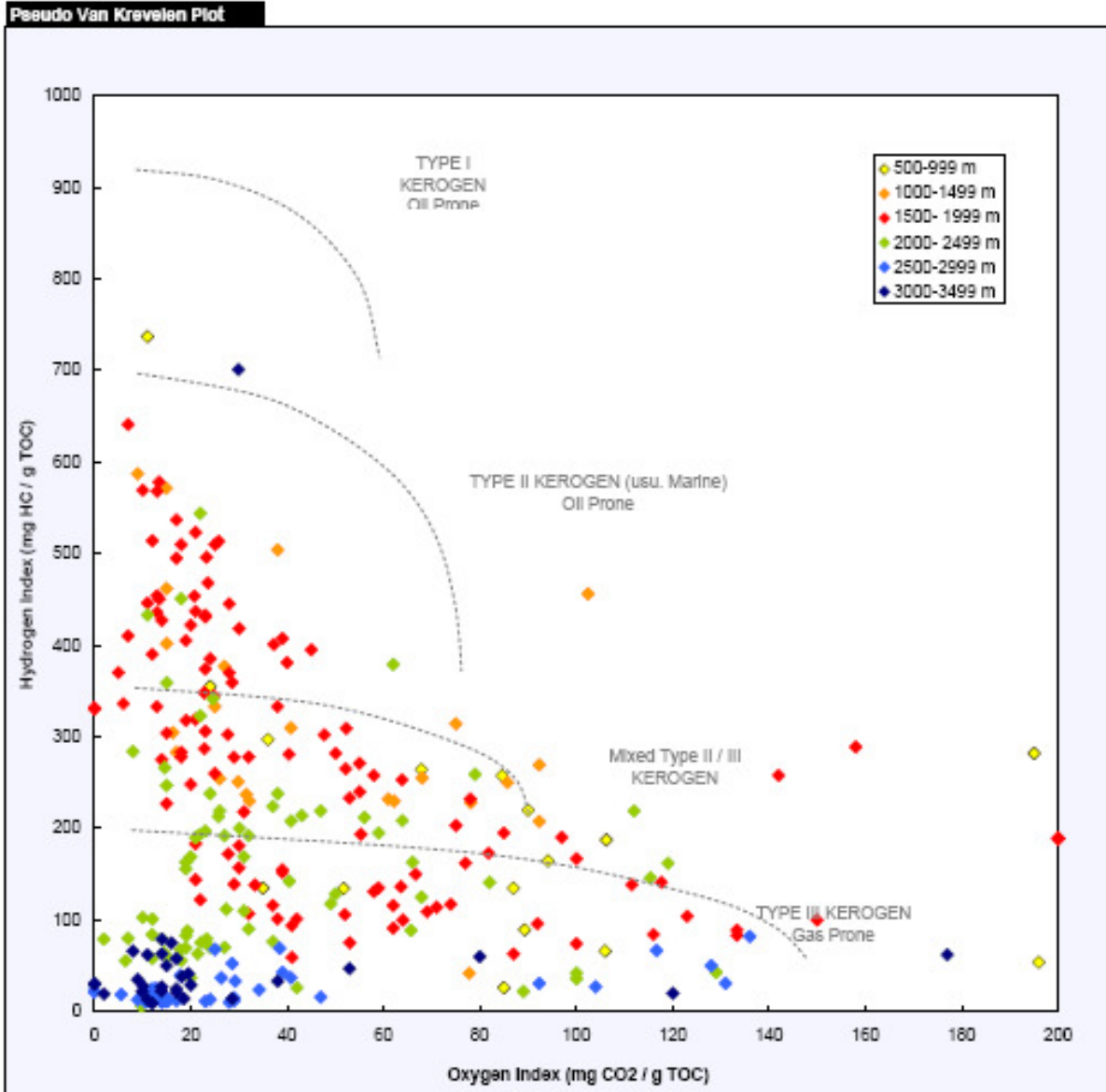


Figure MD-E2. Pseudo-van Krevelen plot of hydrogen index versus oxygen index showing various source rock potential of samples from the Montney and Doig formations, Alberta (source: John Pawlowicz, ERCB). Colour indicates depth range of the samples

### Kerogen Type and Maturity

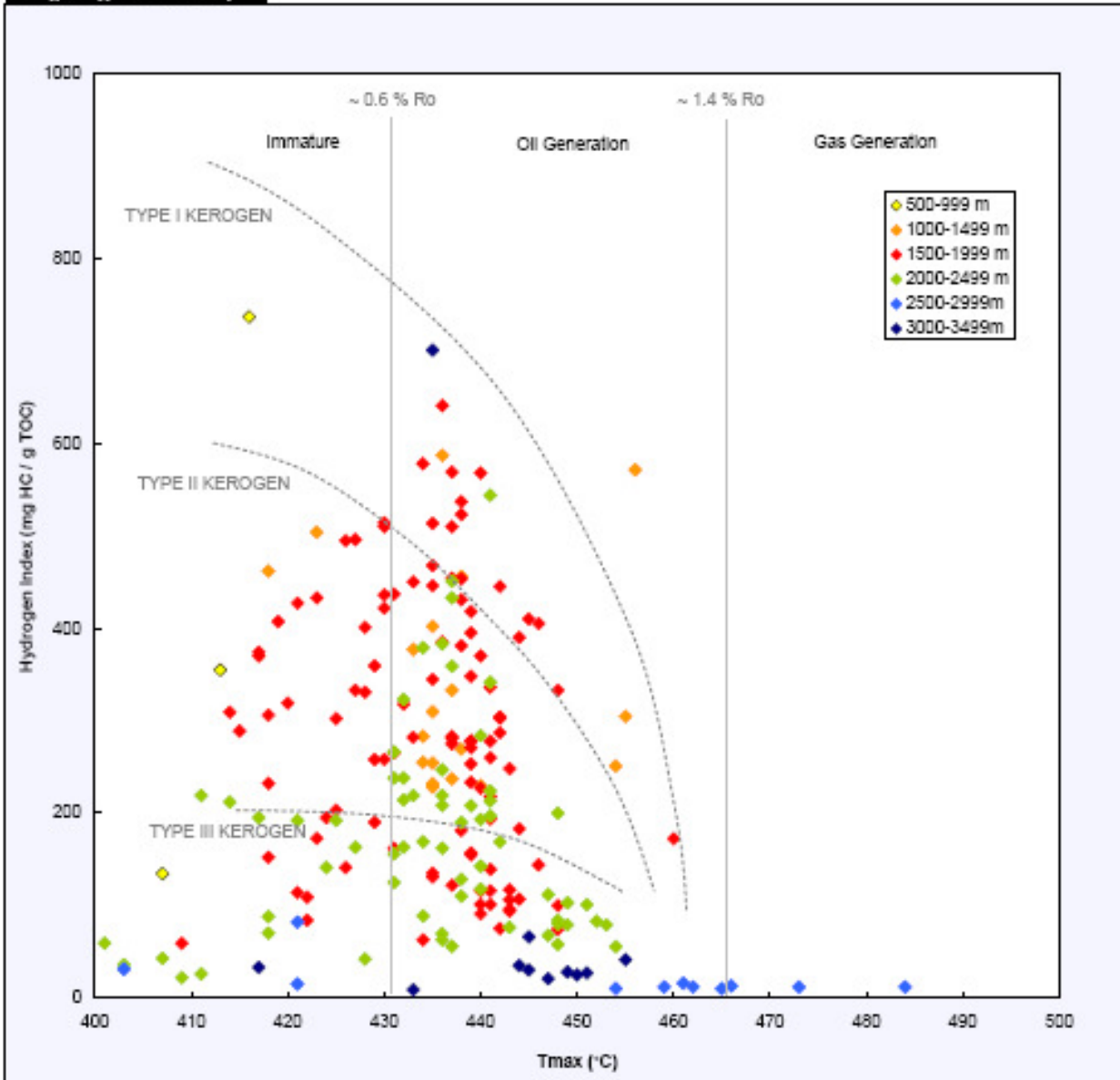


Figure MD-E3. Maturity (using Tmax) versus hydrogen index showing the variability of source rock potential of various source rock samples from the Montney and Doig formations, Alberta (source: John Pawlowicz, ERCB, 2012). Colour indicates depth range of the samples

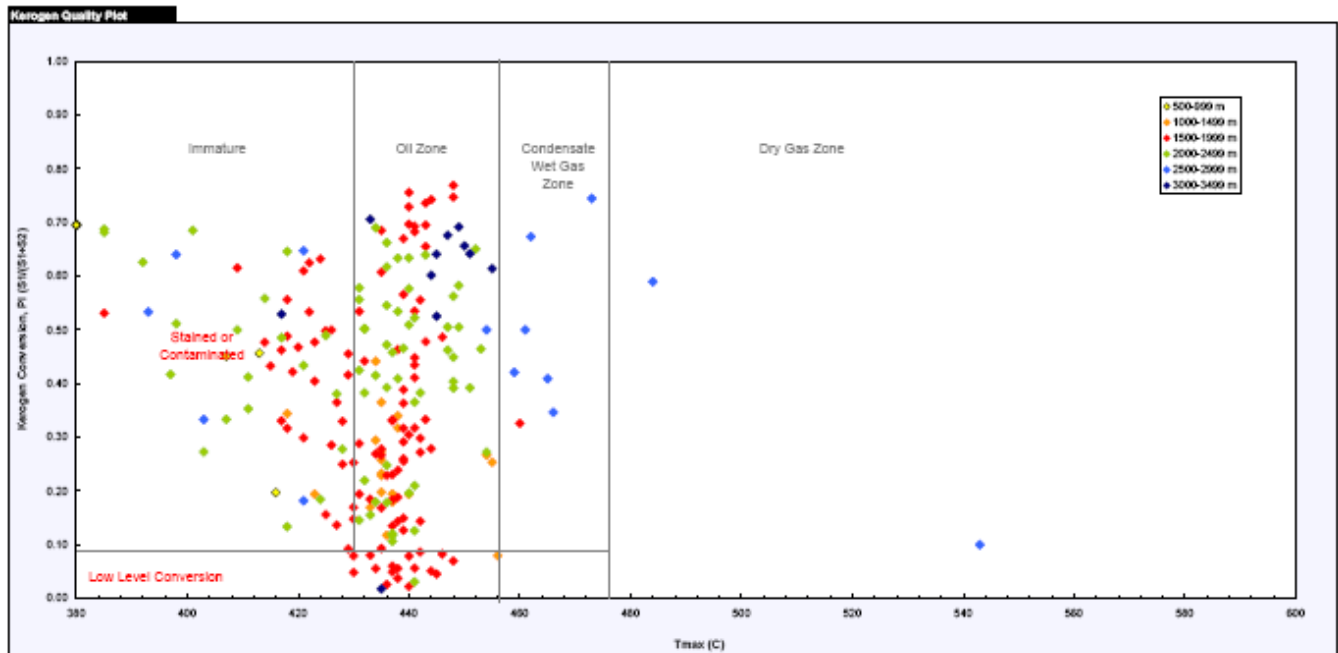


Figure MD-E4. HC transformation versus maturity showing samples connected to immature, oil, condensate and dry gas zones areas of various source rock samples from the Montney and Doig formations, Alberta (source: John Pawlowicz, ERCB, 2012). Colour indicates depth range of the samples

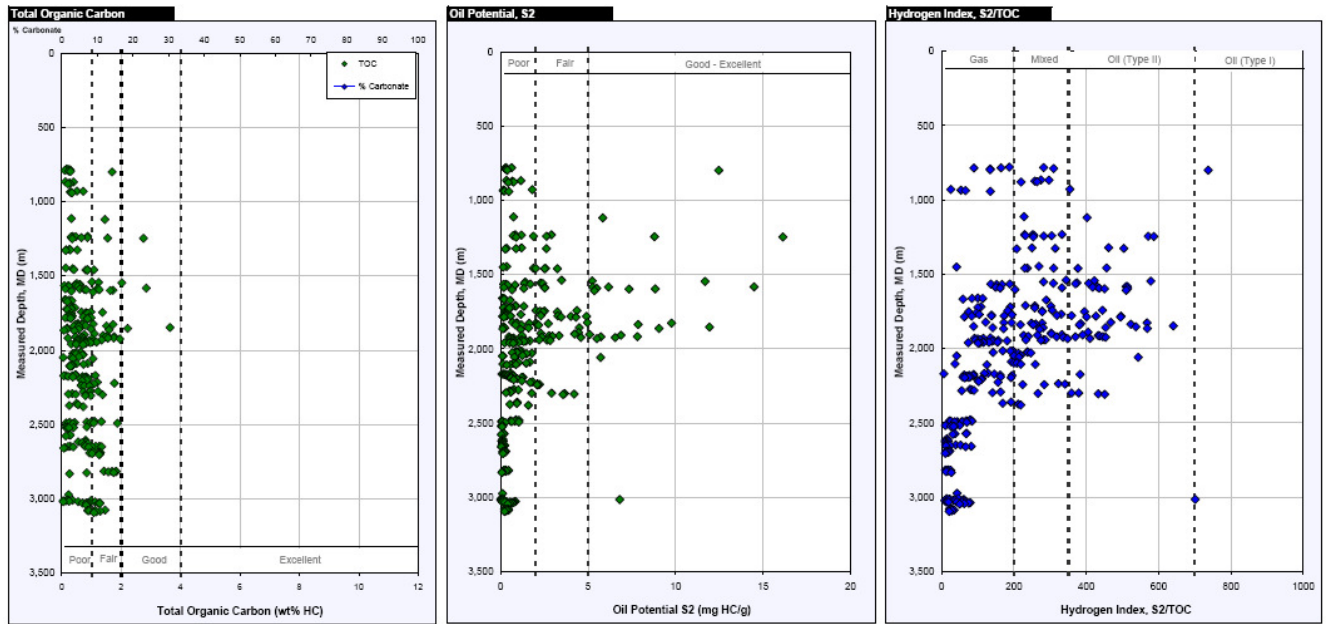


Figure MD-E5. Depthwise plot of TOC, Oil Potential, and Hydrogen Index of various source rock samples from the Montney and Doig formations, Alberta (source: John Pawlowicz, ERCB, 2012)

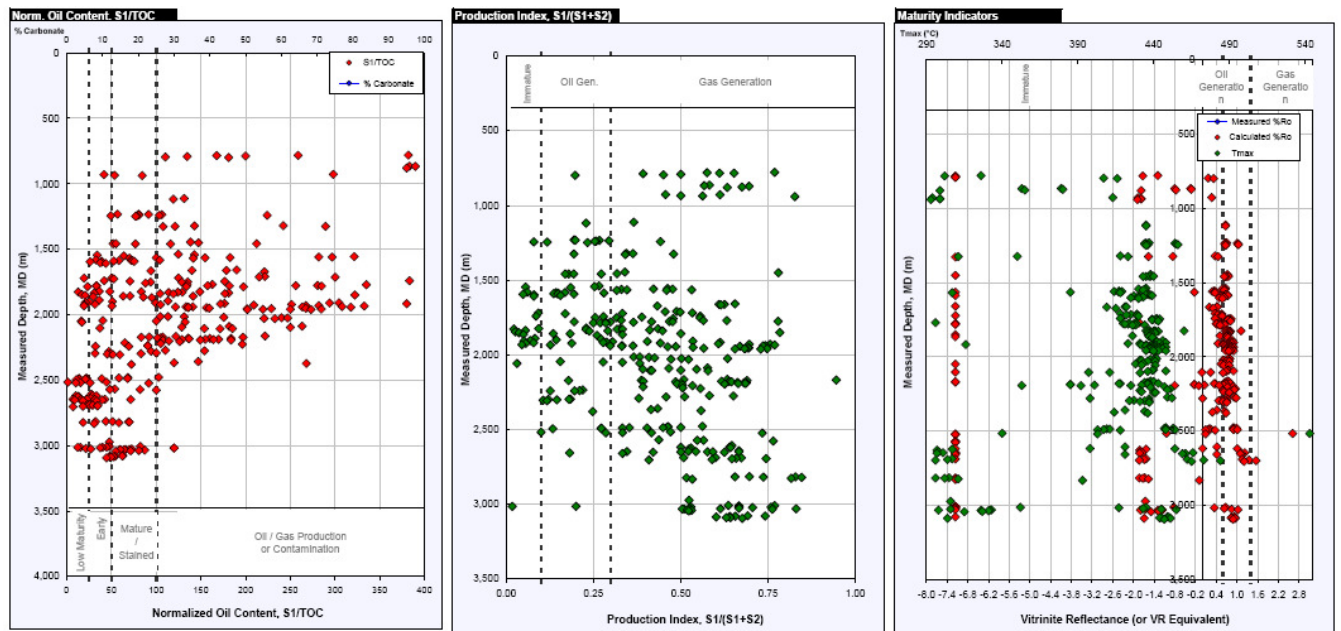


Figure MD-E6. Depthwise plot of normalized oil content, production indices, and maturity of various source rock samples from the Montney and Doig formations, Alberta (source: John Pawlowicz, ERCB, 2012)

# Montney-Doig All Data, Alberta

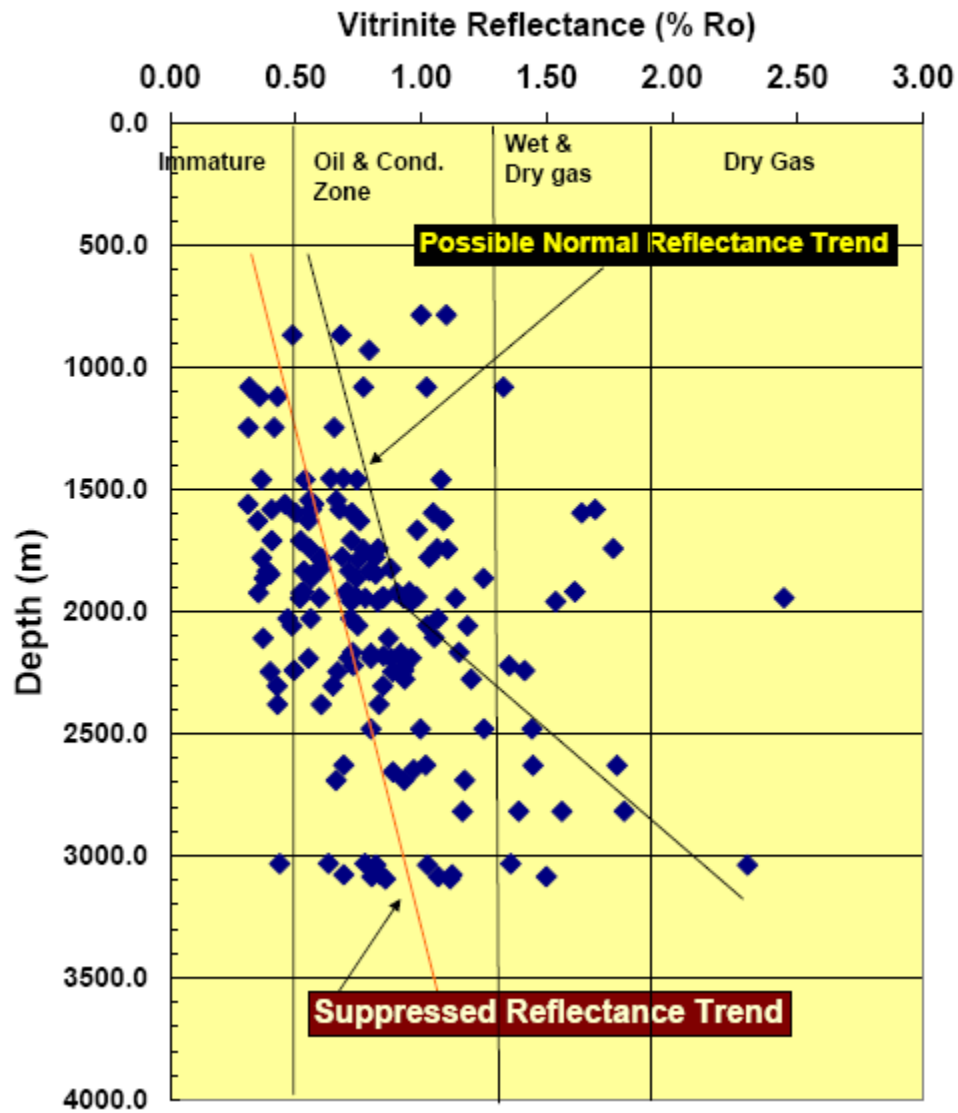


Figure MD-E7. Reflectance versus depth plot of all analyzed samples from the Montney and Doig formation source rocks showing two different reflectance trends: a. normal reflectance gradient; and b. suppressed reflectance gradient

### All Montney-Doig Data: Tmax versus Ro Plot

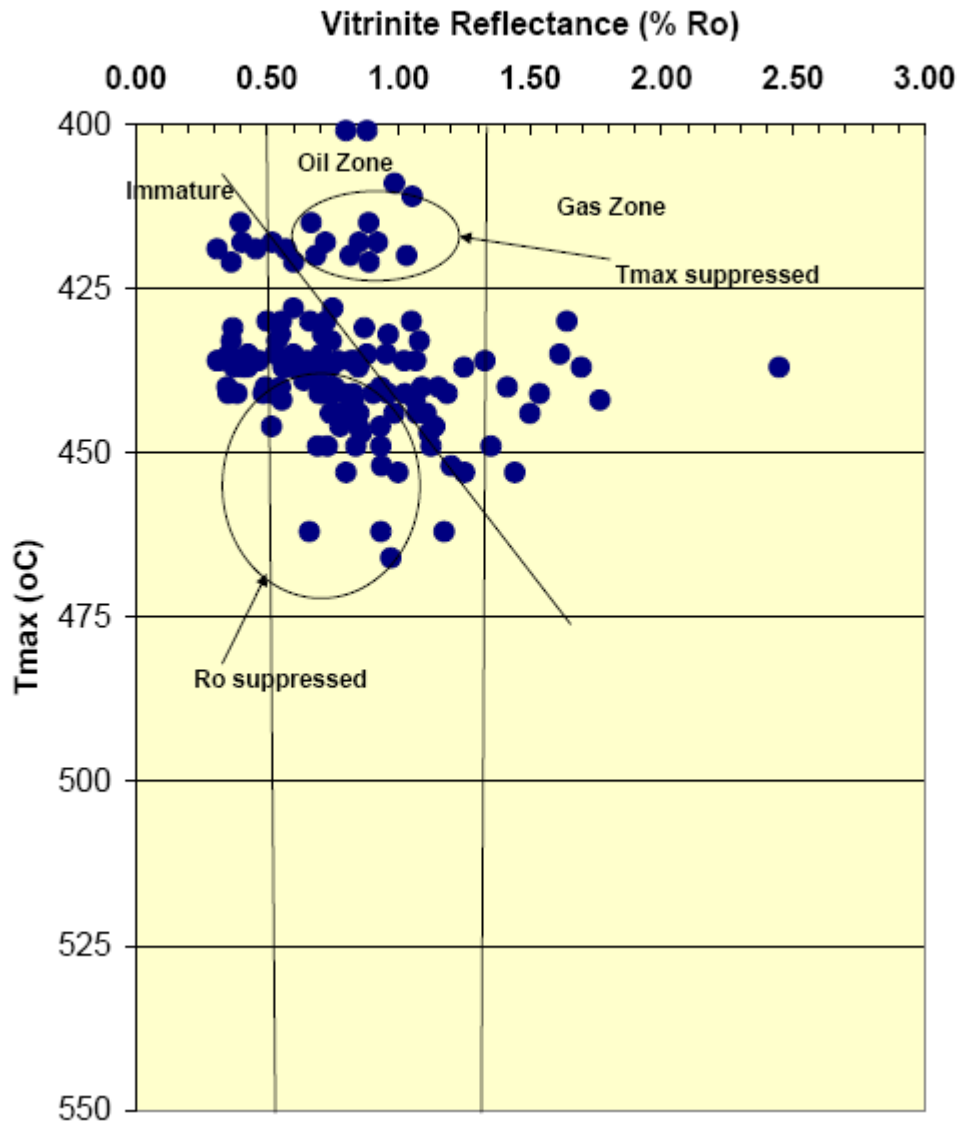


Figure MD-E8. Correlation of two main maturity data (Tmax from Rock-Eval pyrolysis and measured vitrinite reflectance) of various source rock samples from the Montney and Doig formations, Alberta (source: John Pawlowlicz, ERCB, 2012) showing areas where the Ro values are suppressed and other where the Tmax values are suppressed.

Sample No.	Site No.	Quartz	Feldspars			Pyrite	Hem.	Clay Minerals						Carbonates				Sulphate Gyp.	FlAp.	Brkt.	Total						
			Albite	Micro.	Ortho.			Musc.	Bio.	Paly.	Kaol.	Illite	Mont.	ClCh.	Calcite	Dolo.	Ank.					Rhod.					
8126	M23	44.7	9.5	15.1		0.2		3.2				1.7			1.1	1.7	12.9	8.5					0.9	0.5	100.0		
8730	M23	38.5	7.6		14.6	1.7		10.3	2.8			1.4				0.7	9.8	10.5	0.4					0.9	0.6	99.8	
8753	M10	40.6	9.2		9.2	4.7		16.8	1.8		1.0	0.6		1.3	0.1	13.5								0.4	0.7	99.9	
8761	M19	42.5	6.9		7.6	3.0		9.8	1.1			1.7				26.0									1.0	0.5	100.1
8819	M1	38.5	2.6		22.2	2.7		8.5	3.6			3.3				17.4									0.5	0.7	100.0
8854	M2	41.2	7.3		13.9	2.3	0.6	9.1	2.4			0.9		1.4	0.4	19.3									0.5	0.6	99.9
8897	M6	20.7	7.9		13.7	8.9		31.4	4.3	2.0	3.8					4.5									1.6	1.3	100.1
8899	M8	38.2	5.5		8.2	4.4	0.6	20.4	3.2			4.1				13.1			0.1						1.5	0.7	100.0
8905	M39	27.4	3.3		8.4	5.3		20.0	2.1						5.6	9.5	10.4								7.5	0.6	100.1
8919	M35	40.1	10.6		11.8	0.2		9.6				2.0			7.3	8.6	8.6	0.1							0.4	0.7	100.0
9254	M21	23.4	7.6		17.7	8.3		22.5	3.2	0.2	3.0	1.6				9.9									1.5	1	99.9

**Legend**

Column Label	Description	Column Label	Description
Sample No.	AGS sample number	Hem.	Hematite
Site No.	AGS site location number	Kaol.	Kaolinite
Ank.	Ankerite	Micro.	Microcline
Bio.	Biotite	Mont.	Montmorillonite
Brkt.	Brookite	Musc.	Muscovite
ClCh.	Clinocllore	Ortho.	Orthoclase
Dolo.	Dolomite	Paly.	Palygorskite
FlAp.	Fluorapatite	Rhod.	Rhodiocrosite
Gyp.	Gypsum		

All values are in weight per cent (wt.%)

Analysis performed by SGS Minerals Ltd.

Software: Bruker AXS Diffrac Plus EVA

The semi-quantitative analysis of EVA is performed on the basis of relative peak heights and I/lor values of those detected crystalline phases with PDF files. Amorphous or crystalline mineral species present in trace amounts may go undetected.

Figure MD-F1. Mineralogy from XRD for selected Montney Formation source rocks (source: Anderson et al. 2010)

Sample No.	Site No.	SiO <sub>2</sub>	Al <sub>2</sub> O <sub>3</sub>	Fe <sub>2</sub> O <sub>3</sub>	MgO	CaO	Na <sub>2</sub> O	K <sub>2</sub> O	TiO <sub>2</sub>	P <sub>2</sub> O <sub>5</sub>	MnO	Cr <sub>2</sub> O <sub>3</sub>	V <sub>2</sub> O <sub>5</sub>	LOI	Total
		wt. %	wt. %	wt. %	wt. %	wt. %	wt. %	wt. %	wt. %	wt. %	wt. %	wt. %	wt. %	wt. %	wt. %
8126	M33	63.40	6.66	1.86	3.94	7.61	1.09	2.87	0.46	0.35	0.20	0.01	<0.01	10.70	99.2
8730	M23	56.30	8.93	3.40	3.81	6.72	0.90	3.80	0.59	0.31	0.22	0.02	<0.01	11.60	96.6
8753	M10	61.40	10.20	3.50	3.60	4.28	1.09	3.84	0.70	0.15	0.07	0.02	0.00	8.51	97.4
8761	M19	57.10	6.41	2.19	5.43	8.46	0.08	2.76	0.46	0.44	0.18	0.03	<0.01	12.60	96.1
8819	M1	55.90	15.70	5.92	1.99	2.35	1.15	5.18	1.44	0.46	0.09	0.03	<0.01	7.92	98.1
8854	M2	59.50	8.56	3.26	4.30	5.86	0.79	3.48	0.58	0.18	0.12	0.02	<0.01	9.06	95.7
8897	M6	52.40	17.10	6.33	2.07	2.13	0.86	5.94	1.04	0.54	0.04	0.02	0.02	9.03	97.5
8899	M8	59.00	11.00	4.09	3.36	4.19	0.72	4.35	0.72	0.21	0.06	0.02	0.02	9.40	97.1
8905	M39	44.20	8.96	6.34	2.43	10.10	0.28	3.87	0.46	3.08	0.03	0.04	0.13	16.90	96.8
8919	M35	59.90	8.42	2.51	2.24	8.85	1.16	3.20	0.65	0.18	0.07	0.02	0.04	9.36	96.6
9254	M21	51.20	15.20	6.82	2.82	3.22	0.63	5.17	0.80	0.58	0.06	0.02	0.02	10.80	97.3
8854DUP	M2	59.60	8.49	3.24	4.29	5.84	0.81	3.48	0.59	0.18	0.11	0.01	<0.01	8.89	95.5

**Legend**

Column Label	Description	Column Label	Label Description
Sample No.	AGS sample number	TiO <sub>2</sub>	Titanium oxide
Site No.	AGS site location number	P <sub>2</sub> O <sub>5</sub>	Phosphorus oxide
SiO <sub>2</sub>	Silicon oxide	MnO	Manganese oxide
Al <sub>2</sub> O <sub>3</sub>	Aluminum oxide	Cr <sub>2</sub> O <sub>3</sub>	Chromium oxide
Fe <sub>2</sub> O <sub>3</sub>	Iron oxide	V <sub>2</sub> O <sub>5</sub>	Vanadium oxide
MgO	Magnesium oxide	LOI	Loss-on-ignition - amount of material lost due to heating
CaO	Calcium oxide	Total	Total weight per cent
Na <sub>2</sub> O	Sodium oxide	wt. %	Weight per cent
K <sub>2</sub> O	Potassium oxide	DUP	Duplicate

Figure MD-F2. X-ray Fluorescence analysis showing various oxides within some selected Montney & Doig formation source rocks (source: Anderson et al. 2010)

Sample No.	Site No.	Sample Type	Crystalline Mineral Assemblage (Relative Proportions Based on Peak Height)			
			Major (> 30 wt. %)	Moderate (10-30 wt. %)	Minor (<10 wt. %)	Trace (< 1 wt. %)
8730	M23	Core	(quartz)	(ankerite)	illite, (*plagioclase), (*potassium-feldspar)	(*pyrite), (*calcite)
8753	M10	Core	(quartz)	(dolomite)	illite, chlorite, (plagioclase), (potassium-feldspar)	(*pyrite), (*apatite)
8761	M19	Core	(quartz)	(dolomite)	illite, (*plagioclase), (*potassium-feldspar)	(*pyrite)
8819	M1	Core	(quartz)	illite	(mica), (dolomite), (plagioclase), (potassium-feldspar), (pyrite)	(*brookite)
8854	M2	Core	(quartz)	(dolomite)	illite, (plagioclase), (potassium-feldspar)	*chlorite, (*calcite), (*pyrite), (*brookite)
8899	M8	Core	(quartz)		illite, (plagioclase), (potassium-feldspar), (dolomite)	(*gypsum), (*pyrite), (*brookite)
8919	M35	Core	(quartz)	(calcite)	illite, (dolomite), (ankerite), (plagioclase), (potassium-feldspar), (pyrite)	(*rhodochrosite)
9254	M21	Core	(quartz)		illite, (dolomite)	*kaolinite, (*potassium-feldspar), (*apatite), (*pyrite)

**Legend:**

Column Label	Label Description
Sample No.	AGS sample number
Site No.	AGS site location number
Sample Type	Core, outcrop or cuttings
wt. %	Weight per cent (relative proportion of clay sized minerals only)

\* Tentative identification due to low concentrations, diffraction line overlap or poor crystallinity

() Not a clay mineral, according to SGS Minerals Ltd.

Figure MD-F3. Quantitative mineral assemblages from selected source rocks from the Montney and Doig formation source rocks (source: Anderson et al. 2010).

Sample No.	Site No.	Run No.	Vr (cm <sup>3</sup> )	Vc (cm <sup>3</sup> )	P1 (psi)	P2 (psi)	P1/P2	(P1/P2)-1	Vs (cm <sup>3</sup> )	Avg. Vs (cm <sup>3</sup> )	Wt. (g)	Gdensity (g/cm <sup>3</sup> )
8702	M27	1	88.512	147.903	17.296	6.507	2.658	1.658	1.145			
8702	M27	2	88.512	147.903	17.245	6.489	2.658	1.658	1.188			
8702	M27	3	88.512	147.903	17.257	6.493	2.658	1.658	1.169	1.167	3.060	2.622
8764	M19	1	88.512	147.903	17.308	6.524	2.653	1.653	1.595			
8764	M19	2	88.512	147.903	17.320	6.531	2.652	1.652	1.684			
8764	M19	3	88.512	147.903	17.313	6.527	2.653	1.653	1.635	1.638	4.290	2.619
8858	M2	1	88.512	147.903	17.210	6.485	2.654	1.654	1.520			
8858	M2	2	88.512	147.903	17.229	6.493	2.653	1.653	1.551			
8858	M2	3	88.512	147.903	17.360	6.543	2.653	1.653	1.573	1.548	4.000	2.584
8878	M9	1	88.512	147.903	17.319	6.530	2.652	1.652	1.662			
8878	M9	2	88.512	147.903	17.260	6.508	2.652	1.652	1.671			
8878	M9	3	88.512	147.903	17.308	6.526	2.652	1.652	1.667	1.666	4.400	2.640
8904	M8	1	88.512	147.903	17.384	6.533	2.661	1.661	0.889			
8904	M8	2	88.512	147.903	17.254	6.485	2.661	1.661	0.920			
8904	M8	3	88.512	147.903	17.251	6.484	2.661	1.661	0.924	0.911	2.420	2.656
8908	M39	1	88.512	147.903	17.220	6.492	2.652	1.652	1.637			
8908	M39	2	88.512	147.903	17.262	6.508	2.652	1.652	1.643			
8908	M39	3	88.512	147.903	17.297	6.522	2.652	1.652	1.672	1.651	4.300	2.605

**Legend**

Column Label	Label Description
Sample No.	AGS sample number
Site No.	Site location number
Run No.	Number of times each sample was tested
Vr	Reference volume = 88.512 cm <sup>3</sup>
Vc	Volume of sample cell = 147.903 cm <sup>3</sup>
P1	Pressure reading after pressurizing the reference volume
P2	Pressure reading after including Vc
Vs	Volume of the solid
Avg. Vs	Average volume of the solid
Wt.	Weight of the sample
Gdensity	Grain density

Figure MD-G. Measured porosity, permeability, and grain density for selected Montney Formation source rocks (source: Anderson et al. 2010).

In image 8705\_4 (500× magnification), the fabric trends parallel to bedding, with silt-sized particles up to 20 μm in diameter. Mineralogical analysis on the sample yielded the following results, beginning at the bottom of the image: potassium feldspar at site 1, dolomite at site 2, mica at site 3, dolomite at site 4, a possible kaolinite and illite mix at site 5, pyrite at site 6 and quartz at site 7. The next image is taken near the pyrite framboid in the upper left corner.

Microporosity, to use the term loosely, is visible within the framboid of image 8705\_5 (2000× magnification). Surrounding the pyrite are grains up to 10 μm in diameter, although most are less than 5 μm. The linear pores mentioned earlier are visible between clay domains. Core expansion during recovery may enhance or create these features along lines of weakness in the sample, often grain or clay domain contacts. An example of the enhancement or creation of porosity is at the tip of the yellow arrow, where the curvature of the clay domain matches the curvature of the particle. This pore may have been closed at depth. The wavy character of the clay suggests that the clay domains are compacting around the particles, thus reducing porosity. Otherwise, it is difficult in this sample to estimate primary porosity.

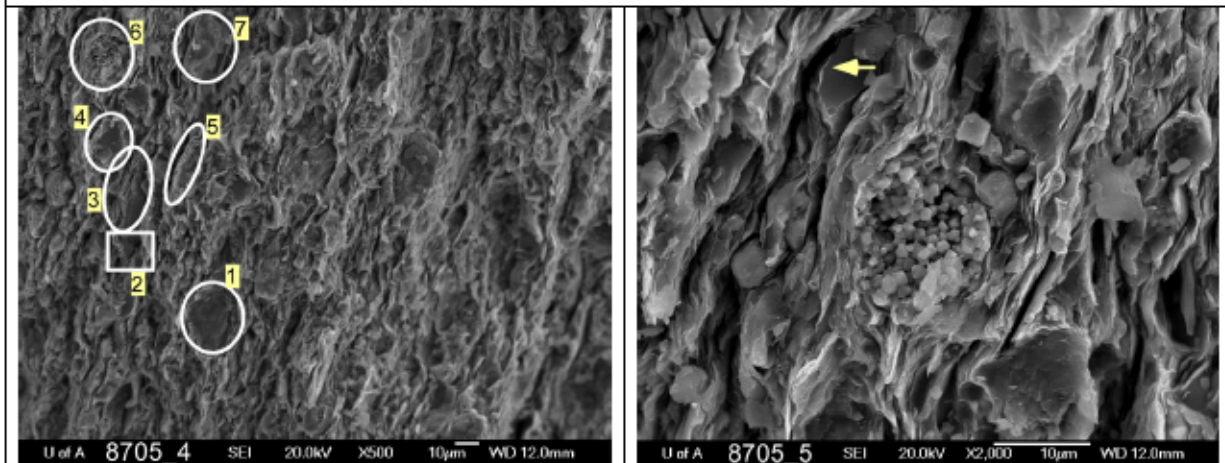


Figure MD-H1. SEM photomicrographs of sample 8705 showing various mineralogical assemblages and porosity distribution; Scale is depicted in the figures and explained above (source: Anderson et al., 2010)

Image 8709\_5 (5500× magnification) of the pyrite framboid (EDX\_8709\_003) was taken just north of the previous image. The framboid and surrounding grains are covered in authigenic illite, which is occluding porosity. There is a smaller framboid just beneath the larger pyrite.

Image 8709\_6 (1300× magnification) contains a large grain of potassium feldspar at site 1 (EDX\_8709\_004), a dolomite crystal at site 2 (EDX\_8709\_005) and a cube of pyrite at site 3 (EDX not saved). The yellow arrows point to what appears to be a late stage of illite growth that occludes porosity. Both grains and overgrowth are well packed in this view.

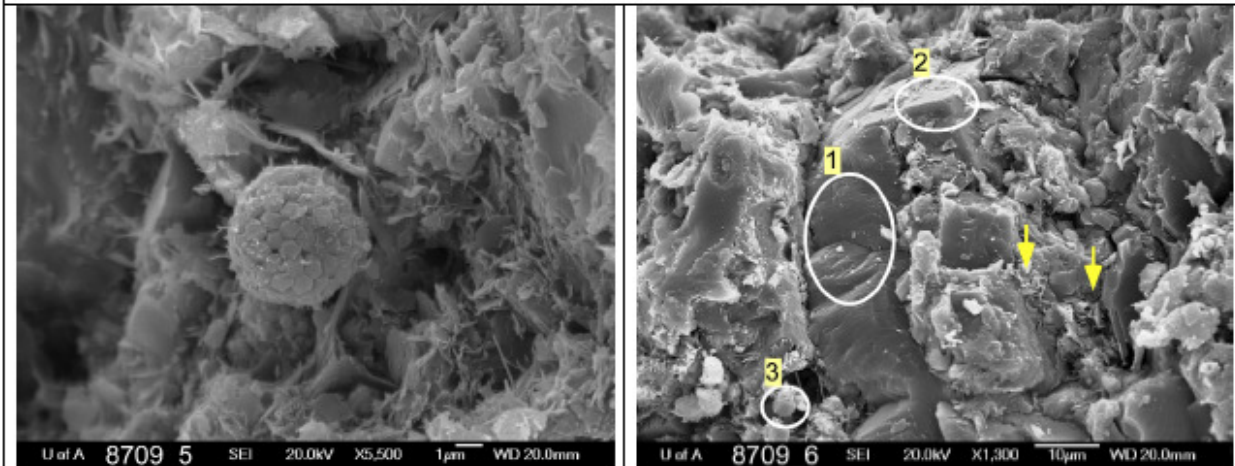


Figure MD-H2. SEM photomicrographs of sample 8709 showing various mineralogical assemblages and porosity distribution; Scale is depicted in the figures and explained above (source: Anderson et al., 2010)  
(source: Anderson et al., 2010)

Image 8731\_5 (8500× magnification) appears to be oil-stained. Grains of unknown mineralogy, approximately 0.5 to 1.0 μm in diameter, are either coated with the oil or, less frequently, lie atop the coating.

An EDX analysis (EDX not saved) on image 8731\_6 (600× magnification) identified mica at site 1, dolomite at site 2 and possibly sodium feldspar and clay at site 3. Dolomite crystals are indicated by the white arrows. There is also a reasonable degree of porosity surrounding the large particles in the centre of the image. The pores are less than 5 μm in diameter.

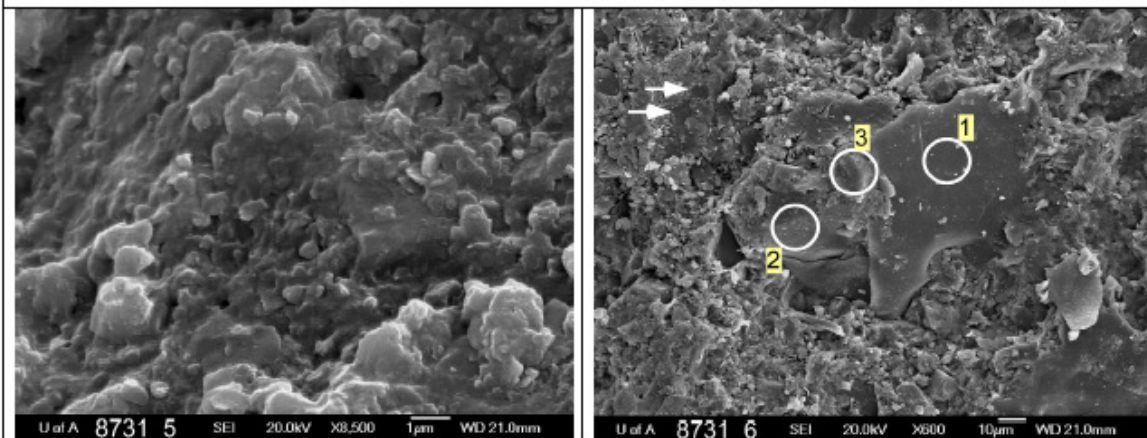


Figure MD-H3. SEM photomicrographs of sample 8731 showing various mineralogical assemblages and porosity distribution; Scale is depicted in the figures and explained above; Sample 8731. Porosity high

Image 8739\_5 (300× magnification) shows dolomite crystals at site 1 (EDX not saved) and smaller rhombic crystals (indicated by the white arrows) that are presumably dolomite. Quartz grains were identified at sites 2 and 3 (EDX not saved). As in many of the images, a large amount of overgrowth at site 4 (presumably quartz) covers the grains and obscures the mineralogy and size of the grains. The largest pores in this image are much greater than 10 μm, unlike the silt-dominated images where pores of this size are relatively rare.

In image 8739\_6 (1000× magnification), the rather large, odd-shaped crystal that spans much of the image (site 1), is dolomite (EDX not saved). Relative to the previous image and the smaller, more pristine dolomite crystal at site 2, we may be seeing ‘old’ and ‘new’ dolomite crystals representing separate stages in the dolomitization of the Montney Formation.

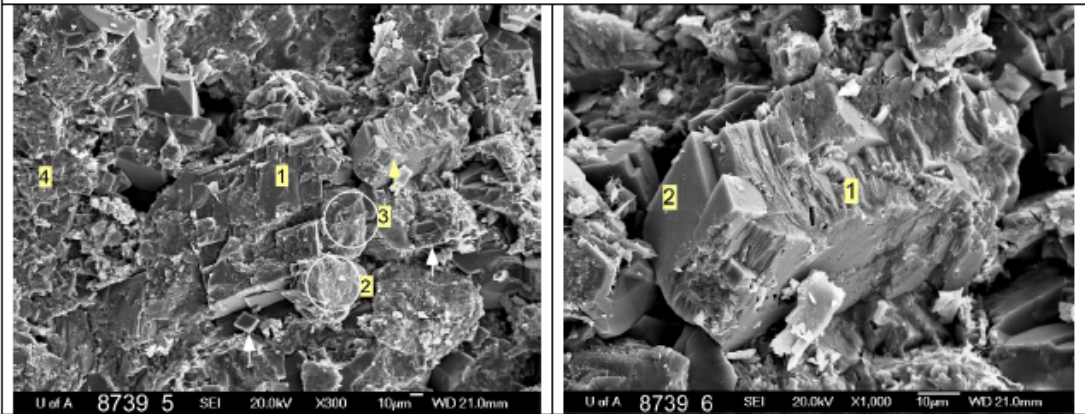
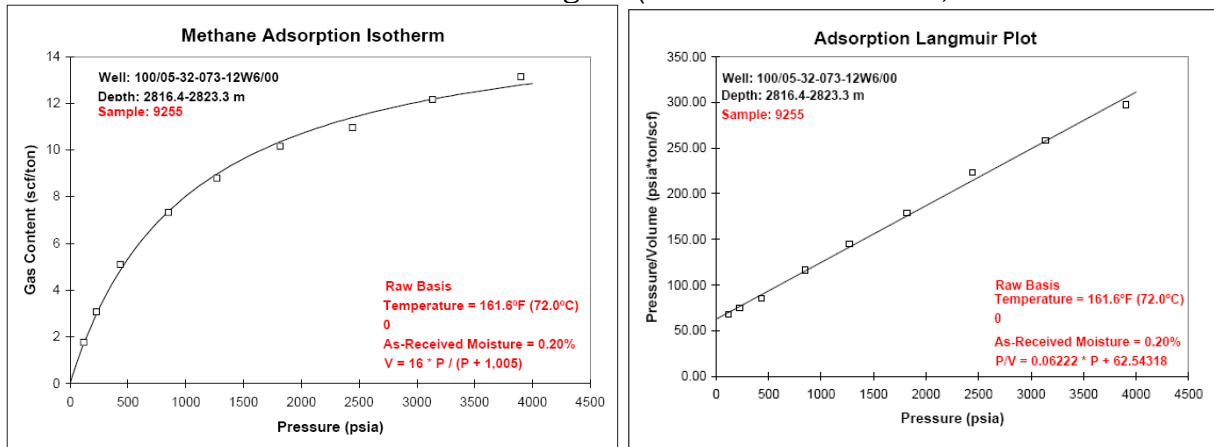
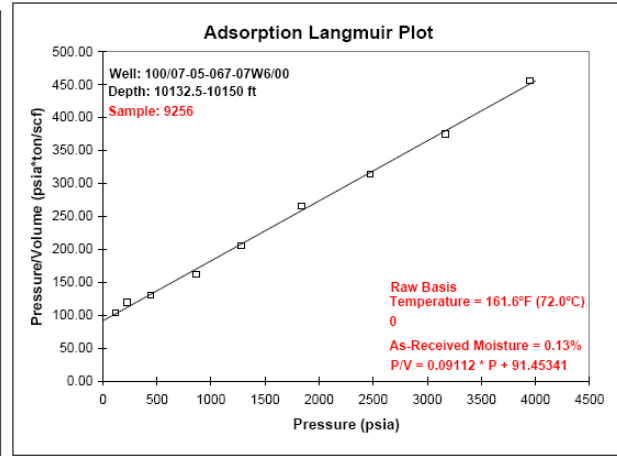
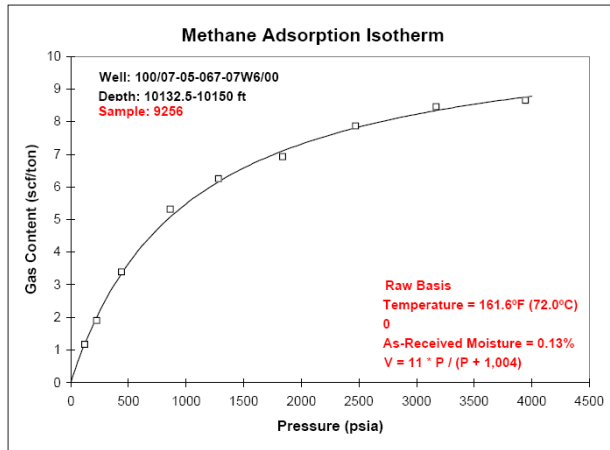


Figure MD-H4. SEM photomicrographs of sample 8739 showing various mineralogical assemblages and porosity distribution; Scale is depicted in the figures and explained above; Figure sample 8739. High porosity retains with dolomite crystal growth.

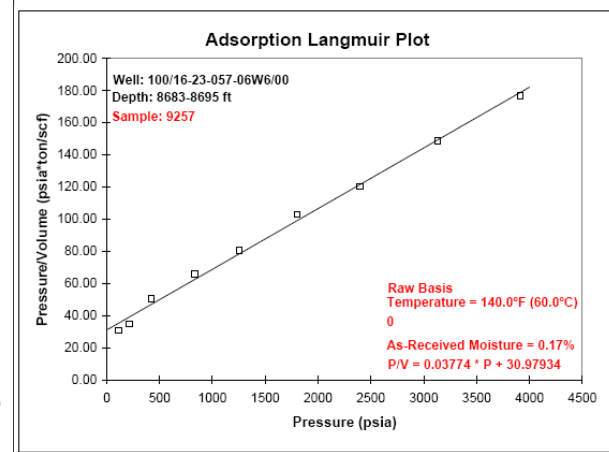
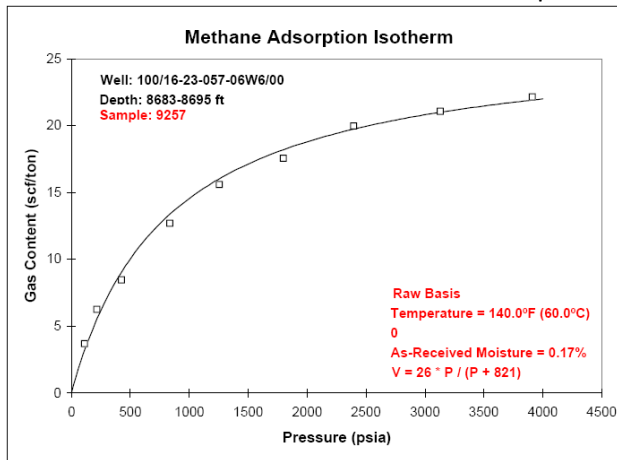
Figure MD-I. Adsorption Isotherm analysis of six selected samples from the Montney Formation [9255, 9256, 9257, 9258, 9259 and 9260). The depths of these samples mentioned in the next Figure (source: Beaton et al., 20100



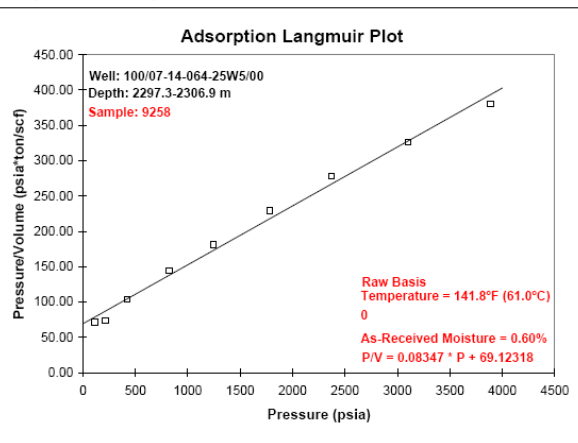
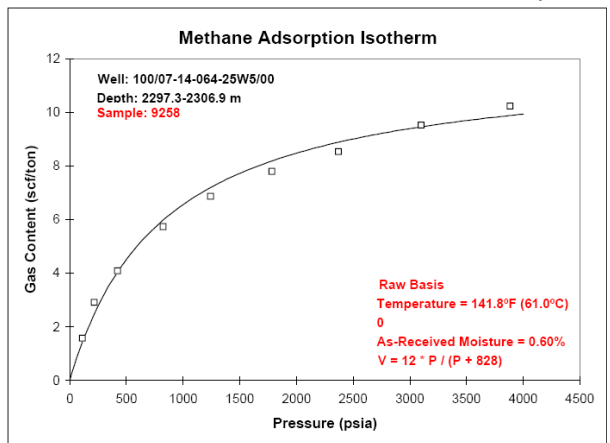
Sample 9255 (2816.4 m)



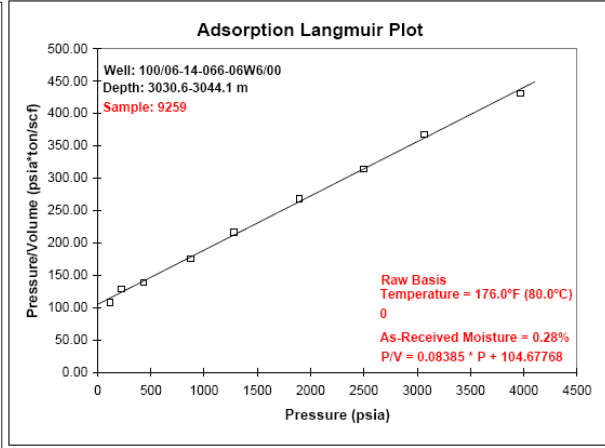
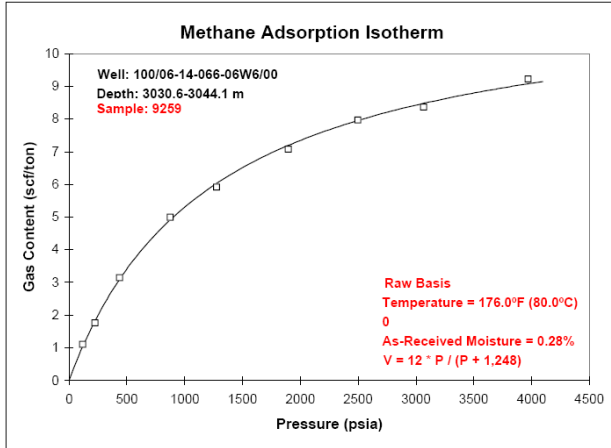
Sample 9256 (3088.4 m)



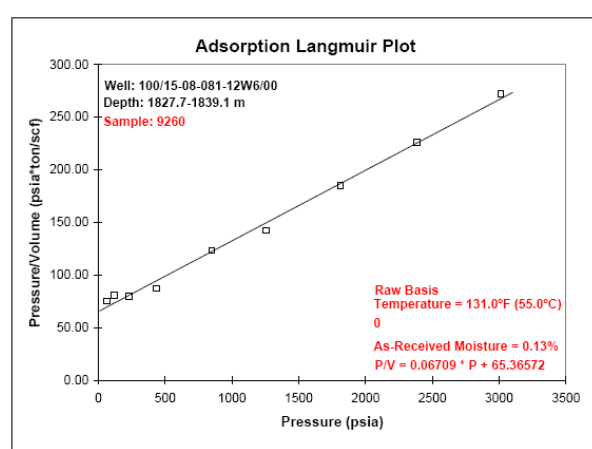
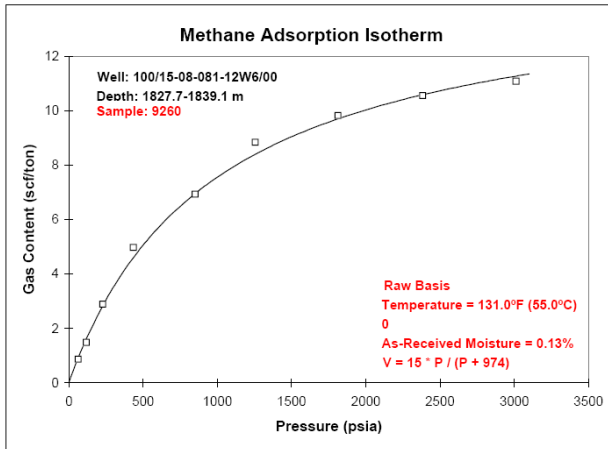
Sample 9257 (2646.6 m)



Sample 9258 (2297.3 m)



Sample 9259 (3030.6 m)



Sample 9260 (1827.7 m)

Sample No.	Site No.	Depth (Metres)	TOC wt. %	Analysis Temperature Celsius	As Received Moisture wt. %	PL Raw Basis MPa	VL Raw Basis scc/g	PL Raw Basis psia	VL Raw Basis scf/ton
9255	M23	2816.4 - 2823.3	1.83	72	0.20	6.93	0.50	1,005.2	16.1
9256	M10	3088.4 - 3093.7	1.17	72	0.13	6.92	0.30	1,003.7	11.0
9257	M2	2646.6 - 2650.2	1.14	60	0.17	5.66	0.80	820.8	26.5
9258	M6	2297.3 - 2306.9	0.47	61	0.60	5.71	0.40	828.1	12.0
9259	M8	3030.6 - 3044.1	0.93	80	0.28	8.61	0.40	1,248.3	11.9
9260	M34	1827.7 - 1839.1	0.66	55	0.13	6.72	0.50	974.3	14.9

Legend

Column Label	Label Description
Sample No.	AGS sample number
Site No.	AGS sample location number
Depth (Metres)	Sample depth in metres (measured from core)
TOC wt. %	Total organic carbon in weight per cent
Analysis Temperature Celsius	Temperature in degrees Celsius
As Received Moisture wt. %	Sample moisture content in weight per cent
PL Raw Basis MPa	Pressure - Langmuir pressure raw basis in megapascals
VL Raw Basis scc/g	Volume - Langmuir volume raw basis in standard cubic centimetres per gram
PL Raw Basis psia	Pressure - Langmuir pressure raw basis in pounds per square inch absolute
VL Raw Basis scf/ton	Volume - Langmuir volume raw basis in standard cubic feet per ton
Point No.	Individual measurement
Gas Content Raw Basis scc/g	Gas content in standard cubic centimetres per gram
Pressure Raw Basis psia	Pressure raw basis in pounds per square inch absolute
Gas Content Raw Basis scf/ton	Gas content in standard cubic feet per ton

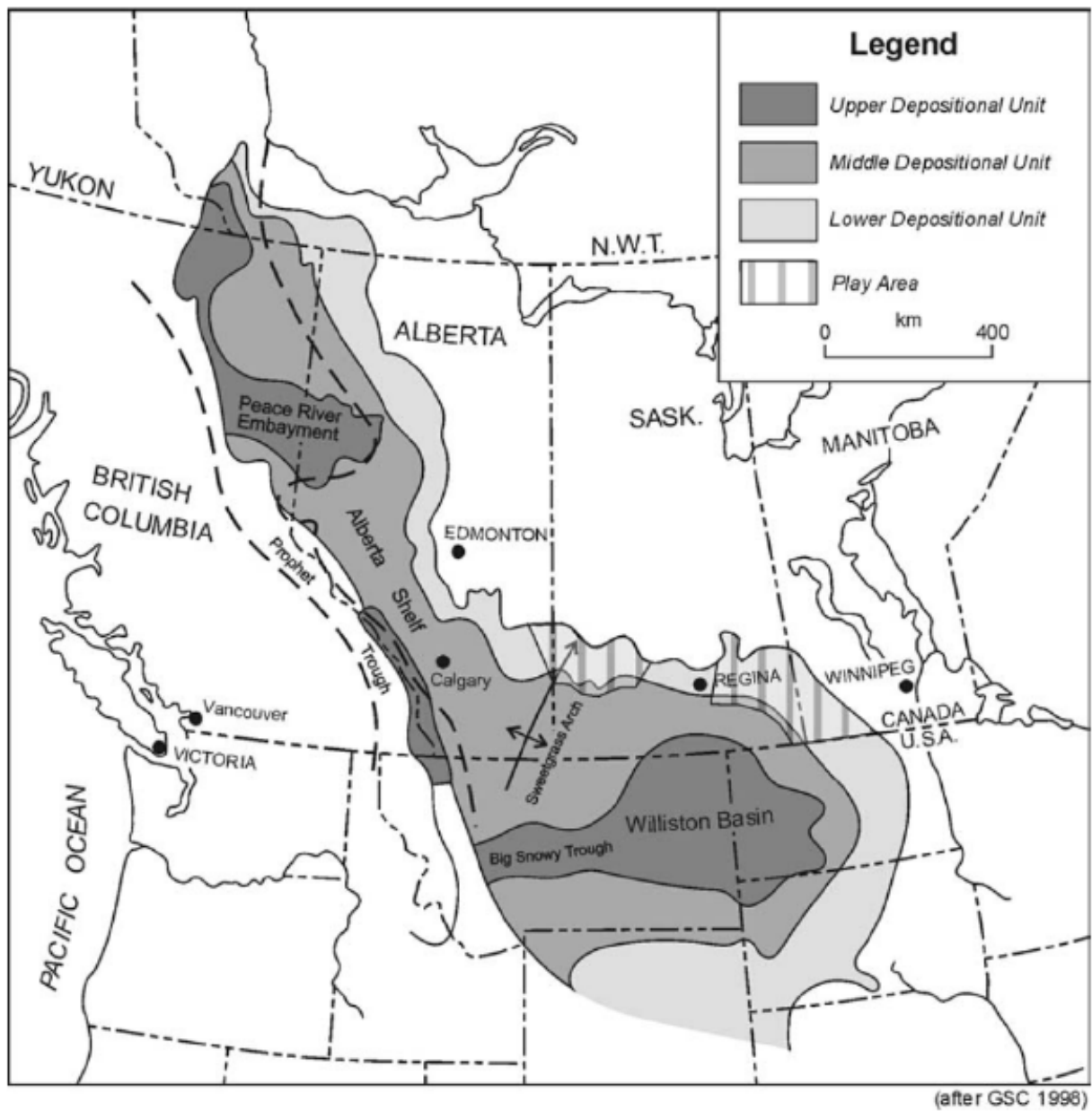
Figure MD-J1. Adsorption Isotherm analysis of samples from various depths (mean data of selected depth intervals).

Adsorption Isotherm Point Data

Sample No.	Point No.	Pressure Raw Basis MPa	Gas Content Raw Basis sc/cg	Pressure Raw Basis psia	Gas Content Raw Basis sc/ton
9255	1	0.82	0.06	119	1.8
	2	1.58	0.10	229	3.1
	3	3.00	0.16	435	5.1
	4	5.87	0.23	852	7.3
	5	8.76	0.27	1,270	8.8
	6	12.53	0.32	1,817	10.2
	7	16.86	0.34	2,445	11.0
	8	21.63	0.38	3,137	12.2
	9	26.90	0.41	3,902	13.2
9256	1	0.83	0.04	121	1.2
	2	1.56	0.06	226	1.9
	3	3.04	0.11	441	3.4
	4	5.95	0.17	863	5.3
	5	8.84	0.20	1,282	6.3
	6	12.68	0.22	1,839	6.9
	7	17.05	0.25	2,473	7.9
	8	21.86	0.27	3,170	8.5
	9	27.21	0.27	3,947	8.7
9257	1	0.78	0.12	113	3.7
	2	1.50	0.20	217	6.3
	3	2.94	0.27	426	8.5
	4	5.76	0.40	835	12.7
	5	8.65	0.49	1,256	15.6
	6	12.42	0.55	1,802	17.6
	7	16.52	0.62	2,396	20.0
	8	21.59	0.66	3,132	21.1
	9	26.97	0.69	3,912	22.2
9258	1	0.77	0.05	112	1.6
	2	1.48	0.09	215	2.9
	3	2.90	0.13	421	4.1
	4	5.69	0.18	825	5.8
	5	8.57	0.22	1,243	6.9
	6	12.31	0.24	1,786	7.8
	7	16.35	0.27	2,372	8.5
	8	21.39	0.30	3,102	9.5
	9	26.79	0.32	3,886	10.2
9259	1	0.82	0.03	119	1.1
	2	1.56	0.06	226	1.8
	3	3.01	0.10	437	3.2
	4	6.03	0.16	874	5.0
	5	8.81	0.18	1,278	5.9
	6	13.08	0.22	1,897	7.1
	7	17.24	0.25	2,501	8.0
	8	21.15	0.26	3,067	8.4
	9	27.38	0.29	3,971	9.2
9260	1	0.45	0.03	65	0.9
	2	0.82	0.05	119	1.5
	3	1.58	0.09	229	2.9

Figure MD-J2. Changes of gas content during pressure changes for the adsorption Isotherm analysis of samples from various depths.

# **Banff-Bakken-Exshaw Formations Figures and Tables**



Source: National Energy Board, *Technical report: Conventional heavy oil resources of the Western Canadian Sedimentary Basin*, August 2001, and adapted from the Geological Survey of Canada, 1998.

Figure BEB-1a. Devonian to Mississippian basins of Alberta, BC, Saskatchewan, Manitoba, and selected states of northeast USA highlighting the Banff-Exshaw-Bakken Depositional Systems (source: Scotia Capital, 2011)

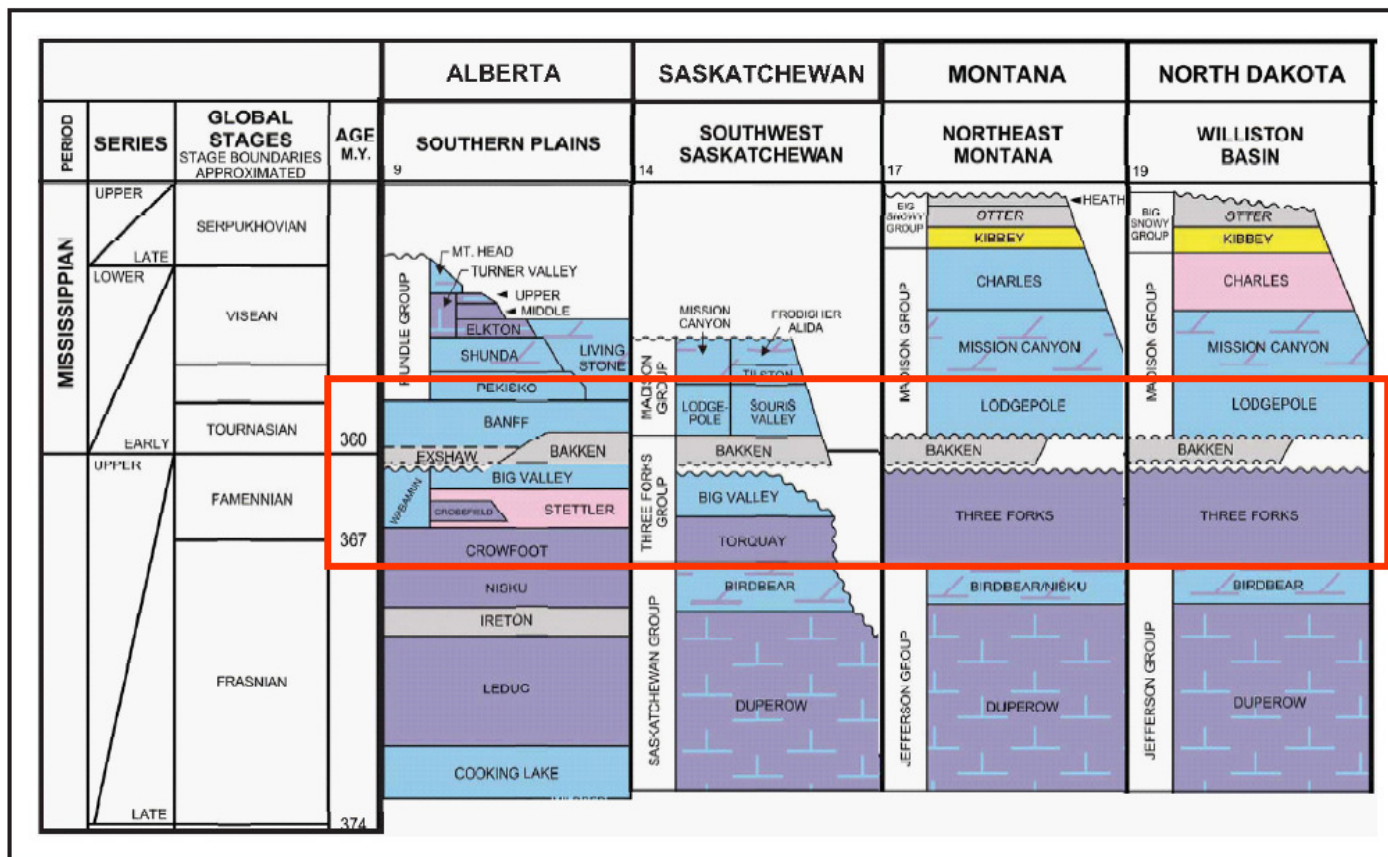
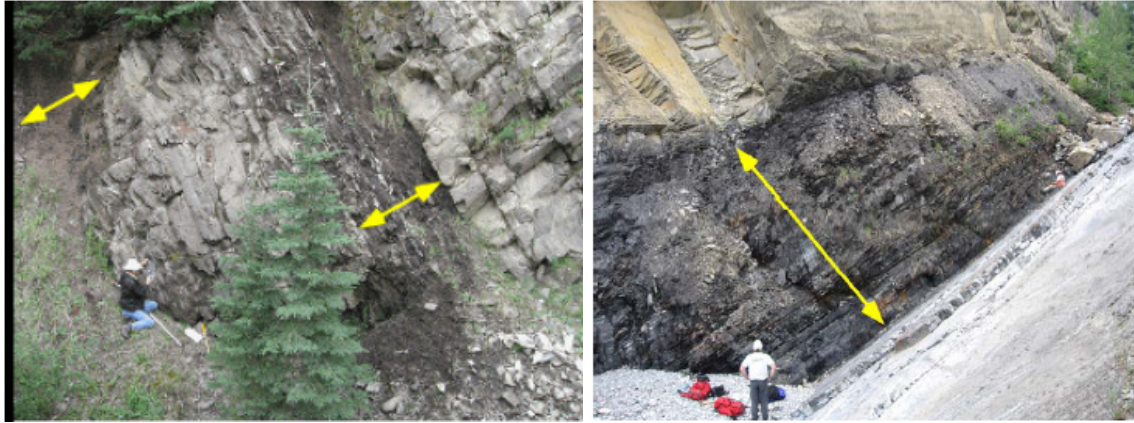


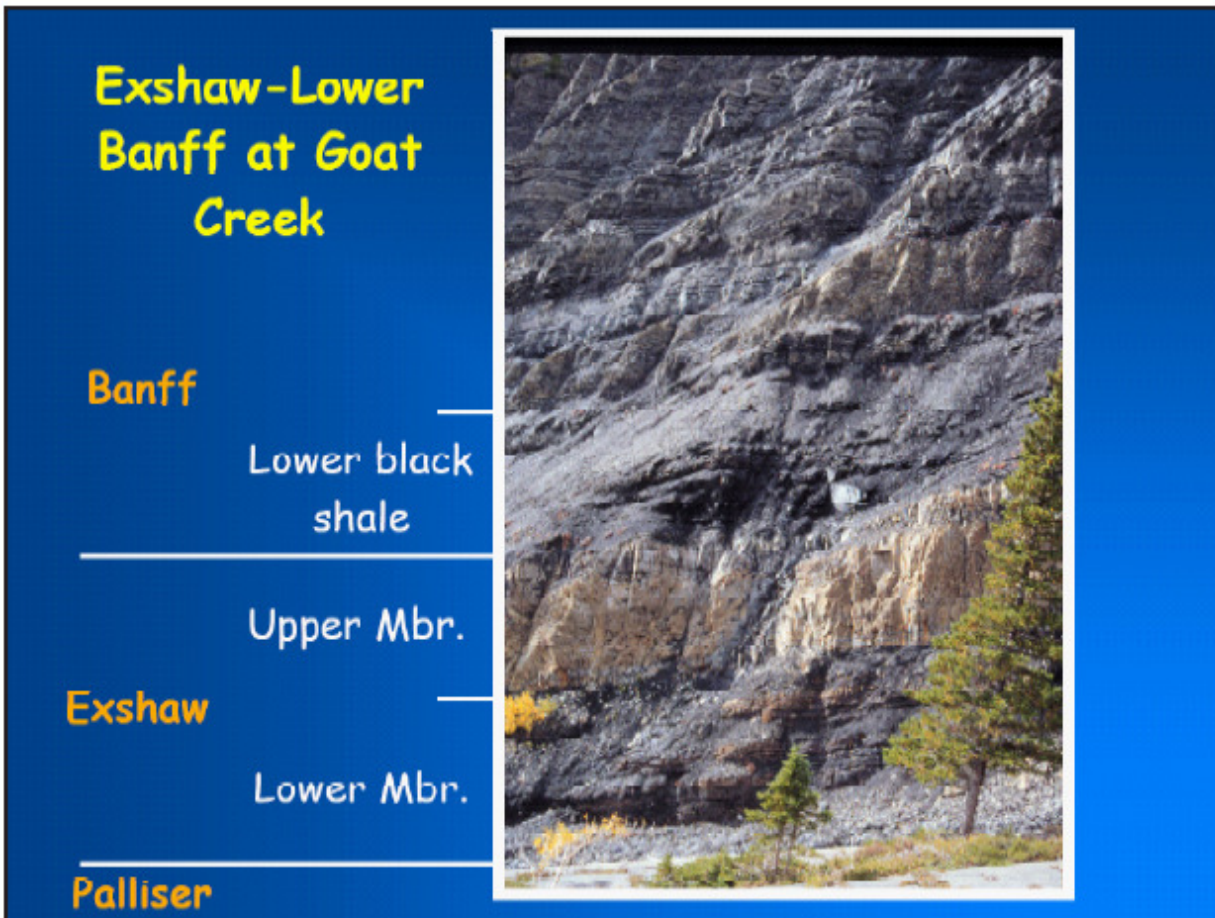
Figure BEB-1b. Stratigraphic correlation of the Famennian to Tournaisian (Upper Devonian to Mississippian) Banff-Bakken-Exshaw formation sediments within western Canada and USA (source: ERCB, 2011)



A

B

Figure BEB-2a. Field photos of Banff and Exshaw Formation source rocks: (A) Banff Formation near Nordegg (arrow 2m in length); (B) Exshaw Formation near type section (at Jura Creek near Kenmore) underlying the Banff Formation source rock (After Rokosh et al., 2009)



Source: Reidiger et al., 2004

Figure BEB-2b. Straigraphic interlayering of Banff and Exshaw formations at Goat Creek, Alberta (source: Scotia Capital, 2011)

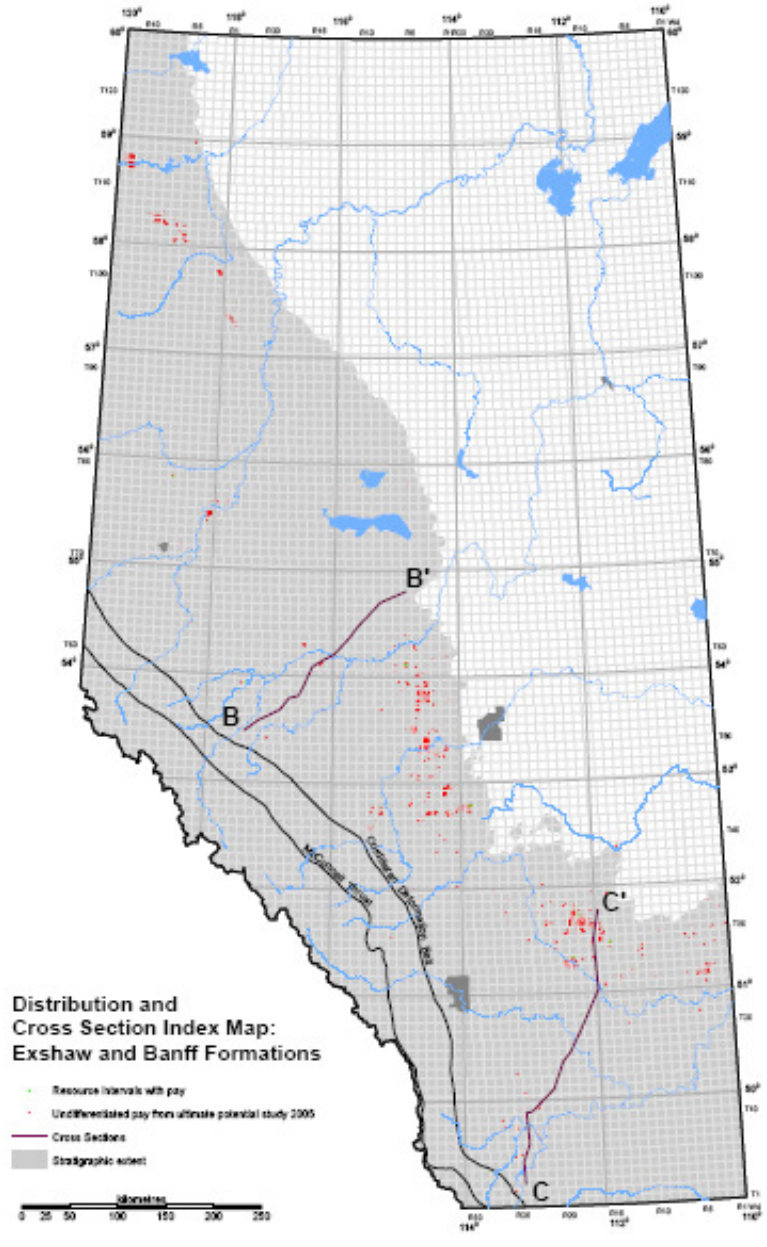


Figure BEB-3a. Geological cross-section index map for Banff-Exshaw-Bakken formations

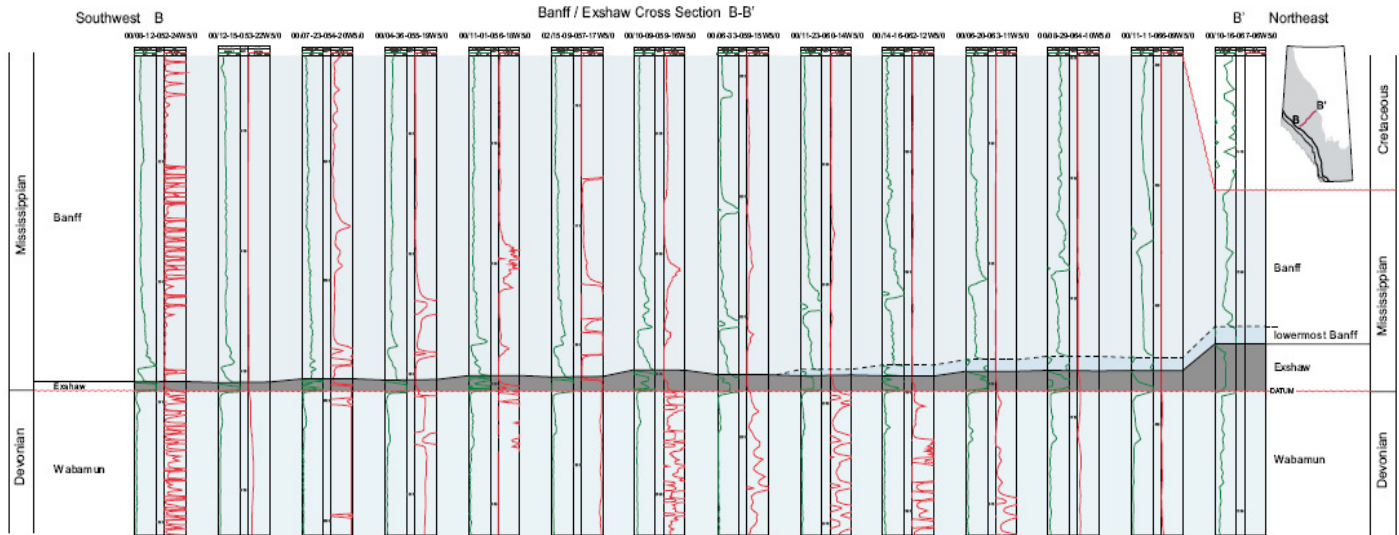


Figure BEB-3b. Stratigraphic cross-section of B-B' line that crosses through various wells highlighting Banff-Exshaw-Bakken formations

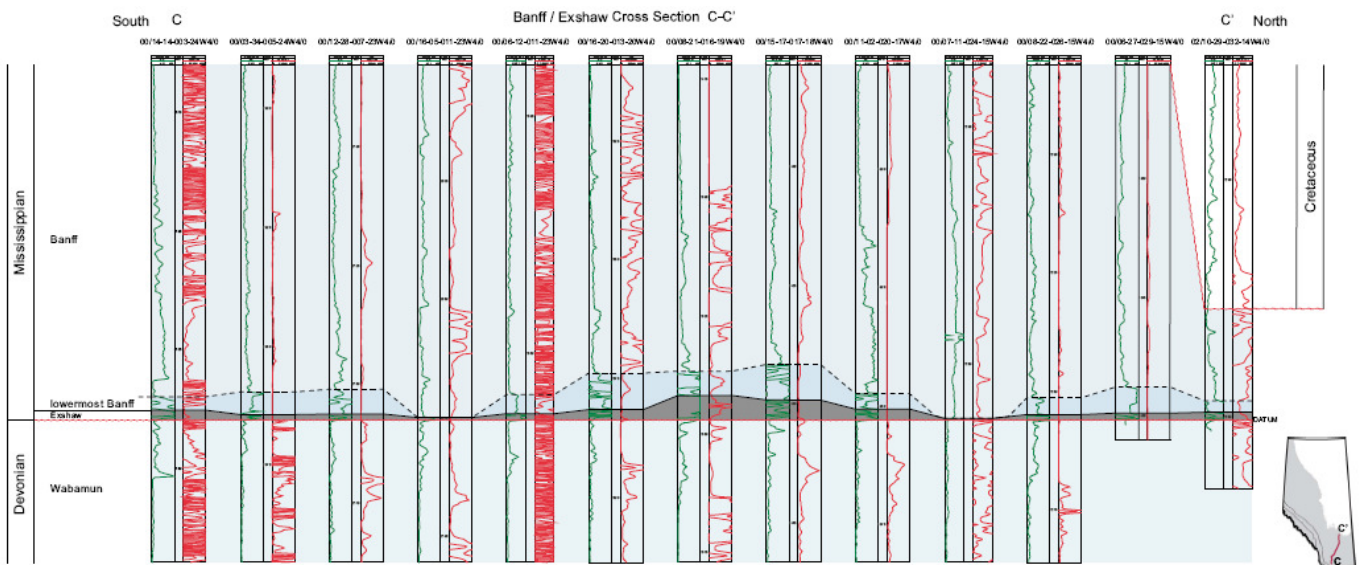


Figure BEB-3c. Stratigraphic cross-section of C-C' line that crosses through various wells highlighting Banff-Exshaw-Bakken formations

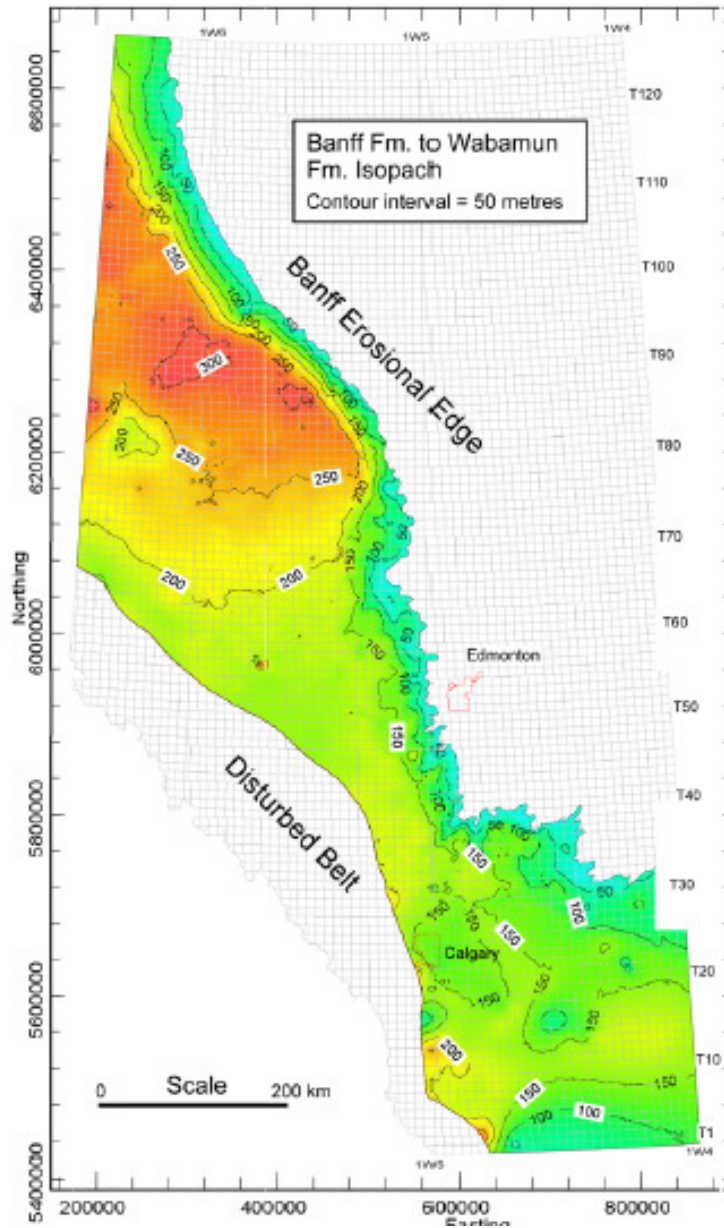


Figure BEB-4. Isopach map of stratigraphic units from the top of Banff Formation to the top of the Wabamun Formation (including Bakken & Exshaw formations)

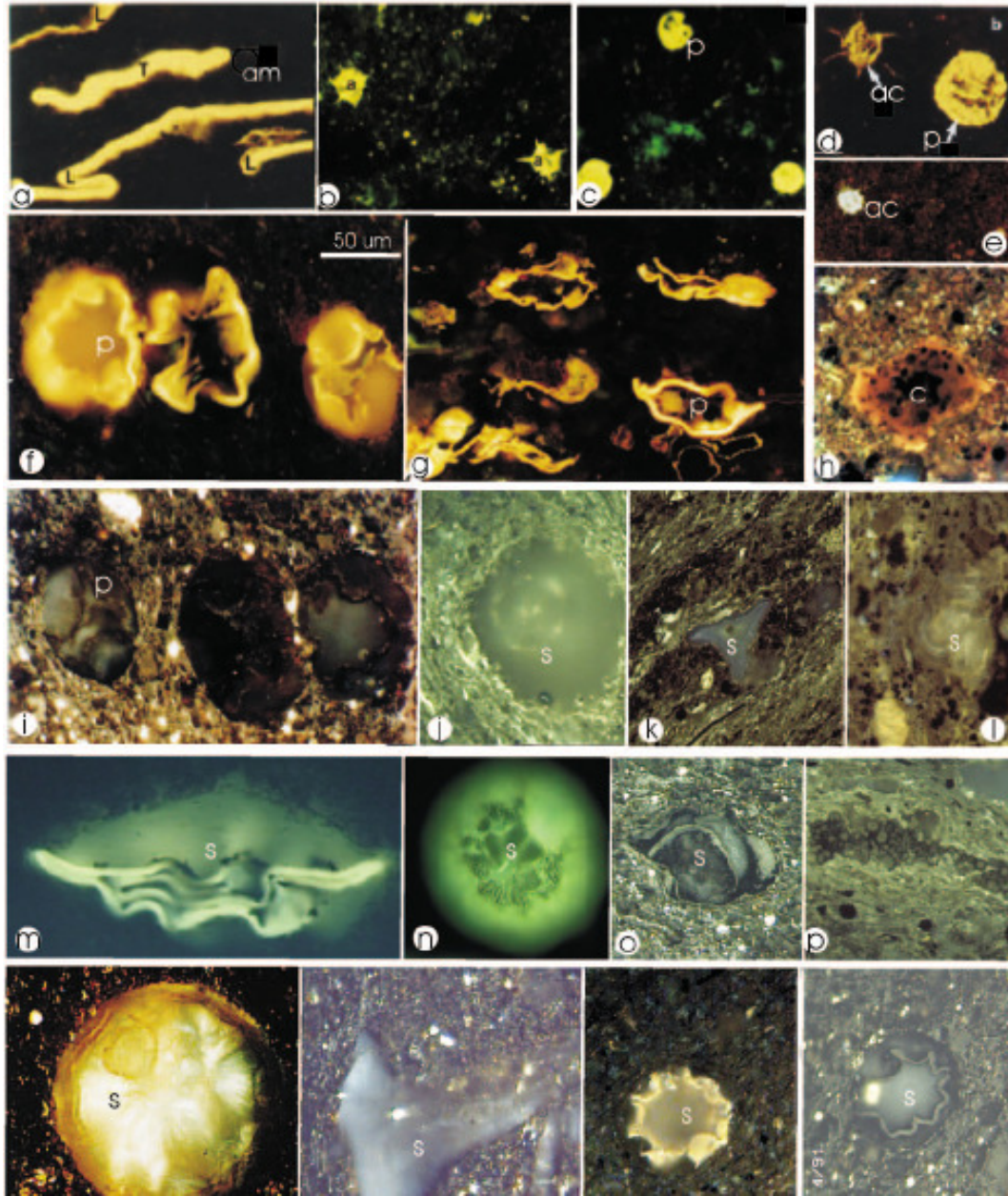


Fig. 8. Macerals and microfossils in organic facies (OF) A, B, C and D of Exshaw and Bakken formations. Fluorescence and reflected white light (i-k, o, r, t), water or oil immersion; scale bar (50 µm) on photo f is for all photos. a. OF A: Large *Tasmanites* (T) and *Leiosphaeridia* (L) prasinophyte alginite within amorphinite matrix (am). b-e. OF B: Small prasinophytes alginites (p) and spiny acanthomorphic acritarchs (ac). f, g. OF A: Silicified prasinophyte alginite (p). h. OF C: Degraded coccoidal alginite (c). i-l. OF D: Siliceous microfossils (s), mainly derived from Radiolaria. m. OF A: Silicified prasinophyte (?). n-t. OF D: Siliceous microfossils (s), mainly derived from Radiolaria.

Figure BEB-5a. Photomicrographs of the organic petrological variability of source rocks within the Banff-Baken-Exshaw source rocks from Alberta and Saskatchewan (after Stasiuk and Fowler, 2004)

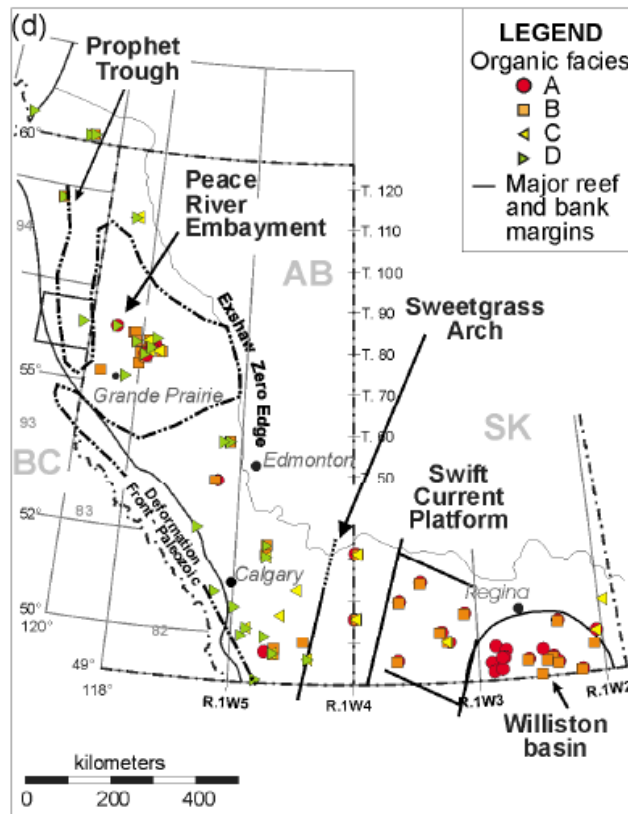


Figure BEB-5b. Model of various subdivisions of the organic facies scheme of the Upper Devonian-Mississippian Banff-Exshaw-Bakken formation source rocks within different regions of Alberta based on organic petrological interpretation (after Stasiuk and Fowler, 2004)

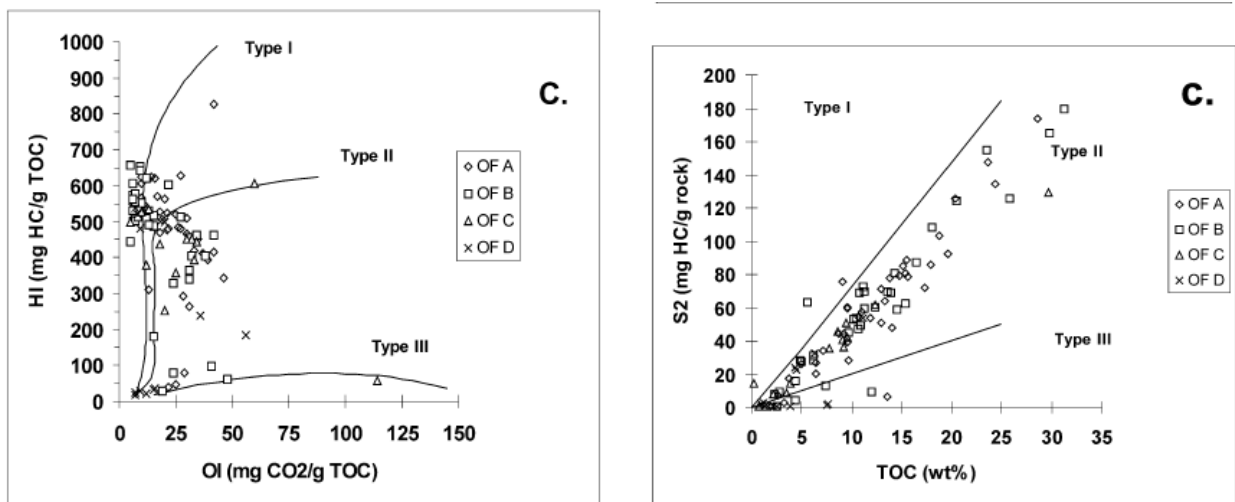


Figure BEB-5c. Rock-Eval pyrolysis data Banff-Exshaw-Bakken source rocks along with their variability in organic facies distribution (after Stasiuk and Fowler, 2004)

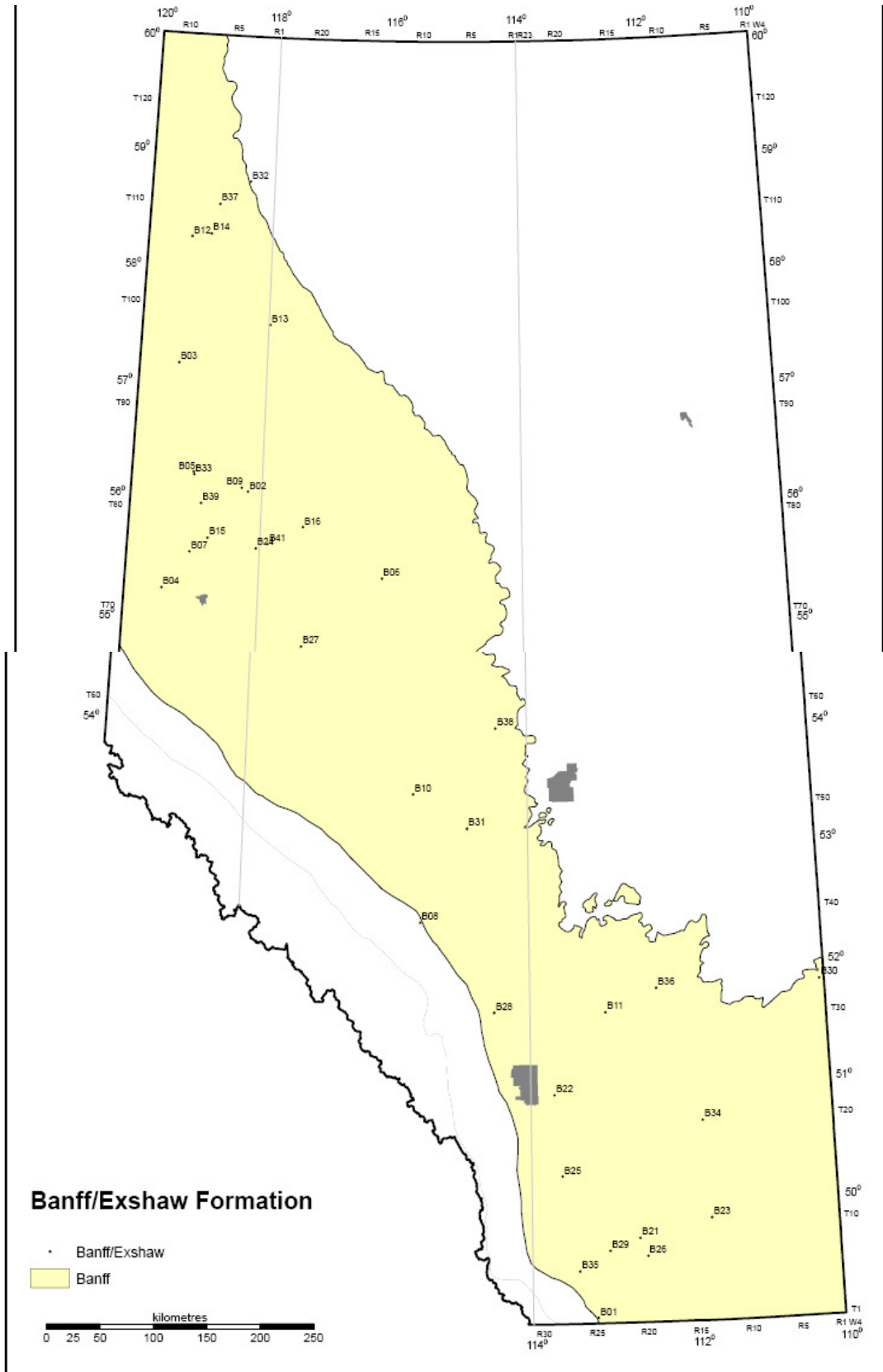


Figure BEB-6. Sample Locations of Banff-Exshaw source rocks within Alberta

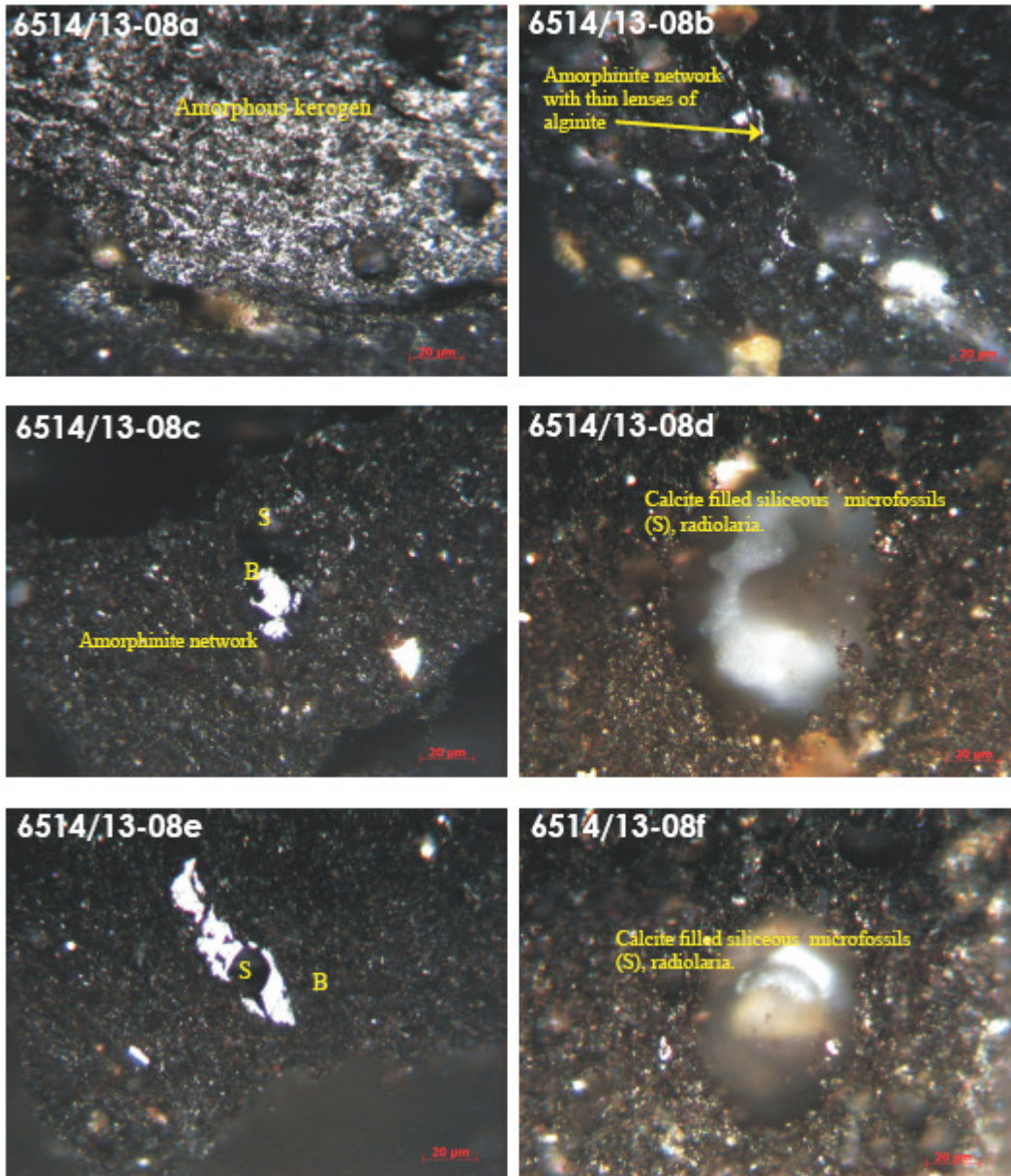


Figure BEB-7a. Photomicrographs of overmature Banff-Exshaw black shale source rocks showing presence nonfluorescent amorphinite and bitumen (sample 6514 (Beaton et al., 2010

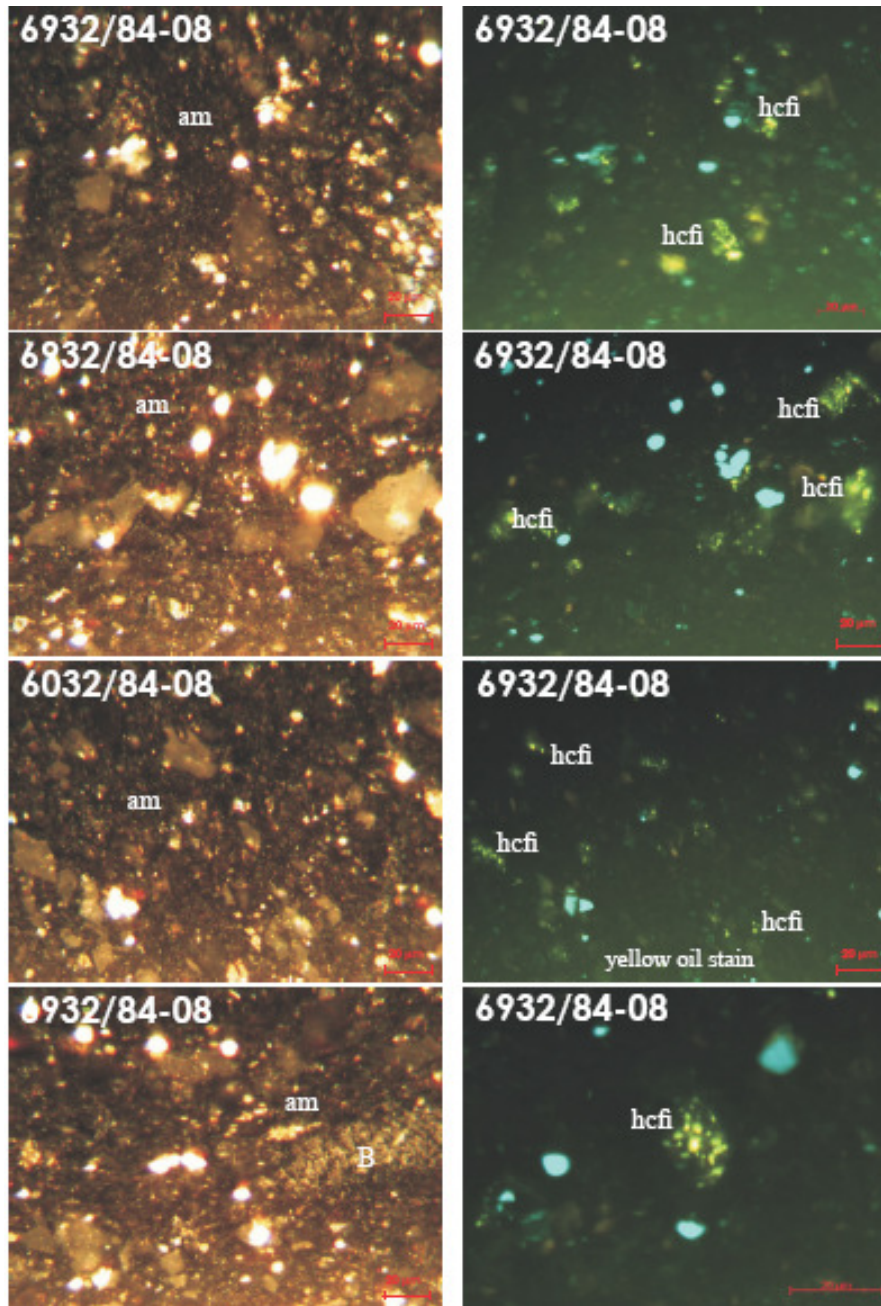
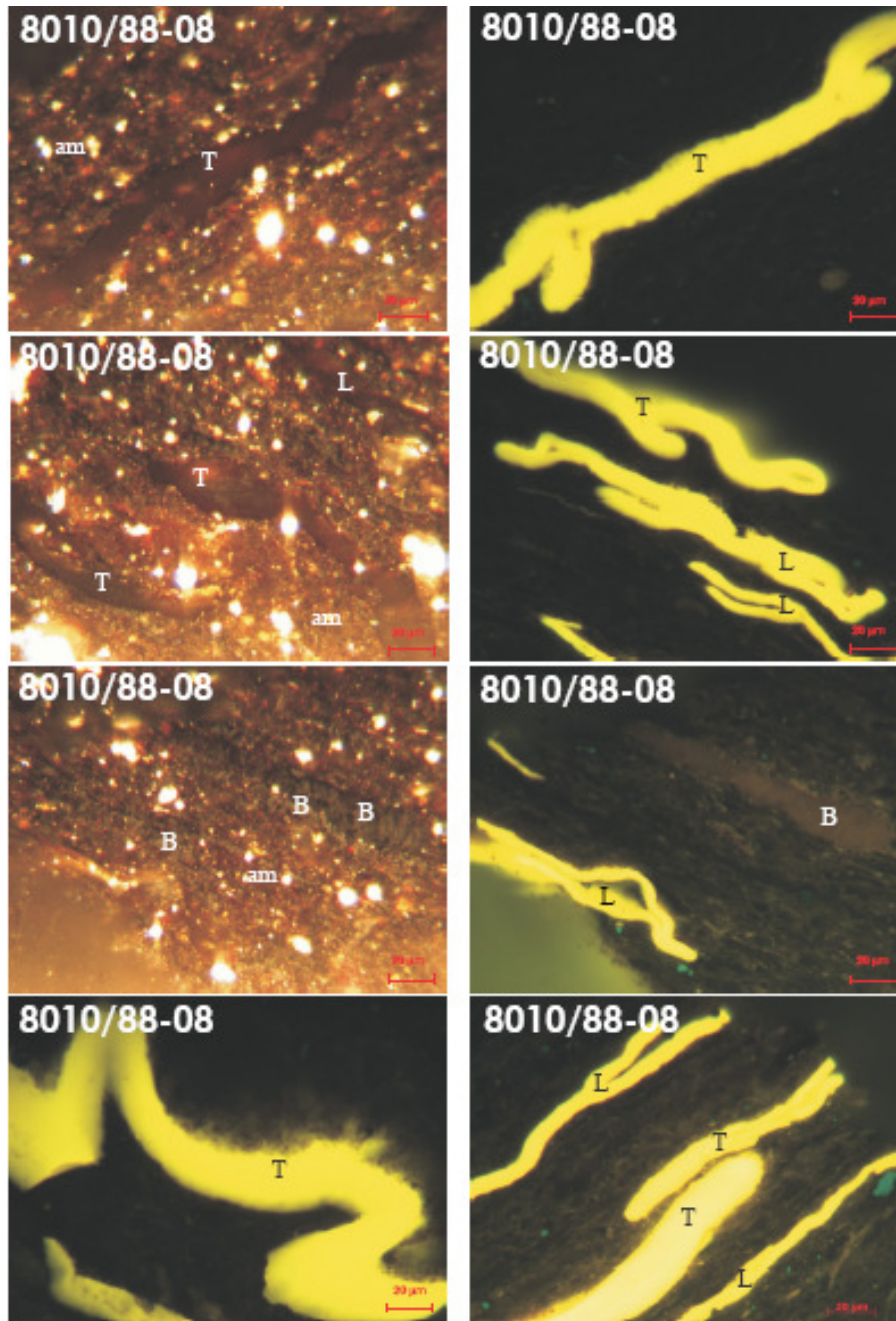
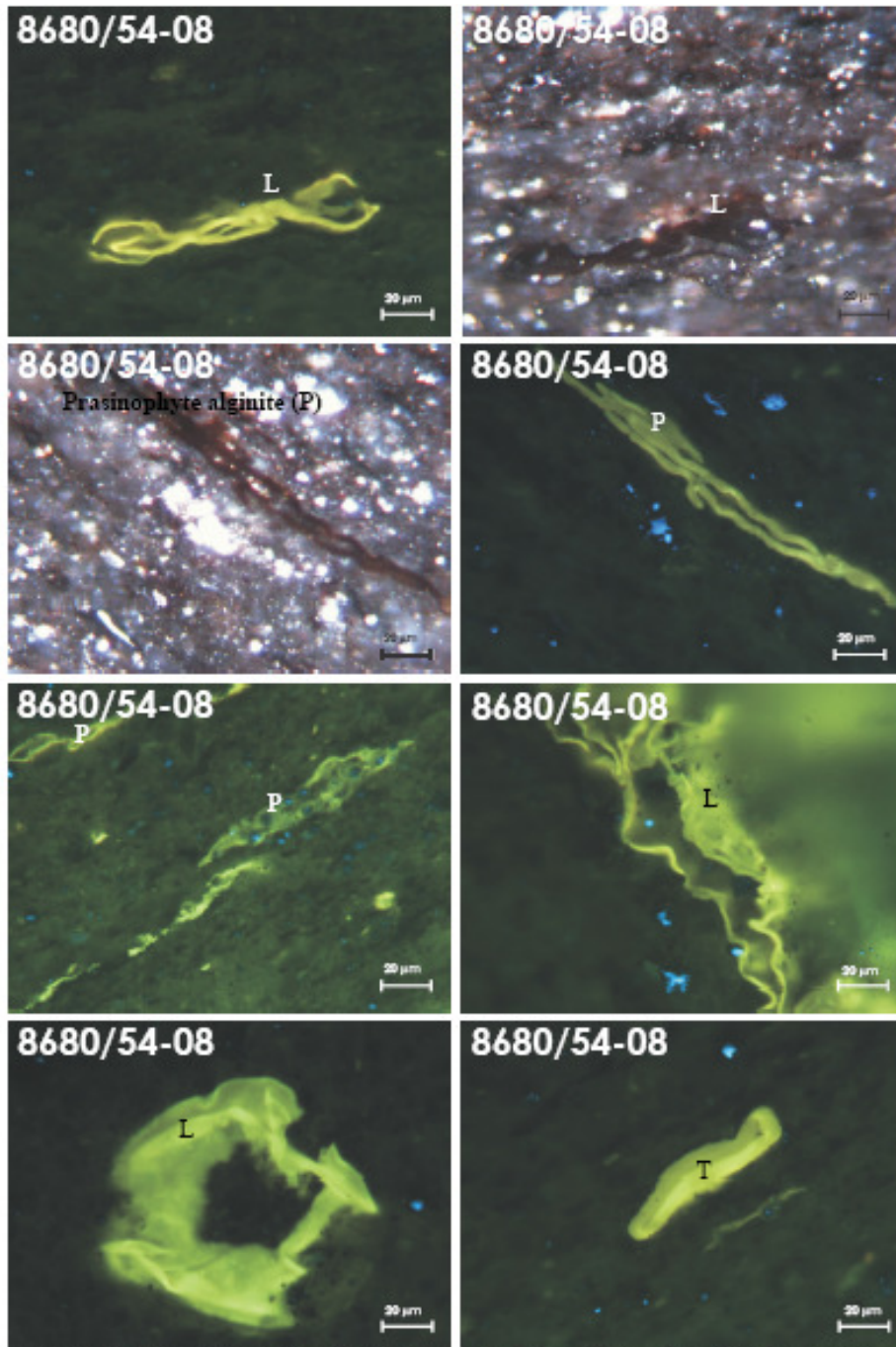


Figure BEB-7b. Amorphous kerogen rich (Amorphinite 2) source rock with solid bitumen (sample 6932) (after Beaton et al., 2009)



8010/88-08. Organic and pyrite rich shale with mainly spent amorphous kerogen (am), bright yellow fluorescing *Tasmanites* (T) and *Leiosphaeridia* (L) alginite, weak fluorescing fluoroamorphinite and bitumen with dull yellow fluorescing alginite (mostly *Prasinophyte* (P)). Orange fluorescing bitumen (B) inclusion also observed. Fluorescent and reflected white light.

Figure BEB-7c. Mixture of amorphinite 2 and Telalginite (*Tasmanites*) source rock from Banff-Exshaw formation (sample 8010) (after Beaton et al., 2009)



8680/54-08. Liptinite and pyrite (framboidal) rich shale, with mostly yellow fluorescing alginite (*Leiosphaeridia* (L) Prasinophytes (P)) and some rare thick-walled unicellular *Tasmanites* (T). Also present are amorphous bitumen (phosphatic) with micrinite inclusion. Fluorescent and reflected white light.

Figure BEB-7d: Photomicrographs of algal dominated (both *Telalginite* and *Lamalginitite* - *Tasmanites*, *Leiosphaeridia*, and *Prasinophyphytes*) source rocks from the Banff-Exshaw Formation black shale (sample 8680) (source: Beaton et al., 2009).

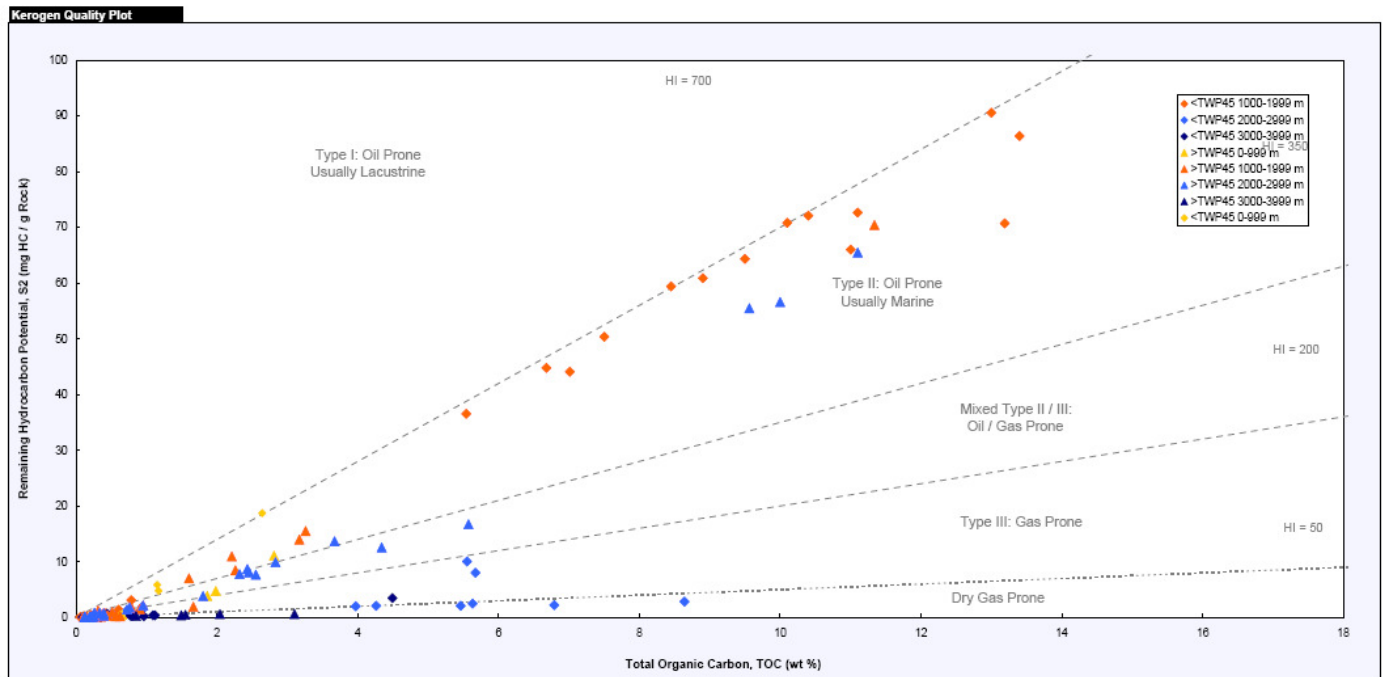


Figure BEB-8a. Kerogen quality plot of total organic carbon and remaining hydrocarbon potential (S<sub>2</sub> in mg/g rock) for only Exshaw source rocks (source: John Pawlowicz, ERCB, 2012). Colour indicates depth range of the samples

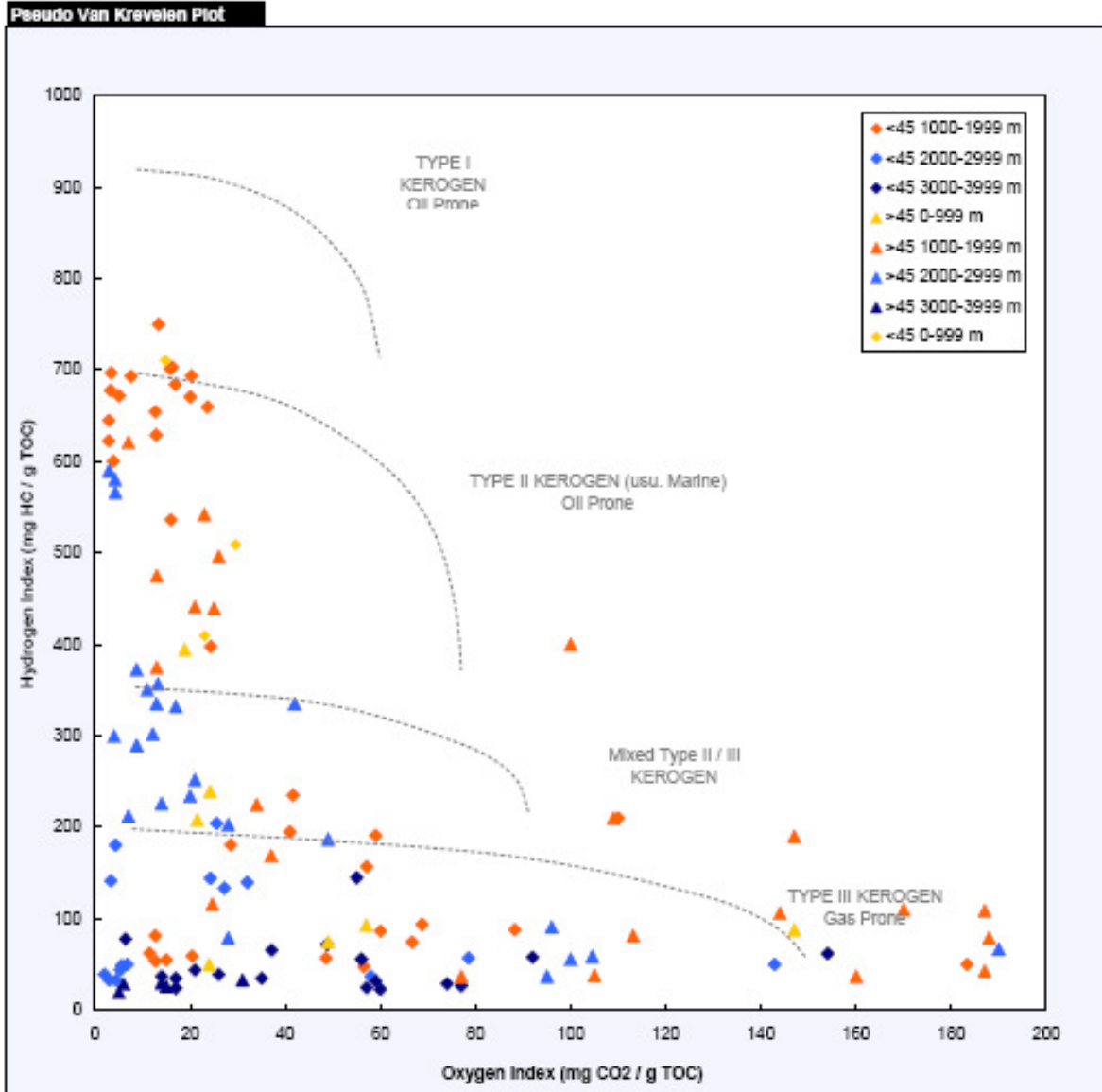


Figure BEB-8b. Pseudo-van Krevelen plot of hydrogen index versus oxygen index showing various source rock potential from various samples analyzed from Banff-Exshaw source rocks, Alberta (source: John Pawlowicz, ERCB, 2012). Colour indicates area depth range of the samples

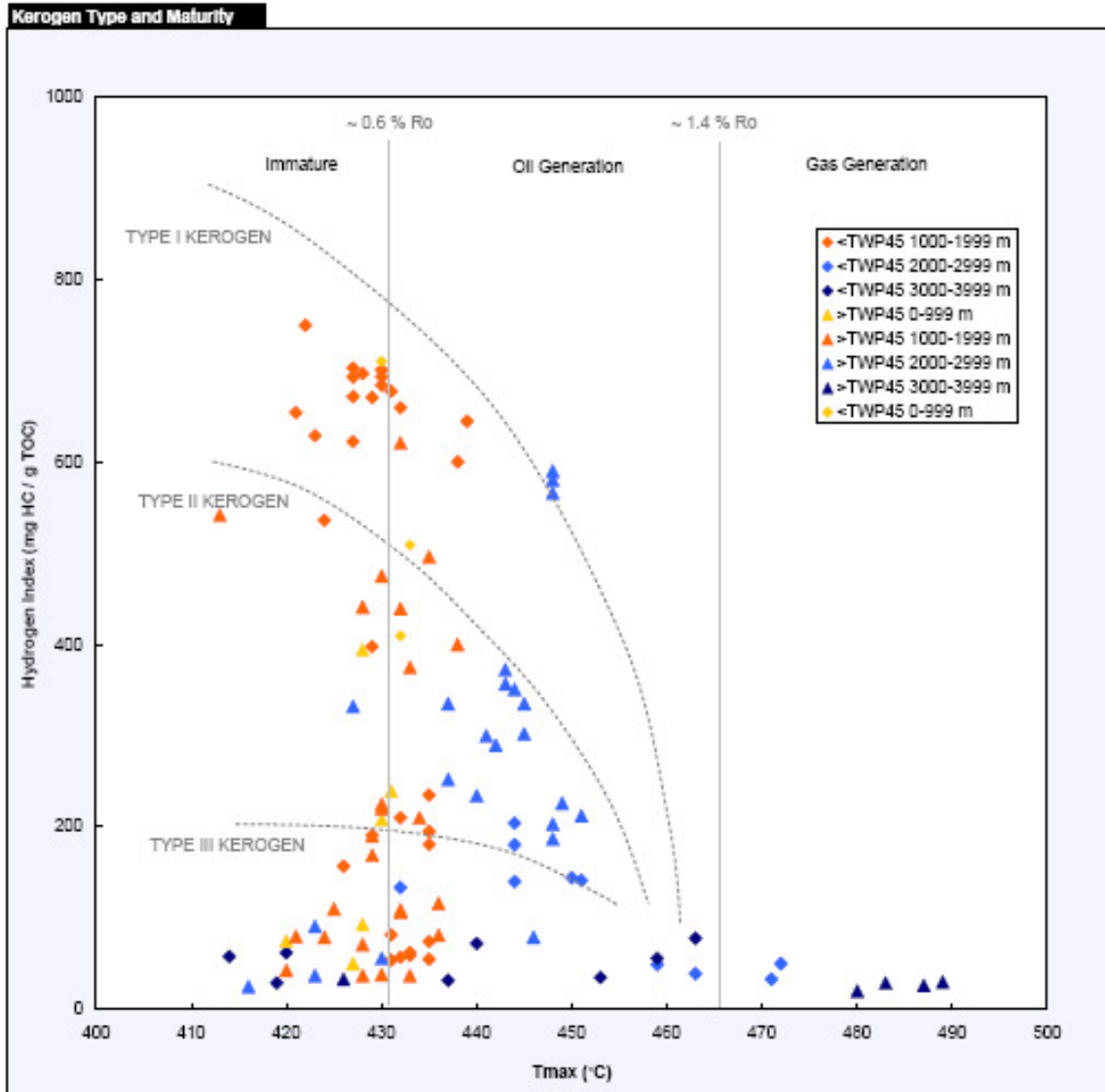


Figure BEB-8c. Maturity (using Tmax) versus hydrogen index showing the variability of source rock potential from various samples from both Banff and Exshaw source rocks, Alberta (source John Pawlowicz, ERCB, 2012). Colour indicates depth range of the samples

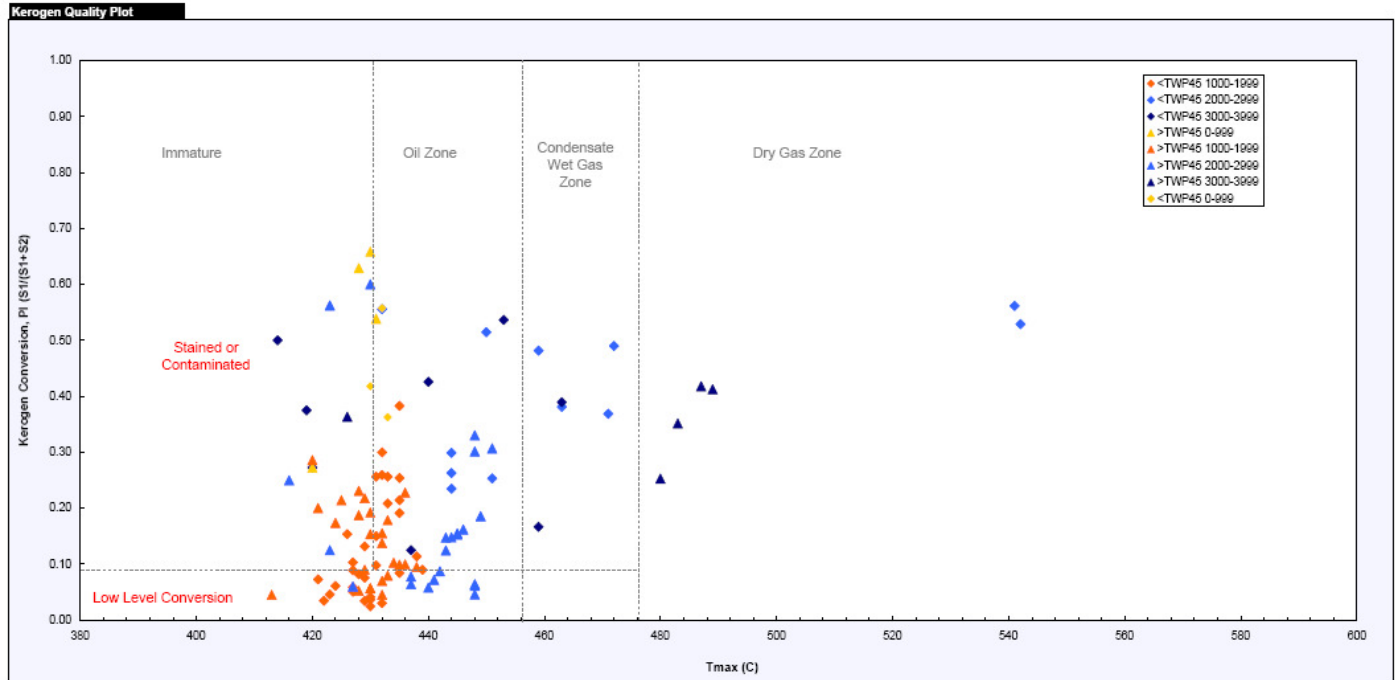


Figure BEB-8d. HC transformation versus maturity showing samples connected immature, oil, condensate and dry gas zones areas (source John Pawlowicz, ERCB, 2012). Colour indicates depth range of the samples

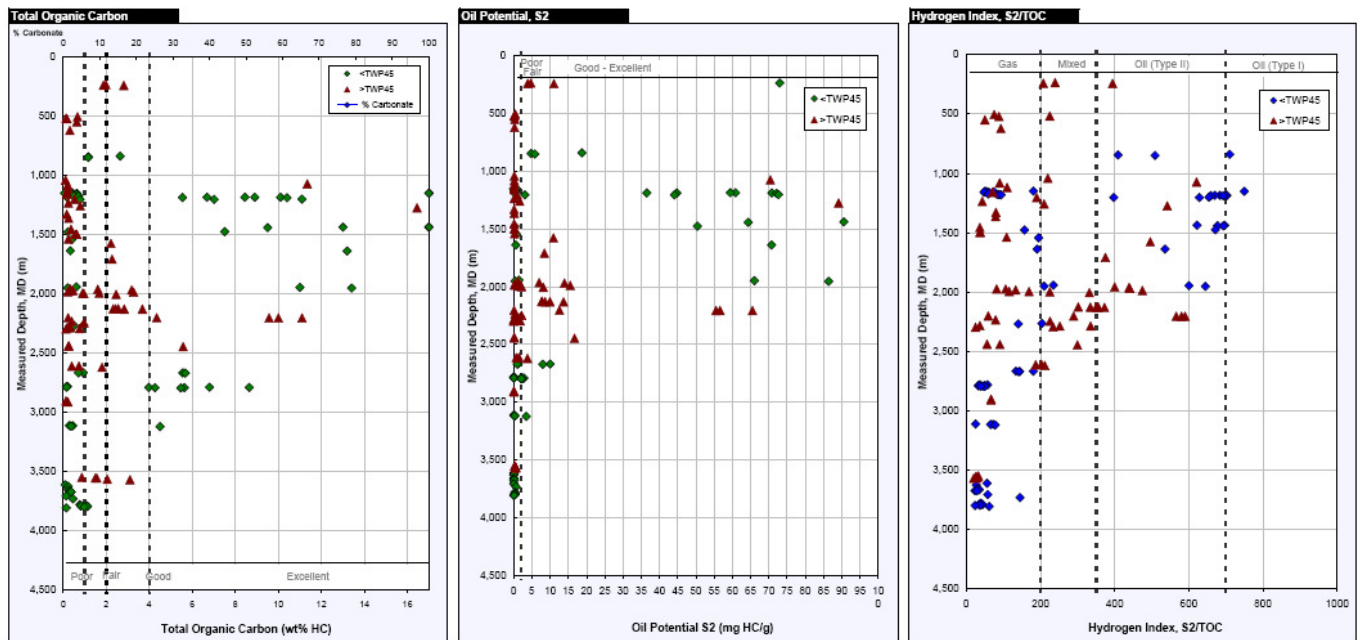


Figure BEB-8e. Depthwise plot of TOC, Oil Potential, and Hydrogen Index of various samples from Alberta (source John Pawlowicz, ERCB, 2012).

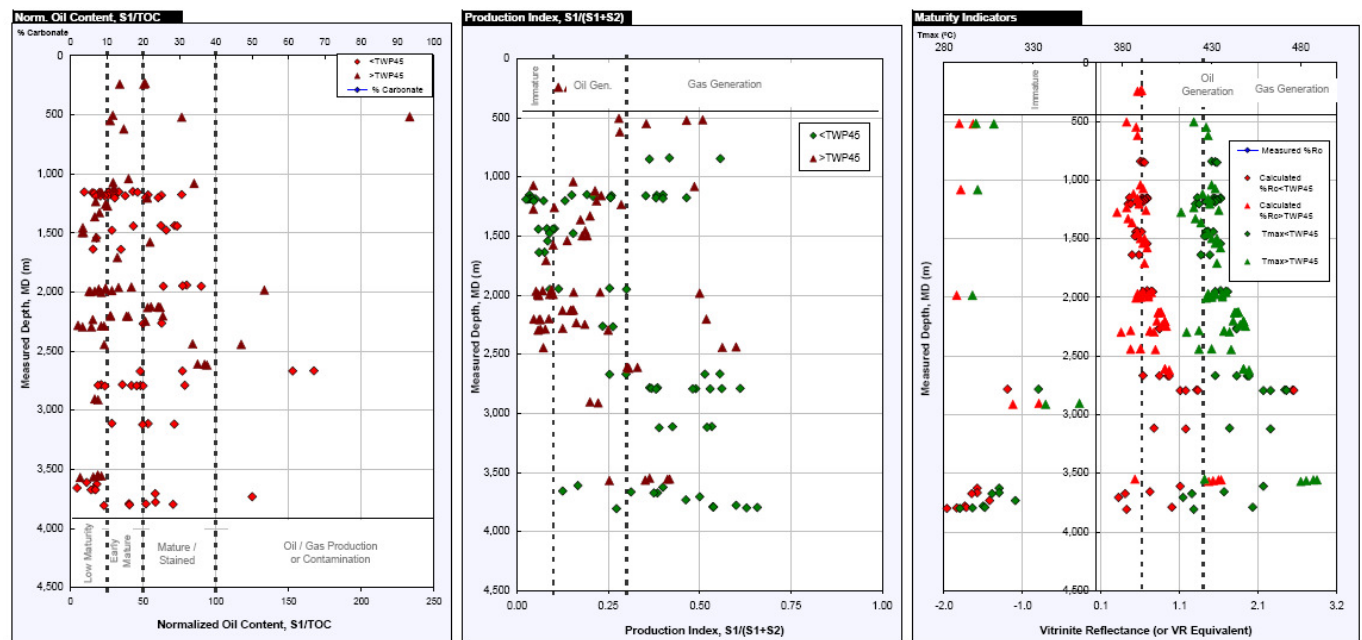
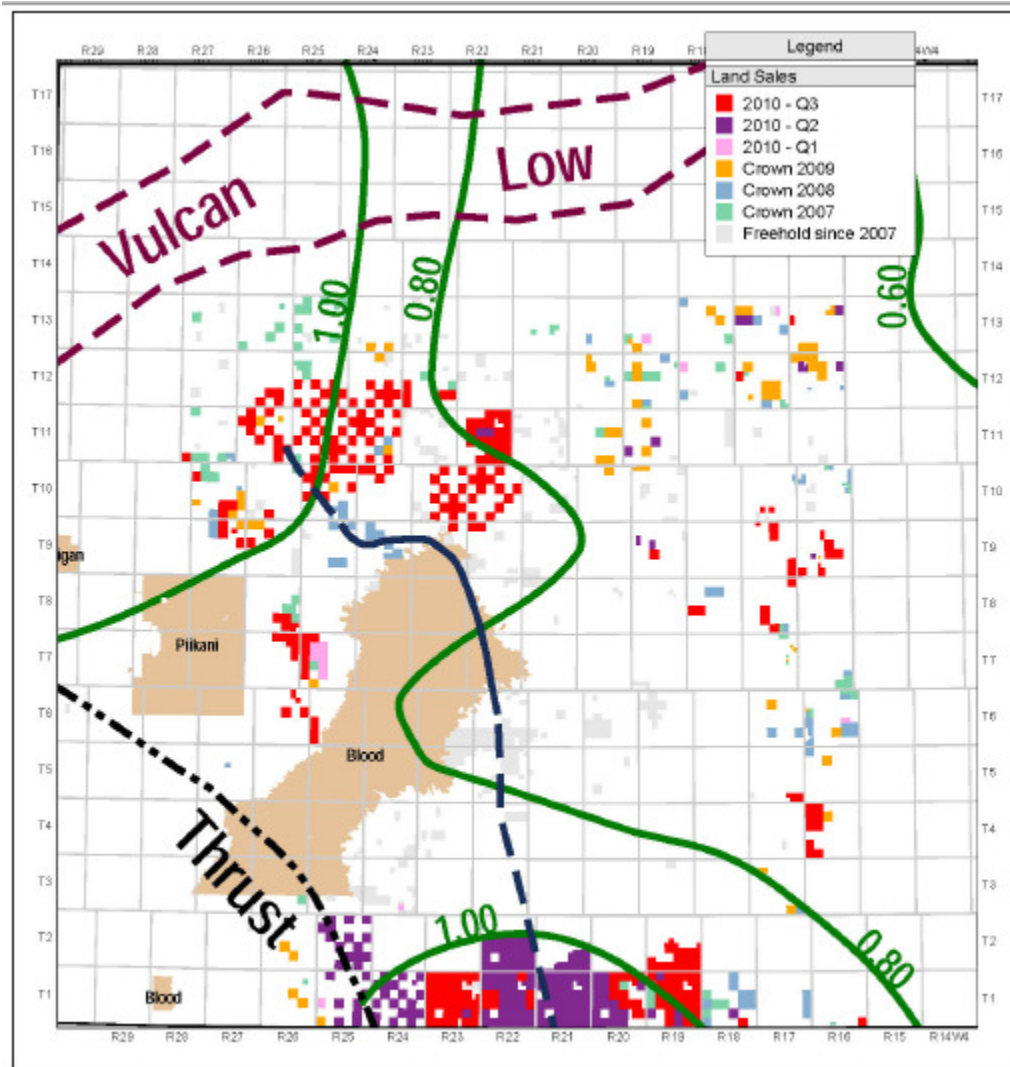


Figure BEB-8f. Depthwise plot of Oil Content, Production Index, and Maturity Index of various samples from Alberta (source John Pawlowicz, ERCB, 2012).



Source: BMO Capital Markets; GeoScout

Figure BEB-9a. Maturation trend of Baken-Exshaw source rocks from Alberta, Saskatchewan, and Montana (USA) (source: Zeitlin et al., 2010)

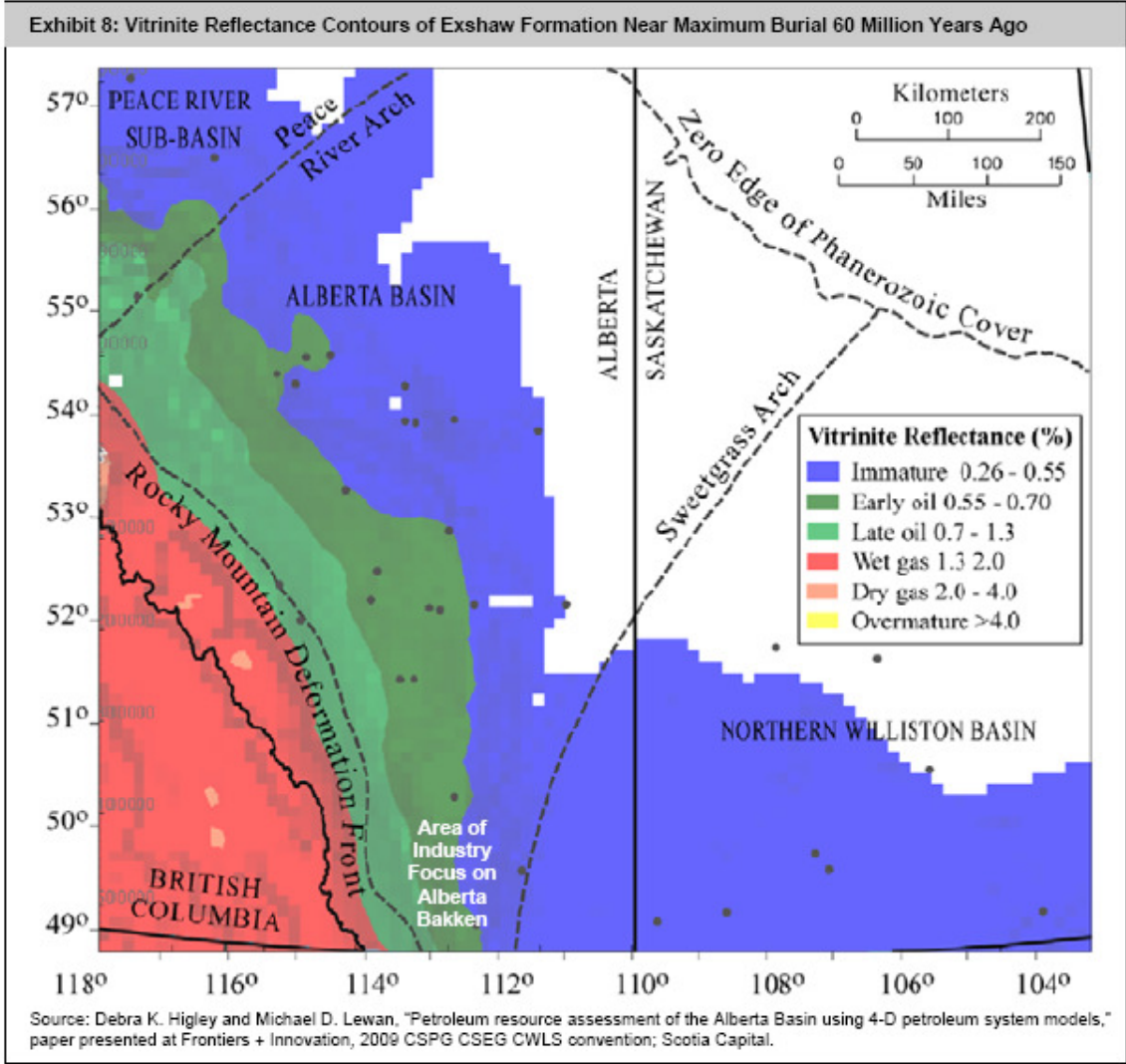


Figure BEB-9b. Maturation windows based on selected vitrinite reflectance (data from Higley and Lewan (2009) (source: Scotia Capital, 2011)

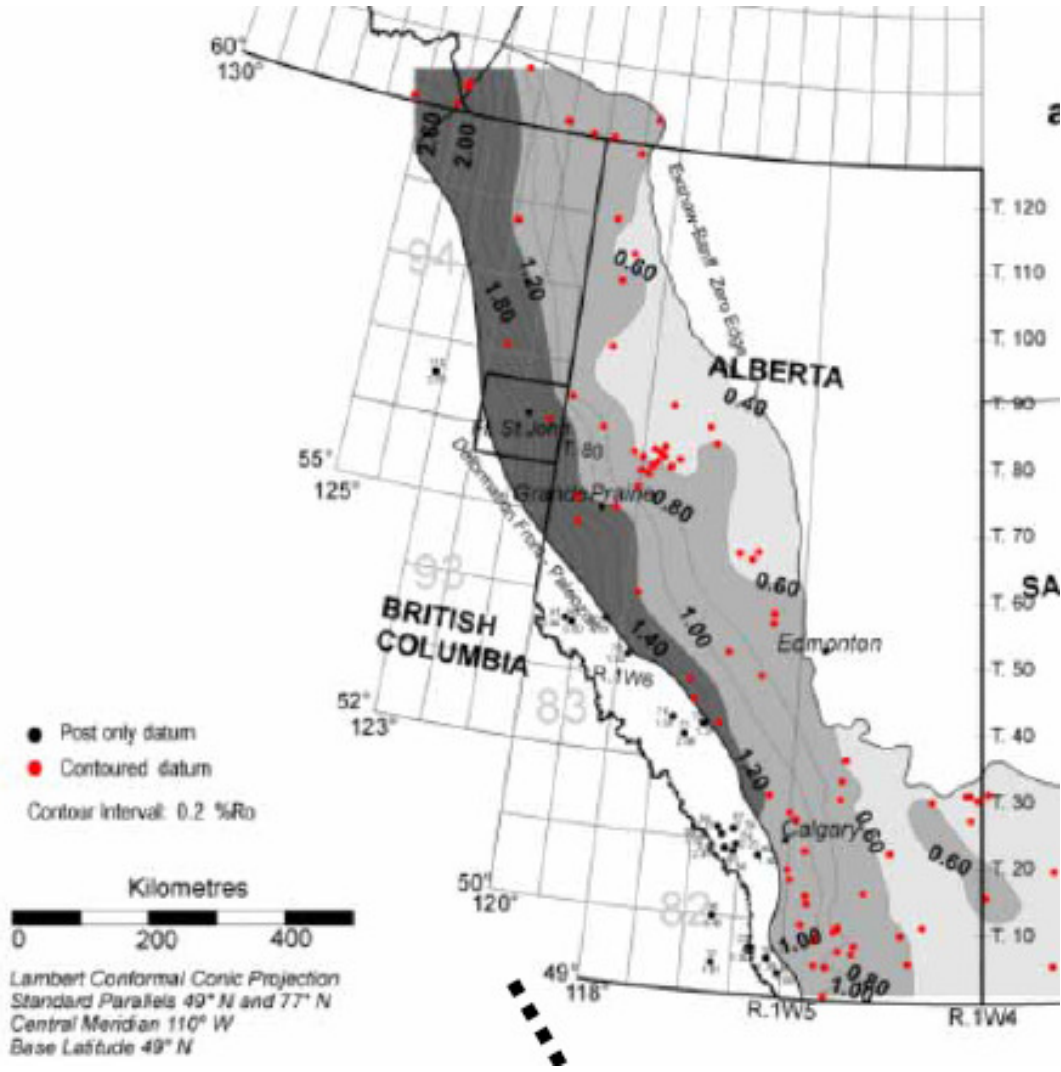


Figure BEB-9c. Vitrinite reflectance contour map of Alberta (from Geological Survey of Canada, 2002; source: Scotia Capital , 2011)

Sample No.	Sample Type	Sample Site	Quartz	Feldspar			Pyrite	Musc.	Clay Minerals							Carbonates			Sulphates Gypsum	Anatase	Brookite	Ilmenite	Hematite	Total		
				Albite	Micro.	Ortho.			Kaol.	Illite	Faly.	Sep.	RM.LC	Mont.	ClCh.	Chlo.	Calcite	Dolo.							Ank.	
6507	outcrop	B19	21.7	3.5		20.3	9.8		1.2								26.0	17.6								100.0
6508	outcrop	B19	40.9			13.1	5.1		1.1	3.4							4.0	32.3								100.0
6509	outcrop	B19	68.1			14.1	2.6		2.2	5.8							4.5	2.6								100.0
6510	outcrop	B19	65.6			13.4	2.8		3.4	6.6							6.5	1.6								100.0
6511	outcrop	B19	71.1			12.2	2.7		2.4	5.9							3.9	1.8								100.0
6512	outcrop	B19	66.2			13.4	1.4		2.9	9.1							4.1	3.0								100.0
6513	outcrop	B19	18.4	4.0		19.6	0.6		10.0	40.6							4.6	2.2								100.0
6514	outcrop	B19	69.5	2.0		5.2	0.3		2.2	11.5							9.3									100.0
6516	outcrop	B19	65.0	1.9		9.2	0.2			16.7							7.0									100.0
6517	outcrop	B19	66.9	4.0		14.7			1.2	7.6							4.5		1.2							100.0
6518	outcrop	B19	45.4	2.3		19.3	0.3		3.0	16.3							13.4									100.0
6519	outcrop	B19	60.9	1.7		13.7	1.0		1.1	11.7							10.0									100.0
6520	outcrop	B19	65.0	1.1		10.8	1.4		1.1	13.6							3.6	3.4								100.0
6521	outcrop	B19	53.0	1.7		17.5	0.5		1.0	24.0							2.1	0.3								100.0
6522	outcrop	B19	68.3	1.2		11.1	0.3		0.9	14.4							3.5	0.4								100.0
6523	outcrop	B19	50.4	2.0		1.0			9.3	32.7							3.8	0.8								100.0
6524	outcrop	B19	34.6	1.3		8.9	1.5			43.3							9.0	1.6								100.0
6525	outcrop	B19	47.4	6.8		19.4			1.0	20.6							1.8	0.0	2.9							100.0
6526	outcrop	B19	22.3	2.1		19.8	3.3			24.1							20.8	7.7								100.0
6527	outcrop	B19	24.2	4.2		19.1	2.9		4.8	29.4							11.7	2.8	1.0							100.0
6528	outcrop	B19	20.8	6.0		13.5	1.8		4.9	27.2							21.2	3.3	1.4							100.0
6529	outcrop	B19	17.8	3.4		15.0	2.5			19.8							37.2	4.3								100.0
6530	outcrop	B19	22.1	3.4		18.3	3.1			28.2							21.8	3.1								100.0
6533	outcrop	B17	36.3	3.7		16.7	0.4		7.1	5.5							10.6	19.6								100.0
6534	outcrop	B17	74.9	1.8		6.9			1.2	6.4							8.9									100.0
6537	outcrop	B17	66.2	0.5		12.5				4.0							16.3	0.5								100.0
6538	outcrop	B17	82.4	0.8		10.1				5.1							1.6									100.0
6539	outcrop	B17	7.2	3.9		71.1	0.3		1.4	4.3							9.1	2.7								100.0
6540	outcrop	B17	30.2	2.0		19.9	0.3			8.7							17.7	21.1								100.0
6541	outcrop	B17	29.2	1.0		12.7	0.4			3.4							10.1	43.3								100.0
6542	outcrop	B17	33.0	2.0		20.4				6.7							14.9	22.9								100.0
6543	outcrop	B17	39.7	4.3		9.7				7.4							11.6	27.3								100.0
6545	outcrop	B17	28.3	1.1		5.6	0.1		3.1								23.9	29.8	1.0							100.0
6546	outcrop	B17	29.2	1.1		5.8	0.1		3.2								24.7	30.7								100.0
6547	outcrop	B17	12.5	0.6		3.3											66.1	17.5								100.0
6548	outcrop	B17	53.0	1.2		0.6											0.1	45.1								100.0
6549	outcrop	B17	45.3			1.4											34.4	18.9								100.0
6550	outcrop	B17	12.1	0.6		3.6											53.9	29.9								100.0

Figure BEB-10a. Bulk mineralogy of Selected outcrop samples from the Banff-Bakkem-Exshaw Formation (after Pawlowicz et al., 2009)

Sample No.	Sample Type	Sample Site	Quartz	Feldspar			Pyrite	Musc.	Clay Minerals							Carbonates			Sulphates Gypsum	Anatase	Brookite	Ilmenite	Hematite	Total			
				Albite	Micro.	Ortho.			Kaol.	Illite	Faly.	Sep.	RM.LC	Mont.	ClCh.	Chlo.	Calcite	Dolo.							Ank.		
6926	core	B08	13.1	2.1		3.2		3.7	0.6								61.9	11.9	3.4							99.9	
6931	core	B01	30.9	4.3	13.4		1.3	9.8										34.5	5.7								99.9
6934	core	B04	26.1	5.0	4.1		0.8	13.3									31.0	7.4	8.2							100.1	
6943	core	B06	26.8	3.2		7.6	0.3	4.8	2.6								34.4	14.2	6.1							100.0	
6947	core	B10	31.6	--		23.4	6.7	26.9			9.4						1.3			0.8						100.1	
7287	outcrop	B19	31.7	4.5		10.0				9.1							36.3		8.3							100.0	
7288	outcrop	B19	28.1	4.8		6.1			1.0	11.8							41.3	6.9								100.0	
7301	outcrop	B17	4.5	1.6													52.9	3.1	37.8							100.0	
7302	outcrop	B17	20.8	3.4			1.2			21.2							42.1	11.3								100.0	
7303	outcrop	B17	16.7	2.6		3.1	1.1			10.0							57.3	9.2								100.0	
7304	outcrop	B17	15.9	0.1		9.1	1.7			8.9							37.3	0.3	26.8							100.0	
7305	outcrop	B17	18.6	1.1		2.6	0.8			9.5							52.4	2.4	12.7							100.0	
7307	outcrop	B17	22.4	2.1		2.8	1.1			17.5							36.0	2.5	15.8							100.0	
7308	outcrop	B17	35.8	0.7		1.5	0.3			7.8							44.0	2.0	7.9							100.0	
7309	outcrop	B17	13.1	1.9		6.2	3.2			9.0							51.5	0.1	15.0							100.0	
7310	outcrop	B17	13.4	1.2		1.9	0.9			4.4							73.5	4.8								100.0	
7311	outcrop	B17	15.0	3.2		5.7			1.7	15.6							47.2	11.6								100.0	
7312	outcrop	B17	27.5														70.9	1.6								100.0	
7313	outcrop	B17	3.9				0.4										91.4	4.3								100.0	
7314	outcrop	B18	7.6	4.7		6.9	2.1			4.1							33.9	5.5	35.2							100.0	
8017	core	B03	24.2	7.2		8.0	2.0	19.7	2.6								10.0	8.5	9.4							100.0	
8021	core	B12	41.1	2.1		13.6	1.8	18.5		10.4	10.3						0.5	1.0		0.8						100.1	
8038	core	B16	32.0	4.7		4.0	2.9	15.5			3.5	4.7					12.3	2.6	4.3							86.5	
8680	core	B09	45.7	7.3		5.3	8.9	20.9			9.3						0.6				0.9					100.0	
8683	core	B02	29.9	5.0	3.1		2.2	27.7	3.9								11.0	6.8	5.3						1.3	99.9	
8684	core	B02	28.1	6.5		7.2	1.4	17.7	2.3			3.4					15.0	9.9	8.5							100.0	
8688	core	B05	46.0			9.1	6.1	23.8	7.4			5.8					0.9			0.6	0.3					100.0	
8692	core	B15	51.3	3.0		5.9	1.1	17.5	1.8								3.9	5.2	5.0						0.5	100.1	

Figure BEB-10b. Bulk mineralogy of selected mixtures of outcrop and core samples from the Banff-Bakkem-Exshaw Formation (after Pawlowicz et al., 2009)

Sample No.	SiO <sub>2</sub>	Al <sub>2</sub> O <sub>3</sub>	Fe <sub>2</sub> O <sub>3</sub>	MgO	CaO	Na <sub>2</sub> O	K <sub>2</sub> O	TiO <sub>2</sub>	P <sub>2</sub> O <sub>5</sub>	MnO	Cr <sub>2</sub> O <sub>3</sub>	V <sub>2</sub> O <sub>5</sub>	LOI	Total
	(%)	(%)	(%)	(%)	(%)	(%)	(%)	(%)	(%)	(%)	(%)	(%)	(%)	(%)
6926	18.40	2.55	0.70	2.40	38.90	0.24	0.86	0.14	0.05	0.01	<0.01	0.02	33.60	97.80
6931	46.10	7.42	2.93	7.41	11.60	0.53	3.24	0.53	0.09	0.08	0.05	<.01	17.30	97.30
6934	38.50	7.37	2.82	3.44	20.70	0.58	2.03	0.35	0.12	0.04	0.02	0.02	22.50	98.50
6943	37.50	4.80	2.03	3.35	24.50	0.47	1.74	0.32	0.08	0.04	0.01	0.01	22.80	97.60
6947	60.80	16.40	4.23	2.13	0.60	0.39	6.85	0.92	0.18	0.01	0.02	0.02	6.12	98.70
8017	46.10	11.30	4.35	4.75	9.97	0.99	2.82	0.60	0.11	0.08	0.02	<.01	18.00	99.10
8021	64.50	14.30	4.76	2.27	0.42	0.42	4.73	0.81	0.19	0.02	0.02	0.01	5.56	98.00
8038	48.30	7.27	3.98	2.08	8.73	0.53	2.44	0.35	0.72	0.04	0.02	0.03	24.60	99.10
8680	64.00	12.90	5.37	1.33	0.16	0.83	3.17	0.61	0.09	0.02	<.01	0.15	10.30	99.00
8683	49.80	12.00	4.23	2.02	7.98	0.64	3.66	0.56	0.08	0.03	0.02	0.13	16.40	98.60
8684	47.20	10.20	4.01	3.33	13.30	0.62	2.68	0.59	0.11	0.06	<.01	0.03	16.60	98.80
8688	66.90	14.00	3.99	1.10	0.48	0.39	3.56	0.77	0.07	0.03	0.02	0.07	7.30	98.50
8692	66.90	9.59	2.61	2.54	4.57	0.62	2.71	0.45	0.13	0.02	0.02	0.07	9.35	99.50
8692DUP	66.30	9.56	2.61	2.53	4.59	0.60	2.73	0.45	0.11	0.03	0.02	0.06	9.41	99.00

Figure BEB-10c. Oxides of various elements of selected mixture of outcrop and core samples (after Pawlowicz et al., 2009)

Sample No.	Sample Site	Sample Type	Crystalline Mineral Assemblage (relative proportions based on peak height)			
			Major	Moderate	Minor	Trace
6934	B04	core	illite	(quartz), (calcite)	kaolinite, chlorite	(*siderite), (*pyrite)
8683	B02	core	illite	(quartz)	kaolinite, (calcite), chlorite	(*ankerite)
8688	B05	core	illite		kaolinite, (quartz)	(*pyrite)

\* Tentative identification due to low concentrations, diffraction line overlap or poor crystallinity

() Not a clay mineral

Figure BEB-10d. Quantitative X-Ray Deffraction of three selected source rocks (after Pawlowicz et al., 2009)

AGS Sample No.	Core Depth (feet) <sup>1</sup>	Core Depth (m) <sup>2</sup>	Unique Well Identifier	Formation	N	Average permeability (mD) <sup>3</sup>	Average permeability (mD)
6919	12000.0	3657.6	100/08-27-039-11W5/00	U. Banff	5	0.648333	
6937	11710.5	3569.2	100/04-23-072-10W6/00	Exshaw/L. Banff	5	0.965	
8691		2612.75	100/16-24-077-06W6/00	L. Banff	5	0.0020667	
6923	12245.0	3732.3	100/08-27-039-11W5/00	M. Banff	6	0.0031325	
6924	12399.0	3760.9	100/08-27-039-11W5/00	M. Banff	5	0.139	
6925	12441.0	3792.0	100/08-27-039-11W5/00	L.-M. Banff	5	0.0203667	
6928	12468.0	3800.2	100/08-27-039-11W5/00	L. Banff	6	0.004228	
6933		2795.3	100/01-20-001-24W4/00	Exshaw	5	0.153	
6935	11668.0	3556.4	100/04-23-072-10W6/00	L. Banff	5	0.002147	
6941	3803.0	1159.2	100/07-08-074-14W5/00	Banff	6	0.04575	
8682	6440	1962.9	100/02-14-082-02W6/00	L. Banff	6	0.0086025	
8688	7373	2247.3	100/06-04-084-07W6/00	L. Banff	6	3.775	
8693		2610	100/16-24-077-06W6/00	L. Banff	6, 3	0.003488	0.013 (layers)

<sup>1</sup> original units

<sup>2</sup> original and converted units

<sup>3</sup> Average permeability (K) for each sample is calculated by removing the high and low recorded values, then averaging the remaining values. Normally, five to six readings were taken on each sample. Contact AGS for a list of the raw results.

Figure BEB-11. Average permeability of selected Banff and Exshaw outcrop and core samples (after Pawlowicz et al., 2009)

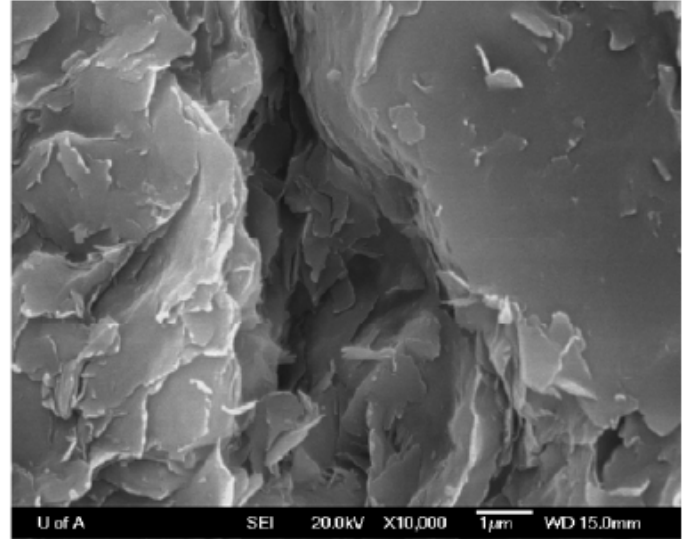
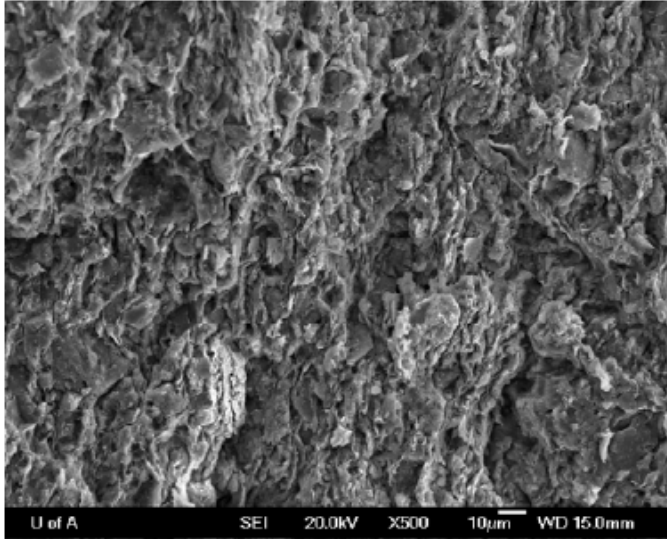
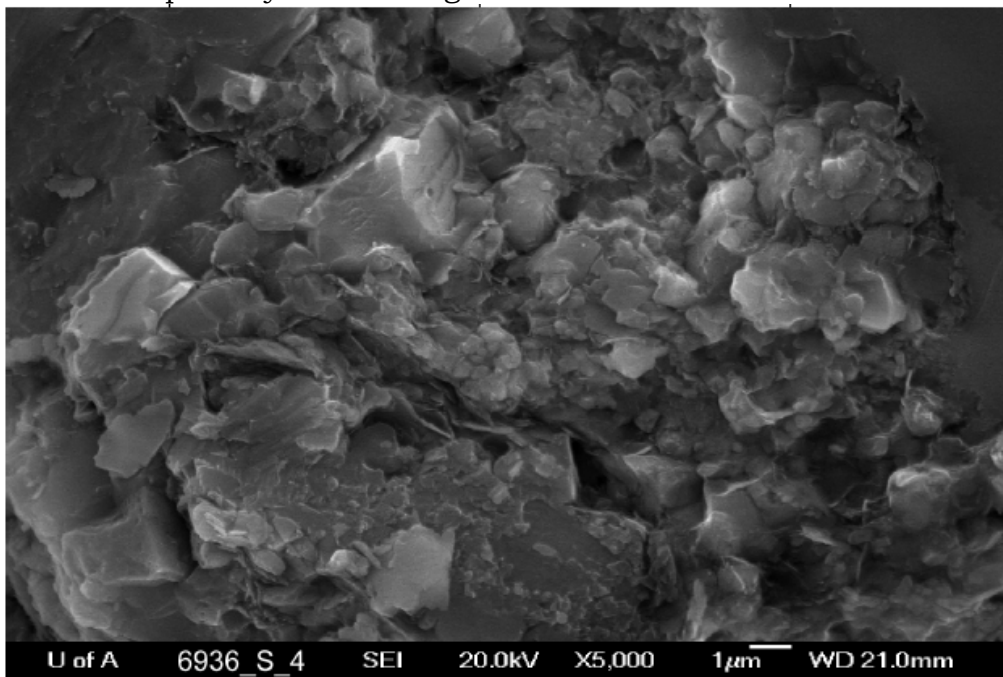
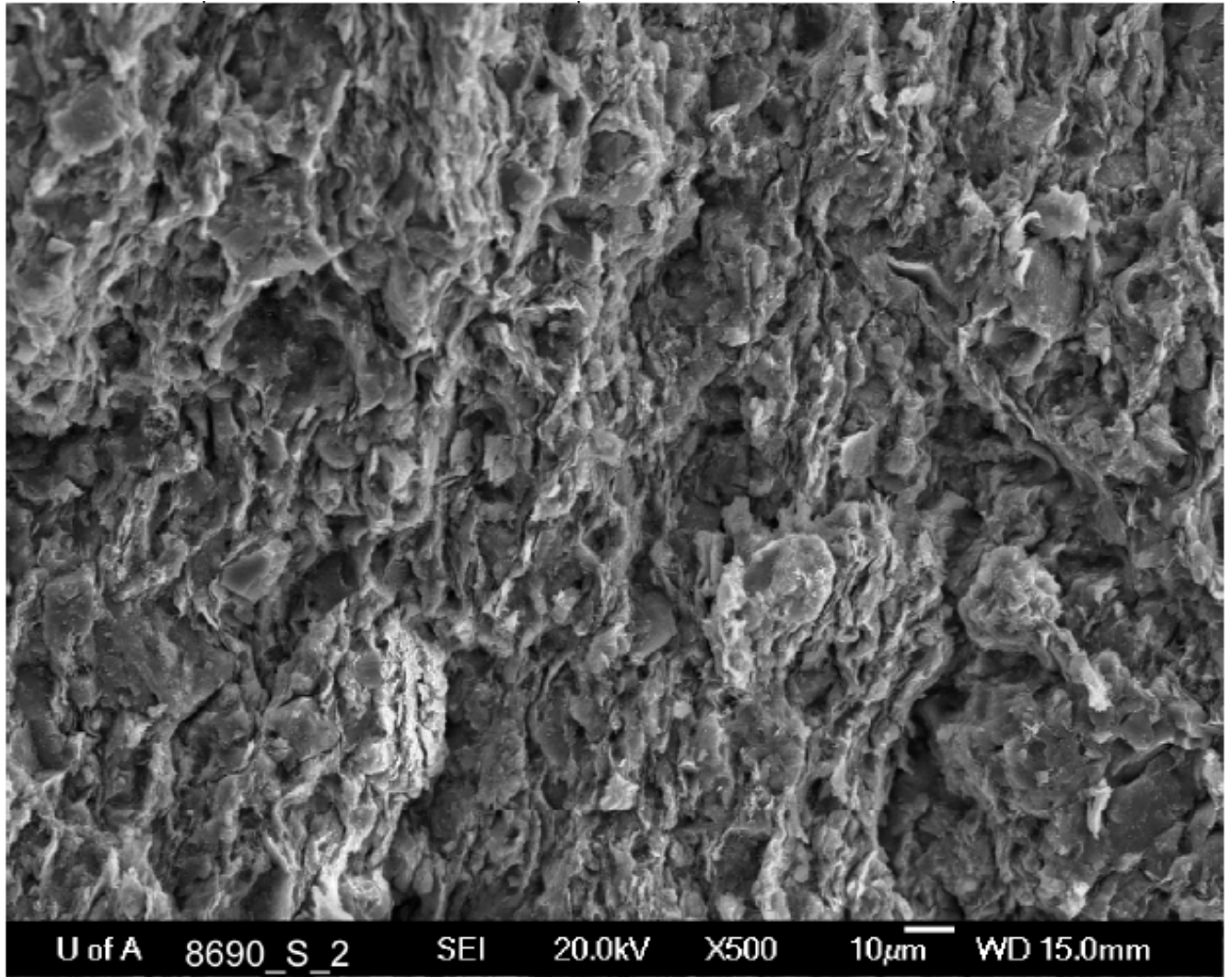


Figure BEB-12a. SEM image of dolomitic lime mudstone (sample 6922) with Banff Formation with less than 5% silt-sized quartz grains and showing dolomitization. The sample show microporosity within the grain boundaries.



This is a high magnification view of the matrix. The matrix is dominated by quartz overgrowth of a variety of morphologies and crystal sizes and, to a lesser extent, clay plates. Quartz overgrowth appears to occur between grains and coating grains, significantly decreasing porosity. Hence, the morphology of the grains viewed in all the photos of sample 6936 (Lower Banff) may not reflect depositional grain morphology. Microporosity is evident between overgrowth crystals. Clay mineralogy was not identified in this photo.

Figure BEB-12b. Porosity Distribution within Lower Banff Formation source rock (Pawlowicz et al., 2009)



This image is taken near the centre of the previous photo. There appears to be an abundance of silt-sized particles that are embedded between clay sheets, giving the sheets a crenulated appearance. The sample is very well fractured, which adds to the observation of a high degree of porosity between clay sheets and at the edges of many particles. Pyrite framboids are occasionally observed when the image is zoomed.

Figure 12c. Porosity Distribution within Lower Banff Formation source rock same image as of Figure 12b in higher magnification (Pawlowicz et al., 2009)

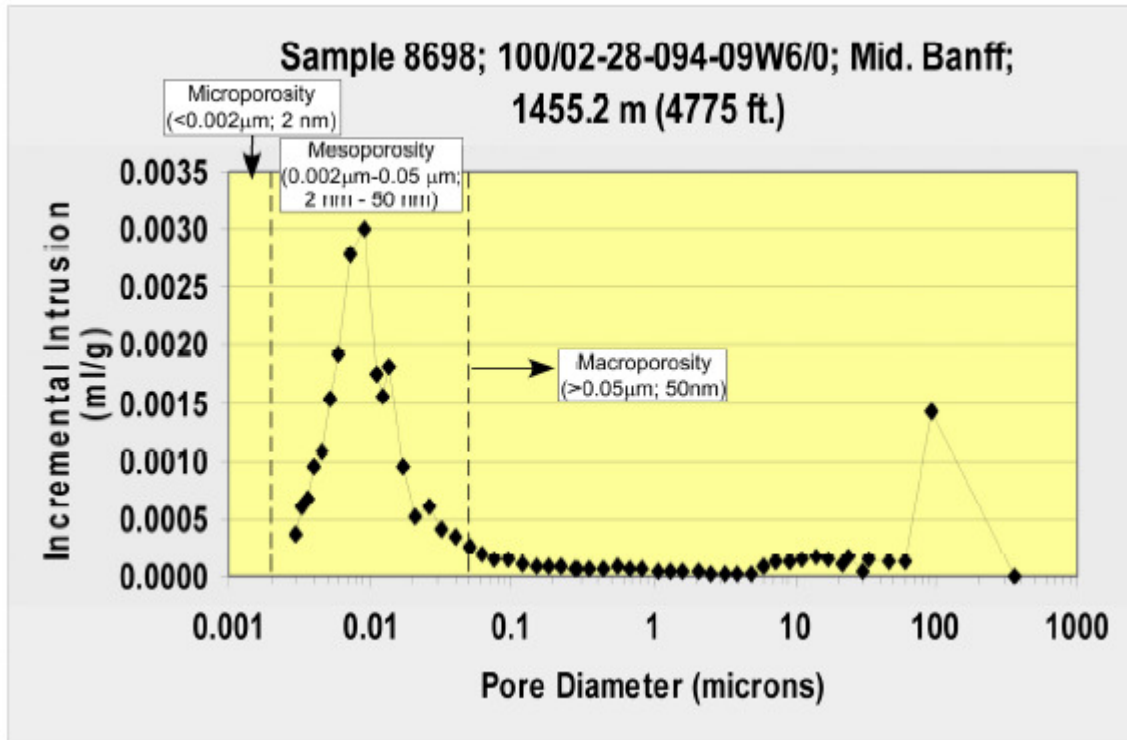


Figure BEB-13a. Pore diameter of selected Middle Banff Fm source rock

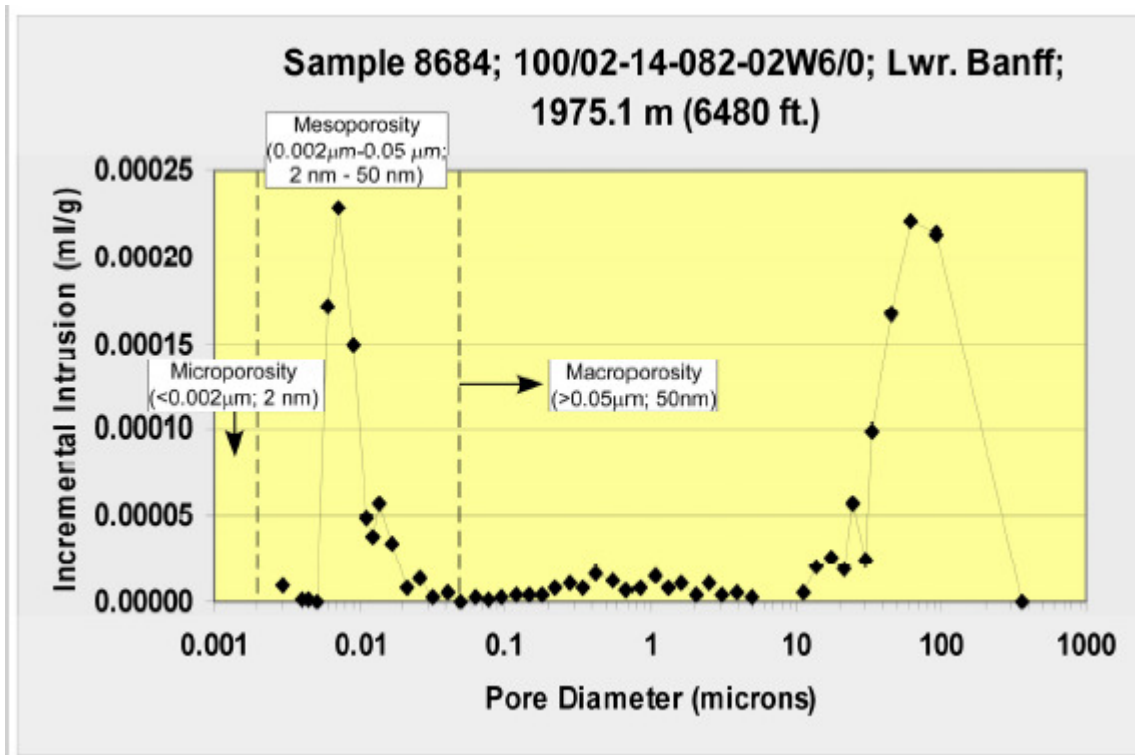
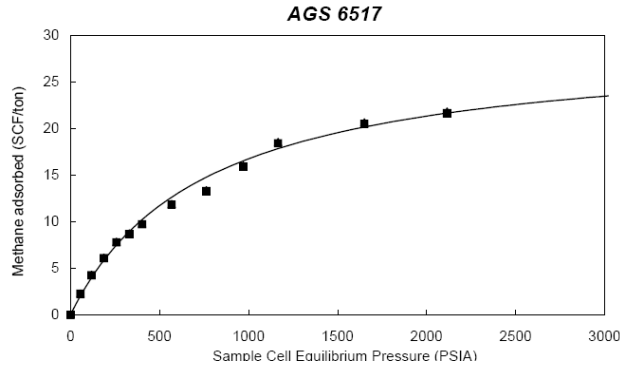
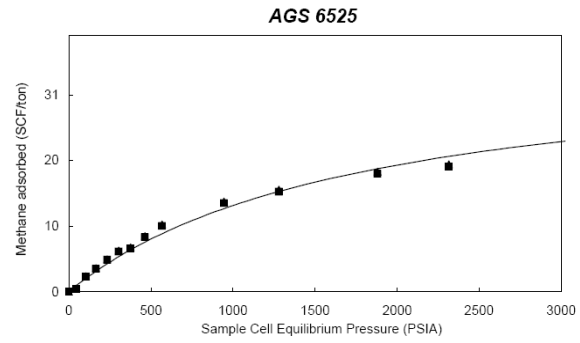


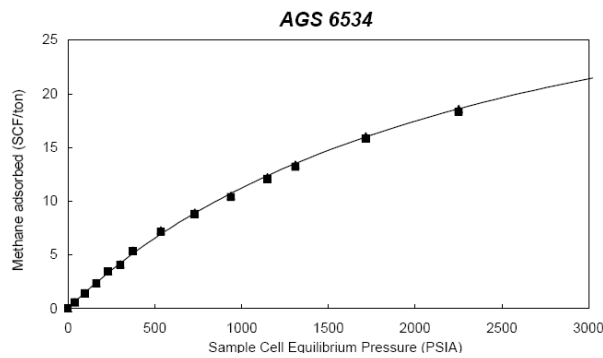
Figure BEB-13b. Pore diameter of selected Lower Banff Fm source rock



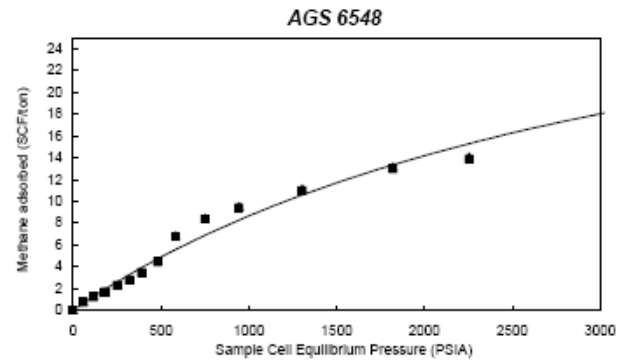
Sample 6517: JuraCreek; Exshaw Fm



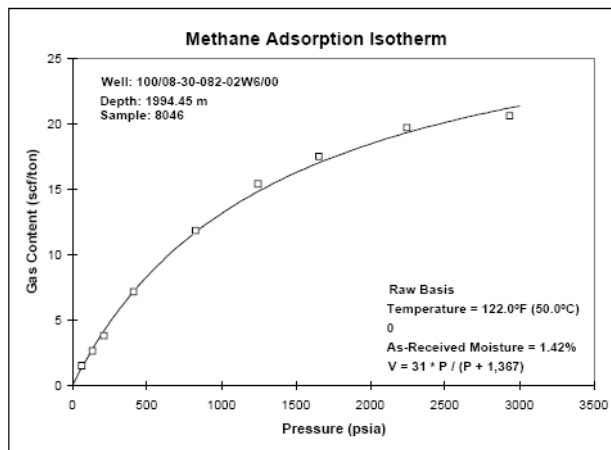
Sample 6525: JuraCreek; Exshaw Fm



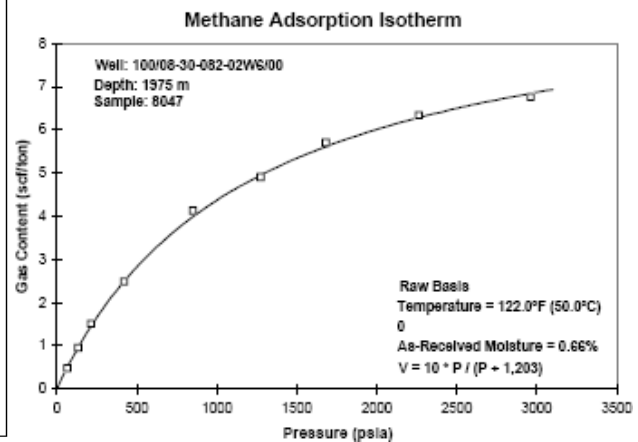
Sample 6534: Nordegg Railway sec. Lwr Banff Fm



Sample 6548 (outcrop same as 6534)



Sample 8046: Lwr Banff. Depth: 1994-1996 m)



Sample 8047:Lwr Banff. Depth:1975-1984m

Figure BEB-14a. Methane adsorption capacity of six selected samples from Lower Banff and Exshaw Formation source rocks (both outcrop & well)(samples: 6517; 6525; 6534; 6548; 8046; and 8047) (after Beaton et al., 2009)

Sample No.	Depth (metres)	TOC (%)	Analysis Temperature (°C)	As Received Moisture (%)	Langmuir Pressure Raw Basis (Mpa)	Langmuir Volume Raw Basis (scc/g)
6517	outcrop	4.48	38	0.77	5.20	0.86
6525	outcrop	0	38	1.87	12.20	1.07
6534	outcrop	3.25	38	1.47	17.17	1.13
6543	outcrop	0.75	38	0.59	15.27	0.66
6548	outcrop	0.09	38	1.51	24.57	1.14
7304	outcrop	0.38	38	1.87	n/a	n/a
8046	1994.45	1.66	50	1.42	9.42	0.97
8047	1975	0.44	50	0.66	8.29	0.30

Figure BEB-14b. Amount of gas from methane adsorption capacity of various samples. (6500 series are high maturity) (after Beaton et al., 2009)

Sample	Depth (m) <sup>1</sup>	Analysis Temperature (°C)	Average Thickness of Shale (m)	Moisture (wt. %)	Langmuir Pressure (MPa)	Langmuir Volume (standard cubic cm/g)	Density	Unit	T <sub>max</sub> (°C)	TOC (wt. %)	Calculated Reservoir Pressure (MPa)	Calculated Gas Volume at Reservoir Pressure (cc/g)	Gas Capacity (Bcf/sq. mi.)	
													Max. Capacity on Organic Matter	Max. Capacity + 25% (for Free Gas)
<b>Core samples</b>														
8678/79	1994.5	50	30	1.42	9.42	1	2.5	banff	436	1.66	19.5461	0.7	4.6	5.8
8684/85	1975.0	50	100	0.66	8.29	0.3	2.5	banff	436	0.44	19.355	0.2	4.8	6.0
<b>Outcrop samples</b>														
6517	2500	38	8	0.77	5.2	0.86	2.558	jc.exshaw		4.48	24.5	0.7	1.3	1.7
6525	2500	38	8	1.87	12.2	1.07	2.583	jc.exshaw		nd	24.5	0.7	1.3	1.7
6534	2000	38	2	1.47	17.17	1.13	2.589	nord.exh	554	3.25	19.6	0.6	0.3	0.4
6543	2500	38	2	0.59	15.27	0.66	2.352	nord.banff	320	0.75	24.5	0.4	0.2	0.2
6548	2500	38	2	1.51	24.57	1.14	2.608	nord.banff		0.09	24.4	0.6	0.3	0.3
<b>Core samples</b>														
Banff 8678/79 (00/08-30-082-02W6/00)		Lower Banff black shale		jc.exshaw		Exshaw black shale at Jura Creek Outcrop Site								
Banff 8684/85 (00/02-14-082-02W6/00)		Lower Banff grey shale		nord.exh		Exshaw black shale at Nordegg Outcrop Site								
				nord.banff		Banff black shale at Nordegg Outcrop Site								

Figure BEB-15. Gas Capacity Banff-Exshaw (after Rokosh et al., 2009)

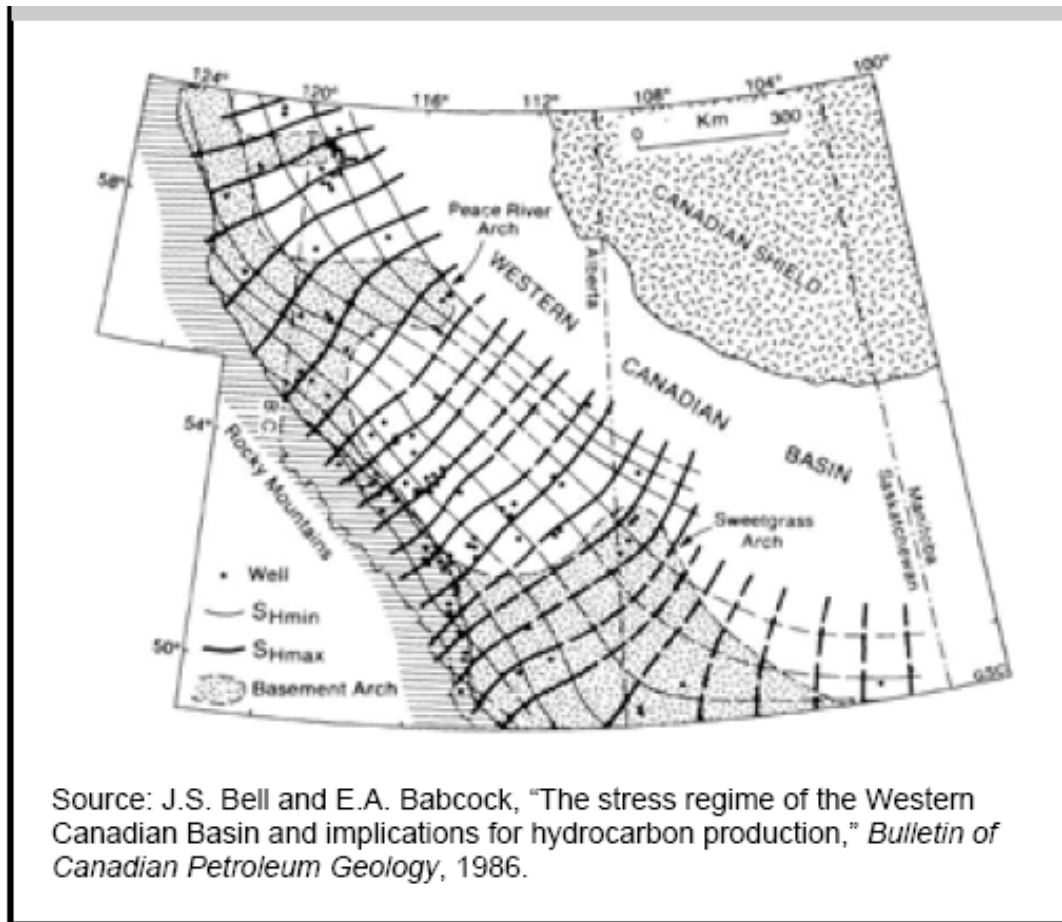


Figure BEB-16. Stress regime of the western Canadian Sedimentary Basin especially highlighting the area around Alberta

# **Duvernay and Muskwa Formations**

## **Figures and Tables**

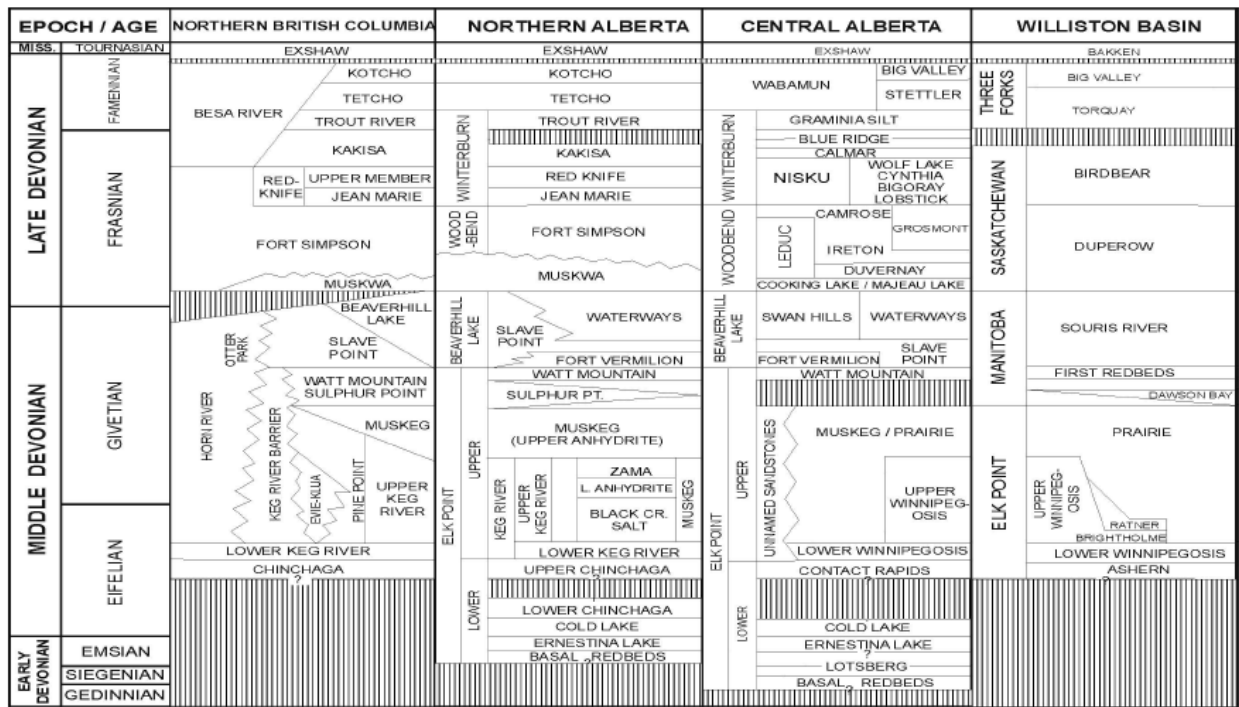


Figure DM-A1. Sedimentary Basins showing the position of Duvernay and Muskwa formations (after Reinson et al., 2003).

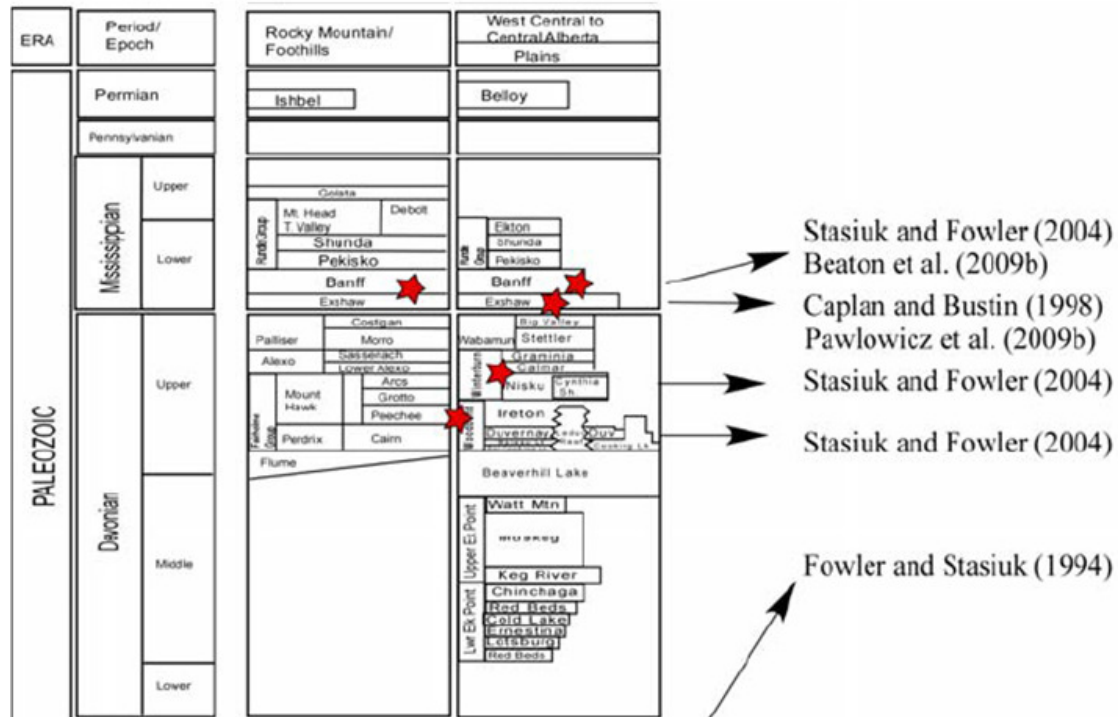


Figure DM-A2: List of potential source rocks from Precambrian to Permian age within Alberta with potential list of publications (after Rokosh et al., 2009)

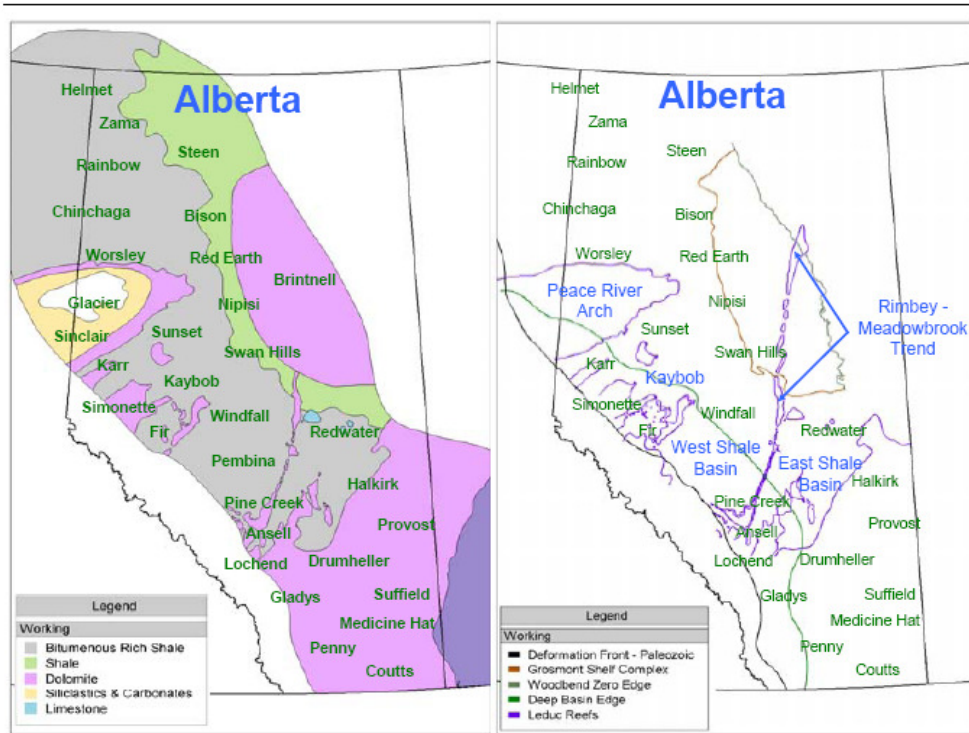


Figure DM-A3. Distribution of Duvernay and Muskwa formation sediments with specific organic shale rich areas within Alberta (source” GeoSCOUT, Macquarie Research, 2011)

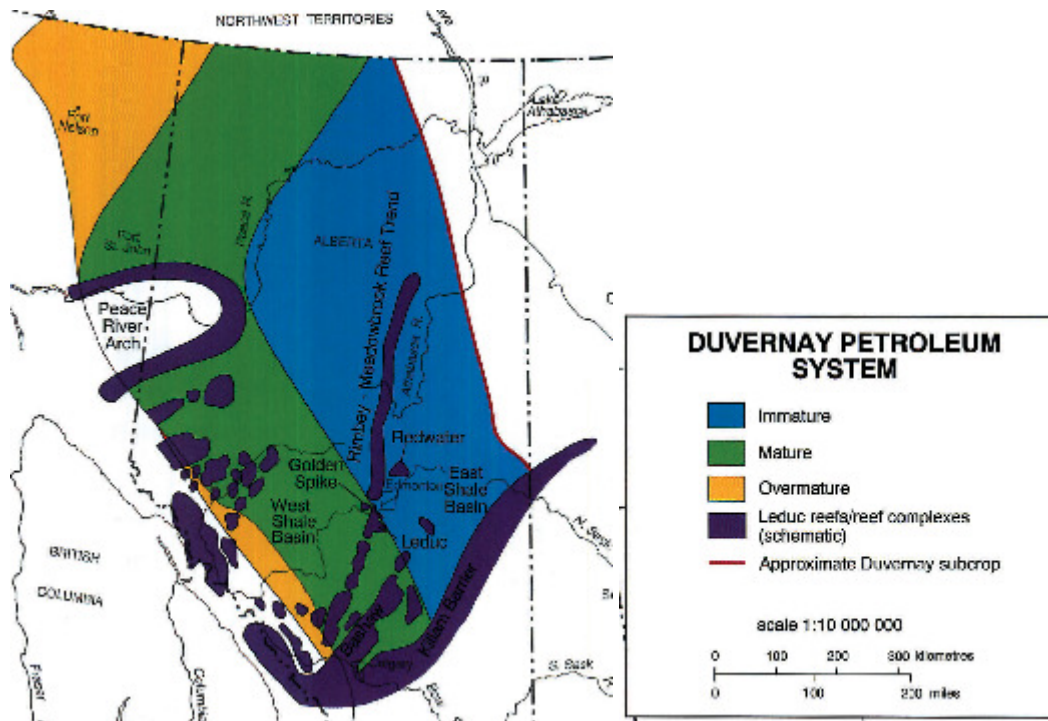
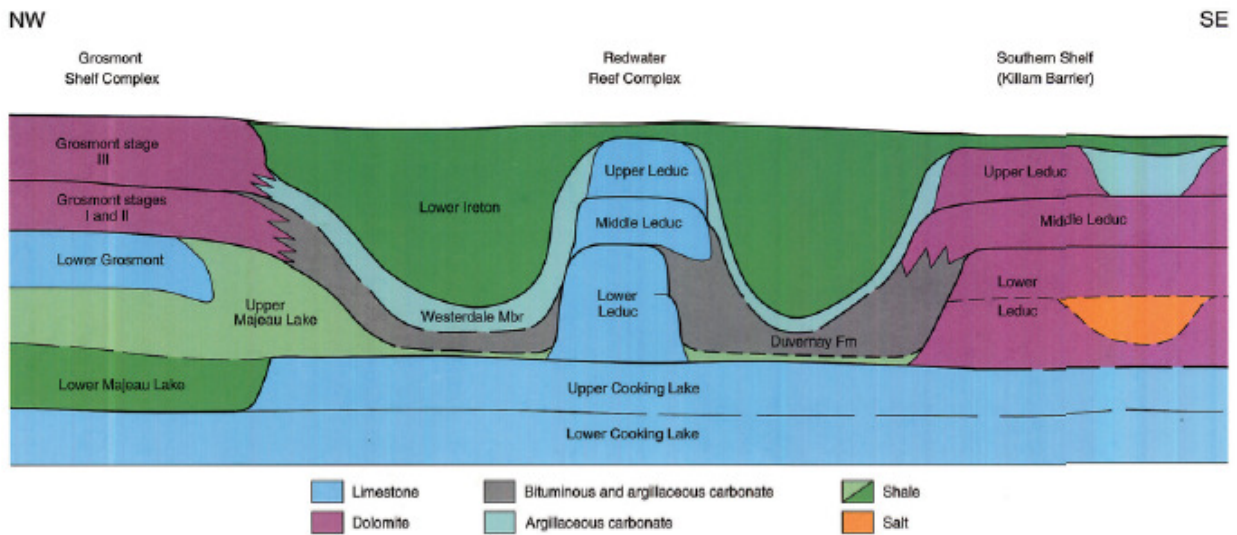


Figure DU-A4. Duvernay Petroleum System after Creaney et al. 1990 (GSC Atlas, WCSB, 1990)



Source: Alberta Geological Survey, Macquarie Research, August 2011

Figure DM-B. Stratigraphic cross section of Duvernay Formation from NW to SE of Alberta (from Alberta Geological Survey, Macquarie Research, 2011) showing the Duvernay shale source rocks occur within basinal part.

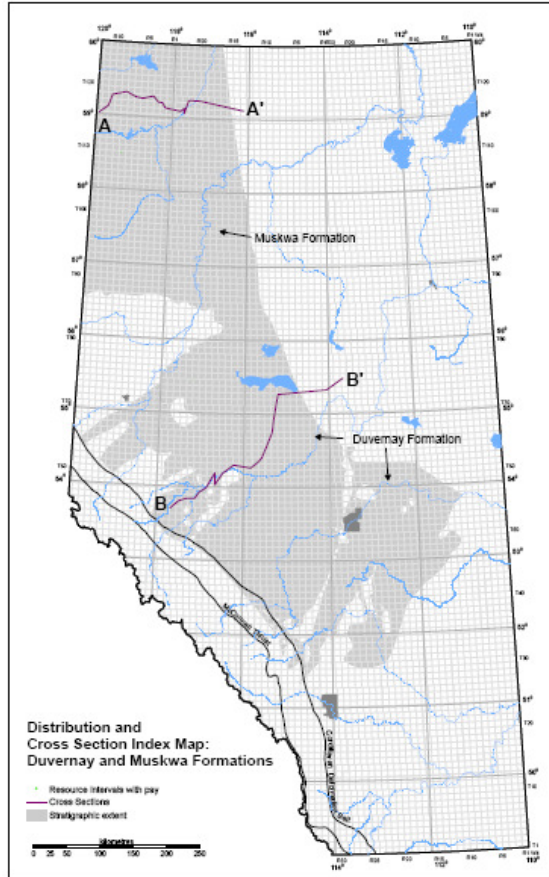


Figure DM-C1. Stratigraphic extent map of both Duvernay and Muskwa formations within Alberta

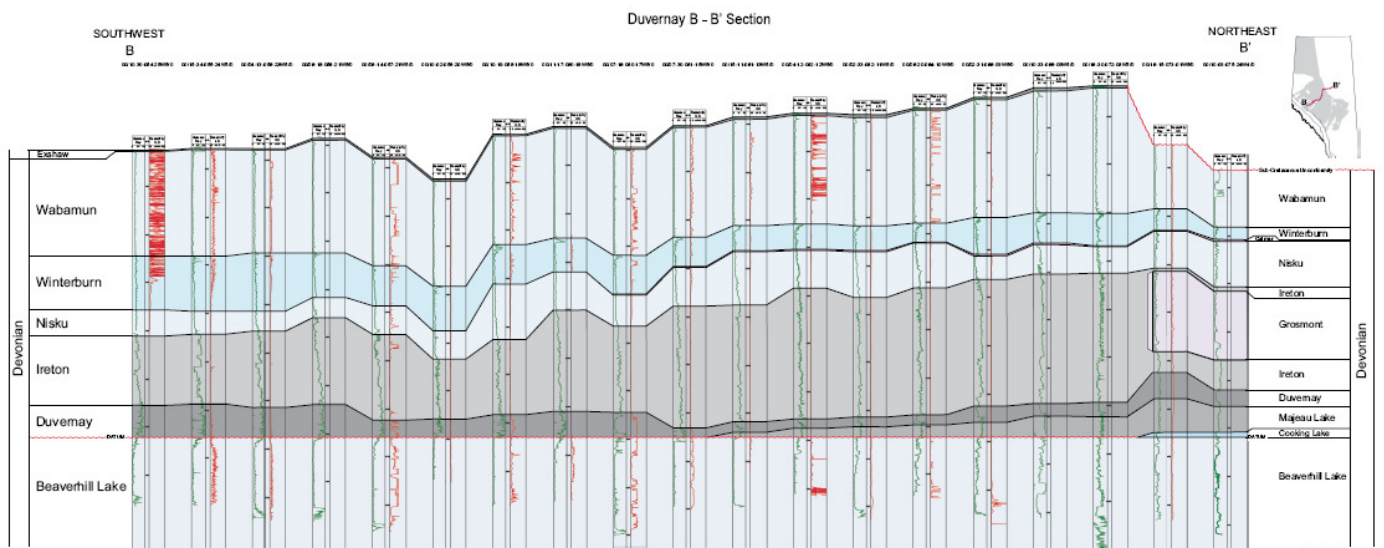


Figure DM-C2. Well log stratigraphic correlation with stratigraphic section B-B' showing the Duvernay Formation shale section

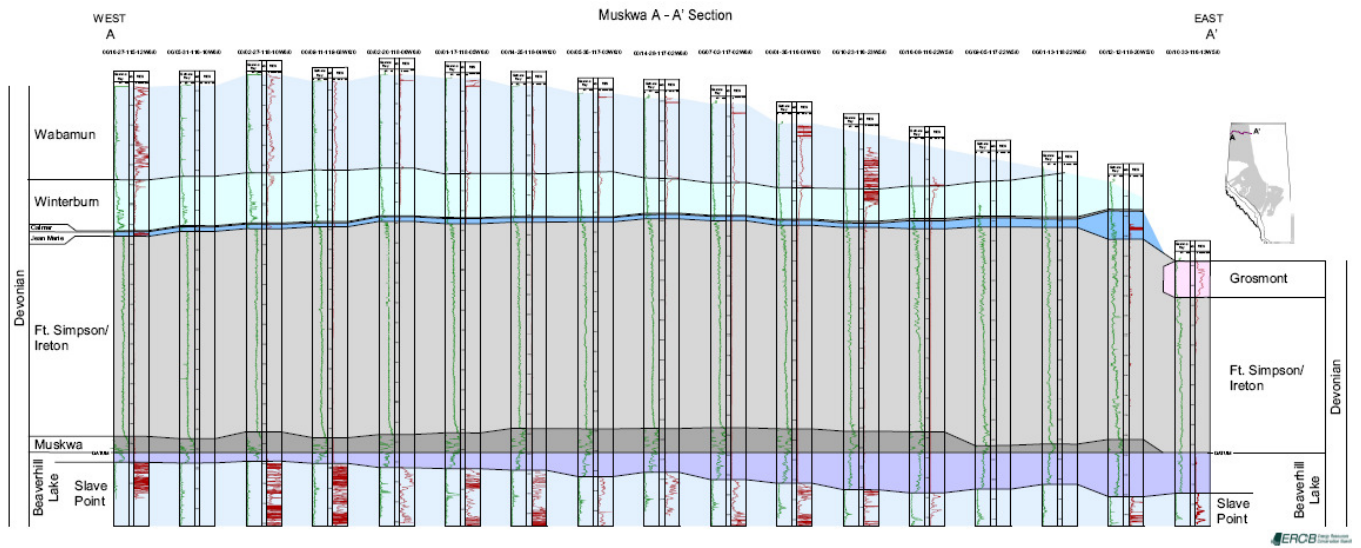


Figure DM-C3. Well log stratigraphic correlation with stratigraphic section A-A' showing the Muskwa Formation shale section

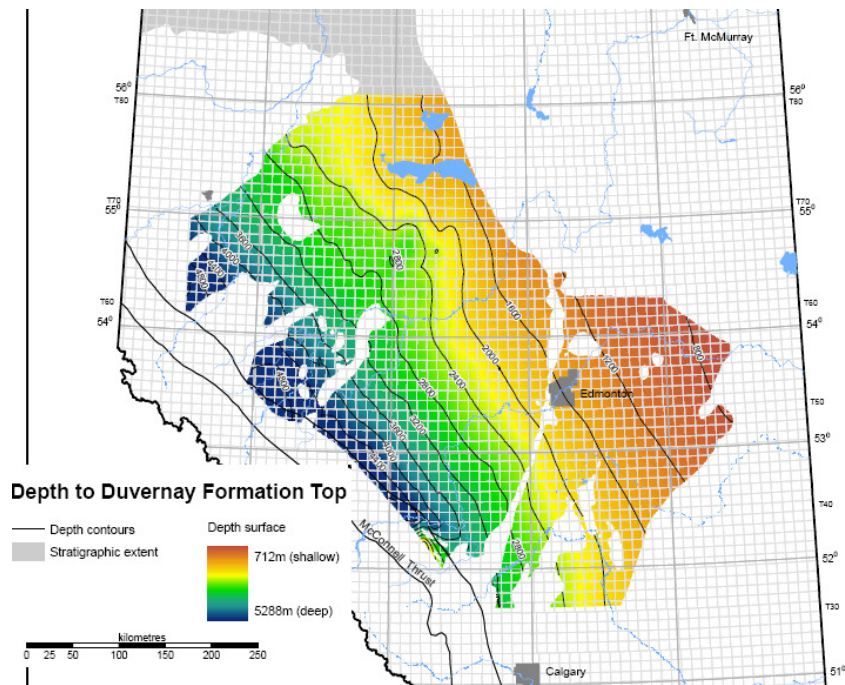


Figure DM-D1. Depth to top of the Duvernay Formation from northwest to southeast section of Alberta

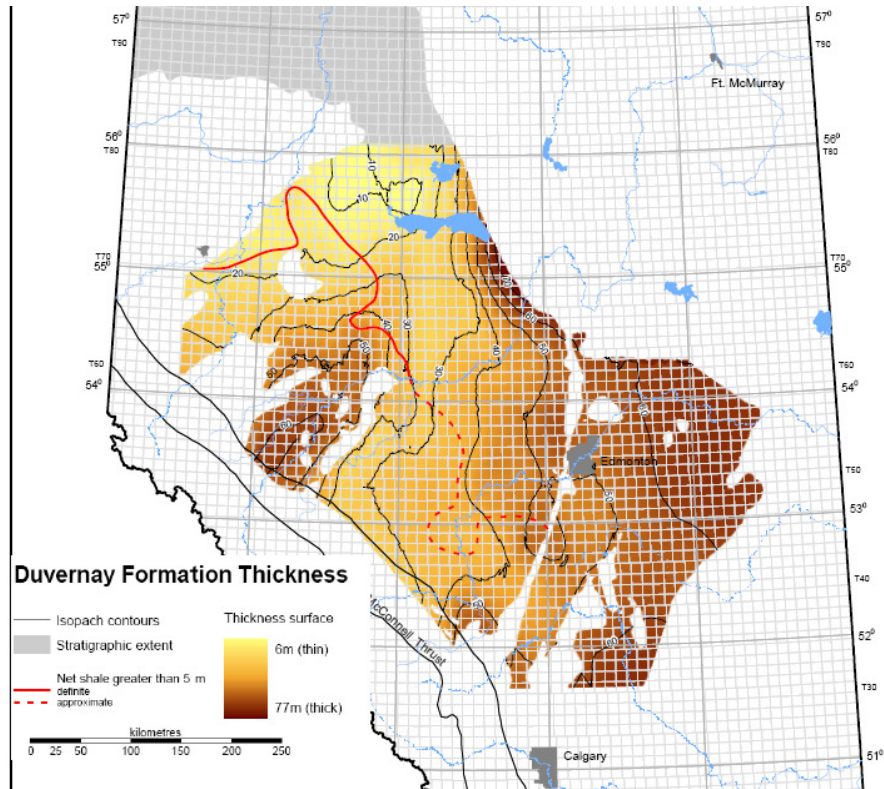


Figure DM-D2. Isopach map of Duvernay Formation from NW-SE of Alberta

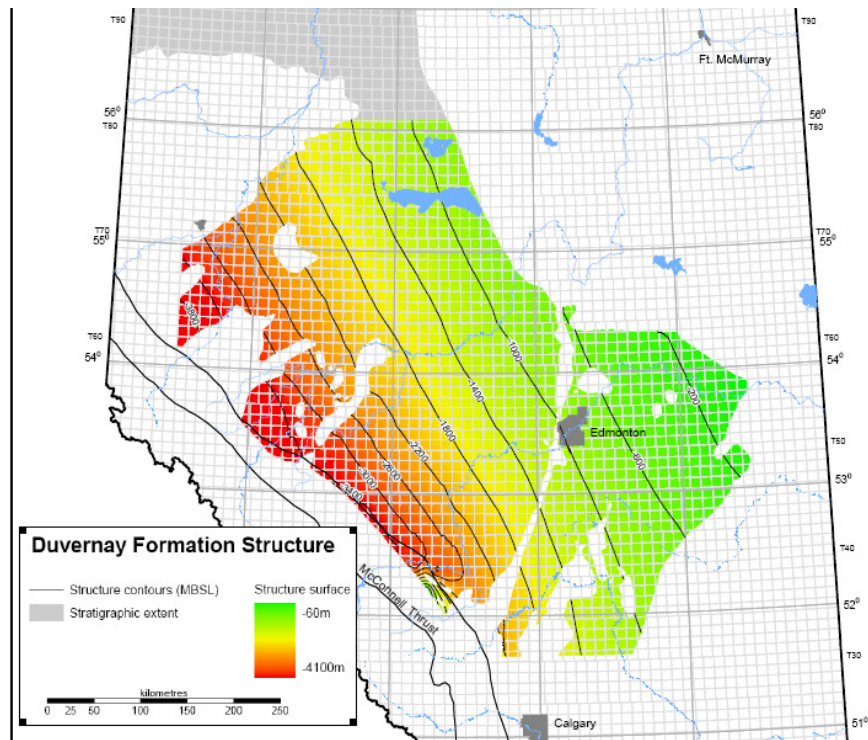


Figure DM-D3. Structure contour map of Duvernay Formation from NW-SE Alberta.

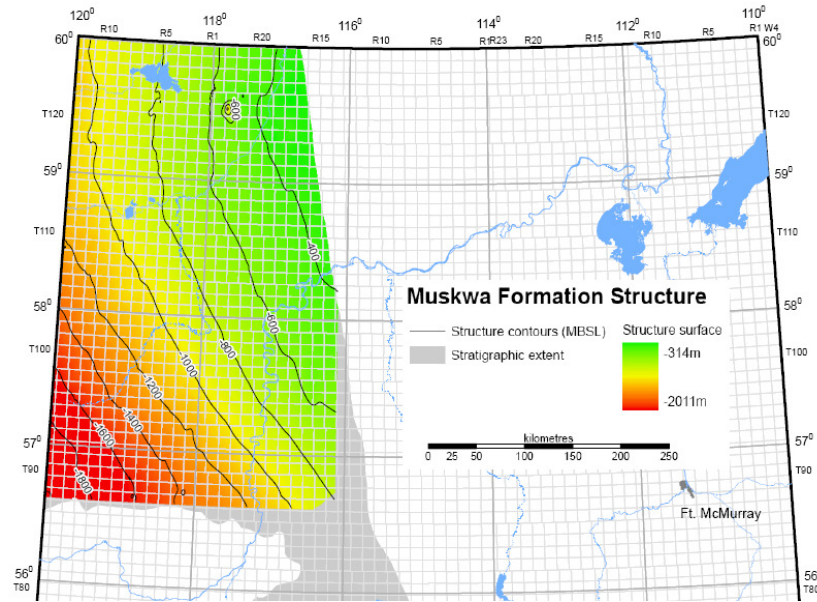


Figure DM-D4. Muskwa Formation structure contour map within the NW of Alberta

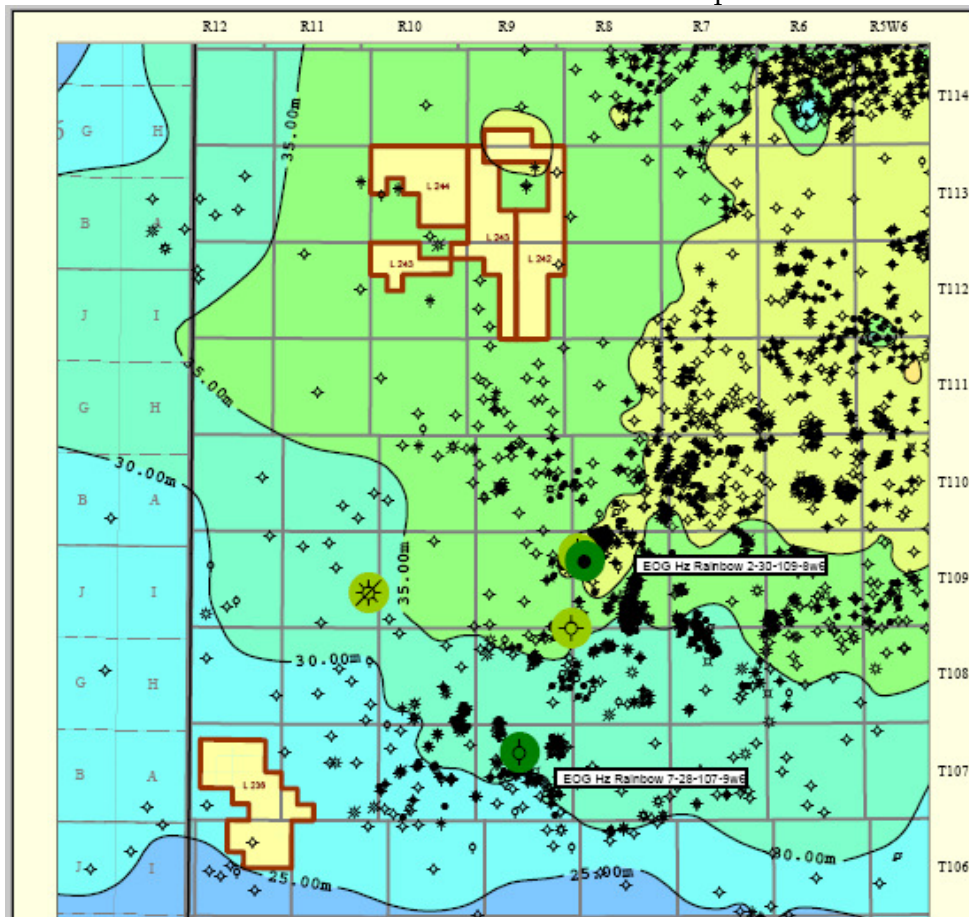


Figure DM-D4a. Muskwa Formation Isopach map Alberta (source: Sayer Energy Advisors Report, October 2011)

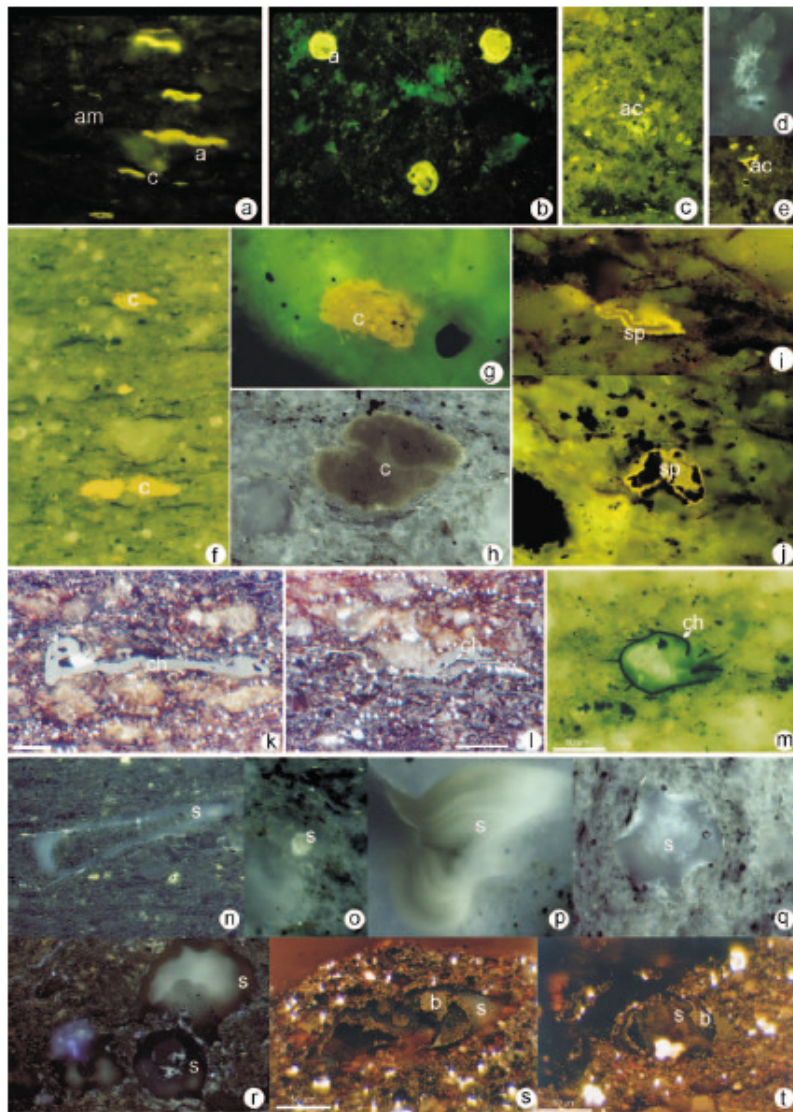


Fig. 6. Macerals and microfossils in organic facies (OF) A, B, C and D of Upper Devonian Woodbend group; scale bar (50  $\mu$ m) shown in "s" is for photos without scale bar. Fluorescence and reflected white light (k, l, s, t), water or oil immersion. a. OF A: Large and small prasinophyte alginites (a), brown-fluorescing amorphinite matrix (am) and carbonate (c); b. Prasinophyte alginites (a). c–e. Acanthomorphic acritarchs (ac) in OF B. f–h. OF C: Coccolidal alginites (c); h shows degraded alginite. i, j. OF C: Sporinite (sp), bisaccate pollen grain in j. k–m. OF B–C: Chitinous microfossils (ch) are probably derived from scolecodonts and chitinozoans. n–r. OF D: siliceous microfossils (s) mainly derived from Chrysophyte alginites like Radiolaria. s, t. OF D: Siliceous microfossils (c) infilled by granular bitumen (b).

Figure DM-E1. Photomicrographs of various source rocks from the upper Devonian Woodbend Group (Duvernay and Muskwa formations) (after Stasiuk and Fowler, 2004)

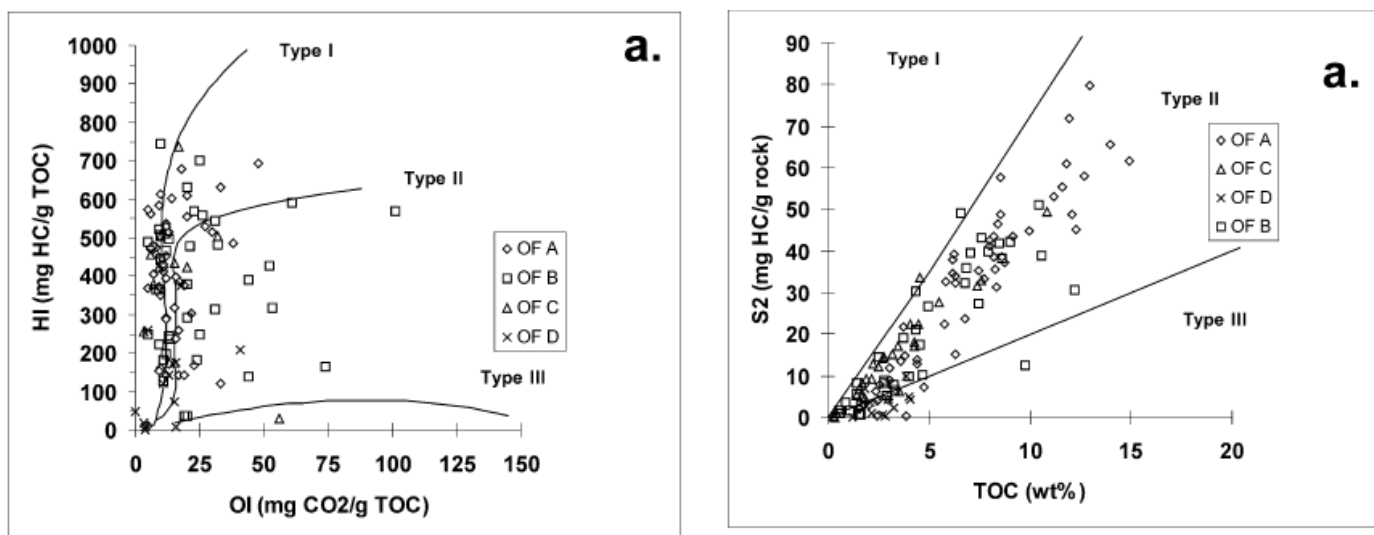


Figure DM-E2. Source rock potential of Duvernay and Muskwa formations from Alberta (after Stasiuk and Fowler, 2004)

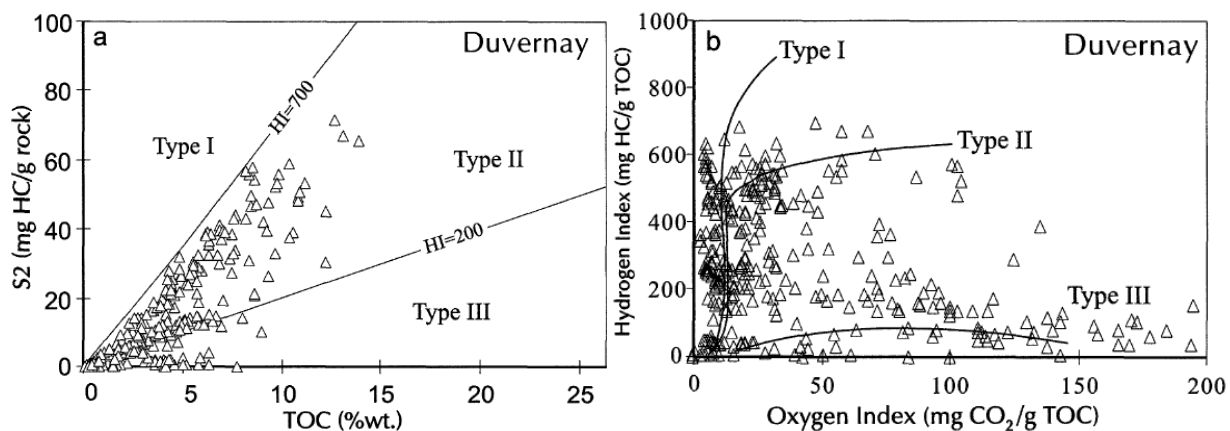
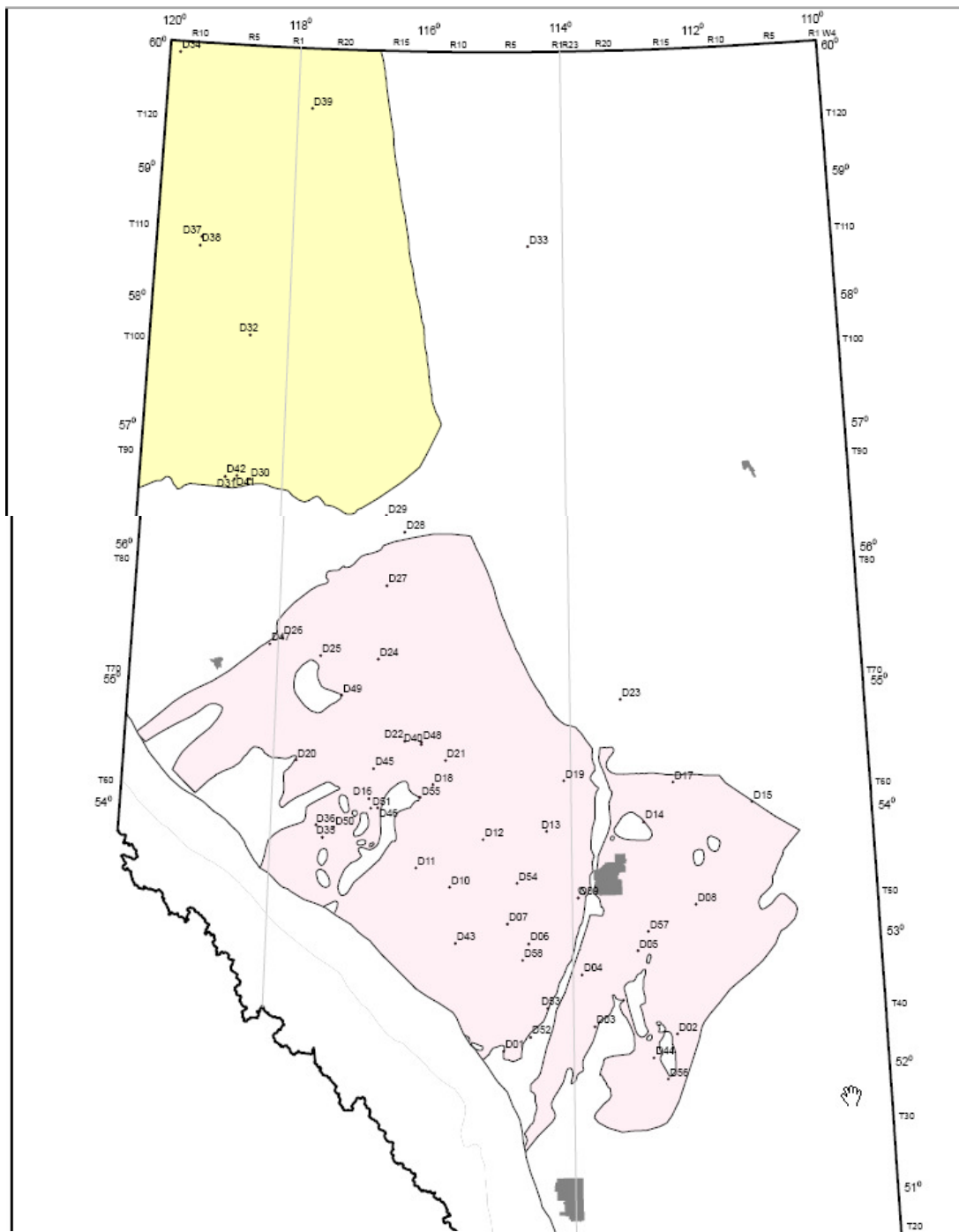


Figure DM-E3. Rock-Eval pyrolysis data of Duvernay Formation source rocks from central Alberta (source: Fowler et al., 2001)



**Muskwa and Duvernay Formations**

- Muskwa/Duvernay
- Duvernay
- Muskwa



Figure DM-F1. Sample Location for Muskwa and Duvernay formations (source: John Pawlowicz, ERCB).

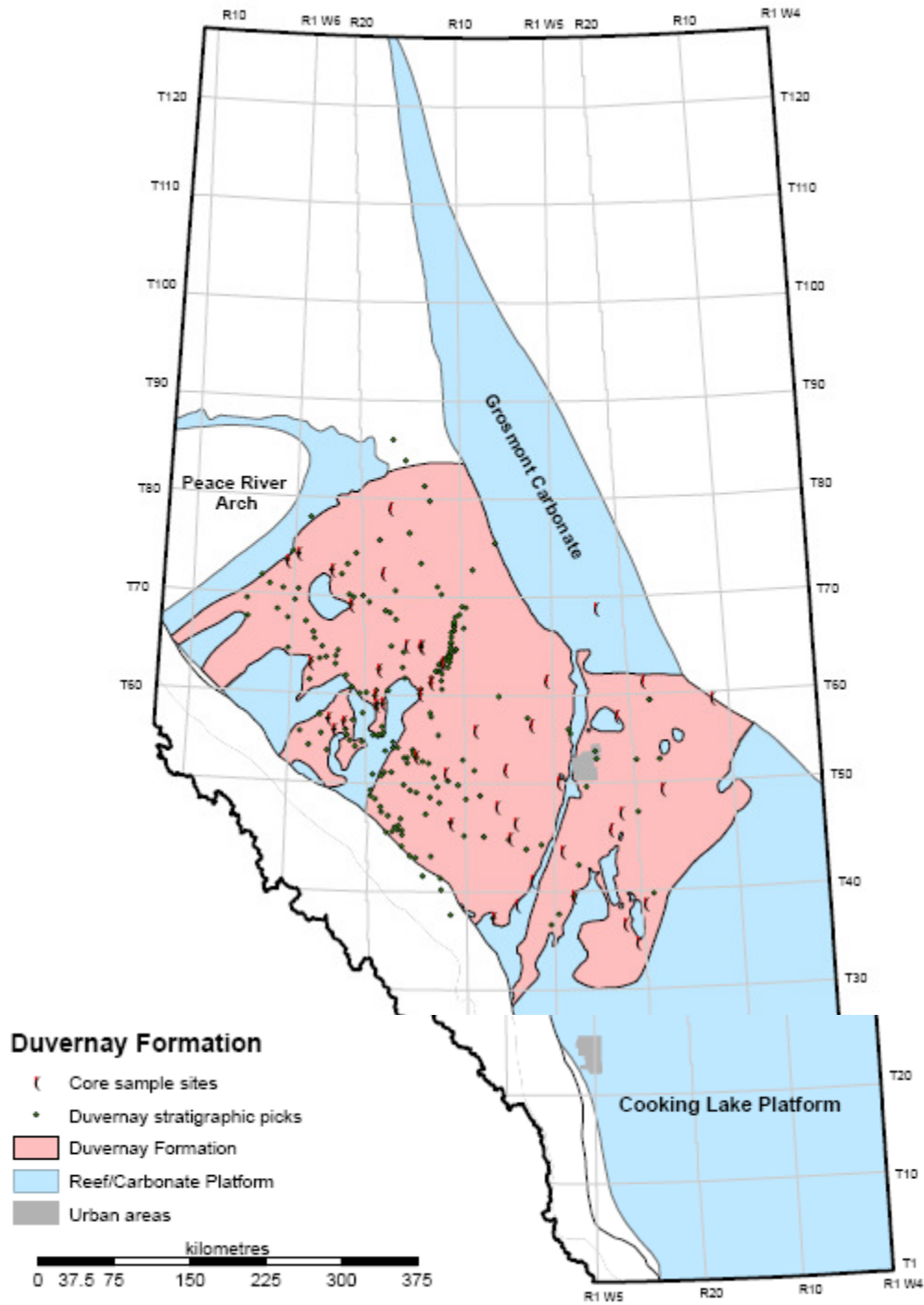
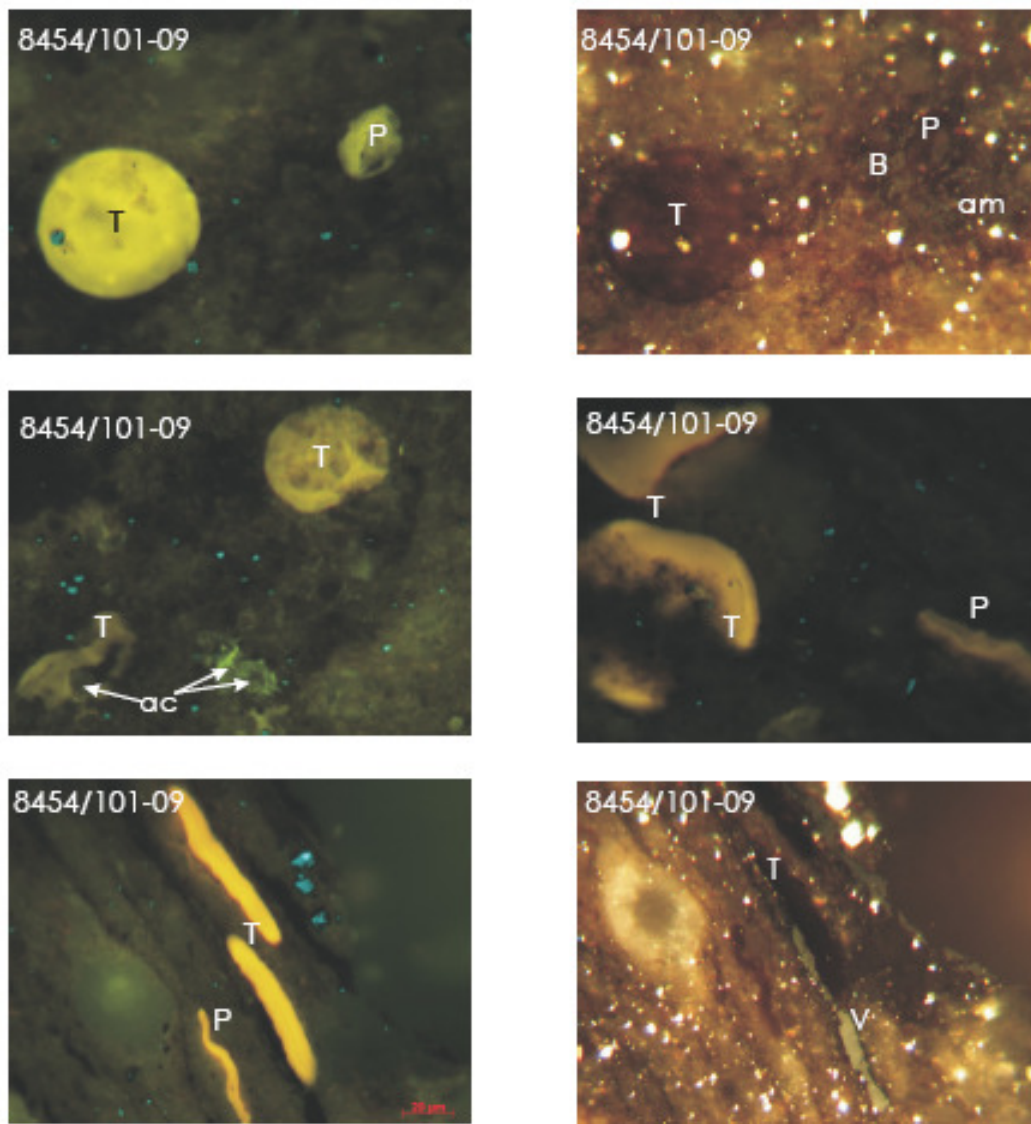
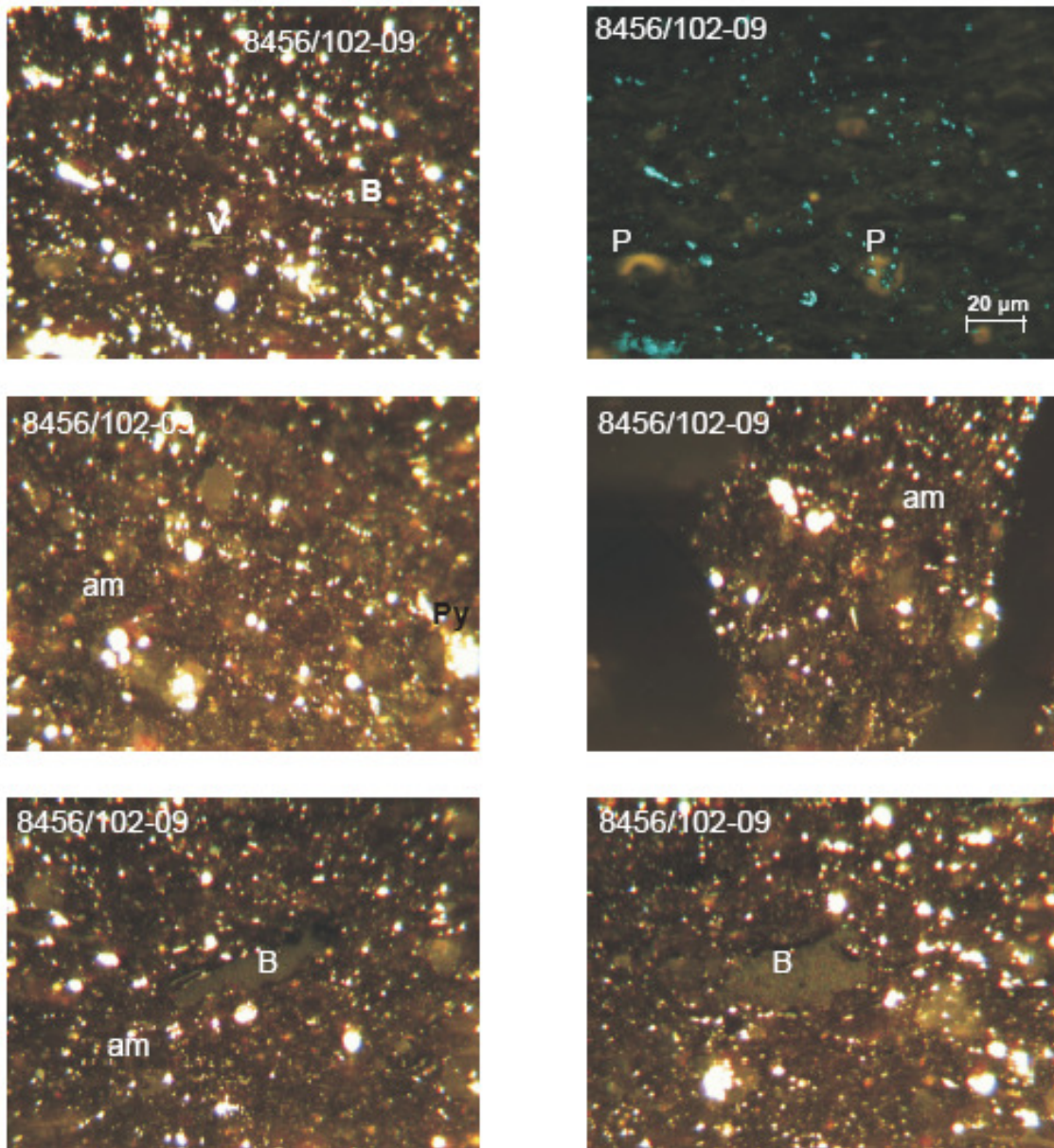


Figure DM-F2. Sample Location for Duvernay formations with Rock-Eval data locations (source: John Pawlowicz, ERCB)



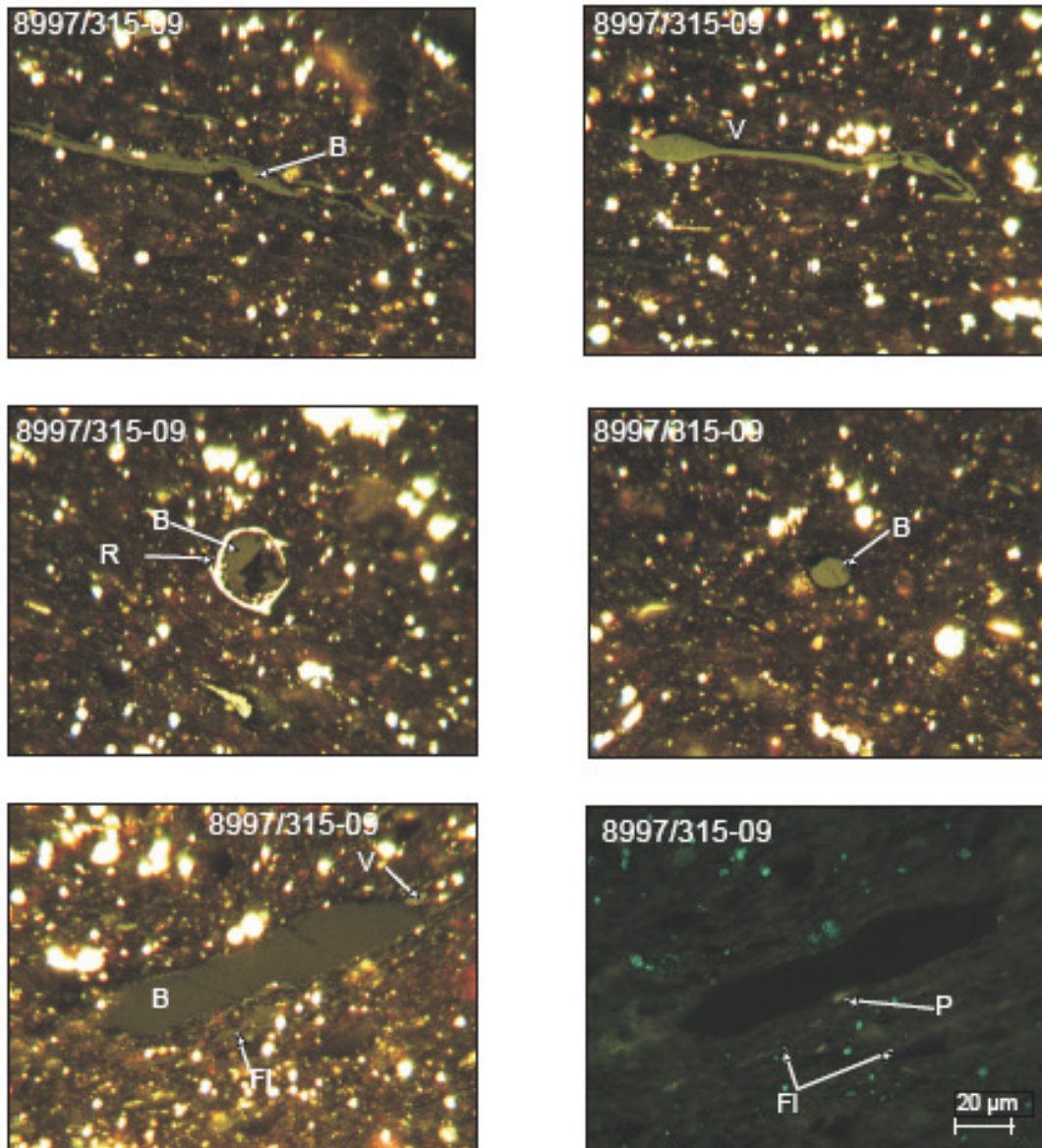
AGS 8454/GSC 101-09 (Duvernay; 100/04-33-068-22W4/00, 1054.6 m core depth). Organic-rich, carbonaceous shale with mostly long thin continuous lenses of dark brown amorphous and non-amorphous kerogen (am) with some pyrite and micrinite inclusions. Orange fluorescing bitumen (B) are also observed proximal to kerogen lenses. Major amount of yellow fluorescing, thick-walled *Tasmanites* sp. (T). Micrhystridium cf. acanthomorphic arcitarchs (ac), and Prasinophyte (P) alginite. V= Vitrinite. Scale bar applies to all images. (In oil, polished surface, fluorescence and reflected white light, 50X magnification).

Figure DM-G1. Photomicrographs of various whole rock kerogen that includes mainly mixtures of Telalginite (*Tasmanites*) and Amorphinite 2 and minor lamalginite (*Prasinophytes*); Duvernay Formation shale – sample 8454 (source: Beaton et al. 2010).



AGS 8456/GSC 102-09 (Duvernay; 100/05-17-058-08W5/00, 2358.8 m core depth). Shale rich in dark brown amorphous kerogen (am) with pyrite and micrinite inclusions in a marl matrix. Minor amount of both yellow fluorescing to non-fluorescing *Prasinophyte* (P) alginite, and chitinous microfossils (ch, possibly from fish remains or bone). Some granular bitumen (B) with a rare amount of allochthonous vitrinite (V) and inertinite (I) macerals. Scale bar applies to all images. (In oil, polished surface, fluorescence and reflected white light, 50X magnification).

Figure DM-G2. Photomicrographs of various whole rock kerogen that includes mainly framboidal pyrite rich amorphinite 2 and solid bitumen and minor lamalginite (*Prasinophytes*); Duvernay Formation shale - sample 8456 (Source: Beaton et al. 2010).



AGS 8997/GSC 315-09 (Muskwa; 100/02-30-088-04W6/0, 2413.4 m core depth). Sieve-like network of weak brown fluorescing fluoramorphinite matrix with high amount of pyrite and thin, golden-yellow fluorescing Prasinophyte (P), Leiosphaeridia (L), orange-fluorescing sporinite (Sp), filamentous alginite (FI) and other alginite (A). Minor to rare amount of measurable small vitrinite (V), bitumen (B) and brown fluorescing bituminite (Bt) lenses, bright yellow-fluorescing soluble hydrocarbon (oil, see arrow) within pores, and bitumen-filled acanthomorphic marine acritarch. Scale bar applies to all images. (In oil, polished surface, fluorescence and reflected white light, 50X magnification). R = Radiolaria. T = Tasminites, I = Inertinite. Some measured %Ro are suppressed due to soluble hydrocarbon present

Figure DM-G3a. Photomicrographs of whole rock kerogen that includes mainly amorphous liptinite (amorphinite 2) with minor algodetrinite, sporinite and solid bitumen; Muskwa Formation carbonate mudstone – sample 8997; depth: 2413.4 m (source: Beaton et al. 2010).

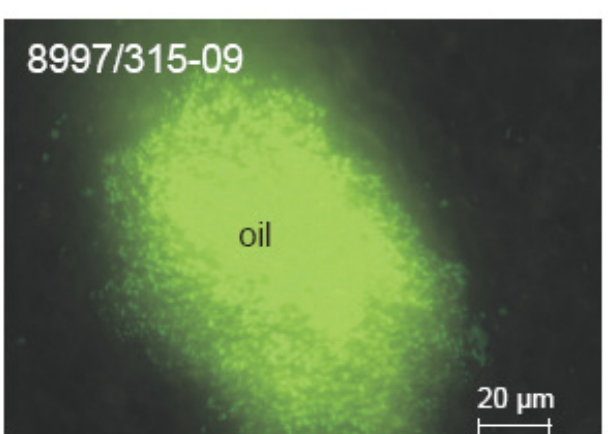
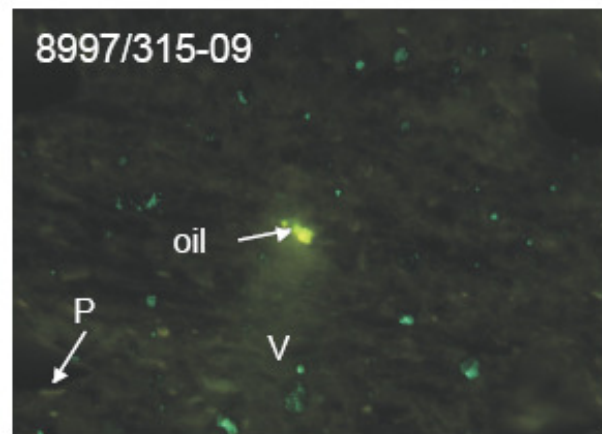
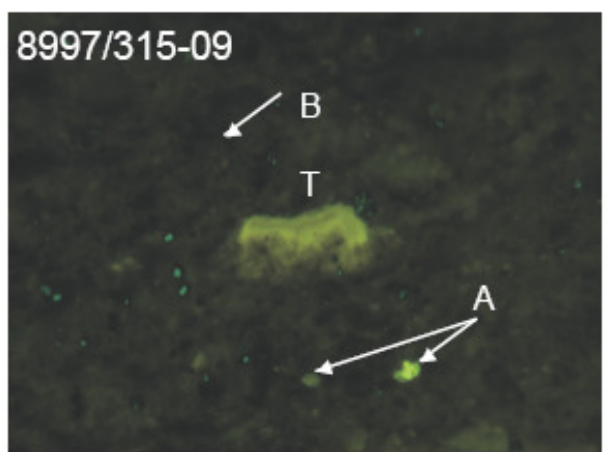
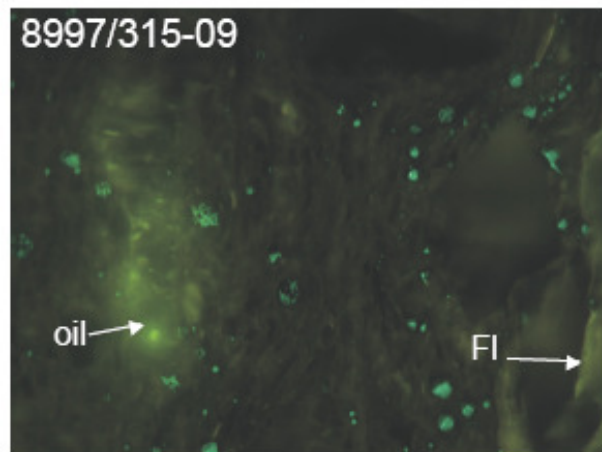
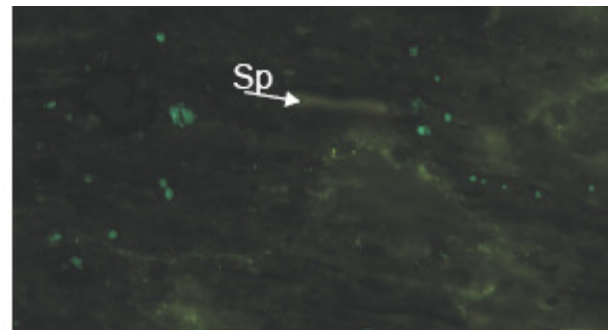
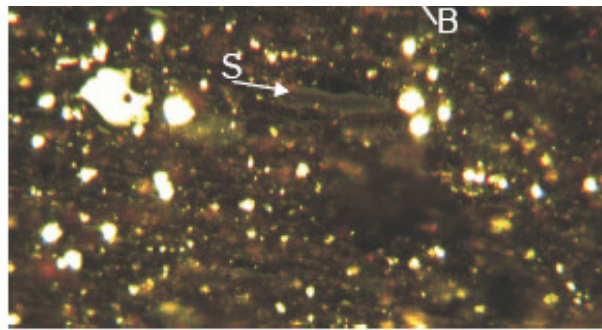


Figure DM-G3a. Photomicrographs of whole rock kerogen in blue light excitation. The photo includes mainly amorphous liptinite (amorphinite 2)(mostly nonfluorescent) with minor telalginite (*Tasmanites*) algodetrinite, sporinite (sp) and abundant oil (oil); Muskwa Formation carbonate mudstone – sample 8997; depth: 2413.4 m (source: Beaton et al. 2010).

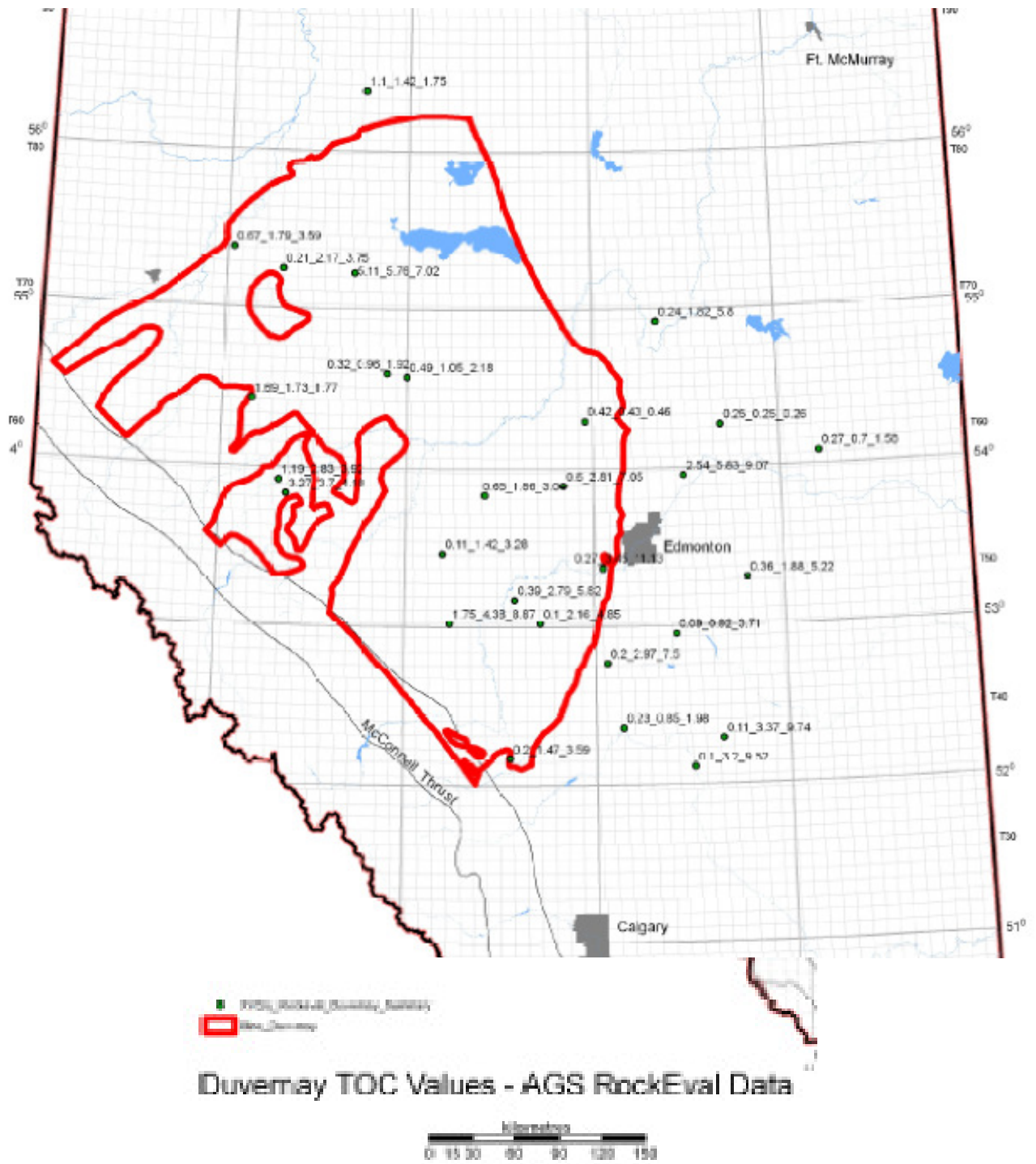


Figure DM-H1. Average distribution of the Total Organic Carbon (TOC) values of the Duvernay Formation within Alberta

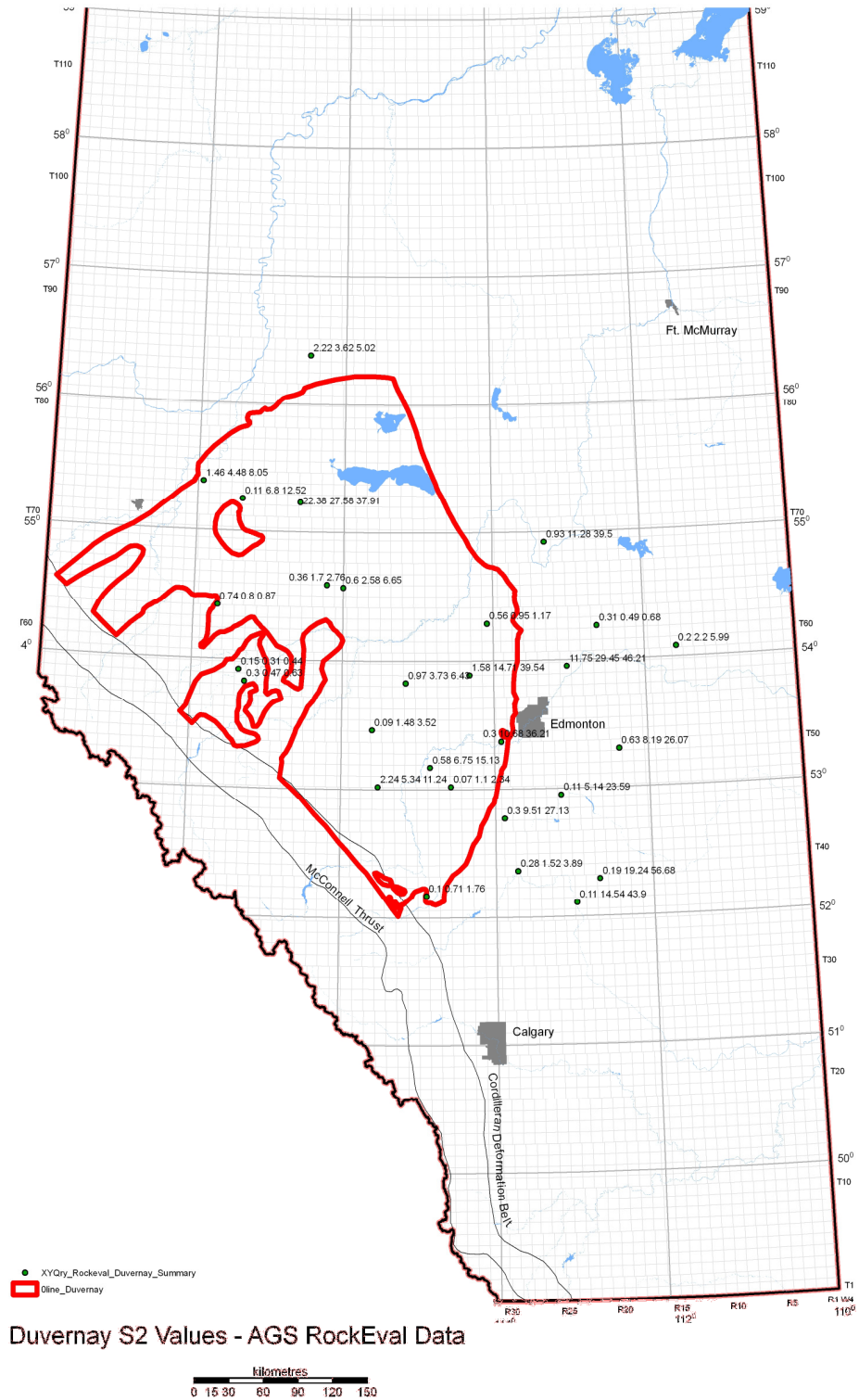


Figure DM-H2. Average distribution of the S2 (mg pyrolyzed hydrocarbons in mg) values from the Rock=Eval pyrolysis of the source rocks from the Duvernay Formation within Alberta

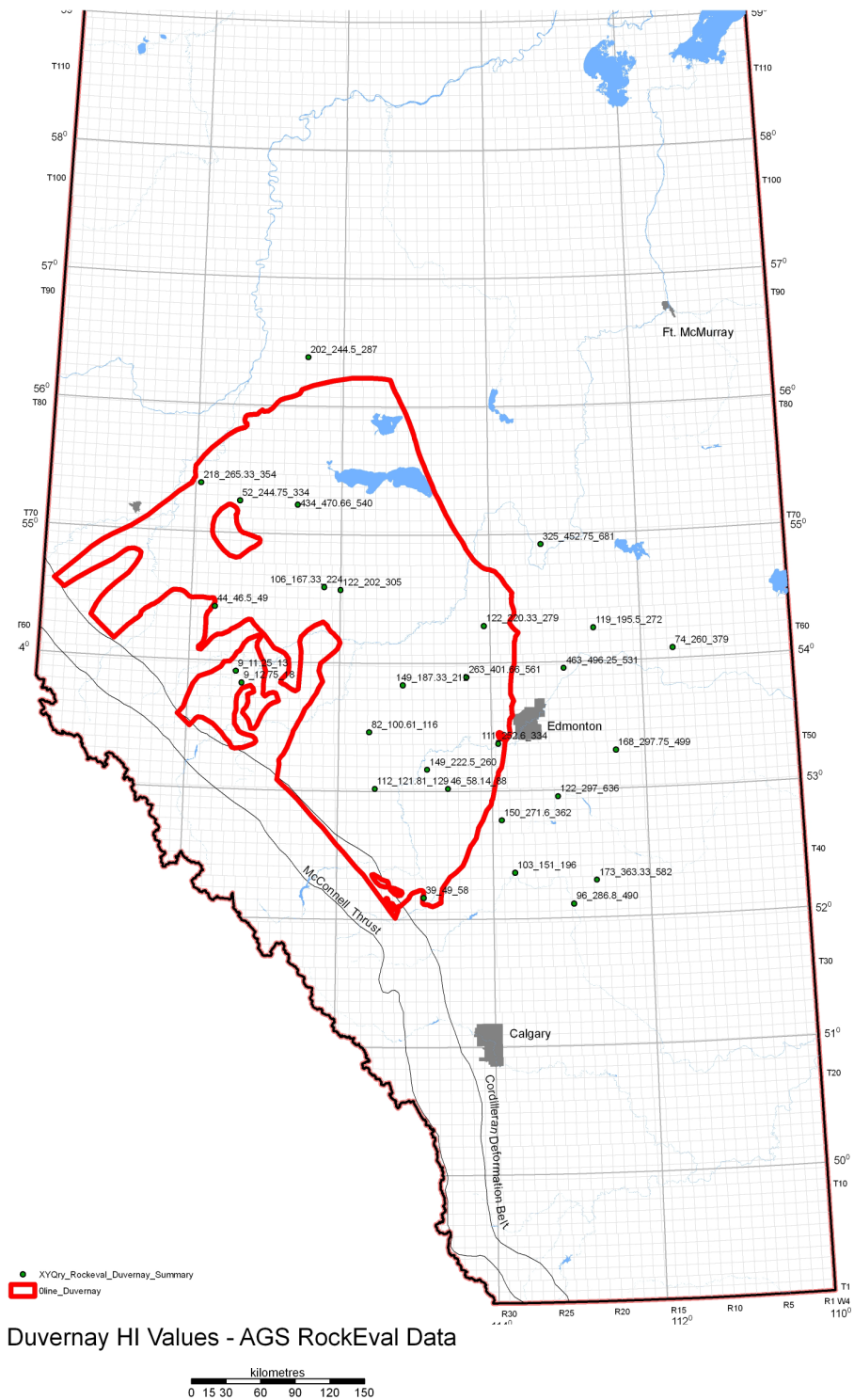


Figure DM-H3. Average distribution of the hydrogen index (mg HC/g TOC) values from the Rock=Eval pyrolysis of the source rocks from the Duvernay Formation within Alberta

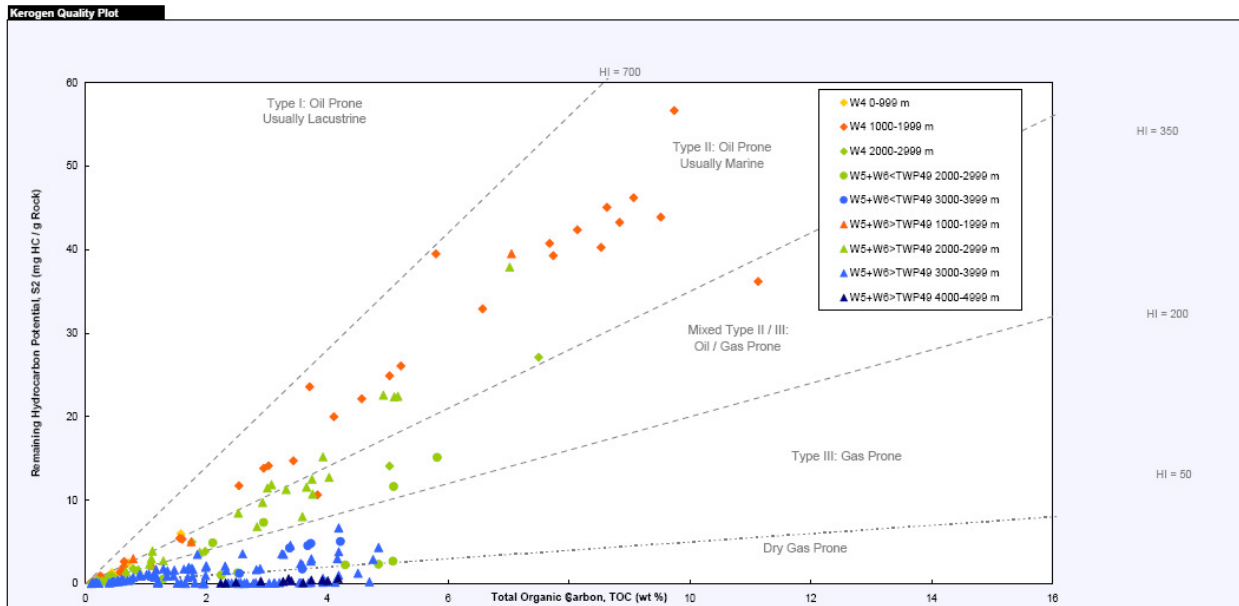


Figure DM-11a. Kerogen quality plot of total organic carbon and remaining hydrocarbon potential (S2 in mg/g rock) from Duvernay Formation source rock. Colour indicates depth range of the samples (Source: John Pawlowicz, ERCB, 2012).

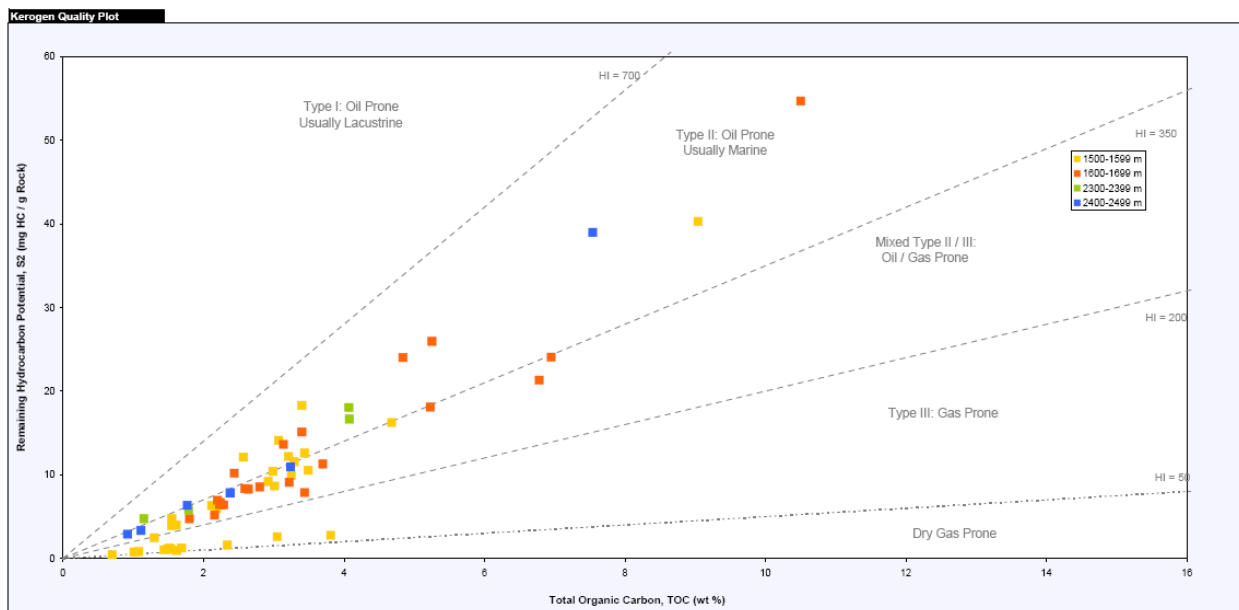


Figure DM-11b. Kerogen quality plot of total organic carbon and remaining hydrocarbon potential (S2 in mg/g rock) from Muskwa Formation source rock. Colour indicates depth range of the samples (Source: John Pawlowicz, ERCB, 2012).

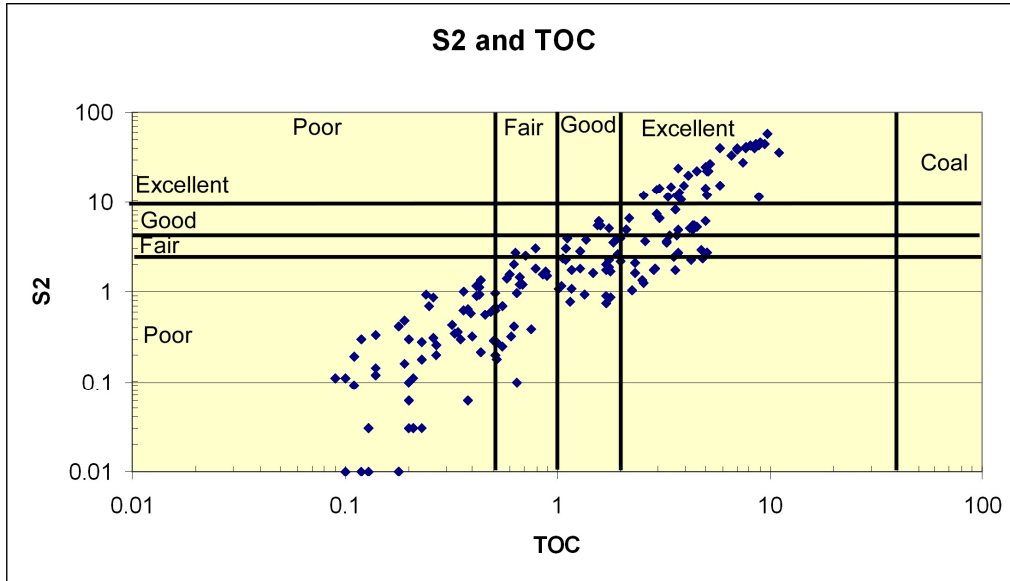


Figure DM-I1c. Cross plots of S2 and TOC values of the sediments from the Duvernay Formation within Alberta showing the quality of the source rock potential (Dean Rokosh, ERCB; 2012)

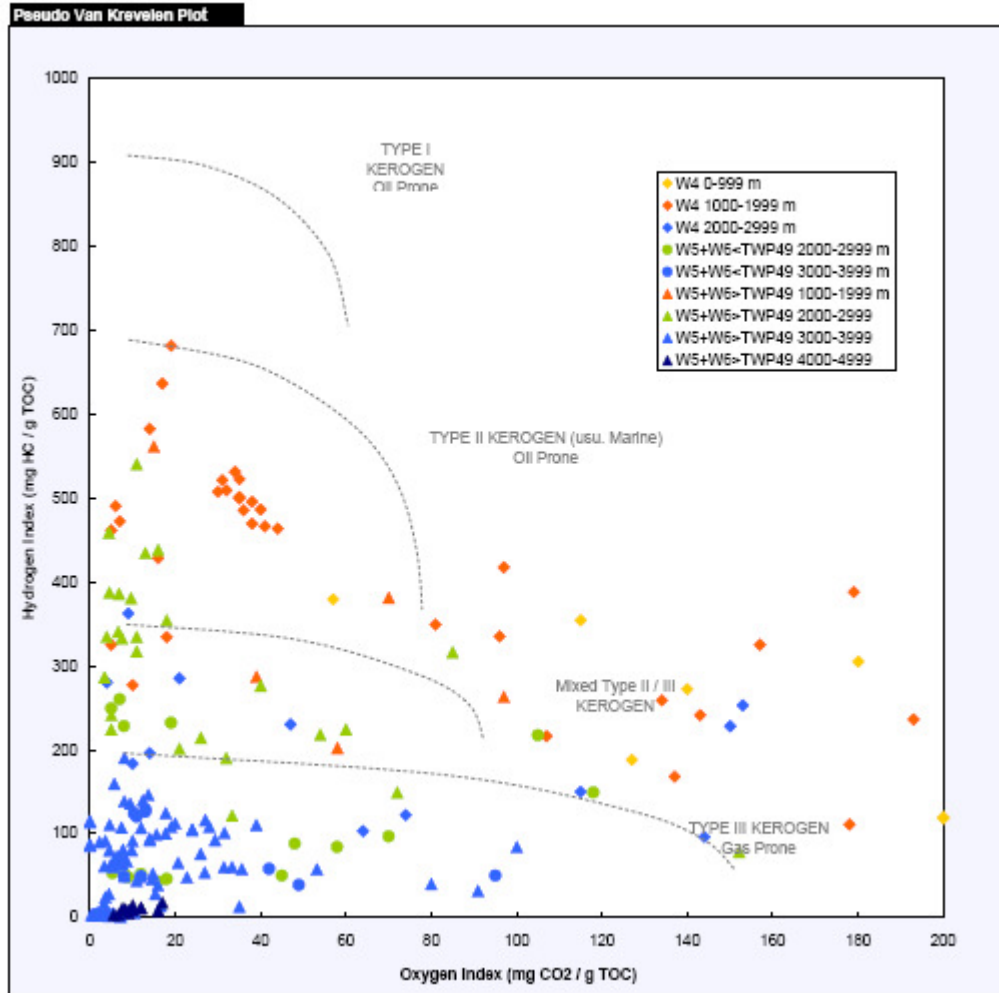


Figure DM-I2a. Pseudo-van Krevelen plot of hydrogen index versus oxygen index showing source rock potential from Duvernay Formation, Alberta (source: by John Pawlowicz, ERCB). Colour indicates depth range of the samples

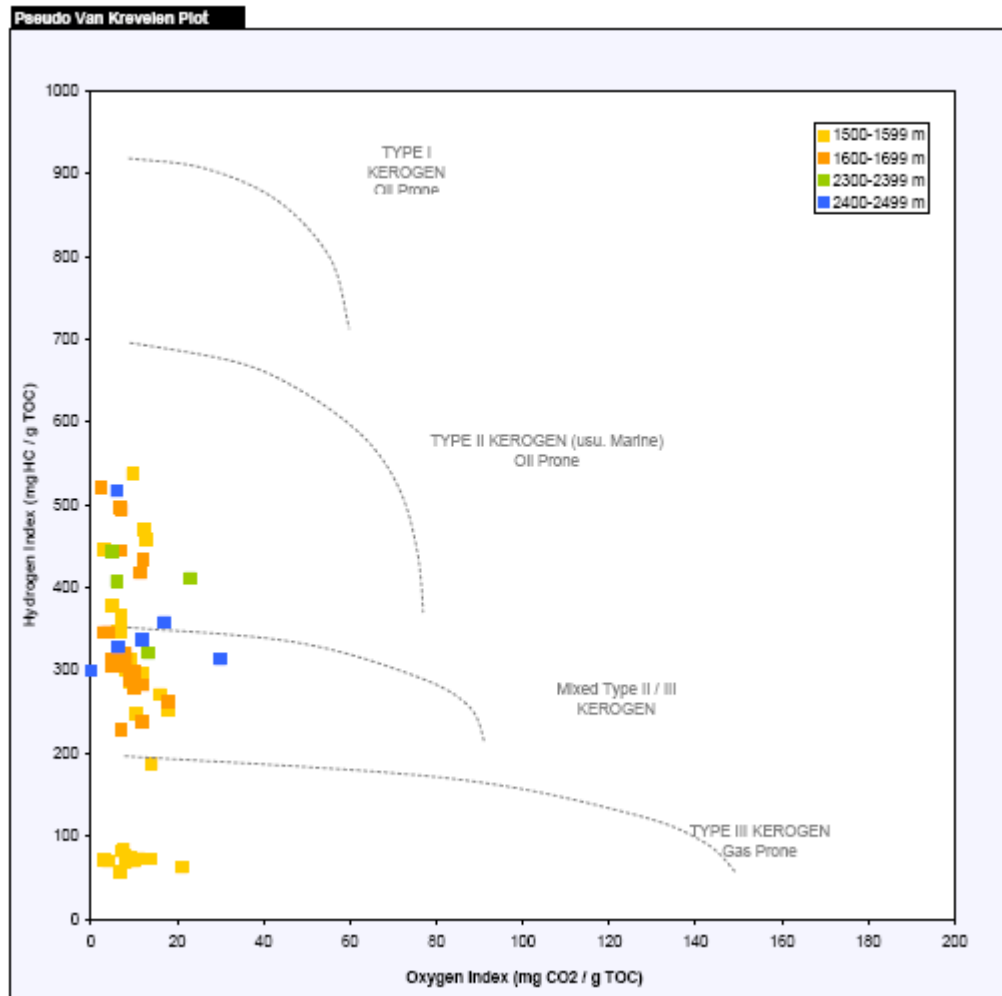


Figure DM-I2b. Pseudo-van Krevelen plot of hydrogen index versus oxygen index showing source rock potential from Muskwa Formation source rocks, Alberta (source: by John Pawlowlicz, ERCB). Colour indicates depth range of the samples

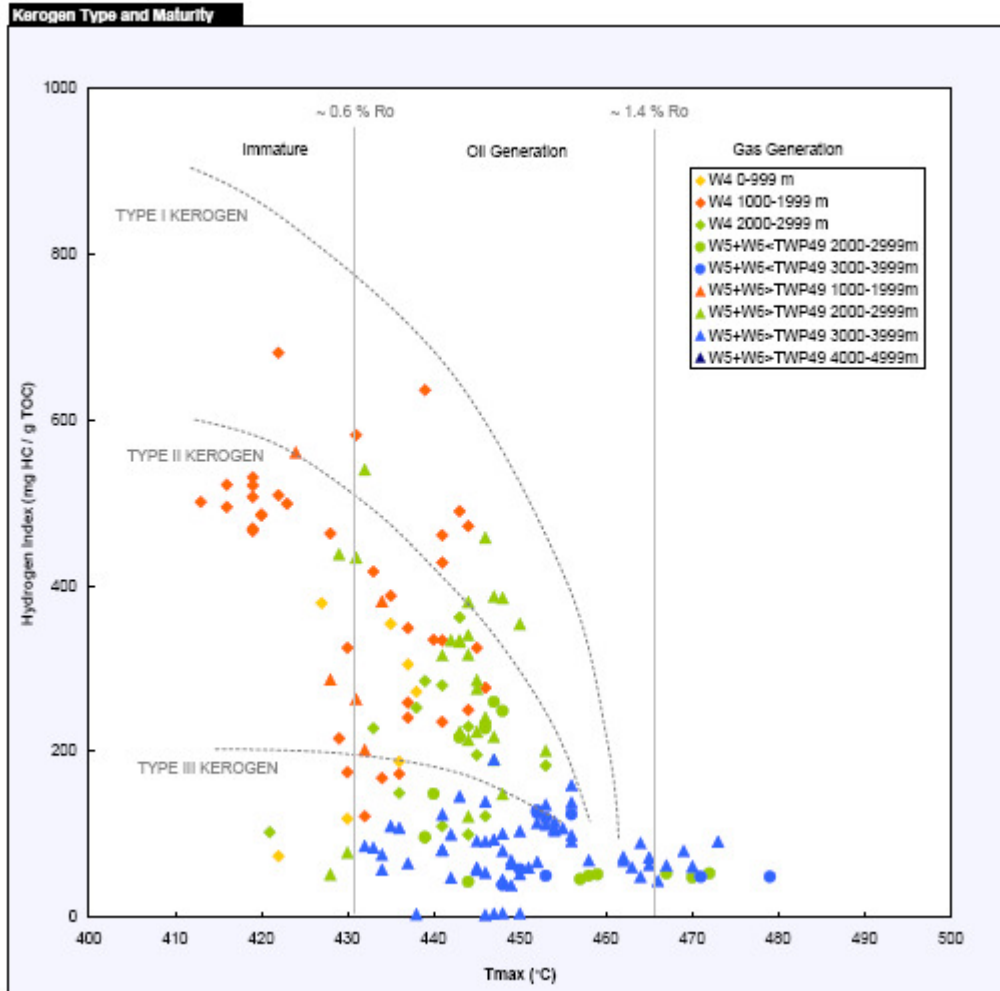


Figure DM-I3a. Maturity (using Tmax) versus hydrogen index showing the variability of source rock potential from various samples from Duvernay Formation, Alberta (source: by John Pawlowicz, ERCB). Colour indicates depth range of the samples

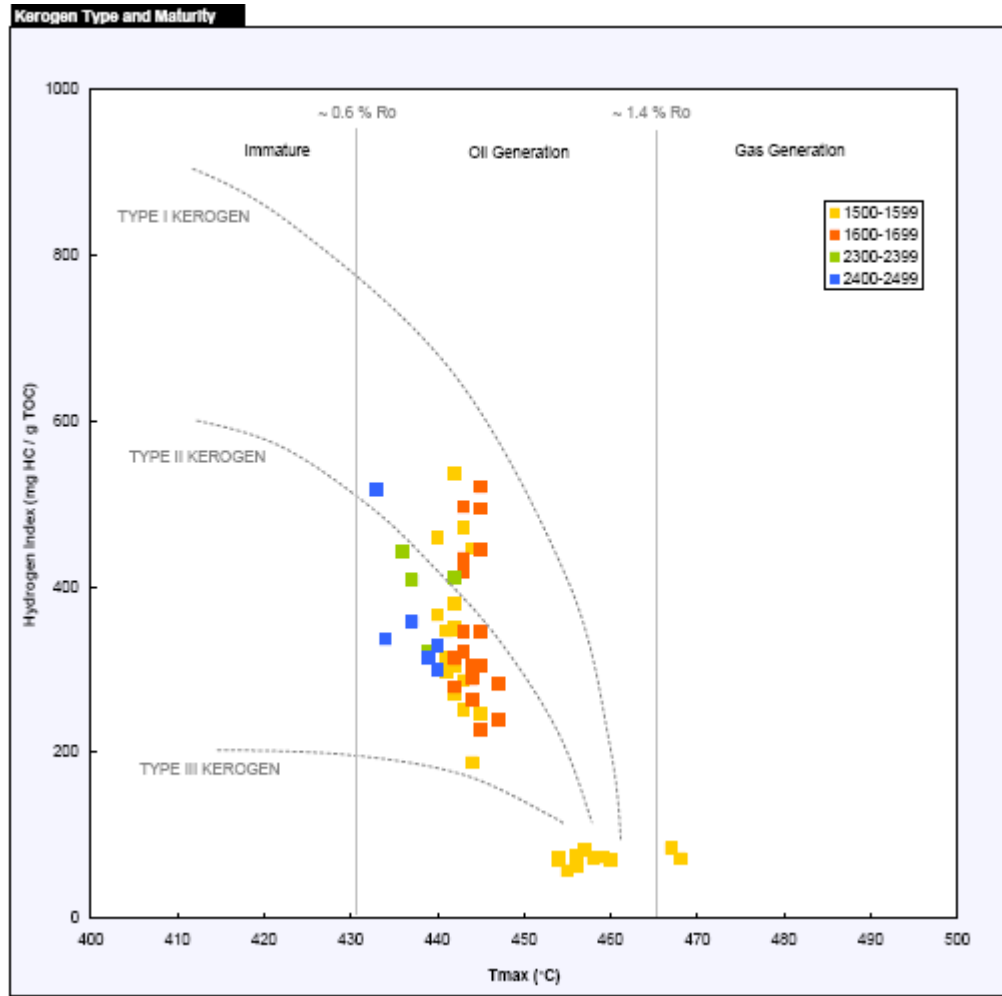


Figure DM-I3b. Maturity (using Tmax) versus hydrogen index showing the variability of source rock potential from various samples from Duvernay Formation, Alberta (source: by John Pawlowicz, ERCB). Colour indicates depth range of the samples

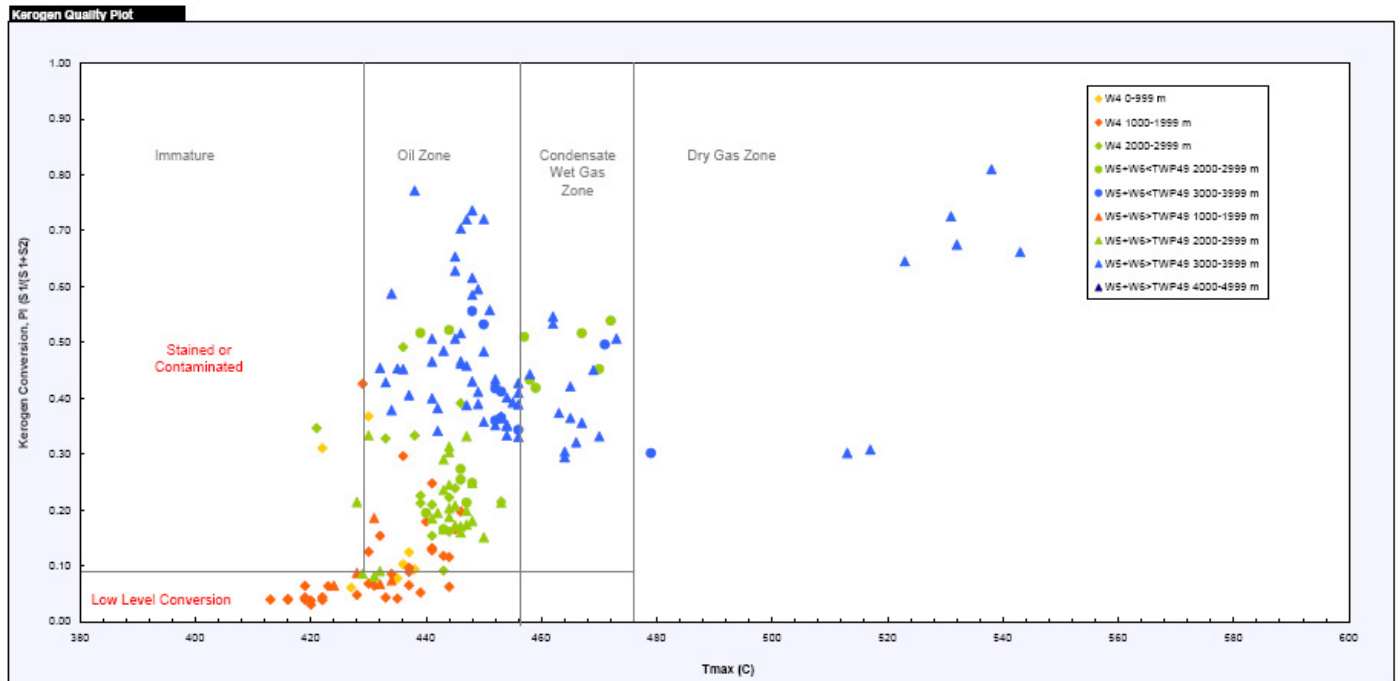


Figure DM-I4a. HC transformation versus maturity showing samples connected immature, oil, condensate and dry gas zones areas from Duvernay Formation, Alberta (source: by John Pawlowicz, ERCB). Colour indicates depth range of the samples

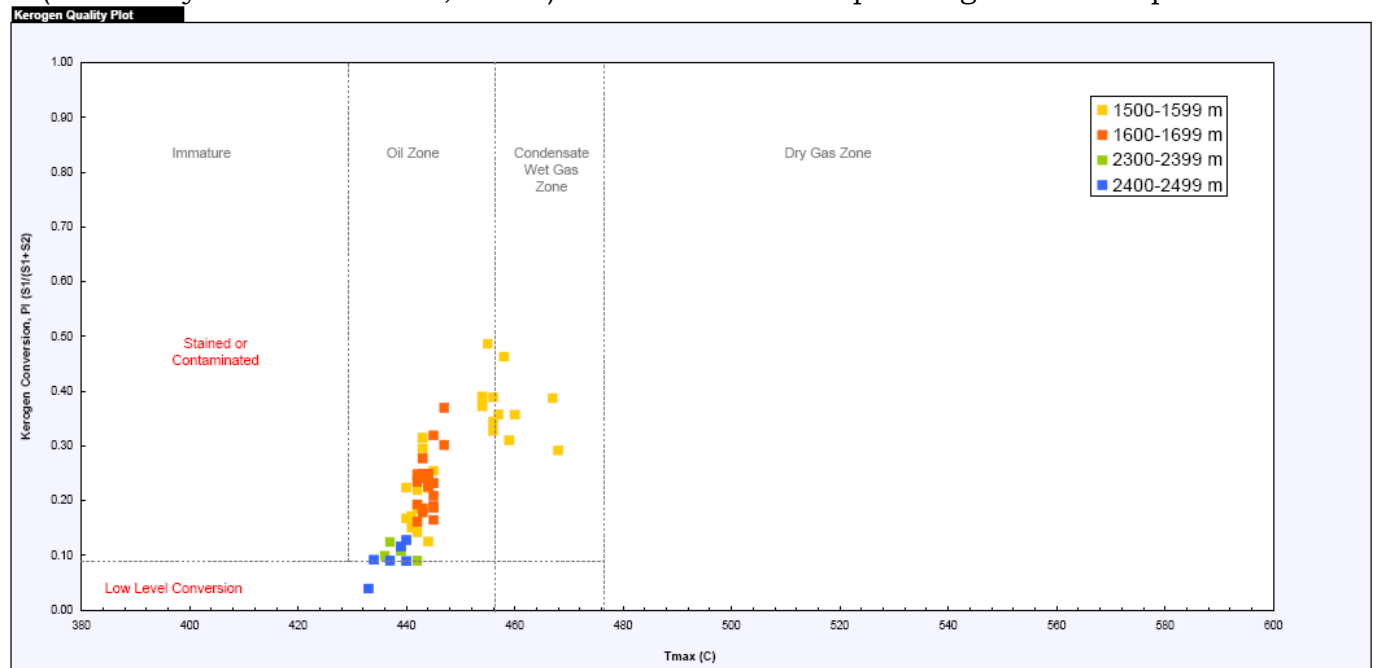


Figure DM-I4b. HC transformation versus maturity showing samples connected immature, oil, condensate and dry gas zones areas from Muskwa Formation, Alberta (source: by John Pawlowicz, ERCB). Colour indicates depth range of the samples

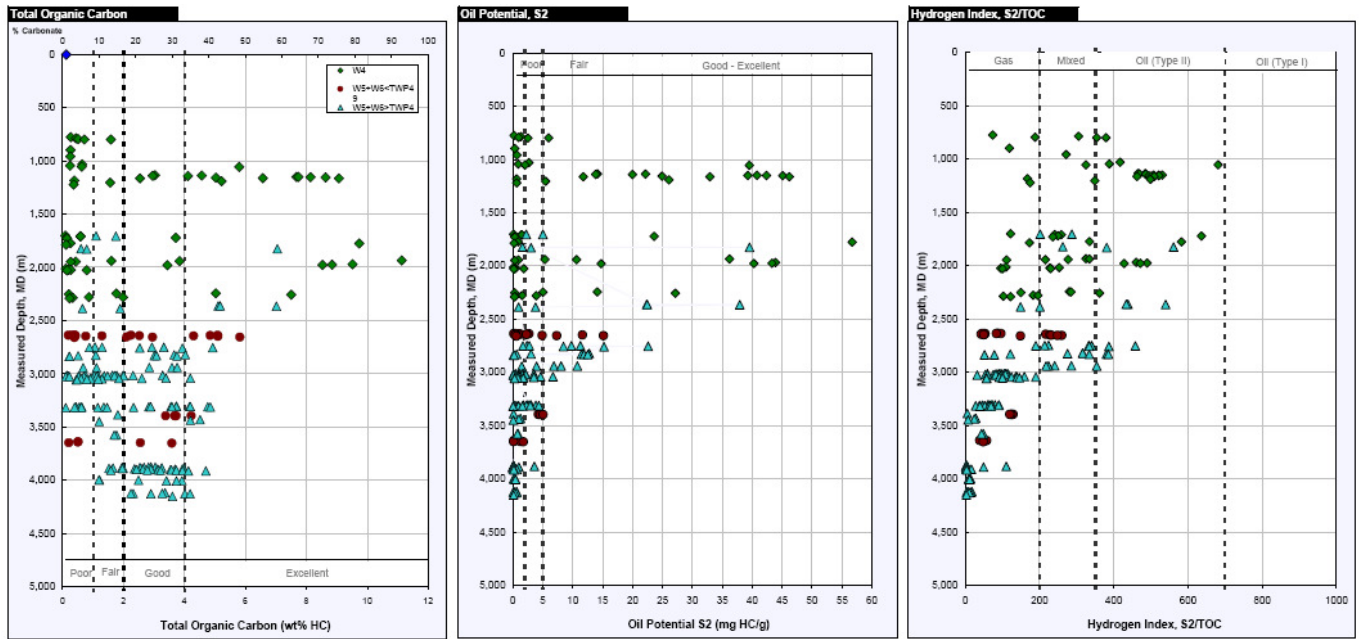


Figure DM-15a. Depthwise plot of TOC, Oil Potential, and Hydrogen Index of various samples from Duvernay Formation, Alberta (source: by John Pawlowicz, ERCB)

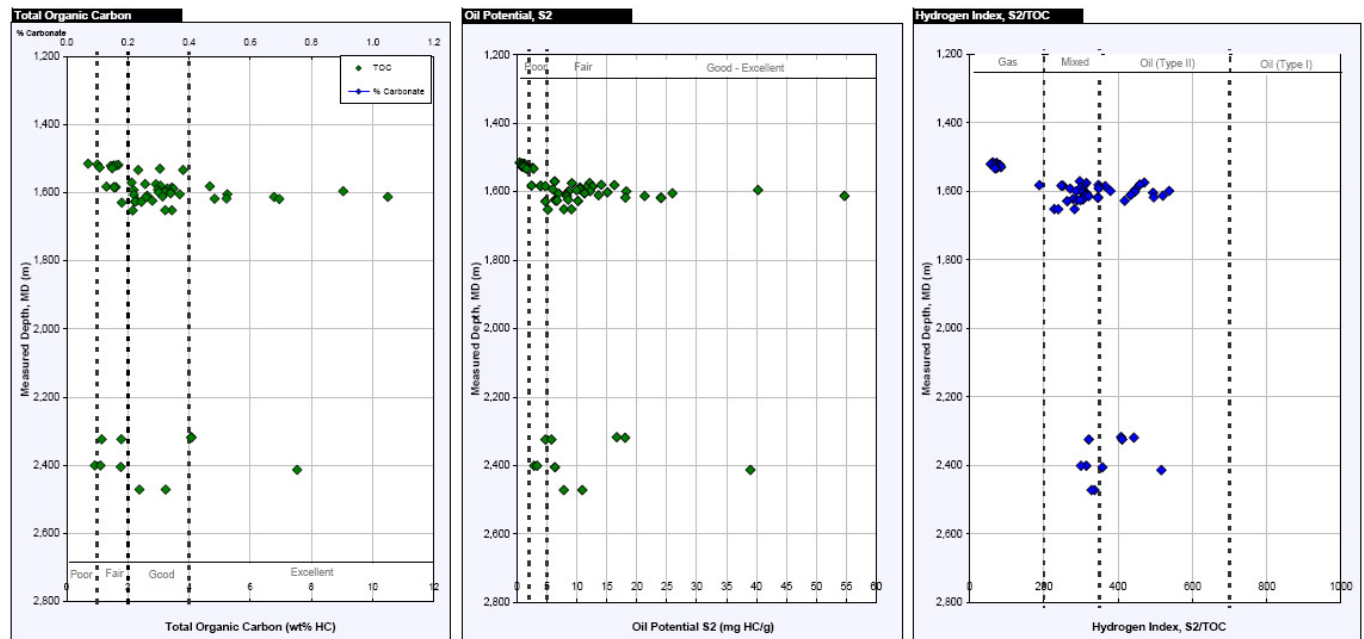


Figure DM-15b. Depthwise plot of TOC, Oil Potential, and Hydrogen Index of various samples from Muskwa Formation, Alberta (source: John Pawlowicz, ERCB)

### Duvernay

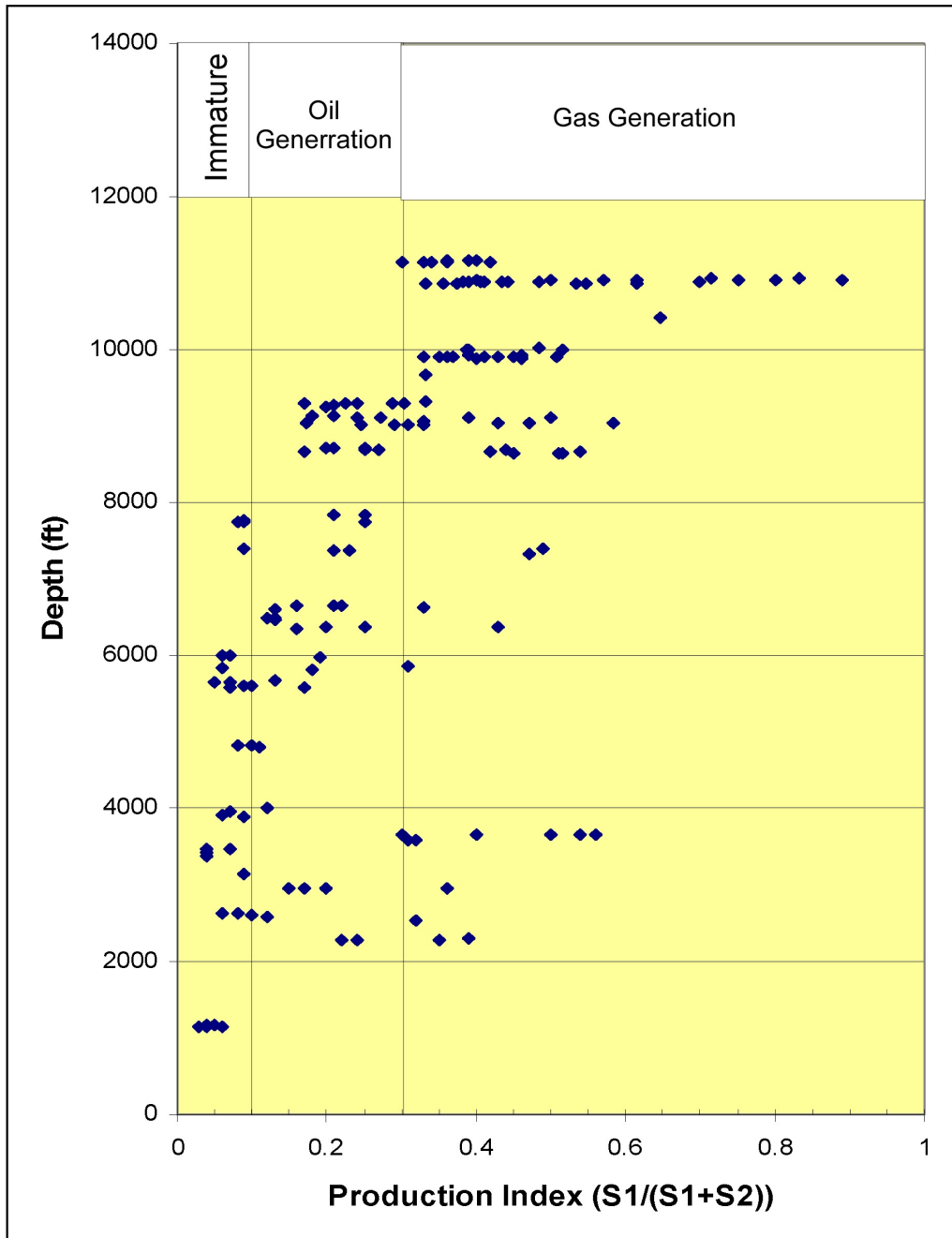


Figure DM-I6. Cross plots of the depth versus Production index values for Duvernay & Muskwa Formation source rock samples

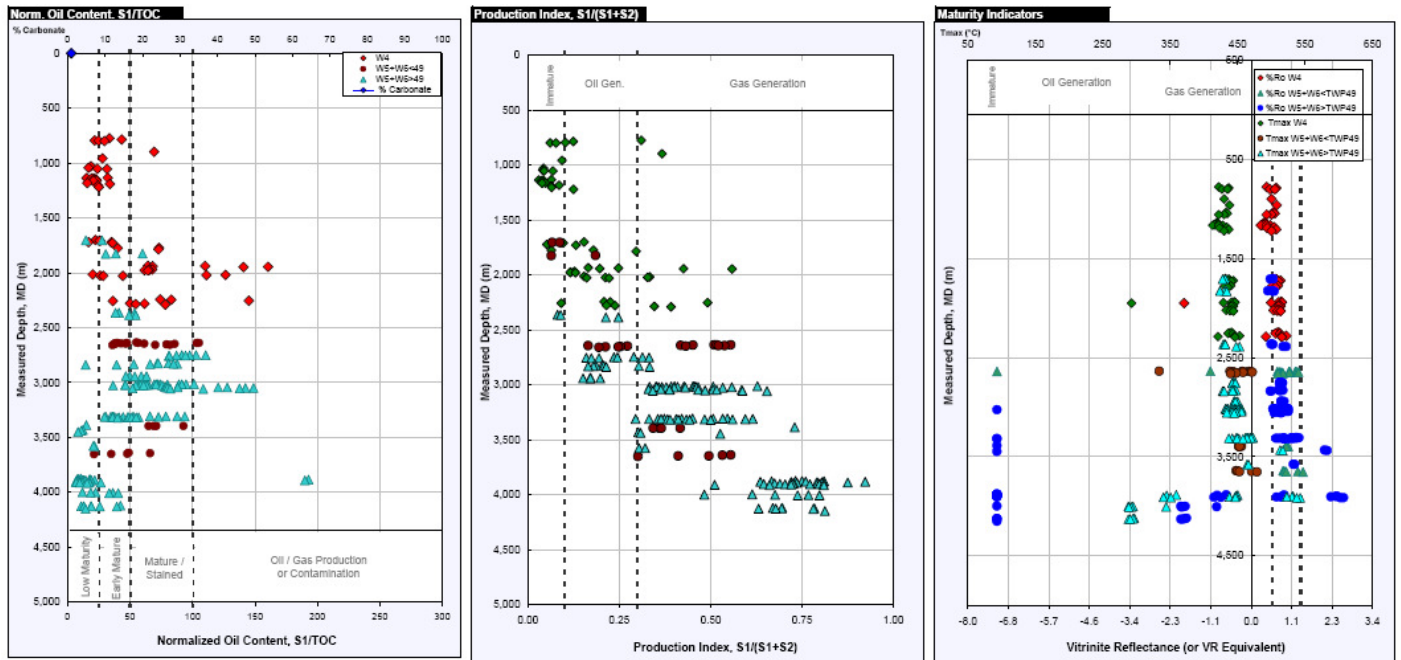


Figure DM-I7a. Depthwise plot of normalized oil content, production indices, and maturity from various samples analyzed with Rock-Eval pyrolysis from Duvernay Formation, Alberta (source: John Pawlowicz, ERCB)

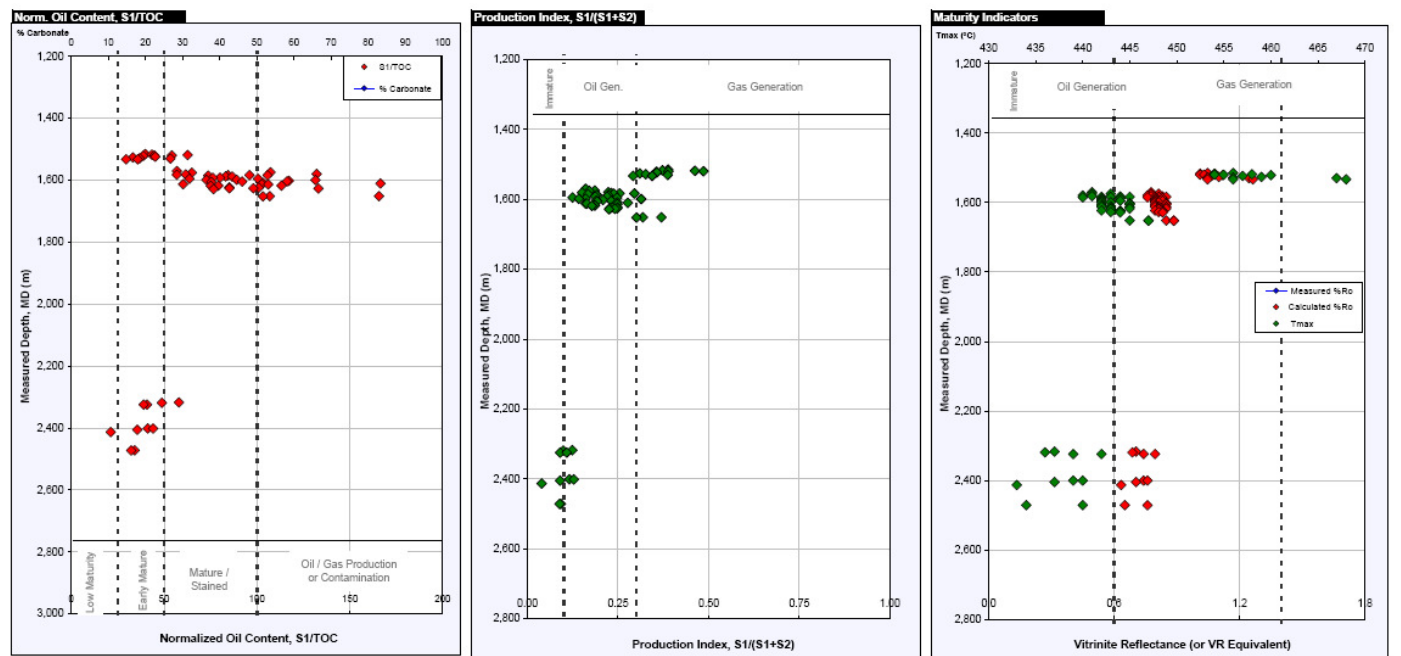
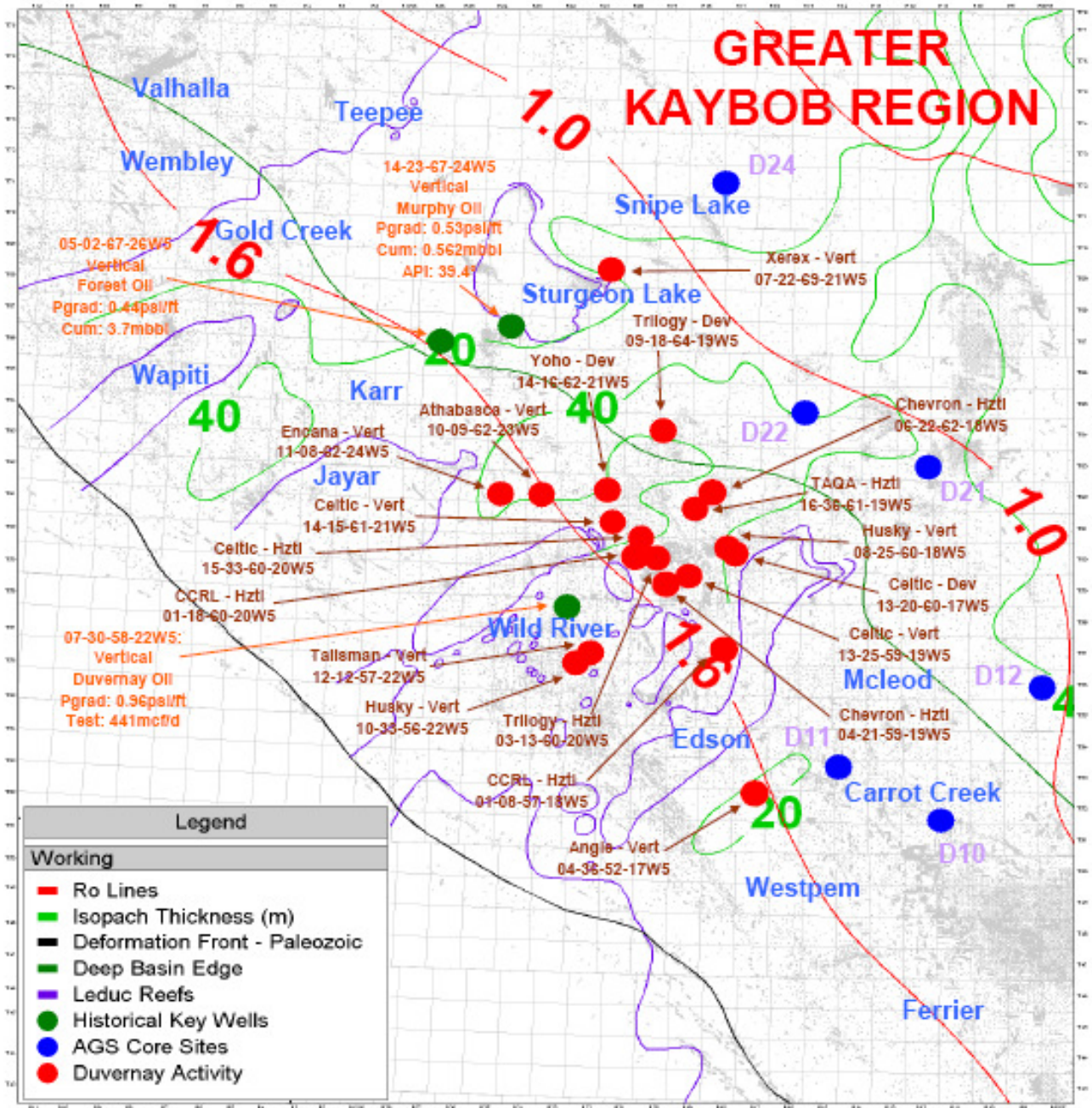
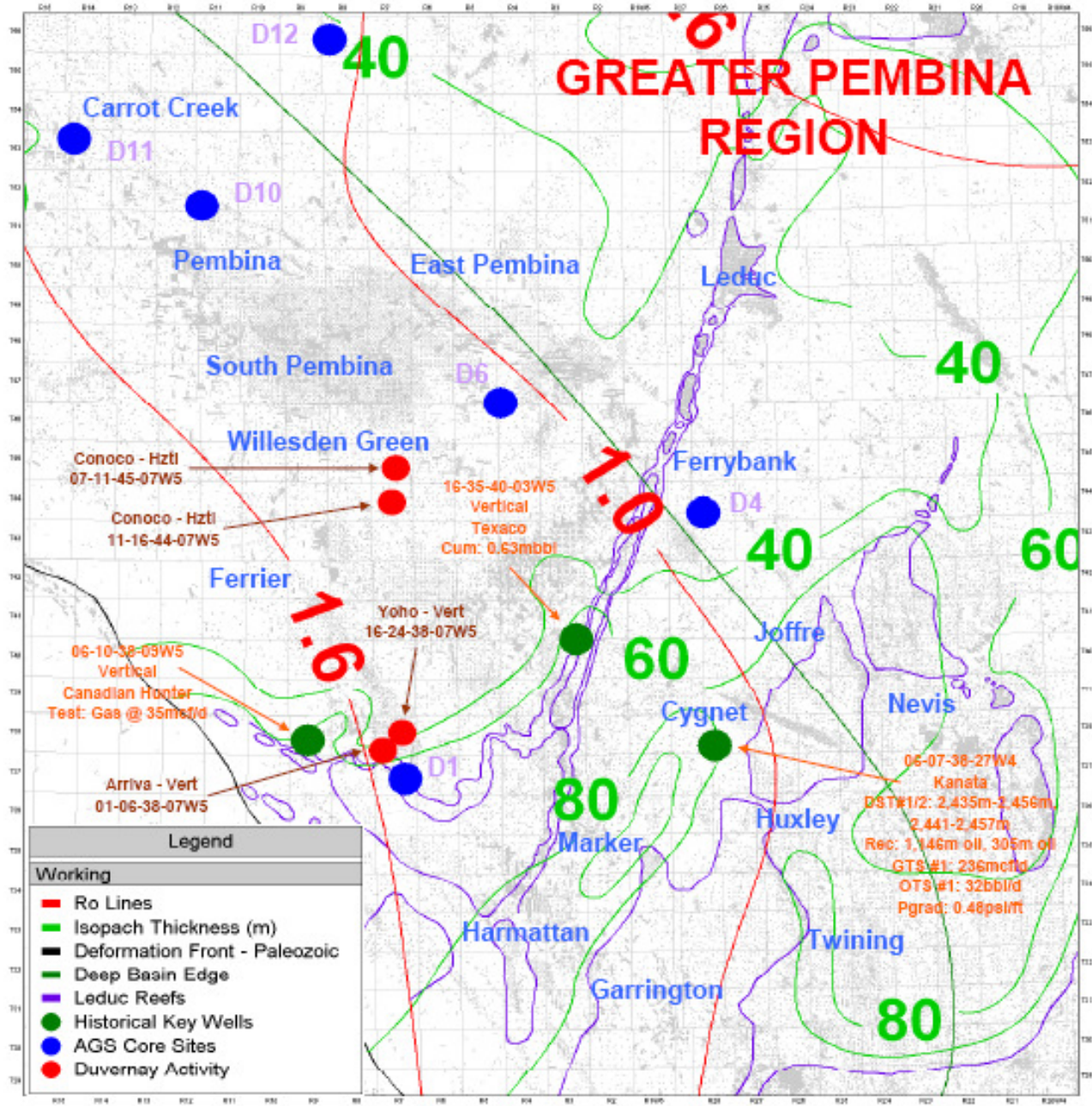


Figure DM-I7b. Depthwise plot of normalized oil content, production indices, and maturity from various samples analyzed with Rock-Eval pyrolysis from Muskwa Formation, Alberta (source: John Pawlowicz, ERCB)



Source: geoSCOUT, Macquarie Research, August 2011

Figure DM-J1. Vitritine Ro (red lines) contours and the isopach thickness (green letters) of the Duvernay Formation along with Land Sales ages within the Greater Keybob area (source: Macquarie Equities Research, 2011)



Source: geoSCOUT, Macquarie Research, August 2011

Figure DM-J2. Vitrinite Ro (red lines) contours and the isopach thickness (green letters) of the Duvernay Formation along with Land Sales ages within the Greater Pembina area (source: Macquarie Equities Research, 2011)

Sample No.	Site No.	Quartz	Feldspars			Pyrite	Hem.	Clay Minerals						Carbonates				Sulphate Gyp.	FlAp.	Brlt.	Total				
			Albite	Micro.	Ortho.			Musc.	Bio.	Paly.	Kaol.	Illite	Mont.	ClCh.	Calcite	Dolo.	Ank.					Rhod.			
8135	D8	12.3	2.5		2.9	3.5		15.4							2.9	54.5	2.1	3.0	0.1			0.7	0.3	100.2	
8456	D12	46.5	3.5		3.5	2.5	0.5	14.4				3.9	3.7		3.0	8.9	3.9	4.7				0.5	0.5	100.0	
8461	D15	5.0	2.0		3.3	3.4		4.6				0.7			3.4	74.9	0.4	1.9	0.3				0.2	100.1	
8480	D21	15.2	3.7	15.6				5.1				11.6	3.3		9.4		3.7	28.0	1.4	2.6				0.6	100.2
8996	D31	31.3	2.4		11.1	3.5	0.5	19.3	1.8			0.5	4.0		1.9		22.5					0.4	0.8	100.0	
9205	D10	24.0	5.5		4.2	1.0	0.3	8.1				2.1			3.0	21.5	18.4	11.7					0.4	100.2	
9228	D22	11.6	2.8		6.8	5.3		12.0				1.5	1.1	2.3	3.6	47.0	1.6	2.7				1.6	0.4	100.3	
9235	D1	1.3			1.9	0.2		1.9							1.0	87.4	0.6	1.7	0.1		3.8			99.9	
9266	D32	46.5	4.1			2.1		17.1				2.8	5.3		5.1	10.5	2.3	3.7					0.5	100.0	
9267	D24	30.5	4.3	6.0		3.4		18.3	4.3			5.2	5.2		4.2	14.5	1.4	1.7				0.4	0.6	100.0	
9268	D19	6.1	0.8		2.0	2.1		11.3				2.4	1.9		3.8	63.0	1.8	2.7	1.9				0.2	100.0	
9362	D6	26.6	1.5			3.7		10.0	1.8			1.9	4.4		2.4	40.7	0.1	0.7	1.7		3.8	0.4	0.2	99.9	
9372	D34	36.2	6.5		5.7	2.1	1.1	26.7	5.2	0.1		2.1	3.9		2.8		3.7	2.7						1.1	99.9
9375	D4	14.5	2.1		8.8	1.9		16.6				4.0	2.7		2.9	41.6	1.7	2.1	0.8					0.3	100.0
9380	D5	15.9	2.0		5.1	4.5		17.4	2.2			5.4	1.9		2.6	38.6	1.1	1.0	1.8				0.4	99.9	
9386	D11	23.2	2.5	10.3		6.3		20.6	2.6			3.7	2.1		3.2	21.6	1.0	1.6	0.7				0.7	100.1	

**Legend**

Column Label	Label Description	Column Label	Label Description
Sample No.	AGS sample number	Hem.	Hematite
Site No.	AGS site location number	Kaol.	Kaolinite
Ank.	Ankerite	Micro.	Microcline
Bio.	Biotite	Mont.	Montmorillonite
Brlt.	Brookite	Musc.	Muscovite
ClCh.	Clinocllore	Ortho.	Orthoclase
Dolo.	Dolomite	Paly.	Palygorskite
FlAp.	Fluorapatite	Rhod.	Rhodochrosite
Gyp.	Gypsum		

All values are in weight per cent (wt %).

SGS Minerals Ltd. performed the analysis.

Software: Bruker AXS Diffrac Plus EVA

The semi-quantitative analysis of EVA is performed on the basis of relative peak heights and I/lor values of those detected crystalline phases with PDF files. Amorphous or crystalline mineral species present in trace amounts may go undetected.

Figure DM-K1. Bulk sample XRD analysis of the Duvernay and Muskwa formations shale (after Anderson et al., 2010 ERCB Report)

Sample No.	Site No.	SiO <sub>2</sub>	Al <sub>2</sub> O <sub>3</sub>	Fe <sub>2</sub> O <sub>3</sub>	MgO	CaO	Na <sub>2</sub> O	K <sub>2</sub> O	TiO <sub>2</sub>	P <sub>2</sub> O <sub>5</sub>	MnO	Cr <sub>2</sub> O <sub>3</sub>	V <sub>2</sub> O <sub>5</sub>	LOI	Total
		wt. %	wt. %	wt. %	wt. %	wt. %	wt. %	wt. %	wt. %	wt. %	wt. %	wt. %	wt. %	wt. %	wt. %
8135	D8	23.40	6.82	2.81	1.74	30.40	0.29	2.39	0.32	0.26	0.04	0.02	0.01	28.00	96.50
8456	D12	58.20	9.79	4.26	2.39	6.46	0.39	2.60	0.47	0.13	0.02	0.01	0.04	12.70	97.46
8461	D15	11.50	3.27	2.84	1.31	40.60	0.17	1.08	0.11	0.08	0.03	<0.01	<0.01	33.30	94.29
8480	D21	40.60	13.20	4.49	2.64	15.50	0.29	4.00	0.54	0.09	0.06	0.02	0.02	16.40	97.85
8996	D18	49.30	11.50	4.36	5.53	6.78	0.24	4.77	0.63	0.14	0.04	0.02	0.01	13.20	96.52
9205	D10	34.30	6.46	3.95	5.26	19.80	0.59	1.77	0.39	0.09	0.06	0.01	0.02	22.80	95.50
9228	D22	25.40	7.41	4.03	1.77	27.90	0.28	2.34	0.29	0.48	0.08	<0.01	<0.01	24.50	94.48
9235	D1	3.67	0.96	0.58	0.71	49.20	<0.01	0.48	0.05	0.07	0.02	0.01	<0.01	40.60	96.35
9266	D32	59.20	9.50	3.84	2.19	6.92	0.44	2.17	0.45	0.09	0.05	0.02	0.03	11.30	96.20
9267	D24	51.00	11.10	4.27	2.06	8.30	0.38	3.08	0.41	0.12	0.03	<0.01	0.02	15.50	96.27
9268	D19	16.70	6.02	2.16	2.07	36.00	0.16	1.52	0.23	0.08	0.06	<0.01	<0.01	31.20	96.20
9362	D6	37.20	5.85	4.15	1.65	22.60	0.17	1.65	0.24	0.16	0.04	0.01	0.03	22.20	95.95
9372	D34	60.80	16.60	4.89	2.05	0.74	0.52	3.47	0.68	0.09	0.03	0.03	0.04	8.30	98.24
9375	D4	32.80	9.34	2.66	1.55	24.60	0.23	3.58	0.30	0.11	0.05	0.01	0.02	21.50	96.75
9380	D5	34.70	11.50	3.31	2.04	21.10	0.25	3.71	0.44	0.10	0.04	<0.01	0.01	20.10	97.30
9386	D11	43.90	13.30	4.27	2.40	13.50	0.28	2.28	0.60	0.09	0.05	0.02	0.02	14.90	95.61
9266DUP	D32	60.00	9.45	3.81	2.22	6.99	0.46	2.16	0.46	0.10	0.04	<0.01	0.03	11.30	97.02

**Legend**

Column Label	Label Description	Column Label	Label Description
Sample No.	AGS sample number	TiO <sub>2</sub>	Titanium oxide
Site No.	AGS site location number	P <sub>2</sub> O <sub>5</sub>	Phosphorus oxide
SiO <sub>2</sub>	Silicon oxide	MnO	Manganese oxide
Al <sub>2</sub> O <sub>3</sub>	Aluminum oxide	Cr <sub>2</sub> O <sub>3</sub>	Chromium oxide
Fe <sub>2</sub> O <sub>3</sub>	Iron oxide	V <sub>2</sub> O <sub>5</sub>	Vanadium oxide
MgO	Magnesium oxide	LOI	Loss-on-ignition (amount of material lost due to heating)
CaO	Calcium oxide	Total	Total weight per cent
Na <sub>2</sub> O	Sodium oxide	wt. %	Weight per cent
K <sub>2</sub> O	Potassium oxide	DUP	Duplicate

Figure DM-K2. Major oxides of the Duvernay and Muskwa formations shale from X-ray Fluorescence analysis (after Anderson et al., 2010 ERCB Report)

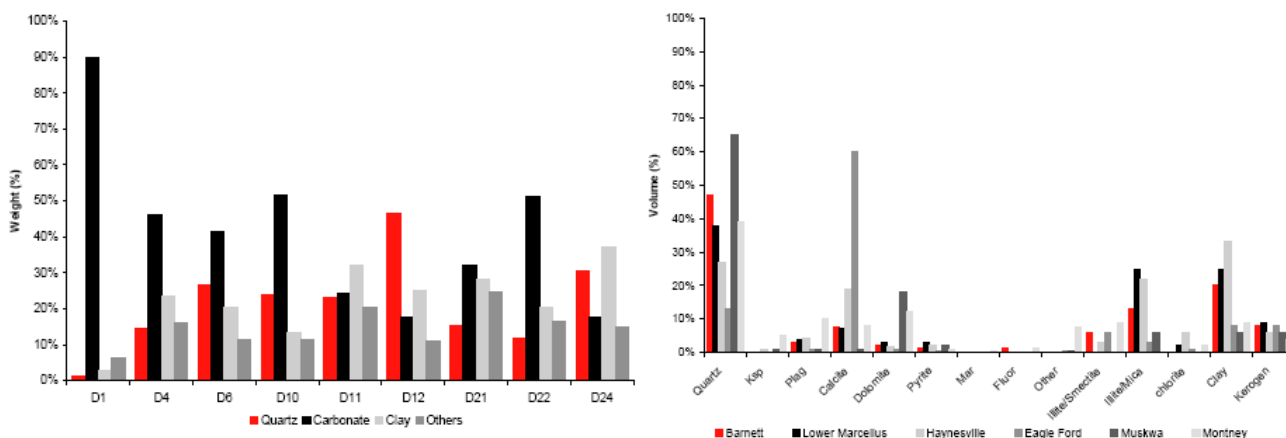
Sample No.	Site No.	Sample Type	Crystalline Mineral Assemblage (Relative Proportions Based on Peak Height)			
			Major (>30 wt.%)	Moderate (10-30 wt.%)	Minor (< 10 wt. %)	Trace (< 1 wt. %)
8996	D31	Core	(quartz)		illite, (dolomite)	*chlorite, (*plagioclase), (*potassium-feldspar), (*pyrite), (*brookite)
9205	D10	Core	(calcite)	(ankerite), (quartz)	illite	*(brookite), *(pyrite)
9228	D22	Core	(calcite)		(quartz)	*illite, *chlorite, (*ankerite), (*brookite), (*pyrite), (*potassium-feldspar)
9235	D1	Core	(calcite)			(*quartz), (*gypsum), (*potassium-feldspar)
9266	D32	Core	(quartz)		illite, kaolinite, chlorite, (calcite)	(*ankerite), (*pyrite)
9267	D24	Core	(quartz)		illite, (calcite)	*chlorite, (*mica), (*plagioclase)
9268	D19	Core	(calcite)		illite, (quartz)	*chlorite, (*ankerite), (*potassium-feldspar)
9362	D6	Core	(quartz)	(calcite)	illite	*chlorite, (*mica), (*pyrite), (*apatite), (*gypsum)
9372	D34	Core	(quartz)	illite/montmorillonite mixed	chlorite	*kaolinite
9375	D4	Core	(quartz)	(calcite)	illite	*chlorite, (*ankerite), (*pyrite)
9380	D5	Core		(quartz), illite, (calcite)	chlorite	(*brookite), (*potassium-feldspar), (*rhodochrosite), (*pyrite)
9386	D11	Core	(quartz)		illite, (calcite)	*chlorite, (*plagioclase)

**Legend**

Column Label	Label Description
Sample No.	AGS sample number
Site No.	AGS site location number
Sample Type	Core, outcrop or cuttings
wt. %	Weight per cent (relative proportion of clay-sized minerals only)

\* Tentative identification due to low concentrations, diffraction line overlap or poor crystallinity.

Figure DM-K3. Clay Mineralogy of the Duvernay and Muskwa formations shale (after Anderson et al., 2010 ERCB Report)



Note: \*designated well cores evaluated by the ERCB/AGS

Source: Core Laboratories (C. Hall, 2010). ERCB/AGS. Company Reports. Macquarie Research, August 2011

Figure DM-K4. Mineralogy of the Duvernay formation shale and its comparison with other important shale gas resources of the world.

Image 8479\_6 is a 10 000 $\times$  magnification image of image 8479\_5 (800 $\times$  magnification) that focuses on the development of apparent porosity between grain surfaces. The material is dominated by clay minerals, likely of the illite-smectite family. The open linear pores, elongated north-south in the image, occur at grain boundaries and may be due to relaxation of the sediment upon unloading, which would fit the 'poker-chip' appearance of the core. Circular pores may be sites of plucked grains, so it is difficult to be certain of porosity development in this image.

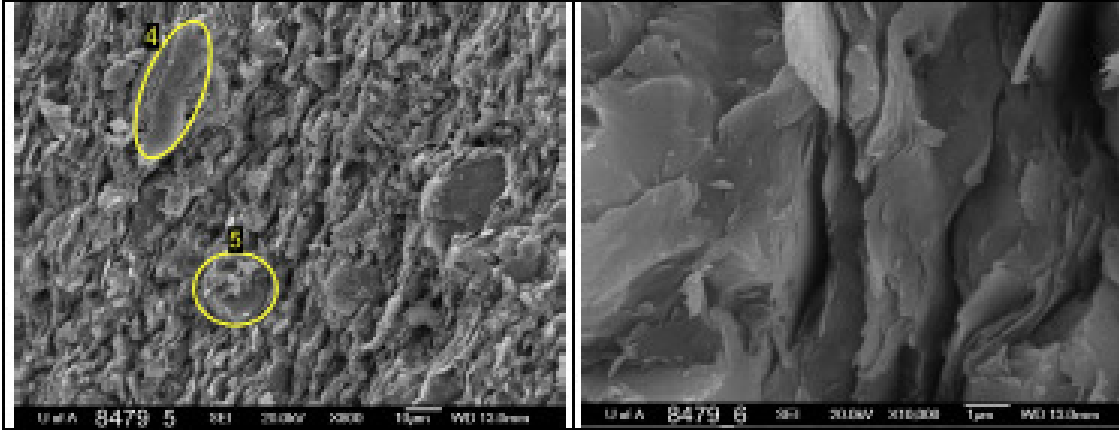
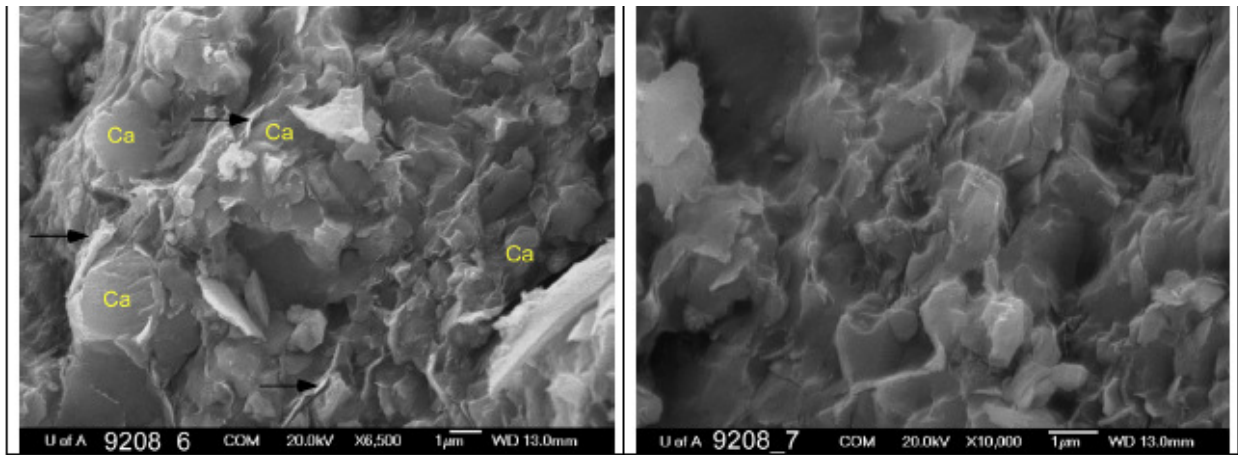


Figure DM-L. SEM images of Duvernay source rock showing the porosity development within Duvernay Shale (sample 8479)



The focal points of image 9208\_8 (3700× magnification) are the large, perhaps authigenic, calcite particles (see image 9208\_4 and 9208\_EDX\_002) surrounded by clay and the quartz particle in the yellow circle. Quartz grains are difficult to locate in this sample. There is a high degree of porosity relative to image 9208\_7. Pore sizes range from <math><1\ \mu\text{m}</math> to 4–5  $\mu\text{m}</math>; porosity is very well distributed.$

Image 9208\_9 is a relatively low magnification (1600×) image of an area of fairly high, well-distributed porosity. Mineralogy is again dominantly calcite and clay of various sizes.

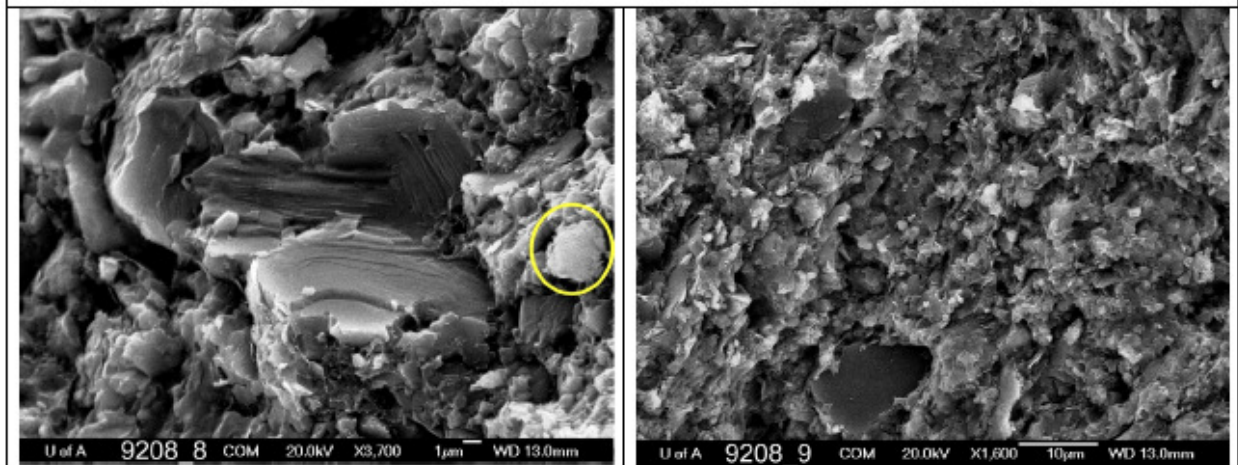
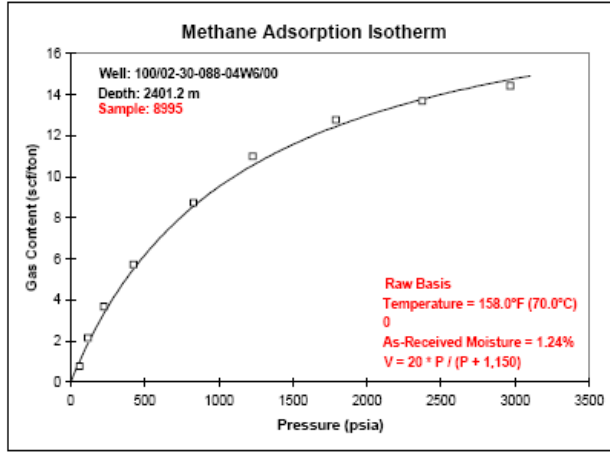
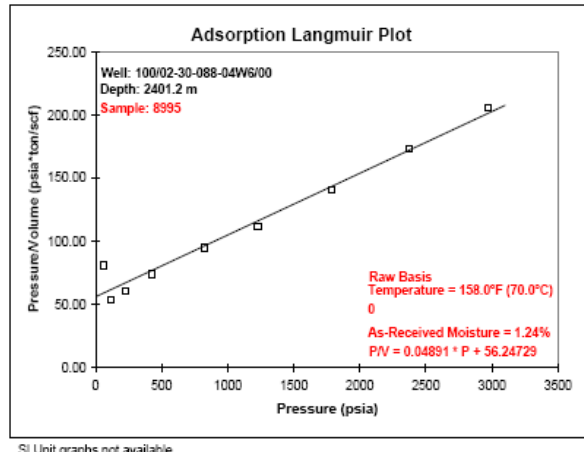


Figure DM-L2. SEM image of Duvernay Formation source rock showing relatively high porosity surrounding the quartz and clay grains.

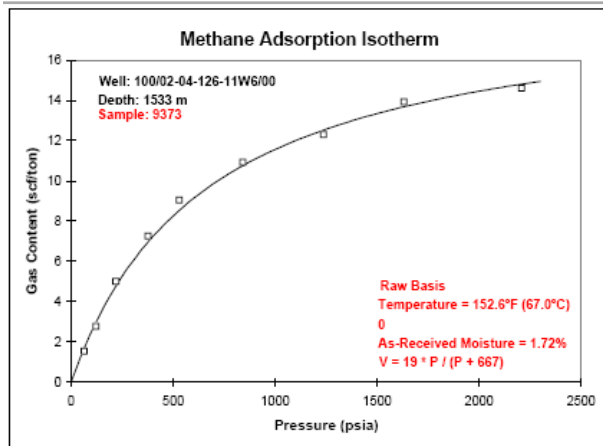


Sample: 8995 (2401.2 m) Muskwa Fm

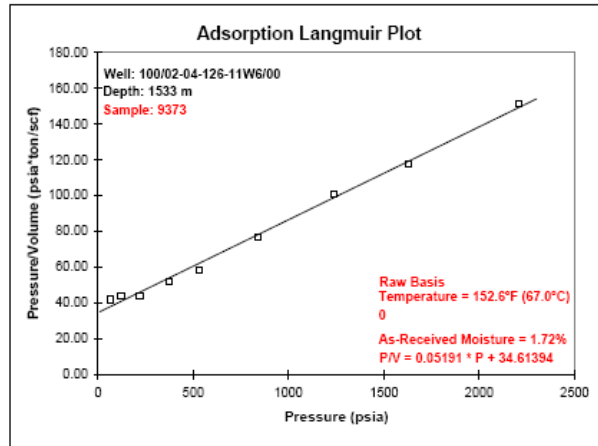


Sample: 8995 (2401.2 m) Muskwa Fm

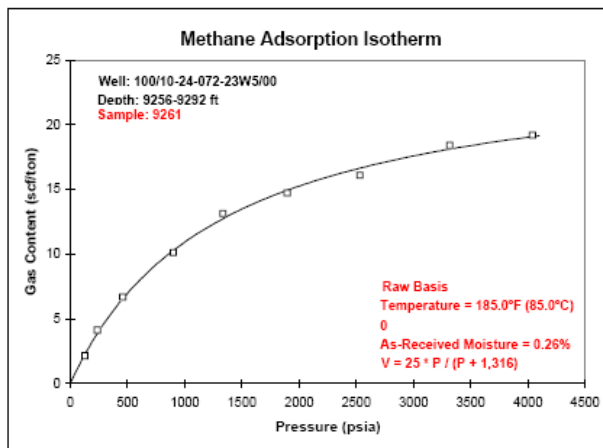
SI Unit graphs not available



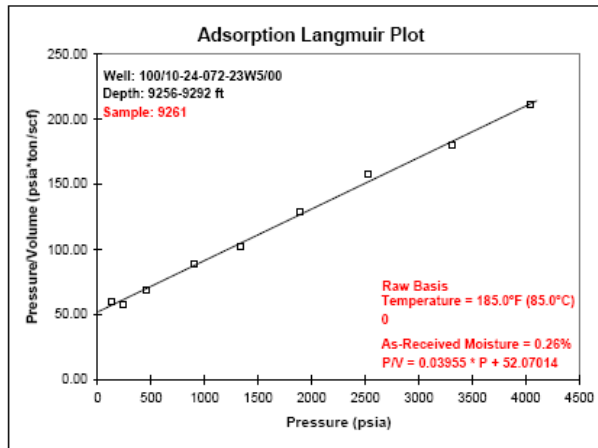
Sample: 9373 (1533 m) Muskwa Fm



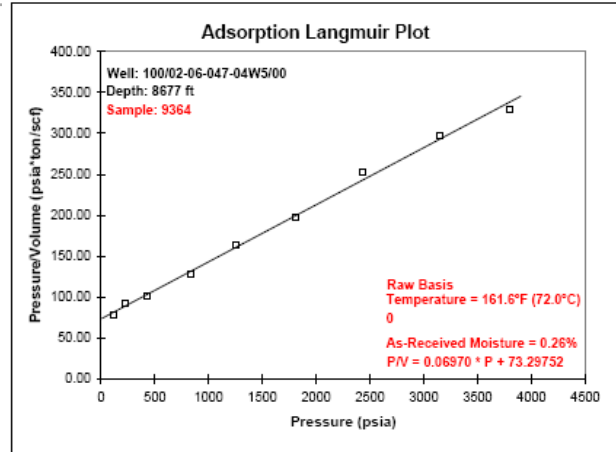
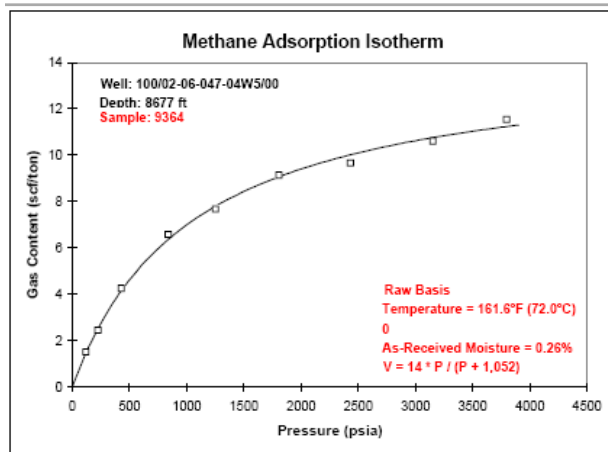
Sample: 9373 (1533 m) Muskwa Fm



Sample: 9261 (9252-9292 ft) (Duvernay)



Sample: 9261 (9252-9292 ft) (Duvernay)



Sample: 9364 (8677 ft) (Duvernay)      Sample: 9364 (8677 ft) (Duvernay)  
 Figure DM-M. Adsorption Isotherms of four samples from the Duvernay and Muskwa Formation source rocks

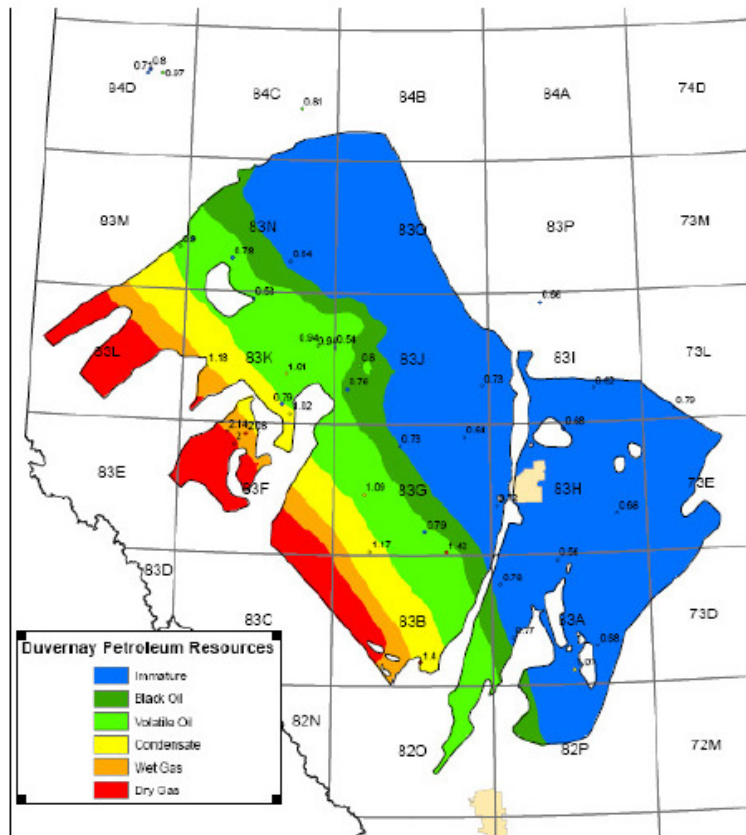


Figure DM-N: The distribution of various type of hydrocarbons (black oil, condensate, and dry gas) within northeast to northwest section of Alberta

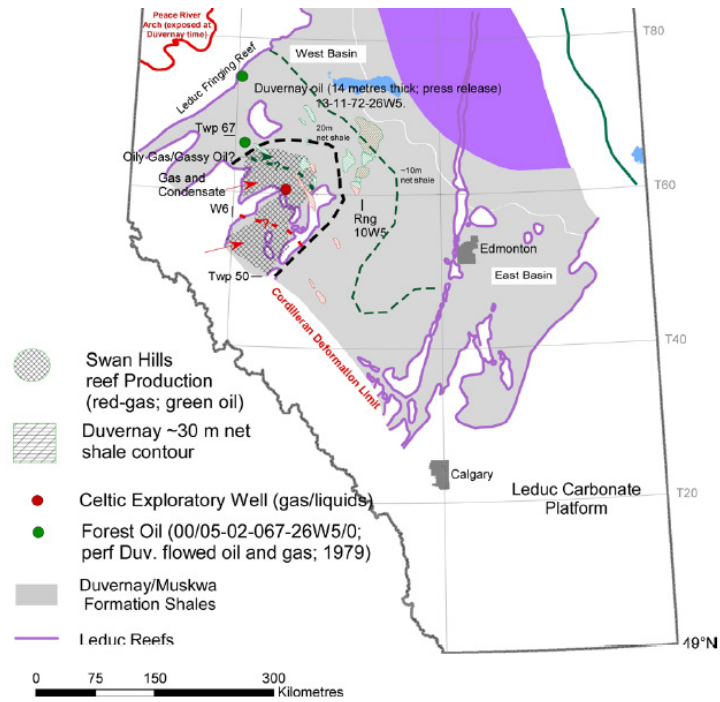


Figure DM-O. The distribution of oil, condensate and gas wells within the northwest